The Dissertation Committee for Amy Lynn Neuenschwander certifies that this is the approved version of the following dissertation:

REMOTE SENSING OF VEGETATION DYNAMICS IN RESPONSE TO FLOODING AND FIRE IN THE OKAVANGO DELTA, BOTSWANA

Committee:

Kelley A. Crews, Supervisor

Kenneth R. Young

Brian H. King

Robert A. Dull

Melba M. Crawford

Susan Ringrose

REMOTE SENSING OF VEGETATION DYNAMICS IN RESPONSE TO FLOODING AND FIRE IN THE OKAVANGO DELTA, BOTSWANA

by

Amy Lynn Neuenschwander, BSASE; MSASE

Dissertation

Presented to the Faculty of the Graduate School of

the University of Texas at Austin

in Partial Fulfillment

of the Requirements

for the Degree of

Doctor of Philosophy

The University of Texas at Austin

December 2007

Acknowledgements

I would like to express my extreme gratitude to my family, friends, and faculty who have helped me complete this dissertation. I feel quite fortunate to have had the opportunities afforded me and I hope that everyone views the work in this dissertation as good science.

The members of my committee have provided me with a tremendous graduate education and have taught me to think critically about problem solving. In particular, this work has made me more aware of the complexity of human-environment systems and that a larger perspective is necessary as we enter into a new era.

First and foremost, I give my deepest gratitude to my best friend and my graduate advisor Kelley Crews. In addition to being a dear friend, Kelley has been a supportive advisor and given me the freedom to pursue my research yet keep me directed along a meaningful path. She has always shown faith in me and my abilities, even when I had lost faith in myself. I have told Kelley multiple times since we met that she has made me a better person. By watching her example, both professionally and personally, I have learned a lot and I continue to strive to improve myself. So, thank you – I couldn't have done any of this without you. I am extremely proud to be Kelley's first PhD student and I hope that this dissertation is just the beginning of a long relationship throughout our careers.

Next I would like to thank the other members of my committee. I selected each person on my committee to serve a particular role, which in sum encompass everything that I wanted this research to represent. Ken Young provided me with the insight on how

to think about ecology particularly in the context of disturbances. Brian King introduced me to the idea regarding how the utilization and distribution of natural resources influences livelihood decisions. Rob Dull showed me the importance and long use of human-induced fires on the landscape. Melba Crawford contributed to my methodological and statistical analysis of the time-series data that I utilized in this research. In addition, I have worked with Melba for many years and I have such an admiration for her that I regard her as my "work mom". It was Melba's encouragement and confidence in me that I enrolled in the graduate program in engineering. Finally, I have to give thanks to Susan Ringrose who is my Botswana connection. Sue was the voice of reason regarding my interpretation of the Okavango landscape.

I would also like to thank the many friends and colleagues in Botswana that I have relied on for my research. First I need to recognize Thoralf Meyer for his fabulous guiding services and knowledge of the Botswana landscape. I think I learned more from Thoralf in one day than reading a handful of articles. Plus, he made our time in the Delta great fun. I'd also like to thank the other members of Solutions for Geographic Information: Colm, Nkadi, Cherie, and Paul. I also need to thank Wilma Matheson and Sue (and Smudgy) for their hospitality during our trips to the Delta. Being in the presence of friends like them makes it easier to be far away from home.

I also need to give great thanks to Michael Heinl and Jan Silva from Techniche Universitaet Muenchen for their collaboration and allowing me to utilize the Landsat time-series. Much of the information that I was able to develop was only made possible by having this extraordinary data set. I would also like to thank Melba Crawford and the

Center for Space Research for use of NASA EO-1 imagery as well as the Harry Oppenheimer Okavango Research Centre for additional information and data.

I would also like to thank the institutional support which provided me with funding allowing me to conduct my research. These include, NASA Earth Systems Science Fellowship, NSF Doctoral Dissertation Research Initiative, University of Texas at Austin Continuing Fellowship (David and Mary Miller), and Department of Geography and the Environment Research Contribution and Veselka Award.

I have to also thank my friends and colleagues from the Center for Space Research. Tim Urban, Roberto Gutierrez, Jenni Bonin, Charles Webb, and Don Chambers have all provided me with excellent feedback and advice on everything from data filtering to defending my dissertation. You all are great and I think CSR is such a special place to work that is supportive and intellectual stimulating.

Lastly, I'd like to thank my parents and friends for understanding when I couldn't always go out because I was working on my dissertation. Mom and Dad, y'all are the best and I know I'm lucky knowing that you'll always be there supporting me. Thanks also to Robert, Talia, and Diane for always being my friends.

AS WE SAY IN BOTSWANA… TSHASA MAHURA!

REMOTE SENSING OF VEGETATION DYNAMICS IN RESPONSE TO FLOODING AND FIRE IN THE OKAVANGO DELTA, BOTSWANA

Publication No. _____

Amy Lynn Neuenschwander, PhD.
The University of Texas at Austin, 2007

Supervisor: Kelley A. Crews

The Okavango Delta, an internationally recognized wetland, is undergoing natural and anthropogenic change at a variety of spatio-temporal scales. The objective of this research was to utilize remotely sensed imagery to assess the spatio-temporal distribution of flooding and fire and their subsequent influences on vegetation as represented by vegetation index trajectories in the Okavango Delta. The characterization of the spatio-temporal dynamics of vegetation spectral response via a time-series of remotely sensed data not only informs ecosystem and disturbance theory but also presents new methodological applications for multi-temporal change analysis. Disentangling these components from a signal is critical for better assessing the interrelationships among climatic oscillations, disturbance regimes, and human management on ecosystem response.

This research tested six hypotheses regarding flooding and fire, and found that the largest number of fires occurred either within 5 km of the border to the Wildlife

Management Areas or within the active (flooded a minimum of every two years) floodplains. These hypotheses indicate that burning is highest where people have access into the management areas and where the natural resources are plentiful. Periodicities from vegetation signal time-series did not confirm published climate-driven periodicities of 3, 8, and 18-years but did reveal seasonal (6 month) and quasi-decadal periodicities. Vegetation trajectories were more predictable with increasing flood frequency and duration, but were less predictable with increased fire frequency. The fact that increased burning resulted in less predictable behavior indicates the potential of quantifying the anthropogenic influence on the landscape using remotely sensed imagery. Flooding and fire were not statistically correlated to the residual dynamics, refuting the conceptualization of flooding and fire as disturbance and supporting the interpretation of flooding and fire as disturbance regimes. This research thus contributes methodologically and theoretically to the ecology literature by operationalizing tests for disturbance versus disturbance regimes via spatio-temporal characterization. Further, this work extends change detection techniques typically implemented with coarser spatial resolution but more frequently acquired imagery by using harmonic regression and wavelet analysis with Landsat data. Lastly, this work provides a temporally rich assessment of recent vegetation, flooding, and fire trends for improving management efforts of the Okavango Delta.

TABLE OF CONTENTS

LIST of FIGURES

LIST of TABLES

1 INTRODUCTION

In a world where major ecological change due to anthropogenically accelerated climate change and land use / land cover change is likely (Vitousek, 1994; Dale, 1997; Midgley et al., 2002; Walther et al., 2002), there is an increasing need to examine the forcing factors and ecological drivers that shape and modify landscapes and ecosystems today (Tilman et al., 2001). Recently, the National Research Council completed a decadal survey of the United States' role in Earth science applications from space. They began their study with the following challenge (NRC, 2007 pg ES-1):

> *Understanding the complex, changing planet on which we live, how it supports life, and how human activities affect its ability to do so in the future is one of the greatest intellectual challenges facing humanity. It is also one of the most important challenges for society as it seeks to achieve prosperity, health, and sustainability.*

Successful monitoring and conservation of the environment requires not only knowledge of ecosystem function but the identification of the social and economic forces that impact the natural environment through societal values, government policies, and pressures of population growth and poverty (Folke et al., 1996; Ogden et al., 2005). Local pressures contributing to changing landscape patterns include regional-scale climate change, hydrological change, and land use / land cover change (Schulze, 2006). Changes to the landscape and biogeochemical and hydrologic cycles may be induced by both natural and anthropogenic factors (Cramer et al., 2001; Arnell et al., 1996). Holling and

Meffe (1996) emphasize that the "Golden Rule" of natural resource management should be to "strive to retain critical types and ranges of natural variation in ecosystems" (pg 334). A thorough understanding of ecosystems requires knowledge not only of physical variables (e.g. soils, climate, topography, etc.) and land use/land cover (Lambin et al., 2001), but also of the disturbance history, as disturbances impact all levels of biologic organization in a system (Peterson et al., 1998).

The three primary ecological theories used as a conceptual framework for this research are equilibrium theory, disturbance theory, and resilience theory. Ecosystem dynamics are often described as falling along a continuum between equilibrium and non-equilibrium properties; however, most ecosystems exhibit properties of both (Briske et al., 2003). The advantage of using a non-equilibrium framework to describe ecosystem behavior is the recognition that ecosystems are dynamic and subject to external forces such as disturbances. Resilience is defined as the ability of a system to absorb a disturbance while maintaining the same function, structure, and feedbacks as a pre-disturbance state (Ludwig et al., 1997; Folke et al., 2004). Thus, the observed behavior of a resilient system would continue on its current trajectory following a disturbance.

Disturbance and disturbance regimes play an important role in vegetation ecology. In addition, local level changes can have a significant impact on larger scale processes (Pickett and White, 1985; Pickett et al., 1989, Wu and Loucks, 1995). For example, trace gases and aerosols released from local fires enter into the atmosphere and contribute to greenhouse gases (Scholes and Andreae, 2000; Korontzi et al., 2003). Recognizing the importance of disturbances on landscapes, Holling (1992) states that

analysis should be conducted on the function of disturbances to link the patch level to the global level for understanding ecological process. Figure 1.1 illustrates dominant vegetation processes at different levels. At the plant level, growth and productivity are influenced by biologic interactions and factors such as water and nutrient availability (Caylor et al., 2004; Corbin and D'Antonio, 2004). Conversely, at the regional or continental level, vegetation productivity is largely driven by climatic patterns of precipitation and temperature (Woodward, 1987; Shugart, 1993). At the landscape level, vegetation productivity is often a result of recovery following disturbances on the landscape, which influences microclimate as well as competition among individual plants (Holling, 1992; Daniels and Veblen, 2003).

In terms of disturbance theory, it is often debated what constitutes a disturbance and what does not; as disturbances occur at a variety of spatio-temporal scales (Pickett et al., 1989; White and Jentsch, 2001). For example, in flood pulse systems such as the Okavango Delta, a lack of flooding (rather than the occurrence of the flood event itself) could be regarded as a type of disturbance (Bayley, 1995). The same argument can be made for savannas that require fire to prevent dominance by woody plants. The concept of disturbance will be described in detail in Chapter 2. For descriptive purposes presented here, flooding and fire regimes will be referred to as a disturbance regime (rather than simply disturbances) in this dissertation.

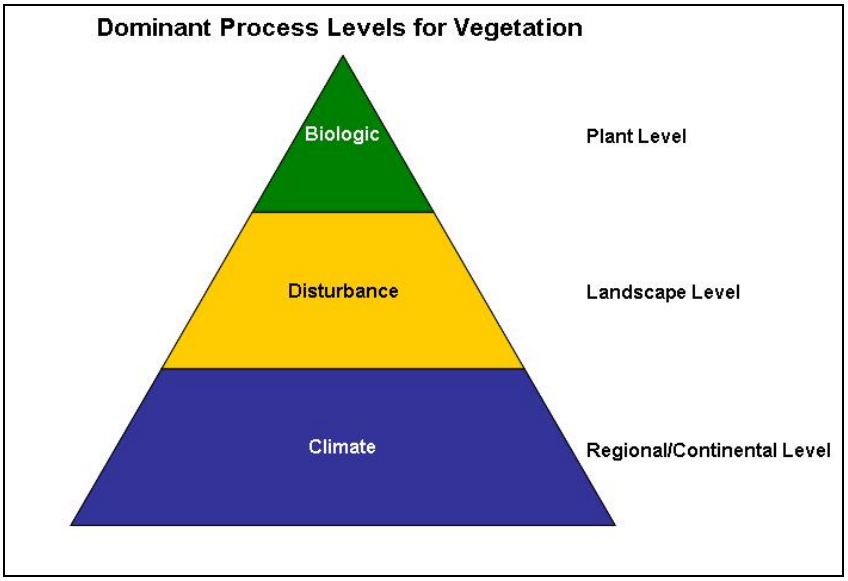

Figure 1.1 Hierarchical levels of dominant processes for vegetation. (Adapted from Holling, 1992 and Peterson et al., 1998)

1.1 Motivation for this research

This research is focused on the Okavango Delta in northern Botswana, one of the world's largest freshwater wetlands (approximately 15,000 km^2) and shown in Figure 1.2. The Delta provides critical habitat and resources to humans and wildlife (including large and endangered mammal populations), and for this reason has been internationally recognized as a wetland of importance by the Ramsar Convention on Wetlands (Kgathi et al., 2005). A fundamental requirement of the Ramsar treaty and the Okavango Delta Management Plan (ODMP) is the wise use and conservation of wetlands while being responsive to the socio-economic needs of local stakeholders (Swatuk, 2003).

The Okavango Delta is a wetland system with many complex ecological processes (Ramberg et al., 2006a). This research examines the relationship among flooding, fire, and observed vegetation spectral response through time as observed via

remotely sensed data. This area is a fitting location to examine the ecological impacts of flooding and fire because the Okavango Delta system has a relatively low amount of anthropogenic pressures (Turton et al., 2003; Ringrose et al., 2005). The benefit of conducting a study in an area of (relatively) low human pressure is that it enables the examination of vegetation dynamics via remote sensing in response to climatic and/or natural fluctuations. It is critical to understand and quantify the natural variability of ecosystems before the impacts from anthropogenic stressors can be determined and fully understood.

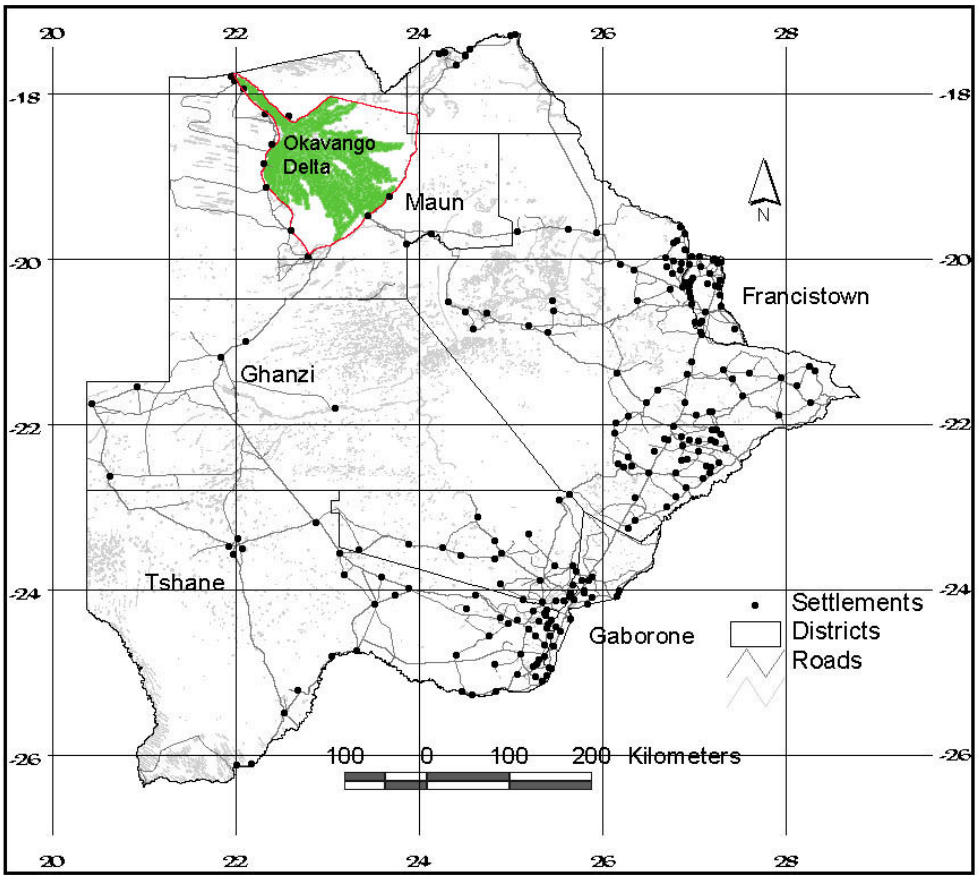

Figure 1.2. Okavango Delta and major settlements and roads in Botswana.

The Okavango Delta is located within a semi-arid savanna system in southern Africa where fire is common (Scholes, 1997). It receives approximately 75% of its total water supply through surface flow from the arrival of the annual floodwaters via the Okavango River (McCarthy et al., 1998a; Gumbricht et al., 2004a), which is fed by the Cubango and Cuito Rivers that originate in the highlands of Angola. Within the Okavango catchment, over 94% of the annual input to the Okavango River originates in Angola, with another 2.9 % originating from Namibia and the remainder originating in Botswana (Ashton, 2003). As the only permanent water source in northern Botswana, the Delta is significant due to its habitat for many threatened species (waterbird, antelope, and the endangered wild dog) and for the livelihood of local peoples dependent upon the Delta for water and veld resources (Kgathi et al., 2005). Understanding the pressures that occur in this relatively undisturbed environment is important for protecting the wildlife and people that utilize its resources. However, changes in land use such as the extraction of resources (water, fish, wood, and reeds), increased burning, overgrazing of domestic livestock, and a growing tourism industry threaten this wetland-savanna environment (Mbaiwa et al., 2002; Kgathi et al., 2006).

The Okavango offers a variety of opportunities for study from both a remote sensing and an ecological perspective. The study area for this research is located in the southeastern distal region of the Delta near the village of Maun at the wetland/savanna interface and is approximately 2,430 km^2 in size. The vegetation within the study area varies considerably and includes sedges, reeds, and grasses found in the channels and floodplains, *Acacia*-dominated savannas of various densities of tree cover in the drylands,

woodlands dominated by *Mopane*, *Combretum*, and *Acacia*, and riparian forest located on the fringes of many small islands and channel edges within the wetlands. Since flooding occurs during the dry (cloud-free) season, seasonal flooding can be monitored readily using optical remotely sensed data. The Delta is a compelling area ecologically in terms of its inter- and intra-annual variability, disturbance regimes, and responsiveness to changing climatic conditions. While the Okavango Delta is especially important to the communities who rely upon its resources and the wildlife that utilize it for habitat, understanding the complex interaction between natural and anthropogenic changes in this area will also contribute to the general understanding of observable vegetation spectral response in the presence of disturbance regimes (in this case, fire and flooding). The research will utilize information derived from remotely sensed imagery to map the spatio-temporal distribution of flooding and fire and to study their associations with the observed vegetative spectral response.

1.2 Environmental Remote Sensing

Disturbance often results in a patchy land cover and this heterogeneity acts to increase the probability of additional disturbance (Forman, 1995). This research quantifies the temporal dynamics of the observed vegetation spectral response to these disturbance regimes. A difficulty in characterizing landscapes in semi-arid regions using remotely sensed imagery is that the land cover within the pixel is often heterogeneous, in part because the spatial and spectral data resolution are coarse (Huete and Jackson, 1987; Diouf and Lambin, 2001; Harris and Asner, 2003). In semi-arid regions, climatic,

topographic, edaphic, disturbance, and land use factors all contribute to landscapes with varying densities of herbaceous cover, bare soil, rock, litter, and patches of woody vegetation. As a result, an important aspect of land cover change and water usage in the Delta involves the examination the relationship among flooding, fire, vegetation distribution, and observable vegetation spectral response.

Changes in land cover can be a result of long-term natural change, climatic variability, anthropogenic alteration of the landscape, and natural vegetation dynamics (Lambin et al., 2003). A common approach to mapping land cover change from medium resolution multispectral data (such as Landsat) is the "from-to" change analysis where relative changes of land cover between two scenes are extracted (Singh, 1989; Ridd and Liu, 1998; Du et al., 2002; Coppin et al., 2004). However, rather than mapping static land cover change between two distinct times, this research will utilize the total temporal signal from the available Landsat dataset and map temporal classes: classes that behave similarly spectrally throughout the time-series. Many multi-temporal studies are now based on time-series analysis of remotely sensed data to infer change and ecological process. To conduct this analysis, a time-series of 85 TM/ETM+ scenes ranging from April 1989 through October 2002 was used, with images spaced roughly every two to three months. By characterizing changes in observed vegetation spectral response as captured by a vegetation index, it becomes possible to assess the relative influence of disturbance on landscape dynamics and variability. This type of monitoring is offered as an alternative to traditional post-classification change detection, allowing for quicker calculation over time-series with frequent observations.

The practicality and the significance of this research lie in the richness of the dataset. Most land use/land cover (LULC) change detection studies utilizing medium resolution imagery (i.e. 30 m spatial resolution) are typically comprised of a few scenes collected one to several years apart (Mas, 1999; Masek et al., 2000; Rogan et al., 2002; Rogan et al., 2003). In contrast, remote sensing studies that utilize temporally rich datasets (observations daily to weekly, such as with MODIS or AVHRR) are limited due to the coarse spatial resolution of the imagery (i.e. 250 m to 1 to 4 km) (Justice et al., 1985; Eastman and Fulk, 1993; Markon et al., 1995; Jakubauskas et al., 2001). These studies typically examine vegetation indices (as a proxy for primary production) at the regional or continental level (Moulin et al., 1997; Gong and Shi, 2003; Stockli and Vidale, 2003). The dataset utilized in this research has sufficient temporal resolution (i.e. ~2 months) to examine intra- and inter-annual vegetation spectral response, but at a significantly improved spatial resolution (i.e. 30 m). Thus, the patterns observed at the landscape level due to disturbances can be measured via observed vegetation spectral response through time, and subsequently provides insight into understanding the underlying pressures on the ecosystem.

1.3 Research Hypotheses

The area's vegetation is affected by two major disturbance regimes, flooding and fire, but is also influenced by herbivory, human activity, and shifting climatic conditions. Humans influence the functioning of the Delta through burning, typically for hunting purposes, accidental fires, and the clearing of vegetation (Heinl et al., 2006). The 14-year

Landsat dataset provides a time-series of vegetation spectral response of the lower Okavango Delta from which the vegetation dynamics can be extracted. In addition, the 14-year spatio-temporal characterization of the flooding and fire regimes can be established.

Vegetation dynamics are here evaluated through the temporal pattern of observable vegetation spectral response. The observed vegetation spectral response through time is a function of multiple factors including climatic fluctuations, phenological differences in vegetation, background soil conditions, herbivory, anthropogenic stress, and flooding and fire. Decomposition of time-series data into seasonal, trends, or other cyclic patterns (referred to as the permanent signal) facilitates inference of the physical pressures contributing to various components of the time-series (Rodriquez-Trelles et al., 1996; West, 1997); stochastic events due to disturbances comprise a transitory or non-cyclic signal (Rodriguez-Arias and Rodo, 2004). This research will investigate whether ecosystem signals derived from remotely sensed imagery can be decomposed into these temporal components and whether the deviations from the decomposed signal are correlated with observed flooding and fire regimes. Again, the advantage of this 14-year Landsat database is the ability to conduct time-series analysis on vegetation at the landscape level rather than at the regional/continental level (Borak et al., 2000).

A concern stated in the Okavango Delta Management Plant (ODMP) as a threat to ecosystem sustainability is the high rate of human-induced fires in the Delta (Kay et al., 1999; Jansen and Madzwamuse, 2003). The study area contains four specific land

management regimes: Moremi Game Reserve, Wildlife Management Areas (which are utilized for consumptive and non-consumptive purposes), and communal areas. Within the wildlife management areas (WMAs), burning is not permitted. In other regions of the Delta, frequent burning is reported to be ecologically damaging resulting in increased erosion and loss of vegetation species (ODMP, 2006). The WMAs are separated from the communal area by a 1.5 m tall fence known as the Buffalo Fence. Settlement density in the communal areas is higher in the portions closest to Maun, and generally decreases as one approaches the Buffalo Fence. However, several settlements have recently been established near the fence crossing checkpoints. People seeking to enter the WMAs for the purposes of extracting resources typically cross on foot, and thus the human activities associated with burning in the WMAs will be highest closer to (within 5km of) the fence.

Hypothesis 1. Within the Delta's management zones, fire frequency is highest in the Wildlife Management Areas closest to the fence where people have easiest access.

A fundamental requirement of the Ramsar treaty and the ODMP is the wise use and conservation of wetlands while being responsive to the socio-economic needs of the stakeholders (Swatuk, 2003). Many communities rely upon harvesting of reeds or wetland-based tourism and fishing to provide the economic resources needed. In the Delta, the majority of fires are anthropogenic in origin, typically applied to small areas prior to harvesting of reeds or for clearing of dead vegetation prior to the arrival of the annual floods (Ringrose, personal communication). Thus the motivation for burning is

greatest in floodplains. Further, the active floodplains (those flooding at least once every two years) provide a greater and more easily ignitable fuel load for the lower intensity (cold) fires typically observed in the area.

Hypothesis 2. The largest number of fires occurs within the active floodplains.

Like most of southern Africa, Botswana's precipitation is highly cyclical. The temporal variability of precipitation in the Delta from year to year is reported to follow precipitation cycles common to southern Africa (McCarthy et al., 2000). McCarthy et al. (2000) reports 3, 8, and 18-year oscillations in precipitation cycles, with the largest oscillation occurring at the 18-year interval. Due to the location of Botswana within the African continent, the ENSO phenomenon is reported to have a negligible (Hulme et al., 2005) to weak (Obasi, 2005) influence on the climate of northern Botswana with below normal precipitation occurring during the warm phase of ENSO. Because the Delta is located in the subtropics and subject to annual flooding and wet/dry seasons, it is also expected that seasonal (6-month) periodicities will be detected.

Hypothesis 3. Periodicities observed from the vegetation signal time-series will be strongest at both (seasonal) and 3-, 8-, and 18-year cycles.

Resilience is defined as the ability of a system to withstand disturbance while maintaining the same function, structure, and feedbacks as a pre-disturbance state (Ludwig et al., 1997; Folke et al., 2004). By implementing a harmonic regression model on each EVI trajectory, the overall R^2, or predictability, serves as a potential indicator of

resilience. Thus, if an area experiences a disturbance yet continues along its trajectory, this predictability is an indicator of resilient behavior. This research will test that increased flooding reduces the predictability of the trajectory. That is, as flooding increases the cyclic nature of the vegetation trends will be disrupted and become less predictable. The motivation for implementing a harmonic regression in this research is to quantitatively describe the trends and patterns of land cover trajectories hypothesized to correspond to cyclical events or pressures. Harmonic regression fits data to a described trend and cycle(s) using harmonics of a sine wave rather than fitting the data to a linear or polynomial function. The overall R^2 of the harmonic regression will be examined for areas experiencing different levels of flooding. Similarly, this research will test the idea that increased burning reduces the predictability of the trajectory. That is, increased burning is associated with destabilizing the temporal trajectory, resulting in a poorer fit of observable vegetation response to cyclic patterns. Again, the overall R^2 of the harmonic regression will be examined for areas experiencing different levels of burning.

Hypothesis 4. As flood frequency increases, the predictability of the temporal trajectory decreases.

Hypothesis 5. As fire frequency increases, the predictability of the vegetation trajectory decreases.

Temporal analysis of ecosystem trajectories can be successfully decomposed into two general categories: permanent and transitory signals (Rodriguez-Arias and Rodo, 2004). Permanent signals are composed of trends, seasonal and annual cycles, and long

term cycles (Jassby and Powell, 1990). Transitory signals, in contrast, are signals that are temporary and discrete within a time series, such as from a disturbance (Rodriguez-Arias and Rodo, 2004). This hypothesis tests whether the deviations from the permanent signal are correlated with observed flooding and fire regimes. That is, if flooding and/or fire act as disturbance (rather than or in addition to more cyclic disturbance regime behavior), then they should be positively associated with an increase in residual (non-cyclic) signals.

Hypothesis 6. Flooding and fire are positively correlated with the residual signal of the EVI trajectories.

1.4 Future Scenarios for the Okavango Delta

From 1900 to 2000, the African continent has experienced an average temperature increase of 0.5ºC (IPCC, 1996). Predicted future climate is harshest in the semi-arid region of southern Africa, with temperature increases ranging from 0.2ºC/decade to 0.5ºC/decade (McCarty, 2001; Hulme et al., 2001; Wigley and Raper, 2001). Temperature increases of this magnitude will increase potential evaporation, decrease soil moisture, and likely extend the severity of droughts that this region of Africa already experiences (Balling, 2005).

The use of global circulation models (GCMs) has been implemented by climatologists to predict climatic outcomes due to increased levels of CO_2 and aerosols in the atmosphere for the near future (Cox et al., 2000; Bonan et al., 2003). The predicted changes in annual rainfall are less certain. In general, GCMs do a poor job at representing changes to precipitation cycles, especially decadal variations, due to the fact that the

models do not take into account many factors such as dynamic vegetation feedback, land cover modification, ENSO events, cloud cover, dust and biomass aerosols, and sea surface temperature variations (Pope et al., 2000; Hulme et al., 2001). If the Okavango catchment were to experience less precipitation, there would be significant changes to the ecosystem functioning, structure, and services as less water would enter the Delta through annual flooding (Ellery and McCarthy, 1994; Junk 2002).

In addition to anticipated climatic shifts, anthropogenic changes also impact ecosystems. The Okavango Delta has already experienced change due to political policy and land use practices (Thomas, 2003; Ellery and McCarthy, 1998). Following twenty-seven years of civil war, displaced Angolans are returning to the upper portion of the Okavango basin (Andersson et al., 2006). For this reason, management plans have been developed and are in the process of being implemented by the government and citizens of Botswana for the wise use and sustainability of the Okavango Delta (Scudder et al., 1993; Turton and Earle, 2003).

1.5 Organization of Dissertation

This dissertation examines the utilization of remotely sensed imagery to quantify the spatio-temporal distribution of flooding and fire and their associations through time to the dynamics of the observed vegetation spectral response. Chapter 2 provides an overview of the theoretical framework for this research, particularly focusing on equilibrium/non-equilibrium concepts for ecosystems, disturbance theory, ecosystem resilience, and the role of disturbance in savanna and wetland ecosystems. Chapter 3

describes the environment (biotic, abiotic, and to a limited degree political) of the Okavango Delta in northern Botswana. Chapter 4 details the research methodology for environmental remote sensing. In particular, it describes the sensor systems used and data processing methods that will be implemented to test the research hypotheses. In addition, this chapter reviews the methods used in the remote sensing community to detect changes on the landscape from simple "from-to" methods to analysis on multi-temporal datasets. Chapter 5 describes the datasets used in the analysis for this research including the 14-year Landsat data. In addition, trends from meteorological and hydrological datasets for Maun and the lower Okavango are presented. Chapter 6 provides a characterization of the spatio-temporal distribution of the flooding and fire regimes in the lower Okavango Delta with respect to different landcover types. Hypotheses one and two are discussed and tested in Chapter 6. Hypotheses three through six along with the results of the multi-temporal analysis are presented in Chapter 7. Finally, Chapter 8 synthesizes the methodologies/results used in this research and describes their contribution to the literature. Further, the contribution of the results to Delta and its stakeholders are presented. Additionally, the last chapter calls for continued monitoring of the Delta using remotely sensed and *in situ* data.

2 THEORETICAL FRAMEWORK

The theoretical framework for this dissertation is based on concepts of equilibrium/non-equilibrium theory and ecosystem resilience with particular attention given to disturbance and disturbance regimes. Resilience theory provides a conceptual framework in which the behavior of complex systems (Levin, 1993; Pickett and Cadenasso, 2002), whether ecological or social systems (Walker et al., 2006), can be explored. The primary components of resilience theory are self-organization, feedback loops, hierarchical structure of the system, and non-linear behavior in response to disturbance (Gunderson, 2000; Cumming et al., 2005). The first section of this chapter will define and discuss fundamental ideas regarding the conceptualization of ecosystems. Next the concepts of ecological resilience and disturbance will be discussed. Finally, since this research will be focused on a wetland/savanna interface, a general review of relevant wetland and savanna theories is presented.

2.1 Conceptualization of Ecosystems

The ecosystem concept came from Arthur Tansley (1935) who described an ecosystem as a complex of organisms linked with their surrounding physical environment. The definition of an ecosystem is purposely vague so as not to be restrictive and to allow for general relationships to be developed (Tilman, 1999). Pickett and Cadenasso (2002) provide a framework for conceptualizing ecosystems as meaning (how it is defined), model (what are the components and their function), and metaphor (what does it represent or to what is it likened). Ecosystem models were developed to

understand functions and fluctuations such as include nutrient/resource allocation (Veenendal et al., 2004; Scholes, 2003), population shifts (Moorecraft et al., 2001; Rodriguez-Arias and Rodo, 2004), and energy flows using thermodynamic laws (Schneider and Kay, 1994; Toussaint and Schneider, 1998). This research primarily focuses on the model component of the ecosystem framework as it describes the physical structure and functioning. Following the ecosystem model architecture, critical components for understanding ecosystem processes include the definition of the spatial and temporal domain as well as the type of system dynamics (e.g. equilibrium or non-equilibrium).

Conceptual definitions of ecosystems evolved from simple models to complex adaptive systems (CAS) (Levin, 1998), which are a mechanism for describing the interactions and feedbacks of complicated structures and patterns in an ecosystem. Specifically, Levin (1998) described four properties of CAS: aggregation, diversity, nonlinearity, and flows. Aggregation refers to how individual components within an ecosystem are grouped (i.e. population, taxonomic, or functional groups) and are dependent upon local environmental conditions in which they exist. The hierarchical patterns that emerge from this aggregation are the result of processes from below and areas constrained from above (O'Neill et al., 1989; Peterson, 2000a). Lower level components within a hierarchical structure are considered homogeneous and are constrained by a higher level. Interactions among lower level components and with higher level components can be weak or strong depending upon the relationship and linking mechanism. The property of non-linearity implies that the system can shift into

alternative pathways depending upon the interactive behavior among components and stochastic events. This behavior of CAS lends itself well to ecological resilience theory, because as systems adapt to change they become more resilient to future change (Gunderson, 2000a; Carpenter et al., 2001). Finally, flows (energy, nutrients, and materials) are the last defining properties of CAS and they can enter, interact, and alter the system at various times and rates. A key concept of CAS as defined by Levin (1998) is that the interactions are localized; thus place (Loreau, 1998; Peterson et al., 1998).

Recently, Pickett et al. (2005) defined a new conceptual framework of biocomplexity that incorporates relationships and dynamics at multiple scales building toward the development of operational models. Within this framework, they identify the three dimensions of biocomplexity as spatial (the patch structure and configuration on the landscape), organizational (the connectivity and dynamics of these patches), and temporal (the interactions to local environment, lagged responses, as well as historical legacies). While the biocomplexity framework provides a strategy for unraveling the complexity within coupled systems, it is often difficult to incorporate conceptual frameworks into practical applications. Despite the challenges, the development and utilization of conceptual frameworks are necessary for describing complex systems such as ecosystems.

2.1.1 Equilibrium Theory

Equilibrium as defined by Merriam-Webster is “a state of balance between opposing forces or actions”. This concept of a balance of nature has been conceptualized

since the days of Aristotle (384-322 BC) (Perry, 2002) and was the common paradigm for ecology until the 1970s (DeAngelis and Waterhouse, 1987). A system in equilibrium can be described as fluctuating around an equilibrium (or steady-state) point (Holling, 1973; Pickett and Cadenasso, 2002). Under this paradigm, ecosystems possess the capacity of internal regulation through negative (Briske et al., 2003). Two fundamental characteristics of a system presumed to be in equilibrium are that the system is closed and that the system is self-regulating. The concept of representing a natural system as being closed is not valid as there are many external variables and forces interacting with an ecosystem at any given time (Wu and Loucks, 1995). Further limitations of the classical equilibrium theory include not accounting for spatial heterogeneity on a landscape, assuming systems are free of disturbance and other stochastic factors, and neglecting spatio-temporal scale. A practical limitation to equilibrium theory is that many processes modeled in an equilibrium framework utilize mean values and assume homogeneity, largely due to analytical convenience (Perry, 2002).

2.1.2 Non-equilibrium Theory

In response to the limitations of classical equilibrium theory, non-equilibrium theories were offered to incorporate the concepts of stochastic processes and nonlinear dynamics of ecosystem processes. Non-equilibrium models incorporate concepts such as multiple steady states and attractors (O'Neill, 1999; Walker et al., 1981; Ludwig et al., 1997), a shifting mosaic of patches (Turner et al., 2001), and ecosystem resilience (Levin, 1998; Pickett and Cadenasso, 2002). Holling (1973) noted that ecosystems could shift to

a new configuration under the influence of significant disturbance. Under a non-equilibrium paradigm, ecosystems are prone to disturbances and the dynamics are less predictable (Briske et al., 2003; Lankford and Beale, 2007). Spatial heterogeneity across a landscape plays a fundamental role in the landscape dynamics and is often incorporated in a non-equilibrium framework.

Characterizing the spatial heterogeneity of a landscape is often operationalized by viewing that landscape as a composite of smaller, homogeneous patches. Patch dynamics, source-sink models, patch boundaries, and metapopulation theories have all recognized and focused on the spatial heterogeneity of a landscape for developing process to pattern linkages (Wu and Loucks, 1995; Aguiar and Sala, 1999). A limitation of a non-equilibrium paradigm is that the dynamics are overly influenced by stochastic events and less sensitive to continuous dynamics and internal regulations from plant-herbivore-nutrient interactions. From their work in rangeland ecosystems, Briske et al. (2003) suggest that ecosystems have aspects of both equilibrium and non-equilibrium paradigms rather than existing along a continuum as suggested by Wiens (1984). In fact, the assessment of ecosystem equilibrium is a function of both temporal and spatial scale (DeAngelis and Waterhouse, 1987). As spatial scale decreases, the dynamics of a system move toward non-equilibrium. For example, disturbances or perturbation to the system can result in population extinction at the species level, (Illius and O'Conner, 1999); thus exhibiting non-equilibrium dynamics at the system level. However, the system can still be considered in equilibrium at the community level, as the extinction of one species may not affect the overall system function in the presence of other species. Equilibrium

dynamics at one level can thus occur with non-equilibrium dynamics occurring at a lower level (Illius and O'Conner, 1999).

2.2 Disturbance

Another key component for conceptualizing ecosystem dynamics is understanding how disturbance affects a system. White and Pickett (1985) provide a general definition of disturbance as "any relatively discrete event in time that disrupts ecosystem, community, or population structure and changes resources, substrate availability, or the physical environment" (pg 7). Shea et al. (2004) define disturbance as "an event which alters the niche opportunities available to the species in a system" (pg 492). Both of these definitions go beyond the concept of destruction of standing biomass to imply a disruption to processes and resources available in an ecosystem.

Disturbances are often characterized by the components that comprise a disturbance regime. These include the frequency (number of events over a given time period), intensity (energy per area per time), residuals (organisms that survive the disturbance), return interval (amount of time between events), extent (amount of area disturbed), and severity (effect of the disturbance on the ecosystem) (White and Pickett, 1985; O'Neill, 1999; White and Jentsch, 2001). These concepts of disturbance are typically associated with a negative connotation. Natural disturbances (i.e. lacking a human factor), however, are recognized as an important component of most landscapes, comprise a normal fluctuation to the system, and may often result in benefits to a system such as nutrient or soil deposition (Pickett et al., 1989). Further, depending upon the

disturbance regime, determining what is normal and what is disturbance can be somewhat ambiguous (White and Pickett, 1985; White and Jentsch, 2001). For example, herbivory is considered a natural and normal occurrence for many landscapes whereas an infestation of locusts that destroys entire crops may be considered a disturbance. The productivity of many ecosystems is often dependent upon the presence of disturbances such as fire, wind, or herbivores. If small disturbances are removed from the system there is an increased risk of large-scale destruction (Costanza, 1999). Finally, the definition of what constitutes a disturbance is also dependent upon the spatial and temporal scale at which it is considered.

The intermediate disturbance hypothesis (IDH) states that species richness will be greatest at intermediate levels of disturbance, resembling a Gaussian distribution (Connell, 1978; Collins et al., 1995; Collins and Glenn, 1997; Shea et al., 2004). The ecological reasoning behind this theory is that at low levels of disturbance, inter-species competition mechanisms will dominate, reducing diversity (Glenn et al, 1992). Conversely, at high levels of disturbance only species that rapidly colonize or are tolerant to disturbance will exist on the landscape (Connell, 1978; Townsend et al., 1997). The definition of intermediate is subjective and relative to the life histories of the vegetation type within the communities in which they exist (e.g. herbaceous versus forest). Shea et al. (2004) describe two underlying mechanisms behind the IDH as storage effect and non-linear response. The storage effect is a buffering mechanism of species (i.e. seed banks) that allow the species to re-emerge after periods of stress.

Results from experimental testing of the IDH are varied (Shea et al., 2004). Collins et al. (1995) tested it at the Konza prairie experimental station and found that species richness within burned grassland plots declined with increasing fire frequency which contradicts the IDH. They suggest, however, that their results were potentially confounded within the spatial scale of the experiments and due to the complexity of interactions among species. Similarly, Beckage and Stout (2000) did not find support of the IDH for species richness and fire for a Florida palm savanna. Sites were burned one to six times during a 16 year period and the authors collected data on the herbaceous understory in each site. Instead of a Gaussian relationship, they report a saturating (asymptotic) relationship between number of burns and species richness. They did, however, show that tree density was inversely related to fire frequency. In contrast, Townsend et al. (1997) found support of the IDH in macroinvertebrate richness in stream beds experiencing flooding related bed movement. While specific disturbance events are shown to impact ecosystems (i.e. hurricane or landslide), it is less certain how a change in disturbance regime impacts the landscape. Clark (1996) examined the fossil pollen and charcoal record to test the hypothesis that a changing fire regime would also change the long term histories of three fire dependent species in Minnesota: the results supported their conclusion that fire was controlling that landscape's diversity. A limitation of the IDH is that a simple variable, such as species richness, does not provide much insight into ecosystem function in response to disturbance. Rather, it is merely a count of the number of species.

2.3 Ecological Resilience

As described earlier in this chapter, the conceptual framework for ecosystems has evolved to recognize that they are complex and adaptive systems driven by both internal and external processes (Levin, 1998; Pickett and Cadenasso, 2002). Ultimately, understanding ecosystem response to these forces is critical for developing land management strategies and decision-making (Ellison, 1996; Wyant et al., 1995; Theobald et al., 2000).

Resistance and resilience are two properties that are widely used when discussing ecosystem dynamics (Peterson et al., 1998; Gunderson, 2000). Resistance is the ability to withstand change, and may be measured as the amount that a variable changes following a disturbance (Pimm, 1984). Resilience is the ability of a system to recover after it experiences a stress or disturbance (Holling, 1973; Walker et al., 1981; Allen et al., 2005; Bennett et al., 2005). Specifically, the definition of ecological resilience is the ability of a system to absorb a disturbance while maintaining the same function, structure, and feedbacks (i.e. a pre-disturbance state) (Ludwig et al., 1997; Folke et al., 2004). Thus, how quickly a system returns to its original state is a measure of its resilience (Pimm, 1984; Ludwig et al., 1997). Resilience was defined by Walker et al. (1981) as the "ability to adapt to change by exploiting instabilities rather than the ability to absorb disturbance by returning to a steady-state after being disturbed" (pg 495). Thus, resiliency is a property of the adaptive capacity of an ecosystem (Holling, 2001). In addition to providing an ability to withstand disturbance, ecological resilience provides the flexibility to respond to change in those disturbances (Nystrom and Folke, 2001).

2.3.1 Threshold Models

Conceptualizing multiple possible states within an ecosystem requires considering thresholds as boundaries that separate the different steady-states (Briske et al., 2003). The ball and cup metaphor, as shown in Figure 2.1, is considered the classic illustration of this concept (Holling, 1973; Noy-Meir, 1975, Scheffer et al., 2001). If the impact of a disturbance exceeds the resiliency of a system, then enough force and/or change is exerted to shift the system into an alternate state. What is initially difficult to grasp when relating this metaphor to ecosystem behavior and response is that the ball does not represent a physical entity per se, but rather a coupled set of ecological processes and components (DeAngelis and Waterhouse, 1987). The crossing of a threshold, also referred to as a regime shift, can be marked with either new, sudden feedbacks of the system where the trajectory of the system changes direction (Foley et al., 2003; Folke et al., 2004; Carpenter and Brock, 2006; Kinzig et al., 2006) or a more subtle trajectory change. A regime shift is comprised of a substantial reorganization of an ecosystem or components within an ecosystem and can be a result of factors operating at multiple scales, thus complicating observation and study (Peterson, 2002a; Carpenter and Brock, 2006). These shifts are commonly found in both savanna and wetland ecosystems (Walker et al., 1981; Bennett et al., 2005).

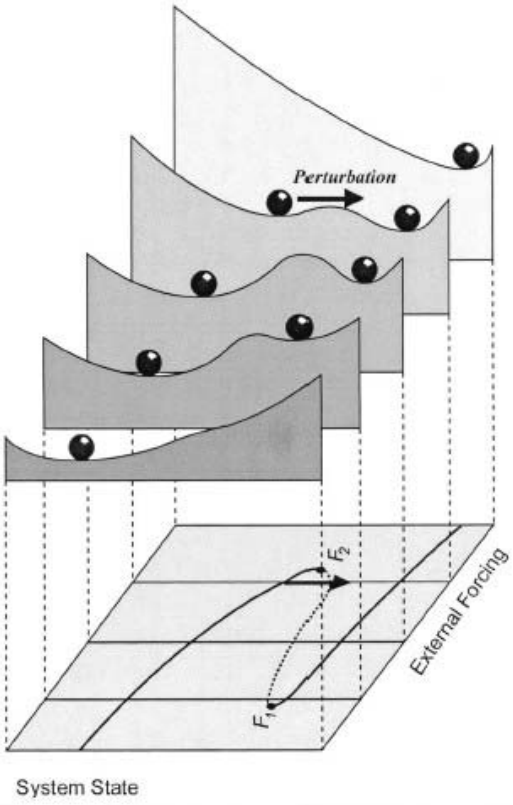

Figure 2.1. Stability of different landscapes ranging from stable to unstable (front to back) and their response to perturbations (from Scheffer et al. 2001).

A regime shift can occur quite rapidly; however, the cumulative effect of disturbances and gradual perturbations to the system is the result of a long history (Scheffer et al., 2001; Villa and McCloud, 2002; Scheffer and Carpenter, 2003). Thus, regime shifts can be misinterpreted to be the result of small events such as drought, disease, or storms, even though these events were only the triggering mechanism (Camill and Clark, 2000; Foley et al., 2001). For example, alternating steady states and regime shifts were presented by Folke et al. (2004) showing that long-term pollen records and

fossil shorelines and lake beds indicate the Sahel region in Africa is subject to shifts of alternating desert and vegetated conditions (Scheffer et al., 2001; Foley et al., 2003).

2.3.2 Indicators of Resilience

In much of the literature, ecological resilience is used as a metaphor rather than as a parameter than can be directly measured or empirically tested (Holling, 1973; Walker et al., 1981; Ludwig et al., 1997; Carpenter et al., 2001; Bennett et al., 2005). A difficulty in representing resilience as a function of time is that different species (in this case in terrestrial vegetation) have different life-cycles. For example, the resiliency of grasses will be much greater (i.e. faster) than trees in response to a fire that destroys above ground biomass. To date, there is no standard of which parameter(s) and which spatio-temporal scale(s) are necessary to determine ecological resilience. Instead, ecosystem resilience is inferred through a variety of indicators (Villa and McCloud, 2002; Bennett et al., 2005; Carpenter and Brock, 2006) or proxy variables that contain relevant information about key properties of the system and that can be directly measured or monitored (Adger, 2000; Schiller et al., 2001; Moss et al., 2001). However, a clear definition of ecosystem properties (in terms of X is resilient to Y over a period of Z) is necessary for successful implementation in the field (Carpenter et al., 2002). Properties linked with ecological resilience include rapid turnover of nutrients and biomass, redundancy of species or species richness at all hierarchical levels, large stocks of soil carbon and nutrients, and negative feedbacks of biologic interaction (Schiller et al., 2001; Turner et al., 2003). Allen et al. (2005) suggest the usage of discontinuous distributions

of system parameters across spatial scales, or hierarchical levels, as an indicator of resilience. Under this framework, complex systems are presumed to be hierarchical in nature and are driven by a few fundamental processes that operate across various spatio-temporal scales. A system that functionally operates at multiple levels in a hierarchical structure is suggested to be resilient (Peterson, 2000b; Carpenter et al., 2001).

The determination of resilience indicators is a function of the complexity of the system under investigation. Bennett et al. (2005) suggest a strategy to determine resilience indicators, or surrogates, for a variety of different ecosystems. While the internal dynamics of complex systems may not be known, knowledge of the feedbacks is necessary so that a threshold of key variables can be determined. For example, the dynamics of a relatively simple system such as a lake should function under oligotrophic (lacking plant nutrients, associated with an abundance of dissolved oxygen) conditions if nitrogen levels are held below a certain value. But if the nitrogen levels exceed some threshold, the lake would shift into a eutrophic state with a new set of dynamics. In this example, nitrogen levels would serve as an indicator, which is ideal as these levels could be easily measured and monitored. Carpenter and Brock (2006) suggest an increase in variability of system behavior as an indicator of a regime shift. It is possible to monitor variability of properties, such as nutrient levels or primary productivity, without full knowledge of the respective threshold value. In complex systems such as an African savanna with several variables potentially acting upon that system (fire, elephants, woodland/grassland competition), the threshold(s) can fluctuate, or can be difficult to

determine. For these types of systems, Bennett et al. (2005) suggest that the rate of change and the direction of that change can be used as a resilience indicator.

In the southern Pacific, the rate of change of coral reef accretion was used as an indicator of resilience (Villa and McCloud, 2002). Another indicator described by Costanza (1999) is the ability of vegetation to maintain vigor (productivity) in the presence of a stressor. The National Research Council (2000) recommends national and local indicators of ecological health that include: land use/land cover, species diversity, nutrient run-off, soil organic matter, vegetation productivity, carbon storage, nutrient use efficiency, foliage-height profiles, light penetration, and soil condition.

Rappaport et al. (1998) suggest three factors that comprise ecosystem sustainability are vigor (production or activity of vegetation), organization (biodiversity and interactions among components), and resilience. To predict the sustainability of an ecosystem, the Environmental Protection Agency (EPA) and the UN Framework Convention on Climate Change (UNFCC) are implementing the concept of vulnerability indicators (Moss et al., 2001). A vulnerability indicator is a composite of sub-indicators in the areas of societal value of the ecosystem, resilience, potential for risk, and scale (Villa and McCloud, 2002). Depending upon the rules established in the decision-making process, each sub-indicator is aggregated using a linear or non-linear weighting. However, there is not a theoretical understanding of how vulnerability is or should be assessed across hierarchical scales. Each sub-indicator is a reflection of processes or conditions that are implicit in the spatial and temporal scales of how it was defined (Niemi and McDonald, 2004). Eighty-nine indicators are currently utilized by the EPA to

assess environmental quality (US EPA, 2007). A few examples of these indicators include avian populations, coastal sediment quality, land use/land cover, nitrogen and phosphorus levels, growth rates in ecosystems, habitat/canopy structure, landscape fragmentation, and productivity (US EPA, 2007). A common thread among all of the suggested indicators from various programs incorporates measures of productivity, ecological function, and resiliency. It is the development of ecosystem health and vulnerability indicators that are entering into ecosystem conservation and restoration programs (Harris and Hobbs, 2001; Cairns, 2000).

2.3.3 Models of Landscape Resiliency

To demonstrate the concept of resiliency in a savanna, Ludwig et al. (1997) present a simple competition model between woody cover and herbaceous cover that is moderated by fire. In this model, fire results in the destruction of woody cover, thus giving the short term competitive advantage to grass and starting the cycle over again. The results from this simple model indicate a cycle between alternate states of woody versus herbaceous cover having a return period of approximately 50 years. However, this behavior could be called into question as many savanna fires are surface fires and typically do not result in tree mortality. This concept of cycling between alternate states is important to bear in mind when examining ecosystem behavior over a shorter time period. Baxter and Getz (2005) developed a model of woody vegetation dynamics in a savanna in response to elephant browsing, fire, and precipitation. While this model simplifies some parameters of the interaction on the landscape, it does indicate a

significant reduction of woody cover due to the introduction of elephants. This type of analysis has been employed in several studies (Walker et al., 1981; Foley et al., 2003; Carpenter and Brock, 2006) to describe the dynamics behind ecosystem shifts.

A limitation of many of the models used to simulate ecosystem dynamics is the lack of spatial interactions from neighboring cells. In a spatially explicit savanna model described by Baxter and Getz (2005), each calculation is computed and iterated on a per cell basis. In modeling, the impacts from elephants and fire do not move around on the landscape (i.e. interact with the landscape) except due to a random number generator cell assignment. Additionally, competition and interactions between woodlands and grasslands in neighboring cells are not implemented, likely due to complexity of characterizing the landscape. The spatial interactions of rainfall on vegetation productivity in arid regions were modeled and compared against aspatial models in a study by van de Koppel and Rietkerk (2004). Here the authors found that spatial heterogeneity on the landscape acted as a buffer to improve the resilience of the ecosystem at local scales. In arid regions, the spatial patterning of vegetation was found to be a self-organizing property linked to water availability as water infiltration rates are higher near vegetation (Rietkerk et al., 2002). In a real ecosystem, disturbances and stressors are located within a spatially varying landscape comprised of various soil and vegetation types (Fuhlendorf and Smeins, 1996; Alder et al., 2001). The result is a spatially heterogeneous landscape that is temporally changing (Wiens, 1989; Holling, 2001; Scholes et al., 2002; Young and Aspinall, 2006).

2.3.4 Ecological Time-series

Originating in population studies, the analysis of ecological time-series data has been implemented to understand the temporal dynamics of predator-prey models (Turchin and Taylor, 1992), climate variability (Heyen et al., 1998), and other factors driving density dependent fluctuations (Berryman, 1992; Berryman and Turchin, 2001). Recently other environmental variables such as sea surface temperature (SST), surface level pressure (SLP) (Barnston and Ropelowski, 1992; Kestin et al., 1998), hydrology (Labat et al., 2004), viral infection levels (Cummings et al., 2004), genetics (Rodriguez-Trelles et al., 1996), oxygen isotope from ice cores (Petit, J.R. et al., 1999; Shackleton et al., 2000) and dendrochronology (Tyson et al., 2002) have been studied using time-series analysis to detect patterns and trends.

One approach implemented in the analysis of ecological time-series data is the utilization of the autocorrelation function (ACF) (Berryman and Turchin, 2001), which computes the correlation of a signal (e.g. population density) with itself at a time lag (Berryman, 1992). The ACF provides information regarding the periodicity and repeating patterns of the fluctuations, but does not specify the number of processes acting on the data (Berryman and Turchin, 2001). Turchin and Taylor (1992) used the ACF to reconstruct the population dynamics of 14 insect species. Their results show that complex responses are present in 1-dimensional population time-series that were attributed to multiple factors influencing the underlying dynamics. Species populations have also been fitted to a curvilinear logistic model; however, this approach dampens to a stable equilibrium over time (Berryman, 1992).

Principal Component Analysis (PCA) is a tool that has been used to reduce the dimensionality of time-varying spatial data by transforming the input data into fewer, uncorrelated variables that capture most of the original variance (Jassby and Powell, 1990; Hirosawa et al., 1996). PCA is utilized to orthogonalize multivariate time-series data (Heyan et al., 1998), compute trends of time-varying spatial distributions such a precipitation and SST (Wallace et al., 1992; Smith et al., 1996), and with change detection using remotely sensed imagery (Eastman and Fulk, 1993; Schowengerdt, 1997; Ferreira and Huete, 2004). By implementing a PCA, each PC band represents the spatial distribution of variance within the data. Another method that is utilized to extract patterns from ecological time-series is canonical correlation analysis (CCA: also known as canonical correspondence analysis) (Barnston and Ropelewski, 1992), a multivariate statistical approach that maximizes the correlations between a set of predictors and predictands. CCA is advantageous to multiple linear regression since the patterns between multiple predictands and predictors are computed simultaneously. Prior to implementing CCA, both predictor and predictand data are often detrended and orthogonalized using the principal components technique. Heyen et al. (1998) utilized a multivariate model to identify relationships between zooplankton population fluctuations and climate indices (e.g. Sea Surface Temperature and North Atlantic Oscillation Index). They first computed the log-abundances of the population data and then determined a variety of measures including the net increase of abundance over different time periods, cumulative abundance in a year, and relative increase in abundance. A CCA was applied

to the population variables with the climate indices. Only a moderate correlation between certain zooplankton populations and climate was found.

An alternate approach is to decompose the time-series data by removing the mean long-term signal and then analyzing the seasonal signal (Jassby and Powell, 1990). Decomposition of time-series data into seasonal patterns, secular trends, or other cyclic patterns provides inference of the physical processes contributing to various components of the series (Rodriquez-Trelles et al., 1996; West, 1997). For example, decomposition of Dengue fever infection levels for Thailand indicates a 3-year component in the underlying signal that is attributed to the pathogen dynamics (Cummings et al., 2004). This periodicity, however, was not observable in the raw data, revealing the value of signal decomposition in understanding system dynamics. Temporal signals of ecological time-series data may be partitioned into two general categories: permanent and transitory (Rodriguez-Arias and Rodo, 2004) that are a mixture of many frequencies (Lundberg et al., 2000). Permanent signals are composed of both trends and seasonal and long term cycles (Jassby and Powell, 1990; Rodriquez-Trelles et al., 1996). Transitory signals, in contrast, are signals that are temporary and discrete within a time-series, such as those caused by a disturbance. The simplest form of a cyclic time-series model can be expressed as:

$$X_t = \mu + A\cos(\omega t + \psi) + e_t \qquad \textbf{Equation 2-1}$$

where μ = mean of the series,

A = amplitude,

ω = angular frequency

ψ = phase shift,

and e_t = random error.

This simple model of a time-series can be modified to include a secular trend and residuals comprised of short-term and long-term cycles. The above formulation of a cyclic time-series will be implemented in this research to decompose the permanent and transitory signals observed in the remote sensing dataset.

2.3.5 Human Role in Ecosystem Resilience

While ecology is often perceived to focus on natural processes occurring on the landscape, humans are the most dominant force on the earth. Approximately 50% of the land surface has been impacted in some way by anthropogenic effects and no ecosystem is "free of pervasive human influence" (Vitousek et al., 1997 pg 494). Although many anthropogenic changes improve human quality of life (e.g. increased agricultural productivity), some have been found to produce negative effects on ecosystems. Human modification of terrestrial ecosystems has resulted in fragmentation and alteration to biogeochemical cycles (Vitousek et al., 1997) as well as changed resource availability for plant/animal communities (Tilman and Lehman, 2001), and disturbance regimes (Chapin et al., 1997; Tilman and Lehman, 2001). Changes in land use/land cover have been linked to localized climate differences. For example, Pielke et al. (1999) modeled precipitation rates in southern Florida based on 1900, 1970, and 1993 land cover and found an 11% decrease in 1993 estimated precipitation compared to the 1900 levels. Similarly, forest fragmentation in the Amazon has been linked to changes in microclimate patterns (Uhl

and Kauffman, 1990; Baiday Roy, 2006) and increased vulnerability to forest fires (Laurance and Williamson, 2001). In addition, land use / land cover change is negatively associated to recovery rates following disturbances. In Puerto Rico, tropical forests that were impacted by human induced land cover change were found to have slower rates of succession following a major hurricane (Turner et al., 2003).

In mathematical models of ecological resiliency, Ludwig et al. (1997) describe ecosystem dynamics as a function of longer term processes and sporadic disturbances. These longer term processes include edaphic conditions, vegetation composition, system hydrology, and topography; however, they also can be altered by human land use. By reducing the strength of the longer term processes, stochastic events are suggested to have a greater impact on the system. Folke et al. (2004) hypothesize an increased probability of ecosystem shift into a new state due to human-induced reduction of ecosystem resilience by alteration of hydrology or vegetation composition. It is suggested that conservation and management issues should focus on managing the longer term processes rather than preventing disturbances if the goal is to maintain ecosystem resilience (Landres et al., 1999; Scheffer et al. 2001). However, the spatial limitation of many reserves is not likely to facilitate conservation of large-scale dynamics of ecosystems (Bengtsson et al., 2003). Resilience of landscapes is dependent not only on the capacity of the ecosystem itself to respond to change, but also by the institutional and environmental management in which they exist (Peterson, 2000; Forbes, et al., 2004).

Foster et al. (1997) compare the impacts of hurricane damage and anthropogenic changes (i.e. nitrogen fertilization and soil warming) on ecosystem processes in the

Harvard forest to investigate whether forests are as resilient to chemical and climatic stressors as they are to natural disturbance. The Harvard forest, and most of New England, was hit by a hurricane in 1938. A substantial lumber salvage operation to harvest 1.5 billion board feet of timber was implemented in the region following the hurricane. The activity of logging, road development, and burning of residual materials resulted in major changes to the landscape. In an experimental simulation of the 1938 hurricane, they found that despite the appearance of significant wind damage, the understory and soil microenvironment suffered little change. Due to the rapid regrowth and sprouting of new trees, the floristic composition was not dramatically changed in the model. To test the forest response to anthropogenic stressors, they conducted experiments to modify the nitrogen levels and soil temperature in field plots. Although the floristic composition of the forest did not change in response to these experiments, ecosystem processes such as nitrogen and carbon cycling were altered. The authors suggest that the changes to internal ecosystem processes from anthropogenic stressors are thus a greater threat to the forest than hurricane blowdown.

2.4 Application Areas for Theoretical Framework

The objective of this research is to investigate flooding, fire, and vegetation assemblages found in the Okavango Delta to lead to a better understanding of the system's vegetation dynamics. For the purposes of this research, the lower Okavango Delta is described as having two major ecosystem components defined by an absence or presence of flooding: upland savanna/woodlands and wetlands/floodplains. The

wetlands/floodplains ecosystem is topographically low and experiences continuous or intermittent flooding with the vegetation adapted to wet conditions. In contrast, the savanna/woodland ecosystem are situated topographically higher in elevation and do not flood. Both ecosystems can burn. The following section outlines ecosystem concepts for both wetland and savanna systems, while the study area itself is described in Chapter 3.

2.4.1 Wetland Ecosystems

In addition to supporting biodiversity, wetlands provide valuable ecosystem services such as a flood control buffer, processing of nutrients or pollutants (Mitsch et al., 2001), and support of fisheries (Barbier, 1994). The amount of global wetland loss since 1900 is estimated to be approximately 50%, with the majority of losses attributed to conversion to agriculture and urban development (Barbier, 1994). The delineation of a parcel of land as being a wetland has significant implications for jurisdictional and regulatory agencies across the world (Tiner, 1991). Recognizing the presence of hydric soils and vegetation, the US Fish and Wildlife Department 1979 definition of wetlands is as follows:

> *"Wetlands are lands transitional between terrestrial and aquatic systems where the water table is usually at or near the surface or the land is covered by shallow water. Wetlands must have one or more of the following three attributes: 1) at least periodically, the land supports predominantly hydrophytes, 2) the substrate is predominantly undrained hydric soil, and 3) the substrate is nonsoil*

and is saturated with water or covered by shallow water at some time during the growing season of each year"

Widely adopted by many governments and NGOs (Turner, R. et al., 2000), the international definition of a wetland as defined at the 1972 Ramsar convention on wetlands is as follows:

"areas of marsh, fen, peatland, or water, whether natural or artificial, permanent or temporary, with water that is static or flowing, fresh, brackish, or salt including areas of marine water, the depth of which at low tide does not exceed 6 meters."

The distribution of vegetation within any wetland system is dependent upon the hydrological regime and the underlying soils (Mitsch and Gosselink, 2000; Ellery et al., 2003a). The hydrologic regime (frequency of flooding, depth of inundation, duration of inundation, and flow rate) is critical to understanding wetland structure and distribution and is largely a function of topography. Having knowledge of the hydroperiod, species turnover, and water budget is required for understanding wetland function (Cassanova and Brock, 2000; Mitsch and Gosselink, 2000). Capon (2005) found that flood frequency was a major determinant in plant community diversity in an arid floodplain. Specifically, areas that were frequently flooded exhibited similarities in plant types whereas areas less frequently flooded showed variability in plant distribution, suggesting that flooding is the dominant control on vegetation distribution within a floodplain. Mitch and Gosselink (2000) present experimental results explaining the relationship between hydroperiod and

species diversity. They found that species diversity was lowest for continuously flooded marshes, whereas continuously moist soils had the highest species diversity. Hydrology directly affects the soil through the movement of nutrients and oxygen availability for plants. Mitsch and Gosselink (2000) defined other specific effects of the hydrology in a wetland environment as contributing to a unique vegetation composition, where primary productivity is enhanced by a flowing or pulsing hydroperiod and where accumulation of organic material is controlled by hydrology.

River-floodplain ecosystems such as parts of the Amazon basin, the Pantanal of the Paraguay River, and the Okavango Delta in Botswana provide critical habitat for a variety of flora and fauna (Sparks, 1995). In each of these systems, the hydrology is seasonal and can be described by the flood pulse concept of Junk et al. (1989). A flood pulse implies a periodic inundation that can be short or long in duration, have variable water levels, and is predictable in some cases and not in others (Junk and Furch, 1993). The flood pulse is recognized as the primary driver controlling the response and adaptations of the vegetation and other biota within the system (Robertson et al., 2001). Floodplains are described as periodically inundated by lateral and overflow of rivers/lakes, in addition to groundwater and localized precipitation (Junk and Furch, 1993). Processes such as nutrient transfer, decomposition, reproduction, and biological productivity are timed to the flood pulse (Bayley, 1995). Thus, a disruption to the hydrologic regime of a river-floodplain system would constitute a disturbance (Bayley, 1995).

In several Australian river-floodplain systems, Kingsford (2000) reports the presence of dams and water diversion has led to a reduction in flooding, the consequences of which include the conversion of floodplains into upland terrestrial ecosystems. In the Florida Everglades, it is hypothesized that increased nitrogen levels and an altered hydrologic regime have led to invasion of cattail at the expense of native sawgrass vegetation (*Caladium jamaicense*), which subsequently has reduced the level of primary and secondary production (Ogden et al., 2005). It is also suggested by Ogden et al. (2003) that the drainage of marshes and the increased intensity of fires have resulted in changes of flow patterns and spatial distribution of plant communities.

2.4.1.1 Disturbance Impacts in Wetlands

Disturbances in wetland ecosystems can originate from both natural and anthropogenic stressors and alter ecological processes as well as ecosystem structure. In a study conducted along a reach of the Missouri River, disturbed wetlands due to non-point source pollution from nearby agriculture experienced decreased levels of species diversity and a higher occurrence of exotic species (Chipps et al., 2006). In a Florida wetland marsh system, fire resulted in an increase of native cattail (*Typha domingensis)* over native sawgrass (*Caladium jamaicense*) for the first two years following the burns; however, species diversity rates restored to pre-burn levels after the second year (Ponzio et al., 2004). In this case, fire provides a pulse of nutrients that the cattail utilize for short-term gains. This finding seems to suggest that other factors, such as hydrology and

nutrient levels, influence the long-term competition and relative abundances of sawgrass and cattail.

In other wetland ecosystems, prescribed burns are used as a management tool to limit the encroachment of woody species (Clark and Wilson, 2001; Lee et al., 2005). On the St. Johns River in Florida, repeated burning (two fires over three years) was found to reduce the Willow cover and minimize woody encroachment into herbaceous marsh compared to a single burn (Lee et al., 2005). Although fire is regarded as an effective management tool for the reduction of woody cover, the impacts of burning on the seedling recruitment of exotic species is not well known (Clark and Wilson, 2001).

2.4.2 Savanna Ecosystems

Savannas are typically regarded as "communities or landscapes with a continuous grass layer and scattered trees" (Scholes and Archer, 1997). Perhaps a less contested description of savanna is as a vegetation type that is co-dominated by both grasses and woody plants (Skarpe, 1992; Scholes, 1997). Savanna ecosystems have a wide distribution and can be found from arid climates with precipitation less than 100 mm/year to moist climates with rainfall averaging over 1500 mm/yr (Jeltsch et al., 2000). Savannas are geographically extensive, occupy over one eighth of the global land area, and comprise over half of the African continent (Scholes and Archer, 1997; Jeltsch et al., 2000). These areas serve as important locations for economic activities such as raising domestic livestock (Fuhlendorf and Smeins, 1997; Fuhlendorf and Smeins, 1998). However, since much of the grazing activities occur on bioclimatically and edaphically

marginal lands, it has been suggested that many savannas, grasslands, and rangelands in semi-arid regions are predisposed to either desertification or woody encroachment (Asner et al., 2004).

Savannas are common in tropical and sub-tropical regions where pronounced wet and dry seasonal shifts sustain this landscape structure; however they also occur in temperate climates. What makes savannas such an interesting biome is that these two different vegetation life forms (grass and trees) coexist without one dominating over the other (Knoop and Walker, 1985). This coexistence is regarded as the "savanna question". There are several theories debated today regarding this coexistence. Specifically, the relationships among herbivory (grazing and browsing), fire, soil type, nutrient availability, water availability, and climate contribute to complex vegetation dynamics that dictate the proportion of grass and tree cover in the savanna (van Langevelde et al., 2003). Landscape dynamics within arid and semi-arid systems are often considered as existing in a non-equilibrium state (Scholes, 1997; Briske et al., 2003; Lankford and Beale, 2007). In arid and semi-arid regions, primary productivity is linearly related to precipitation (Scholes and Archer, 1997) and changes in rainfall can significantly alter the vegetation at a broad scale (Fuhlendorf and Smeins, 1998).

Non-equilibrium dynamics are used to describe a savanna ecosystem where the balance between grasses or trees shifts due to variability in a factor such as fire or precipitation. Competition-based theories regarding the competition between grasses and trees in a savanna are based on traditional niche separation of these two vegetation forms. A simple model that was the foundation of savanna ecosystem theory is the two-layer

water theory (also known as the root-niche theory) (Walter, 1971). Here it is presumed that grasses derive all the available water in the upper layer of the soil and that the trees penetrate deeper into the soil. While this is possible, it is not commonly observed in many areas and this theory of water usage is typically rejected in lieu of life history/disturbance or demographic based models (Higgins et al., 2000; Scholes and Archer, 1997; Wiegand and Jeltsch, 2000). Many field experiments show that both trees and grasses compete for water and nutrients in the upper soil zone and many trees are shallow-rooted (Knoop and Walker, 1985; Higgins et al., 2000).

Most other class of models describing the coexistence between trees and grasses in savanna ecosystems are demographic-based. These models are based on variables such as climatic variability, as well as fire and grazing, to determine the seedling recruitment of tree species (Sankaran et al., 2004). In the demographic models, young tree saplings and grasses compete for the same resources, which can prevent the tree saplings from reaching maturity (Bond and van Wilgen, 1996). In addition to the direct competition for resources with grasses, young tree saplings are also vulnerable to fire. Thus, fire is a major factor that allows for the persistence of grasslands over trees. Frequent fires in this scenario would kill young tree saplings, while grasses quickly resprout after a burn. However, if the grassland does not experience frequent fire, then the tree saplings reach a size large enough to escape mortality due to a surface fire. Once this occurs, trees have a competitive advantage due to shading and begin to prevail over grasses. In areas with fire suppression or lack of sufficient fuel to sustain a surface fire, dense thickets of woodlands can develop. A lack of fuel (herbaceous layer) due to increased grazing practices has

been documented as a factor in woody encroachment (Fuhlendorf and Smeins, 1997; Fuhlendorf and Smeins, 1998; Rogues et al., 2001).

Jeltsch et al. (2000) suggest a concept where buffering mechanisms prevent the savanna system from transitioning into pure grasslands or pure woodlands. In this construction, savannas are non-equilibrium systems are affected by disturbance factors such as fire and herbivory, or by sporadic rainfall. For example, in an arid savanna where grass dominates, the buffering mechanism preventing the savanna from transitioning into grassland and allowing for the establishment of trees is would be the highly variable rainfall and random seed dispersal by animals. Here, sporadic rainfall produces enough moisture to allow a tree seeding deposited in animal dung to germinate and reach a height where it is able to escape competition from grasses. In savannas where precipitation is not the limiting factor, the buffering mechanisms that prevent the savanna from transitioning into pure woodlands are fire and/or herbivory (Barnes, 2001; van Langvelde et al., 2003). In Africa, a combination of browsing by elephants and small ungulates was found to limit sapling establishment (Barnes, 2001). It is argued by van Langvelde et al. (2003) that these indirect effects of fire and herbivory determine the dominance of grasses and trees. The following two sections describe the role of fire and herbivory on a savanna landscape.

2.4.2.1 Fire

Fire plays a significant role in modifying landscapes and can occur naturally, ignite accidentally, or can be used intentionally as a management tool in the form of

prescribed burns. Many studies have examined the role of fire on plant traits (Whelen, 1995; Bond and van Wilgen, 1996; Scholes and Archer, 1997), the recovery of vegetation after fire (Collins, 1992; Collins et al., 1995; DeBano et al., 1998; Heinl et al., 2004), the role of fire by ancient man on landscapes (Bird and Cali, 1998; Bond et al., 2003b), and the distribution of fire-prone ecosystems (DeBano et al., 1998; Bond et al., 2003b; Bond and Keeley, 2005; Bond et al., 2005). The components necessary for fire are simple: an ignition source, oxygen, and fuel. Fires, as with any disturbance, can be characterized by its regime, which includes severity, frequency, and size. In addition to regime behavior, fires are also described by their individual behavior, which is the way that a fire responds to topography, available fuels, or weather conditions (e.g. wind, humidity). Surface fires refer to fires where only the fuels at the surface are burned, whereas crown fires advance from tree to tree and are considered more destructive. In northern Botswana, many of the fires are cool surface fires where primarily the herbaceous vegetation is burned (Heinl et al., 2006). The ability for a fire to alter vegetation is dependent upon the legacy of previous fires, removal of fire-sensitive species, and the establishment of fire-tolerant species. Woody plants considered fire-tolerant have traits that include a thick or flaky bark (>1cm), protected buds or seeds, or fire stimulated seed dispersal or germination (Whelen, 1995; DeBano et al., 1998), whereas other species grow quickly above the height considered to be susceptible to surface fires (Gignoux et al., 1997). Graminoids are typically less impacted by fire than woody species and they usually do not suffer mortality from fire.

In southern Africa, humans have also influenced savanna structure through the use of fire. Recently, evidence of early hominid utilization of fire in southern Africa over 1 million years ago has been discovered indicating man has used fire as a tool for modifying the landscape (Brain and Sillent, 1988). On the African savanna, Blackmore et al. (1990) attribute pockets of *Acacia* developing within *Burkea* savannas to charcoal and manure from a period of Iron Age settlements. Currently, fire is widely used by pastoralists in southern Africa to maintain an herbaceous cover and by the *San* people in the Kalahari to attract game (Sheuyange et al., 2005). However, despite the increase in human utilization of fire, many paleoecological and contemporary studies indicate that fire closely tracks climate (Bond and van Wilgen, 1996; Mensing et al., 1999; Brown et al., 2004). The impact of humans on the landscape through the use of fire is superimposed on the climatic patterns.

2.4.2.2 Herbivory

In addition to fire, the impact of large mammals (both grazers and browsers) on the African landscape is a critical component of tree-grass competition in savannas (McNaughton et al., 1988; Scholes, 1997). In African savannas, grazing from indigenous herbivores (e.g. buffalo, rhinoceros, elephants, and ungulates) is estimated at 6 – 13 % of the herbaceous annual primary production depending upon soil fertility (Owen-Smith and Danckwerts, 1997). In contrast, the consumption rate of browsers is estimated to be 4 – 7% of annual primary productivity of woody foliage (Owen-Smith and Danckwerts, 1997). Heavily grazed savannas were found to have lower species diversity than areas

undergoing a light or moderately grazing intensity (Fuhlendorf and Smeins, 1998). Additionally, the heavily grazed regions were more susceptible to severe drought suggesting a reduction in resiliency. The impacts of large browsers (i.e. elephants) on savannas include tree mortality and the inhibition of growth from established woody vegetation (Cumming et al., 1997; Ben-Shahar, 1998). In addition to herbivory, trampling of seedlings by large herds (such as wildebeest or buffalo) is also a limitation on the growth of tree species (McNaughton, 1985).

While the effects of large mammals should factor into an understanding of African savanna dynamics, the largest impacts result from domestic grazing (Hiernaux et al., 1999). An estimated 76% of lands in Botswana are dedicated to livestock grazing (Ringrose et al., 2002a). Livestock grazing is typically regarded as the primary factor for shrub encroachment due to reducing the cover and competitive ability of the grass layer (Perkins, 1996; Weber et al., 1998) or by reducing the amount of fuel available to sustain surface fires (Rogues et al., 2001). Studies indicate areas lightly grazed show a slight increase in woody cover, whereas areas highly grazed show a dramatic increase in woody vegetation (Asner et al., 2004). Once an area has experienced bush encroachment, it will not revert to grasslands once the grazing pressure is removed without fire or sustained drought (Bond and van Wilgen, 1996; Rogues et al., 2001). Ringrose et al. (2003) examined the vegetation distribution along a 1000 km transect across the Kalahari and found evidence of bush encroachment in arid regions, associated with extensive cattle grazing.

Another possible contributor to bush encroachment is increasing levels of atmospheric CO_2. In fact, low levels of CO_2 are thought to explain the rapid expansion of C_4 grasses during the Tertiary and Pleistocene periods (Bond et al., 2003a) because C_4 grasses require extra energy to process CO_2 during photosynthesis (Huang et al., 2001). This increase in C_4 grasses implies the development of fire-prone grassy ecosystems. Today, however, CO_2 levels have increased from 180 ppm at the last interglacial to 270 ppm pre-industrial levels to the present 370 ppm resulting in a "fertilization effect" on tree growth. The fertilization effect of higher levels of CO_2 would result in trees reaching a height of 2.5 m quicker, which is stated as the height necessary to escape mortality from surface fires (Bond et al., 2003a).

It is evident that multiple factors contribute to the dynamics within the wetland and savanna ecosystems. The research in this dissertation is concentrated at the interface between a wetland and savanna ecosystem. Next, Chapter 3 will describe the environment within the study area to provide the reader with a foundation of the local ecology for the research presented in this dissertation.

3 THE OKAVANGO DELTA

The Okavango Delta, located in northern Botswana, is often referred to as the "Jewel of the Kalahari" and is one of the world's largest wetland environments (Ross, 1987). Botswana lies within a savanna biome that occupies 60% of sub-Saharan Africa (Scholes and Walker, 1993; Cowling et al., 1997). Located in the Ngamiland District, the Okavango Delta shown in Figure 3.1 forms a vast wetland environment approximately 8,000 km^2 in size during the non-flood season and expanding to approximately 20,000 km^2 during the flood season (McCarthy and Ellery, 1993; Gumbricht et al., 2004a). It is a complex ecosystem impacted by a variety of forces that influence its vegetation composition and overall function (Ellery et al., 2003b; Ramberg et al., 2006b). The Delta serves an important role in sustaining the lives of the people living in the region as well as providing critical habitat for numerous wildlife species (Ramberg et al., 2006a; Mbaiwa and Mbaiwa, 2006; Kgathi et al., 2006). The relationship of the components within the Okavango ecosystem will be discussed in the following sections. A major goal of this research is the better understanding of these relationships and the linkages that describe their functionality. A gap in the overall knowledge regarding the ecosystem functioning in the Okavango revolves around the variability in the spatio-temporal distribution of the annual floodwater and other disturbance regimes.

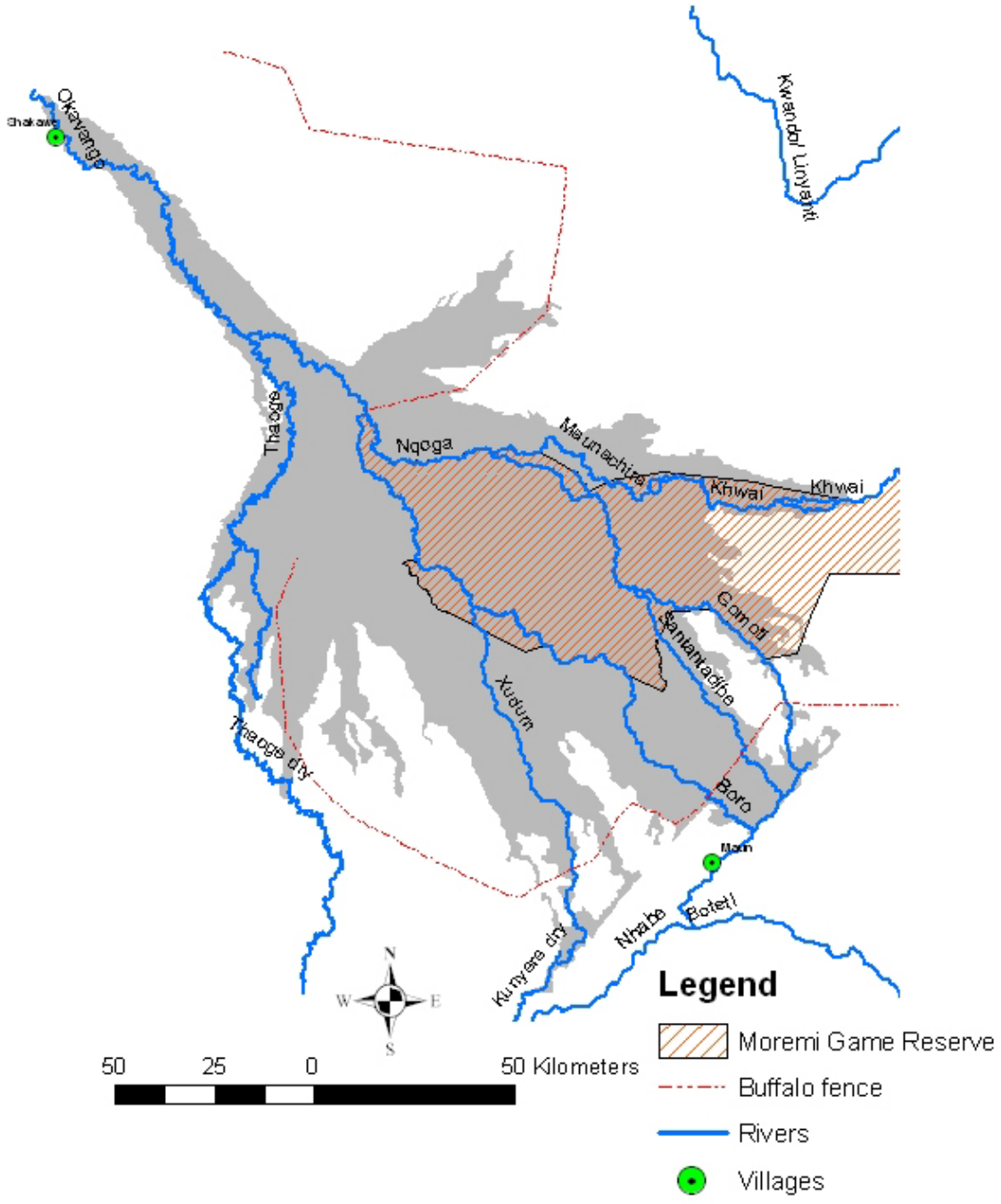

Figure 3.1. Map of the major rivers, Moremi Game Reserve, and veterinary fence in the Okavango Delta, Botswana. Also depicted are the villages of Maun and Shakawe, from which general climatic conditions of the Delta are derived.

3.1 Ecology of the Okavango Delta

3.1.1 Climate of the Okavango Region

Located at 19º S and 23º E, the Okavango Delta region has a semi-arid climatic regime driven by subsiding air with an average annual rainfall of 460 mm (Source data Botswana Meteorological Services, 2006). The precipitation typically originates from localized thunderstorms during the summer months (November through March). The amount of rainfall during these five months accounts for 90% of the total annual precipitation, and droughts in Botswana are common during the winter dry season (May through August). The Okavango Delta is 950 m above sea level and average maximum temperatures and minimum temperatures are known to fluctuate from 25° C to 38° C in the summer months and 8° C to 21° C during the winter months (Botswana Meteorological Services, 2006). There is a lack of meteorological data across the Delta, but general meteorologic measurements are recorded at Maun (located at the distal end of the Delta) and at Shakawe (located at the entry of the Okavango River into the panhandle) (Kgathi et al., 2006). Averages from these two sites are used to represent the climate of the Delta. Rainfall data in the Angolan catchment area have not been collected since the 1970s due to civil war (Andersson, 2006).

The temporal variability of precipitation in the Delta from year to year is reported to follow precipitation cycles common to southern Africa (McCarthy et al., 2000). Like most of southern Africa, Botswana's precipitation is highly cyclical. Tyson et al. (1975) report precipitation cycles of 16 – 20 years in South Africa and observed a weak 10 – 12

year cycle in the Cape region of South Africa. Similarly, McCarthy et al. (2000) reports 3, 8, and 18-year oscillations in precipitation cycles, with the largest oscillation occurring at the 18-year interval; however, the rainfall over the Delta has been below the long-term average since the 1970s. Botswana's position within the African continent, means the ENSO phenomenon has a negligible (Hulme et al., 2005) to weak (Obasi, 2005) influence on the climate of northern Botswana, with below normal precipitation occurring during the warm phase of ENSO (El Niño).

Botswana experienced droughts during the 1960s, to which the deaths of numerous wild animals are partially attributed (Ross, 1987). Recently, Botswana endured a significant drought during 1982 – 1988 and below average precipitation during 1993 – 1994 and 1996 – 1999. A quasi-twenty year cycle was noted for South Africa with wet periods centered in 1921, 1940, 1958, and 1975 (Dyer and Tyson, 1977). This approximate 18-year rainfall oscillation for southern Africa has been confirmed in other geophysical data, such as river discharge along the Zambezi and Cuito Rivers as well as dendrochronological data dating back at least 600 years (Tyson et al. 2002). Further analysis of climate patterns using tree ring dendrochronology, $\delta^{18}O$ dating of cave stalactites and recent stream flow measurements show the most pronounced climate pattern is an 80-year oscillation dating over the past 3500 years (Tyson et al., 2002). Similarly, solar sun spot activity has been found to follow a short term 11-year cycle coupled with a long term 80-year oscillation (Friis-Christensen and Lassen, 1991). The coincidence of solar activity cycles "may be the underlying cause of many climatic cycles that are preserved in the geophysical record" (Perry and Hsu, 2000 pg. 12433). Currently, the Delta

is reported to be in a period of relatively high precipitation that is forecasted to continue through 2010 based upon an 18-year cycle, with 80-year oscillations predicted to contribute to peak precipitation in 2020 (McCarthy et al., 2000).

3.1.2 Flooding

The Okavango Delta has seen significant fluctuations in water discharge into the system (Gumbricht et al., 2004). Over a 60-year period, the annual discharge from the Okavango River into the Delta recorded at Mohembo has ranged from a low of $6x10^9$ m^3 to a high of $1.64x10^{10}$ m^3, with the average annual discharge of $1.01x10^{10}$ m^3 (McCarthy et al., 2000; Botswana Meteorological Services, 2004). The average discharge of the Okavango River at Mohembo during the period 1933 to 1947 was estimated to be approximately 1.2×10^{10} m^3 (Wellington, 1949). The base flow from the Okavango River is adequate to sustain the permanent swamps in the panhandle and upper fan year round (Ellery and McCarthy, 1994).

The Delta is fed by both local summer rains and by the annual flooding of the Okavango River (Wolski and Murray-Hudson, 2006) during the winter. The peak of the annual flood typically reaches the panhandle between February and May but the flood waters usually do not reach the distal portion of the Delta near the village of Maun until June or July, which is winter and peak of the dry season. The annual variation in both rainfall and the advancing floodwaters is high, and the extent of the flooding is not well understood (Gumbricht et al., 2004a). The spatial and temporal flooding patterns in the Delta are constantly changing. In spite of the high sand volume and associated infiltration

rates, it was speculated that all the flooding occurs at the surface level (McCarthy, 1998a). Recent work, however, has indicated that as much as 85% of the infiltrated floodplain water moves laterally to a distance of 10 m to the adjacent drylands (Ramberg et al., 2006b). The groundwater level below the sandy river channels is relatively shallow (typically 1 – 2 m) and may allow some infiltration of water into the soils in advance of the surface floodwaters (McCarthy et al., 1997; Ellery et al., 2003b). The pan evaporation rates in the Delta have been determined to be ~2172 mm/year (Wilson and Dincer, 1976; McCarthy et al., 2000), while hydrologic models have estimated the evapotranspiration at 2400 mm/year (Thangarajan et al., 1999; Bauer et al., 2004). An estimated 98% of the water entering the Okavango Delta is lost through evapotranspiration (Wilson and Dincer, 1976; McCarthy et al., 1998a), however Ashton (2003) estimates that 16% of the 98% water loss is in the form of groundwater recharge rather than evapotranspiration.

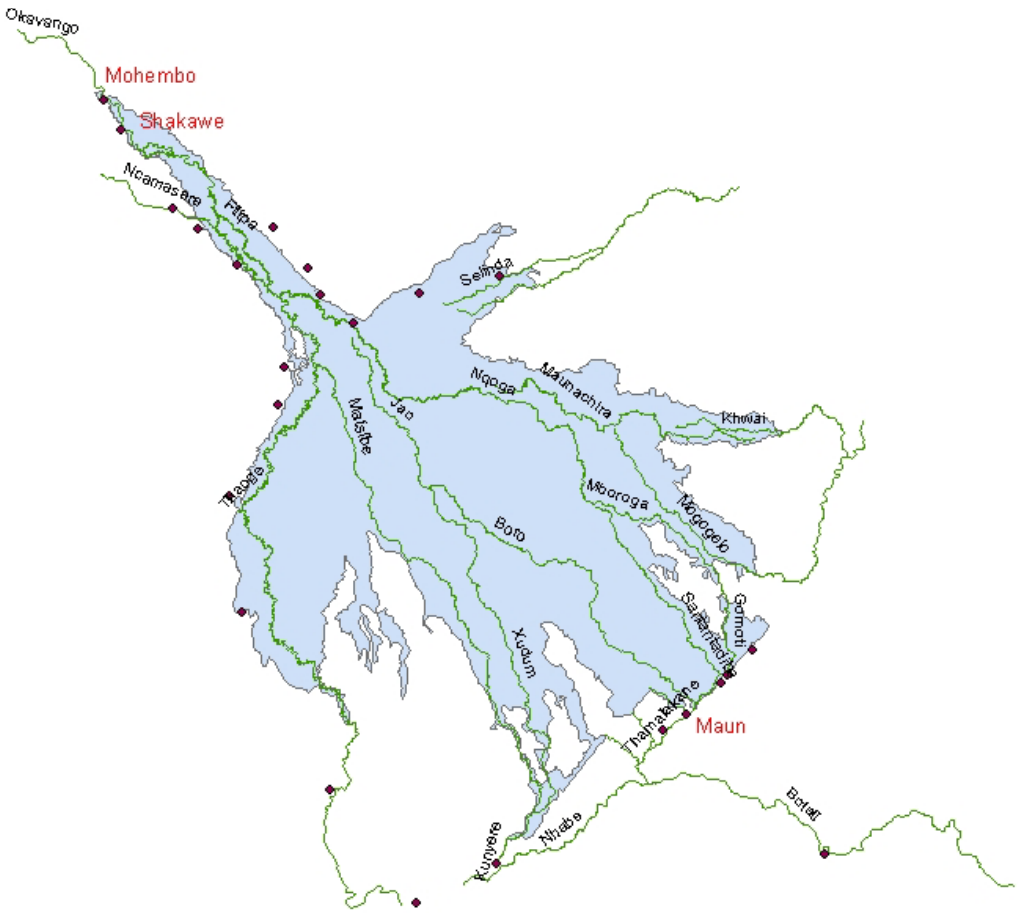

Figure 3.2. Map of primary channels in the Okavango Delta

The primary channel of the upper fan is currently the Nqoga, which is a continuation of the Okavango River (Figure 3.2). The Jao-Boro and Thaoge are the two distributaries of the Nqoga, and it is estimated that these three receive only 60% of the water inflow measured at the entry point, Mohembo, to the panhandle (McCarthy et al., 1998a; Gieske, 1999). Historical documents show that the Thaoge was once the primary distributary channel, a large supplier of water to the western portion of the fan, and supplied Lake Ngami (Rey, C., 1932). However, by 1888 the gradual choking of the Thaoge channel due to papyrus growth was noted as avulsion processes began to take

place and the channel became essentially closed (Wellington, 1949). It was also noted that during this period the greatest concentration of water occurred on the eastern side of Chief's Island. The impact of papyrus on the channels and water flow is highlighted by Wellington (1949) who describes an account of part of the Thaoge channel that was blocked for 2.5 miles due to dead papyrus mats that required eight days for 14 men to clear the passage. Today the Thaoge is considered to be only a minor channel and is all but dormant (dry) at the lower end. Prior to World War II, the Nqoga-Santantadibe channel was considered to be the main distributary of the Okavango Delta as it was relatively free of obstructions and carried most of the water to the Thamalakane River (Wellington, 1949). Today, the Jao-Boro River is considered to be the major distributary within the Delta; however, the Nqoga-Santantadibe system is still very active.

A major concern of people living along the Okavango Delta stems from the variability of flooding extent which had led to channel failure for some reaches. A channel failure results in no groundwater recharge, the necessity to develop new livelihood strategies, and potentially the relocation of settlements. Originally, channel failure along the Thaoge was linked to thick mats of vegetation that restricted water flow leading to a dormant channel. Today, however, the process leading to channel failure in the upper Delta is known to be an aggradation of sediment (Smith et al., 1997; Wolski and Murray-Hudson, 2006), which in turn facilitates vegetation establishment as water velocity has been reduced, subsequently leading to a further reduction in water flow.

The aquifer system under the Delta consists of a shallow unconfined aquifer ranging 5 to 25 m in thickness overlaying a semi-confined aquifer (Linn et al., 2003). The

freshwater zone in the aquifer varies from 25 to 120 m below ground level with sudden changes in water salinity (i.e. fresh or brackish) in both the horizontal and vertical directions (Bauer et al., 2006). The depth of the water table is related to local rainfall and the extent of prior seasonal flooding; localized rainwater raises the water table to the surface annually prior to the occurrence of overland flow (McCarthy et al., 2000). However, based on rainfall loss due to evapotranspiration, Thangarajan et al. (1999) asserts that the hydrology of the Delta is only dependent upon the floodwaters and not linked to the local precipitation events. Further they note that water infiltration occurs along the longitudinal axes of the Delta. The water infiltration rates on the seasonal floodplains were measured at an average 5 cm/day with a rate as high as 17 cm/day (Ramberg et al., 2006b). It is suggested that the freshwater recharge to the aquifer is primarily due to the annual flooding and the rainfall recharge is considered insignificant (Linn et al., 2003). Similarly, the depth of the freshwater pools within the aquifers is attributed to the frequency and extent of the annual flood events. Areas without flood recharge over many years have seen a significant decrease in water quality, as the water has become brackish. It is expected water quality can be degraded without freshwater recharge in periods less than 10 years (Linn et al., 2003). In 2006, however, it was noted that the residual flooding from the rainfall during the wet season was so great that the arrival of the annual floodwaters could not be detected in many channels (personal observation). The rainfall during the 2005/2006 wet season was more than 300 mm above the mean annual amount.

The general movement of the annual flood pulse in the upper Delta is via the channels (McCarthy, 2006). The elevation of the channels is higher than the flanking

floodplains, however, the channel walls are porous and water also flows into and over the floodplains via sheetflow (McCarthy, 2006; Ramberg et al., 2006b). In the lower Delta, the channels are less defined and water flow is a gentle distribution across the floodplains. The various channels within the Delta appear to have very different dynamics. Thirty years of hydrological data were interpreted by Wolski and Murray-Hudson (2006) indicating that the Jao-Boro system responds to seasonal and inter-annual climatic fluctuations, whereas the Santantadibe system is relatively stable and experiences little seasonality of its water levels. At various portions along the Santantadibe and Nqoga, a quasi-decadal cycle was observed in water flow velocity and was suggested to be vegetation related by Wolski and Murray-Hudson (2006) as the channel dimensions are not changing.

The water feeding the Okavango Delta has an extremely low salinity, with half of the dissolved solids comprised of silica (McCarthy et al., 1998a). While low salinity is characteristic of the Okavango system, the electrical conductance used to determine dissolved salts indicates a two-fold increase along the major axis of the Delta ranging from 60 – 80 mS/cm2 near Mohembo to 100 – 120 mS/cm2 in the distal Delta (Bonyongo and Mubyana, 2004). This increase is attributed to the evaporative concentration of salts associated with evaporation and the transpiration of wetland plants (reeds, grasses and sedges). The pH of water throughout the Delta is at or near neutral. The soils within the Okavango Delta system are generally considered to be nutrient-poor containing low levels of nitrogen (Ellery and McCarthy, 1993). Other soil nutrients such as phosphorus (P), calcium (Ca), and magnesium (Mg) were found to decrease with

distance from the river, while pH, potassium (K) and sodium (Na) levels increased with distance from the river (Garstang et al., 1998; Mubyana et al., 2003; Bonyongo and Mubyana, 2004). While the macronutrient levels followed this general elevation trend, the associations of nutrients with different vegetation assemblages was highly variable. There is additional evidence that significant amounts of nutrients are also deposited into the Delta via dry deposition through Aeolian (wind-borne) transport (Krah et al., 2004; Krah et al., 2006).

3.1.3 Vegetation in the Okavango

Much of the vegetation in the Okavango Delta is highly dependent upon the arrival of the annual floodwaters and the plant community organization is a function of the duration and depth of flooding (Ramberg et al., 2006a). As shown in Figure 3.3, the Delta is typically subdivided into four regions, based primarily upon the duration of flooding: the panhandle, permanent swamps, seasonal swamps, and occasional swamps (McCarthy and Ellery, 1993; Rogers, 1997). Each of these regions is in turn associated with particular vegetation communities, although some plant species may occur in more than one physiographic region. This research is concentrated at the wetland/savanna interface due to the presence of multiple disturbance regimes in the seasonal and occasional floodplains near Maun.

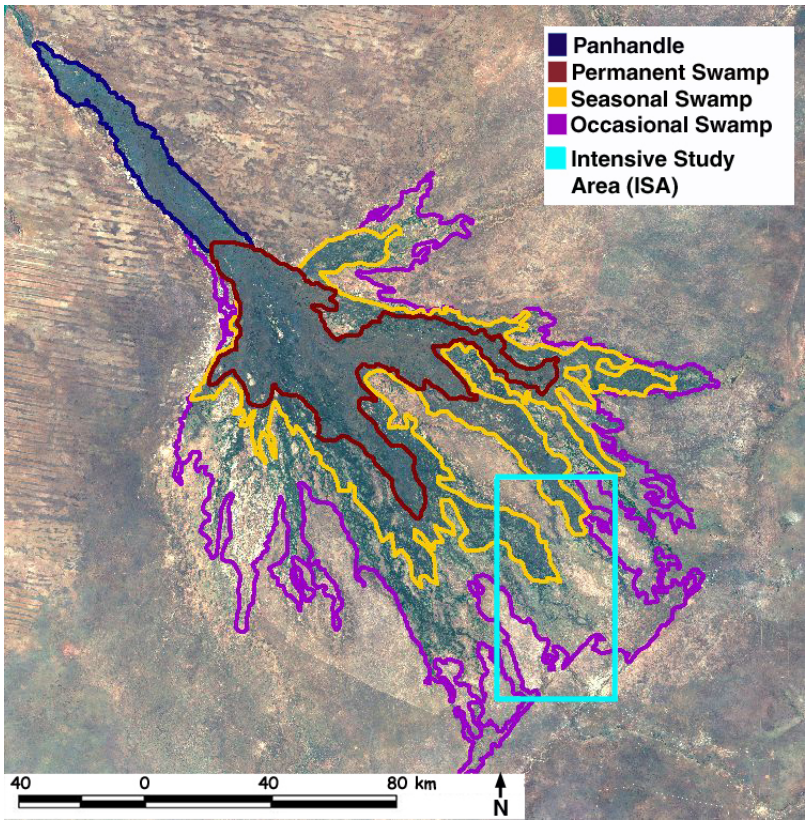

Figure 3.3. Flooding regions and study area.

The vegetation in the Delta exhibits defined zonation patterns depending upon the frequency, depth and duration of the inundation (Ellery et al., 1991; Rogers, 1997; Ellery and McCarthy, 1998). Vegetation plays a key role in the distribution of water in that the channels are defined by thick stands of papyrus in the panhandle and thick stands of sedges in the lower Delta. These channel banks are sturdy enough to trap sandy sediments, which help to define the channel banks, yet are porous enough to allow water to filter into the wetlands (Smith et al., 1997; Tooth and McCarthy, 2002). The permanent swamps of the upper Delta consist of grasses and sedges that produce peat, and the base flow from the Okavango River is sufficient to sustain the permanent swamps year round (Rogers,

1997). Seasonal swamps are characterized by less organic matter and are comprised of grasses and sedges (Ellery and McCarthy, 1993). The reeds and sedges found in this area coexist with grasses that need some period of dryness to survive (Ellery et al., 2003; Nash et al., 2006). Occasional swamps do not flood each year, are dominated by grasses, and can transition to woody shrub and tree species that can tolerate sporadic inundation within a few years (Knoop and Walker, 1985; Ellery and McCarthy, 1998; Personal observation, 2007). Less documented and potentially more important in the Delta is the vegetation response of occasional swamps to sporadic flooding (every two to ten years). In all, twenty-six plant communities have been defined for the permanent swamps, floodplains, and islands in the Delta (Ramberg et al., 2006a).

Wetland vegetation in the panhandle, upper swamps, and marshes has been classified into eight communities including *Pennisetum glaucocladum* reedbed, *Phragmites mauritiamus* reedbed, *Cyperus papyrus* swamp, *C. papyrus/Miscanthus junceus* swamp, *M. junceus* swamp, *Imperata cylindrica* marsh, *Pycreus nitidus* marsh, and mixed bog based upon field surveys (Bonyongo et al., 2000; Ellery et al., 2003). Ellery et al. (2003b) report the vegetation distribution follows a pattern of community change downstream of the longitudinal axis. A similar pattern of community change is observed perpendicular to the channels, most likely attributed to changes in nutrient and water supply (Bonyongo and Mubyana, 2004).

The floodplains of the seasonal swamps are characterized by large stands of sedges including *Schoenoplectus corymbosus* and *Cyperus articulatus*. Also common in the seasonal swamp are reeds (*Phragmites communis*), bulrush (*Typha capensis*) and

grass (*Miscanthus junceus*). The more distal portions of the seasonal swamps (or the secondary floodplains) are large grasslands that include species such as *Panicum repens*, *Sorgastrum friesii* and *Imperata cylindrica*. The drier portions of the occasional swamp also contain dryland grass species such as *Panicum repens*, *Andropogon*, and *Stripagrostis uniplumis* as well as shrubs such as *Pechuel-loeschea leubnitziae*. Habitat density and diversity are greatest in the distal portions of the Delta (Ramberg et al., 2006a). The woodlands, typically dominated by Mopane *(Colosphernum mopane),* Leadwood *(Combretum imberbe),* Silver Terminalia *(Terminalia sericea)* or Acacias *(Acacia* spp.*)*, are located on well drained soils (Cowling et al., 1997; Roodt, 1998). The woodlands are typically named for the dominant species in the area (e.g. Mopane Woodland) and the dominant species are typically a function of soil type. Figure 3.4 shows the relation between soil type and vegetation within the Okavango Delta.

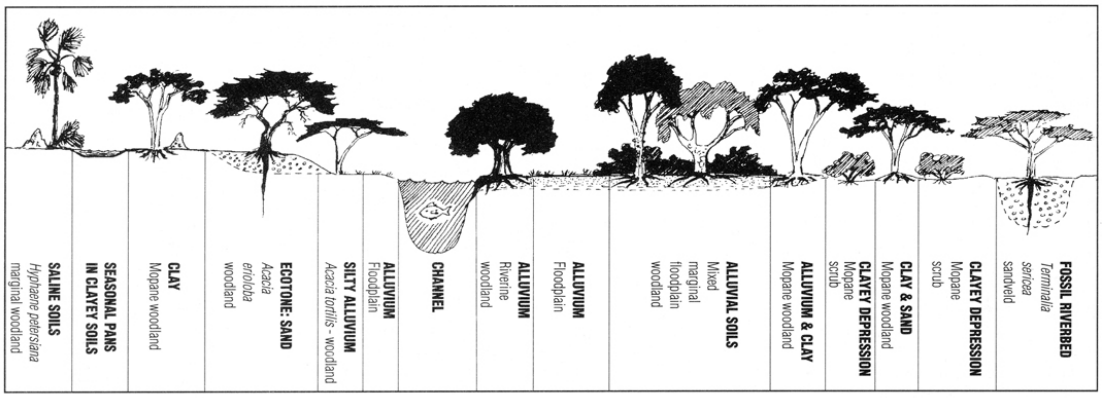

Figure 3.4. Ecotones in relation to floodplain elevation (source Roodt, 1998)

At the southern end of the Delta, regions of savanna and woodlands extend into the Delta in between the channels and floodplains. *Mopane* woodlands are common on clayey soils, and they tend to have a shallow root system that takes advantage of the

water stored within the clay soil horizon (Roodt, 1998). The scrub *Mopane* is the same species found in the *Mopane* woodlands; however, the maximum height of the scrub *Mopane* is limited to approximately 1.5 – 2 m. The *Mopane* scrub is usually associated with depressions, and the physiognomy is linked to hydrology, fire (Kennedy and Potgieter, 2003; Mlambo and Mapaure, 2006), and lack of nutrients (Mlambo, 2007). However, there is no clear consensus on the cause of the physiognomic difference. *Mopane* leaves are a favorite of elephants, which have destroyed much of the *Mopane* woodlands in northern Botswana near Chobe National park (Ben-Shahar, 1996). Additionally, soils in *Mopane* woodlands are also typically alkaline near water holes where elephants dig searching for salts and subsequently there is more drying. The wood from *Mopane* trees is preferred by humans for building of fences, roofing support, and for fuel wood as the wood is harder than the *Acacias* (Mlambo and Mapaure, 2006).

Acacias dominate nutrient rich savannas of southern African with a mean annual precipitation of < 500 mm/yr whereas broadleaf trees dominate more temperate savannas (Scholes, 1997; Scholes et al., 2002). The *Acacias* are not tolerant of flooding and will die under this condition. *Acacias* are also known to die if the groundwater table falls below the reach of the tap root (Scholes et al., 2002). *Acacia* trees are nitrogen fixing, creates an ideal situation for the development of grasses. The *Acacia* sandveld dominated by Camelthorn *(Acacia erioloba)* can be found on deep sandy soils. In the Moremi Game Reserve, the *Acacia* sandvelds are commonly found between *Mopane* woodlands and permanent water sources (Roodt, 1998). The mixed marginal woodlands as described by Roodt (1998) are found on alluvial soils (silts), and the knobthorn (*Acacia nigrescens*) is

common. Like the *Acacia* sandveld, this woodland is also rich in nitrogen due to the dominance of nitrogen fixing *Acacia*. Thus, this area is considered good grazing land due to the palatable grasses. The *Acacia tortillis* woodland is dominated by the umbrella thorn tree (*Acacia tortillis*). While the umbrella thorn tree is often a savanna woodland component, it can also be found in homogeneous stands. The umbrella tree favors alluvium and is not found in sandy soils (Moleele et al., 2005). *Acacia tortillis* is often associated with overgrazing as it rapidly moves into a disturbed area; these trees are also very sensitive to the water table depth (Knoop and Walker, 1985).

3.1.4 Geology of the Okavango

One of the factors that sets the Okavango apart from most depositional systems is the low abundance of clayey soils and silts common to alluvial systems (McCarthy et al., 1997a; Smith et al., 1997). The sediments in the Okavango River catchment are comprised of almost entirely Aeolian Kalahari sediments, resulting in a high amount of sand transported into the system (Ellery et al., 1998). The clastic sediment load is derived from weathered granite that occupies a small portion of the catchment area. Active channels in the panhandle of the Okavango system transport mainly medium- and fine-grained sands and an estimated 15% of the total sediment input is characterized as suspended load (Smith, et al., 1997). The clay and silt alluvium that does exist in the Delta is typically deposited at the apex of the alluvial fan and is usually covered with a shallow layer of sand.

A consequence of the low amount of clayey soils in the upper Delta is the lack of firm channel banks. Instead, the river and channel banks in the panhandle are comprised of peat with thick stands of papyrus rooted in the peat, which typically extend to the channel floor (Smith et al., 1997; McCarthy et al., 1997a; Tooth and McCarthy, 2004). The porous nature of the channel banks in the panhandle and upper fan allows a slow dispersion of water into the adjacent swamps where they remain permanently flooded. In the upper fan, vegetation traps sediment load, decreasing the turbidity of the water downstream. Channels in the panhandle and upper fan have a water depth around 3 – 4 m and a width around 100 m (Tooth and McCarthy, 2004). Over time, the water distribution and the general flooding pattern of the Delta appear to be moving from west to east with the major flow diversions attributed to tectonic activity (McCarthy et al., 1997b; McCarthy et al., 1998a). While the physical controls that govern the variability of the spatial distribution from the annual flooding are known (i.e. rainfall upstream, topography, sediment aggradation, vegetation growth, and channel avulsion), flooding extent and duration each year can not currently be predicted (Scudder et al., 1993; Gumbricht et al., 2004a). However, advances in hydrology modeling are improving these efforts (Wolski et al., 2005; Bauer et al., 2006). This variability in flooding, both in terms of extent and duration, has serious implications for both ecosystem health and human utilization of resources.

At the distal portions of the Delta, the sedimentation that occurs consists of solute materials rather than clastic materials (McCarthy et al., 1997a). Here most of the water transport is via overland flow with very little water transported through the channels

themselves (McCarthy, 2006). In some areas of the Delta, it is speculated that the primary function (or origin) of the channels is for hippo and elephant movement rather than water transport (McCarthy et al., 1998b). The channels in the lower Delta consist of a sandy substrate and are typically 1 – 2 m in depth and < 40 m in width. These channels are highly vegetated, often kept open by boat and animal traffic. The 2 m escarpment height of the Kunyere fault limits the flooding extent at the distal end of the Delta (McCarthy et al., 1997).

The fan of the Delta has relatively low relief (1:3300), but localized topography on the order of 1 meter is common (McCarthy et al., 1998c; Gumbricht et al., 2001; Gumbricht et al., 2005). Floodwater flows slowly across the surface, gradually filling depressions before advancing farther downstream. Trona islands are common within the myriad of channels in the Delta. They are hypothesized to be formed by alluvial processes or initiated from a nucleus formed by abandoned termite mounds (Ellery et al., 1998; McCarthy et al., 1998c). As these elevated areas develop, they provide suitable forage for grazing animals. As the islands continue to develop they become fringed by woody vegetation and shrubs seeded and fertilized by animal droppings (Gumbricht et al., 2004b). As these trees from the riparian forest tap into groundwater, the water table becomes increasingly concentrated with dissolved solids that ultimately precipitate upward into the island interiors as silica and calcite (McCarthy et al., 1998c; Gumbricht et al., 2004b; Bauer et al., 2006).

3.1.5 Animal Impacts

The Okavango Delta provides habitat for many animal species, and in turn the animals play an important role in the functioning of the Delta. The Delta is home to 650 bird species including the globally threatened Wattled Crane and Slaty Egret (Jansen and Madzwamuse, 2003). The Delta also has a high floral diversity including 208 aquatic species, 675 herbaceous species, and 195 woody species (Ramberg et al., 2006a). Due to the abundance of water and food, the Delta also has a large mammal population, including elephant, Sitatunga antelope, and the African wild dog. The large megafauna populations provide critical ecological functions including seed dispersal, island formation, herbivory, and channel modification (McNaughton et al., 1988; McCarthy et al., 1998b, McCarthy et al., 1998c). The African continent is the only continent where megafauna are still prevalent and the great migratory herds of wildebeest, zebra, and buffalo are supported by vast, seasonal grazing-tolerant grasslands (Ross, 1987). The Okavango Delta is the southern most source of surface water in the Kalahari Basin, making it a focal point for wildlife during the dry season when local floods are at their peak.

The elephant is one of the most influential animal species in southern Africa. In 1995, the elephant population in northern Botswana was estimated to be 80,000 (Mosugelo et al., 2002), roughly equal to the human population. Elephants play a role in ecosystem processes through seed dispersal and cycling of nutrients. Despite these positive properties, elephants can also have a negative impact on the local environment especially in conservation areas where the populations have exceeded the carrying

capability of the land (Ben-Shahar, 1998). Limited browsing encourages plant growth. However, intensive browsing of leafy vegetation on trees limits the growth of trees and provides a means to prevent total densification of woody vegetation. In addition, elephants can easily modify habitats by knocking over trees in search of leaves, fruit, and bark. The sustainability of woodlands in Northern Botswana is spatially varying with distance to water and influenced by elephant browsing, fire, and climatic factors (Mosugelo et al., 2002). The combination of extensive browsing of elephants and fire is hypothesized to describe the shifts of woodlands within savanna ecosystems on the timescale of two decades (Ben-Shahar, 1996; Dublin et al., 1990; Baxter and Getz, 2005).

Both the termite and the hippo have been considered as keystone species for the Okavango Delta (McCarthy et al., 1998b). The hippopotamus is important in the wetlands of the Okavango due to its ability to create and maintain channels. As described in previous sections, large mats of papyrus and reeds can form in the channels and create blockages leading to channel avulsion. Hippos are herbivores and graze on the grasses during the night; however, during the day they remain mostly submerged to protect their skin from the harsh sun. The continual movement in and out of the water each night creates new flow paths for water movement. A favorite grass of the hippo is *Cynadon dactylon* (Bermuda grass*).* Another animal species critical to the Okavango wetlands is the termite. Termites collect the small amounts of clay that enter the Delta for the creation of their mounds (McCarthy et al., 1998c). The combination of saliva and silts/clays create an extremely sturdy mud and many mounds can reach heights of >3 m.

Once abandoned, these termite mounds serve as a nucleus for many of the islands within the mosaic of wetlands (McCarthy et al., 1998c).

3.2 Land use within the Okavango Delta

People have inhabited the Okavango Delta region for more than 100,000 years (Butzer, 1984; Ramberg et al., 2006a). The presence of tsetse fly, which carries a deadly parasite, has limited the amount of more recent development in the Delta (Jansen, 2002; Meyer and Bendsen, 2003). The earliest records of domestic livestock are dated in the Toteng region (just North of Lake Ngami and out of the Tsetse fly zone) at approximately 2000 years ago (Robbins et al. 2005). Historical accounts of people living during the first half of the twentieth century paint a different picture of life in the Delta than what is observed today. Older inhabitants along the Gomoti River perceive that the present day decline in river health is attributed to a lack of rainmakers, government restrictions on access to lands leading to reduced river management, and safari/tourist camps (Bernard and Moetapele, 2005). During the early twentieth century, travel by mokoro (dug-out canoes) by villagers to hunt, fish, and trade with other villages was so common that the traffic might have kept many of the tributaries open (Wellington, 1949). In addition, villagers removed vegetation or fallen trees blocking channels to ensure water flow. Bernard and Moetapele (2005) quote one informant as saying "We depended upon this river, and we took care of it" (pg.268). Local villages are also known to have burned vegetation in the channels to clear choked channels and to encourage new growth. Today's fires are thought to be more extensive than when local chiefs controlled the

location and timing (Bernard and Moetapele, 2005). In addition, burning of dense brush was recommended as a method for establishing a tsetse fly-free buffer for livestock grazing as the flies are found in dense scrub (Clifford, 1929). The establishment of the Moremi Game Reserve in the 1960s and wildlife management areas in the early 1990s changed the way in which local inhabitants could access resources in the Delta. Restrictions have been placed on hunting, fishing, and harvesting of veld products (reeds and thatch) by local communities residing within the management areas (Cassidy, 2000).

3.2.1 Land Management Designation

The majority of lands within the Okavango Delta are protected for conservation under the designation of the Moremi Game Reserve (MGR) or the Wildlife Management Areas (WMAs) as shown in Figure 3.5. Moremi Game Reserve is Botswana's first wildlife reserve: in 1966 (the year of Botswana independence), land was given by the Ba Tswana people to the Botswana government for the preservation and conservation of wildlife (Ross, 1987; Bolaane, 2005). The lands within the MGR exist under the highest levels of protection whereby "no person shall hunt or capture any animal, or species or variety, specimen or sex of any animal" (Botswana Government, 1992). Permits and a small fee (US$20 for visitors, US$2 for Botswana residents) are required for entry into the game reserve. There are no fences or borders restricting access to the game reserve from the adjacent wildlife management areas. The extraction of resources, possessing and raising domestic livestock, cultivation, and setting fires are not permitted within the game reserve.

The communal lands, designated on the map in Figure 3.6 as pastoral/arable/residential, are home to most of the approximately 120,000 people of the Okavango Delta. Within the communal areas, there is no restriction on where a person can extract resources as long as they are extracted for subsistence and not profit. The extraction of materials is not enforced, leading to the over-extraction of some resources (Kgathi et al., 2006). The traditional practice however, for accessing resources is to gain permission from the *kgosi* (chief) of the nearby settlement (Twyman, 2001). Many locals possess small herds of goats and donkeys; wealthier citizens may also possess a few cattle. Additionally, some ethnic groups such as the Batawana often raise livestock (Meyer and Bendsen, 2003).

Possession of up to 15 head of cattle enables citizen rights to water boreholes and grazing lands. The expansion of the livestock industry into the two-thirds of the country covered by the Kalahari is possible due to digging wells and placement of boreholes to extract groundwater (Sporton et al., 1999). Owners possessing more than 15 head are required to place their herd in one of several commercial livestock ranches, one of which is located approximately 75 km south of Maun. Cattle are a highly valued commodity in Botswana for many rural people as a source for meat or cash in times of economic hardship (Twyman, 2001).

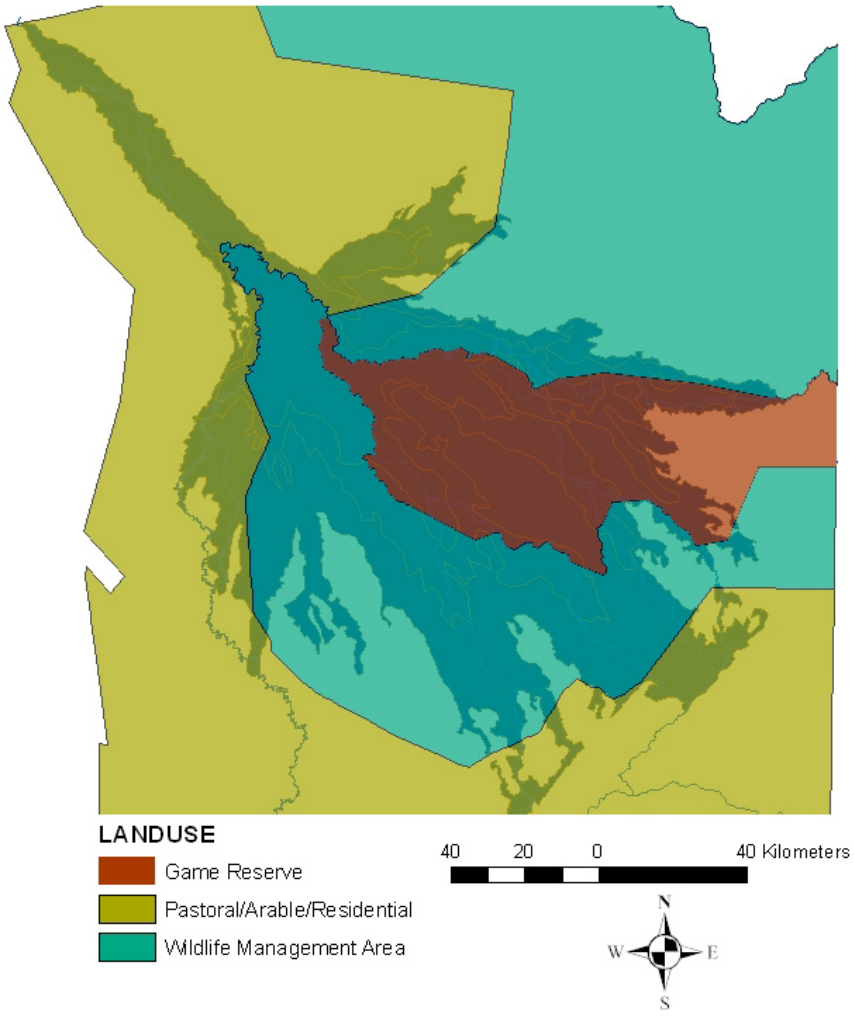

Figure 3.5. General land use designation within the Okavango Delta

The wildlife management areas were established in 1975 under the Tribal Grazing Land Policy and reformalized in 1992 in the Wildlife Conservation and National Parks Act. The WMAs, however, were established with limited stakeholder participation (Jansen, 2002). In the Okavango Delta the WMAs function as a buffer between the communal areas and the Moremi game reserve. Access into the WMAs requires a permit and fee (approximately US$25) for entry, and they are designated as photography or

hunting concessions for both commercial or community usage. The vast majority of safari camps in the Delta exist in a WMA. Cultivation within the WMAs is heavily restricted and the raising and grazing of domestic livestock (cattle and goats) are forbidden. A 1.5 m veterinary fence, referred to as the "Buffalo Fence", separates the WMAs from the communal lands of the villages. The 250 km fence was erected in 1982 to separate the wildlife populations from the domestic livestock populations in an effort to avoid disease. Today the WMAs are almost entirely fenced on the periphery (Mbaiwa and Mbaiwa, 2006).

The WMAs are divided into Controlled Hunting Areas (CHA) and are designated for commercial or community managed photographic or hunting activities. The three general categories of land management within the study area are shown in Figure 3.6, which includes a portion of the Moremi Game Reserve, WMAs, and communal lands. The concession areas are numbered for the Ngamiland district (i.e. NG/32).

Livestock and veterinary cordoned fencing throughout the country are known to be detrimental to the natural migration patterns of southern Africa's wildlife and thus are a source of controversy in Botswana (Boone and Hobbs, 2004; Ramberg et al., 2006a). The Buffalo fence around the Okavango Delta has apparently protected domestic cattle from hoof and mouth disease (Mbaiwa and Mbaiwa, 2006). Following the erection of the fences, however, the death of many wild animals was reported due to entanglement, stress, and lack of access to water (Ross, 1987; Albertson, 1998). In the central Kalahari, the disruption of migration routes combined with severe drought and competition with

domestic cattle led to the local demise of the zebra, buffalo, elephant, and wildebeest herds (Mbaiwa and Mbaiwa, 2006).

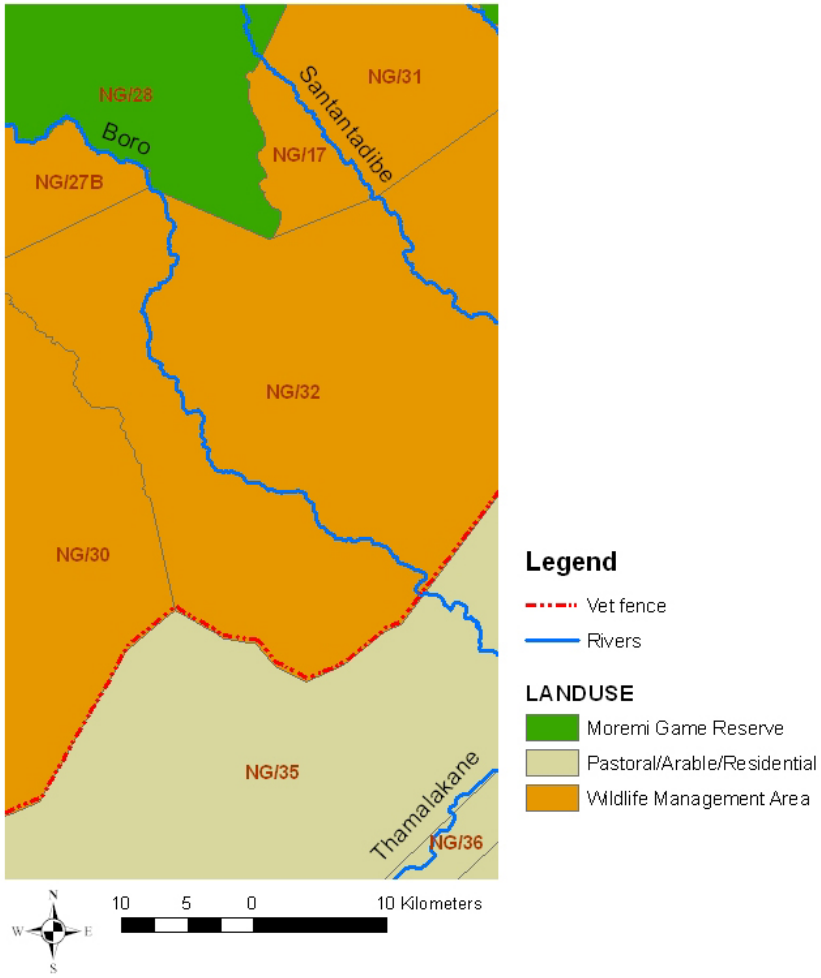

Figure 3.6. General land use of controlled hunting areas within study area.

3.2.2 Tourism

The tourism industry is second only to diamonds in Botswana in economic impact and employs more people than any other industry; it has been steadily growing in

economic importance over the past two decades. It is estimated that 60% of the population in Ngamiland is linked to the tourism industry (Kgathi et al., 2006). Tourism into the Okavango Delta began to flourish in the early 1980s when the Botswana government began a program to eradicate tsetse fly (Bolten, 1998). In 1989 there were 32 camps and lodges operating in and around the Delta; by 2001 the number had increased to 63 (Mbaiwa et al., 2002). At the start of 2003, there were 91 camps and lodges operating in the Delta. Currently, over 100 tourist camps are estimated to be operating in the Delta (Drotsky 2006, personal communication). In addition to guiding, the tourism sector provides employment alternatives through lodge staffing and food service, as well as for the sale of handicraft products such as basket making (Mbaiwa, 2004b). Botswana currently promotes a low volume-high dollar tourism policy in an effort to limit the environmental impact of tourism in the Okavango Delta (Mbaiwa, 2003). This policy is achieved by restricting the number of issued licenses that in turn restrict the number of camps and beds at each facility (Mbaiwa et al., 2004c).

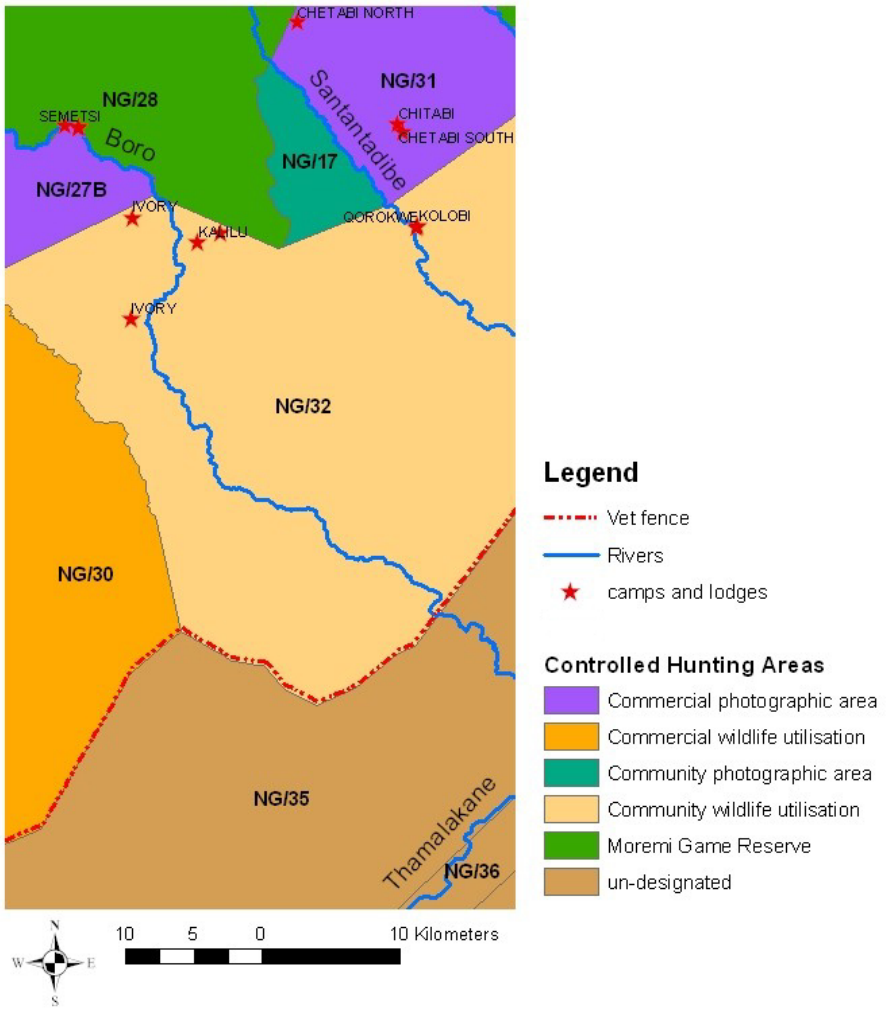

Figure 3.7. Concessions within the study area and the location of camps and lodges.

The largest concession in the study area is NG/32, which is designated for community utilization of hunting as shown in Figure 3.7. Although designated for hunting, several hunting concessions are also incorporating photographic activities into the concession to increase the economic potential. Hunting activities are generally restricted to the drier regions, whereas photographic activities are focused within the floodplains and marshes. For NG/32, the region between the Boro River and the

Santantadibe River is used for photography only (Sheller 2007, personal communication). Within the study area, four of the fourteen camps exist in the hunting concessions and the others are located in the photography concessions.

Since the tourist camps are located in either photography or hunting concessions, they are typically managed as such. Hunting camps are small and do not support a large staff. Most hunting patrons occupy the camps in small groups and track the desired animals for several days. The fees for hunting vary depending upon the trophy and can range from US $200 (steenbuck) to $25,000 (elephant) to $100,000 for an adult male lion. The total cost of a hunting expedition for a trophy elephant cost almost of $200,000 US dollars including trophy, taxidermist, processing, and safari fees. In some cases, a fraction of the fee and all of the meat are split among the communities within the operating WMA. This level of support provided to the communities depends upon the relationship among the safari companies, the North West District Council (NWDC), and the communities. In contrast, photographic based camps are larger in size and employ a larger support staff. While photography based camps are economically favored (in that local people are hired and more of the income stays within the Botswana economy), they have environmental consequences. In order to support the larger photography based tourist camps, temporary camps are established nearby for the support staff. These camps, however, are often not as sanitary or safe as they should be (2006 personal observation). The photographic camps also result in a densification of a trail network in the WMAs. This results from local guides attempting to find wildlife for tourists by driving off road and creating new trails. These new trails result in increased accessibility

into remote areas and destruction of vegetation. Large trucks, previously not able to travel into the remote areas, are used to collect large amounts of reed out of the floodplains for sale in Maun (2006 personal observation). Mbaiwa et al. (2004b) report the immediate concerns of camp and lodge managers are "off-road driving, high traffic in lagoons and airstrips during the high season, and too many mud-holed illegal tracks" (pg 326). While tourism is the second largest industry in Botswana, it is often criticized due to the inequity in redistributing financial benefits back to the community and an over-reliance on foreign safari ownership (Mbaiwa, 2004c; Kgathi et al., 2006).

3.2.3 Natural Resource Extraction

The Okavango Delta has provided natural resources for the people of Botswana for thousands of years. Recent surveys indicate that 65% of the people living in or near the Delta depend on fishing to subsidize their livelihood (Kgathi et al., 2005). Household surveys indicate a local perception that the abundance of natural resources in the Delta is declining for products such as reeds (roof thatching material), palm leaves (basket making), fruits for medicinal purposes, and fuel wood (Mbaiwa, 2004b). This perceived decline of local resources is attributed to over-exploitation of resources for commercial gains and a lack of conservation policies (Kgathi et al., 2006). In contrast, local citizens view fish availability, wildlife, and bird populations as increasing in recent years. In addition to utilizing vegetation products, almost all of the surveyed houses extract water directly from the Delta for household uses such as cooking, washing, and livestock watering (Kgathi et al., 2005).

The majority of the people in the villages and settlements are poor and rely upon small scale cultivation of corn, millet, melons, and beans for subsistence. However, many Botswana rely upon drought relief from the government to subsidize the purchase of food. The soil quality in the study area is regarded as poor and unsuitable for large scale agriculture. Arable farming of millet, corn, and sorghum is practiced; however, yields are often low to fair due to variable precipitation and damage from birds, rodents, or livestock (Meyer and Bendsen, 2003). A type of traditional farming in the Ngamiland region, known as molapo farming, occurs on the floodplains on the Delta. The percentage of farmers in Ngamiland who practice molapo farming, however, has decreased from 27% in 1979 to 16% in 1998. Molapo crops are planted when the flood waters recede and typically consist of corn, beans, or melons (Kgathi et al., 2005). Lands used for molapo farming are not allocated by the government; rather they are under a traditional land tenure system.

3.3 Development History of the Okavango Delta

The presence of permanent water in the Okavango Delta located within the semi-arid Kalahari has challenged development of Botswana during British control over the Bechuanaland Protectorate period circa 1870 until Botswana gained independence in 1966. During this period, there were several reports and assessments regarding the development and utilization of the land under British control. Because of the abundant grasses in many regions of Botswana, cattle raising was the livelihood for the majority of the people (Rey, 1932). Livestock is still the third-largest industry in Botswana. Despite

the abundance of palatable grasses, the lack of surface water is a major difficulty for domestic livestock. Thus over the years, many water development plans and strategies were proposed to increase and or divert flow from the Okavango River/Delta. Some of these strategies, shown in Figure 3.8, included the erection of a dike from the northern end of Chiefs Island to the village of Saboro, which lies at the apex of the alluvial fan. This embankment would divert much of the water to the Nqoga-Santantatibe system leaving the western portion of the Delta available for agriculture (Wellington, 1949).

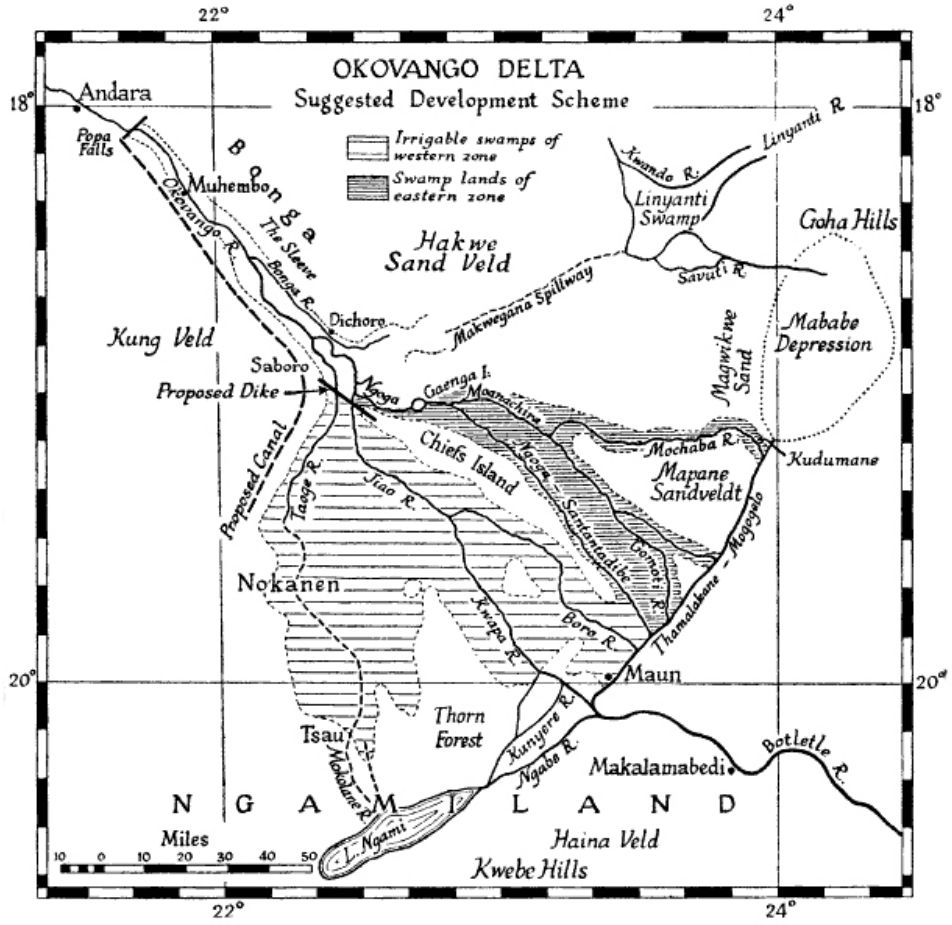

Figure 3.8. Map of suggested development plans for the Okavango Delta in 1949. The proposed plan included a dike from Saboro to Chief's Island to divert the majority of water flow leaving the western zone available for agriculture (from Wellington, 1949)

Currently, many of the estimated 120,000 people who live around or within Okavango Delta reside within the lower Delta. The largest village, Maun, has a present-day population of approximately 50,000 (Linn et al., 2003). The United Nations sponsored two studies to investigate the utilization of water in the Delta in 1960 and the mid-1970s. This sponsorship resulted in proposals to dredge the Boro River in the lower Delta to meet the consumption needs of the citizens as well as to support the Orapa diamond mine (Ellery and McCarthy, 1994; Ellery and McCarthy, 1998). The lower reach of the Boro River was dredged between 1971 and 1974 in an attempt to straighten the outflow channels into Maun. The results of the dredging included decreased channel stability and loss of channel vegetation. In addition, adjacent floodplains were converted into dry terrestrial habitat (Ellery and McCarthy, 1994). The discovery in 1974 of ground water near Maun temporarily halted dredging efforts. The water demands of the growing population of Maun in the mid-1980s led the Botswana government to consider new water diversion measures. These water diversion proposals were postponed due to harsh criticism by Greenpeace and the World Conservation Union (Ellery and McCarthy, 1994). The rapidly growing region near Maun currently relies on groundwater extraction to meet the water needs of its citizens and to sustain the tourism industry.

3.3.1 Water policies in the Okavango Catchment

As previously described, the Okavango Delta is considered to be a near pristine ecosystem that supports a vast habitat for both wildlife and humans. The Okavango Delta

is fed by the Okavango River, which provides a riparian corridor through two other countries, Angola and Namibia. The Okavango Delta is currently considered a relatively undisturbed wetland; however, future anthropogenic usage could alter this system. Management and conservation of wetland ecosystems require a scientific knowledge of hydrologic and ecosystem functioning in order to facilitate practical and informed management decisions (IUCN, 2000). The issues at the forefront of management and conservation efforts are associated with wetland hydrology and consist of monitoring water quality and water quantity. A significant threat to the Delta is increased water demands and usage along the Okavango River in Angola and Namibia. The Okavango Delta is one of two permanent bodies of water for the entire country of Botswana and the utilization of this resource is of utmost concern to many parties and agencies, such as the Botswana Department of Water Affairs. As with most developing countries, water is a critical resource for both survival and economic growth (Neme, 1997). Recent political regime changes and subsequent population relocations in neighboring Angola resulting in increasing water demands on the Okavango River caused the United Nations to denote the Delta's condition as one of the most pressing international concerns for both water management and sustainable development (Nichol, 2003; Ashton, 2003).

3.3.1.1 Treaties for the Protection of the Okavango Delta

The catchment for the Okavango River consists of over 413,000 km^2 and is actually a sub-basin within the larger Makgadikgadi system (approximately 725,000 km^2) (Turton et al., 2003). Within the Okavango catchment, over 94% of the annual input to

the Okavango River originates in Angola, with another 2.9 % originating from Namibia and the remaining 2.62 % originating in Botswana (Ashton, 2003). Recognizing the importance of the Okavango River, all three countries signed treaties in 1994 forming the Permanent Okavango River Basis Water Commission (OKACOM). The objective of OKACOM is to serve as a technical advisor to the three states in the areas of conservation, development, and resource utilization. While the formation of OKACOM has been received as an indicator of potential improved water management, it has not solved the underlying problem: an equitable utilization of water from the Okavango River for all three countries (Turton et al., 2003). In 2003, Angola ended a 30-year civil war, and has begun to develop industrial infrastructure, including irrigated agriculture along the Okavango River.

At the inaugural OKACOM meeting, Namibia declared its plan for establishing a 700 km pipeline to extract water from the Okavango River to its capitol, Windhoek, with links along the way for agriculture and settlements (Turton and Earle, 2003). While development of the pipeline for Namibia has been delayed, it is estimated that increased groundwater extraction and recycling of wastewater will only sustain the Namibian population demands until 2009 (Ashton and Neal, 2003). Meanwhile, communities along the Delta such as Maun are also experiencing population growth. Increased population in the entire catchment area translates into increased demands on water (Ashton, 2003). Ashton (2003) estimates a 44% increase in water needs by 2020, based only on growing population trends and current land use patterns in the catchment area. If increased irrigation demands are projected with the population increase and a proposed water

pipeline is constructed to supply water to Namibia, Ashton (2003) estimates the water demands could be thirteen times the current level by 2020.

In addition to the formation of OKACOM, all three countries have signed, ratified, or are considering five international treaties for establish a framework for cooperation of water management decisions. The Ramsar Convention on Wetlands of International Importance requires participant states to designate at least one wetland to be included on a list of important wetlands. Botswana and Namibia have ratified the Ramsar treaty and each party has designated the Okavango Delta as a wetland of importance. Angola has not yet ratified the Ramsar treaty and is currently considering its position (Ashton and Neal, 2003). The Convention on Wetlands, signed in Ramsar, Iran, in 1971, is an intergovernmental treaty that provides the framework for national action and international cooperation for the conservation and wise use of wetlands and their resources. There are presently 141 contracting parties to the Convention, with 1387 wetland sites totaling 122.7 million hectares designated for inclusion in the Ramsar List of Wetlands of International Importance. The Ramsar treaty requires parties to promote the wise use and conservation of wetlands and to consult with other parties regarding water usage when the water system extends over multiple territories (Ashton and Neal, 2003). Lands designated by both Botswana and Namibia totaling over 55,000 km^2 make the Okavango Delta the largest inland Ramsar site.

While the Okavango Delta warrants protection and conservation, it has been suggested that the Botswana government signed on to the Ramsar designation of the Okavango Delta as a wetland of importance in 1997 partially to place its water disputes

with Namibia and Angola into the global spotlight (Turton and Earle, 2003; Ashton and Neal, 2003). It is estimated that more than one million of the citizens displaced by the war in Angola and forced into refugee camps will be returning to areas adjacent to the Cubango and Quito Rivers that form the Okavango River (Andersson et al., 2003). The increased water demands for agricultural irrigation as well as the establishment of dams along the Okavango River could have drastic impacts on the overall functioning of the Delta.

In addition to the Ramsar treaty, all three riparian countries have ratified or are considering the following four treaties from the United Nations: The United Nations Convention on Biological Diversity (UNCBD) of 1992, The United Nations Convention to Combat Desertification (UNCCD) of 2001, The United Nations Convention on the Law of Non-navigational Uses of International Watercourses (UNCSW) of 1997, and the United Nations Framework Convention on Climate Change (UNFCCC) of 1992. In addition, Botswana and Namibia have ratified the revised protocol on the Shared Watercourse Systems in the South African Development Community (SADC) of 2001. Under this treaty, member states must maintain a proper balance between economic development to improve the standard of living of their people and conservation of the environment. Under these provisions, member states are allowed to utilize their resources as best needed, with the stipulation that they must ensure that environmental degradation is minimized or avoided (Ashton and Neal, 2003). While the ratification and establishment of these treaties are encouraging in terms of wise use of the water from the Okavango River, the fact remains that both Namibia and Botswana reside in semi-arid

climates and are facing water shortages. Thus, each riparian state has a different set of requirements and development priorities for the Okavango River (Turton and Earle, 2003). It is likely that increased water utilization will occur in the future. Due to this impending scenario, it is important to understand the ecological processes and functions as they currently exist to determine the impact from future change.

In late 2006, the Botswana government finalized the Okavango Delta Management Plan (ODMP) project for the wise use of natural resources in the Delta while being responsive to the socio-economic needs of stakeholders. The ODMP utilizes an ecosystem approach to management that has the objective of balancing human benefit of resources from the Delta while sustaining ecosystem processes and function (Jansen and Madzwamuse, 2003). Five operational principles of the ecosystem approach as outlined by the IUCN (2000) include focusing on the functional ecosystem relationships and processes, increasing benefit sharing for local stakeholders by maintaining biological diversity, utilizing adaptive management decisions, applying management strategies at the appropriate scale and decentralizing decision-making to the lowest level possible, and incorporating multiple sectors such as fishing, agriculture, and forestry since they can indirectly impact biodiversity. Challenges facing the Delta recognized by the ODMP include lack of understanding of climate change, high rates of human-induced fires, uncoordinated research activities, inequity of land management for stakeholders, tourism, over-exploitation of veld products, and unsustainable agricultural practices (Jansen and Madzwamuse, 2003).

4 REMOTE SENSING AND RESEARCH METHODOLOGY

Since 1972, the use of digital remotely sensed data from airborne and spaceborne systems has been utilized to monitor the Earth's terrestrial and aquatic ecosystems (Field et al., 1995). Data collected from optical sensor systems, such as Landsat Thematic Mapper (TM), Advanced Very High Resolution Radiometer (AVHRR), and the Moderate Resolution Imaging Spectroradiometer (MODIS), have been used to map land cover from regional to global scales (DeFries and Townsend, 1994; Loveland and Belward, 1997; Friedl et al., 2002; Slayback et al., 2003). Additionally, active remote sensor systems such as radar and lidar have been used to characterize topography and surface structure (Hoekman and Quiriones, 2000; Lefsky et al., 2002). Because of its systematic ability to view the earth from above, remotely sensed imagery offers a unique vantage point to assess and quantify land cover from the local to regional/continental level. Additionally, remote sensing systems are capable of collecting data in various regions of the electromagnetic spectrum beyond the limits of the human eye. For example, the near infrared and middle infrared portions of the spectrum can provide information about vegetation productivity and/or stress that would otherwise be unobservable to an unaided eye. For these reasons, the utilization of remote sensing has been adopted into many ecological monitoring programs (Goward et al., 1994; Shuman and Ambrose, 2003; Roberts et al., 2003). The field of remote sensing has advanced significantly during the past twenty years in the areas of information extraction, classification methods, and image processing techniques (Moon, 1996; Myneni et al., 1995; Schowengerdt, 1997;

Crawford et al., 1999; Muchoney and Williamson, 2001; Tso and Mather, 2001; Liang, 2004; Richards and Jia, 2006).

However, remotely sensed data have some limitations for environmental applications. First, ecosystems are dynamic, but many ecological processes such as succession or forest degradation require multiple years if not decades to occur (Trodd and Dougill, 1998; Song and Woodcock, 2003; Tottrup and Rasmussen, 2004). Remotely sensed imagery provides a snapshot yielding information at one point in time (Crews-Meyer, 2006). Depending upon the time within the vegetation phenological cycle or successional trajectory, the use of a few satellite images can lead to a misinterpretation of land cover change (Lambin, 1996; Lambin, 1999; Du et al., 2002). A second limitation is the scale (both spectral and spatial) of the observation that spaceborne sensor systems can detect and the resulting information that can be derived from those measurements. For example, it is possible to determine land cover type or estimate biophysical parameters such as fraction of photosynthetically active radiation (fPAR) based upon the measured surface reflectance from optical sensors (Asrar et al., 1992; Field et al., 1995). However, the ability to do so is a function of both the spatial and spectral resolution of the data (Leprieur et al., 2000).

Traditional optical sensors detect upwelling radiance, which is a function of electromagnetic (EM) energy interaction with the surface as well as the scattering and absorption of that energy with the atmosphere. Neglecting the atmosphere, the spatial resolution of a pixel is a function of the instantaneous field of view (IFOV) of the detector, the altitude, and pointing of the satellite (Richards and Jia, 2006). The reflected

radiance from the small portion of the Earth that is detected by the sensor array is reflected by components within it such as vegetation, man-made features, and soil. Because of the broad spectral width and placement of bands on spaceborne multispectral sensors and the relatively coarse spatial resolution, it is typically not possible to identify species composition or to know the vegetation community structure (trees:shrubs:grass) within each pixel. Spectral un-mixing techniques have been developed and have been used with some success with hyperspectral sensors with a greater number of narrowly constructed spectral bands (Manolakis et al., 2001; Keshava and Mustard, 2002; Thai and Healey, 2002).

Temporal resolution of remotely sensed data is important for observing land cover change because many temporal processes occur at different time scales (Lambin, 1999; Eva and Lambin, 2000; Lunetta et al., 2004). Lambin and Ehrlich (1997) utilized a multi-temporal sequence to examine seasonal properties of African land cover. They determined that land cover change in Africa is mostly driven by droughts, modifications to seasonality, and shifts in precipitation events. Lunetta et al. (2002) examined the impact of image temporal frequency (three, seven, and ten years) to capture land cover change in North Carolina. They found that a minimum time-step of three years is required to capture the rapid regeneration of clear cut forest but recommended a higher image frequency (one to two year) to reduce change omission errors.

4.1 Sensor Systems

Numerous Earth observing sensor systems in operation today collect information in several portions of the EM spectrum; the primary datasets used in this research come from medium resolution passive optical systems such as Landsat Thematic Mapper, Landsat Enhanced Thematic Mapper (ETM+), and Advanced Land Imager (ALI). Because of the 30 m spatial resolution and the spectral coverage, data from Landsat TM, ETM+, and ALI are often considered the link between local processes and global distributions of environmental phenomena (Cullinan et al., 1997; Gupta et al., 2000; Liang, 2004). Many ecological processes at the field level are too detailed to be accurately represented by 30 m multispectral data. Conversely, regional and continental patterns of vegetation are driven by climatic patterns. Data at the landscape level provide a means to relate field-based information to data in a larger regional context.

4.1.1 Landsat

Since the launch of the Earth Resources Technology Satellite (ERTS - later renamed Landsat) on July 23, 1972 by NASA, Landsat has provided the longest time-series of systematically collected remotely sensed data to the scientific and civilian communities (Masek et al., 2001; Cohen and Goward, 2004). In the early 1980s, NASA developed the Thematic Mapper (TM) system as an improvement to its predecessor, the Multispectral Scanner (MSS). The TM instrument collects data in 7 spectral bands compared to four by MSS (blue, green, red, near infrared (NIR), two middle infrared, and a thermal infrared band) at an improved IFOV of 42.5 μradians resulting in a nominal 30

m spatial resolution (120 m for thermal). The TM bands were modified from the MSS predecessor to maximize detection and improve monitoring of the Earth's surface. The TM also has improved radiometric resolution (8 bit) relative to MSS (6 bit). The TM instrument was first launched in 1982 on the Landsat-4 satellite and many scientific applications began to shift to exploit the newly available resource. Because of the early success of TM and problems associated with the Landsat-4 satellite, the Landsat-5 satellite was launched early in 1984 to meet the demands of the scientific community and provide continuous acquisition of data.

To meet new science demands, an Enhanced Thematic Mapper (ETM) sensor was developed which incorporated a panchromatic band with a spatial resolution of 15 m and two radiometric scaling sensitivities were developed (Masek et al., 2001). The two radiometric gain states provide a trade-off in sensitivity. The low gain setting records a greater radiance range but with decreased sensor sensitivity, whereas the high gain has a smaller radiance range but greater sensitivity. Landsat bands 1 – 7 (excluding 6 –thermal) are acquired with only one gain setting while band 6 is recorded with both low and high gain.

The ETM sensor was onboard the Landsat-6 satellite, but the satellite failed to successfully launch in 1993. The failure of Landsat 6 to achieve orbit raised concerns regarding data continuity for the science communities. The quickest remedy to launch a new system was to utilize the ETM sensor design. ETM+ was developed and did offer some improvements to the ETM design, including increased spatial resolution of the thermal channel (60 m) and the addition of sensor calibrators to allow full calibration of

the instrument once on orbit (Masek et al., 2001). Additionally, the use of precise ephemeris data to compute the orbital position of the Landsat 7 satellite resulted in a geometric positional accuracy of +/- 80 m that is superior to TM data (NASA Landsat 7 Handbook). The ETM+ sensor was successfully launched in 1999 on Landsat 7 and operated without fault until May 2003 when the scan line corrector component of the sensor failed resulting in approximately 25% data loss in every scene. Both TM and ETM+ use cross-track scanning, where a mirror scans perpendicular to the satellite motion. A telescope focuses the energy onto a pair of motion compensation mirrors which directs the energy to the array of detectors positioned on the focal plane. The Landsat-5 and Landsat-7 satellites are in a near polar, sun synchronous orbit at an altitude of 705 km above the Earth's surface. The designed orbit results in slightly more than 14 orbits per day and 16 days are required to image the entire Earth (from 81 degrees north to 81 degrees south). The Landsat-7 satellite crosses the equator at approximately 10:15 AM local time, with a swath width of 185 km. The spectral, spatial, and radiometric characteristics of TM, ETM+ will be compared to ALI in the following section.

4.1.2 Advanced Land Imager (ALI)

The ALI sensor was developed as prototype for the Landsat Data Continuity Mission and launched on the Earth Observing-1 (EO-1) satellite. In November 2000, the EO-1 satellite was placed into orbit slightly east of and approximately one minute behind the Landsat 7 satellite. Since the ALI sensor was developed as a technology demonstration instrument and not an operational land imager, the sensor array was not

fully populated and thus only one-quarter of the swath width available with ETM+ is covered by an ALI acquisition (~37 km). The EO-1 satellite attitude changes as the satellite is rolled to point the instrument at a designated ground target to compensate for the partially populated focal plane and provide decreased revisit time. The ALI instrument collects data in nine multispectral bands with a ground resolution of 30 m and a single panchromatic band with a ground resolution of 10 m. The ALI sensor uses pushbroom imaging, as opposed to a cross-track scanning system like TM and ETM+. Pushbroom imaging results in greater dwell time and higher signal to noise ratio (SNR), but it is more difficult to maintain good inter-detector calibration. The EO-1 satellite has outlived its original mission design (Ungar, 2002), and the satellite is projected to remain on-orbit to collect supplemental imagery through 2010 in light of the limited image acquisitions of ETM+.

The ALI bands are similar to those of the Landsat ETM+, with the exception of three additional visible/infrared bands but the exclusion of a thermal band. A band by band comparison between ALI and ETM+ is listed in Table 4.1. ALI has higher spectral sensitivity than ETM+, as indicated by its dynamic range of 12-bit data compared to 8-bit from ETM+. In addition to the increased dynamic range, the ALI sensor has an improved signal-to-noise ratio: four to ten times better than ETM+ depending on the band (Ungar, 2002). Additional bands were added in the blue (442 nm), the near-infrared (866 nm), and the middle infrared (1244 nm) portions of the spectrum. By splitting the broad spectral coverage of ETM+ band 4, a portion of the EM spectrum that is not favorable for remote sensing due to atmospheric absorption is excluded. The addition of ALI band 5p

provides information in the 1200-1288 nm range that is useful for detecting water content within vegetation. The ALI panchromatic band is improved in that it covers the spectral range (480 – 690 nm) at 10 m spatial resolution compared to the 15 m spatial resolution of Landsat ETM+ panchromatic band (520 – 900 nm). By reducing the spectral range to the visible region, the image is crisper than that of ETM+ which spans the vegetation red edge. The ALI panchromatic band also has an increased signal-to-noise ratio relative to that of the Landsat ETM+ panchromatic band.

Table 4-1. Comparison of TM, ETM+, and ALI visible and infrared bands

Landsat TM Bands	TM wavelength (nm)	Landsat ETM+ Bands	ETM+ Wavelength (nm)	ALI Bands	ALI Wavelength (nm)
				1p	432 - 451
1	450 - 520	1	450 - 520	1	458 - 511
2	530 - 610	2	530 - 610	2	532 - 602
3	630 - 690	3	630 - 690	3	632 - 688
4	760 - 900	4	780 - 900	4	775 - 805
				4p	844 - 888
				5p	1200 - 1288
5	1550 - 1750	5	1550 - 1750	5	1554 - 1725
7	2080 - 2350	7	2090 - 2350	7	2090 - 2362

4.2 Data Pre-processing

The use of remotely sensed data for detecting evidence of environmental change has taken place since the mid-20th century though aerial photography and since 1972 with the launch of earth observing satellites (Coppin et al., 2004; Lyon et al., 1998; Petit and Lambin, 2001; Huete et al., 2002). Many change detection methods involve pairwise comparison of one date relative to another, commonly known as from-to detection. Recently, change detection methods utilizing a time-series of scenes have been developed

(Lambin and Ehrlich, 1997). While some change detection techniques are patch based (Crews-Meyer, 2002; Petit and Lambin, 2002), most are pixel-based. The quality of the change detection is therefore affected by the quality of the pixels (Price, 1987; Du et al., 2002; Steven et al., 2003). Regardless of which methods are used to detect change, there are fundamental requirements for data pre-processing data prior to the change analysis: image registration, radiometric calibration, and sensor calibration (Du et al., 2002; Song et al., 2001; Chen et al., 2005; Masek et al., 2005). Errors within the datasets are inevitable; thus the goal is to minimize them such that the output of the change detection represents a true change and not noise or processing artifact. Data acquired at different times include the effects of differences in scattering due to atmospheric water vapor and aerosols, differences in illumination due to relative sun angle positions, and differences due to sensor calibration and degradation over time (Kaufman, 1989; Nicholson and Farrar, 1994). In order to produce accurate results, the scenes must be registered (i.e. so that they directly overlay) and corrected for radiometric differences. This helps ensure that the values in each scene represent the same targets and that detected changes are not due to acquisition conditions (Vogelmann et al., 2001; Masek et al., 2001; Steven et al., 2003).

4.2.1 Geometric Correction

Geometric correction involves specifically relating the radiance received at sensor to a geographic location on the earth. Image rectification is the process of applying geographic coordinates to a grid-based image through an application of scaling and

rotation parameters. This step requires resampling and is often implemented by the data provider (such as the USGS Eros Data Center -EDC) where satellite ephemeris data, satellite attitude, and pointing information are combined to geolocate the detector radiance. As a method of convenience, the radiance data are resampled to a standard uniform grid spacing, such as a 30 m pixel for Landsat. Depending upon the level of geometric processing requested, distortion caused by topography can be eliminated or reduced by correcting for topographic relief using a digital elevation model (DEM).

Although data purchased from providers such as USGS EDC are typically projected into either geographic or projected coordinates, it is usually necessary to perform an image to image or image to map registration to accurately position the image into a correct geographic space. Registration refers to co-aligning two or more images and may or may not require resampling of pixels. User registration of the imagery is often necessary to correct/adjust for topographic distortion that may not have been implemented by the data provider and to compensate for less accurate satellite positioning of older satellite systems such as Landsat 5. Biases in estimated land cover change due to misregistration of imagery have been tested with both medium (30 m) and coarse resolution (1 km) imagery resulting in errors ranging from 5% for a 5-class AVHRR classification to 33% for a 20-class Landsat TM classification (Verbyla and Boles, 2000). To achieve accurate change detection using Landsat ETM+, registration accuracy is suggested to within one-fifth pixel root mean square error (RMSE); with Landsat TM and ETM+, the accuracy standard would be one-fifth of 30 m, or 6 m (spatial resolution 30 m) (Dia and Khorram, 1998).

4.2.2 Radiometric and Atmospheric Correction

Radiometric and atmospheric correction is an often neglected pre-processing step; however it is critical when using multi-temporal remotely sensed imagery for change detection (Pons and Sole-Sugranes, 1994; Teillet et al., 1997; Canty et al., 2004). When multi-temporal data are analyzed, the data should maintain consistency between dates by using either absolute or relative correction (Song et al., 2001). As mentioned previously, at-sensor radiance is affected by reflected energy interactions at the surface of the earth as well as atmospheric scattering and absorption caused by aerosols and water vapor, respectively (Kaufman et al., 1997). In addition, the sun/sensor viewing geometry and sensor degradation over time can change the observed radiance. As a method to reduce data space yet preserve the dynamic fidelity of the radiance, the sensor radiances are linearly scaled from floating point numbers into integer numbers referred to as brightness values (BV) or digital numbers (DNs). The radiometric resolution of the data (i.e. 6 bit, 8 bit, 12 bit) varies from sensor to sensor and has generally increased due to improved computing abilities. Retrieval of radiance data from DNs is possible using the following linear equation.

$$L_\lambda = DN \times GAIN_\lambda + OFFSET \qquad \textbf{Equation 4-1}$$

The scaling parameters for each satellite system are different and often vary at different times throughout year or satellite lifetime. For example, the scaling parameters changed from low gain to high gain for Landsat ETM+ data after July 1, 2000 to incorporate

decreased sensitivity of sensor detectors over time. Thus, the raw DN values from different sensors or same sensor/different date are not directly comparable. Despite this fact, many people neglect accounting for the various factors or convert their data into radiances when extracting features or classifying thematic information from a single image.

Once the DN values are converted into radiance, there is a simple formulation to correct for the sun/sensor viewing geometry and convert the data into top-of-atmosphere (TOA) reflectance. The equation to convert radiance data from multispectral sensors such and Landsat TM and ETM+ is

$$\rho_\lambda = \frac{L_\lambda \times \pi \times d^2}{E_\lambda \cos\theta} \qquad \textbf{Equation 4-2}$$

where L is radiance, ρ is reflectance, d is Earth-Sun distance at the specified date, θ is the solar zenith angle, and E is the wavelength dependent exoatmospheric constant (mean solar irradiance). By normalizing the data by the mean solar irradiance, between scene variability is reduced.

4.2.2.1 Relative Correction using the Dark Object Subtraction Method

The debate to atmospherically correct remotely sensed data is still active in the literature (Song et al., 2001; Coppin et al., 2004; Chen et al., 2005), particularly when a thematic classification of single date imagery is the desired output. By applying an atmospheric correction, assumptions regarding the state of the atmosphere and the

amount of scattering are made (Richards and Jia, 2006). These assumptions may be incorrect or incomplete and the application of a correction to the data may introduce more error than is necessary (Song et al., 2001). When working with continuous (versus thematic), multi-temporal imagery, atmospheric correction is a necessary processing step to make the data as consistent as possible in spectral response through the time-series (Song et al., 2001; Schroeder et al., 2006). There are two types of atmospheric correction: absolute and relative. Absolute correction assumes atmospheric properties such as the aerosols concentration and optical depth are known and can be successfully removed using radiative transfer models. Unfortunately, the conditions and parameters of the atmosphere at the time of image acquisition are seldom known (Kaufman, 1989, Du et al., 2002). Thus, most atmospheric correction involves relative correction models, such as the ridge or pseudoinvariant method (Hall et al., 1991; Chen et al., 2005) or PCA normalization method (Du et al., 2002), which normalize differences between multiple scenes and a base image using a linear transformation to fit the scenes relative to the base image.

Dark object subtraction (DOS) (Chavez, 1988), one of the oldest relative correction methods, uses observed DN(s) of a dark-object (typically a deep, still body of water or cloud shadow) to estimate the amount of scattering in the atmosphere. Once the atmospheric scattering model has been estimated, the user can predict and adjust for the amount of haze present in each wavelength. The DOS method defines a starting haze value (SHV) as the minimum value in either TM band 1 or TM band 2. The SHV is used to predict one of five relative scattering models: very clear, clear, moderate, hazy, and

very hazy. The very clear atmospheric models assume that the scattering is Rayleigh and is inversely proportional to λ^{-4} (where λ = wavelength). In contrast, a moderate atmosphere is presumed to be dominated by Mie scattering which is inversely proportional to λ^{-1}. The relative scattering models are listed in Table 4.2 and utilized multiplication factors are listed in Table 4.3.

Table 4.2. Relative Scattering Models for predicted atmospheric conditions as implemented by Chavez (1988).

Atmospheric Conditions	Relative Scattering Model
Very clear	λ^{-4}
Clear	λ^{-2}
Moderate	λ^{-1}
Hazy	$\lambda^{-0.7}$
Very Hazy	$\lambda^{-0.5}$

Table 4.3. Multiplication factors used to predict haze values in other bands given a starting haze value determined in Band 1.

Band	Very Clear	Clear	Moderate	Hazy	Very Hazy
1	1.0	1.0	1.0	1.0	1.0
2	0.563	0.750	0.866	0.905	0.930
3	0.292	0.540	0.735	0.807	0.857
4	0.117	0.342	0.584	0.687	0.765
5	0.075	0.086	0.294	0.424	0.542
7	0.002	0.048	0.219	0.345	0.468

Using the method outlined by Chavez (1988), the relative haze corrections must be normalized for each Landsat band and he provides corrections for TM data collected on Landsat 4. The haze correction for each TM band is estimated using the following equation.

$$DN_{HAZE} = SHV_{Band1} \times SCAT_{norm} \times RAD_{norm} + OFFSET \qquad \textbf{Equation 4-3}$$

The data used in this research come from Landsat 5 TM and Landsat 7 ETM+: the normalization parameters derived for this project are listed in Table 4.4. In this research, the data were corrected to both TOA reflectance and apparent surface reflectance using the DOS method. Data corrected to apparent surface were ultimately used in this research as the trajectories of pseudoinvariant targets were more consistent through the time-series.

Table 4.4. Normalization and Scattering Parameters for Landsat 5 TM and Landsat 7 ETM+ relative to Band 1.

	Radiometric Normalization		**Offset**	
Band	Landsat 5 TM	Landsat 7 ETM+	Landsat 5 TM	Landsat 7 ETM+
1	1.0	1.0	-1.52	-6.2
2	0.516	0.974	-2.84	-6.4
3	0.747	1.253	-1.17	-5.0
4	0.734	0.802	-1.51	-5.1
5	5.56	6.714	-0.37	-1.0
7	10.59	18.093	-0.15	-0.35

4.3 Vegetation Indices

Spectral indices, especially those targeting vegetation, have been widely utilized in remote sensing applications as a means to detect, map, and monitor terrestrial ecosystems (Leprieur et al., 2000). Spectral indices are popular because they are easy to implement while serving as a surrogate for a biophysical parameter such as vegetation health, leaf area index/fPAR (Privette et al., 2002; Privette et al., 2004; Wang et al., 2005), water stress (Fensholt and Sandholt, 2003; Cheng et al., 2006), or snow/ice cover (Salomonson and Appel, 2004). There are, however, several considerations regarding the interpretation and proper application of spectral indices. Remote sensing data are subject to several parameters that can impact the at-sensor radiance including atmospheric scattering,

sun/sensor viewing geometry, topography, and sensor degradation over time (Richards and Jia, 2006). These factors should be accounted for prior to the utilization of spectral indices, especially when conducting multi-temporal analysis. Additionally when working with multi-temporal data, vegetation indices should be derived from radiances rather than DN values to eliminate band dependent sensor calibration/degradation issues over time (Price, 1987; Teillet et al., 1997).

A weakness or criticism of utilizing vegetation indices is that they are both scene and data dependent (Myeni et al., 1995). For example, an index value of 0.4 in one region of the world does not have the same implication or meaning in another region. Further, pixel values having an index value of 0.4 within the same scene also does not imply anything except a similar index value. Vegetation indices have been shown to depend upon the spatial and spectral characteristics of the sensor that collected them (Teillet et al., 1997). In addition to the variability of the width and center wavelengths of spectral bands for different sensor systems, the spectral response function of each band can also vary between sensor systems. Therefore, unless corrections are applied to the data that account for radiometric calibration and conversion to surface reflectance, vegetation indices from different sensor systems are not directly comparable (Teillet et al., 1997). The differences of top-of-atmosphere Normalized Difference Vegetation Index (NDVI) values from Landsat TM and ETM+ were found range from 1 – 4%, and while small, these inconsistencies could be problematic for longer time-series of data (Steven et al., 2003).

The red (~650 nm) and near infrared (~800 nm) portions of the electromagnetic spectrum are reported to be a strong indicators of the amount of photosynthetically active radiation (PAR) in the vegetation, since actively photosynthesizing vegetation absorbs red energy and reflects near infrared energy (Choudhury, 1987; Goward and Huemmrich, 1992; Yang and Prince, 1997). While other vegetation indices have been developed to exploit other regions of the EM spectrum (such as the short wave infrared –SWIR ~1600 nm), the vast majority of indices utilize these two portions of the spectrum. The Normalized Difference Vegetation Index (NDVI) is one of the most widely applied spectral indices and it is defined as

$$NDVI = \frac{\rho(\lambda_{NIR}) - \rho(\lambda_{RED})}{\rho(\lambda_{NIR}) + \rho(\lambda_{RED})} \qquad \textbf{Equation 4-4}$$

A limitation of NDVI is its sensitivity to atmospheric scattering and absorption as well as differences in soil. A common mitigation method is to include the blue band of the EM spectrum to correct for atmospheric aerosols (Miura et al., 2001). The use of NDVI and other vegetation indices has been implemented in many studies of semi-arid and arid regions of the world; however, they have been shown to be sensitive to soil background (including soil moisture) and not as sensitive to a weaker vegetation signal (Yang and Prince, 1997; Leprieur et al., 2000). In arid or semi-arid environments, vegetation indices that are adjusted for the soil are more strongly correlated to ground-derived properties such as leaf area index and above ground biomass (Broge et al., 2000). Fuller et al. (1997) found that NDVI poorly modeled *Mopane* canopy radiative scatter in Zimbabwe and that the soil background dominated the signal. In addition, Fuller et al.

(1997) found that the tree canopy was more accurately modeled during the dry season when the herbaceous layer was dormant.

Nicholson and Farrar (1994) evaluated the relationship between AVHRR NDVI and rainfall for vegetation and soil types in Botswana. They found that the relationship between NDVI and precipitation was largely linear. However, the results indicate differences in NDVI-rainfall relationships were not supported for different soil types, indicating the influence of soil background and soil moisture on the index value. Bradley and Mustard (2005) used NDVI to examine inter-annual variability of vegetation spectral response in semi-arid regions in the Great Plains of the United States and showed the seasonality of vegetation in these areas could be misinterpreted as land cover change. Ringrose (2003) used a normalized difference infrared index (NDII) (Gao, 1996) which emphasizes the near- and mid-infrared portions of the spectrum (NIR-MIR)/(NIR+MIR) and a ratio of NIR/MIR to assess riparian tree coverage in the Okavango Delta. Both indices are considered to be correlated to water content in vegetation and soil; however Ringrose found inconsistent trends relating the water content indices to vegetative cover in the Okavango Delta. A suggested reason why these water content indices may not correlate well with observed vegetation spectral response was that they do not account for the bright soil background common in this particular region.

The Enhanced Vegetation Index (EVI) (Huete et al., 1997) was selected for use in this study as it was developed to minimize both soil background and the atmospheric scattering signal. EVI, originally defined as Soil Atmospherically Resistant Vegetation

Index (SARVI2) and an extension of the Soil Adjusted Vegetation Index (SAVI), is defined as

$$EVI = G\frac{\rho(\lambda_{NIR}) - \rho(\lambda_{RED})}{\rho(\lambda_{NIR}) + C_1\rho(\lambda_{RED}) - C_2\rho(\lambda_{BLUE}) + L}$$ **Equation 4-5**

where *G* is a gain factor, *C1* and *C2* are aerosol coefficients developed to minimize the aerosol scattering effect, and *L* is a canopy adjustment factor (Huete et al., 2002). The canopy adjustment factor adjusts for differential extinction of the red and near infrared reflectance in vegetation canopy (Huete et al., 1997). The empirically derived coefficients utilized in the EVI algorithm are *G* = 2.5, *C1* = 6, *C2* = 7.5, and *L*=1 (Huete et al., 2002; Fang et al., 2005). The *C1* and *C2* aerosol coefficients used in this study were defined for TM/ETM+ apparent TOA reflectance (Huete et al., 1997). The *C1* and *C2* coefficients depend on the level of atmospheric processing applied to the data. The use of atmospherically resistant vegetation indices, such as EVI, has been shown to reduce the variations in NDVI that are attributed to atmospheric aerosols by 60% (Miura et al., 2001). Additionally, EVI has been reported to be more sensitive to weak vegetation signals in semi-arid savannas by minimizing the soil background (Huete et al., 1997) and more sensitive to canopy structure variations (Gao et al., 2000). Changes in EVI values have been found to be inversely related to woody cover and directly related with grass coverage (Fang et al., 2005). EVI was utilized in this research as it is a widely accepted indicator of vegetation productivity/vigor and minimizes some of the weaknesses encountered with NDVI (Xiao et al., 2003).

4.4 Change Detection of Vegetation

Previous chapters provided a framework for conceptualizing vegetation change across a landscape in response to disturbance as it pertains to ecosystem change and resilience. The focus for the remainder of this chapter is to examine the methods for land cover change detection using remotely sensed data. Changes on the landscape are a result of both natural and anthropogenic forces and are differentially observable at various scales. Land cover and land use respond dynamically to the complexities inherent in human-environment systems (Lambin et al., 2003). Change can be abrupt (such as fire or hurricane impacts) or subtle (such as woody encroachment) (Coppin et al., 2004). Land cover conversion is generally considered as resulting from change of one vegetation class to another (e.g. forest to agriculture) whereas land cover modification is a within class change (e.g. selective logging in forest).

4.4.1 Simple Change Detection (Two Scenes)

The most common approach to change detection is the "from-to" change analysis where relative changes between two scenes are extracted on a per-pixel basis (Schowengerdt, 1997; Richards and Jia, 2006). To detect change and to minimize the amount of change due to seasonality, near-anniversary dates are used when possible. Here, images are collected at approximately the same time of year to minimize the differences of phenology of the vegetation and illumination differences of sun angle position. Differences in the scenes due to non-change (such as cloud cover) must be masked out prior to analysis so that they do not bias the results.

How the land cover change is actually extracted varies depending upon which algorithm/method is used (Singh, 1989; Coppin and Bauer, 1996). Image differencing is a common approach and is relatively simple to implement (Ridd and Liu, 1998; Lunetta et al., 2004). Respective bands from two dates are differenced to examine the amount of change. Since the different bands in a multispectral image contain different information, a vegetation index or a linear combination of the bands is often used. Differences based on the red band or NDVI between two dates have been implemented in several studies (Lyon et al., 1998; Hayes and Sader, 2001; Coppin et al., 2004) with varying degrees of success. A limitation of image differencing is that it only provides an indication of change but does not provide information regarding the type of the detected change.

An alternative to image differencing is post-classification change, sometimes referred to as either thematic change detection or delta (Δ) change (Mas, 1999; Coppin et al., 2004). In this technique, each image is classified and the thematic outputs are compared to determine the change. While image differencing is often used to provide a binary representation of change, the utilization of post-classification change analysis does provide insight into the types of land cover conversion occurring on the landscape. A benefit of using this method is that radiometric differences between the two dates are less problematic since each date is classified separately (Song et al., 2001). However, the quality of the change detection depends upon the accuracy of the initial classification products. The traditional means of assessing error in land cover change estimates is by multiplying error matrices. Thus, any error from the land cover classification translates

into an error in estimating the amount and type of land cover change (Crews-Meyer, 2006).

Finally, a third method to detect change on the landscape is to use a composite dataset, whereby all the bands from both dates are concatenated into one image to highlight change (Mas, 1999). Using this method, however, puts equal weight on the spectral and temporal features from each scene thereby increasing the difficulty of class separability (Schowengerdt, 1997). Often, instead of using all the bands, linear combinations of the bands such as those generated by using a tasseled cap transformation, principal component analysis (PCA) or minimum noise fraction (MNF) transformation are used, as they contain information of variance within the scenes and are represented as orthogonal components. The motivation behind utilizing a linear transformation for change detection is to represent the variance between dates in a reduced number of orthogonal bands (Lasapanora, 2006). PCA is also frequently used for multi-temporal studies; a more detailed description will be given later in this chapter.

4.4.2 Multi-temporal change detection

The classic change detection techniques of "from-to" that are based on a comparison of two dates (or a pairwise comparison of multiple dates) are limited in the types of change that can be detected. A limitation of these types of change detection is it becomes increasingly more difficult to relate landscape change to a process when the time between scenes becomes too long (Lunetta et al., 2004; Crews-Meyer, 2006). As mentioned previously, changes in land cover can be a result of long-term natural change,

climatic variability, anthropogenic alteration of the landscape, or natural vegetation dynamics (Lambin et al., 2003). Many multi-temporal studies are now based on time-series analysis of remotely sensed data to infer change and ecological process. Most time-series work has involved broad scale sensor systems such as the Advanced Very High Resolution Radiometer (AVHRR) or the Moderate resolution Imaging Spectroradiometer (MODIS) since they acquire data at least once a day over all areas of the world and have been operational for extended periods. While these sensor systems provide a high temporal resolution, the spatial resolution is coarse at 1 km for both systems (although MODIS operates at higher spatial resolution for certain wavelengths). Thus, some of the finer details of land cover change are often overly aggregated due to the spatial resolution of the data.

4.4.2.1 Vegetation Phenology in Multi-temporal Data

Lambin and Ehrlich (1997) used a change vector analysis to map subtle change for broad land cover classes in Africa. The basic purpose of change vector analysis is to compute a monthly average of a land cover indicator for the entire time-series, and then identify monthly change for a given year. A change may be represented as

$$c(i) = p(i, ref) - p(i, y) \qquad \textbf{Equation 4-6}$$

where *c(i)* is the change vector between a pixel in the reference year and the y^{th} year (Lambin and Ehrlich, 1997). Once a change vector is computed, the principle components of the directional change vector can be computed to determine the most

significant change processes. In the above described project, the authors used a ratio of surface temperature and NDVI as their land cover indicator. As mentioned previously, the use of NDVI may not be well suited to certain regions, particularly those with a significant soil background such as semi-arid environments. However, other indices of change such as EVI or a disturbance index can be substituted. Mildrexler et al. (2007) utilized a MODIS based disturbance index (defined as the ratio of land surface temperature to EVI) to identify continental scale disturbance. A disturbance is identified as a departure of the disturbance index from a multi-year mean. The primary limitation to the methods described by Lambin and Ehrlich (1997) and Mildrexler et al. (2007) is that they are subject to the temporal extent of the time-series by making the assumption that all the changes encountered are represented within the time-series. This method also assumes that an appropriate reference state (i.e., the mean) can be determined and that it represents the norm. Additionally, while these methods identify the patterns of temporal change, they do not attempt to quantify the processes contributing to the observed temporal patterns.

4.4.2.2 Change Curve Fitting

Rodrigues-Arias and Rodo (2004) described ecological processes as having trends, cycles, and structured residuals, which is typical for time-series decomposition. The detection of trends and characterization of phenological cycles has been a recurrent theme in many multi-temporal analysis studies (Andres et al., 1994; Rogan et al., 2002; Lunetta et al., 2006). Curve fitting using linear functions was used by Lawrence and

Ripple (1999) to estimate the change in vegetation cover and rate of recovery following the eruption of Mt. St. Helens. Eight TM scenes were used in the analysis, and the linearly transformed data were clustered using an ISODATA algorithm. First and second order polynomials were fit to clustered mean values and were found to identify and represent three types of vegetation recovery rates based upon the disturbance recovery from Mt St. Helens. Tottrup and Rasmussen (2004) utilized a time-series of AVHRR NDVI data to investigate temporal trends on the landscape in Senegal. The authors integrated NDVI values over an annual period and computed a linear trend on the annual NDVI summations. There were positive, negative, and neutral tendencies that varied spatially across the landscape. However, the land cover change associated with negative trends occurred in areas that were heavily cultivated (peanuts) and was attributed to possible soil degradation.

Harmonic regression is not typically regarded as a methodology employed by the remote sensing community for detecting land cover change using medium spatial resolution optical imagery (Braswell et al., 1997; Zhang et al., 2003). It is simply a regression technique used to fit data to a described trend and cycle. Rather than fitting the data to a linear polynomial function (Braswell et al., 1997; Lawrence and Ripple, 1999), harmonic regression utilizes a sine wave (or a series of sine waves) function(s) to the data. The motivation for implementing a harmonic regression in this research is to quantitatively describe the vegetation dynamics through time. Vegetation dynamics can be defined as the temporal behavior of vegetation spectral response at various time-scales (e.g. seasonal or annual) (Roerink et al., 2003). By fitting vegetation dynamics with a

harmonic regression, this research will extract the vegetation cycles rather than the identification of a deviation from the temporal norm via change-vector analysis.

4.4.2.3 Spectral Analysis

Spectral analysis of multi-temporal data has traditionally involved the utilization of a Discrete Fourier Transform (DFT) within the frequency domain to assess vegetation dynamics and phenology (Andres et al., 1994; Ricotta and Avena, 2000). A time-series of surrogates for vegetation productivity (e.g. NDVI) is constructed to represent the input vegetation signal. By decomposing the time-series data in the frequency domain, the periodicity and magnitude of dominant signals (such as seasonal and annual patterns) can be extracted. The DFT essentially decomposes the waveform (or input signal) into sinusoids (sine waves) of different frequency components that sum to the original waveform. The DFT is defined as

$$F_r = \sum_{k=0}^{N-1} f_k \exp(-ir\Omega k) \qquad \textbf{Equation 4-7}$$

where $\Omega = 2\pi N^{-1}$ and where N is the period of the fundamental frequency. The DFT approach provides a method for detecting inter- and intra- annual variability across landscapes. Mapping vegetation phenology using AVHRR data, Moody and Johnson (1997) note the separation of rapidly responding grasslands from slowly responding shrublands, woodlands, and irrigated areas in response to precipitation from the extracted frequencies. Similarly, Menenti et al. (1993) utilized Fourier analysis on two years of

NDVI datasets in Zambia to quantify ecological and agricultural zones having similar growth dynamics, and found the results from NDVI were more robust than available maps. Roerink et al. (2003) implemented a Fourier analysis on two years of AVHRR NDVI data over Europe and found that the annual mean NDVI value was correlated with climatic variables and could be used as an indicator of climate variability. They found the semi-annual NDVI was not a suitable indicator of climate variability as it was heavily smoothed in the data analysis. However, they cautioned that the climatic impact on vegetation response is difficult to assess from two years of data. Hay et al. (1998) implemented Fourier analysis on multi-temporal AVHRR data to determine the seasonality of malaria in Kenya. Fourier analysis has also been implemented in climatic and geologic studies such as determining the primary wet and dry phases in the geologic record (Tyson et al., 2002) or precipitation cycles (Tyson et al., 1975; Dyer and Tyson, 1977).

Wavelet analysis has been widely used in many fields including geophysics, ecology studies (Saunders et al., 2004; Mi et al., 2005), hydrology (Labat et al., 2004), and climate studies (Kestin et al. 1998) in order to characterize the temporal and frequency variability in time-series data. Wavelets have been shown to be a powerful tool for detecting both permanent and transitory signals (Rodriguez-Arias and Rodo, 2004). Similar to Fourier analysis, wavelets work by decomposing the input signal into a set of dominant frequencies and then determining when in time the variability fluctuations occur (Kestin et al., 1998; Torrence and Compo, 1998). The continuous form of a wavelet transform is defined as

$$W_n(s) = \sum_{n'=0}^{N-1} x_{n'} \psi^* \left(\frac{(n'-n)\delta t}{s} \right)$$ **Equation 4-8**

where s is the wavelet scale and n represents a localized time index (Torrence and Compo, 1998). Rather than using a sine or cosine function to decompose the signal, wavelets use a template applied over a finite portion of the time-series (Fortin and Dale, 2005). A guide to understanding wavelets is provided by Torrence and Compo (1998) and the full derivations will not be listed here. However, a brief description of wavelets is that a signal, x_n, can be convolved with a set of wavelets, Ψ, which are derived from a mother wavelet. In discrete form, the wavelet transform is defined as

$$W(b, x_n) = \frac{1}{\sqrt{b}} \sum_{j=1}^{n} f(x_j) g \left(\frac{x_j - x_n}{b} \right)$$ **Equation 4-9**

where g represents the mother wavelet function and b represents the tested wavelet scale centered at x_n and at position x_j along the time-series. There are many types of mother wavelets, each with different properties (shape, width, orthogonal versus non-orthogonal, and complex or real). It is advised that the mother wavelet shape should resemble the type of features or patterns in the input signal (Torrence and Compo, 1998). Since climatic patterns are cyclical, a Morlet wavelet is often used in climate studies and will be used in this research since vegetation phenology also follows a cyclical pattern. The Morlet wavelet is the result of a sine wave multiplied by a Gaussian function and is illustrated in Figure 4.1.

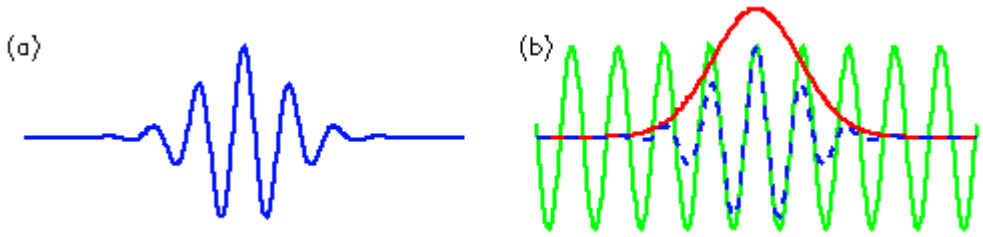

Figure 4.1a) Morlet wavelet and b) the derivation of a Morlet wavelet as a sine wave (green), Gaussian function (red). (Figure provided by Torrence and Compo (1997); http://atoc.colorado.edu/research/wavelets/wavelet2.html).

The Morlet wavelet function is defined mathematically as

$$g(x) = \pi^{-1/4} e^{i\omega x} e^{-x^2/2} \qquad \textbf{Equation 4-10}$$

where ω is the frequency. The width of the wavelet is a compromise in resolution. A fine width (in time) increases the temporal resolution; however, it reduces the number of points being utilized in the frequency analysis. A convenient way to visualize the detected patterns in the time-series at the tested frequencies is the wavelet power spectrum. The wavelet power spectrum (WPS) is defined as

$$WPS = \left\langle W(b, x_i)^2 \right\rangle \qquad \textbf{Equation 4-11}$$

The global wavelet spectrum (GWS) is defined as the time-averaged wavelet spectrum over all wavelet scales. The GWS indicates the dominant scales that are evident in the data and can be written as

$$\overline{W}^2(s) = \frac{1}{N} \sum_{n=0}^{N-1} \left| W_n(s)^2 \right| \qquad \textbf{Equation 4-12}$$

Wavelet analysis for this research was conducted using Matlab programs modified from Torrence and Compo (1998). Software is available for free download at http://atoc.colorado.edu/research/wavelets. A limitation of wavelets is the edge effect at the end of the data series. To minimize the edge effect, the input time-series of length N is zero padded to the next higher power of 2 prior to computing the Fourier transform. The zeros are then removed once the wavelet transform has been completed. However, since the data are of finite length, only frequencies within the limits of the data can be determined. To visualize which frequencies are significant and not due to random noise in the data, Torrence and Compo (1998) include a cone of influence (COI) into their software's output. Thus, signals falling outside the cone are considered not valid as they may be influenced by the edge effects of the zero padding. Wavelet analysis will be a fundamental component of this research to detect dominant periodicities in the time-series data.

4.5 Methodology Used in this Research

This chapter outlines the major issues associated with the utilization of multi-temporal remote sensing imagery for the detection of change and dynamics on the landscape. The Landsat dataset available for this research facilitated the investigation of vegetation dynamics apparent at the landscape level in response to disturbance. In particular, this research employed analytical techniques commonly used with coarse resolution imagery (due to the high temporal frequency of image acquisition) with medium resolution imagery. A general overview of the Landsat dataset utilized in this

research will be described in Chapter 5; however the remainder of this chapter is dedicated to a description of the data-processing and analysis techniques utilized.

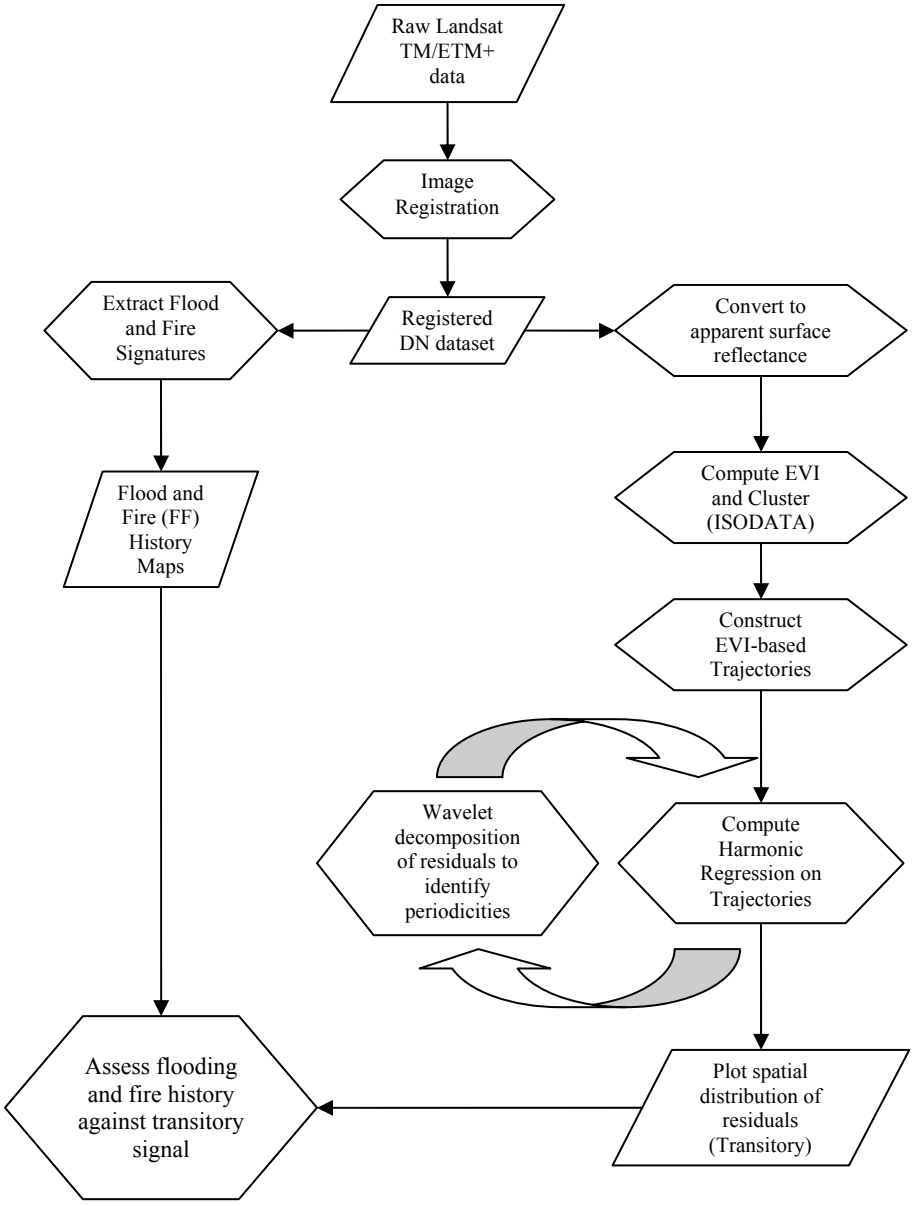

Figure 4.2. Flowchart of processing and analytical steps utilized in this research.

A flow chart of the processing and methodologies is shown in Figure 4.2. Through a collaborative arrangement with Technischen Universität München (TUM), the Landsat dataset was co-registered and the flooding and fire extents were extracted as part of a previous project (Heinl et al., 2006). For the current study, the flooding and fire maps were compiled into composite flooding and fire maps and simple statistics computed, described in greater detail in Chapter 6. Once this analysis was completed, the dataset was radiometrically corrected using the specified gains and offsets and atmospherically corrected using the dark object subtraction method. With the data radiometrically and atmospherically corrected, the vegetation dynamics were studied. The goal is to apply multi-temporal analysis techniques such as harmonic regression and wavelet decomposition to describe the vegetation dynamics. By developing a harmonic based regression model, the dynamics of the landscape can be characterized without making assumptions of change based upon the long-term mean which is dependent on the time-series extent. Knowledge of the vegetation dynamics yields a greater understanding of the pressures contributing to the observed vegetative patterns on the landscape.

5 LANDUSE/LANDCOVER DATA

5.1 Remotely Sensed Data

An extensive set of remotely sensed data acquired for the Okavango Delta are available for this research through the University of Texas Center for Space Research (CSR), collaboration with the University of Botswana Harry Oppenheimer Okavango Research Center (HOORC -located in Maun, Botswana and proximate to the study area), and other international partners. Many of these scenes were made available through the NASA Safari2000 project and by the NASA EO-1 scientific validation team (EO-1 SVT). These data include scenes from Landsat 5 TM (70 scenes), Landsat ETM+ (17 scenes), EO-1 Advanced Land Imager, ALI (26 scenes), EO-1 Hyperion (16 scenes), IKONOS (3 scenes), and MODIS (over 100 scenes). This archive represents a dataset that is temporally rich in both intra-annual and inter-annual information. The Landsat and EO-1 archive represents a sequence of data beginning from April 1989 to 2002 with an average time step of one scene every two months. ALI and Hyperion data acquisitions were positioned over the study area as part of the NASA EO-1 Science Calibration/Validation mission. The majority of the research in this dissertation is conducted using the Landsat TM and ETM+ time-series. When appropriate, other datasets such as ALI and IKONOS served as independent sources of information to complement results.

Table 5.1. Landsat TM and ETM+ Dataset. Atmospheric conditions (VC=very clear, C=clear, MOD=moderate) See Chapter 4 for details.

Date	Sun Elev.	DOY	Sensor	ATM	Date	Sun Elev.	DOY	Sensor	ATM
29-Apr-89	43.8	119	TM5	VC	16-Apr-96	46.3	107	TM5	VC
16-Jun-89	36.4	167	TM5	VC	19-Jun-96	36.2	171	TM5	VC
18-Jul-89	37.4	199	TM5	VC	5-Jul-96	36.3	187	TM5	VC
4-Sep-89	48.5	247	TM5	C	22-Aug-96	45	235	TM5	VC
27-Feb-90	54.2	58	TM5	C	23-Sep-96	54.7	267	TM5	C
16-Apr-90	46.5	106	TM5	VC	12-Dec-96	61.7	347	TM5	C
3-Jun-90	37.6	154	TM5	VC	21-May-97	39.6	141	TM5	VC
21-Jul-90	37.7	202	TM5	VC	24-Jul-97	38.2	205	TM5	VC
22-Aug-90	44.7	234	TM5	VC	9-Aug-97	41.3	221	TM5	VC
23-Sep-90	54.4	266	TM5	VC	26-Sep-97	55.3	269	TM5	C
12-Dec-90	61.8	346	TM5	C	15-Dec-97	61.5	349	TM5	C
2-Mar-91	53.9	61	TM5	C	5-Mar-98	53.5	64	TM5	C
3-Apr-91	49.1	93	TM5	VC	25-Jun-98	36.1	176	TM5	VC
22-Jun-91	36.2	173	TM5	VC	27-Jul-98	38.7	208	TM5	VC
24-Jul-91	38.2	205	TM5	VC	13-Sep-98	51.3	256	TM5	C
29-Nov-91	63	333	TM5	MOD	19-Jan-99	57.7	19	TM5	C
21-Apr-92	45.3	112	TM5	VC	9-Apr-99	47.9	99	TM5	VC
8-Jun-92	37	160	TM5	VC	11-May-99	41.4	131	TM5	VC
11-Aug-92	42	224	TM5	VC	12-Jun-99	36.7	163	TM5	VC
12-Sep-92	51.3	256	TM5	C	10-Oct-99	59.1	283	ETM+	C
14-Oct-92	60.4	288	TM5	C	30-Jan-00	56.8	30	ETM+	C
15-Nov-92	63.6	320	TM5	C	3-Apr-00	48.9	94	ETM+	C
18-Jan-93	57.8	18	TM5	C	29-May-00	38.2	150	TM5	VC
7-Mar-93	53.3	66	TM5	VC	14-Jun-00	36.5	166	TM5	VC
11-Jun-93	36.8	162	TM5	VC	9-Aug-00	41.5	222	ETM+	VC
29-Jul-93	39	210	TM5	VC	25-Aug-00	45.8	238	ETM+	C
30-Aug-93	47	242	TM5	VC	10-Sep-00	50.7	254	ETM+	MOD
20-Dec-93	60.9	354	TM5	C	5-Nov-00	63.3	310	TM5	C
26-Mar-94	50.5	85	TM5	C	8-Jan-01	58.8	8	TM5	C
13-May-94	41	133	TM5	VC	16-May-01	40.4	136	TM5	VC
1-Aug-94	39.6	213	TM5	VC	17-Jun-01	36.4	168	TM5	VC
2-Sep-94	47.9	245	TM5	VC	19-Jul-01	37.5	200	TM5	VC
4-Oct-94	57.7	277	TM5	C	12-Aug-01	42	224	ETM+	VC
5-Nov-94	63.3	309	TM5	C	13-Sep-01	51.3	256	ETM+	C
7-Dec-94	62.3	341	TM5	C	15-Oct-01	60.4	288	ETM+	MOD
24-Jan-95	57.3	24	TM5	C	3-Jan-02	59.4	3	ETM+	C
14-Apr-95	46.9	104	TM5	VC	24-Mar-02	50.8	83	ETM+	C
1-Jun-95	37.9	152	TM5	VC	9-Apr-02	47.9	99	ETM+	C
19-Jul-95	37.5	200	TM5	VC	11-May-02	41.4	131	ETM+	VC
20-Aug-95	44.1	232	TM5	VC	14-Jul-02	36.6	165	ETM+	VC
21-Sep-95	53.8	264	TM5	C	31-Aug-02	47.3	243	ETM+	C
23-Oct-95	61.8	296	TM5	C	2-Oct-02	57	275	ETM+	C
26-Dec-95	60.3	360	TM5	C					

The dates and image atmospheric conditions for the Landsat TM and ETM+ dataset used in this research are listed in Table 5.1. Each Landsat TM and ETM+ image was rectified to a UTM 34S WGS-84 projection using cubic convolution resampling. While cubic convolution does change the original DN values, it was deemed necessary to minimize the amount of geolocational error typically encountered with a nearest neighbor resampling due to the large number of images in the database. The estimated atmospheric conditions as computed from the DOS method (Chavez, 1988 -described in Chapter 4) are listed as very clear, clear, moderate, hazy, and very hazy.

5.2 Climatic Data

The spatial distribution of meteorological stations in Botswana is unfortunately rather sparse. While several climatic stations exist in the vicinity, a time-series of measurements from all stations is not complete. The meteorological station at the Maun and Shakawe airports were used to provide climatic estimates for the Okavango Delta. Monthly precipitation records for Maun airport dating from 1922 to 2003 and monthly temperature records from 1965 to 2003 were collected and a subset from 1989 to 2002 was extracted for comparison to the Landsat time-series. Figure 5.1 indicates an average annual temperature increase at the Maun airport since 1965 of approximately 0.4ºC/decade. The long-term (1922 to 2003) annual precipitation recorded at Maun is 450.05 mm. The precipitation recorded at the Maun airport is not necessarily an indicator of the size of the impending flood (as that water originates upstream in Angola) and does

not indicate how much precipitation fell across the region; but it does provide a limited sense of the climatic conditions in the lower Delta.

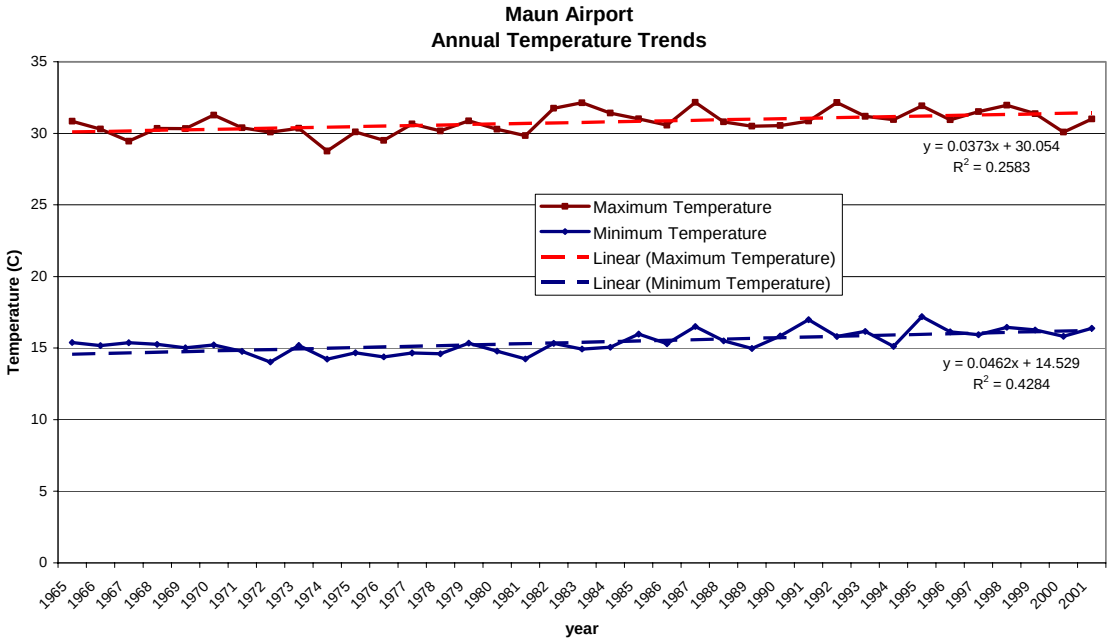

Figure 5.1. Temperature Trends recorded at Maun Airport of Annual Maximum and Annual Minimum. Both trends show an average increase of ~0.4° C / 10 years since 1965.

During 1989 to 2002, the wettest month on record at the Maun airport was February 1996 with 281 mm followed by January 1994 with 275 mm, January 2000 with 255 mm, and January 1989 with 215 mm. As shown in Table 5.2, many of the wettest months are not represented in the Landsat image sequence due to persistent cloud cover during the wet season. This timing is thought to be significant in that many of the perennial grasses should have a green-up following a rain event, and that initial response is likely to be missed since (cloud-free) remotely sensed data are typically not available.

An exception to this limitation of optical data occurred in January 2000 as a clear scene was acquired on January 30, 2000 during one of the wettest months within the time-series. The annual precipitation totals were computed for precipitation years rather than calendar years since a distinct rainy/dry season exists. As evidenced by the monthly totals, the months of May to September are typically extremely dry in the lower Delta.

Table 5.2. Monthly precipitation (mm) totals at Maun Airport from 1989 to 2002. Highlighted boxes indicate a co-incident Landsat scene.

Year	OCT	NOV	DEC	JAN	FEB	MAR	APR	MAY	JUN	JUL	AUG	SEP	TOTAL
88/89	12.9	14.5	46.0	215.5	180.0	44.3	96.3	0.0	0.0	0.0	0.0	7.6	617.1
89/90	17.4	5.5	41.5	87.1	110.0	33.3	17.3	0.0	0.0	0.0	0.0	0.0	312.1
90/91	28.5	13.3	78.4	177.6	134.0	123.0	0.0	0.0	0.0	0.0	0.0	5.8	560.6
91/92	6.7	40.7	55.1	50.1	7.4	87.9	5.0	0.0	0.0	0.0	0.0	1.4	254.3
92/93	14.3	23.9	155.0	66.5	122.0	15.4	47.4	0.0	0.0	0.7	0.0	8.2	453.4
93/94	0.0	44.0	15.2	275.0	50.0	6.2	0.0	0.0	0.0	0.0	0.0	0.0	390.4
94/95	16.6	54.1	10.4	27.0	14.4	0.0	2.0	0.0	0.0	0.0	22.0	11.0	146.5
95/96	3.5	105.0	46.1	189.3	281.0	9.0	0.4	2.9	0.0	0.0	0.0	0.5	637.2
96/97	26.6	24.8	67.8	153.8	19.2	64.8	1.8	5.1	0.0	0.0	0.0	13.0	363.9
97/98	1.7	50.5	109.0	150.2	18.6	28.4	32.6	0.0	0.0	0.0	0.0	0.0	391.0
98/99	7.9	14.2	63.5	110.0	56.5	41.2	3.8	10.0	0.0	0.0	0.0	0.0	307.1
99/00	5.7	43.7	45.0	255.0	183.5	31.2	21.7	2.3	2.6	0.0	0.0	0.0	590.7
00/01	0.0	126.2	29.3	34.0	103.8	47.7	87.8	3.5	0.0	0.0	0.0	0.0	432.3
01/02	22.3	126.4	41.4	58.6	36.0	15.3	6.0	0.0	0.0	0.0	12.8	0.0	318.8
02/03	31.2	69.1	54.9	30.5	51.1	5.5	30.4						

5.3 HOORC Derived Landuse/Landcover Products

Several GIS layers for the Okavango Delta were made available for this research through HOORC. These include land management, soils, political boundaries, and landcover. The landcover map produced by HOORC was developed based upon local knowledge of the landscape and Landsat ETM+ imagery from 1999. The HOORC landcover classification consists of 46 classes mapped by dominant species and

vegetation structure. For this project, the HOORC landcover product was aggregated into three vegetation types consisting of herbaceous, mixed savanna, and woodland dominated savanna. In addition, a 14-class vegetation structure product was aggregated from the HOORC landcover map (Jellema et al., 2001). The vegetation structure classification is based upon a 4-part descriptor adapted from Grunblatt et al., (1989) used by HOORC and is depicted in Figure 5.2. The relationships between vegetation type and structure classes are listed in Table 5.3.

HEIGHT	STRUCTURE	2º LIFE FORM	1º LIFE FORM
Low	**O**pen	**B**are	**G**rassland
Tall	**C**losed	**G**rassed	**S**hrubland
	Dense	**S**hrubbed	**W**oodland
	Sparse	**T**reed	**B**are

Figure 5.2. 4-part coding for HOORC vegetation structure classes. Under this scheme, a class comprised of tall open woodlands with an understory of shrubs would be labeled TOSW.

Table 5.3. Vegetation Type and Vegetation Structure Classes adopted from HOORC landcover map with structure descriptor given by HOORC

Vegetation Type	*Vegetation Structure Code*	*Structure Descriptor*
Herbaceous	LOBG	Low Open Bare Grasslands
Herbaceous	LOGG	Low Open Grassed Grasslands
Mixed Savanna	LOSG	Low Open Shrubbed Grasslands
Mixed Savanna	LDSG	Low Dense Shrubbed Grasslands
Mixed Savanna	TOTG	Tall Open Treed Grasslands
Herbaceous	TDGG	Tall Dense Grassed Grasslands
Mixed Savanna	LOGS	Low Open Grassed Shrublands
Mixed Savanna	LOTS	Low Open Treed Shrublands
Mixed Savanna	LDBS	Low Dense Bare Shrublands
Woodland Savanna	LOBW	Low Open Bare Woodlands
Woodland Savanna	LOSW	Low Open Shrubbed Woodlands
Woodland Savanna	TOSW	Tall Open Shrubbed Woodlands
Woodland Savanna	TOTW	Tall Open Treed Woodlands
Herbaceous	WATER	Water, Reeds and Sedges

The mapped spatial distribution of the HOORC vegetation type and vegetation structure classes is shown in Figure 5.3 and Figure 5.4 respectively.

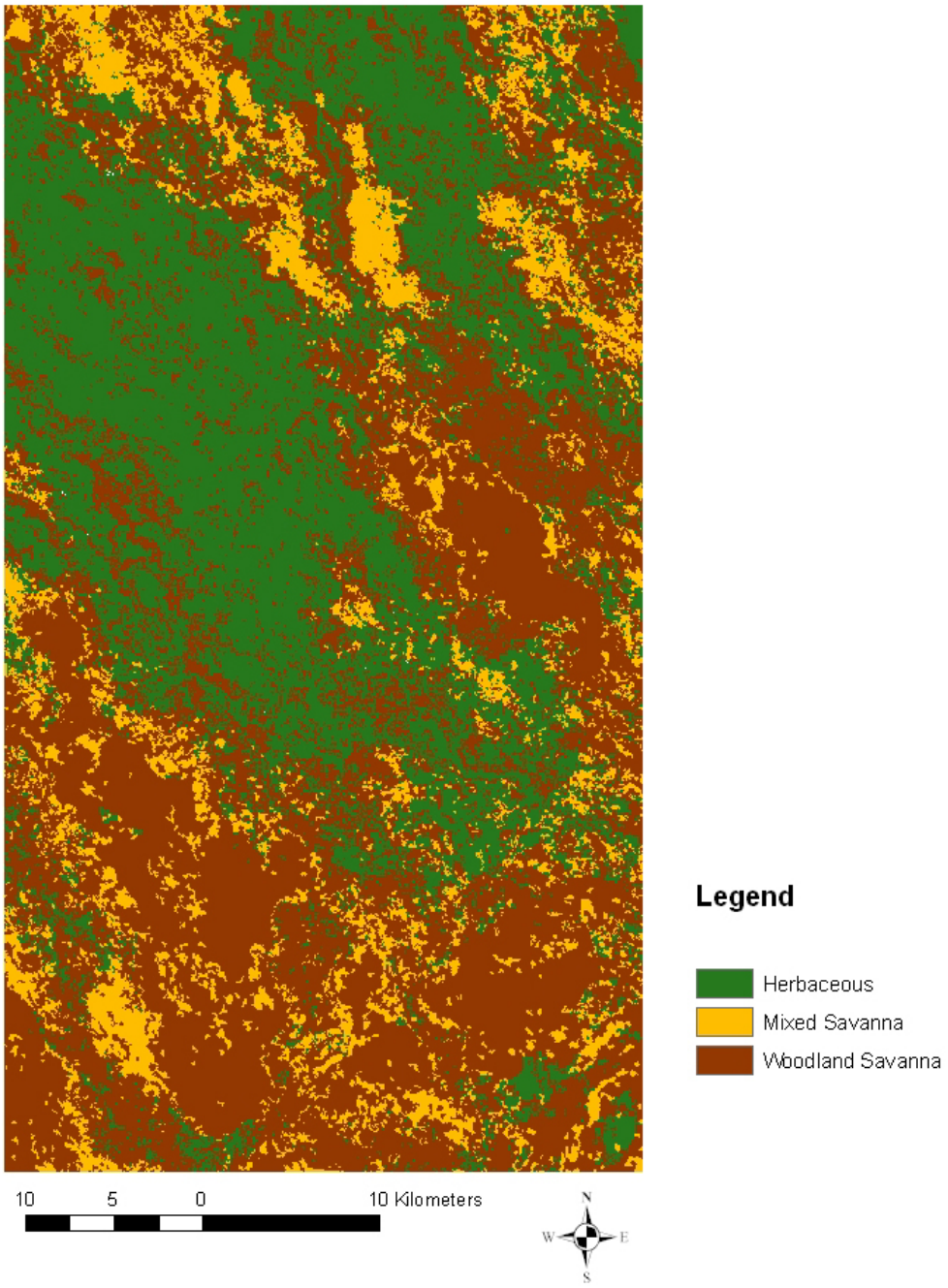

Figure 5.3. HOORC Landcover classification product aggregated to vegetation type.

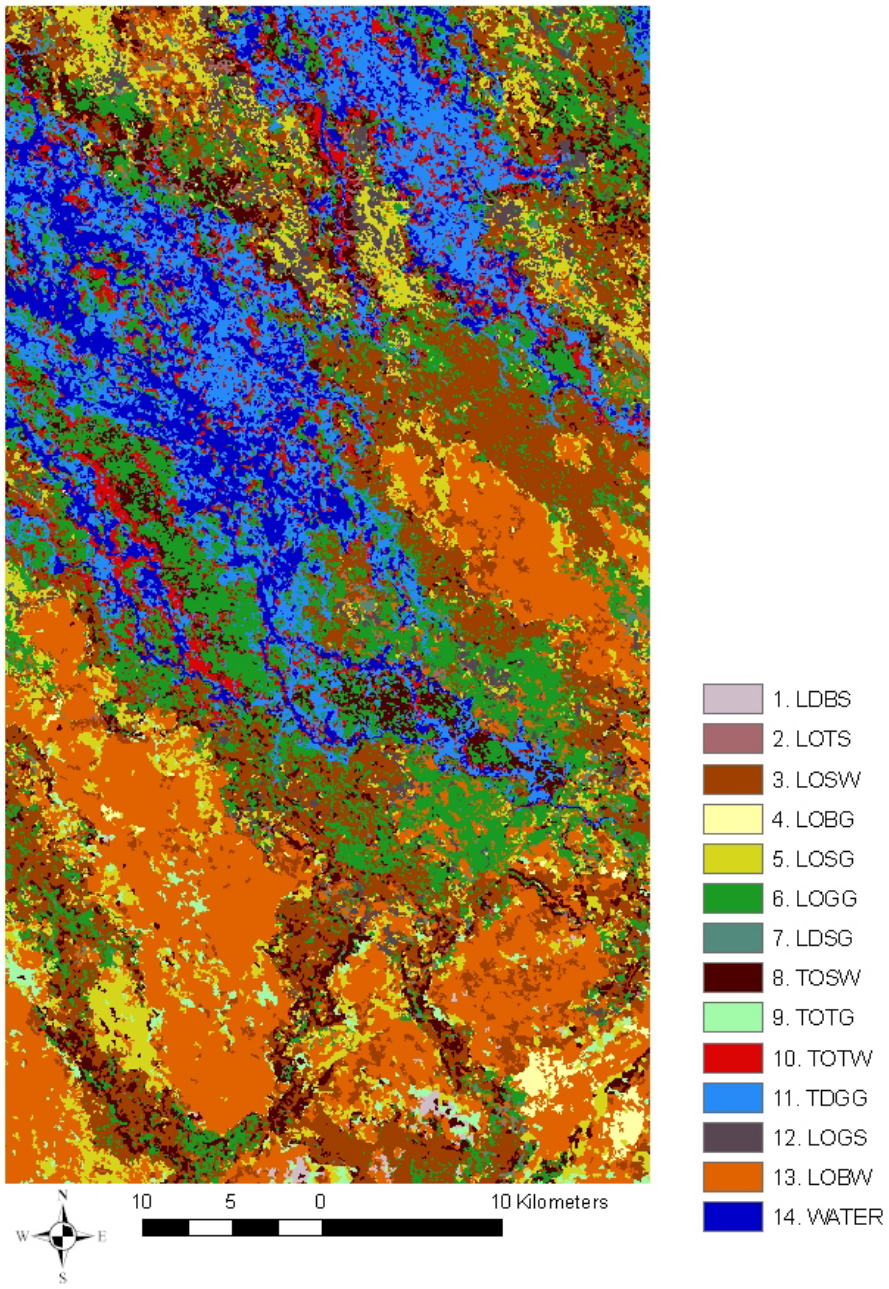

Figure 5.4. HOORC Landcover classification product aggregated to vegetation structure. Abbreviations of vegetation structure classes are given in Table 5.3.

The vegetation type and structure products derived from HOORC were used to stratify the flooding and fire regimes. Since the HOORC vegetation product represents

the land cover conditions in 1999, the channels and water class was regarded as herbaceous for subsequent analysis because water is spatially varying in the time-series.

For purposes of evaluating the potential influence of land management on ecosystem resilience, the area's management zones were also used to stratify data and are depicted in Figure 5.5. As detailed in Chapter 3, the Moremi Game Reserve experiences the highest level of protection, followed by the Wildlife Management Areas (WMAs) that are partitioned into hunting or photography concessions, and finally the communal areas that have few restrictions on access of resources. The Moremi Game Reserve occupies approximately 10.4% (25,396 hectares) of the study area, followed by communal areas accounting for 26.6% (64,789 hectares), hunting concessions with 25.6% (62,150 hectares), and photography concessions occupying 37.1% (90,127 hectares) of the study area. The overall distribution of hunting and wildlife concessions in the Delta are shown in Figure 5.6. The majority of lands in the Okavango Delta are designated as hunting concessions with the photographic concessions limited to the swamps and floodplains.

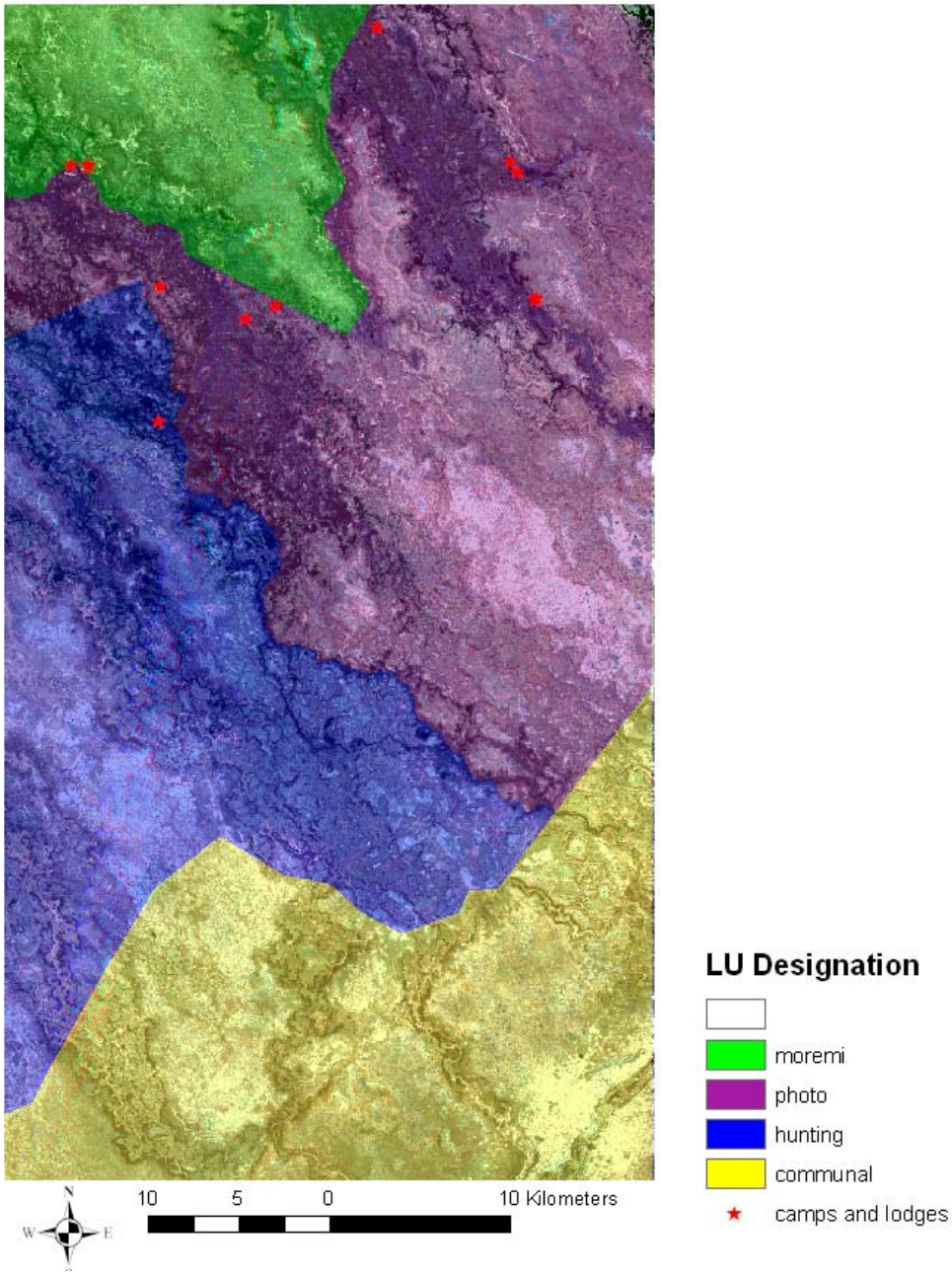

Figure 5.5. Land management designation in study area. Wildlife Management Areas are designated as photography or hunting concessions restricting where hunting can occur.

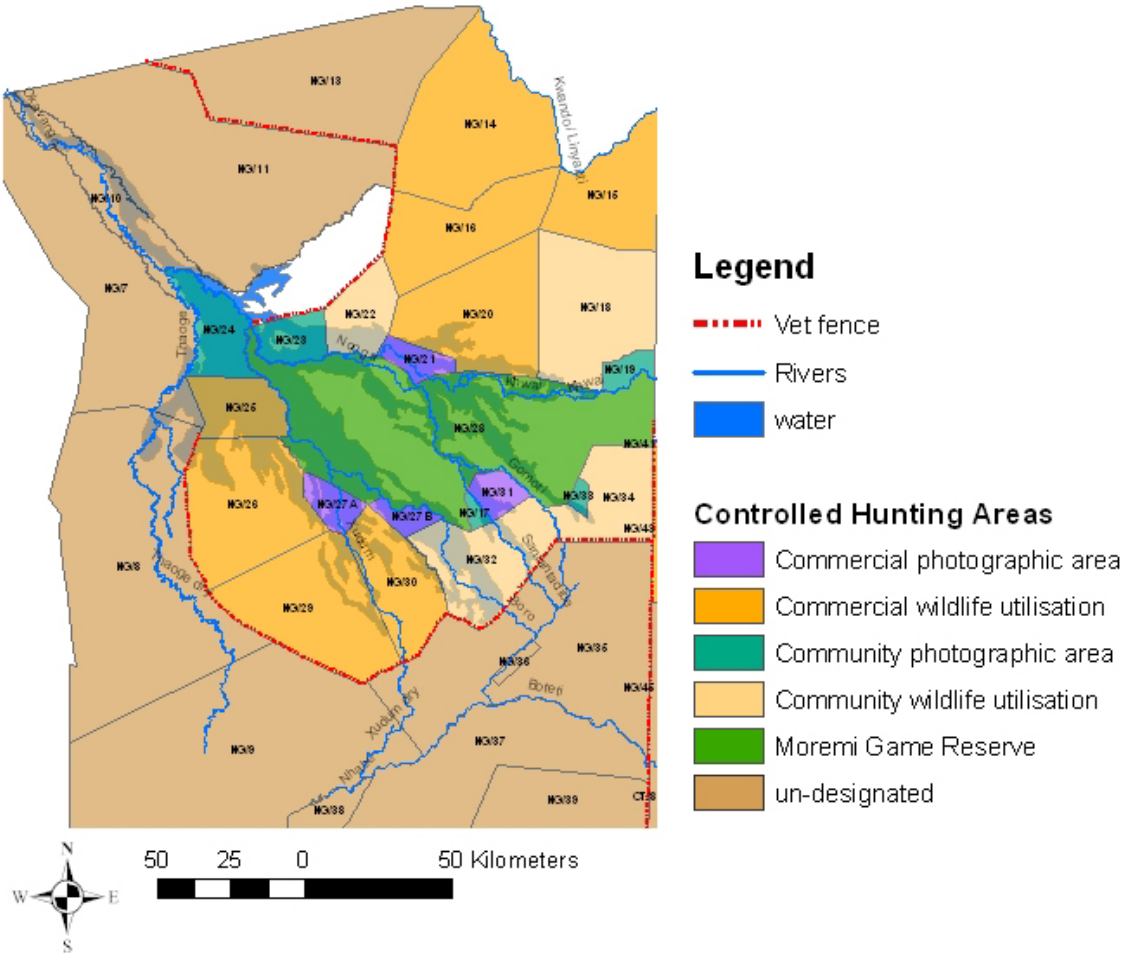

Figure 5.6. Land management designation for Okavango Delta. Wildlife Management Areas are designated as photography or hunting concessions restricting where hunting can occur. Photographic concessions typically occur in the swamps and floodplains, whereas hunting concessions occur in drier environs.

5.4 Field Data Collection

Field data were collected during two two-week campaigns in June 2006 and May 2007, and complemented by observations during a four-week campaign in March 2001. Due to the wide diversity of vegetation cover types, a primary goal of the fieldwork was

to visit as much of the area as possible during the allowed time in order to observe as many cover types as possible. A limitation of conducting a field survey at this time of year (local winter) was that the arrival of the annual flood pulse made many of the roads into the Delta inaccessible. The 2006 wet season was extraordinarily high (over 700 mm of recorded precipitation) such that many of the channels were already full of water, making it difficult to detect the arrival of the flood pulse. In contrast, the 2007 flood arrived early in some portions of the Delta, dissipated, and then returned approximately two weeks after the field study.

The company Solutions for Geographic Information (SGI) was contracted to provide transportation and guiding services during both field campaigns. The local guides, including both residents and Botswana citizens, had excellent knowledge of the landscape and the vegetation of the Okavango environs. Due to danger associated with animal population inside the Buffalo Fence, field surveying was limited to a road survey where the dominant landcover type and general density were recorded and geolocated for locations along a road. Most roads within the Delta are sandy trails that are the width of one car. Some trails are traveled more frequently than others as evidenced by the large ruts in portions of the trails. For the communal areas outside the Buffalo Fence where animal threats are less common, the vegetation sampling added a combined line intercept/plot method designed for recording vegetation structure to road surveys. The road survey method was efficient and fast and provided a way to see and sample more regions within the study area. GPS points were collected as land cover changed and differences were noted. Vegetation was visually assigned to general class types (e.g.

scrub *Mopane* or *Acacia* savanna) while recording each GPS location. While conducting the road survey, when possible a GPS position was marked at the center of a patch along the road. This strategy for GPS collection was done in an effort to minimize any positional errors with remotely sensed data. In addition, a boat survey (analogous to road survey) was conducted along the Boro River to see the wetland vegetation in the study area.

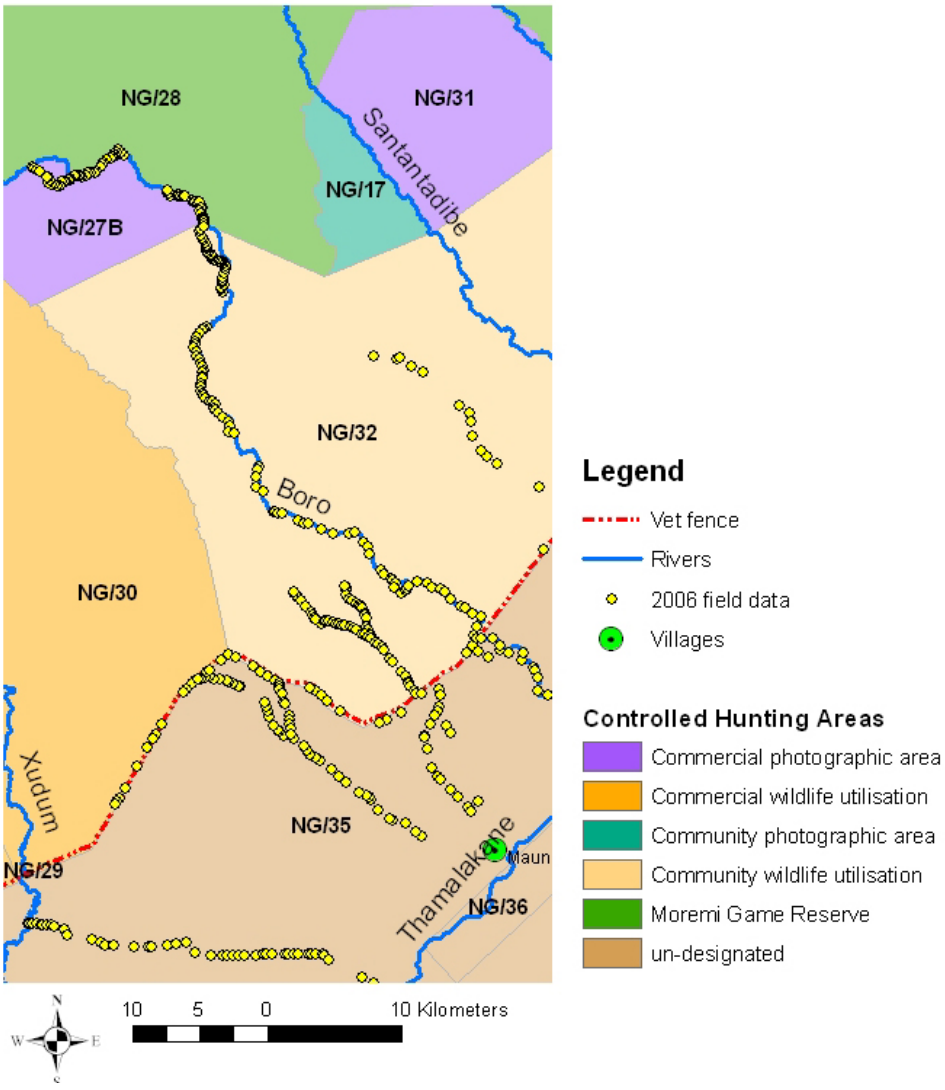

Figure 5.7. Location of vegetation points collected during 2006 road surveys.

5.4.1 Vegetation Structure Line Intercept/Plot Method

This method was developed as a way to quantify the various levels of vegetation structure. Transects were chosen in locations that were representative of various land cover types, with direction/azimuth determined randomly. Transect lines were sampled in 100 m lengths and points were recorded every 5 m. Species (if known) were recorded at height increments of <1m (distinguished between low and tall grass (0.5m)), <2m, <3m, <5m, and 5m and above. For a point to be recorded, a leaf or branch must cross within the vertical plane of the transect line at each 5 m sampling location. Upon the collection of the first transect line, it was apparent that in many cases the line transect may not accurately represent the amount of woody cover in the region and what would be represented in a pixel. For this reason, two 10 x 10 m grids on either side of the main transect line were sampled. The first 10 x 10 m grid was located at the 15- 25 m location on the right side of the line and the second grid was located at the 60 – 70 m location along on the left side of the transect line. Within each grid, a stem count of woody species over one third of a meter in height was made to estimate woody cover. The results from the line transect and road surveys were used to interpret land cover and land cover change in the time-series data.

6 FLOODING AND FIRE: SPATIAL AND TEMPORAL PATTERNS

The results presented in this chapter address the two hypotheses regarding the spatial association of flooding and fire. Specifically, Hypothesis 1 tests whether fire frequency is highest in the Wildlife Management Areas closest to the fence as compared to other management zones. Hypothesis 2 tests whether the higher fire frequency occurs within the active floodplains as compared to other physiographic regions.

6.1 Mapping of Flooding and Fire Regimes

Flooding and fire signatures were extracted from each Landsat TM and ETM+ image using an unsupervised ISODATA classification as described in Heinl et al. (2006). The spectral reflectance of a fire scar is a function of both combustion completeness and the fraction of the area that burns within a pixel, and is wavelength dependent (Roy and Landmann, 2005). The typical reflectance values for most fire scars are low and reported as 0.05 (blue; 400 nm) and 0.10 (mid-infrared; 2500 nm) (Roy et al., 2005). Patterns of flooding and fire from individual scenes were combined to create annual flooding and fire extent maps. Visual interpretation of the data indicates that the flooding and fire regimes are spatially coincident within the floodplains. Individual flood and fire extent maps were combined to create annual flooding and annual fire maps, thus providing 14 flooding maps and 14 fire maps. These annual disturbance maps were then combined to create a 14-year flooding and 14-year fire history map. The average return time in years for flooding and fire during the study period was also computed using the results from the 14-year history maps. In addition to the average return time, the maximum time between

events in years was also computed. The spatial distribution of 14-year flooding history, average return time, and maximum time between floods are shown in Figure 6.1 a) – c). Since the temporal extent for this study is 14 years, the possible average return intervals are 1, 2, 3, 4, 5, and 7 years. Similarly, 14-year history, average return time for fire, and maximum time between fires are shown in Figure 6.2 a)-c).

The three major channels and associated floodplains represented in the study area from NE to SW are the Santantadibe, Boro, and Marophe. From Figure 6.1a, the effect of the Kunyere fault (running northeast to southwest) on the hydrology in the distal Delta creates a damming effect to the water and forming a boundary between the floodplains and drylands. Water levels and flow rates in the Boro are reported to be seasonally dynamic, whereas the water levels in the Santantadibe are more stable and not impacted by climatic fluctuations (Wolski and Murray-Hudson, 2006). From Figure 6.1c, it is observed that the Santantadibe and upper sections of the Boro are frequently flooded as the maximum time between years ranges from one to two years, whereas the Marophe channel (at the southern end of the study area) sustained a period of eight years between floods. Regions that are mapped with a large time between flood events are more likely to experience shifts in vegetation. *Acacia* spp. and other woody species often encroach into less frequently flooded floodplains (also referred as occasional floodplains) when flooding is no longer present on the landscape. The encroachment of woody vegetation into the floodplains is partially kept in check by recurring floods or fire.

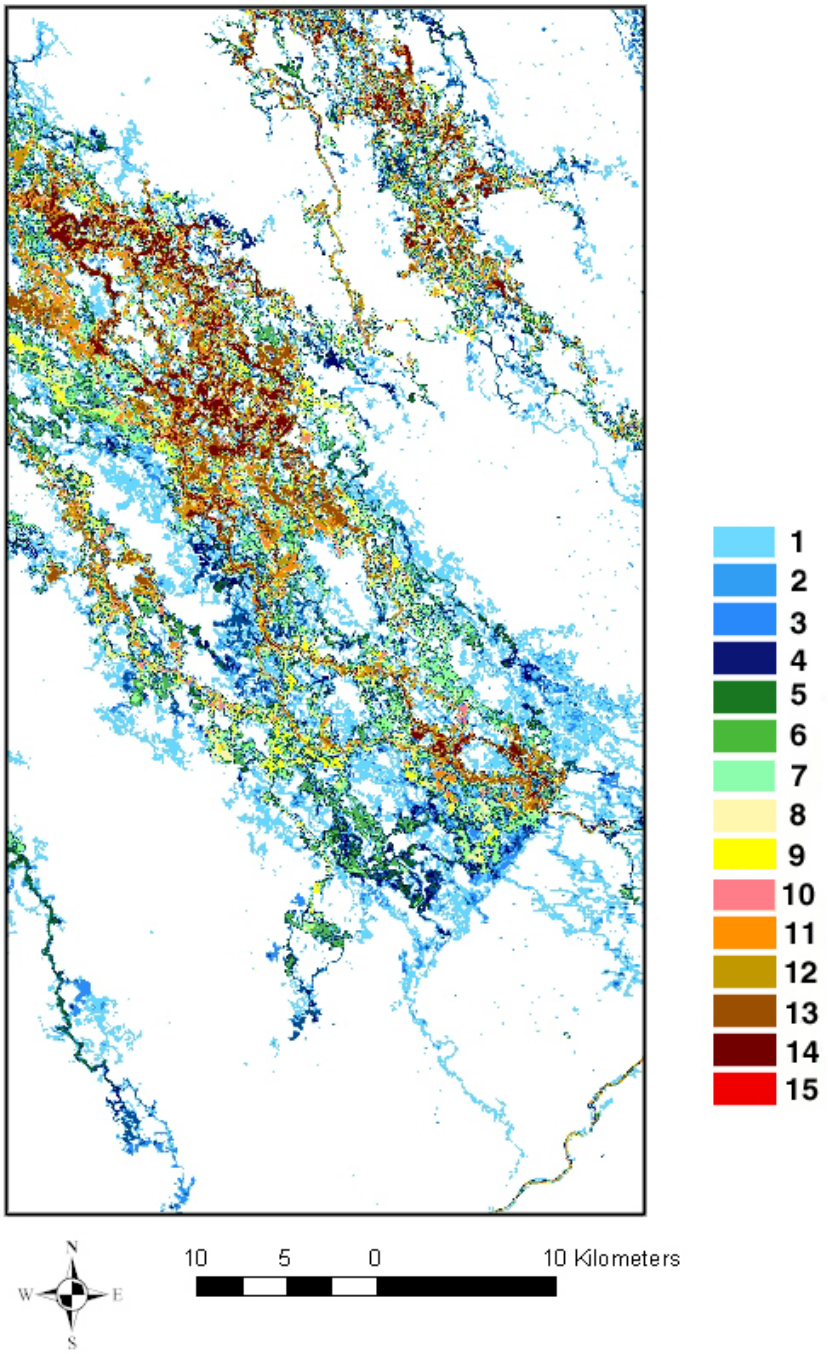

Figure 6.1 a) 14-year flooding history (number of years that flooding was observed),

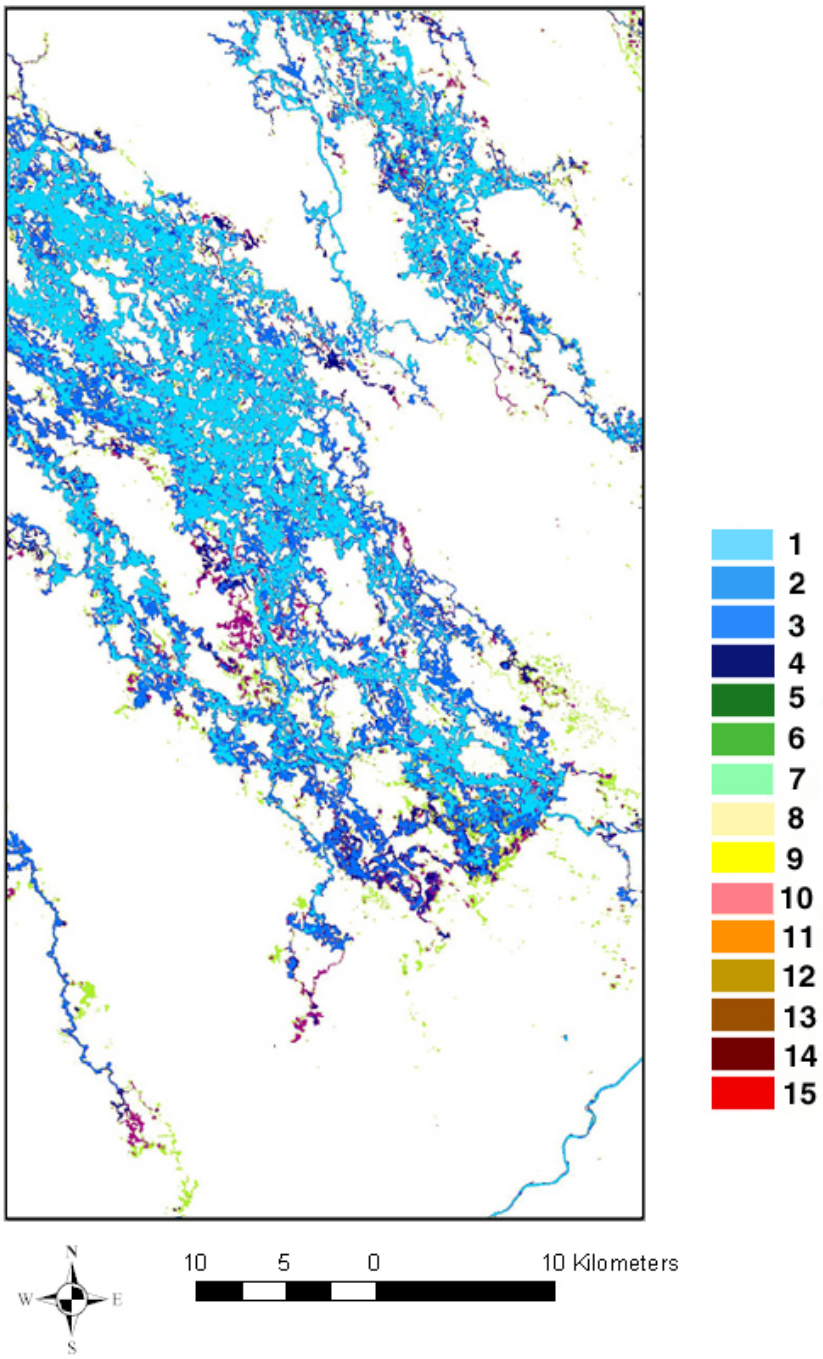

Figure 6.1 b) Average return time in years for flooding during the 14-year history

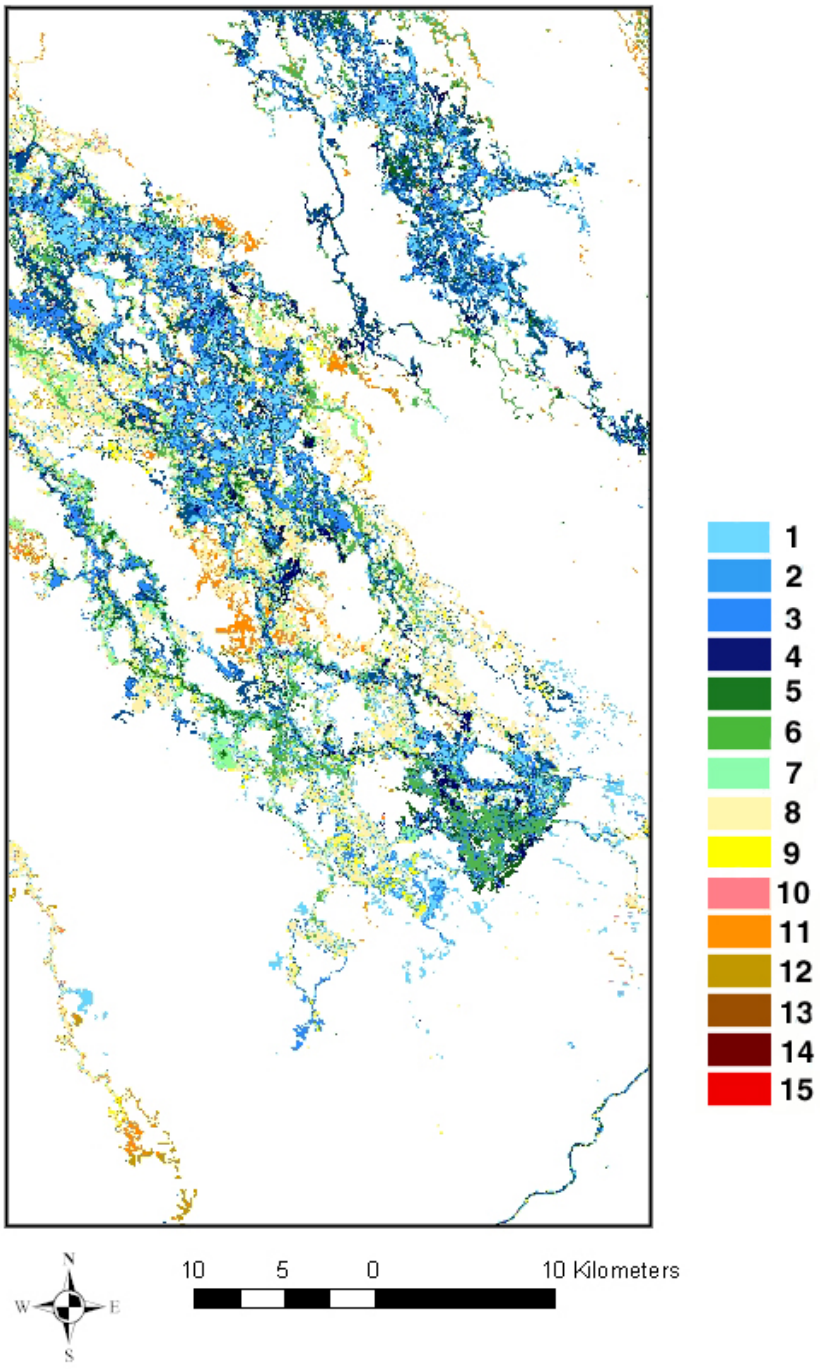

Figure 6.1 c) Maximum time in years between floods.

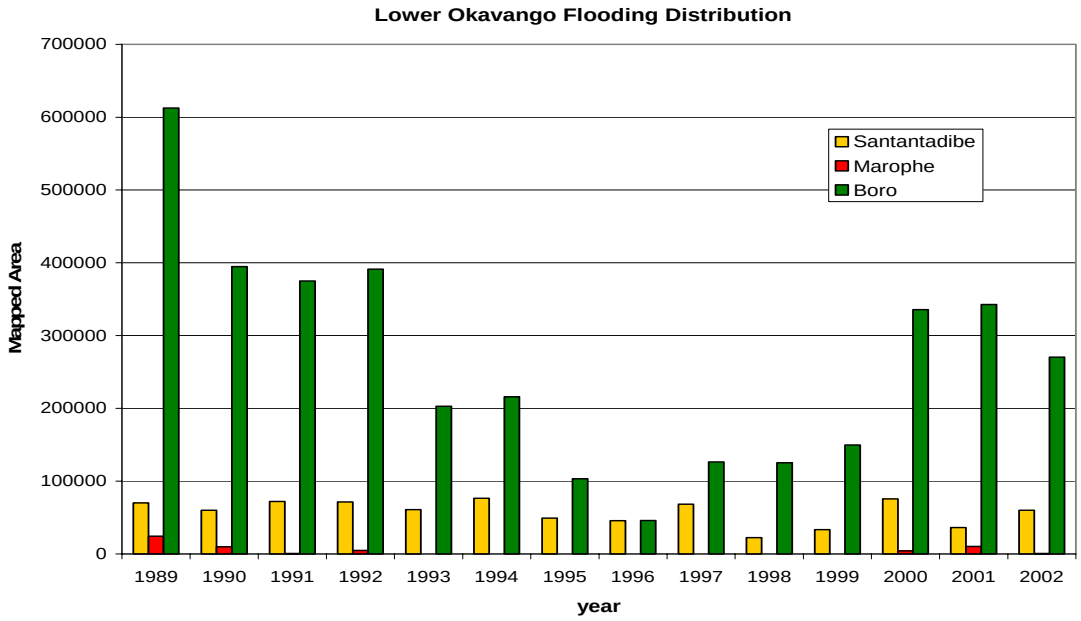

Figure 6.2 Distribution of flooding extent (m^2) in study area from 1989 to 2002 for Boro, Marophe, and Santantadibe channels.

In Figure 6.2, the spatial extent of mapped annual flooding is presented for each channel/floodplain. The Boro receives the majority of flood waters within the lower Delta during the high flood years (early 1990s, early 2000s); however it is subject to greater fluctuations. In contrast, the Santantadibe channel experiences similar amounts of flooding throughout the time-series. The Marophe channel (which is hydrologically connected to the Xudum) experiences the least amount of flooding, and never received floodwaters during the drought of the mid-90s.

Figures 6.3 a-d represent the spatial patterns of the fire regime in the distal Okavango. In Figure 6.3a, it can be seen that the heaviest amount of burning occurs in the floodplains of the Boro and at an average distance of 5 km from the Buffalo fence. Although the majority of burning occurs in the floodplain, the average fire return interval

image (Figure 6.3b) is characterized by small patches, whereas the maximum time between fires (Figure 6.3c) has a larger patch size. This difference in patch size shown between these two images may be an important variable for understanding which factors of the fire regime are controlling the successional pathways. The fire return interval (FRI) results shown in Figure 6.2b depict a FRI of every 2- to 3- years in the lower floodplains, transitioning to 4- to 5- year intervals upstream and as high as every 5- to 7- years in regions adjacent to the floodplains or drylands. The majority of the savanna and woodlands in the drylands did not burn more than once during the 14-year time period; thus, the fire return interval or a maximum time between burns for savanna and woodlands in this region was not able to be determined. Figure 6.3d represents the spatial history of burning with a 5 km buffer zone around the Buffalo fence. People seeking to enter the WMAs for the purposes of extracting resources (with or without a permit) typically cross on foot, and thus the human activities associated with burning in the WMAs will be highest closer to (within 5km of) the fence. Areas having the highest number of burns (more than 7 years in the 14-year history) fall within the 5km buffer zone. This relationship confirms the first hypothesis that fire frequency is highest in the Wildlife Management Areas closest to the fence where people have the easiest access.

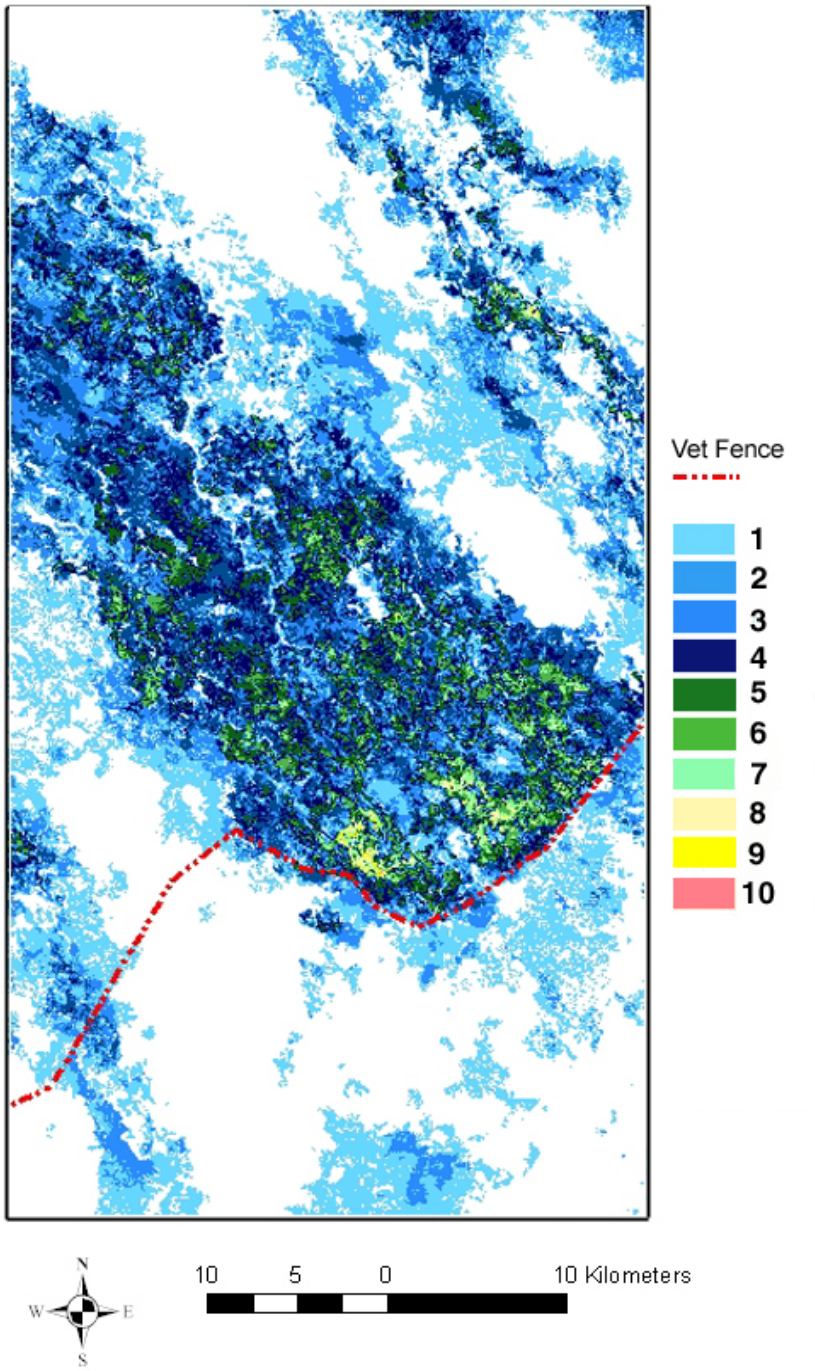

Figure 6.3 a) 14-year fire history (number of years that fire was observed) from 1989 - 2002.

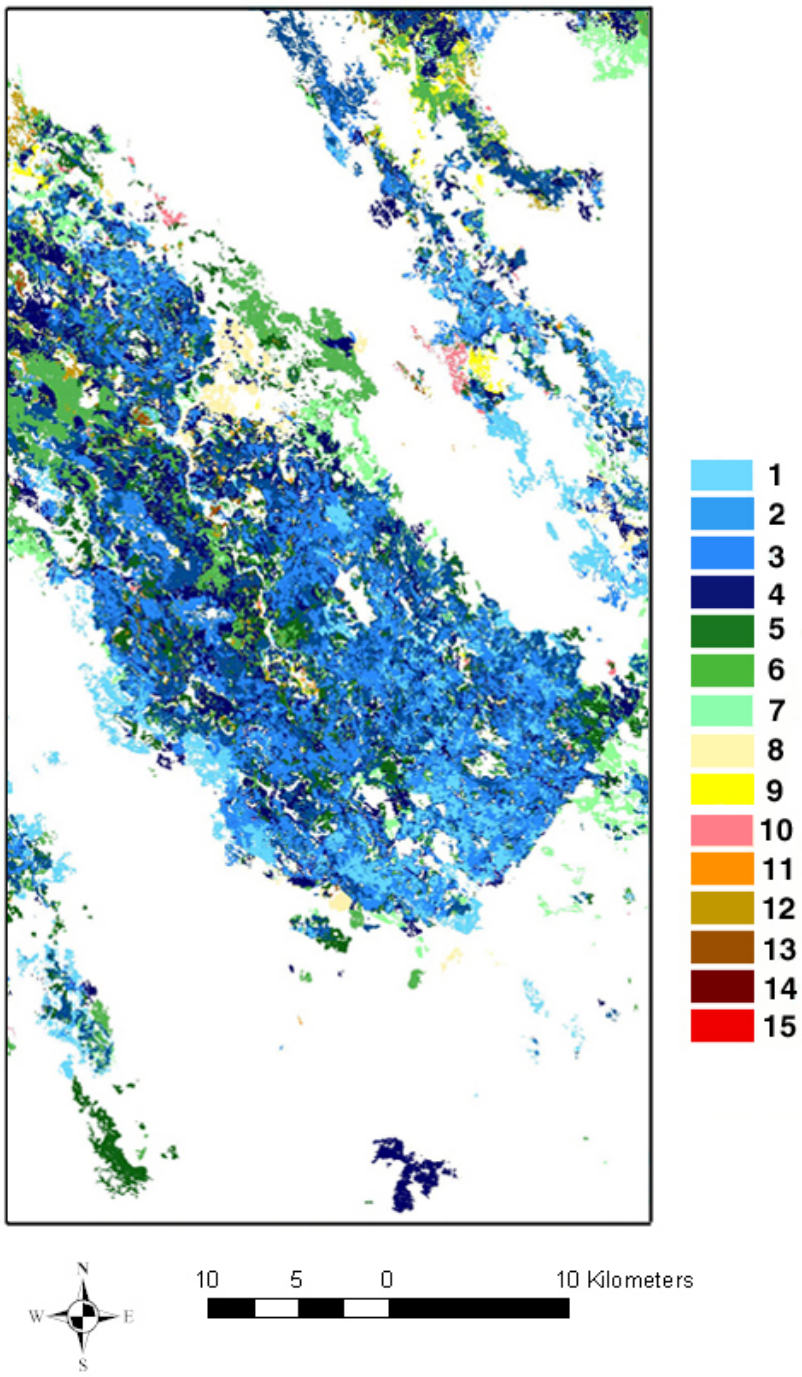

Figure 6.3 b) Average return time in years for fire during the 14-year history

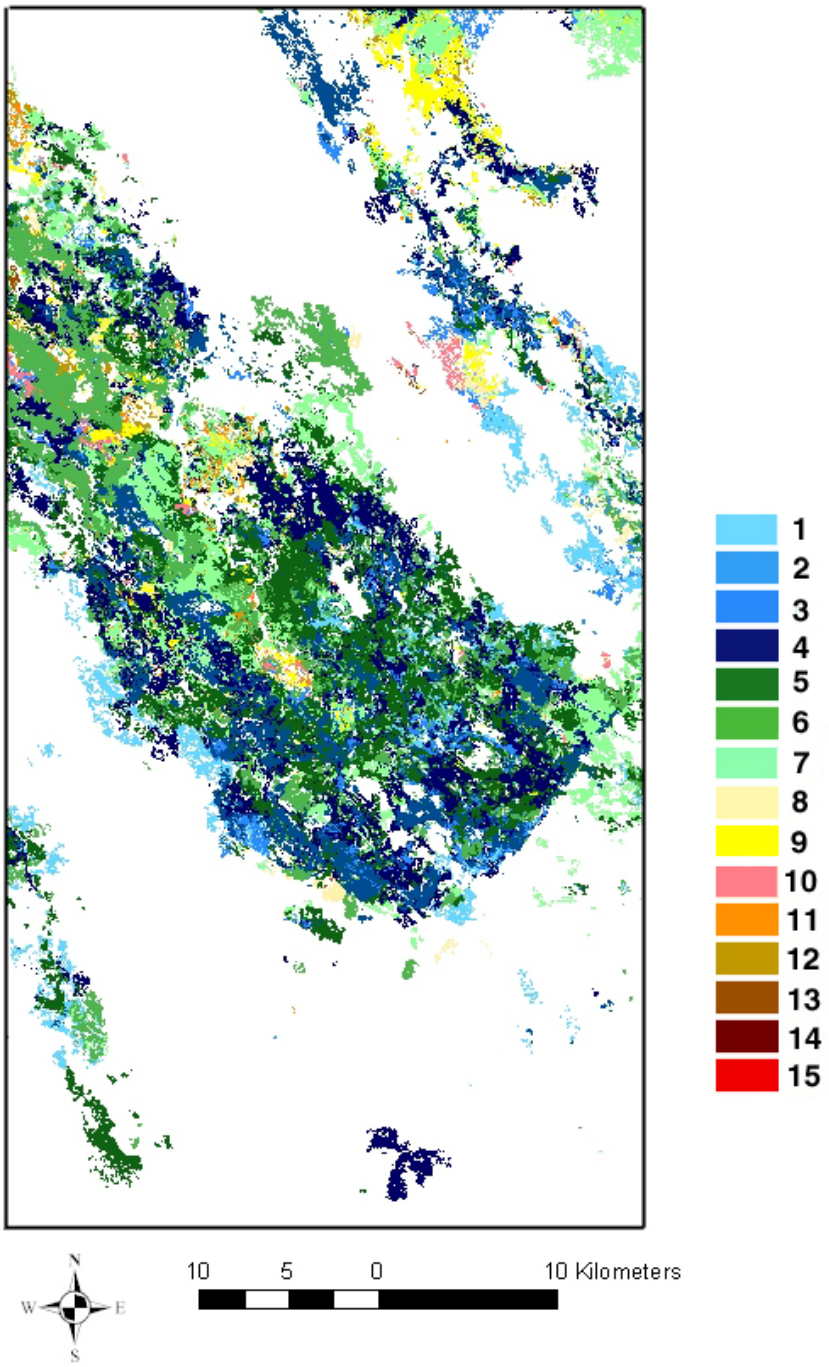

Figure 6.3 c) Maximum time in years between fires.

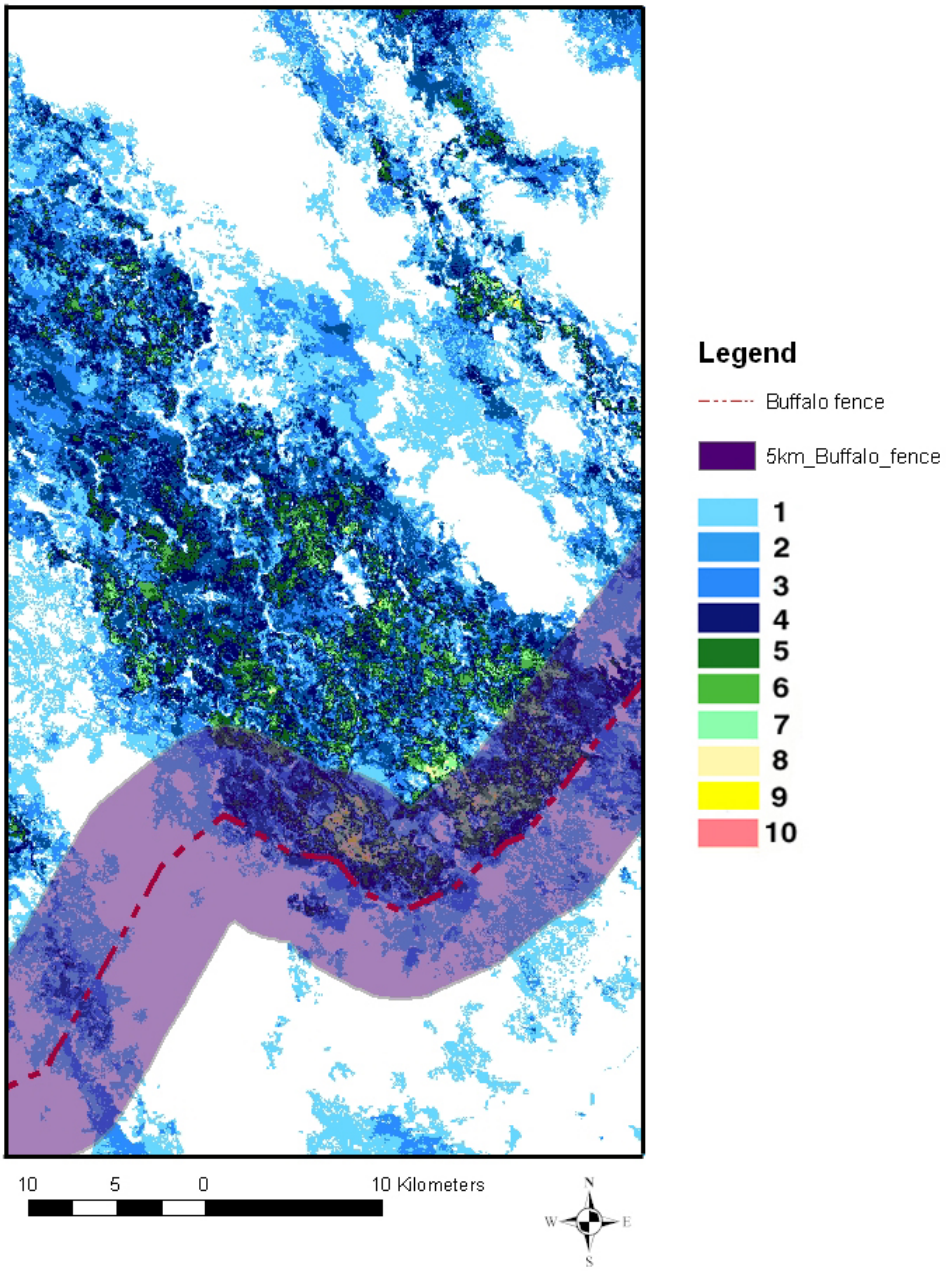

Figure 6.3 d) 5-km buffer around the Buffalo fence with the 14-year fire history (number of years that fire was observed) from 1989 to 2002.The areas with the greatest number of fires occur within this buffer zone.

The average monthly extent of flooding and fire for the lower Okavango Delta are shown in Figure 6.4. Precipitation amounts shown are the monthly average for Maun

from 1922 to 2002. The peak of the flooding in the lower Delta occurs in the months of July through September. In Botswana, a natural fire regime (that is, a natural ignition source) typically occurs at the beginning of the wet season as available fuels are sufficiently dry to support burning and lightening is sparked by dry thunderstorms (Bond and van Wilgen, 1996; Roy et al., 2005). In addition, dry winds are strong in September and October helping to spread the advance of fires. As shown in Figure 6.4, 72% of the mapped fires in the lower Okavango Delta occur during the winter dry season (April through September) when there is little precipitation prompting the hypothesis that most of these fires are anthropogenic in origin. The ignition origin of the fires that occur during the rainy season (October through March) cannot be determined based upon these results.

To quantify the number and spatial extent of fires that occur annually in the floodplains/wetlands *versus* those that occur in the savanna/drylands, a segmentation of the annual fire maps was conducted to identify individual fires. A fire patch was defined as having a minimum size of 10 pixels or 0.9 km^2. The fires were separated into floodplain or upland fires using the 14-year flooding history to define the extent of the floodplains. Thus, if a pixel has flooded at any point during the 14-year history, it is defined here as a floodplain. The total area burned within the floodplains and drylands for each year in shown in Figure 6.5. The number of floodplain fires is lowest in 1989, due to the large amount of standing water from the large flood event. The largest amount of upland burning occurred in 1996 and 1997 and the lowest amounts of burning occurred in 1993 to 1995 and 1998.

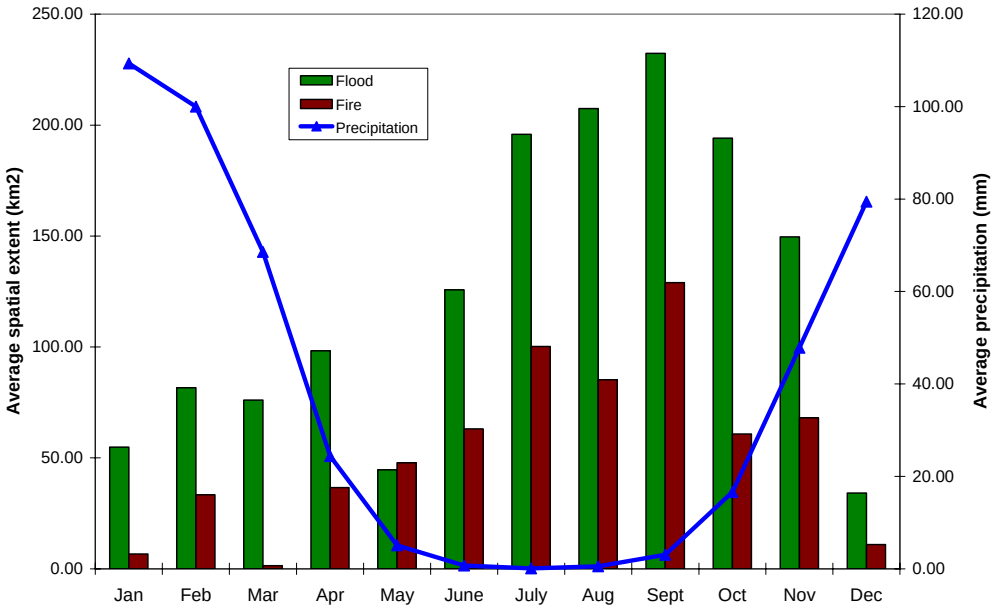

Figure 6.4 Seasonality of flooding and fire in the lower Okavango Delta from 1989 to 2002 based upon 14-year time-series. Average precipitation values generated from 1922 to 2002 precipitation data collected at the Maun airport.

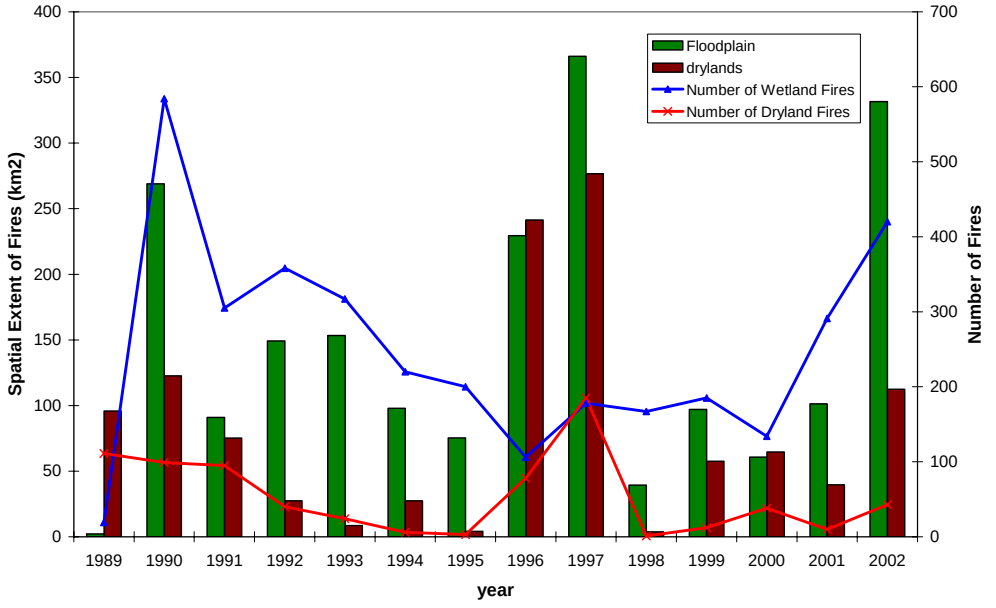

Figure 6.5. Annual fire spatial extent and numbers of fires for the lower Okavango Delta delineated by floodplain and drylands/savanna.

Similar statistics were computed for the average patch size of fires and area shown in Figure 6.6. In general, fires occurring in the floodplains had an average patch size of 0.648 km^2 per fire and on average the floodplains experienced 248.85 fires per year. In contrast, fires in the drylands were larger with an average patch size of 1.92 km^2 per fire and experienced on average 53.2 fires per year.

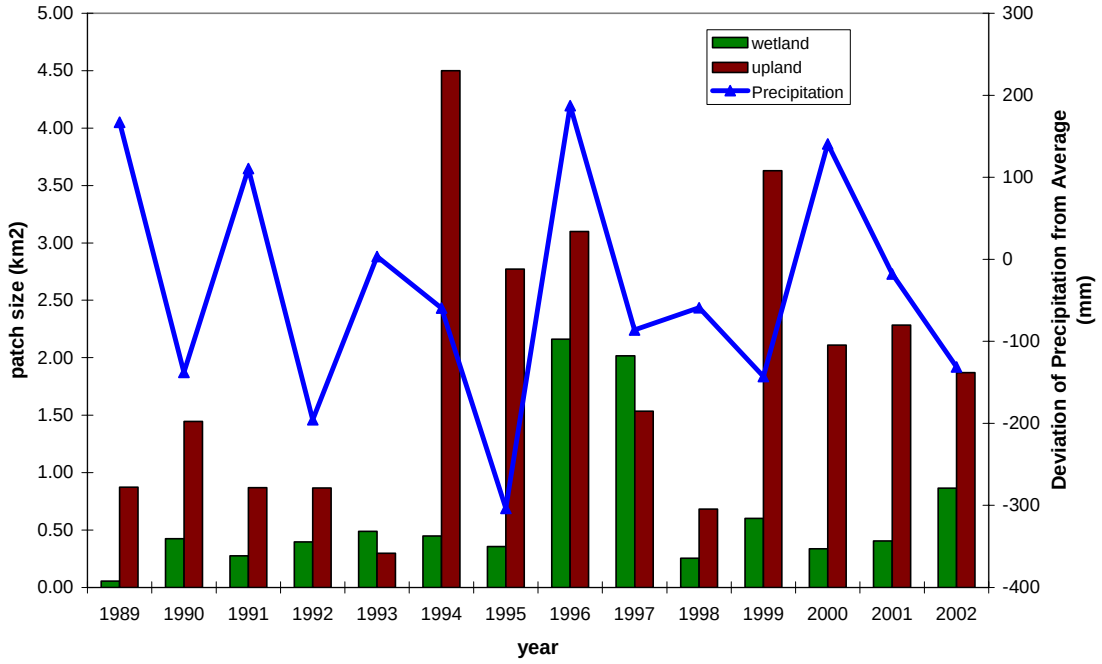

Figure 6.6. Annual fire mean patch size for the lower Okavango Delta delineated by floodplain and drylands/savanna and deviation of precipitation from mean 455 mm/yr.

6.2 Spatial Association of Flooding and Fire Regimes

One of the objectives of this research is to describe the spatial association of flooding and fire regimes on the landscape. Hypothesis 2 proposed that the largest number of fires occurs within the active floodplains. The 14-year flood maps were used to define dry floodplains, active floodplains, and less active floodplains. A dry floodplain

is defined as having flooded at least once since 1989 but did not flood after 1992 (i.e., 10 years of no flooding). An active floodplain is defined as having a flood return time of at least every other year. Less active floodplains are defined as all areas that experience a flood in the 14-year history and do not fall under the active or dry floodplain mask. The study area was also stratified in terms of different burning levels with low fire corresponding to 1 – 2 fires over the 14-years, intermediate burning corresponds to 3 – 7 years of burning, and high levels of burning corresponding to more than 7 years burned in the study period. The three floodplain zones were characterized against the three levels of fire and vegetation type.

Table 6.1 lists the characterization of fire with respect to the floodplains. Intermediate levels of burning account for the maximum percentage of landscape at 48.2%, 45.6%, and 50.3% for the drying, less active, and active floodplain. Low levels of fire occupied 35.5%, 38.8%, and 31.4% of the landscape in the drying, less active, and active floodplains. Approximately 75% of the areas experiencing high amounts of burning (7 or more times) occurred in the active floodplains confirming Hypothesis 2.

Table 6.1. Flooding and fire interactions on the floodplains.

	Dry floodplains		**Less Active Floodplains**		**Active Floodplains**	
Fire Level	**hectares**	**Percent**	**hectares**	**Percent**	**hectares**	**Percent**
Low fire	7,378.9	35.6	4,987.7	38.8	12,026.9	31.5
Intermediate fire	10,001.5	48.3	5,856.4	45.6	19,220.5	50.3
High fire	207.7	1.0	180.3	1.4	1,129.2	2.9

Table 6.2. Fire Regime with respect to Floodplains versus Drylands

	Floodplains				Drylands			
	Fire History		Max Time Between Burns		Fire History		Max Time Between Burns	
Fire Level	hectares	Percent	Hectares	Percent	hectares	Percent	hectares	Percent
Null	12,146.4	15.0	25,451.5	31.4	97,858.2	60.3	133,519.6	82.4
1	13,305.2	16.4	1,273.9	1.5	35,661.5	22.0	4,369.2	2.6
2	15,921.1	19.6	2,255.2	2.7	14,622.4	9.0	1,425.5	0.8
3	15,627.5	19.3	7,801.7	9.6	8,258.6	5.0	3,160.4	1.9
4	11,917.3	14.7	11,153.1	13.7	3,742.3	2.3	3,429.6	2.1
5	7,151.0	8.8	12,620.9	15.5	1,486.7	0.9	4,583.4	2.8
6	3,273.8	4.0	10,083.9	12.4	334.3	0.2	4,423.0	2.7
7	1,161.2	1.4	5,935.2	7.3	65.7	0.0	4,666.1	2.8
8	378.9	0.4	1,118.8	1.3	2.2	0.0	719.3	0.4
9	81.5	0.1	1,618.5	1.9	0.0	0.0	877.8	0.5
10	4.4	0.0	361.9	0.4	0.0	0.0	490.9	0.3

6.3 Association of Flooding and Fire Regimes with Vegetation Type

Vegetation types within this study area consist of herbaceous, savanna, and woodland classes. The percentage of vegetation types (as defined by HOORC) are as follows: herbaceous class comprises 35% of the study area (84,829 hectares), mixed savanna comprises 13.9% of the study area (33,777 hectares), and woodland savanna comprises the remaining 51.1% (124,375 hectares).

Table 6.3 lists the percentage of vegetation type (herbaceous, mixed savanna, or woodland savanna) within each floodplain type. An important qualification is that the statistics for vegetation types that do not experience flooding are not included in Table 6.3. For pixels within the drying floodplains, the percentage was highest for woodland savanna vegetation at 47.4% followed by herbaceous at 38.6%, and 13.9% defined as

mixed savanna. The dominance of woodlands under the drying floodplain mask is logical as woody species such as *Acacia* spp move in quickly into former floodplains. Again, the definition of the vegetative cover was derived from 1999 imagery toward the end of the time-series. The relative abundance of herbaceous vegetation to woodlands switches for the less active floodplains. Here, herbaceous vegetation is the most dominant at 68.4% of the landscape, with woodland savanna occupying 28.5% of the landscape and mixed savanna comprising only 3.1% of the landscape. As expected, vegetation within the active floodplains mask was more strongly skewed toward herbaceous-dominated at 85.8% of the landscape, with 13.1% labeled as woodland savanna and the remaining 1% is defined mixed savanna.

Table 6.3. Vegetation Type and Floodplain Relations.

	Dry floodplains		**Less Active Floodplains**		**Active Floodplains**	
Veg. Type	**hectares**	**Percent**	**hectares**	**Percent**	**hectares**	**Percent**
Herbaceous	8,022.2	38.6	8,781.0	68.4	32,825.61	85.8
Mixed Savanna	2,886.1	13.9	400.7	3.1	377.21	0.9
Woodland Savanna	9,844.7	47.4	3,660.4	28.5	5,031.36	13.1

Figure 6.7 casts the statistics presented in Table 6.3 above as the percentages of floodplain levels for each vegetation type. Again, the data in Table 6.3 and Figure 6.7 are for pixels that experienced flooding at least once in the time-series. The majority (66%) of the herbaceous vegetation occurred within the active floodplains followed by the less active floodplains (17%) and the drying floodplains (16%). The mixed savanna class was generally split between the drying floodplains (41%) and the active floodplains (52%)

with only 6% occurring on the less active floodplains. The majority of woodland savanna vegetation (53%) occurred on drying floodplains followed by active floodplains (27%) and less active floodplains (20%). This association confirms the hypothesis that an increase in woody cover would be expected for these drying floodplains.

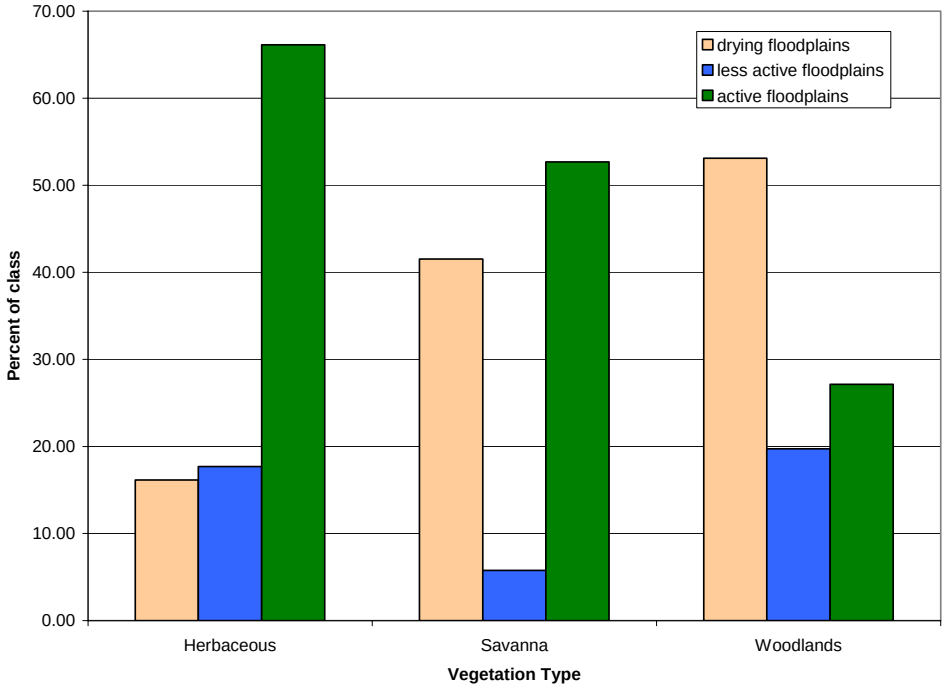

Figure 6.7. Association of HOORC Vegetation Type with Floodplain type

The relationship between vegetation type and fire, shown in Table 6.4, is nearly the same relationship as vegetation type and flooding. Again, the statistics listed in Table 6.4 and Figure 6.8 are only for vegetation types that experienced a fire during the 14-year time-series. For low fire levels (1-2 times), the majority (49%) of the vegetation type belonged to the woodland savanna class, followed by herbaceous (38%) and then mixed savanna (12%). At the intermediate fire levels of 3-6 times over 14 years, fire was more

prevalent on the landscape and herbaceous vegetation dominated at 65%, followed by woodland savanna (30%) and mixed savanna (4%). At the highest levels of burning (7+ times), 72% of the vegetation was herbaceous, followed by 24% for woodland savanna and 4% of mixed savanna. One possible explanation for the high percentage of woodland savanna fire occurring in the highest fire levels is due to the proximity of many woodland species (riparian forest) to the floodplains where burning does frequently occur.

Table 6.4. Vegetation Type and Fire Relations

	Low Fire		Intermediate Fire		High Fire	
Veg. Type	**hectares**	**Percent**	**hectares**	**Percent**	**hectares**	**Percent**
Herbaceous	30,239.6	38.0	33,774.4	65.2	1,221.6	72.1
Mixed Savanna	9,979.8	12.5	2,118.7	4.1	65.5	3.8
Woodland Savanna	39,280.3	49.4	15,893.5	30.7	406.8	24.0

Figure 6.8 depicts the statistics presented in Table 6.4 above as the percentages of burning levels for each vegetation type. The herbaceous vegetation was associated with intermediate (52%) or low (46%) levels of burning with only 2% of the herbaceous vegetation burned at the highest levels. Over 82% of the mixed savanna class that experienced a burn experienced low levels of burning followed by intermediate (17%) and high (0.5%). The majority of woodland savanna vegetation was also associated with low levels of burning (71%) followed by intermediate (28%) and high (0.7%).

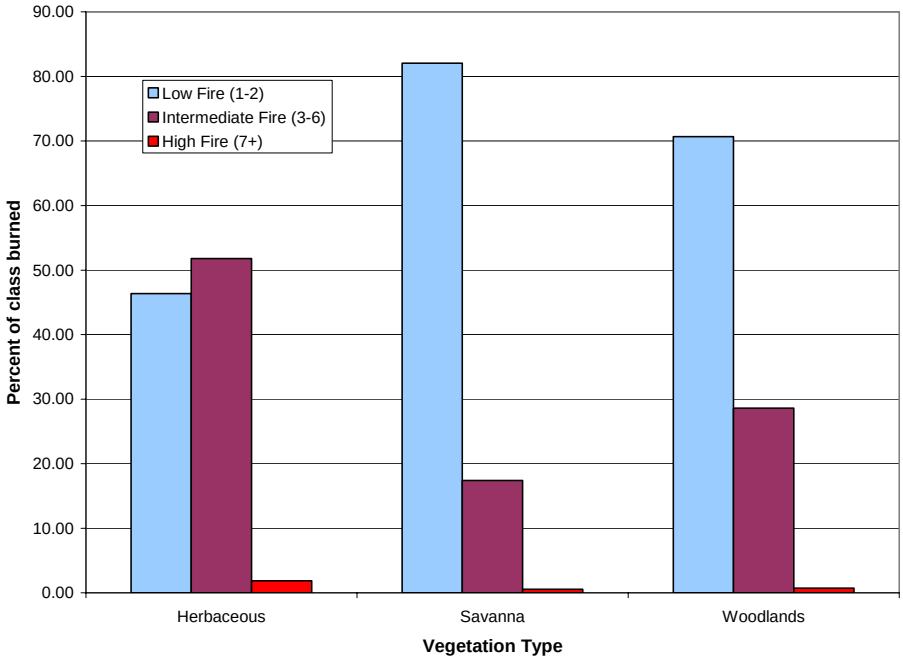

Figure 6.8. Association of Vegetation Type with burning levels

The flooding and fire statistics (history, average return time, and maximum time between events) for each vegetation type are shown in Figure 6.9 (history), Figure 6.10 (average return time), and Figure 6.11 (maximum time between events). The results indicate that both flooding and fire are spatially coincident with herbaceous vegetation. Of note, however, is the fact that woodlands have a higher percentage of class occupied by flooded pixels than the shrublands, albeit by a small difference. However, these interpretations are under the assumption that the HOORC vegetation product is accurate and that the vegetation type is not changing through time. In Figure 6.10, the average return time for each vegetation type is similar to the results in Figure 6.9. Here, a greater proportion of the herbaceous vegetation experienced frequent flooding and fire return times compared to mixed savanna and woodland savanna.

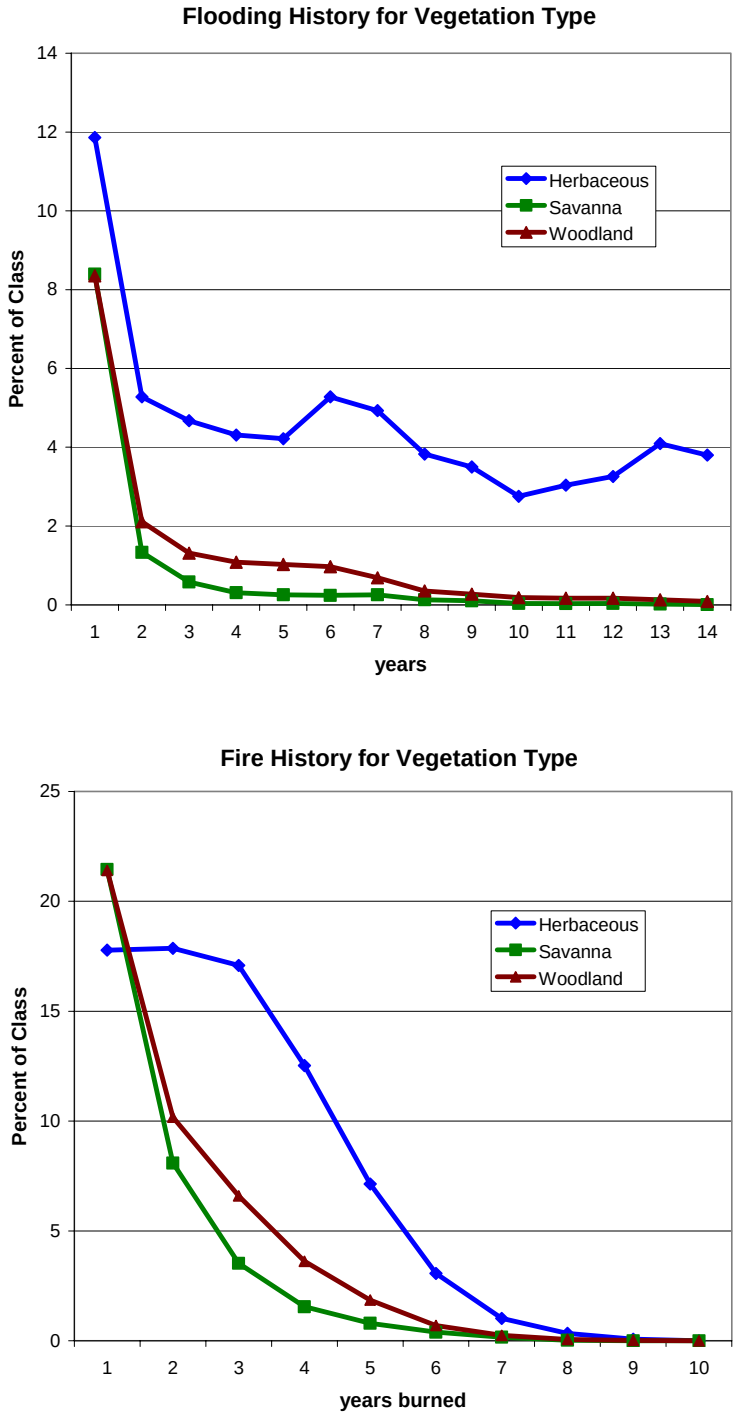

Figure 6.9. Flooding and Fire history for Vegetation Type

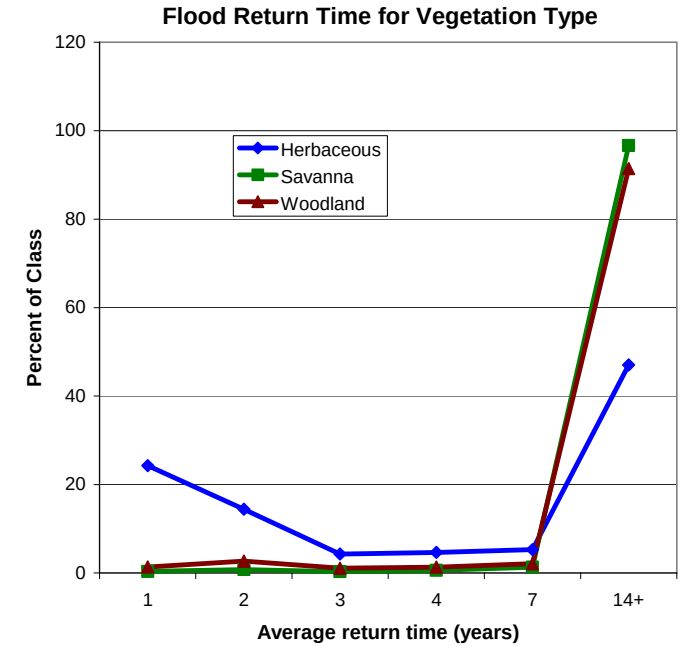

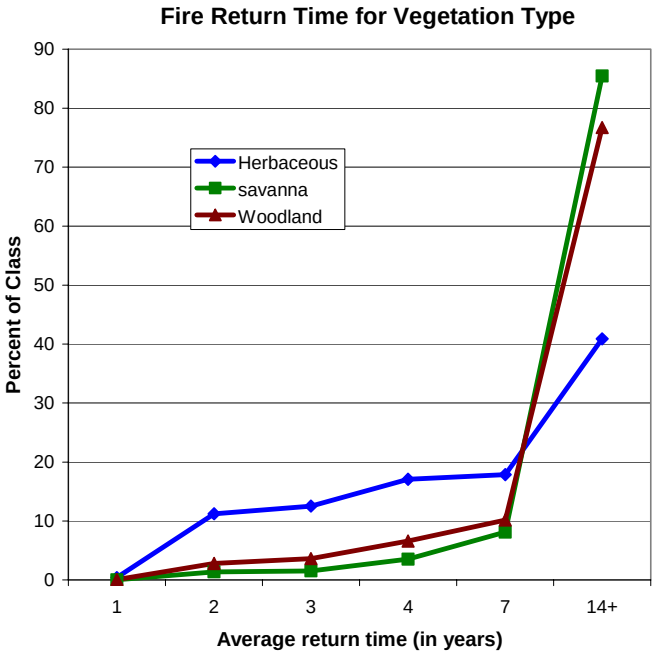

Figure 6.10. Average Flooding and Fire Return Time for Vegetation Type

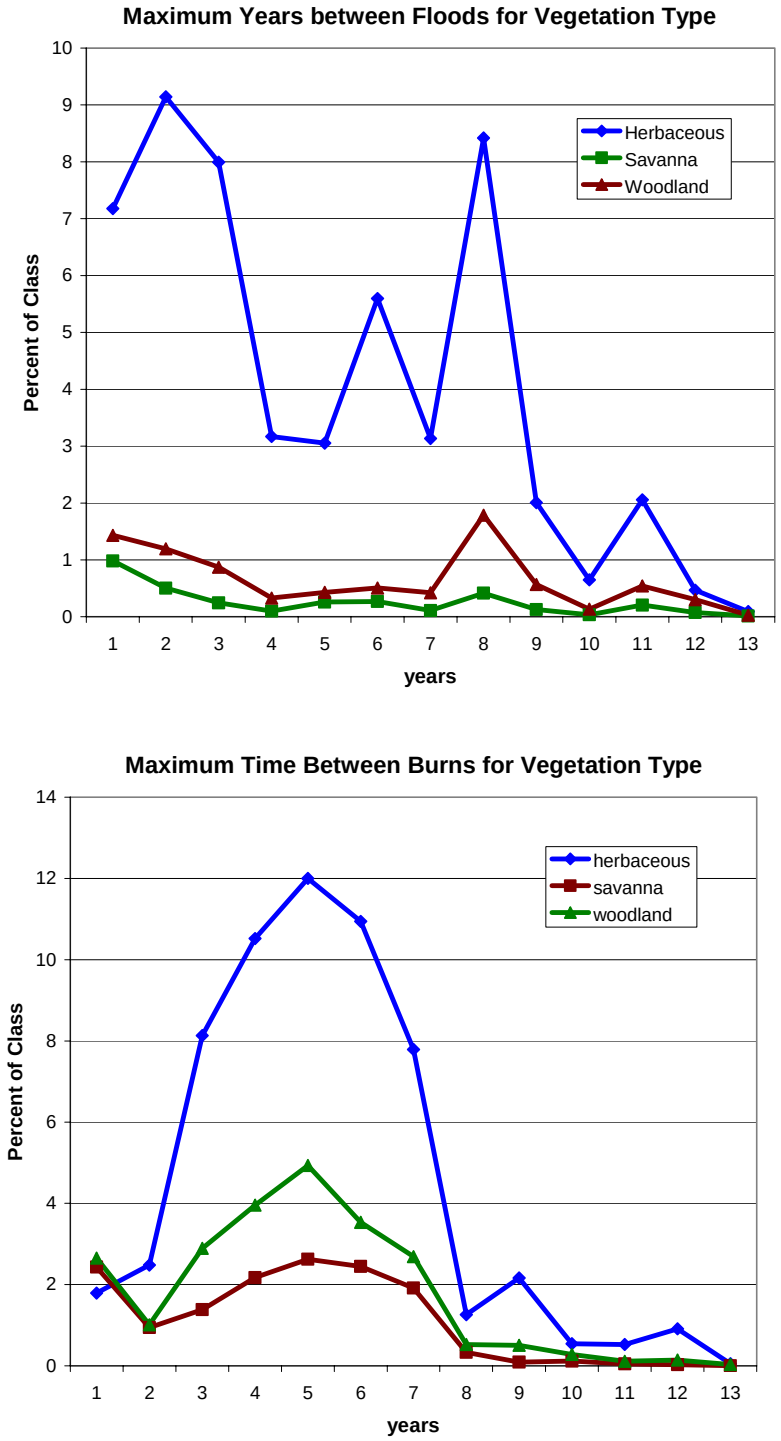

Figure 6.11. Maximum time between flooding or burning events for vegetation type

Figure 6.11 plots the maximum time between either a flooding or fire event for each vegetation class. For flooding and the herbaceous class, the maximum time between floods is not directly related to the percentage of class; perhaps indicating the aspatial representation of annual differences in flood extent. Additionally for fire, all three vegetation types exhibit a curved shape with the maximum time of five years between burns dominating the landscape.

6.4 Association of Flooding and Fire Regimes with Vegetation Structure

The presence of disturbance during the 14-year time-series for each HOORC vegetation structure class (see Figure 5.2 for HOORC vegetation structure class codes) is shown in Figure 6.12.

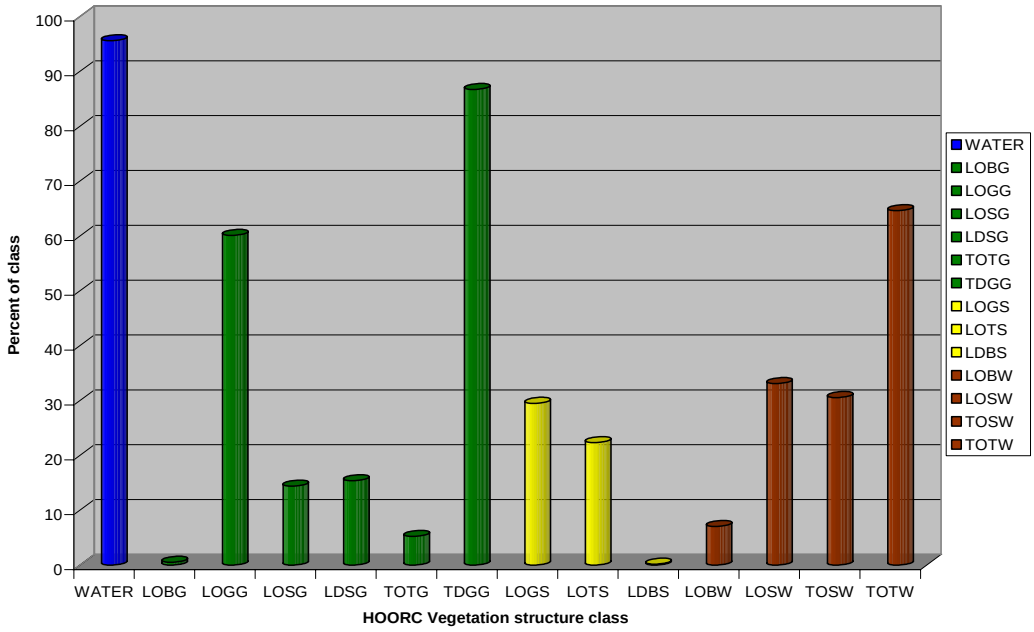

Figure 6.12. Percentage of HOORC structure classes experiencing disturbance during the 1989-2002 time-series. Grasslands are grouped as green, shrublands grouped as yellow, and woodlands groups as brown.

To obtain a nuanced understanding of the relationships between flooding and fire with vegetation, each regime was computed for the vegetation structure classes as defined by HOORC. Table 6.5 lists the percentage of structure class for each floodplain with percentages from 5 – 10% highlighted as green and above 10% highlighted yellow. Areas in the drying floodplains were dominated by low open shrubbed woodlands and low open grasses grasslands that accounted for 29.2% and 33.1% of the vegetation cover respectively. The less active floodplains were dominated by five structure classes: low open shrubbed woodlands, low open grassed grasslands, tall open treed woodlands, tall dense grassed grasslands, and water (that also contained vegetation similar to tall dense grassed grasslands). The active floodplains were dominated by low open grassed grasslands, tall dense grassed grasslands, and water.

Table 6.5. Vegetation structure associated with floodplain position. (green = 5 – 10%, yellow >10%)

	Dry floodplains		**Less Active Floodplains**		**Active Floodplains**	
CLASS	*hectares*	*Percent*	*hectares*	*Percent*	*hectares*	*Percent*
LDBS	0.0	0.0	0.0	0.0	0.0	0.0
LOTS	68.2	0.3	9.2	0.1	46.8	0.1
LOSW	6,055.4	29.2	1,553.7	12.1	2,010.6	5.2
LOBG	18.7	0.1	1.5	0.0	0.0	0.0
LOSG	1,759.3	8.5	181.8	1.4	130.0	0.3
LOGG	6,867.5	33.1	3,798.6	29.6	5,017.9	13.1
LDSG	280.4	1.3	92.5	0.7	55.8	0.1
TOSW	1,793.0	8.6	483.0	3.7	826.0	2.1
TOTG	45.9	0.2	5.8	0.0	2.8	0.0
TOTW	767.3	3.7	1,246.9	9.7	1,964.1	5.1
TDGG	1,004.2	4.8	3,686.0	28.7	13,252.8	34.6
LOGS	800.3	3.8	120.5	0.9	188.5	0.5
LOBW	1,160.6	5.6	367.4	2.8	183.7	0.4
WATER	131.7	0.6	1,294.8	10.0	14,554.8	38.0

The vegetation structure class relationship with fire, listed in Table 6.6 provides a different characterization than the floodplain relationships. Areas labeled as having low levels of fire (one or two burns) contained a mixture of woodlands (LOSW, TOSW, TOTW, and LOBW) comprising 48% of the area and grasslands (LOSG, LOGG, and TDGG) comprising 37% of the landscape. Intermediate fire (three – six years burned) was largely comprised of grassed landcover (LOGG, TDGG, and water), accounting for over 65% of the vegetation. Woodlands were also found to have intermediate fire with LOSW, TOSW, and TOTW accounting for almost 28% of the area. Regions experiencing high burns were associated with grasslands (LOGG and TDGG) for 69% of the total area. Interestingly, several structure classes did not show a significant relationship with either flooding or fire. These include all the structure classes where shrublands are the primary cover (LDBS, LOTS, and LOGS) as well as the grassland classes (LOBG, LDSG, and TOTG). Presuming that the vegetation structure classification is correct, this observation is not unexpected for some classes such as LDBS and LOTS which may lack a sufficient understory of grasses capable sustaining fire. However, for other classes such as TOTG and LOGS that presumably have a sufficient grass layer, there are other explanations (such as grazing rates or lack of ignition) as to why fire was not more frequently observed.

Table 6.6. Vegetation structure and fire relations. (green = 5 – 10%, yellow >10%)

	Low Fire (1-2 burns)		Intermediate Fire (3-6 burns)		High Fire (7-10 burns)	
CLASS	*hectares*	*Percent*	*hectares*	*Percent*	*hectares*	*Percent*
LDBS	143.2	0.2	0.0	0.0	0.0	0.0
LOTS	227.8	0.3	106.3	0.2	6.2	0.3
LOSW	20,534.2	25.8	7,613.3	14.7	246.8	14.5
LOBG	87.9	0.1	2.34	0.0	0.0	0.0
LOSG	6,632.4	8.3	986.8	1.9	15.3	0.9
LOGG	13,067.1	16.4	15,407.7	29.7	959.4	56.6
LDSG	653.0	0.8	95.7	0.1	3.1	0.1
TOSW	4,424.8	5.5	3,035.8	5.8	56.9	3.6
TOTG	864.4	1.1	26.4	0.1	0.0	0.0
TOTW	4,370.5	5.5	3,713.3	7.1	39.3	2.3
TDGG	9,783.1	12.3	10,388.4	20.0	217.3	12.8
LOGS	1,686.6	2.1	1,009.6	1.9	46.9	2.7
LOBW	9,722.9	12.2	1,424.7	2.7	57.4	3.4
WATER	7,301.5	9.1	7,975.9	15.4	44.8	2.6

6.5 Association of Fire Regimes with Land Management

To begin to assess the level of human influence on the landscape, the fire regime was evaluated against the four general land management types in the lower Okavango Delta: communal regions, hunting concessions in the WMAs, photography concessions in the WMAs, and the Moremi Game Reserve. As discussed in Chapter 3, there are restrictions on burning and natural resource extraction within the Moremi Game Reserve as well as the concession areas. The photography and hunting concessions within the study area are comprised of seasonal and occasional floodplains as well as dryland interfluves. The hunting concessions tend to occur on the drier portions of the landscape (floodplains and drylands), whereas the photography concessions occupy more of the

floodplains, marshes and some drylands. The bulk of the tourist activities take place on the concessions. The percentages of each fire level (low, intermediate, or high) with respect to the land management categories are listed in Table 6.7. Of the regions that experienced low fire (one – two burns); the majority (42.3%) occurred in the photography concessions followed by the hunting concessions (28.7%) and communal (22%) areas. Once the fire levels increased to the intermediate (three – six burns) or high (seven or more burns) levels, the majority of them took place within the hunting concessions areas.

Table 6.7. Fire regime and land management.

	Low Fire		**Intermediate Fire**		**High Fire**	
Land Use	**hectares**	**Percent**	**hectares**	**Percent**	**hectares**	**Percent**
Communal	17,519	22.	681.5	1.3	0.0	0.0
Hunting	22,816.2	28.7	25,897.7	50.0	1135.5	67.0
Photography	33,677.4	42.3	24,452.1	47.2	558.2	32.9
Game Reserve	5,319.0	6.7	591.0	1.1	0.0	0.0

6.6 Disturbance Clusters

Flooding and fire have been shown to be important ecological pressures in the savanna/wetland environment of the lower Okavango Delta. As presented in the previous sections, flooding and fire are often spatially concomitant. The flood waters typically arrive into the lower Delta by June and often reach the maximum spatial extent in August and September. During this time, vegetation in the floodplains is extremely dry and the water from the annual flooding permits growth. Fires in the floodplains occur for a variety of reasons. Reed cutters will burn the vegetation to improve the ease of cutting the

reeds for harvesting. Fires are also purposely set in advance of the floodwaters to remove old vegetation in an effort to improve quality of grazing or in an attempt to improve flow. In addition to purposeful fires, many fires are accidentally ignited and, due to the dry conditions, easily spread. In areas where floods occur only occasionally (i.e. every five to ten years), *Acacias* and other woody species will quickly encroach. The seasonal fires reduce woody development within the floodplains and also provide a quick growth and resurgence of grasses. In addition to the local impacts from fire, the impact of fire may reach a global scale through increased CO_2 and other trace gases emissions into the atmosphere. Savanna and floodplain fires are thought to be a significant contributor to the Southern Africa regional source of trace gases and aerosols (Korontzi et al., 2003).

To assess how flooding and fire are related to vegetation distribution, disturbance information from observed fire and flooding signatures from multispectral, remotely sensed data were combined to create a spatially explicit map of disturbance clusters: that is clusters of similar flooding and fire histories. These disturbance clusters serve as a new strategy for class stratification that is ecologically driven. As previously described, the annual flooding and fire maps were combined to create a 14-year flooding and fire history map. The 14-year disturbance histories were composited to create an overall disturbance history (DH) map where 148 unique clusters were defined based on the number of times a pixel burned and was flooded. For example, a given pixel within the Boro floodplain may have a disturbance history value as burned 3 times and flooded 8 times out of the 14-year temporal window. Similarly, disturbance return (DR) clusters were also defined based upon the 14-year return time of flooding and fire. The average

return interval for each regime (flooding and fire) was computed by round(14/x), where x is the number of annual occurrences on a per-pixel basis. This resulted in six possible return interval classes: 1 = every year, 2 = every other year, 3 = every third year, 4 = every fourth year, 7 = every seventh year, and 14 = once in the sequence. By combining the flooding and fire disturbance return (DR) maps, 35 unique classes were identified and the clusters were labeled based upon their return interval. Here, a pixel that had a burn 3 and flood 8 history would have a return code of burn 4 – flood 2. This implies that, on average, the pixels in that cluster burned every four years and floods every other year.

The disturbance history and disturbance return maps are presented in Figure 6.13. These disturbance clusters provide an ecologically meaningful method of defining regions that exhibit similar disturbance patterns. For the study area, 148 unique DH clusters (shown in Figure 6.13a) were mapped covering approximately 60% of the landscape in the study area. Of these, the DH clusters defined as being influenced only by fire were the most dominant on the landscape with burn1 accounting for 14.89%, burn2 for 6.42%, burn3 for 3.57%, and burn4 for 1.44%. This finding is attributed to the relatively large upland fires during the drought years of 1996 and 1997. Additionally, approximately 2% of the study area was annually flooded. Within the study area, 52% of the mapped DH clusters were influenced by either flooding or fire, while 48% were influenced by a combination of both flooding and fire.

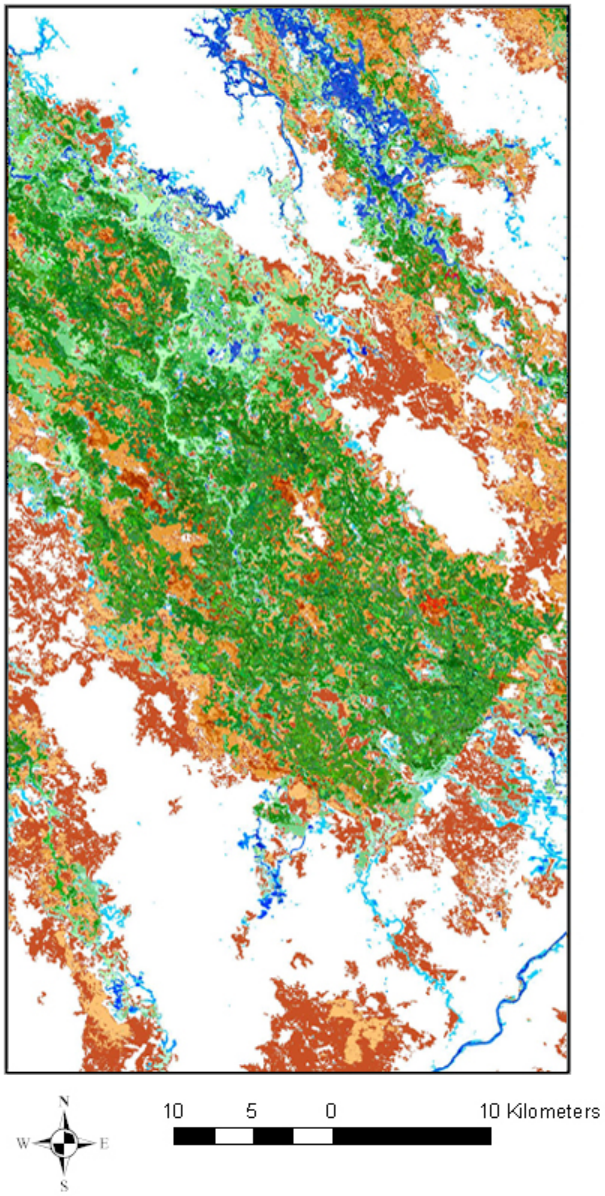

Figure 6.13. a) Disturbance history clusters. Shades of blue indicate locations in the study area influenced only by flooding. Shades of yellows, oranges, and reds indicate locations in the study area influenced only by fire. Shades of green indicate the co-location of both flooding and fire.

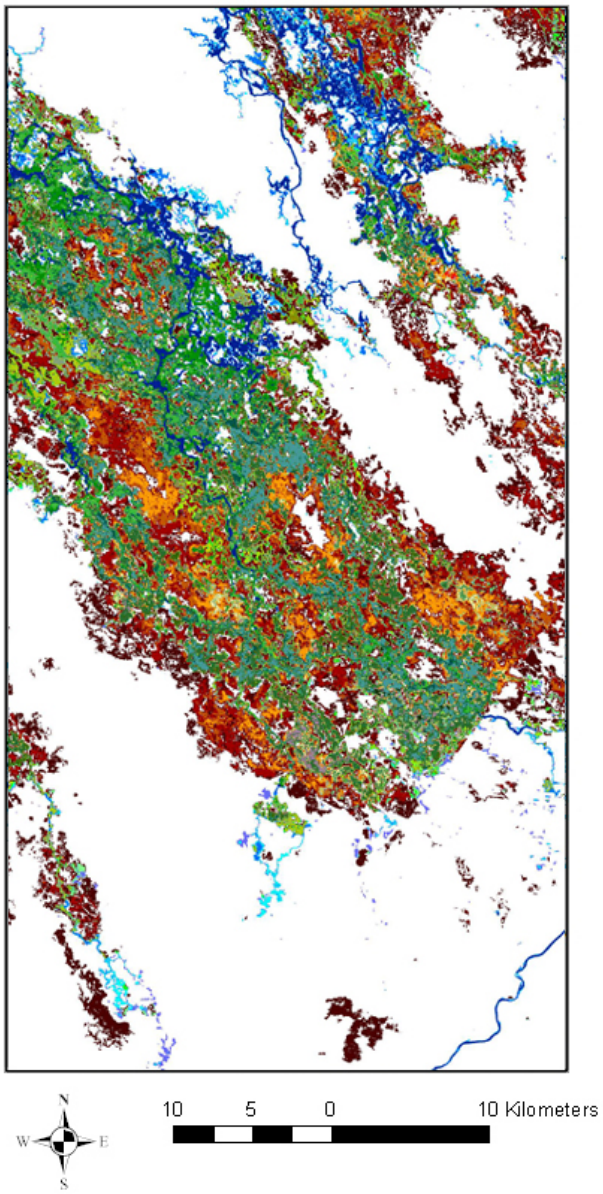

Figure 6.13 b) Disturbance return clusters. Shades of blue indicate locations in the study area influenced only by flooding. Shades of yellows, oranges, and reds indicate locations in the study area influenced only by fire. Shades of green indicate the co-location of both flooding and fire.

The statistics of disturbance return clusters were cross-tabulated against the vegetation types (as defined by HOORC) and plotted in Figure 6.14. The lower x-axis

represents the average return time in years for fire and the upper x-axis represents the average return time in years for flooding. The y-axis is the percentage of vegetation type that experiences a particular disturbance regime. For example, approximately 2.5% of savanna has an average fire return time of two years and a flood return time of three years. The trends for both the woodlands and savanna were as expected: fire is common for these two vegetation types and flooding does not appear to be a significant factor. The herbaceous vegetation, however, showed different trends where flooding with a return time of 1 (i.e., floods on average every year) was the most prevalent for all average fire return intervals.

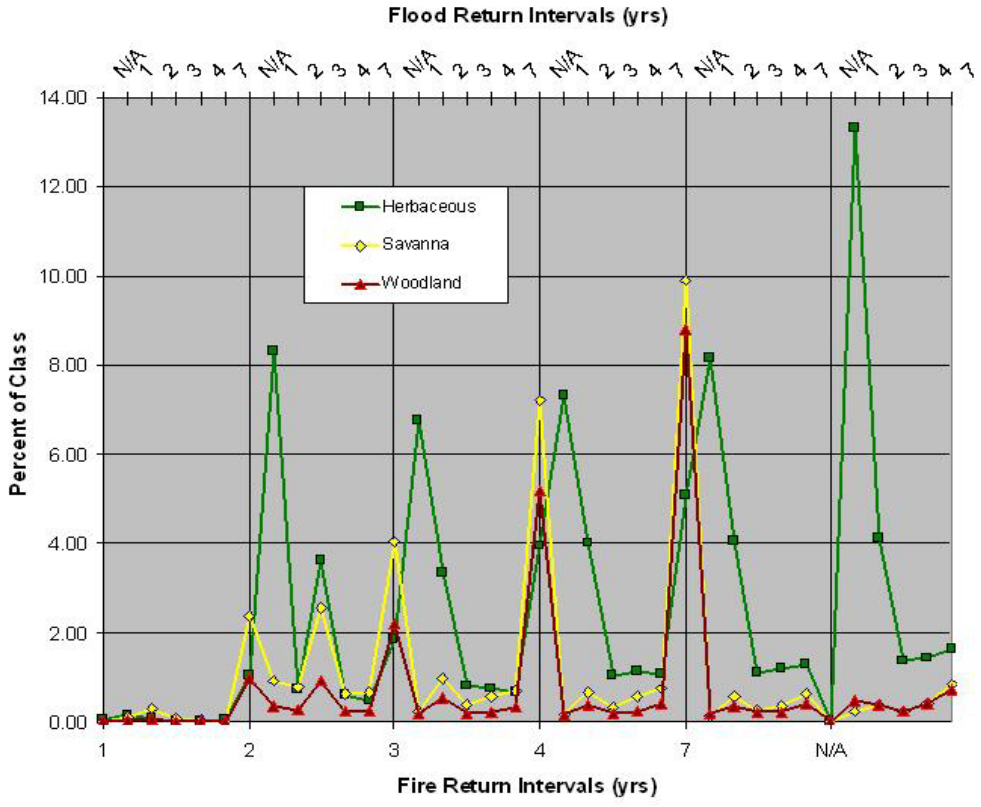

Figure 6.14. Percentage of vegetation type classes as a function of Disturbance Return clusters.

A similar analysis of the disturbance clusters was implemented on the HOORC vegetation structure classification. Figure 6.15 depicts the disturbance return trends for the woodland classes of LOSW, TOSW, TOTW, and LOBW. Again, all the woodland classes have a general trend of fire-only disturbances (with the exception of TOTW). While fire-only did account for the largest percentage of trends for this structure class, approximately 10% of this class was affected by flooding-only. Since much of the TOTW class consisted of riparian vegetation fringing the saline islands in the Boro and Santantadibe floodplains; there are three possible explanations for these results. It is conceivable that some of the pixels in this class were misclassified (classified as woodlands, but should be reeds/sedges), that flooding does periodically get high enough onto these islands, or that there is a slight misregistration error at some portion in the time-series. In Jellema et al. (2002), one of the biggest misclassification problems involved riparian zones and reeds in flooded areas due to the inseparability of the spectral signatures.

The disturbance trends for the shrubland classes (LDBS, LOTS, and LOGS) are shown in Figure 6.16. The LDBS (low dense bare shrubland) had virtually no disturbance trends in the 14-year period. This lack of disturbance is likely due to little herbaceous vegetation in this class necessary to sustain a surface fire (Whelen, 1995). The grassed and treed shrublands were associated with fire and seldom flooded with burning accounting for a larger percentage of the grassed shrublands over the treed shrublands.

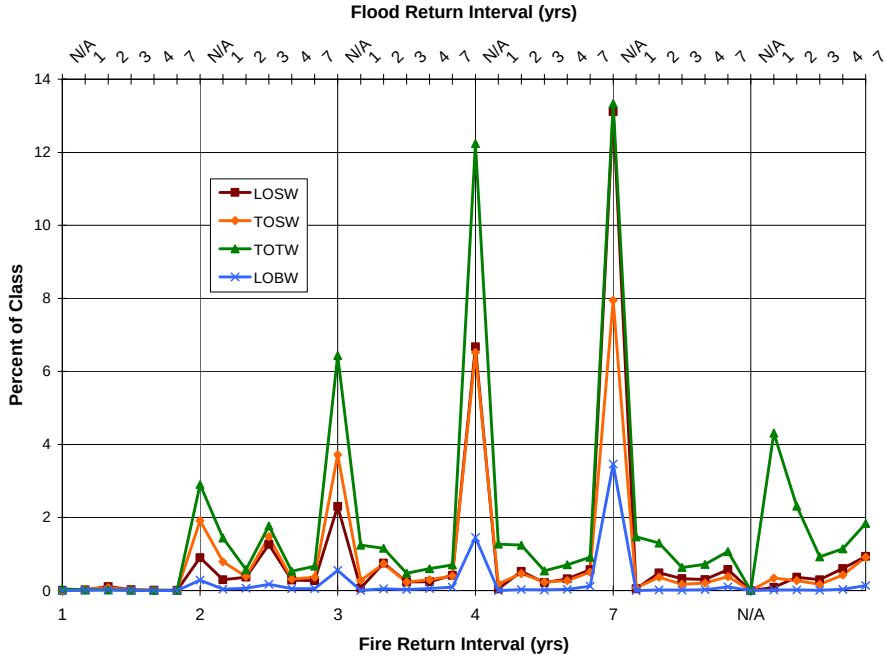

Figure 6.15. Percentage of HOORC structure WOODLAND classes as a function of Disturbance return clusters.

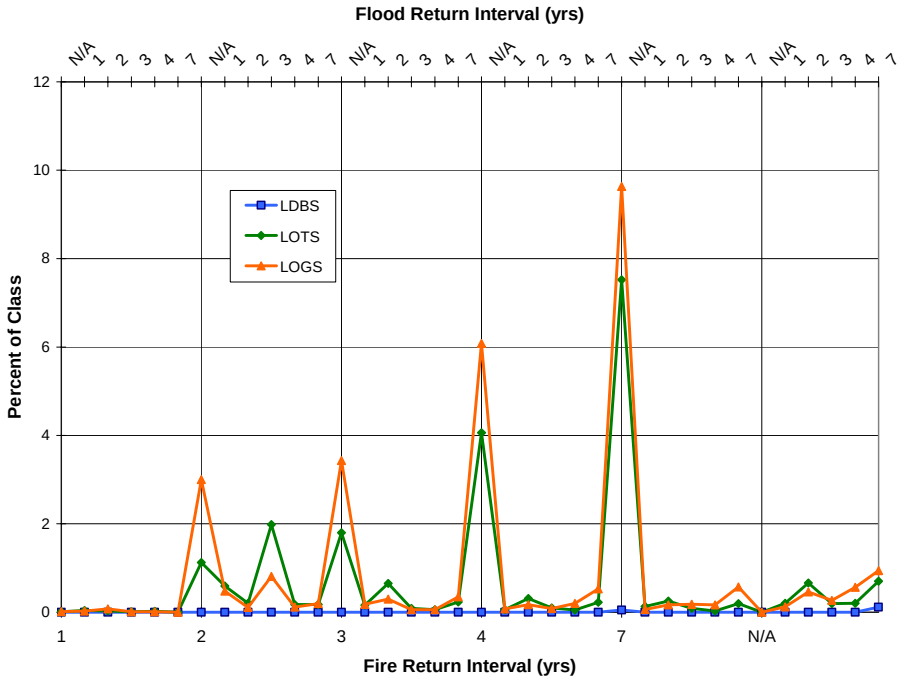

Figure 6.16. Percentage of HOORC structure SHRUBLAND classes as a function of Disturbance return clusters.

The disturbance trends associated with the grassland structure classes (LOBG, LOSG, LOGG, LDSG, TOTG, and TDGG) are perhaps the most interesting and are shown in Figure 6.17. The LOBG class showed virtually no association with either flooding or fire, again likely due to the low amount of herbaceous vegetation in this class. The low open shrubbed grassland, low dense shrubbed grassland, and tall open treed grassland were associated with fire only. These classes likely occur in the upland areas and are not located within the floodplains. The low open grassed grassland was associated primarily with fire, but approximately 14% of this class also experienced flooding. Approximately 16.4% of the tall dense grassed grasslands class was associated fire-only and 20.7% was associated with flooding-only: the remaining 49.5% of the class was associated with both flooding and fire.

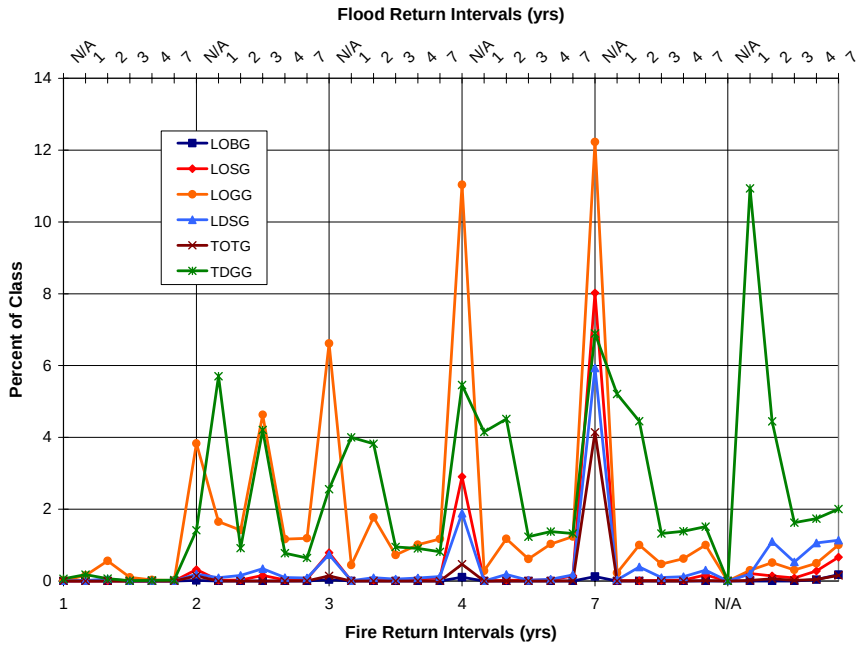

Figure 6.17. Percentage of HOORC structure GRASSLAND classes as a function of Disturbance return clusters.

The results indicate that the grasses within the floodplains experience a greater frequency of burning than the grasses in savanna. Since the seasonality of the floodplain fires occur during the dry winter months, this finding is an indication that the floodplain fires are likely ignited by people, whether purposely or accidental. Since fire seems to be a frequent occurrence on the floodplains, it is suggested here that fire is a major ecological driver for shifting plant functional types in these areas. Additionally, the presence and history of fire has established fire tolerant communities.

In all, the association of flooding and fire regimes with various vegetation type and structure met expectations. Floodplain grasslands experienced the greatest amount of burning and flooding and most of the shrublands and woodlands were impacted only by fire. However, aspatial analysis of disturbance patterns provides one piece of information regarding how this ecosystem functions. The utilization of vegetation type and structure maps derived from one point in time ignores the spatio-temporal configuration of the landscape. As such, subtle shifts or trends within a landcover class are missed. Further, the intricate role that flooding and fire play on vegetation dynamics is not captured. The following chapter will examine vegetation dynamics of the landscape to assess the impact of the flooding and fire regimes on the vegetation from a multi-temporal perspective.

The results presented in this chapter addressed the two hypotheses that fire frequency is highest in the Wildlife Management Areas closest to the Buffalo Fence and that the largest number of fires occurs within the active floodplains. The burning and flooding histories in the study area confirm both hypotheses and that the pixels having the greatest fire frequency in the 14-year history occur with 5 km of the Buffalo fence within

the WMAs. In addition, approximately 75% of the pixels that burned 7 or more times fall within the active floodplain. These results have potential implications on the management and burning policies of the ODMP, discussed in Chapter 8.

7 MULTI-TEMPORAL CLASSIFICATION

The objective of this chapter is to examine vegetation spectral response through time at the landscape level *via* remotely sensed imagery. The results presented in this chapter provide insight into the extent to which cyclical flooding and fire are related to ecosystem change and/or resilience (no change) in the Delta environment.

The input dataset consisted of surface reflectances using the Dark Object Subtraction (DOS) method. The Enhanced Vegetation Index (EVI) was selected for use as it is a widely used and accepted indicator of vegetation vigor that minimizes some of the weakness common with NDVI (see Chapter 4). EVI has been reported to be more sensitive to weak vegetation signals in semi-arid savannas by minimizing the soil background (Huete et al., 1997). EVI was derived for each date and served as a surrogate for vegetative productivity or vigor. Pixels having a similar EVI value through the time-series were grouped using an ISODATA clustering algorithm. The ISODATA was run such that 35 output clusters were output with a maximum of 20 iterations, a minimum of 5000 pixels per cluster, and a maximum class standard deviation of 0.25. Thirty-five output clusters were selected based upon spectral and information classes previously identified in landcover mapping studies of the area (12 classes in McCarthy, J. et al., 2003; 23 classes in Neuenschwander et al., 2005). Further, both a reduction and threshold in class separability supported the cutoff at 35 clusters, yielding a manageable and interpretable set of clusters and results. The output product from this clustering represents regions on the landscape that are temporally and spectrally statistically similar, though not necessarily spatially contiguous. The spatial distribution of the 35 EVI-based

temporal clusters is mapped in Figure 7.1. The results from the ISODATA were used to derive landscape trajectories to provide information regarding the vegetation dynamics. Table 7.1 summarizes the average existence of flooding and fire for each EVI cluster. A *yes* corresponds to a percentage of disturbed pixels above 25% (25% threshold was arbitrarily chosen) for any time in the time-series, *weak* corresponds to a percentage less than 25%, *once89* indicates a significant influence but only in 1989, and *no* indicates no presence of flooding or fire for that class.

Table 7.1. Average existence of flooding and fire for each EVI cluster between 1989 - 2002.

EVI Cluster	Flood	Fire	EVI Cluster	Flood	Fire
1	yes	yes	**19**	no	weak
2	yes	yes	**20**	no	no
3	yes	yes	**21**	weak	yes
4	yes	yes	**22**	no	no
5	yes	yes	**23**	no	no
6	yes	weak	**24**	no	no
7	yes	weak	**25**	no	no
8	once89	yes	**26**	no	no
9	weak	yes	**27**	no	no
10	once89	yes	**28**	no	no
11	weak	weak	**29**	no	no
12	weak	weak	**30**	no	no
13	no	weak	**31**	no	no
14	no	weak	**32**	no	weak
15	no	yes	**33**	yes	yes
16	no	yes	**34**	no	no
17	no	yes	**35**	no	no
18	no	yes			

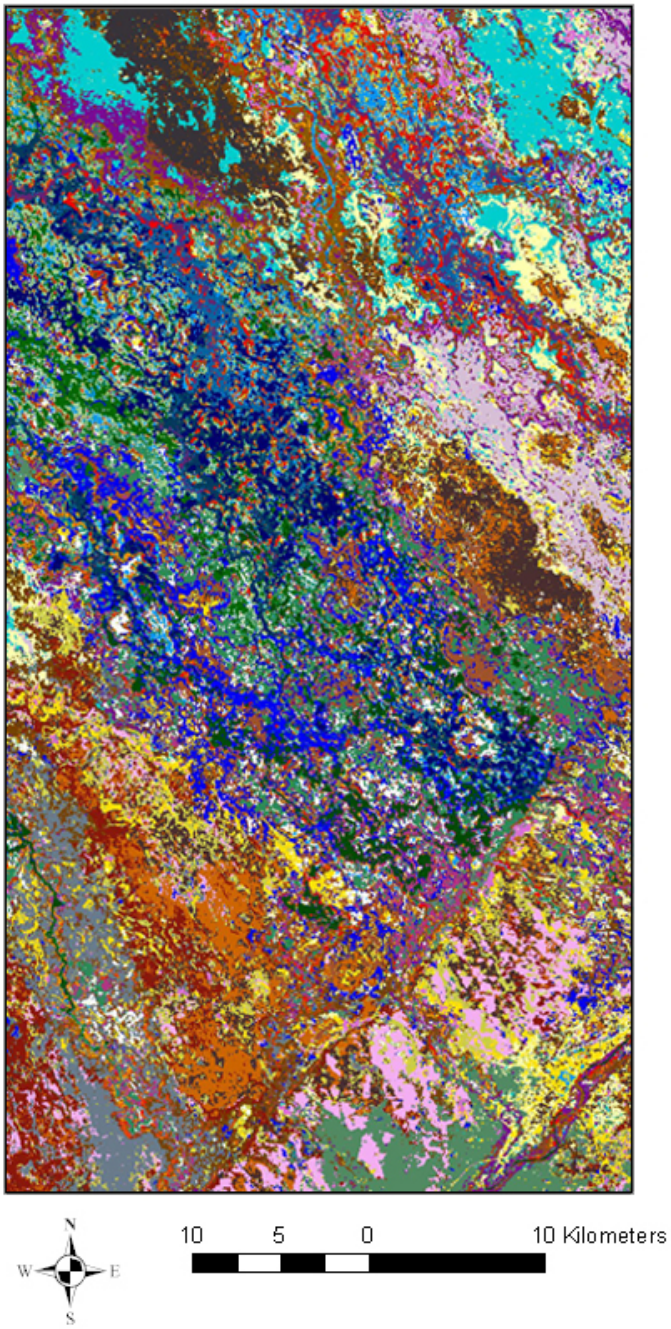

Figure 7.1. Thirty-five EVI-based temporal clusters result of ISODATA classification

Statistics were computed for each spatio-temporal class on the EVI time-series to create cluster trajectories shown in Figure 7.2. The ISODATA method, as implemented

in the ENVI software, clusters pixels into groups based upon statistics (mean and separability distance) such that the resulting groups will tend to be ordered. That is, cluster 1 will have the lowest mean EVI value and cluster 35 will have the highest mean EVI value.

General trends of the EVI time-series include a seasonal variation with highest EVI values occurring during the wet, summer months (November through March) and lowest EVI values occurring during the dry, winter months of May through August. Again, the annual flood pulse typically reaches this region of the Delta during the winter months. Since EVI is typically regarded as an indicator for photosynthesizing vegetation, it is presumed here that low EVI values are a result of water (in some capacity), bare soil, or non-photosynthesizing vegetation. Thus in a general sense, it is presumed that signatures that maintain the lower third of the time-series envelope have different slope/lags, compared to the general harmonic nature of the signal, are water and wetland classes (e.g. vegetation in a periodically flooded channel). Signatures that appear to follow an annual cycle are generally considered to be vegetation. EVI clusters 1 through 7 form the lower envelope of the temporal trajectories and they are associated with channels and the seasonal floodplains. Both cluster 34 and 35 which form the upper envelope of EVI trajectories were associated with riparian vegetation along the Boro and Santantadibe channels at the northern extent of the study area. The vegetation in these two clusters is a combination of trees only found along the islands (i.e. *Hyphaenae, Ficus* spp.) as well as a presence of reeds.

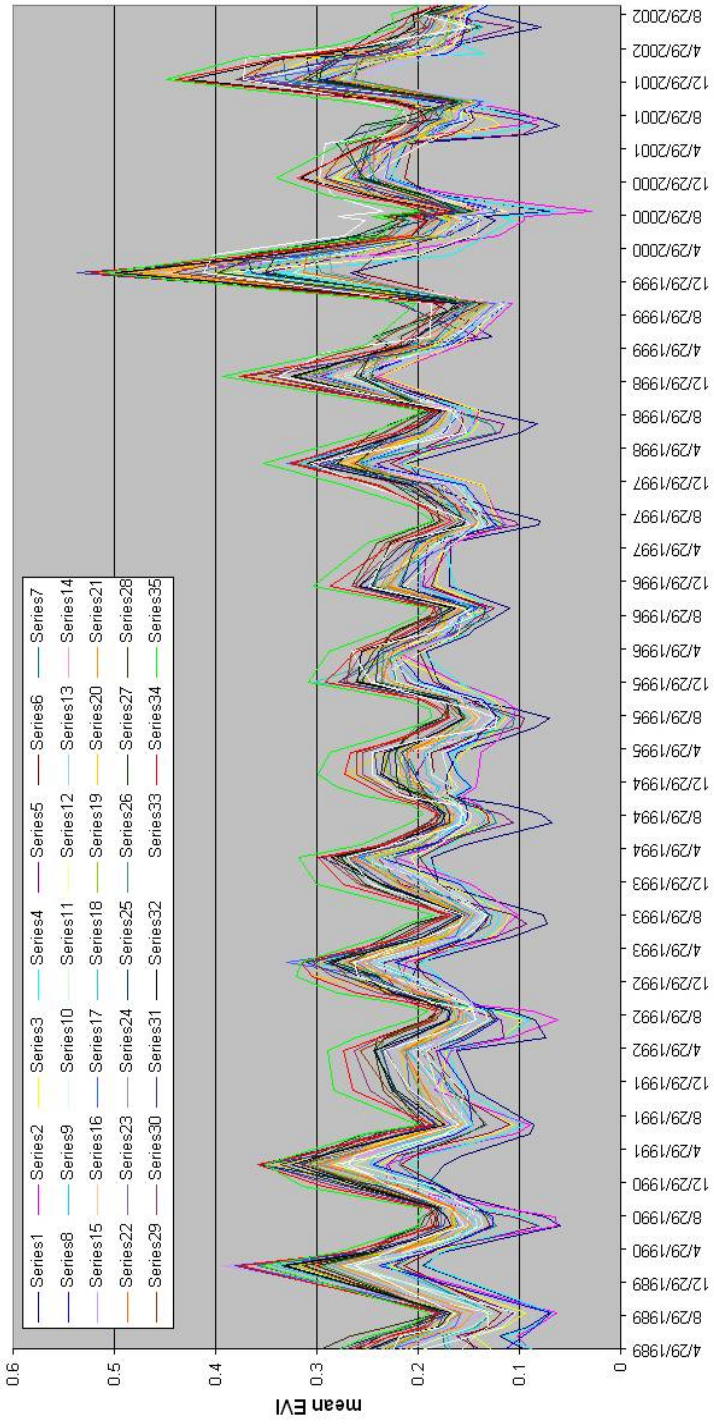

Figure 7.2. Trajectories based on mean EVI values for 35 EVI clusters.

Table 7.2 indicates the association of EVI clusters with different floodplain types (drying, less active, and active). The landcover type associated with each EVI cluster is defined based upon recent fieldwork (2006 and 2007), interpretation of pan-sharpened ALI imagery from September 2003, and the 1999 vegetation map produced by HOORC. The floodplains were designated such that drying floodplains flooded at least once between 1989 through 1992, but did not flood anytime afterward. Active floodplains correspond to areas that flood at least every other year. Less active floodplains have flooded at least once in the 14-year history. In the calculation of EVI, pixels dominated by water, soil, sparse vegetative cover, or non-green vegetation biomass will result in low EVI values. Thus, the first few ISODATA clusters are located in areas that are periodically wet. This is apparent by examining the percentage of pixels in each floodplain against the EVI cluster. The active floodplain largely consisted of pixels from EVI cluster 1 – 5 and 7. The largest contributor to pixels within the less active floodplains was EVI cluster 6. Similarly, the largest percentages of pixels within the drying floodplains were EVI clusters 8 and 9.

Table 7.2 Spatial extent of EVI clusters for different floodplain levels during 1989 - 2002. Drying floodplains did not flood in the last 10 years of the study, active floodplains flood at least every other year, and less active floodplains are floodplains that did not fit the other two categories. (Green 5 – 10%, yellow 10-20%)

		Drying floodplain		Less Active Floodplain		Active Floodplain	
EVI Cluster	**Landcover**	**Hectares**	**Percent**	**Hectares**	**Percent**	**Hectares**	**Percent**
1	channel	0.0	0.0	0.1	0.0	5,117.0	13.4
2	floodplain grasses	237.2	1.1	224.9	1.7	6,072.2	15.9
3	sedge	36.1	0.2	129.6	1.0	4,845.0	12.6
4	floodplain grasses	599.8	2.9	1,046.4	8.1	3,132.1	8.2
5	sedge/hippo grass	6.3	0.0	17.6	0.1	6,432.3	16.8
6	secondary floodplain	3,850.7	18.5	1,719.7	13.4	612.0	1.6
7	miscanthus/sedge	241.6	1.1	680.9	5.3	4,281.7	11.2
8	acacia grassland	4012.1	19.3	733.2	5.7	88.1	0.2
9	island shrub vegetation	3,659.4	17.6	780.0	6.1	308.8	0.8
10	grasses	1,471.1	7.1	1,121.5	8.7	1,235.5	3.2
11	grasses/sage	488.1	2.3	690.4	5.4	1,189.8	3.1
12	treed grassland	494.7	2.4	661.8	5.1	202.7	0.5
13	grasses	418.2	2.0	92.6	0.7	5.8	0.0
14	acacia grassland	118.6	0.6	115.9	0.9	42.6	0.1
15	shrubbed woodland	940.3	4.5	205.1	1.6	12.6	0.0
16	acacia thickets	301.5	1.4	203.6	1.6	169.1	0.4
17	shrubbed woodland	71.6	0.3	33.9	0.2	6.4	0.0
18	acacia shrubbed savanna	383.8	1.8	231.2	1.	45.7	0.1
19	grasses/savanna	59.9	0.3	20.1	0.1	4.9	0.0
20	acacia savanna	580.9	2.8	646.	5.0	392.7	1.0
21	shrubbed islands	941.9	4.5	930.8	7.2	444.9	1.1
22	mopane woodlands	152.8	0.7	28.5	0.2	3.3	0.0
23	grasses	139.9	0.7	69.5	0.5	23.5	0.0
24	mopane woodlands	31.1	0.1	30.4	0.2	21.7	0.0
25	scrub mopane	11.1	0.0	24.2	0.2	19.4	0.0
26	mopane woodlands	7.2	0.0	2.5	0.0	2.5	0.0
27	mixed mopane	0.5	0.0	3.1	0.0	0.0	0.0
28	mixed mopane on CI	3.7	0.0	4.0	0.0	2.4	0.0
29	riparian island fringe	7.0	0.0	7.6	0.0	2.5	0.0
30	riparian woodlands	304.0	1.4	134.1	1.0	14.7	0.0
31	acacia thickets	124.0	0.6	882.9	6.9	1,182.1	3.1
32	riparian woodlands	393.0	1.9	265.4	2.1	94.3	0.2
33	hippo grass	21.4	0.1	134.9	1.0	1,832.9	4.8
34	riparian woodlands	465.1	2.2	509.7	3.9	169.7	0.4
35	riparian woodlands	178.0	0.8	459.5	3.6	229.2	0.6

Table 7.3. Spatial extent of EVI clusters for different fire levels during 1989 – 2002. Low fire are 1 -2 burns, intermediate fire is 3 – 7burns, and high fire indicates pixels burned 8 or more times between 1989 – 2002.(Green 5 – 10%, yellow 10-20%)

		Low Fire		Intermediate Fire		High Fire	
EVI Cluster	**Landcover**	**Hectares**	**Percent**	**hectares**	**Percent**	**hectares**	**Percent**
1	channel	1,698.7	2.1	2,828.9	5.4	69.8	4.1
2	floodplain grasses	692.1	0.9	4,986.1	9.6	813.9	48.0
3	sedge	1,601.2	2.0	3,309.9	6.4	24.9	1.5
4	floodplain grasses	1,346.6	1.7	3,618.7	7.0	237.8	14.0
5	sedge/hippo grass	2,654.1	3.3	2,906.0	5.6	90.6	5.3
6	secondary floodplain	1,555.6	1.9	4,654.5	9.0	123.1	7.2
7	miscanthus/sedge	2,897.6	3.6	1,798.1	3.5	31.5	1.9
8	acacia grassland	2,697.4	3.4	870.4	1.7	0.9	0.0
9	island shrub vegetation	2,023.5	2.5	5,340.4	10.3	76.5	4.5
10	grasses	1,596.3	2.0	3,510.0	6.8	99.3	5.9
11	grasses/sage	2,204.7	2.8	1,082.8	2.1	2.9	0.2
12	treed grassland	3,241.6	4.0	1,548.8	3.0	0.0	0.0
13	grasses	4,870.4	6.1	1,247.0	2.4	2.7	0.1
14	acacia grassland	3,835.9	4.8	252.2	0.5	0.0	0.0
15	shrubbed woodland	3,482.3	4.	3,723.4	7.1	21.8	1.3
16	acacia thickets	3,511.3	4.4	553.7	1.0	1.4	0.1
17	shrubbed woodland	3,509.3	4.4	166.1	0.3	0.1	0.0
18	acacia shrubbed savanna	3,448.4	4.3	912.4	1.7	1.0	0.0
19	grasses/savanna	1,355.7	1.7	108.7	0.2	0.0	0.0
20	acacia savanna	1,755.2	2.2	2,500.7	4.8	19.1	1.1
21	shrubbed islands	3,642.4	4.6	1,626.3	3.1	4.2	0.2
22	mopane woodland	4,639.1	5.8	218.7	0.4	0.0	0.0
23	grasses	2,444.2	3.0	437.4	0.8	0.4	0.0
24	mopane woodlands	2,199.7	2.7	73.2	0.1	0.3	0.0
25	scrub mopane	2,227.2	2.8	79.3	0.1	5.4	0.3
26	mopane woodlands	1,101.3	1.4	21.1	0.0	0.0	0.0
27	mixed mopane	201.1	0.2	0.7	0.0	0.0	0.0
28	mixed mopane on CI	536.8	0.7	4.0	0.0	0.0	0.0
29	riparian island fringe	107.2	0.1	16.2	0.0	0.0	0.0
30	riparian woodlands	2,307.9	2.9	468.9	0.9	1.7	0.1
31	acacia thickets	1,817.4	2.3	901.9	1.7	41.9	2.5
32	riparian woodlands	2,760.5	3.4	603.0	1.1	6.4	0.4
33	hippo grass	816.9	1.0	505.9	0.9	13.3	0.8
34	riparian woodlands	3,273.4	4.1	690.3	1.3	1.4	0.1
35	riparian woodlands	1,456.4	1.8	224.3	0.4	0.0	0.0

Similar statistics of the EVI clusters were computed and compared to fire levels. The fire levels correspond to low levels of burning in the time-series (one - two years burned), intermediate levels of burning (three – seven years burned), and high levels of burning (more than seven years). Areas of low levels of burning generally tended to be evenly distributed across EVI clusters. The EVI clusters that were associated with intermediate levels of burning occurred in EVI clusters 2, 6, and 9. These clusters are associated with the floodplains. Areas that experienced high levels of fire are associated with EVI cluster 2 and 4, with 48% of the pixels that were burned frequently in cluster 2. The association between intermediate and high levels of burning and EVI clusters in the floodplains is not unexpected. As described in the previous chapter, a significant portion of the burning on this landscape occurs with the floodplains.

7.1 Multi-temporal Landcover Trajectory Results

Rodriguez-Arias and Rodo (2004) describe ecosystem trajectories as comprised of permanent signals (consisting of a trend and cycles) and transitory signals (consisting of stochastic behavior). For each cluster identified in the EVI ISODATA results, the mean EVI value was computed for each date in the time-series. The mean EVI values were subsequently used to create an 85 element vector for each cluster resulting in 35 unique EVI-based landcover trajectories. Harmonic regression was used to determine the parameters of the permanent signal for each land cover trajectory.

7.1.1 Harmonic Regression Results

A harmonic regression was implemented on each EVI-based trajectory to extract general trends and dynamics for each EVI class. The motivation for implementing a harmonic regression in this research is to quantitatively describe the trends and patterns of land cover trajectories hypothesized to correspond to cyclical events or processes. The harmonic regression model used in this research takes the form

$$y = \beta_0 + cT + \sum_{i=1}^{m} A_i \sin\left(\frac{2\pi i}{s} T + \phi_i\right) \qquad \textbf{Equation 7-1}$$

where β_0 is an offset, c is the trend, A_i is the amplitude of the i^{th} oscillation, ϕ_i is the phase component of the i^{th} oscillation, s is the fundamental frequency (in this case, one year), and T is the dependent time variable. First, a bias, trend, semi-annual and annual cycles were fit to the data. An annual cycle was modeled to account for annual variability in the signal. Similarly, since the Okavango Delta is located within the subtropics, a semi-annual (6 months) cycle was included to represent the distinct wet/dry seasonality of the region. The t-test and 2-tailed significance of each model coefficient (i.e. trend, semi-annual, and annual terms) for each EVI cluster are listed in Table 7.4. The annual cycle was statistically significant for all EVI clusters. The semi-annual cycle was statistically significant for all but four EVI clusters, each of which was located in the Boro River floodplain. The trend, whether positive or negative, was statistically significant for nineteen of the EVI clusters.

Table 7.4. Two-tailed t-test and significance of each model coefficient term for all 35 EVI clusters. Significant coefficients are highlighted in yellow.

EVI Cluster	Trend		Semi-annual		Annual	
	t-test	p	t-test	p	t-test	p
1	5.82	< 0.0001	1.93E+00	0.0286	15.34	< 0.0001
2	3.65	0.0002	-1.55E+00	0.0614	10.70	< 0.0001
3	4.43	< 0.0001	-1.56E+00	0.0614	9.81	< 0.0001
4	3.64	0.0002	9.45E-01	0.1738	10.48	< 0.0001
5	5.43	< 0.0001	2.25E+00	0.0137	14.36	< 0.0001
6	6.92	< 0.0001	2.29E+00	0.0124	19.68	< 0.0001
7	8.92	< 0.0001	1.75E+00	0.0421	14.38	< 0.0001
8	4.43	< 0.0001	3.27E+00	0.0008	11.77	< 0.0001
9	5.31	< 0.0001	2.78E+00	0.0034	13.95	< 0.0001
10	3.54	0.0003	-3.43E+00	0.0005	12.15	< 0.0001
11	2.38	0.0099	-4.20E+00	< 0.0001	14.94	< 0.0001
12	1.19	0.1189	6.32E+00	< 0.0001	17.74	< 0.0001
13	-0.28	0.3901	-4.24E+00	< 0.0001	12.57	< 0.0001
14	-1.08	0.1418	5.21E+00	< 0.0001	17.62	< 0.0001
15	0.09	0.4643	5.22E+00	< 0.0001	12.09	< 0.0001
16	-0.25	0.4016	4.25E+00	< 0.0001	12.69	< 0.0001
17	-0.60	0.2751	5.28E+00	< 0.0001	14.39	< 0.0001
18	1.52	0.0663	4.48E+00	< 0.0001	14.14	< 0.0001
19	-1.15	0.1269	6.20E+00	< 0.0001	17.30	< 0.0001
20	-0.36	0.3599	-6.22E-03	< 0.0001	16.34	< 0.0001
21	4.57	< 0.0001	-3.32E+00	0.0009	14.16	< 0.0001
22	1.65	0.0515	-4.28E+00	< 0.0001	17.29	< 0.0001
23	0.95	0.1725	4.90E+00	< 0.0001	16.62	< 0.0001
24	1.82	0.0363	-4.52E+00	< 0.0001	17.00	< 0.0001
25	0.13	0.4485	2.63E+00	0.0052	13.97	< 0.0001
26	-0.25	0.4094	-4.10E+00	< 0.0001	15.30	< 0.0001
27	2.24	0.0140	-4.14E+00	< 0.0001	15.25	< 0.0001
28	0.23	0.4094	-4.07E+00	< 0.0001	13.96	< 0.0001
29	4.56	< 0.0001	3.93E+00	0.0001	18.33	< 0.0001
30	-0.99	0.1626	-5.01E+00	< 0.0001	16.18	< 0.0001
31	0.25	0.4016	5.00E+00	< 0.0001	14.61	< 0.0001
32	3.43	0.0005	-3.59E+00	0.0003	14.98	< 0.0001
33	6.96	< 0.0001	1.36E+00	0.0889	13.48	< 0.0001
34	1.94	0.0280	-4.05E+00	< 0.0001	17.70	< 0.0001
35	3.63	0.0003	-3.85E+00	0.0001	18.81	< 0.0001

7.1.2 Residual Analysis of EVI Clusters

As noted earlier, ecological time-series data may consist of longer term signals in addition to the seasonal and annual signals. For each EVI-based trajectory, the residuals from the semi-annual and annual fit were extracted and subsequently examined to identify any additional cycles beyond the initial fit. An example of a residual trajectory after removing a semi-annual and annual fit is shown in Figure 7.3. In each of the residual trajectories, an annual pattern was observed superimposed on a longer-term curve. The observed annual pattern exists in the residual signal because the regression model assumes constant amplitude for the annual signal. Since the amplitude of the annual signal varies, there is a residual annual term. The periodicities, however, of a longer-term trend are not known but they can be determined via wavelet analysis.

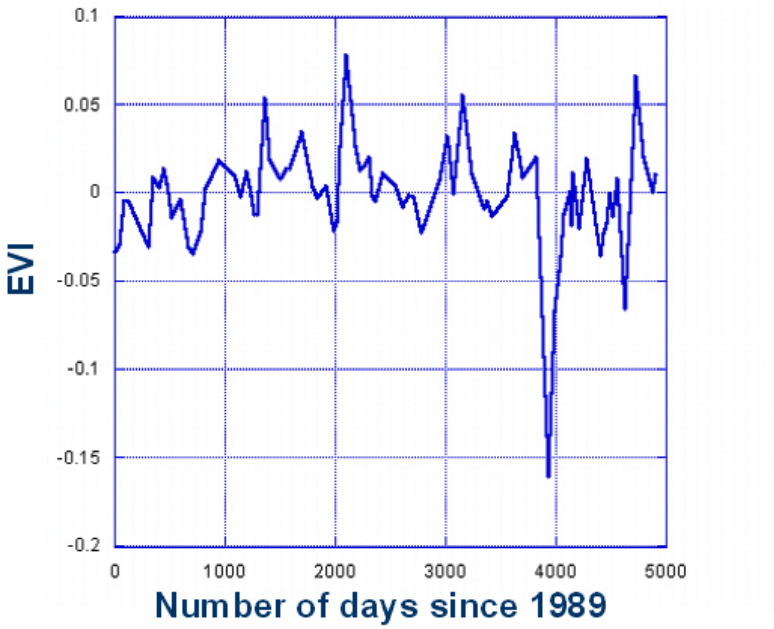

Figure 7.3. Example of residual signal of EVI trajectory after removing semi-annual and annual harmonic fit.

7.2 Wavelet Analysis

An instrumental tool in understanding the patterns (the key frequencies and when they occur) for time-series analysis is wavelet analysis. Wavelet analysis using a Morlet mother wavelet was implemented on the EVI-based trajectories as well as on precipitation records and climate indices to characterize the temporal variability of cyclic behavior in time-series. Due to the uneven temporal spacing of the satellite EVI time-series, the EVI-based trajectories were interpolated into 15.5-day intervals using Kaleidagraph software for subsequent analysis.

7.2.1 EVI Cluster Vegetation Analysis

Each interpolated EVI-trajectory and EVI-residual trajectory was analyzed using wavelet analysis with the Morlet wavelet as the mother wavelet. In addition, trajectories for both flooding and fire were created for each EVI cluster. The value of flooding and fire for each date range from 0 – 1 and represent the percentage of pixels identified as either flooding or fire for a given cluster. The wavelet power spectrum and global wavelets for all 35 EVI trajectories are located in Appendix A.1. As an example, the wavelet power spectrum for the residual trajectory as well as the flooding and fire trajectories for EVI cluster 2 are shown in Figure 7.4a-c. Cluster 2 was chosen as an example because it lies within the floodplain but experienced drought during the mid-90s. Figure 7.4a indicates a decrease in annual vegetation productivity from 1994 – 1998. Figure 7.4b indicate however that flooding was strong for this class during the years of 1989 – 1992 and 1999 – 2002 and was not a factor during the period of 1993 – 1998.

Additionally, while fire occurred in cluster 2 in roughly every year to every other year, the fire signal is strongest in the years where flooding was not present.

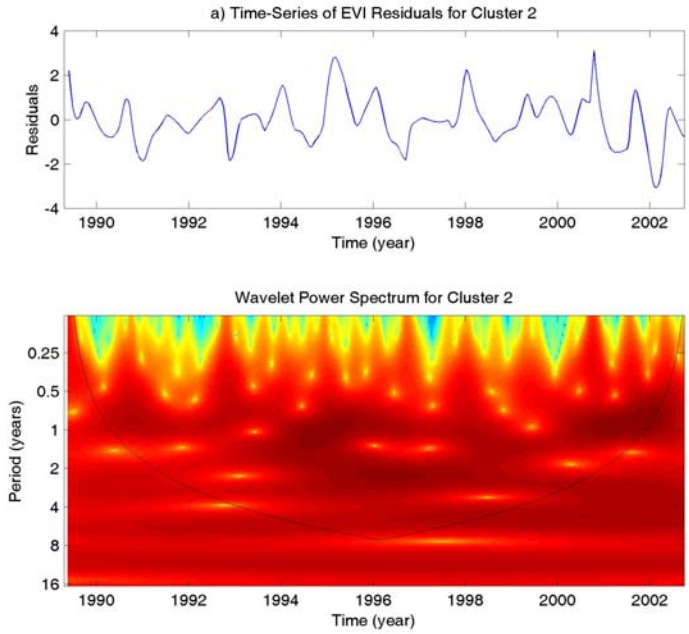

Figure 7.4a. Wavelet power spectrum for EVI cluster 2 for Residual EVI trajectory

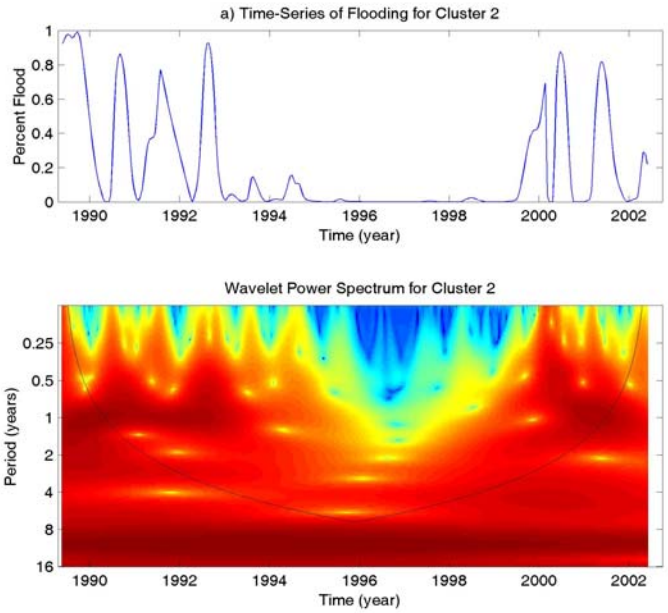

Figure 7.4b. Wavelet power spectrum for EVI cluster 2 for flooding trajectory

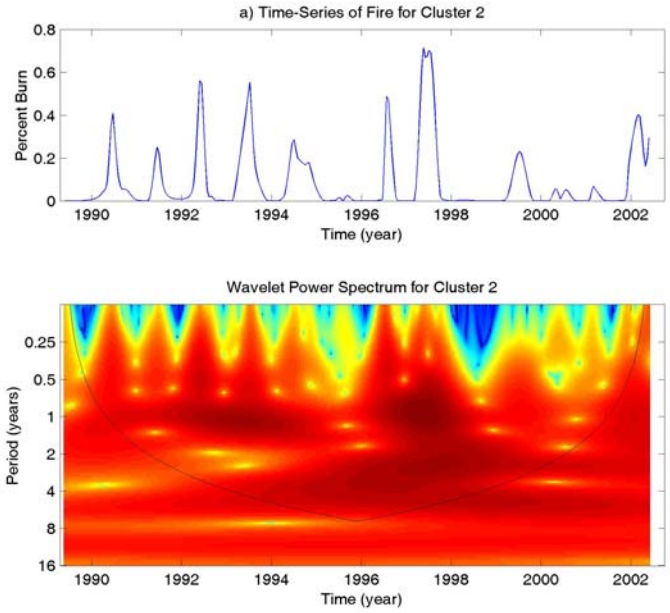

Figure 7.4c. Wavelet power spectrum for EVI cluster 2 for fire trajectory

The utilization of wavelet analysis on time-series data allows for the extraction of dominant periodicities in the data. The global wavelet can be regarded as the time average of the periodicities and is roughly equivalent to the periodicities obtained using Fourier analysis. The global wavelet for the EVI cluster 2 residuals is shown in Figure 7.5. A large oscillation of 1.0 years dominates the residual signal with additional oscillations occurring at 2.6, 5.1 and 10.9 years. The 2.6 year cycle in the residual signal is strongest during the mid 90s when there was no flooding for this cluster.

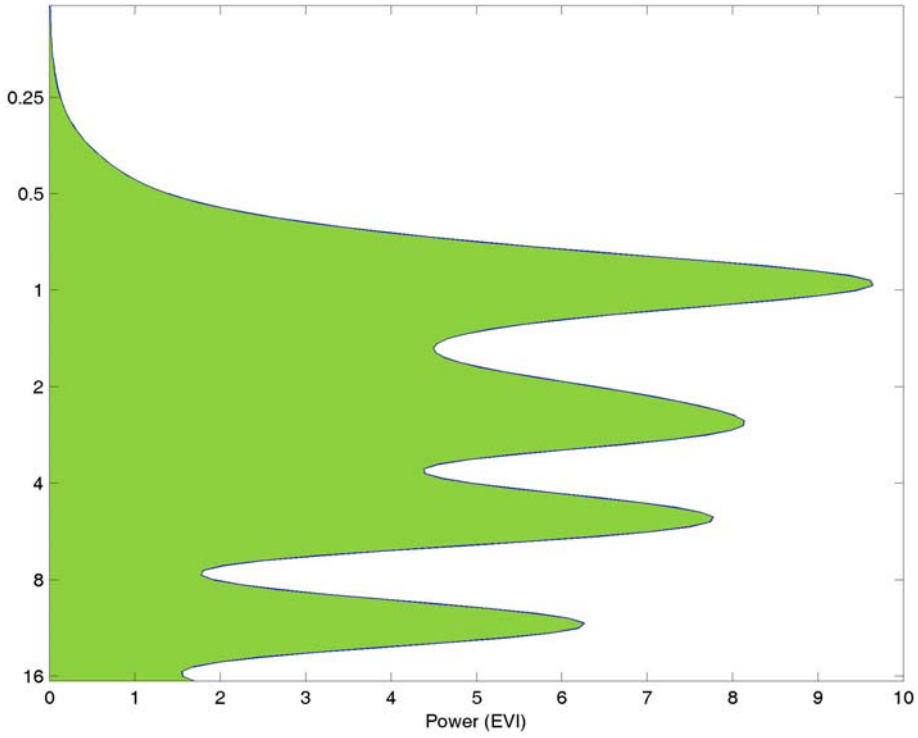

Figure 7.5. Global wavelet for EVI cluster 2 residuals. Periodicities of 1, 2.6, 5.1, and 10.9 years were identified.

McCarthy et al. (2000) report 3, 8, and 18-year oscillations in precipitation cycles, with the largest oscillation occurring at the 18-year interval. Hypothesis 3 tests whether periodicities from vegetation signal time-series exhibit published climate periodicities of 3-, 8-, and 18-years. The dominant periodicities for each EVI-residual cluster are reported in Table 7.5. Since the temporal extent of this dataset is only 14 years, the presence of an 18 year oscillation could not be tested. For eight of the EVI-clusters, a ~3 year cycle was detected. The 8 year cycle reported by McCarthy was not evident in any of the EVI clusters. In all but six of the EVI-residual trajectories, a 10.9 year signal was detected as the dominant frequency from the wavelet analysis results. Of the six trajectories where

the 10.9 year signal was not the dominant signal, two had a dominant frequency of approximately 1 year, one had a dominant frequency of 1.7 years, two had a dominant frequency of 2.5 years, and 1 had a dominant frequency of 5.9 years; these are spatially presented in Figure 7.6. It is important to note that to have statistical confidence in the detected frequencies, the time-series should be at least twice as long as the cycles. The results here indicate that Hypothesis 3 is refuted since only eight EVI clusters had an approximately 3-year cycle. Further, the 8-year cycle was not observed for any of the EVI clusters and the 18-year cycle could not be tested due to the length of the time-series.

Table 7.6 reports the average disturbance return time for each of the EVI-residual clusters where the quasi-decadal signal did not have the greatest power. Clusters having a dominant frequency of 1 year were found to be associated with high levels of flooding (flooding approximately every year) and frequent burning (burning every one to two years), whereas the dominant 1.7 year residuals were associated with intermediate levels of burning (burning every three to four years) and no flooding. Similarly, clusters having the 2.5 year and 5.9 year dominant residual frequency were associated with low to intermediate amounts of burning (two to four times in the 14-year time-series) and flooding approximately every other year. These six classes are located in both the hunting and photography concessions, so management type is likely not an influencing factor. The fact that the dominant residual frequencies are not the quasi-decadal cycle for these six classes is an indication that flooding and fire may be affecting the vegetation dynamics differently than on other portions of the landscape.

Table 7.5. Periodicities (in years) of EVI residual global wavelets for each EVI cluster.

cluster	MAX	ALL Frequencies				
1	10.9	0.8	2.8	10.9	**	**
2	1.1	1.0	2.6	5.1	10.9	**
3	10.9	0.9	1.8	5.3	10.9	**
4	1.0	0.9	2.6	**	**	**
5	10.9	0.9	1.6	2.7	10.9	
6	10.6	1.0	1.6	10.9	**	**
7	10.9	1.0	1.5	3.9	10.9	**
8	1.5	2.5	4.9	**	**	**
9	10.6	1.0	1.5	10.9	**	**
10	10.9	2.4	4.9	10.9	**	**
11	1.6	0.7	1.7	4.4	10.9	**
12	10.9	0.6	1.3	2.7	5.9	11.3
13	10.9	0.7	1.5	5.5	10.9	**
14	10.9	0.6	1.4	2.3	10.9	**
15	10.9	1.1	2.3	5.9	10.9	**
16	10.9	0.6	1.6	5.3	10.9	**
17	10.9	0.4	1.5	2.8	10.9	**
18	10.9	0.6	1.4	2.6	10.9	**
19	10.9	0.6	1.5	10.9	**	**
20	10.9	0.6	1.5	4.9	10.9	**
21	10.9	1.0	1.7	5.3	10.9	**
22	10.9	0.7	1.6	3.7	5.3	10.9
23	10.9	0.6	1.5	10.9	**	**
24	10.9	1.6	3.3	5.5	10.9	**
25	10.9	1.6	10.9	**	**	**
26	10.9	1.6	3.0	10.9	**	**
27	10.9	1.6	3.3	10.9	**	**
28	10.9	0.7	1.5	2.8	10.9	**
29	10.9	0.7	1.6	10.9	**	**
30	10.9	0.6	1.6	10.9	**	**
31	10.9	0.6	1.5	6.1	10.9	**
32	10.9	1.0	1.7	5.5	10.9	**
33	10.9	1.5	3.9	10.9	**	**
34	10.9	0.7	1.6	10.9	**	**
35	10.9	1.0	1.7	10.9	**	**

While the disturbance return clusters were associated with the residual signals, the periodicities were not a direct match. For example, 54% of the pixels under the 1.7 year residual mask were only influenced by fire burning every third, fourth, and seventh year. However, there are several factors such as land management regime, plant competition, and floodplain location within each management regime that confound the interpretation of these clusters. For the 1-year residual case, 60% of the pixels flood on average every

year (with various levels of burning). However, in both of these cases the results presented are based upon cluster averages. Despite using an average, this method provides nuanced information that is not observable with traditional change detection techniques.

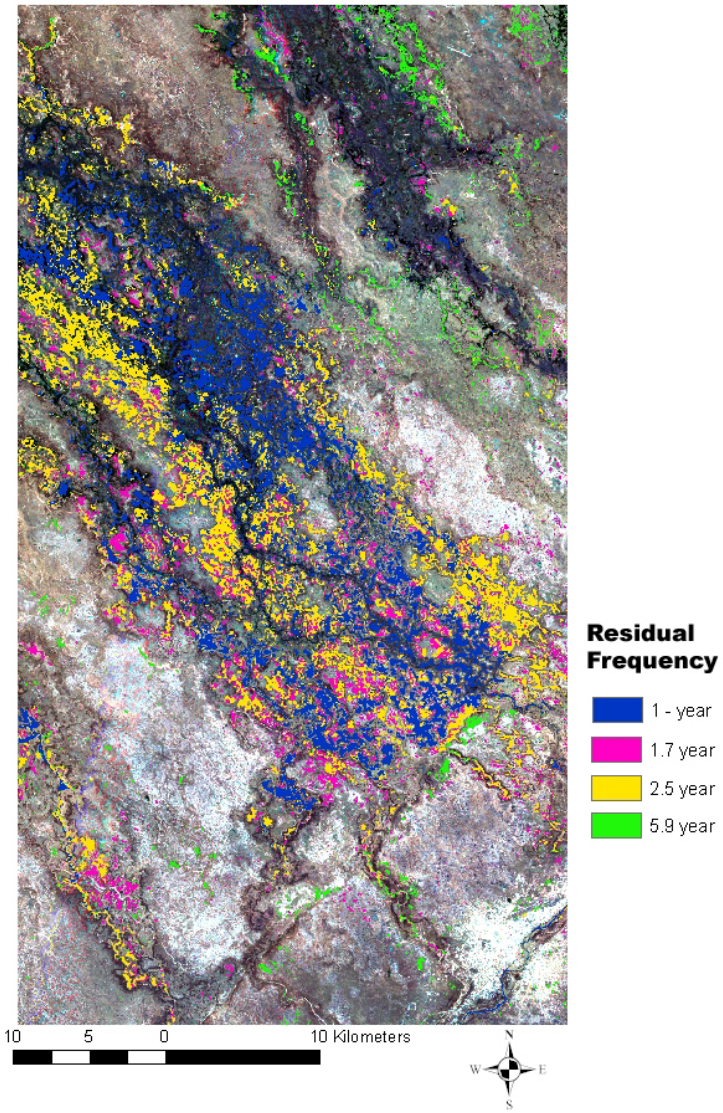

Figure 7.6. Portions of the distal Okavango where the dominant residual frequency was not 10.9 years.

Table 7.6. Distributions of disturbance return (average return time) clusters with 1-year, 1.7-year, 2.5-year, and 5.9-year residual signal. (green 5 – 10 %, yellow 10 – 20%, orange >20%)

	1-year		1.7 year		2.5-year		5.9 year	
	Pixels	%	Pixels	%	Pixels	%	Pixels	%
null	16	0.0	25181	35.5	8019	5.3	16750	49.2
B1F1	999	0.7	0	0.0	45	0.0	0	0.0
B1	1	0.0	4	0.0	31	0.0	0	0.0
B1F2	2511	1.8	0	0.0	86	0.0	0	0.0
B1F3	277	0.2	0	0.0	41	0.0	0	0.0
B1F4	52	0.0	3	0.0	48	0.0	0	0.0
B1F7	4	0.0	1	0.0	31	0.0	0	0.0
B2	13	0.0	3191	4.5	8271	5.4	82	0.2
B2F1	27211	19.9	17	0.0	3880	2.5	118	0.3
B2F2	3095	2.3	94	0.1	2348	1.5	90	0.2
B2F3	21330	15.7	59	0.01	5539	3.6	209	0.6
B2F4	943	0.7	188	0.2	3152	2.1	82	0.2
B2F7	109	0.1	416	0.6	4132	2.7	69	0.2
B3	13	0.0	7612	10.7	12351	8.1	316	0.9
B3F1	15519	11.4	8	0.0	3582	2.3	47	0.1
B3F2	9535	7.0	41	0.0	6438	4.2	367	1.1
B3F3	1172	0.8	53	0.0	2289	1.5	348	1.0
B3F4	378	0.3	122	0.1	4096	2.7	188	0.5
B3F7	56	0.0	573	0.8	4413	2.9	112	0.3
B4	18	0.0	14822	20.9	16076	10.6	1527	4.5
B4F1	13390	9.8	37	0.0	3869	2.5	163	0.4
B4F2	5692	4.2	45	0.0	8961	5.9	484	1.4
B4F3	806	0.6	28	0.0	2257	1.4	347	1.0
B4F4	264	0.2	85	0.1	4689	3.1	387	1.1
B4F7	64	0.0	577	0.8	5003	3.3	290	0.8
B7	7	0.0	15565	21.9	10429	6.8	3572	10.5
B7F1	13238	9.7	61	0.1	2550	1.6	290	0.8
B7F2	4098	3.0	79	0.1	8838	5.8	813	2.4
B7F3	857	0.6	37	0.0	1948	1.3	363	1.1
B7F4	171	0.1	75	0.1	2339	1.5	527	1.5
B7F7	45	0.0	463	0.6	3481	2.3	407	1.2
F1	12201	8.9	142	0.2	1547	1.1	853	2.5
F2	1597	1.1	86	0.1	3360	2.2	2314	6.8
F3	275	0.2	37	0.0	1552	1.0	847	2.5
F4	72	0.0	298	0.4	2379	1.5	1027	3.0
F7	36	0.0	933	1.3	3771	2.5	1070	3.1

The quasi-decadal signal was found to be the dominant cycle in 29 of the 35 EVI-residual trajectories. The length of the time-series, however, raises concern regarding the validity of including this cycle into the model. A quasi-decadal signal has been recently noted (though not quantified) in flow velocity data for a few hydrography stations in the Okavango Delta (Wolski and Murray-Hudson, 2006). Since decadal oscillations have been observed in solar and climatic indices (Friis-Christensen and Lassen, 1991; Hurrell, 1995; Wang and Wang, 1996), the quasi-decadal signal was added to the harmonic regression equation in order to remove any effects of a long-term cycle from the overall trend. The detection of a quasi-decadal signal in vegetative response from remotely sensed imagery indicates a new and exciting capability for linking trends and patterns observed in climate and oceanic data with vegetation in terrestrial ecosystems (e.g., teleconnections). The significance and t-test values of each cycle coefficient within the harmonic regression are indicated in Table 7.7. The annual cycle was statistically significant for all EVI clusters. The addition of the quasi-decadal cycle into the regression resulted in a statistically significant semi-annual model coefficients for all but three EVI spatio-temporal clusters. Additionally, the quasi-decadal cycle was statistically significant for all but five of the EVI clusters. The trend was statistically significant in eighteen of the 35 EVI clusters. Non-significant terms were removed from the final harmonic model and the coefficients and their standard errors are reported in Table 7.8.

Table 7.7. Two-tailed t-test and significance of each model coefficient term (trend, semi-annual, annual, and quasi-decadal) for all 35 EVI clusters. Significant coefficients are highlighted in yellow.

EVI	Trend		Semi-annual		Annual		Quasi-decadal	
Cluster	t-test	p	t-test	p	t-test	p	t-test	p
1	5.19	< 0.0001	-1.96	0.0268	15.31	< 0.0001	-1.21	0.115
2	3.49	0.0004	-1.55	0.0626	10.57	< 0.0001	-0.62	0.2692
3	4.18	< 0.0001	1.52	0.0063	99.79	< 0.0001	-2.43	0.0087
4	3.43	0.0005	0.98	0.1663	10.40	< 0.0001	0.79	0.2157
5	4.88	< 0.0001	2.21	0.015	14.84	< 0.0001	-2.67	0.0046
6	6.21	< 0.0001	2.21	0.015	20.62	< 0.0001	-3.27	0.0008
7	8.75	< 0.0001	1.80	0.0365	16.58	< 0.0001	-5.40	< 0.0001
8	3.99	0.0001	3.41	0.0005	11.58	< 0.0001	-0.47	0.3198
9	4.66	< 0.0001	2.69	0.0044	14.14	< 0.0001	-2.51	0.0071
10	3.11	0.0013	-3.41	0.0005	12.27	< 0.0001	-2.35	0.0107
11	1.58	0.0591	-4.11	< 0.0001	15.12	< 0.0001	2.18	0.0162
12	0.87	0.1943	-6.22	< 0.0001	17.66	< 0.0001	-1.23	0.1112
13	-1.15	0.1269	-4.17	< 0.0001	12.84	< 0.0001	-2.71	0.0041
14	-1.73	0.0438	5.17	< 0.0001	17.87	< 0.0001	-2.41	0.0092
15	-0.68	0.2480	5.21	< 0.0001	12.41	< 0.0001	-2.69	0.0044
16	-1.11	0.1352	-4.23	< 0.0001	13.12	< 0.0001	-3.08	0.0014
17	-1.08	0.1418	5.21	< 0.0001	14.49	< 0.0001	-1.96	0.0268
18	0.76	0.2257	4.50	< 0.0001	14.62	< 0.0001	-3.10	0.0014
19	-1.95	0.0274	6.22	< 0.0001	17.85	< 0.0001	-2.76	0.0036
20	-1.19	0.1189	6.26	< 0.0001	16.98	< 0.0001	-2.85	0.0028
21	4.10	< 0.0001	-3.35	< 0.0001	14.71	< 0.0001	-3.24	0.0009
22	1.02	0.1555	4.36	< 0.0001	17.91	< 0.0001	-3.19	0.001
23	0.14	0.4453	5.01	< 0.0001	17.39	< 0.0001	-3.41	0.0005
24	1.15	0.1269	4.70	< 0.0001	17.62	< 0.0001	-3.33	0.0007
25	-0.62	0.2692	-2.79	0.0033	15.23	< 0.0001	-4.87	< 0.0001
26	-0.98	0.1639	-4.55	< 0.0001	16.19	< 0.0001	-4.24	< 0.0001
27	1.82	0.0363	-4.60	< 0.0001	16.31	< 0.0001	-4.45	< 0.0001
28	-0.73	0.2353	-4.22	< 0.0001	14.72	< 0.0001	-3.78	0.0002
29	3.75	0.0002	3.99	0.0001	19.33	< 0.0001	-3.50	0.0004
30	-1.58	0.0591	-5.06	< 0.0001	16.65	< 0.0001	-2.91	0.0024
31	-0.44	0.3317	5.08	< 0.0001	15.23	< 0.0001	-3.12	0.0013
32	3.01	0.0018	-3.78	0.0002	16.08	< 0.0001	-4.03	< 0.0001
33	6.70	< 0.0001	1.23	0.1112	15.43	< 0.0001	-5.42	< 0.0001
34	1.52	0.0663	4.19	< 0.0001	18.84	< 0.0001	-3.65	0.0002
35	3.23	0.0009	4.09	< 0.0001	20.16	< 0.0001	-3.65	0.0002

Table 7.8. Final model coefficient and standard error of statistically significant terms for all 35 EVI clusters.

EVI	Trend		Semi-annual		Annual		Quasi-decadal	
Cluster	coeff	SE	coeff	SE	coeff	SE	coeff	SE
1	1.14E-05	1.96E-06	8.25E-03	4.27E-03	6.69E-02	4.36E-03	N/A	N/A
2	1.11E-05	3.10E-06	N/A	N/A	7.08E-02	6.60E-03	N/A	N/A
3	1.32E-05	3.15E-06	1.04E-02	6.86E-03	6.62E-01	6.63E-03	-1.44E-02	5.94E-03
4	7.93E-06	2.17E-06	N/A	N/A	4.98E-02	4.65E-03	N/A	N/A
5	1.15E-05	2.36E-06	1.00E-02	4.52E-03	7.36E-02	4.96E-03	-1.20E-02	4.51E-03
6	6.27E-06	1.01E-06	4.82E-03	2.18E-03	4.41E-02	2.14E-03	-6.61E-03	2.02E-03
7	1.54E-05	1.76E-06	6.02E-03	3.34E-03	6.15E-02	3.71E-03	-1.86E-02	3.45E-03
8	9.61E-06	2.17E-06	1.75E-02	5.35E-03	5.70E-02	4.84E-03	N/A	N/A
9	8.29E-06	1.78E-06	1.04E-02	3.85E-03	5.32E-02	3.76E-03	-8.80E-03	3.50E-03
10	8.27E-06	2.66E-06	-1.98E-02	5.81E-03	6.89E-02	5.61E-03	-1.18E-02	5.00E-03
11	N/A	N/A	-1.46E-02	3.68E-03	5.29E-02	3.55E-03	1.02E-02	3.60E-03
12	N/A	N/A	2.38E-02	3.80E-03	6.50E-02	3.68E-03	N/A	N/A
13	N/A	N/A	-2.02E-02	4.76E-03	5.94E-02	4.61E-03	1.14E-02	4.60E-03
14	-2.39E-06	1.38E-06	1.56E-02	3.02E-03	5.22E-02	2.92E-03	-7.09E-03	2.94E-03
15	N/A	N/A	3.07E-02	5.80E-03	7.01E-02	5.62E-03	1.41E-02	5.30E-03
16	N/A	N/A	2.20E-02	5.10E-03	6.50E-02	4.94E-03	1.04E-02	4.65E-03
17	N/A	N/A	-2.96E-02	5.59E-03	7.86E-02	5.41E-03	8.80E-03	4.97E-03
18	N/A	N/A	1.98E-02	4.44E-03	6.30E-02	4.30E-03	1.38E-02	4.02E-03
19	-3.24E-06	1.66E-06	2.25E-02	3.62E-03	6.27E-02	3.51E-03	-9.90E-03	3.58E-03
20	N/A	N/A	-2.91E-02	4.59E-03	7.55E-02	4.40E-03	1.12E-02	4.26E-03
21	9.11E-06	2.22E-06	-1.63E-02	4.85E-03	6.90E-02	4.69E-03	-1.36E-02	4.19E-03
22	N/A	N/A	-1.33E-02	3.09E-03	5.34E-02	2.99E-03	9.49E-03	2.72E-03
23	N/A	N/A	-1.88E-02	3.72E-03	6.33E-02	3.61E-03	1.20E-02	3.34E-03
24	N/A	N/A	-1.14E-02	2.48E-03	4.37E-02	2.50E-03	8.41E-03	2.28E-03
25	N/A	N/A	1.23E-02	4.32E-03	6.43E-02	4.18E-03	1.80E-02	3.70E-03
26	N/A	N/A	-1.21E-02	2.63E-03	4.47E-02	2.75E-03	-1.02E-02	2.44E-03
27	2.77E-06	1.52E-06	-1.46E-02	3.18E-03	5.25E-02	3.22E-03	-1.27E-02	2.86E-03
28	N/A	N/A	-1.63E-02	3.80E-03	5.65E-02	3.81E-03	1.33E-02	3.54E-03
29	6.30E-06	1.68E-06	1.46E-02	3.66E-03	6.84E-02	3.54E-03	-1.19E-02	3.41E-03
30	N/A	N/A	-2.40E-02	4.65E-03	7.53E-02	4.55E-03	-1.08E-02	4.04E-03
31	N/A	N/A	-2.82E-02	5.48E-03	8.14E-02	5.31E-03	1.51E-02	4.82E-03
32	6.80E-06	2.26E-06	-1.87E-02	4.94E-03	7.67E-02	4.77E-03	-1.72E-02	4.26E-03
33	1.45E-05	2.17E-06	N/A	N/A	6.96E-02	4.20E-03	-2.32E-02	4.20E-03
34	N/A	N/A	-1.95E-02	4.80E-03	8.70E-02	4.67E-03	-1.61E-02	4.14E-03
35	6.37E-06	1.97E-06	1.70E-02	4.17E-03	8.35E-02	4.14E-03	-1.35E-02	3.68E-03

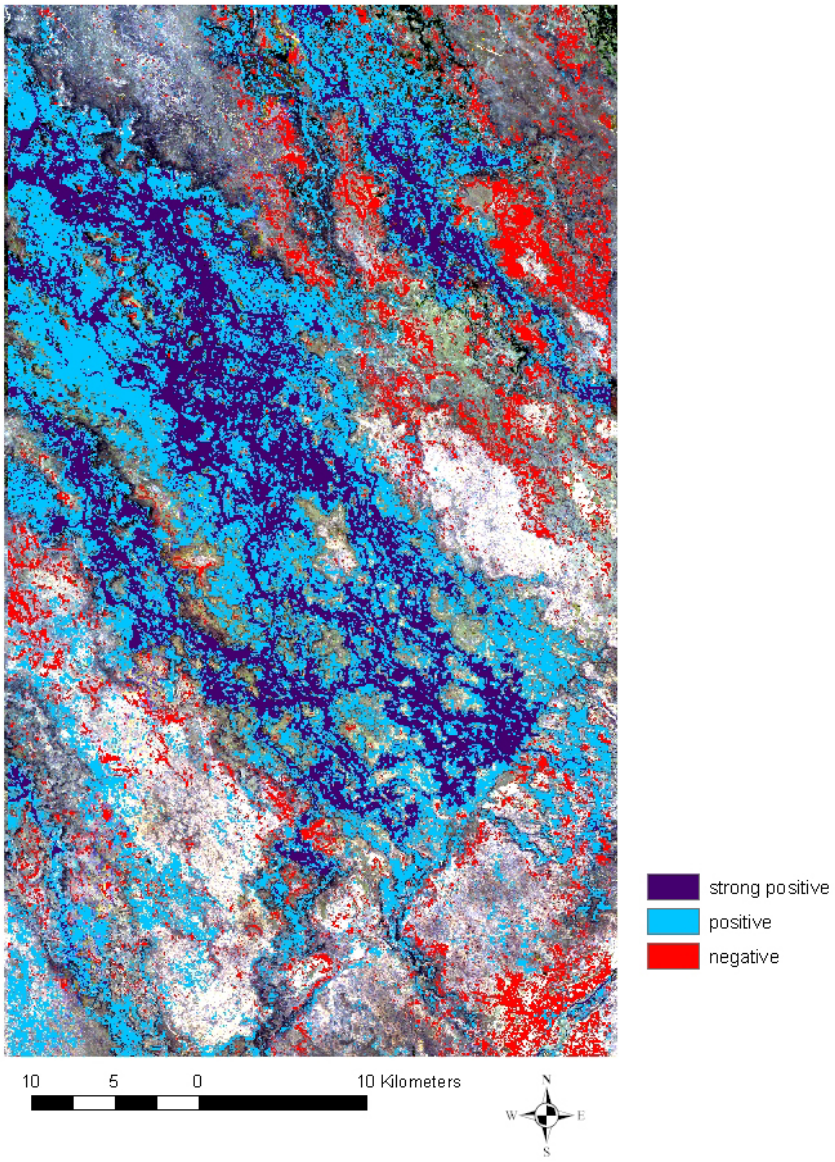

Figure 7.7. Colored areas indicate portions of the landscape associated with statistically significant trend of EVI values during 1989 – 2002 period. Purple indicates Strong positive trend ($+10e^{-5}$), Blue indicates positive trend ($+10e^{-6}$), and Red indicates negative trend ($-10e^{-6}$).

Figure 7.7 illustrates the portions of the landscape with respect to the general detected trend in EVI value that were identified as statistically significant. A positive slope indicates that during the time-series the vegetation spectral response increased

potentially indicating more growth, whereas a negative slope indicates a decline in vegetation spectral response from 1989 to 2002. More specifically, EVI has been found to be negatively associated with an increase in woody vegetation and positively associated with increasing herbaceous productivity (Fang et al., 2005). The relationship of each general trend and the flooding history and fire history is summarized in Table 7.9 and Table 7.10 respectively. Regions having a strong positive slope occurred in the active floodplain with 99 % of the pixels flooded at least once and 80.6% of pixels flooded more than four times in the 14-year history. Sixty four percent of the landscape associated with a positive slope was also found in the floodplains, however, 23% of the pixels flooded only once. Additionally, other areas with a positive trend were associated with *Acacia* savanna of various densities in rural regions. Regions associated with a negative EVI trend through the 14-year time-series consisted of patches of *Acacia* woodland near Maun. These findings suggest an increase in woody cover in the savannas during the time-series. Additionally, 63% of the pixels with a negative trend did not burn during the 14 years. The lack of fire and proximity to human activities is also a potential indicator of woody encroachment. Figure 7.8 indicates that much of the negative trending regions did occur near human activities. Near villages, over-grazing of domestic livestock has resulted in a near depletion of grasses (personal observation, 2006 and 2007). A large region of negatively trending EVI values occurred near Maun, along trails, and between the camps of Chetabi to the north and Qorokwe and Kolobi to the south.

Table 7.9 Statistics for slope classes against 14-year flooding history (green = 5 – 10%, orange >10 – 20 % yellow = >20%)

	Strong Positive Mask		Positive Mask		Negative Mask	
Flood History (Years)	**Hectares**	**Percent**	**hectares**	**Percent**	**hectares**	**Percent**
0	128.5	0.4	18134.3	36.0	18422.8	95.6
1	250.8	0.8	11812.5	23.4	555.1	2.9
2	447.6	1.5	4948.1	9.8	66.4	0.3
3	891.2	3.0	3664.1	7.3	32.0	0.2
4	1715.9	5.8	2554.7	5.1	25.5	0.1
5	2380.8	8.0	1907.9	3.8	24.5	0.1
6	3254.5	10.9	1992.9	4.0	22.5	0.1
7	3186.8	10.7	1511.4	3.0	19.6	0.1
8	2410.0	8.1	1024.5	2.0	21.8	0.1
9	2359.4	7.9	757.0	1.5	20.0	0.1
10	1917.4	6.4	510.6	1.0	19.1	0.1
11	2207.4	7.4	462.6	0.9	14.4	0.1
12	2470.1	8.3	411.1	0.8	12.1	0.1
13	3275.6	11.0	298.3	0.6	10.3	0.1
14	2892.0	9.7	433.2	0.8	3.1	0.0
Total		**99.9**		**100.0**		**100.0**

Table 7.10 Statistics for slope classes against 14-year fire history (green = 5 – 10%, orange = 10 – 20%, yellow = >20%)

	Strong Positive Mask		Positive Mask		Negative Mask	
Fire History (Years)	**hectares**	**Percent**	**hectares**	**Percent**	**hectares**	**Percent**
0	3860.9	13.0	16142.8	28.5	12086.0	62.7
1	4055.0	13.6	9195.1	16.2	5150.7	26.7
2	4488.2	15.1	10503.5	18.5	1429.3	7.4
3	4985.2	16.7	9772.0	17.2	441.3	2.3
4	4954.9	16.6	6617.5	11.7	99.3	0.5
5	3948.3	13.3	3082.5	5.4	55.2	0.3
6	2193.6	7.4	1069.7	1.9	6.4	0.0
7	893.6	3.0	248.0	0.4	0.9	0.0
8	329.0	1.1	37.7	0.1	0.0	0.0
9	75.2	0.3	3.4	0.0	0.0	0.0
10	4.3	0.0	0.0	0.0	0.0	0.0
total		**100.0**		**100.0**		**100.0**

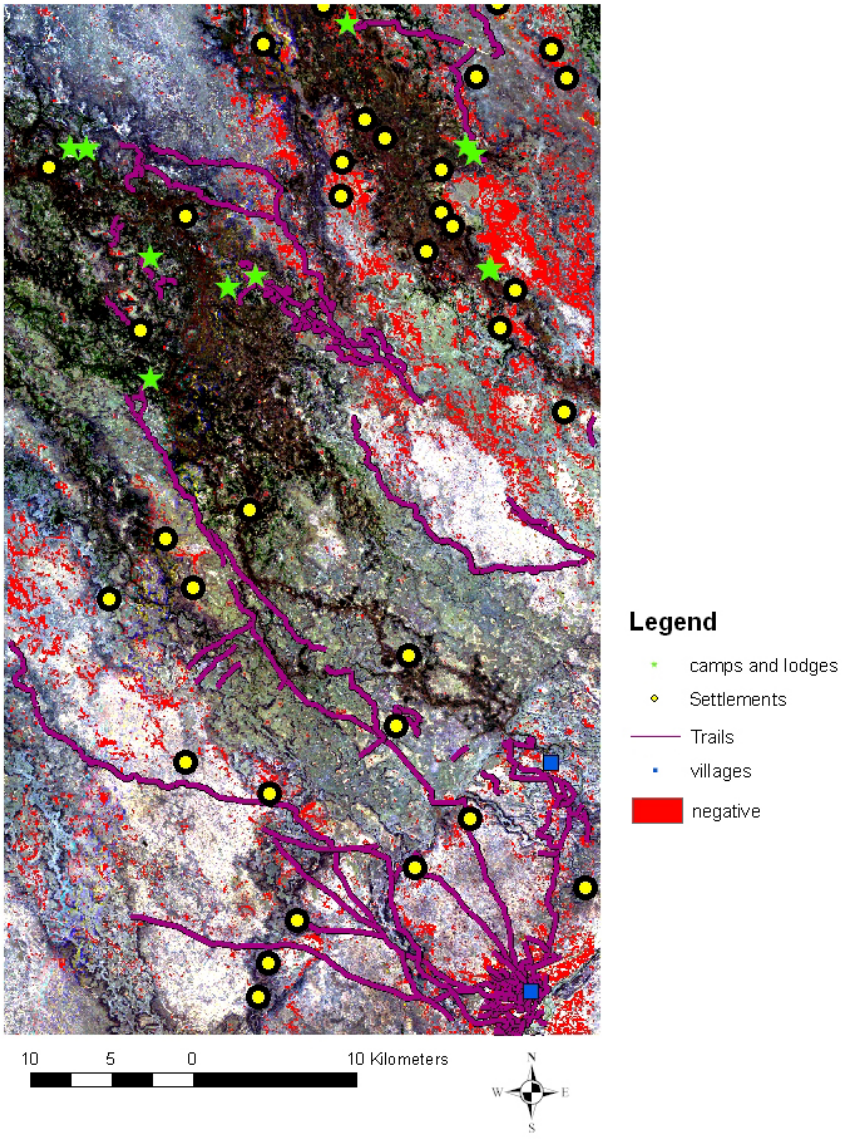

Figure 7.8. Negative trending EVI values (shown as red) from 1989 to 2002 and human activities such as villages, trails, camps, lodges, and small settlements.

The spatial distribution of clusters having a non-significant semi-annual term and non-significant quasi-decadal term are depicted in Figure 7.9a and Figure 7.9b respectively. EVI clusters 2 and 4 contain floodplain grasses and were located in the

floodplains of the lower Boro River. Both of these classes are associated with frequent burning, which could explain why the semi-annual and quasi-decadal cycles were not statistically significant.

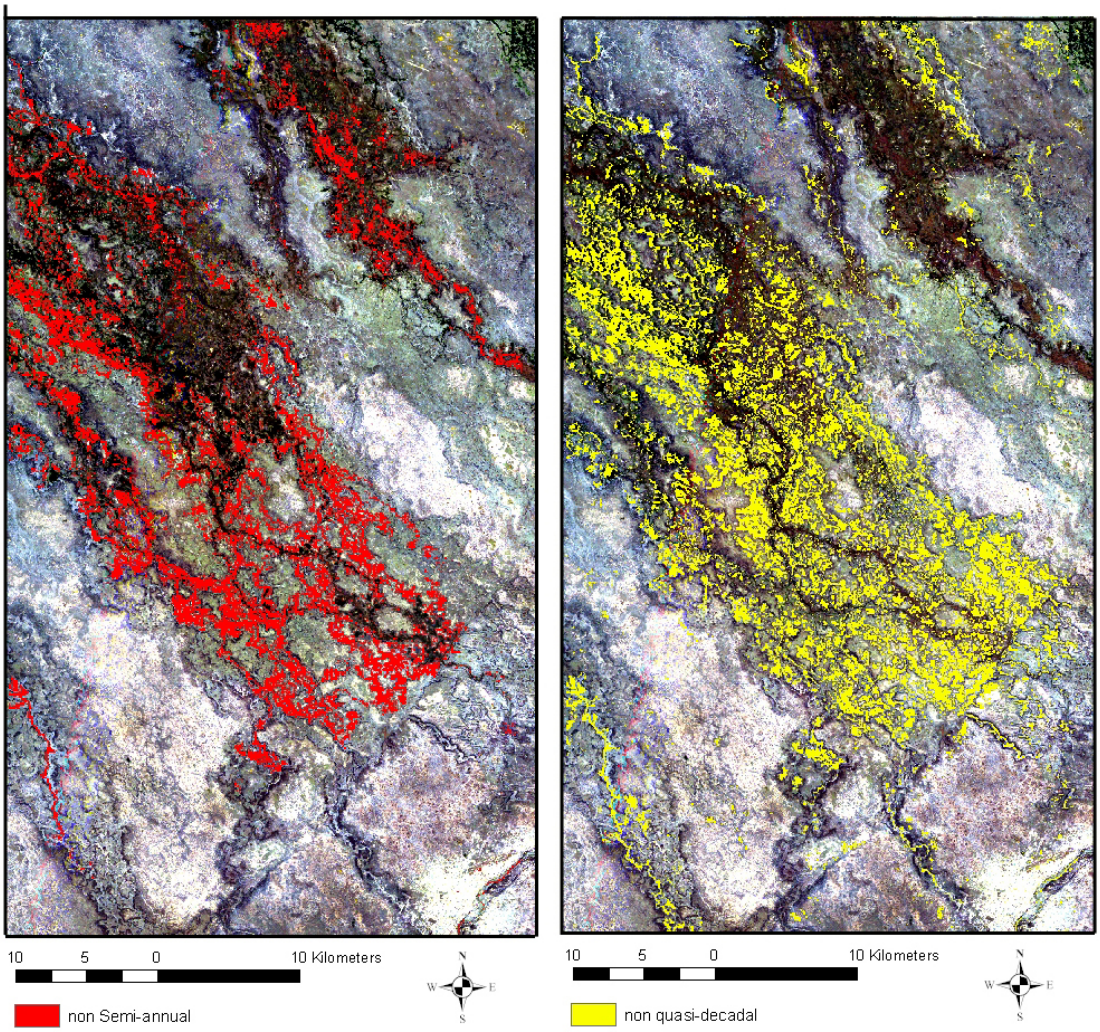

Figure 7.9a. Portions of the landscape where the semi-annual term was not statistically significant, and b) portions of the landscape where the quasi-decadal term was not statistically significant.

Table 7.11. Total variance accounted for using harmonic model with statistically significant terms. Clusters having an R^2 value less than 70% are highlighted yellow.

EVI Cluster	Landcover	Total R^2	EVI Cluster	Landcover	Total R^2
1	Channel	0.79	19	grasses/savanna	0.81
2	floodplain grasses	0.61	20	acacia savanna	0.79
3	Sedge	0.62	21	shrubbed islands	0.76
4	floodplain grasses	0.61	22	mopane woodlands	0.81
5	sedge/hippo grass	0.78	23	Grasses	0.81
6	secondary floodplain	0.87	24	mopane woodlands	0.82
7	miscanthus/sedge	0.85	25	scrub Mopane	0.78
8	acacia grassland	0.66	26	mopane woodlands	0.81
9	island shrub vegetation	0.75	27	mixed Mopane	0.81
10	Grasses	0.68	28	mixed mopane	0.76
11	grasses/sage	0.75	29	riparian island fringe	0.84
12	treed grassland	0.79	30	riparian woodlands	0.79
13	Grasses	0.69	31	acacia thickets	0.76
14	acacia grassland	0.81	32	riparian woodlands	0.79
15	acacia shrubbed woodland	0.68	33	hippo grass	0.82
16	acacia thickets	0.70	34	riparian woodlands	0.82
17	acacia shrubbed woodland	0.73	35	riparian woodlands	0.85
18	acacia shrubbed savanna	0.75			

The overall variability in observed vegetation spectral responses appears to be both largely cyclical and well defined by the semi-annual, annual, and quasi-decadal fits: 61 to 87 percent of the variance was explained using this simple harmonic model. The total variance for each EVI cluster is listed in Table 7.11 along with the landcover as defined by fieldwork from 2006 and 2007. Generally, clusters that fell within the floodplains but were only occasionally flooded or regions that were frequently burned

were less well predicted. Clusters 2, 3, and 4 are floodplain/wetland classes that did not experience flooding during the mid-1990s (see Appendix for flooding power spectrum), which explains the reduced ability to fit the trajectories with a harmonic regression. This disruption to the annual flooding regime likely resulted in the poorer overall fit. In contrast, clusters that were consistently flooded or less frequently burned resulted in the highest overall R^2. The lower R^2 values can be attributed to influences not represented such as anthropogenic factors, as well as changes or anomalies to the natural regimes. The overall R^2 is represented spatially in Figure 7.10 where it is evident that the highest R^2 values (0.87) were associated with annually flooded channels and marshes as well as riparian vegetation whereas the worst fit classes (0.61) were associated with drought-influenced floodplains.

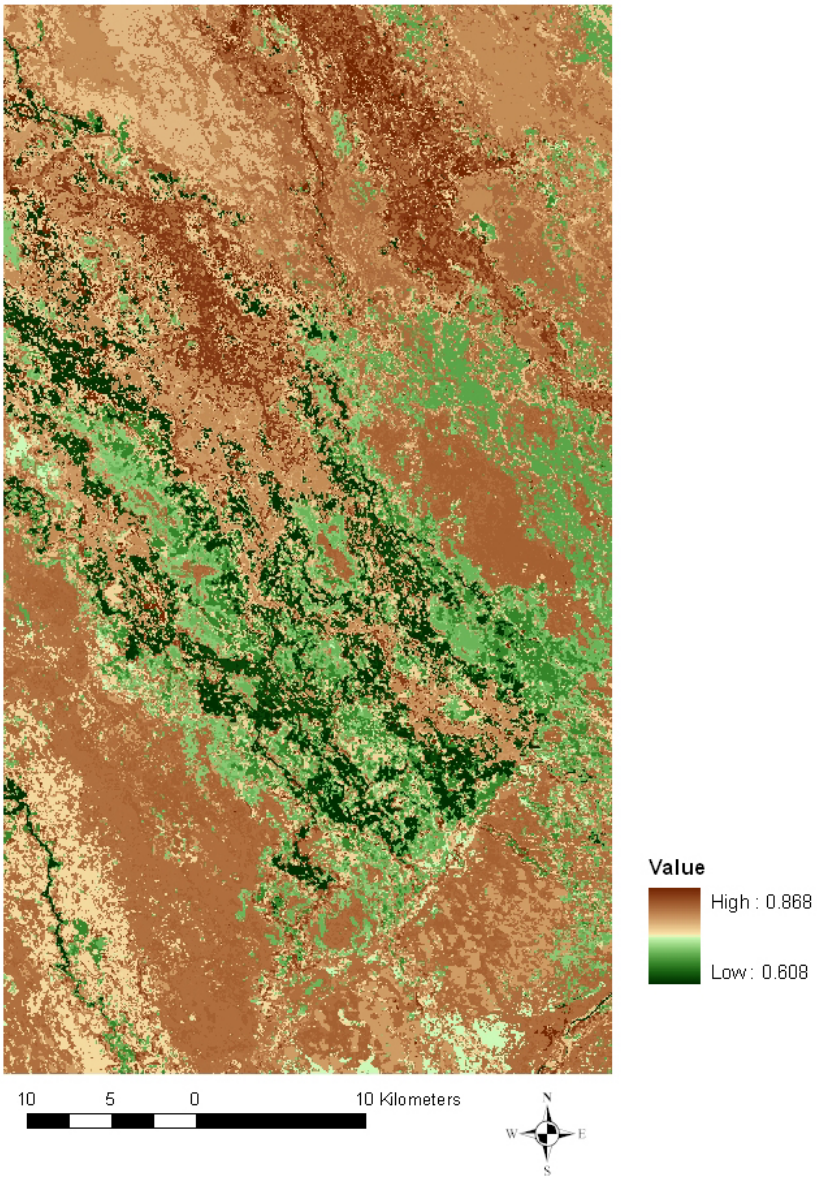

Figure 7.10. Overall R^2 of harmonic regression applying statistically significant terms including semi-annual, annual, and quasi-decadal cycles to 35 EVI-based trajectories in the study area.

7.2.2 Transitory analysis of EVI Clusters

As defined previously, a transitory signal relates to temporary dynamics resulting from a stochastic event such as disturbance. Hypothesis 6 in this research posited that

flooding and fire are positively correlated with the residual signal of the EVI trajectories. The transitory signal was computed by removing the semi-annual, annual, and quasi-decadal regression fit from the EVI-based trajectories. To determine the relationship, if any, of disturbance on vegetation productivity as detected via remotely sensed EVI, the pairwise correlation at the 0^{th} lag between the transitory signals and the flooding and fire trajectories of each class were computed; they are reported in Table 7.12, with statistically significant correlations highlighted in yellow. Fire was positively correlated with positive transitory EVI values for eight of the clusters. EVI cluster 5, 6, 7, and 33 were located within the floodplain and is logical since fire is common to the floodplains. The relationship between flooding and the transitory signal was essentially negligible except for EVI cluster 8 which shows a negative correlation. Although eight of the correlation values between fire and the transitory signal were statistically significant, the correlation values themselves were quite low. Thus, the hypothesis was rejected for both flooding and fire. Limitations of the correlation analysis between the transitory signal and the observed flooding and fire regimes include weak signals that may not be observable and a non-uniform temporal spacing. It is also possible that the 35 ISODATA-based temporal clusters obscured vegetation changes related to more local-scaled processes, such as microclimatic conditions or local as opposed to regional management strategies.

Table 7.12. Correlations and significance between transitory signals from EVI cluster trajectories and flooding and fire trajectories as well as between flooding and fire. Correlations with a statistical significance better than 0.05 are highlighted yellow.

EVI cluster	fire/transitory R	fire/transitory P	Flood/transitory R	Flood/transitory P	fire/flood R	fire/flood P
1	0.2485	0.0232	-0.0127	0.9089	-0.3161	0.0032
2	-0.0229	0.8362	0.1034	0.3492	-0.2219	0.0413
3	0.1827	0.0962	-0.0236	0.8309	-0.2280	0.0358
4	-0.0365	0.7418	0.1397	0.2051	-0.1824	0.0948
5	0.3693	0.0005	-0.0691	0.5322	-0.1976	0.0699
6	0.2514	0.0211	0.0289	0.7939	-0.0430	0.6960
7	0.4483	<0.0001	0.0965	0.3826	0.1230	0.2620
8	-0.0048	0.9656	0.3477	0.0012	-0.0764	0.4869
9	0.2959	0.0063	0.0431	0.6969	-0.1111	0.3115
10	0.0126	0.9098	0.1021	0.3555	-0.0690	0.5304
11	0.1975	0.0718	0.1043	0.3453	-0.0230	0.8343
12	0.0717	0.5166	0.2092	0.0561	-0.0820	0.4557
13	0.2196	0.0447	0.0917	0.4070	0.1036	0.3454
14	0.1199	0.2773	0.0139	0.9004	0.2953	0.0061
15	0.2053	0.0611	0.0443	0.6890	0.2289	0.0351
16	0.2123	0.0525	0.0515	0.6417	-0.0003	0.9979
17	0.1128	0.3070	0.0670	0.5448	-0.0250	0.8201
18	0.0814	0.4614	0.0491	0.6571	-0.0186	0.8658
19	0.1365	0.2156	-0.0413	0.7092	0.4395	< 0.0001
20	0.1148	0.2985	-0.0706	0.5233	0.0708	0.5196
21	0.2185	0.0458	-0.0995	0.3679	-0.0442	0.6881
22	0.1185	0.2832	0.0120	0.9136	0.3789	0.0003
23	0.1114	0.3131	0.0866	0.4336	0.1254	0.2528
24	0.0682	0.5376	-0.1201	0.2764	0.1255	0.2524
25	0.0298	0.7878	0.0359	0.7460	0.2887	0.0074
26	0.0935	0.3975	-0.0319	0.7735	0.1118	0.3085
27	0.1365	0.2156	0.0253	0.8191	-0.0038	0.9724
28	0.1252	0.2565	0.1113	0.3137	0.2950	0.0061
29	0.2709	0.0127	0.1349	0.2212	0.3192	0.0029
30	0.1448	0.1889	0.1130	0.3062	0.0077	0.9442
31	0.0856	0.4386	-0.0550	0.9607	0.0690	0.5303
32	0.1203	0.2756	-0.0216	0.8455	-0.0337	0.7596
33	0.4454	<0.0001	0.1872	0.0881	0.3661	0.0006
34	0.0923	0.4035	0.0394	0.7220	0.0042	0.9699
35	0.1462	0.1845	0.1211	0.2727	0.1567	0.1520

7.3 Influence of Humans on Vegetation Dynamics

7.3.1 Land Management

The land management zones (shown in Figure 7.11) are the Moremi Game Reserve, photographic concessions within the wildlife management areas, hunting concessions within the wildlife management areas, and communal areas where most of the settlements occur and which presumably have the greatest amount of human influence. When drawing comparisons among ecosystems within the land management regimes in this study area, Moremi Game Reserve and the communal areas are regarded as comprised of upland vegetation (however, some wetlands and channels do exist within these two management types). Similarly, the photography and hunting concessions are comprised of both wetland and upland environments. The hunting and photography concessions are split along the Boro River with the north side designated as photography and the south side designated as hunting. It is important to note that the drier sections of the Boro and the Marophe channel occur in the hunting concessions whereas the areas more consistently flooded (upper Boro and Santantadibe) occur in the photography concessions.

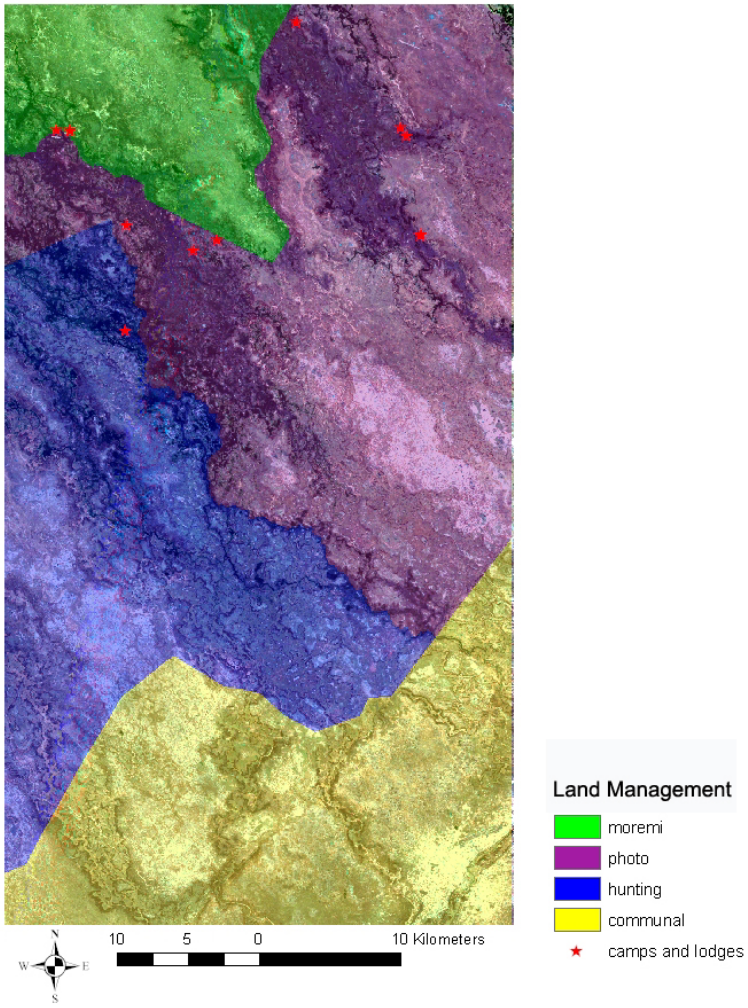

Figure 7.11. Land Management designation in the study area.

A similar analysis as implemented above was conducted but with EVI stratified by land management type instead of EVI clusters, creating four EVI trajectories that each represented a land management regime. The mean EVI values for each date were derived for each management type and stacked into four vectors. The results of applying a semi-annual, annual, and quasi-decadal harmonic fit to each land management regime are reported in Table 7.13. The trend was not statistically significant for any land

management regime. For all four management regimes, the quasi-decadal signal was the dominant frequency. In addition, all management regimes had residual frequencies of 1.5 years, ~4 years, and 10.9 years (Table 7.14). The overall R^2 indicated that lands in the Moremi Game Reserve were better described by climatic signals than lands within the communal regions. This result makes sense as there should be much less or limited human impacts in the game reserve. The hunting concessions had the lowest (but still informative) R^2 with 76.7% of the variance explained. Again, it was shown earlier in this chapter than regions experiencing drought were not well described by the climatic signals. The hunting concessions are located on drier portions of the floodplains than the photography concessions and experienced a large amount of burning. Thus, the results from the land management provide some insight into the understanding of the multiple variables that influence the observed vegetation spectral response. A next step to understanding the vegetation dynamics is to isolate the response to various levels of disturbance within each management zone. This effort is described later in this chapter.

Table 7.13. Overall variance for statistically significant model coefficients for land management classes.

	R^2
Moremi	0.82
Photo	0.83
Hunting	0.76
Communal	0.79

Table 7.14. Wavelet results on land management trajectories

	MAX	ALL Frequencies			
Moremi	10.9	1.4	3.8	10.9	
Photo	10.9	1.5	4.9	10.9	
Hunting	10.9	1.5	3.3	10.9	
Communal	10.9	0.6	1.5	3.3	10.9

7.4 Wavelet Analysis on Environmental Data

7.4.1 Meteorological Data

To compare the temporal signals of environmental variables with those in observed vegetation spectral responses, wavelet decomposition was implemented on the precipitation records and climate indices for the region. Precipitation impacts vegetation growth and determining whether cycles observed in the vegetation spectral response directly correspond to precipitation cycles is critical for interpreting vegetation trends and cycles. As a means to establish confidence in the quasi-decadal cycle detected in the temporal dynamics of the vegetation spectral response, a wavelet transform was implemented on the 80 year precipitation record from the Maun airport. The airport is only one point within the study area and precipitation is quite localized, but the extraction of its precipitation historical patterns and cycles could still provide an important context for interpreting vegetation trends and cycles. Rather than examining the raw data or the raw data minus the mean, a semi-annual and annual harmonic regression were fit to the data and subsequently removed. The motivation for examining the residual signal is the strong annual signal that tends to diminish the power of the other climatic cycles. Figure 7.12 a) and b) depict the wavelet power spectrum and global wavelet for the precipitation residuals. The wavelet analysis of the residuals indicates a strong biennial oscillation (1.91 years) followed by longer term oscillations of approximately 6.2, 10.8, 18.8, and 26.6 years. While the 10.8 year cycle is the weakest of the long-term cycles identified, it does occur in the 1990s and overlaps with the Landsat time-series. The 18.8 year cycle is

presumed to correspond to the 18-year precipitation cycle for southern Africa reported in the literature (Tyson et al. 2002, McCarthy et al., 2000).

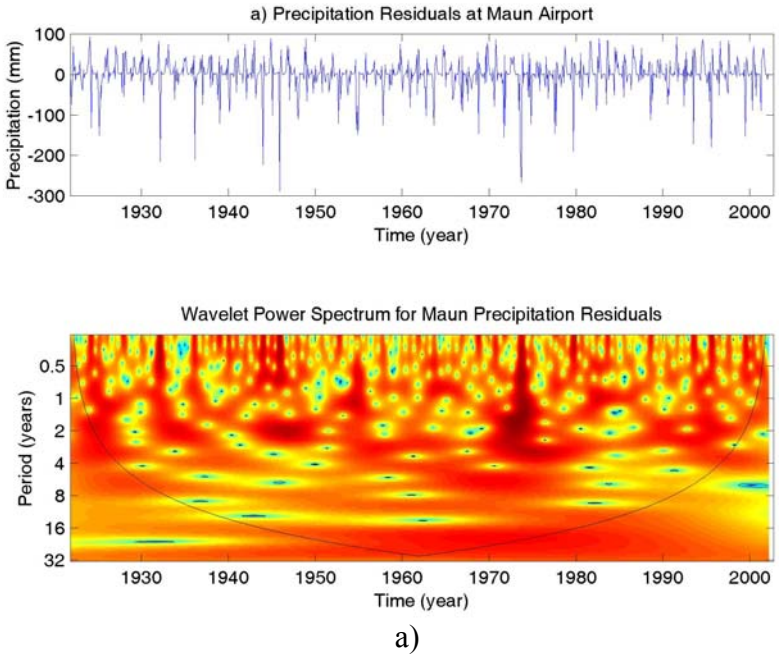

a)

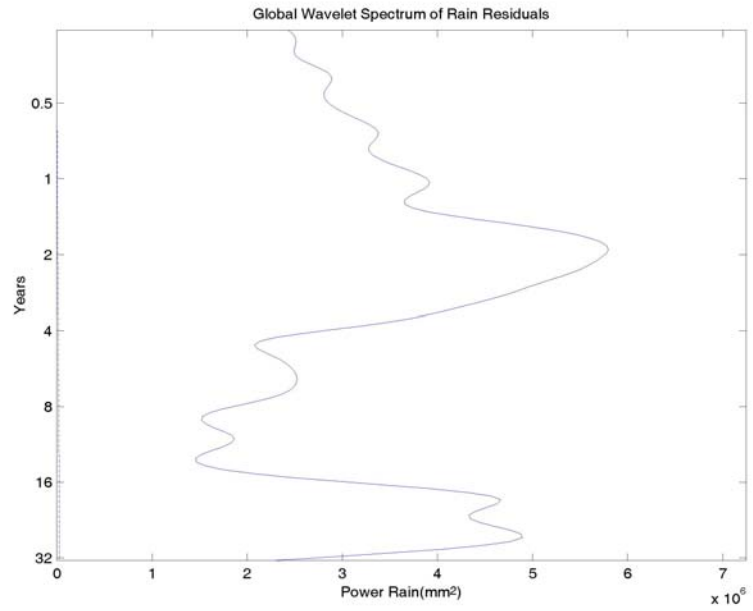

b)

Figure 7.12. Wavelet analysis for Maun Precipitation Residuals. a) Wavelet power spectrum and b) global wavelet

7.4.2 Confirmation of a Quasi-Decadal Signal

The presence of a quasi-decadal signal as the dominant frequency in all but six of the residual trajectories in the vegetation spectral response is a surprising result. This quasi-decadal signal has been recently noted but not quantified in flow velocity data for a handful of hydrography stations in the Okavango Delta (Wolski and Murray-Hudson, 2006). The detection of a quasi-decadal signal in vegetative response from remotely sensed imagery indicate a new and exciting capability for linking trends and patterns observed in climate and oceanic data with vegetation in terrestrial ecosystems. Decadal trends such as the Pacific Decadal Oscillation (PDO), North Atlantic Oscillation (NAO), Southern Oscillation (Wang and Wang, 1996), and global temperature anomalies have been observed for as long as records have been reliably available (Hurrell and Trenberth, 1996). While the majority of studies linking decadal oscillations have been developed for the northern hemisphere, there is recent evidence that anomalies associated with the PDO may impact the southern hemisphere (Mantua and Hare, 2002). The Southern Oscillation, which is linked with El Niño patterns for the equatorial Pacific, also exhibits decadal oscillations and variability (Wang and Wang, 1996). The quasi-decadal trends observed in climate indicators such as PDO and NOA have been linked to variance in solar irradiance (Friis-Christensen and Lassen, 1991); however, the variability of solar irradiance on observed climate change has been questioned due to the short timeline of satellite observations (Waple, 1999).

In addition, wavelet analysis was implemented on other climatic indicators to determine if there are any relationships with patterns detected in the observed vegetation spectral response. The other climatic indicators include the Tropical Southern Atlantic Index (TSA), Indonesian Sea Level Pressure Anomalies (IND), Southern Oscillation Index (SOI), Western Hemisphere Warm Pool (WHWP), and Global Temperature Anomalies (GLOTEMP). All of these indices were retrieved from the NOAA Climate Analysis Branch at http://www.cdc.noaa.gov/ClimateIndices/List/, with most of the climatology for these indices covering a ~50 year period (1948 – 2000). Prior to wavelet analysis, each time-series was detrended using a linear function. The Southern Oscillation (shown in Figure 7.13) has a dominant frequency of 13.1 years with the peak of energy occurring in approximately 1983. The wavelet power spectrum and global wavelet for all tested climate indices are located in Appendix A.2. The extracted oscillations for each climate index are listed in Table 7.15.

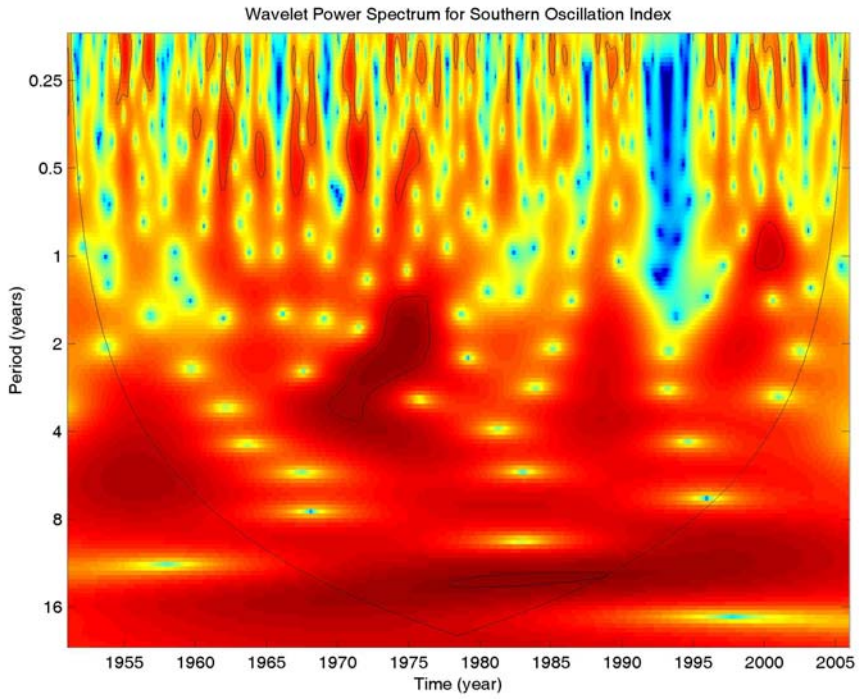

Figure 7.13. Wavelet power spectrum of the Southern Oscillation.

Table 7.15 Results of dominant periodicities of various climate indices (shown in years).

	MAX	ALL Frequencies (years)						
TSA	11.8	0.2	0.8	2.5	5.1	11.8		
IND	14.5	0.2	0.4	0.8	2.3	5.1	8.9	14.5
SOI	13.1	0.2	0.4	2.5	3.7	4.9	6.5	13.1
WHWP	5.5	0.2	0.5	1.0	3.6	5.5	13.5	
GloTemp	20.5	0.2	0.3	0.9	1.8	3.6	5.1	9.9
SOLAR	10.9	5.2	10.9	35.4	100.2			

Data containing the number of sun spots since 1700 (known as Wolf numbers and used as an indicator of solar activity) were retrieved from ftp://ftp.ngdc.noaa.gov/STP/SOLAR_DATA/SUNSPOT_NUMBERS/YEARLY.PLT. An offset and trend were removed from the dataset and were subsequently processed

using the same Morlet wavelet parameters that were implemented on the EVI-residual trajectories. The dominant periodicity of the solar activity was 10.9 years and the wavelet power spectrum and global wavelet are shown in Figures 7.15 a and b, respectively. This periodicity agrees well with the 10.9 years cycle found in the temporal dynamics of the vegetation spectral response. In addition, a 100 year cycle was also found within the sun spot activity which confirms long-term oscillations reported in the literature (Friis-Christensen and Lassen, 1991; Perry and Hsu, 2000). Recent measurements of solar irradiance indicate a range of 0.1% over the 11 year cycle (Perry and Hsu, 2000).

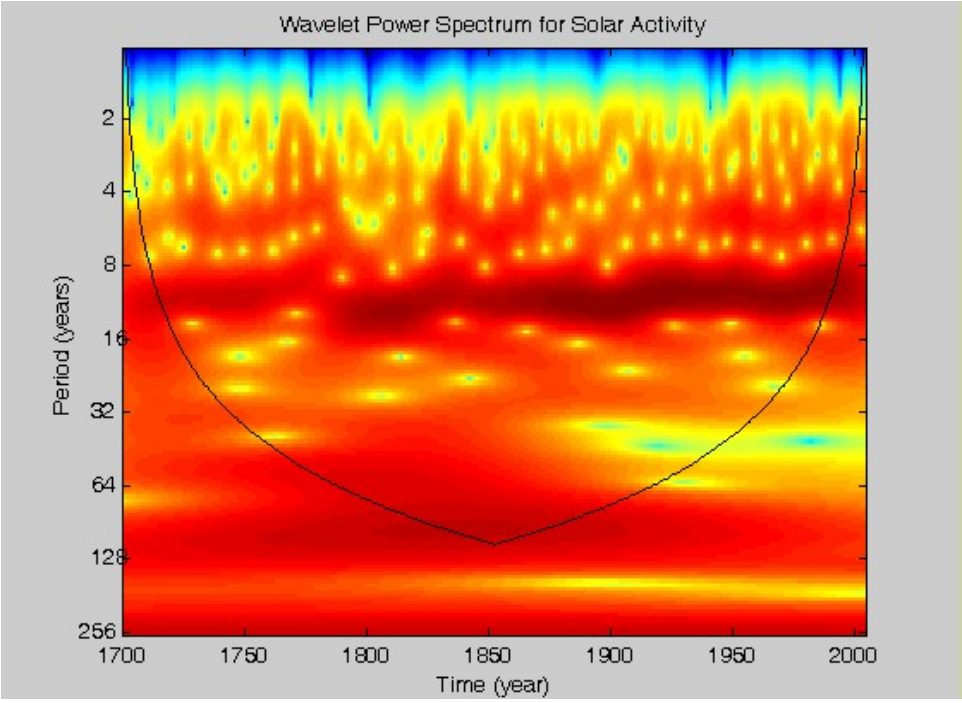

Figure 7.14a. Wavelet Power Spectrum for Solar Activity since 1700. Dominant periodicity was found to be 10.9 years.

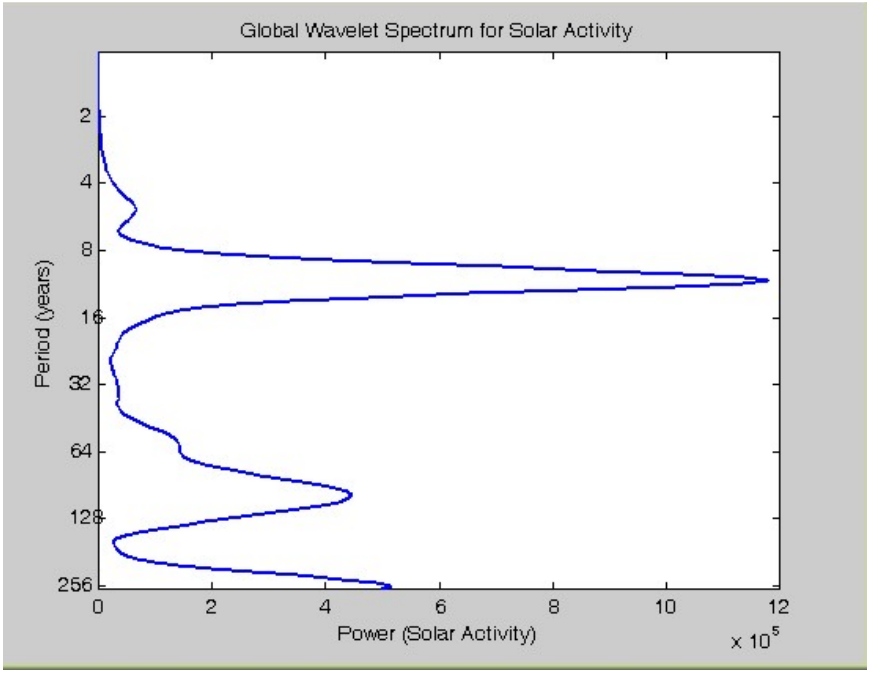

Figure 7.14b. Global wavelet for Solar Activity since 1700.

7.5 Trajectory Analysis of Disturbance Histories

Analysis similar to that described in the previous sections was implemented on a sampling of the disturbance history (DH) clusters rather than EVI clusters. A limitation of using DH clusters is that the entire landscape is not considered in the analysis, but rather only those sets of pixels that have a similar disturbance history. By definition here, a disturbance history is a general term for the individual number of flooding and fire events in the 14-year history. Thus a pixel that experienced six floods and two burns would be coded B2F6. It is important to note that pixels having the same DH label do not necessarily have a similar sequencing between flooding and fires, similar vegetation assemblages, or management strategies. Since there are over 130 DH clusters, only a subset of the DH clusters were utilized for subsequent analysis. To examine the potential impact of land management on ecosystem dynamics and resilience, the DH clusters were

partitioned by land management type as shown in Table 7.16. By definition, the disturbance history clusters that are comprised of both flooding and burning are located within the floodplains. Each Disturbance History/Management cluster was used as a mask and the mean EVI value at each date were computed to create trajectories.

Table 7.16. Disturbance history clusters stratified by land management.

DH – Land Management	Hectares	DH – Land Management	Hectares
B1 – Moremi	1,615.7	B1F13 – Hunting	96.5
B1 – Photo	12,513.2	B2F9 – Moremi	32.8
B1 – Hunting	9,363.9	B2F9 – Photo	169.6
B1 – Communal	11,820.9	B2F9 – Hunting	45.2
B2 – Moremi	641.9	B3F1 – Moremi	67.9
B2 – Photo	6,936.5	B3F1 – Photo	1,871.0
B2 – Hunting	4,813.4	B3F1 – Hunting	1,964.4
B2 – Communal	2,326.0	B3F1 – Communal	167.6
B3 – Moremi	94.9	B3F6 – Photo	233.7
B3 – Photo	3,840.3	B3F6 – Hunting	332.7
B3 – Hunting	3,831.3	B4F3 – Photo	144.7
B3 – Communal	206.0	B4F3 – Hunting	377.7
B4 – Photo	1,383.1	B4F7 – Photo	302.9
B4 – Hunting	1,664.1	B4F7 – Hunting	297.9
B4 – Communal	28.5	B5F11 – Photo	217.2
B5 – Photo	508.0	B5F11 – Hunting	87.4
B5 – Hunting	618.4	B6F8 – Photo	100.3
B6 – Photo	148.1	B6F8 – Hunting	182.2
B6 – Hunting	72.7	B7F12 – Photo	36.9
B1F1 – Moremi	305.1	B7F12 – Hunting	6.5
B1F1 – Photo	1,024.0	F1 – Moremi	786.1
B1F1 – Hunting	989.1	F1 – Photo	956.9
B1F1 – Communal	1,166.3	F1 – Hunting	412.8
B1F13 – Moremi	74.4	F1 – Communal	1,588.7
B1F13 – Photo	374.0		

The same analysis as described for the EVI-clusters was implemented on the EVI disturbance history/management (DH) trajectories. First, a semi-annual and annual harmonic regression was run on each trajectory. The DH-residuals were examined using

wavelets to detect periodicities in the signal. The identified periodicities for each DH-residual class are listed in Table 7.17. For classes that burned only once, the dominant frequency in the residual signal was 10.9 years. This quasi-decadal frequency was again the dominant frequency for classes that were only burned twice, except for those pixels under the communal areas. In fact, for all the other disturbance classes under the communal mask, the dominant frequency was not the quasi-decadal signal but rather a frequency of approximately 1.5 years. One possible explanation is that in the communal regions, other factors are over-riding the climatic signal. These factors could be plant competition among herbaceous vegetation, over-grazing, or harvesting of fuelwood. If so, as the levels of burning increase within the photographic or hunting concessions, the dominant frequency would shift from the quasi-decadal climate signal to other weaker signals. However, this explanation is speculative and other factors (such as topographic relationship within floodplain) would need to be examined further.

The model coefficients and standard errors for a semi-annual, annual, and quasi-decadal harmonic regression are reported in Table 7.18. The semi-annual, annual, and quasi-decadal terms were statistically significant for all DH classes tested in this research. The trend values were statistically significant for only the DH classes that were flooded more than seven years out of the 14-year history. By implementing a harmonic regression model on each EVI trajectory, the overall R^2, or predictability, serves as a potential indicator of resilience. Hypothesis 4 posited that as the number of floods increases, the predictability of the trajectory decreases. Similarly, hypothesis 5 posited that as the number of fires increases, the predictability of the trajectory decreases.

Table 7.17 Periodicities (in years) of DH-residual global wavelets for each disturbance history/management class. Classes with a non-quasi-decadal dominant periodicity are highlighted in yellow.

CLASS	Max	All Frequencies				
B1 - Moremi	10.9	1.5	4.7	10.9	***	***
B1 - Photo	10.9	1.4	4.7	10.9	***	***
B1 - Hunting	10.9	0.6	1.4	3.6	5.4	10.9
B1 - Communal	10.9	0.6	1.5	10.9	***	***
B2 - Moremi	10.9	1.5	4.9	10.9	***	***
B2 - Photo	10.9	1.5	4.9	10.9	***	***
B2 - Hunting	10.9	0.6	1.5	3.7	5.3	10.9
B2 - Communal	1.5	0.6	1.5	3.6	10.9	***
B3 - Moremi	10.9	1.5	5.1	10.9	***	***
B3 - Photo	10.9	1.5	5.1	10.9	***	***
B3 - Hunting	10.9	0.6	1.5	4.6	10.9	***
B3 - Communal	1.4	1.4	3.6	10.9	***	***
B4 - Photo	10.9	0.6	1.5	4.2	10.9	***
B4 - Hunting	10.9	1.5	5.1	10.9	***	***
B4 - Communal	1.5	3.6	5.6	10.9	***	***
B5 - Photo	10.9	1.5	4.7	10.9	***	***
B5 - Hunting	1.5	0.6	1.5	4.2	10.9	***
B6 - Photo	10.9	1.5	4.7	10.9	***	***
B6 - Hunting	1.5	1.5	4.1	10.9	***	***
B1F1 - Moremi	10.9	1.0	1.4	4.6	10.9	***
B1F1 - Photo	10.9	1.1	4.6	10.9	***	***
B1F1 - Hunting	10.9	0.7	1.5	3.1	4.4	10.9
B1F1 - Communal	1.5	1.5	3.1	4.7	10.9	***
B1F13 - Moremi	10.9	0.9	3.3	10.9	***	***
B1F13 - Photo	10.9	0.9	3.1	10.9	***	***
B1F13 - Hunting	10.5	0.9	1.8	3.2	10.5	***
B2F9 - Moremi	10.9	1	1.7	2.7	10.9	***
B2F9 - Photo	10.9	0.9	1.5	2.6	10.9	***
B2F9 - Hunting	10.9	1.0	10.9	***	***	***
B3F1 - Moremi	10.5	1.0	1.6	4.6	10.5	***
B3F1 - Photo	10.9	1.4	4.6	10.9	***	***
B3F1 - Hunting	1.5	1.5	3.1	4.2	10.5	***
B3F1 - Communal	1.5	1.5	3.2	10.5	***	***
B3F6 - Photo	1.0	1.0	10.9	***	***	***
B3F6 - Hunting	0.9	0.9	2.5	7.4	***	***
B4F3 - Photo	10.9	1.0	2.9	4.9	10.9	***
B4F3 - Hunting	1.5	1.5	2.8	4.7	10.5	***
B4F7 - Photo	1.0	1.0	4.9	10.9	***	***
B4F7 - Hunting	1.0	1.0	2.8	8.3	10.9	***
B5F11 - Photo	10.9	0.9	2.6	10.9	***	***
B5F11 - Hunting	0.9	0.9	2.6	10.9	***	***
B6F8 - Photo	1.0	1.0	1.8	5.2	10.9	***
B6F8 - Hunting	10.9	1.0	3.0	10.9	***	***
B7F12 - Photo	2.7	0.9	2.7	5.1	10.9	***
B7F12 - Hunting	10.9	1.1	2.8	5.1	10.9	***
F1 - Moremi	10.5	1.4	4.6	10.5	***	***
F1 - Photo	10.5	1.3	4.6	10.5	***	***
F1 - Hunting	10.9	1.5	3.0	4.6	10.9	***
F1 - Communal	1.4	1.4	3.0	8.2	10.2	***

Table 7.18. Coefficient and standard errors for harmonic terms for disturbance history classes partitioned by land management. All cyclic terms were statistically significant for all disturbance history classes.

Disturbance History Class	Semi-Annual Coef	SE	Annual Coef	SE	Quasi-decadal Coef	SE
B1 - Moremi	-1.96E-02	4.53E-03	7.56E-02	4.37E-03	-1.43E-02	4.20E-03
B1 - Photo	2.22E-02	4.08E-03	6.57E-02	3.95E-03	-1.13E-02	3.95E-03
B1 - Hunting	1.86E-02	3.92E-03	6.17E-02	3.79E-03	-1.48E-02	3.56E-03
B1 - Communal	-1.97E-02	4.08E-03	6.49E-02	3.95E-03	-1.13E-02	3.59E-03
B2 - Moremi	1.76E-02	4.16E-03	6.89E-02	4.03E-03	-1.32E-02	4.00E-03
B2 - Photo	-2.39E-02	4.40E-03	6.71E-02	4.26E-03	-1.21E-02	4.29E-03
B2 - Hunting	-1.91E-02	4.40E-03	6.42E-02	4.27E-03	-1.46E-02	4.05E-03
B2 - Communal	2.27E-02	4.63E-03	6.84E-02	4.47E-03	-9.55E-03	4.28E-03
B3 - Moremi	1.81E-02	4.47E-03	6.84E-02	4.35E-03	-1.27E-02	4.20E-03
B3 - Photo	2.30E-02	4.60E-03	6.75E-02	4.45E-03	-1.29E-02	4.50E-03
B3 - Hunting	-1.92E-02	4.77E-03	6.29E-01	4.60E-03	-1.41E-02	4.57E-03
B3 - Communal	1.87E-02	4.42E-03	6.09E-02	4.30E-03	-1.02E-02	4.10E-03
B4 - Photo	-2.22E-02	4.75E-03	6.71E-02	4.59E-03	-1.33E-02	4.65E-03
B4 - Hunting	2.00E-02	5.00E-03	6.34E-02	4.84E-03	-1.36E-02	4.96E-03
B4 - Communal	2.26E-02	5.32E-03	6.09E-02	5.18E-03	-1.12E-02	5.48E-03
B5 - Photo	-1.96E-02	4.80E-03	6.74E-02	4.71E-03	-1.39E-02	4.80E-03
B5 - Hunting	-2.15E-02	5.30E-03	6.49E-02	5.10E-03	7.37E-03	1.26E-02
B6 - Photo	1.93E-02	5.25E-03	6.77E-02	5.08E-03	-1.20E-02	5.37E-03
B6 - Hunting	-2.20E-02	5.33E-03	6.67E-02	5.10E-03	-9.70E-03	5.50E-03
B1F1 - Moremi	1.69E-02	4.10E-03	6.43E-02	3.90E-03	-1.02E-02	3.70E-03
B1F1 - Photo	2.11E-02	4.17E-03	6.46E-02	4.03E-03	-7.93E-03	3.86E-03
B1F1 - Hunting	1.69E-02	4.30E-03	6.18E-02	4.17E-03	-1.03E-02	3.87E-03
B1F1 - Communal	-2.00E-02	4.80E-03	6.58E-02	4.70E-03	-8.24E-03	4.30E-03
B1F13 - Moremi	1.00E-02	4.60E-03	7.30E-02	4.84E-03	-1.81E-02	4.30E-03
B1F13 - Photo	8.40E-03	3.90E-03	6.45E-02	4.06E-03	-1.50E-02	3.70E-03
B1F13 - Hunting	-1.12E-02	5.59E-03	8.27E-02	5.63E-03	-1.22E-02	5.06E-03
B2F9 - Moremi	6.82E-03	4.18E-03	6.48E-02	4.64E-03	-1.13E-02	4.30E-03
B2F9 - Photo	3.36E-03	3.46E-03	6.07E-02	3.82E-03	-5.21E-03	3.41E-03
B2F9 - Hunting	2.24E-03	6.80E-03	7.45E-02	7.13E-03	-9.00E-03	6.40E-03
B3F1 - Moremi	1.69E-02	4.24E-03	6.44E-02	4.14E-03	-7.87E-03	3.67E-03
B3F1 - Photo	1.85E-02	4.78E-03	6.15E-02	4.62E-03	-7.44E-03	4.50E-03
B3F1 - Hunting	-1.69E-02	4.75E-03	5.80E-02	4.59E-03	-7.35E-03	4.32E-03
B3F1 - Communal	1.76E-02	5.10E-03	6.26E-02	4.94E-03	-7.28E-03	4.65E-03
B3F6 - Photo	9.10E-03	5.20E-03	6.17E-02	5.07E-03	-2.60E-03	4.90E-03
B3F6 - Hunting	6.70E-03	6.10E-03	5.43E-02	5.96E-03	1.08E-03	6.00E-03
B4F3 - Photo	1.66E-02	4.79E-03	6.24E-02	4.60E-03	-6.43E-03	4.10E-03
B4F3 - Hunting	1.66E-02	5.59E-03	5.84E-02	5.39E-03	-3.74E-03	5.31E-03
B4F7 - Photo	8.18E-03	5.87E-03	6.15E-02	5.68E-03	-2.06E-03	5.78E-03
B4F7 - Hunting	6.54E-03	6.29E-03	6.26E-02	6.13E-03	1.06E-03	5.90E-03
B5F11 - Photo	8.80E-03	4.67E-03	6.45E-02	4.94E-03	-3.70E-03	4.56E-03
B5F11 - Hunting	-7.80E-03	5.20E-03	6.68E-02	5.18E-03	-3.30E-03	4.95E-03
B6F8 - Photo	6.09E-03	6.39E-03	6.88E-02	6.35E-03	-5.82E-03	6.70E-03
B6F8 - Hunting	-5.34E-03	6.80E-03	7.19E-02	6.50E-03	-8.48E-03	5.83E-03
B7F12 - Photo	6.74E-03	5.59E-03	7.69E-02	6.09E-03	-4.92E-05	6.60E-03
B7F12 - Hunting	8.70E-03	5.24E-03	7.58E-02	5.78E-03	-8.23E-03	5.22E-03
F1 - Moremi	1.69E-02	4.14E-03	6.91E-02	3.99E-03	-9.65E-03	3.70E-03
F1 - Photo	-2.08E-02	3.70E-03	6.76E-02	3.59E-03	-7.77E-03	3.37E-03
F1 - Hunting	1.68E-02	3.90E-03	6.43E-02	3.79E-03	-1.03E-02	3.40E-03
F1 - Communal	-1.94E-02	4.60E-03	6.55E-02	4.47E-03	-7.67E-03	4.15E-03

Table 7.19. Total variance accounted for using only statistically significant terms semi-annual, annual, and quasi-decadal. R^2 values less than 0.7 highlighted in yellow.

Disturbance Class	R^2	Disturbance Class	R^2
B1 - Moremi	0.80	B1F13 - Hunting	0.78
B1 - Photo	0.79	B2F9 - Moremi	0.76
B1 - Hunting	0.79	B2F9 - Photo	0.81
B1 - Communal	0.79	B2F9 - Hunting	0.61
B2 - Moremi	0.80	B3F1 - Moremi	0.78
B2 - Photo	0.77	B3F1 - Photo	0.71
B2 - Hunting	0.76	B3F1 - Hunting	0.69
B2 - Communal	0.76	B3F1 - Communal	0.69
B3 - Moremi	0.77	B3F6 - Photo	0.68
B3 - Photo	0.76	B3F6 - Hunting	0.55
B3 - Hunting	0.72	B4F3 - Photo	0.72
B3 - Communal	0.73	B4F3 - Hunting	0.63
B4 - Photo	0.74	B4F7 - Photo	0.64
B4 - Hunting	0.70	B4F7 - Hunting	0.61
B4 - Communal	0.66	B5F11 - Photo	0.73
B5 - Photo	0.74	B5F11 - Hunting	0.72
B5 - Hunting	0.68	B6F8 - Photo	0.65
B6 - Photo	0.71	B6F8 - Hunting	0.65
B6 - Hunting	0.69	B7F12 - Photo	0.72
B1F1 - Moremi	0.79	B7F12 - Hunting	0.74
B1F1 - Photo	0.77	F1 - Moremi	0.80
B1F1 - Hunting	0.75	F1 - Photo	0.83
B1F1 - Communal	0.73	F1 - Hunting	0.80
B1F13 - Moremi	0.80	F1 - Communal	0.74
B1F13 - Photo	0.83		

The overall R^2 of the best harmonic fitting for each disturbance history class are shown in Table 7.19. The disturbance/management classes with the lowest R^2 of the harmonic regression were B3F6-Hunting (55%), B4F7-Hunting (61%), B2F9-Hunting (61%), and B4F3-Hunting (63%). In general, the classes falling within the hunting concessions and communal areas had lower R^2 values. The higher R^2 values tended to be associated with classes experiencing lower amounts of observed burning, higher amounts of flooding, and did not exist within the communal areas. Thus, hypothesis 4 which tested

whether as the number of floods increases, the predictability of the trajectory decreases was rejected. In contrast, hypothesis 5 which tested whether as the number of fires increases, the predictability of the trajectory decreases was confirmed.

Again, the earlier results from the 35 EVI-based trajectories suggest that a lack of flooding in floodplains results in a lower R^2. The R^2 in hunting concessions were generally lower than in the photography concession. Similarly, R^2 values in the game reserve were generally higher than communal areas. The explanation is that humans are impacting the vegetation in the communal areas (in non-cyclic ways) and the harmonic regression using the semi-annual, annual, and quasi-decadal cycles do not fit as well as in Moremi where humans have less of an impact. Thus, there are several variables likely affecting the interpretation of the modeled dynamics, including an interaction of the flooding and fire regime, anthropogenic factors, floodplain position within hunting and photography concessions, vegetation type under each DH cluster, and lag times between flooding and fire.

These results reveal new utility for using remotely sensed imagery to assess vegetation spectral response as a function of predicted climatic patterns, land management, and disturbance regimes. In the Okavango Delta, portions of the landscape that were found to fit well with climatic cycles include channels, reeds/sedges, riparian vegetation, and woodlands. In contrast, portions of the landscape that did not fit as well to detected climatic patterns include floodplains that were dry for several years, as well as grasslands and woodlands located near settlements. The ability to quantify vegetation spectral response to climatic patterns as well as disturbance via time-series analysis can

be used to identify regions at risk or vulnerable to future climate or land use change scenarios. As the results indicate, the residual signals also contain frequencies that may be a combination of climatic and anthropogenic effects.

8 SUMMARY OF FINDINGS AND FUTURE RESEARCH

In 2007, the National Research Council identified "understanding shifts in ecosystem structure and function" as "an emerging global challenge" (pg 2-1) (NRC, 2007). The objective of this research was to utilize remotely sensed imagery to examine the spatio-temporal distribution of flooding and fire, and the temporal dynamics of the vegetation spectral response as represented by a vegetation index in the Okavango Delta. Although this research was located in Botswana, the methodologies utilized in this study are generalizable and can be implemented in other regions and systems. Harmonic regression and wavelet analysis, methodologies not typically used in traditional remote sensing change detection studies, were applied to an EVI time-series to extract trends and patterns from the temporal dynamics of the vegetation spectral response across this landscape; this study showed the developed methodologies are robust enough to warrant application and testing elsewhere. The results from this study area present the opportunity to examine fluctuations to natural variability, facilitated by the (relatively) low human population density and natural flow regime that currently exists on the Okavango River. This research tested six hypotheses regarding flooding and fire and are as follows:

1) ***Within the Delta's management zones, fire frequency is highest in the Wildlife Management Areas closest to the fence where people have easiest access.*** This hypothesis was confirmed with the majority of high burn areas occurring within the WMAs and within a 5 km buffer from the Buffalo fence.

2) *Among the Delta's ecological zones, fire frequency is highest within the active floodplains.* This hypothesis was confirmed, with approximately 75% of the high burn areas falling in the active floodplains.

3) *Periodicities observed from the vegetation signal time-series will be strongest at 3-, 8-, and 18-year cycles.* This hypothesis was largely rejected save for the 18-year cycle which could not be adequately tested given the temporal depth of the dataset. In fact, an approximately three year cycle was observed for eight of the 35 EVI clusters. None of the EVI clusters were associated with an eight year cycle. A cycle of 10.9 years was observed for all EVI clusters.

4) *As the flood frequency increases, the predictability of the temporal trajectory decreases.* This hypothesis was rejected as higher R^2 values were associated with increased amounts of flooding.

5) *As the fire frequency increases, the predictability of the temporal trajectory decreases.* This hypothesis was confirmed as lower R^2 values were associated with increased amounts of burning.

6) *Flooding and fire are positively correlated with the residual signal of the EVI trajectories.* This hypothesis was rejected as the transitory signal was not significantly correlated with flooding and only minimally correlated with burning for eight of the EVI clusters.

8.1 Contributions of this Research

The characterization of the spatio-temporal distribution of flooding and fire regimes and the temporal dynamics of vegetation spectral response via a time-series of remotely sensed data informs not only ecosystem and disturbance theory but also presents new methodological applications for multi-temporal change analysis. The availability of the multi-temporal Landsat dataset facilitated the exploration of many ecological questions regarding disturbance theory at the landscape level. Regarding multi-temporal data, sampling theory states that if a signal is sampled at an interval *d*, then frequencies less than *2d* cannot be detected (Li et al., 2005). Thus, to capture a semi-annual (six months) signal in a remote sensed dataset, the temporal spacing between images should be no greater than three months. This dataset has sufficient temporal resolution (approximately one scene every two months over 14 years) to examine both intra- and inter-annual vegetation spectral response to stationary processes, but at a significantly improved spatial resolution (30 m) over sensor systems whose high frequency return time is concomitant to coarser spatial resolution to observe landscape level patterns and change. Local pressures contributing to changing landscape patterns include regional-scale climate change, hydrological change, and land use / land cover change (Schulze, 2006). Thus, patterns observed at the landscape level can be examined through the temporal dynamics of the vegetation signal that subsequently provides insight into the underlying local pressures.

The specific contributions of this research include 1) a contribution to the ecology literature via spatio-temporal characterization of the flooding and fire regimes in the

lower Okavango Delta, 2) implementation of non-traditional change detection techniques using harmonic regression and wavelet analysis for the detection of subtle (e.g. increasing *Acacia* density in a savanna class) trends and patterns of change, and 3) recommendations to the stakeholders and citizens of the Okavango Delta. Each of these contributions is detailed in turn in the following sections.

8.1.1 Contribution to the Literature

8.1.1.1 Equilibrium Theory

The three primary ecological theories used as a conceptual framework for this research include equilibrium theory, disturbance theory, and resilience theory. Ecosystem dynamics are often described as falling along a continuum between equilibrium and non-equilibrium properties; however, most ecosystems exhibit properties of both (Briske et al., 2003). The advantage of using a non-equilibrium framework to describe ecosystem behavior is the recognition that ecosystems are dynamic and subject to disturbances. As such, static conditions or the placement of stringent thresholds are not appropriate when contemplating management of ecosystems. This research indicated that while the observed vegetation spectral response was reasonably predictable to presumed climatic cycles (61 to 88 percent across this landscape), the source of the remaining uncertainty on the landscape, whether climatic or anthropogenic in origin, is still unclear. This uncertainty, however, is the motivation for suggesting continued monitoring and investigation.

The ability to quantify and predict the temporal dynamics of the vegetation spectral response presumes some equilibrium properties (Fuhlendorf and Smeins, 1998; Briske et al., 2003) but within a non-equilibrium framework, which is appropriate for savanna environments (Sullivan, 1996; Lankford and Beale, 2007). Equilibrium concepts imply that, through a set of feedbacks, the vegetation behavior is predictable. However, a non-equilibrium framework recognizes a dynamic system and that external forces (such as a variable climate, fire, and herbivory) influence the system (Lankford and Beale, 2007). That is, the vegetation productivity, density, community structure, and species diversity are, in theory, dynamically responding to their environment. By modeling the vegetation spectral response to climate cycles and trends, human impacts can potentially be extracted from the impacts of natural systems, allowing for better prediction of future ecological function in an environmentally sensitive area. That is, human impacts could be identified as deviations from the predicted "natural" model.

8.1.1.2 Disturbance Theory

Disturbance theory as typically described in the literature, examines the influence of disturbance at the individual level rather than at the landscape level (Collins, 1987; Turner, 1988; Chaneton and Facelli, 1991). This research characterized the flooding and fire regimes in the lower Okavango Delta and found a general spatial association between the two. At the landscape level, differences in residual dynamics were observed with different disturbance histories and frequencies indicating a potential interaction with vegetation dynamics. Due to the spatial and spectral resolving power of the imagery, the

intermediate disturbance hypothesis (IDH) was not a useful framework for this study. A limitation of the IDH is that a simple variable, such as species richness, does not provide much insight into ecosystem function in response to disturbance particularly at the landscape level. However, there is little ecological theory regarding the relationship of disturbance on ecosystems at the landscape level as compared to the individual level. Results from this research identified different periodicities and dynamics in the EVI-residual trajectories for areas that experienced burning and/or flooding. In particular clusters having a dominant frequency of 1 year were found to be associated with high levels of flooding (flooding approximately every year) and frequent burning (burning every one to two years), whereas the dominant 1.7 year residuals were typically associated with intermediate levels of burning (burning every three to four years) and no flooding. Similarly, clusters having the 2.5 year and 5.9 year dominant residual frequency were associated with low to intermediate amounts of burning (two to four times in the 14-year time-series) and flooding approximately every other year. Deviations of the residual dynamics may prove to be a better indicator of ecosystem response compared to the IDH; however, this new notion needs to be tested further.

A 14-year construction of the flooding and fire histories was established for the lower Okavango Delta from 1989 through 2002. Within the study area, 27.7% (67,466 hectares) of the landscape was impacted by both flooding and fire, 5.15% (12,512 hectares) by flood-only, and 26.96% (65,529) by fire-only. The largest flood occurred in 1989 with ~1575 km^2 followed by 2000 and the early 90s with annual flooding extents of ~1000 km^2. The 14-year flooding history revealed different spatio-temporal patterns for

the channels within the study area. The largest channel, the Boro, had the greatest fluctuation in flooding extent (~50 km^2 in 1996 to 610 km^2 in 1989). In contrast, the Santantadibe was mapped with annually consistent flood extent of approximately 70 km^2. These observations are consistent with stream flow measurements reported during the same time period (Wolski and Murray-Hudson, 2006). The Marophe channel (which is hydrologically connected to the Xudum) had only limited amounts of flooding (< 20 km^2 in 1989 and < 10 km^2 in 1990, 2000, and 2001) during the 14-year period. The map product of maximum time between flood events revealed an apparent delineation of the seasonal floodplains from the occasional floodplains. Regions that were mapped with a large time between flood events were more likely to experience shifts in vegetation. *Acacia spp*. and other woody species will often encroach in floodplain margins (also referred as occasional floodplains) within just a few years when flooding is no longer present on the landscape. The encroachment of woody vegetation into the floodplains is partially kept in check by recurring floods and/or fire.

A limitation to the understanding the influence of fire on this landscape is that the spatial patterns and frequency of fire were previously not known (Heinl, 2001; Roy et al., 2005). One of the concerns outlined in the Okavango Delta Management Plan as a threat to the ecosystem sustainability is the high rate of human-induced fires (Jansen and Madzwamuse, 2003). Disturbance frequency is regarded as one of the most important variables in assessing resiliency within an ecosystem (Turner et al., 1993) and a change in frequency can alter the successional trajectory. While fire is considered to be common (every 3 to 4 years) in the Okavango Delta (Ringrose et al., 2005), an increase of

frequency and/or severity can alter the overall productivity, species composition, and vegetation structure (Collins et al., 1995; Pickett and Cadenasso, 1995). For example, a significant increase in the fire frequency can reduce the amount of nitrogen and phosphorus in the soil resulting in decreased fertility (Bonyongo and Mubyana, 2004). In the work presented by Ringrose et al. (2005), it is suggested that fires occur at a 3- to 4-year interval throughout the Okavango Delta. The fire return interval (FRI) results in this research indicate a FRI of every 2- to 3- years in the lower floodplains transitioning to 4- to 5- year intervals upstream and every 5- to 7- years in regions adjacent to the floodplains.

In the Delta, the majority of fires are thought to be anthropogenic in origin, typically applied to small areas prior to harvesting of reeds, for clearing of dead vegetation prior to the arrival of the annual floods, or as accidental fires from camps (Ringrose et al., 2005; 2007 personal observation). Occasionally, these fires spread uncontrolled when in areas of high (vegetative) fuel load that lack firebreaks (Heinl et al., 2004). The seasonal fires reduce woody development within the floodplains and also provide a quick growth and resurgence of grasses (Ringrose et al., 2005). The proximity of an area to the primary floodplains seems to be a major factor in the characterization of the fire regime for the lower Okavango Delta.

8.1.1.3 Resilience Theory

Resilience theory proved to be an appropriate and useful theoretical framework for conceptualizing the impact of disturbances on ecosystem dynamics. Resilience is

defined as the ability of a system to absorb a disturbance while maintaining the same function, structure, and feedbacks (i.e. a pre-disturbance state) (Ludwig et al., 1997; Folke et al., 2004). Thus, the observed behavior of a resilient system would continue on its current trajectory following a disturbance. However, there are important caveats when implementing this approach to a remotely sensed dataset. First, various vegetative components of an ecosystem (e.g. grasses versus trees) have different life cycles, different adaptations to disturbance, and thus different resiliencies. At the spatial extent of most remotely sensed products, the spectral response is an integrated effect from the multiple constituent components on the landscape. An example of this phenomenon would be an *Acacia* savanna that is a combination of a continuous herbaceous layer with varying densities of *Acacia* tress. The observed spectral response is dependent upon the density of trees, grasses, and soil background within the sensor instantaneous field of view. Next, the observed temporal dynamics of the vegetation are a function of which vegetation surrogate was used (e.g. EVI) and what that vegetation index is responsive to. In this work, EVI was selected as the vegetation index as it is reported to be most sensitive to herbaceous vegetation (Fang et al., 2005). In addition, the EVI-trajectories used in this research represent the mean EVI response for each cluster that could obscure the interpretation of resiliency. Therefore, it is suggested that other indices or statistics be utilized to test the robustness of the results. Finally, the temporal resolution of a time-series dataset should be sufficient to capture the effective dynamics on the landscape. In this study, the average time step between successive images was 2.5 months. At this temporal resolution, the overall dynamics of different portions of the landscape were able

to be determined. However, the return time to disturbance (and thus the resilient behavior) was in some cases potentially missed due to a large time step between some scenes. Resilience, as with many concepts, is a function of scale –both temporal and spatial, and datasets must be adequately comprised in order to effectively address these concepts.

The utilization of multi-temporal imagery for the development of resilience indicators also holds promise for future studies. By definition, resilience is the ability of a system to withstand disturbance. By implementing a harmonic model on each EVI trajectory, the overall R^2 can act as a potential indicator of resilience. In the lower Delta, portions of the landscape that were found to fit well with reported climatic cycles (semi-annual, annual, and quasi-decadal) include frequently flooded channels, reeds/sedges, riparian vegetation, and woodlands. In contrast, portions of the landscape that did not fit as well to the cycles include floodplains that experienced drought as well as savannas located near settlements. In general, the higher R^2 values tended to be associated with classes experiencing lower levels of observed burning, higher levels of flooding, and located outside the communal areas. Landscapes that are less resilient (i.e. having a lower R^2) to disturbances such as drought, fire, or insect outbreak could experience dramatic shifts in the vegetation assemblages and ecosystem services. It remains to be seen whether these less poorly fit areas are less resilient, as even a fourteen-year time-series may be inadequate to capture the cycles and dynamics at work in such a complex mosaic (Rappaport et al., 1998; Turner et al., 2001).

8.1.2 New Perspective to Observe Land Cover Change

The time-series of imagery used in this study provided a unique opportunity to examine ecosystem response to disturbance at the landscape level with a seasonally rich time frame. The motivation for implementing a harmonic regression was to quantitatively describe the trends and patterns of land cover trajectories hypothesized to correspond to cyclical events (i.e. semi-annual and annual cycles). Rather than using Fourier analysis to segment the landscape based upon identified periodicities (i.e. seasonality), a harmonic regression was employed to assess how well different portions of the landscape fit with known periodicities. Time-series data from satellite imagery typically consist of a vegetation index for each time step and can be mathematically represented as a signal comprised of a Fourier series. Wavelets are often used for the studies of natural systems because the pressures (both natural and anthropogenic) occur at a variety of spatio-temporal scales (Pickett et al., 1989; Wiens, 1989; Braswell et al., 1997; Alpin, 2006). Wavelet analysis has been widely used in many fields including geophysics, ecological studies (Saunders et al., 2004; Mi et al., 2005), hydrology (Labat et al., 2004) and climate studies (Kestin et al. 1998) for characterizing temporal and frequency variability in time series data. Additionally, wavelets have been utilized for decomposing spatial structure across 2-D images (Mi et al., 2005; Murwira and Skidmore, 2006) yielding information about landscape pattern. An advantage over Fourier analysis is that wavelets not only decompose the input signal into a set of dominant frequencies but also determine where or when the variability fluctuations occur in space or time (Torrence and Compo, 1998;

Kestin et al., 1998). Wavelets were used in this study to identify periodicities beyond the semi-annual and annual climatic cycles, such as quasi-decadal cycles.

However, only recently are decadal trends in the terrestrial vegetation spectral response as observed from remotely sensed imagery being reported, since remotely sensed data archives are now sufficiently long to identify long-term trends. Stockli and Vidale (2004) report phenological variations derived from AVHRR in northern Europe are statistically correlated with the Northern Atlantic Oscillation (NAO) index. Similarly, Gong and Shi (2003) associate decadal trends in global NDVI with NAO and Southern Oscillation Index (SOI). The detection of a quasi-decadal signal in the residuals of the vegetation spectral response for terrestrial ecosystems is a novel contribution of this research. Although the extent of these time-series data is short to have statistical confidence in a quasi-decadal cycle, a quasi-decadal signal has been recently noted (though not quantified) in flow velocity data for a few hydrography stations in the Okavango Delta (Wolski and Murray-Hudson, 2006). Since decadal oscillations have been observed in solar/climatic indices (Friis-Christensen and Lassen, 1991; Hurrell, 1995; Wang and Wang, 1996), the quasi-decadal signal was included in the harmonic regression in order to remove any effects of the long-term cycle from the overall trend.

This research reveals that quasi-decadal trends are also observed (given the previous caveat regarding length of time-series) at the higher spatial resolution of Landsat. Further, the temporal richness of this Landsat time-series indicates differential vegetation spectral response to multiple forcing factors (such as climate, management, and disturbance) across the landscape. The observed quasi-decadal trend could be

associated with variability in solar sun spot activity. In particular, analysis of the annual number of sun spots (Wolf numbers) and precipitation data from the Maun airport show a 10.5 year and 10.8 year periodicity respectively, which is also observed in the EVI-residual vegetation signal. It is not known whether the quasi-decadal signal detected in the EVI residual signals is a result of precipitation cycles or cycles in solar activity; however, there is an apparent climate/vegetation interaction.

Variability in solar radiance at short-term (decadal) and long-term (centuries) timescales has been linked to climate fluctuations observed in ice cores (Waple, 1999) and variability of solar radiance likely influences other climate indices (e.g. PDO and NAO) (Friis-Christensen and Lassen, 1991). In this study area, the mapped annual flood extent exhibited significant correlation ($r = 0.88$) with the solar sunspot activity shown in Figure 8.1. In addition to the impact of climate on the observed vegetation spectral response, the terrestrial vegetation also directly interacts with climate through the exchange of gases, heat, and moisture. Factors such as leaf area index, surface albedo, and landcover and soil characteristics can significantly influence land-climate exchanges on time scales ranging from seasonal to decadal (Pielke et al., 1998; Hurtt et al., 1998). Thus, it is imperative that changes in landcover continue to be monitored and their dynamics integrated into models of land-climate interactions.

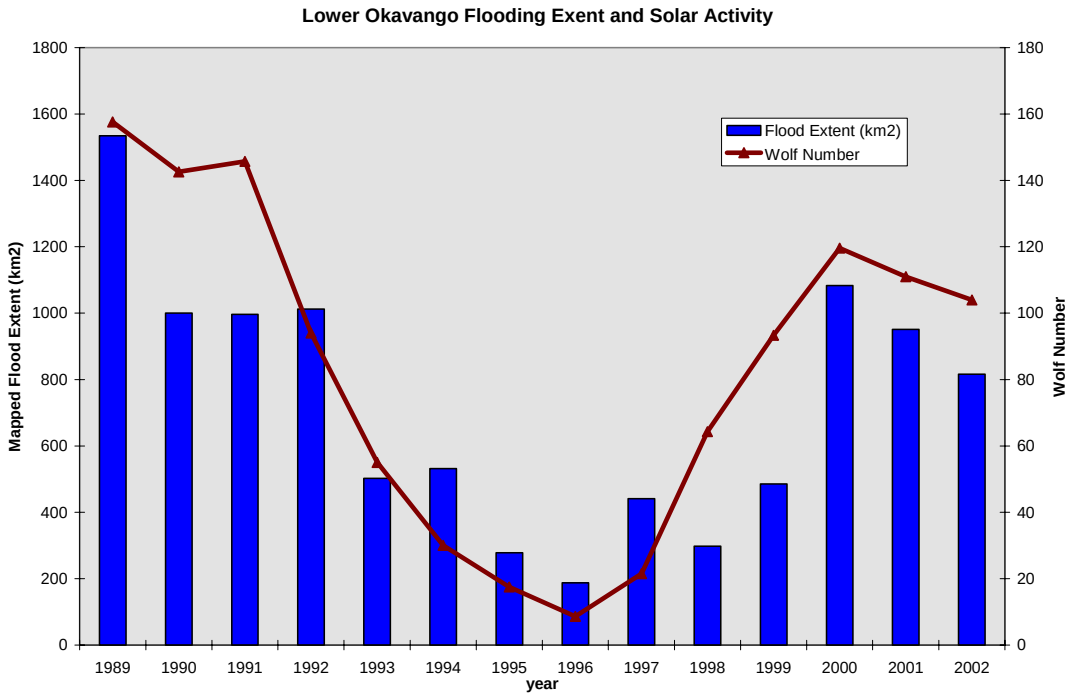

Figure 8.1. Relationship between flooding extent within study area and solar activity.

This research reveals new possibilities in the way remotely sensed imagery is utilized to assess the temporal dynamics of the observed vegetation spectral response as a function of predicted climatic patterns, disturbance, and potentially anthropogenic factors. The creation and analysis of a seasonally rich TM/ETM+ multi-temporal dataset may not always be practical or even possible. To continue the analysis of remotely sensed time-series for future research, it is imperative that the fusion of medium resolution data (e.g. Landsat) to the dynamics derived from MODIS time-series products be developed. The fusion of time-series information from multiple resolutions could improve operational regional scale monitoring and mapping efforts across the Delta or other regions (Song and Woodcock, 2002). The results from this research support the growing

body of evidence that many things in nature are cyclic (Waple, 1999; McCarthy et al., 2000; Tyson et al., 2002). Therefore, it is important that cyclic behavior be both methodologically and theoretically incorporated into the understanding of ecosystem response.

8.1.3 Contributions to the Delta

A goal of many remote sensing studies is to systematically monitor and observe change through time for an area. For several reasons, the Okavango Delta is an ideal place to examine and separate natural and anthropogenic change. The Delta is a compelling location because the amount of anthropogenic influence in many areas is limited. To model and predict the impacts of climate change or land use scenarios on the landscape, it is critical to establish a baseline of ecosystem structure and behavior that have minimal amounts of human input. Although much socio-ecologic research has taken place in the Delta, the results have not translated into policy or action. Several attempts, such as the Okavango Delta Management Plan (ODMP) have been developed, yet they have not been realized into policy. The ODMP was developed to fall within the context of the Ramsar convention as well as policies and treaties under the Southern African Development Community (SADC) and Vision 2016. Vision 2016 is a long term plan developed by the government of Botswana toward poverty reduction, natural resource development and utilization, and sustainable growth. In particular, Vision 2016 recognized the urgent need of a plan for the Delta due to the complexity and fragility of its ecosystem.

Water availability and resources in the Delta have been modeled for changes due to climate change and upstream water extraction (Andersson et al., 2006; Murray-Hudson et al., 2006). The projected flood extent is one of the most sensitive parameters in the hydrology models (Wolski et al., 2006; ODMP, 2006). The mapped spatial distribution of the flood extent has significant implications on the ecosystem functionality of the Delta but also on the people relying upon its resources for their livelihoods. For example, the annual floodwaters are reported to contribute to groundwater recharge. Thus, mapping the flood distribution can increase knowledge regarding where to install boreholes for increased population growth in the vicinity of Maun. The Botswana Department of Water Affairs currently extracts 3.84 MCM per year (~0.0038% mean annual flow) with a projected increase of 11 MCM per year (0.011% mean annual flow) by 2025 (ODMP, 2006). While the projected off-take of water from Botswana does not appear to threaten the annual flooding, upstream issues also of concern may change the system's sensitivity to local off-take. The construction of dams along the Okavango River would also result in the trapping of sediments, a necessary component to channel switching and the resiliency of the Delta (Ellery and McCarthy, 1994; O'Conner, 2001; Bunn and Arthington, 2002). Another concern is the use of fertilizers that would result in eutrophication, increasing the likelihood of invasive aquatic species such as water lettuce *(Eichhornia crassipes)* and African weed (*Salvinia molesta*) (Ellery and McCarthy, 1994; Ellery et al., 2003b).

Another concern stated in the ODMP as a threat to the ecosystem sustainability is the high rate of human-induced fires in the Delta (Kay et al., 1999; Jansen and Madzwamuse, 2003). Within the wildlife management areas (WMAs), burning is not

permitted. However, it was shown in this research that a large number of fires occur within the WMAs, particularly along the Buffalo Fence. In other regions of the Delta, frequent burning is reported to be ecologically damaging resulting in increased erosion and loss of vegetation species (ODMP, 2006). The mapped flood and fire distribution could provide the ODMP with information necessary to monitor and implement policy within the Delta. In other areas of the world, fire is an effective management tool and as such a fire permitting system could be implemented for controlled burns and known locations. While a fire permitting system could be implemented, a difficulty arises when determining how and who will enforce the policy, but all of these questions require a baseline of fire frequency and impact.

A fundamental requirement of the Ramsar treaty and the ODMP is the wise use and conservation of wetlands while being responsive to the socio-economic needs of the local stakeholders. Many communities rely upon harvesting of reeds and other veld products, wetland-based tourism activities, and fishing (Mbaiwa, 2003; Meyer and Bendsen, 2003; Mbaiwa, 2004b). These uses require that the communities or individual citizens have rights and access to resources in the Delta; however landuse practices have been haphazardly implemented (ODMP, 2006). Factors complicating the sustainability of the Delta include climate change, over-exploitation of natural resources, negative impacts from tourism activities, inequity of land management and resources, and improper agricultural practices. Over-harvesting of thatching reeds and harvesting at improper times of the year is thought to be one of the major socio-economic concerns facing the livelihoods of many Delta communities (Kgathi et al., 2005; Kgathi et al., 2006).

Additionally, over-grazing of cattle and donkeys has led to a depletion of herbaceous cover and woody encroachment in many areas surrounding the Delta (Ben-Shahar, 1998; Barnes, 2001; Ringrose et al., 2002d). Trampling of vegetation and soil around waterholes has resulted in poor soil quality (Pietola et al., 2005). A reason for the historically low human population in the Delta is the presence of tsetse fly which carries a deadly parasite (Bolten, 1998; Meyer and Bendsen, 2003). The near eradication of tsetse fly raises concern regarding domestic grazing moving into the Delta. As human encroachment into natural areas increases, it is critical that places like the Delta are conserved and protected.

Habitat quality in the Delta is a complex interaction of flooding, precipitation, fire, and wildlife population levels. Although non-equilibrium properties of ecosystems are recognized in the academic sector, they often do not influence management practices (Gillson and Lindsay, 2003; Gillson and Hoffman, 2007). Remote sensing could provide a critical tool for assessing habitat quality in a near real-time basis. Efforts are underway to integrate wildlife management strategies with habitat management. Hunting and safari camps are currently being asked to provide wildlife counts on gridded habitat maps of the Delta (Sheller, personal communication). This information will help concession owners negotiate hunting quotas for concession areas that are beneficial to the vegetation and to ensure sustainability of ecosystem services provided by the Delta (Campbell et al., 2006). A weakness in this management strategy is that habitat structure associated with different wildlife quotas in the concession areas are based upon vegetation conditions and spatial configuration at one point in time: based upon the HOORC landcover product of 2000.

However, habitat structure and forage quality fluctuate due to changing precipitation, flooding, and burning conditions. This lack of temporal information regarding the temporal dynamics of the vegetation spectral response is one area where the results from this research can be immediately incorporated.

Establishment of baseline vegetation behavior (as observed via remote sensing) is critical for future capabilities of extracting the impacts of wildlife within a dynamically changing natural system, thereby allowing for better prediction of future ecological function in an environmentally sensitive area. A management plan based upon non-equilibrium concepts should consider and incorporate ecological function and processes as well as the range of fluctuating vegetation patterns into the model design (Gillson and Lindsay, 2003; Sammy and Opio, 2005). The near real-time assessment of potential forage using remotely sensed data could offer wildlife officials increased information for negotiating hunting quotas. In rangeland studies, stocking rates and grazing regimes are reported to be influenced by environmental variability and predictability, degradation, property rights, and market stability and prices (Campbell et al., 2006). Long-term studies of rangeland productivity indicate that the profit maximizing stocking rates of cattle fall well below those rates which would degrade the landscape (Holechek et al., 1999). Additionally, information regarding the flooding and fire histories is critical for interpreting and modeling suitable wildlife habitat.

The Okavango Delta plays a significant ecological, hydrological, biological, and socio-economic role in northern Botswana. The future ecologic and economic productivity of the Delta remains uncertain, as many outside forces may severely alter its

existence. The Okavango Delta is the only permanent source of surface water in semi-arid Botswana. As competition for this scarce resource intensifies, the absence of proper water management increases the likelihood of degradation of this wetland system. These findings will help to establish a baseline for integrated ecological assessment, monitoring, and conservation planning in an internationally important environment. Moreover, the results from this research as well as proposed work will help environmental managers and policymakers in regards to natural resource management of seasonally flooded or fire-prone areas. In addition, this research contributes to better understanding the dynamics of one of the world's largest RAMSAR wetland sites before its functionality and the surrounding flora, fauna, and humans are altered by upstream settlement and water policies.

8.2 Future Research

The availability of the Landsat time-series used in this research provided an opportunity to investigate observed vegetation spectral response at a high resolution for an ecologically compelling region. In the course of this analysis, issues and questions regarding further testing and implementation arose that warrant immediate investigation. These include 1) improving the interpretation of the temporal dynamics of the vegetation signal by examining other factors/components on the landscape such as biophysical variables (topography), lagged correlations between flooding and fire, testing the robustness of other statistics or other vegetation indices for creation of trajectories, and collecting additional *in situ* data; and 2) increasing the continuity of the time-series.

Scaling dynamics extracted from medium resolution EVI data (30 m Landsat) could be scaled and linked to coarse resolution EVI data (1 km MODIS) to extend the time-series to present day. Each of these suggestions is discussed in greater depth in the following sections.

8.2.1 Improving the Interpretation of the Temporal Dynamics of the Vegetation Signal

There are several biophysical variables to include in future research to extend the interpretation of the dynamic behavior of the Okavango system. In particular, topography is a key factor for understanding and modeling surface water flow. A digital elevation model derived from the Shuttle Radar Topography Mission (SRTM) having an elevation precision of 1 m is available for international areas with a grid spacing of 90 m. Much of the spatial variability is the lower Delta is caused by small changes (~1 - 2 m) in local topography. Although the spatial resolution of the DEM is coarse and the elevations from SRTM are biased in the presence of vegetation (due to the scattering phase center for C-band radar), the SRTM DEM is the only elevation product available for many regions of the world, including the Delta. One method to incorporate topography into the analysis is to stratify the landscape in the study area based upon sub-catchments and floodplain delineations and examine the vegetation dynamics.

Fleshing out lag times between flooding and fire is a second important way this research should be augmented. This research described the spatial association of flooding and fire and the ratio of number of floods to number of fires between 1989 and 2002 is shown in Figure 8.2. In the distal floodplains closer to the Buffalo fence, the number of fires is greater than the number of flooding events (shown as shades of green). In

contrast, approximately 20 km from the Buffalo fence the number of floods outweighs the number of fires. In addition to examining the ratio between flooding and fire, the 0^{th} lag correlation between flooding and fire with the transitory dynamics was computed. While the correlation between flooding and fire was small at the 0^{th} lag, there is a potential correlation at a distinct lag time. For example, fire may be positively correlated with flood the following year. Although correlation between flooding and fire does not indicate causation, it does improve knowledge regarding how these two regimes interact on this landscape. To assess the potential lagged correlation, the time-series data should be sampled at a uniform time step and the time-series used in this research would require interpolation. Interpolation schemes could include a simple linear fit from point to point or a spline fitting function. One limitation in the interpretation of ecological process using a lagged correlation analysis is the unknown effect of interpolation on the results.

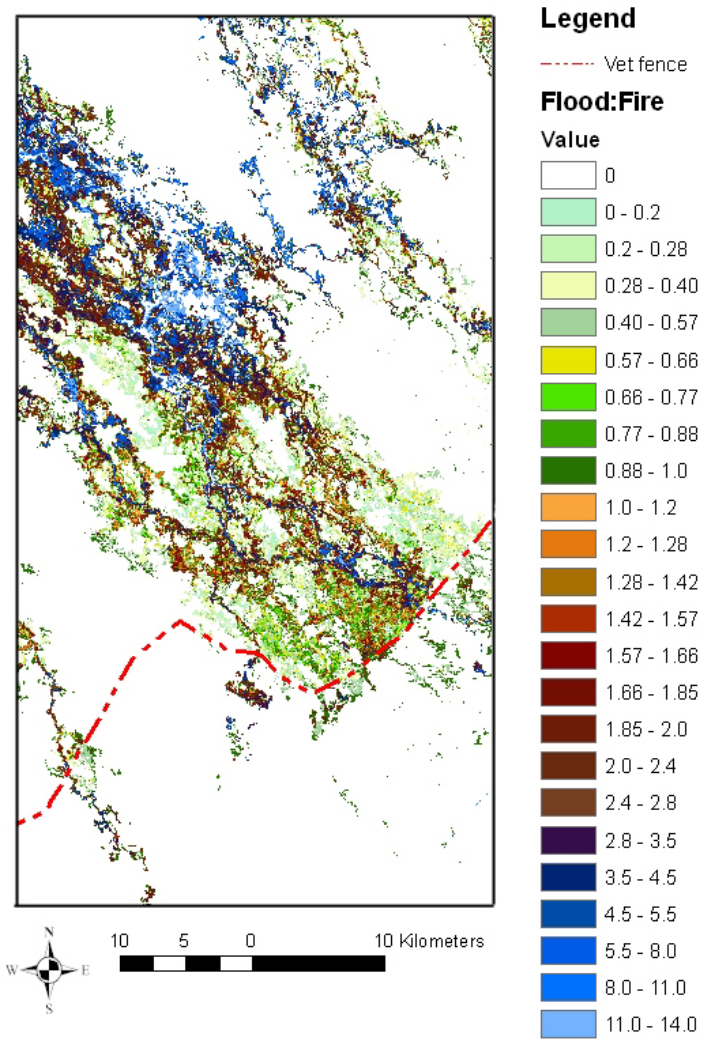

Figure 8.2. Ratio between Flooding and Fire in the study area.

A third approach to continue with this analysis is to examine the robustness of results and interpreted dynamics using different indices and/or methods for creating the trajectories. That is, the robustness of results is increased if similar results are achieved using different trajectories. An alternative method to examine the vegetation dynamics is to analyze the standard deviation of the EVI values within each cluster in addition to the

cluster means. The mean EVI value, though a necessary starting point, may not be the best indicator of subtle change on the landscape; the change in cluster variability through time may yield interesting results, particularly regarding disturbance and resilience. In particular, the standard deviation of the EVI clusters may indicate a departure from normal, providing additional understanding of trajectory behavior.

As discussed earlier, EVI has been shown to be positively correlated with herbaceous productivity (Fang et al., 2005) whereas other bands/derived products (Red and surface albedo) have been suggested to be a better indicator for woody vegetation in semi-arid regions (Fuller et al., 1997; Fuller, 1999; Yang and Prince, 1997). From the harmonic regression results in this study, the maximum canopy response occurs during the latter portion of the rainy season whereas the end of the rainy season represents the peak time for wetland vegetation. This phenology of the herbaceous vegetation in the lower Delta, however, differs from the phenology of the trees in the Delta. The *Acacia* trees are in full leaf-out by early September and *Mopane* trees will leaf-out mid-October (Ringrose, personal communication). The phase component of the annual trend for each EVI trajectory was converted into day of year (DOY) and is plotted spatially in Figure 8.3. Specifically, the peak DOY for the herbaceous layer in the *Mopane* woodlands occurs between day 2 through 6 (Jan 2 – Jan 6). The peak DOY for the herbaceous layer in the *Acacia* dominated savanna occurs between days 24 - 28 (Jan 24 – Jan 28). The peak DOY for the annual grasses and shrubs within the less active floodplain occurs between day 15 – 23 (Jan 15 – Jan 23). Regarding the active floodplains, the peak DOY for the main channels occurs on day 32 - 43 (Feb 2 – Feb 11). A recommended area for

further study is to compute the peak vegetation signal using an indicator that is sensitive to woody cover such as the red band or broadband albedo. That is, different ecological zones of an area may require different vegetation indices, rather than using one vegetation index throughout an entire study area. Decoupling the herbaceous signal from the woody signal would improve the characterization of the habitat in the Delta and provide a mechanism to assess the relationship of disturbance on both herbaceous and woody components on the landscape.

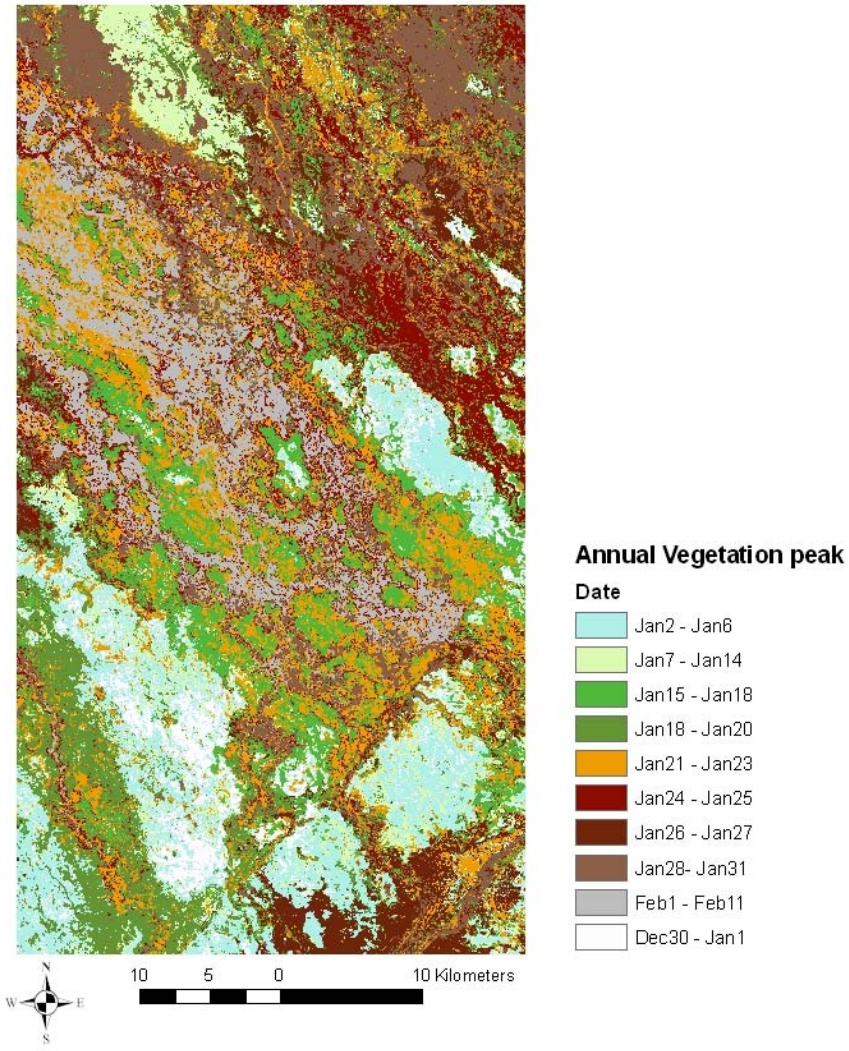

Figure 8.3. Annual peak DOY of landscape trajectories

Finally, the results from this research should be evaluated against field data. In particular, do the areas where the R^2 was less well fit or where the residual dynamics behave differently characterized by different vegetation. Due to the accessibility of the Okavango Delta at certain times of the year, it is difficult to match conditions of archival data. To increase the interpretability of the analysis, it is recommended that future field campaigns be planned at the time of acquisition of new imagery. The utilization of time-series analysis on remotely sensed imagery in conjunction with *in situ* derived knowledge can be a powerful tool for mapping and monitoring vegetation spectral response to anthropogenic and climate change (Cullinan et al., 1997; Kerr and Ostrovsky, 2003).

8.2.2 Increasing the Continuity of the Time-Series

Over the next four years, the number of Earth observing satellites will decrease 40% as satellites age past their expected lifetime of operation and missions for replacement sensors continue to go unfunded (NRC, 2007). The ETM+ sensor onboard Landsat 7 has been operating in a limited capacity since May 2003 due to the failure of the scan line corrector (SLC) resulting in data gaps in all subsequently acquired imagery. This limitation has significantly impacted the civilian scientific community that relies heavily upon this dataset (Markham et al., 2004; Trigg et al., 2006). As such, it is imperative that methodologies be established that can utilize data from multiple sensor systems, such as MODIS. The National Academies of Science (2007) recently recommended that NASA secure a replacement to Landsat 7 by 2012 and provide a

continuity of land cover measurements. However, it remains uncertain whether this deadline for a new Landsat system will be met.

Early in this research, a data search was implemented to assess whether medium spatial resolution imagery is available to extend the time-series in the study area. According to the Earth Explorer search engine for the USGS archive, there are no Landsat TM scenes available from the USGS EDC national archive beyond the year 2000. There are many Landsat ETM+ scenes available; however, the failure of the scan line corrector (SLC) on the ETM+ sensor has resulted in a data product unsuitable for change detection. Specifically, the SLC-off products exhibit large gaps, particularly at the edges of the scanning swath for the sensor. The study area is located at the edge of the Landsat path and the gap-filled products are not a viable alternative. An alternative to Landsat TM or ETM+ are data from ALI, designed and launched as a technology demonstration for a Landsat follow-on mission. Several ALI scenes are available for the study area; however, they overlap during the same temporal window as the Landsat archive used in this research and thus do not improve the frequency of observation during the study period. A few scenes from ALI were acquired in 2004 and 2005; however, the satellite was targeted to collect data along the Linyanti system and only the northern third of the study area was covered. There are seven ASTER scenes that are of good quality available from May 2003 through October 2006 covering a majority of the study area in the lower Delta. While these medium spatial resolution products are available, the temporal resolution is not sufficient to continue the extraction of the vegetation dynamics. As mentioned previously in this chapter, capturing a semi-annual signal in a

remotely sensed dataset requires that the temporal spacing between images be no greater than three months (Li et al, 2005).

Although applied in a different manner, this work extends methods previously developed for coarser spatial resolution datasets such as MODIS and AVHRR (Moulin et al., 1997; Moody and Johnson, 2001) to higher spatial resolution image data (Landsat TM/ETM+) due to the depth of time-series available. Monitoring at a finer landscape level improves previous efforts unable to adequately capture the spatial heterogeneity inherent in this savanna/wetland system. The creation and analysis of a seasonally rich TM/ETM+ multi-temporal dataset may not always be practical or even possible, and as such the verification of when such an endeavor is required will help inform future studies for acquisition (spatial, spectral, and temporal), preprocessing, and analysis methods. Thus, the fusing of such medium resolution data (either from Landsat TM, Landsat ETM+, ALI, or ASTER) with the dynamics derived from AVHRR/MODIS could provide one alternative to establishing an operation monitoring approach applicable for multiscale regional monitoring, mapping, modeling, and management efforts (Gupta et al., 2000). The establishment of baseline studies of ecosystem dynamics using AVHRR (since the early 1980s) and current-day acquisition of MODIS will provide over twenty-five years of data to investigate trends and patterns needed for future research efforts.

The MODIS sensors onboard the NASA Aqua and Terra satellites have been collecting data operationally since 2000. Global MODIS products include EVI, NDVI, albedo, leaf area index (LAI), and gross primary production (GPP). At coarse scales as well

as what this research shows, vegetation productivity is highly related to climate (Moody and Johnson, 2001; Xiao and Moody, 2004; Lunetta et al., 2006). Xiao and Moody (2004) report an 11% increase in LAI in China that is consistent with an increase in temperature. The overlap of two years (2000 through 2002) between the Landsat time-series used in this research and the launch of MODIS provides an opportunity to quantify the trade-offs regarding the quality of information contained within the vegetation dynamics (i.e. decreased spatial resolution for improved temporal resolution). Linear mixture models of land cover and soil reflectances have been used to upscale field based measurements to 1 km observations from MODIS (Barnsley et al., 1997; Doraiswamy et al., 2004) and a similar approach could be implemented to study vegetation dynamics (Teillet et al., 1997).

Final Thoughts

The future of the Delta remains uncertain, as many outside forces may severely alter its existence. The Okavango Delta is the only permanent source of surface water in semi-arid Botswana. As competition for this scarce resource intensifies, the absence of proper water management increases the likelihood of degradation of wetland system. This research has investigated the relationship of flooding and fire on the temporal dynamics of the observed vegetation response in at wetland/savanna interface of the lower Okavango Delta. Changing local pressures such as regional-scale climate change, hydrological change, and land use / land cover change will determine the fate of the Okavango Delta (Petit et al., 2001; Allan, 2004; Schulze, 2006). As this research has shown, patterns observed at the landscape level can be examined through the temporal

dynamics of the vegetation signal that subsequently provides insight into the underlying local pressures. Further, the use of multitemporal remotely sensed imagery provides a mechanism for the practical application of concepts such as ecosystem resilience into an assessment of system conditions. Resilience of landscapes is dependent not only on the capacity of the ecosystem to respond to change, but also by the institutional and environmental management in which they exist (Peterson, 2000; Forbes, et al., 2004; Anderies et al., 2006). These findings will help to establish a baseline for integrated ecological assessment, monitoring, and conservation planning in an internationally important environment. Moreover, the results from this research, as well as proposed future work, will help environmental managers and policymakers in regards to natural resource management of seasonally flooded or fire-prone areas.

Appendix A.1 Wavelets of EVI Clusters

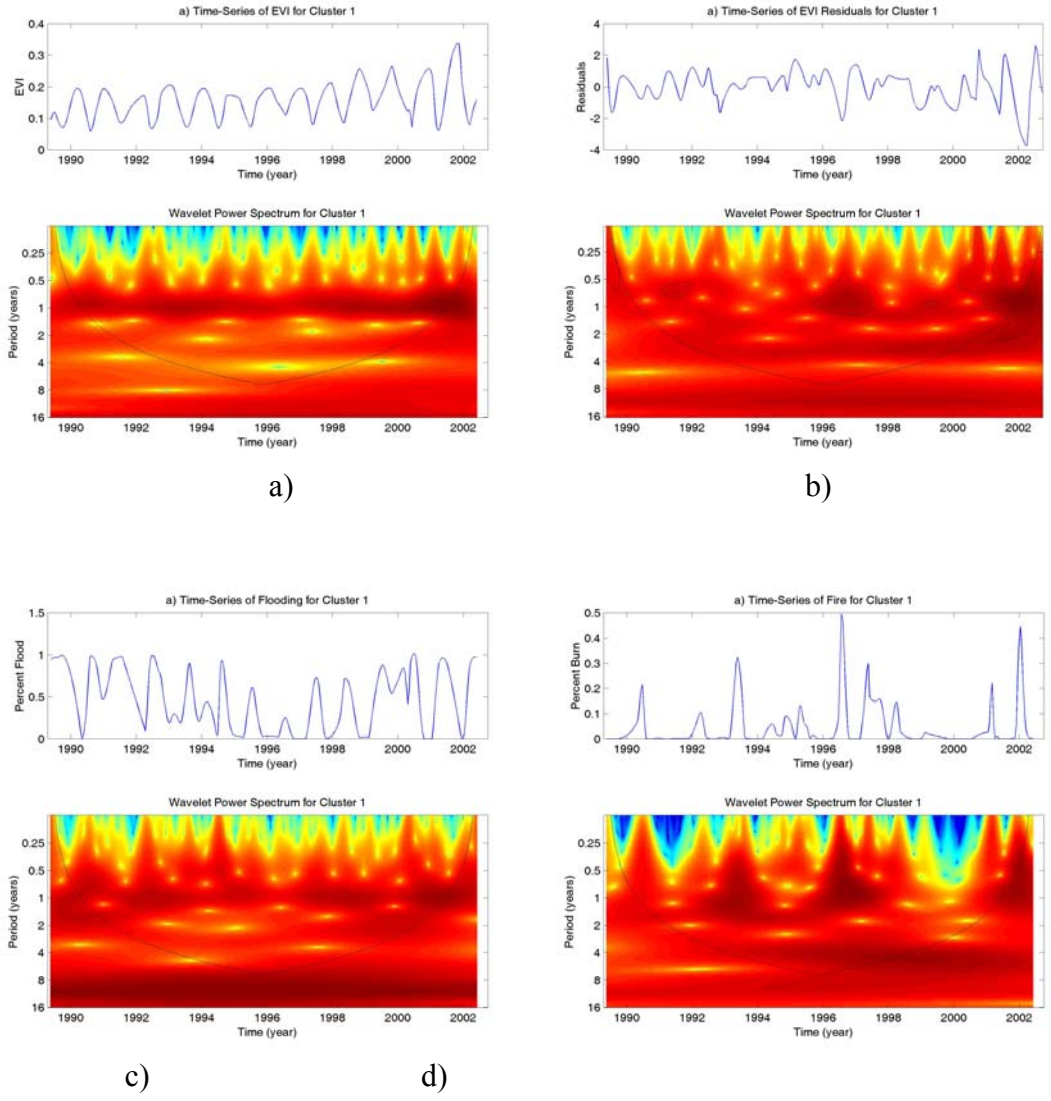

Figure A.1-1 Wavelet power spectrum for EVI cluster 1 for a) Mean EVI trajectory b) Residual EVI trajectory c) Flooding trajectory, and d) Fire trajectory

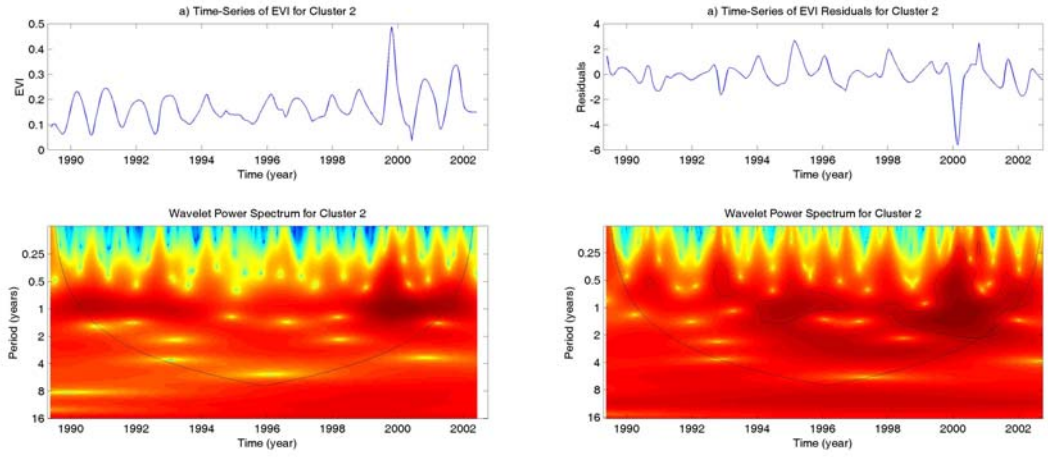

a) b)

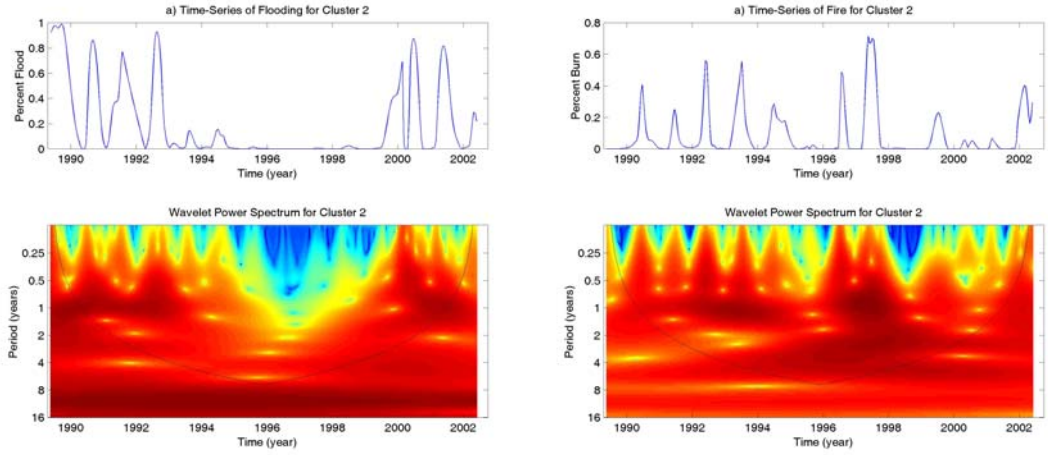

c) d)

Figure A.1-2 Wavelet power spectrum for EVI cluster 2 for a) Mean EVI trajectory b) Residual EVI trajectory c) Flooding trajectory, and d) Fire trajectory

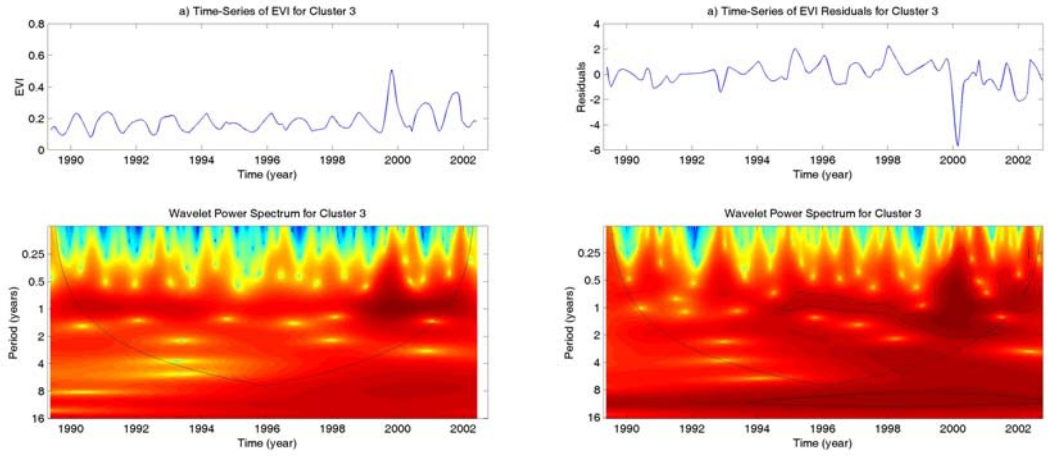

a) b)

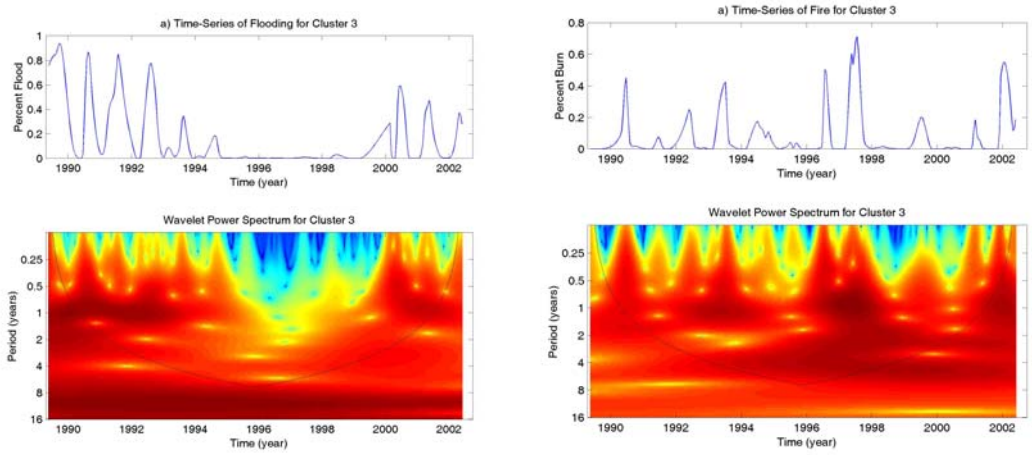

c) d)

Figure A.1-3 Wavelet power spectrum for EVI cluster 3 for a) Mean EVI trajectory b) Residual EVI trajectory c) Flooding trajectory, and d) Fire trajectory

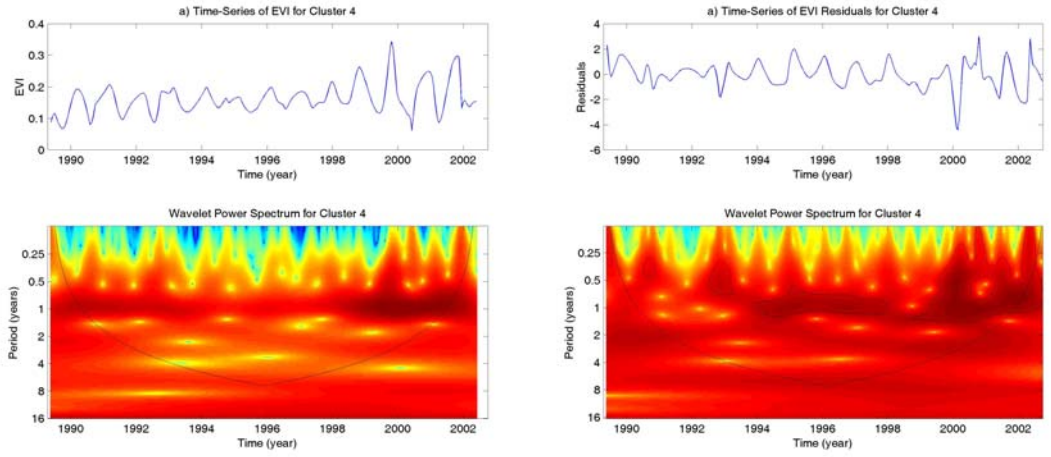

a) b)

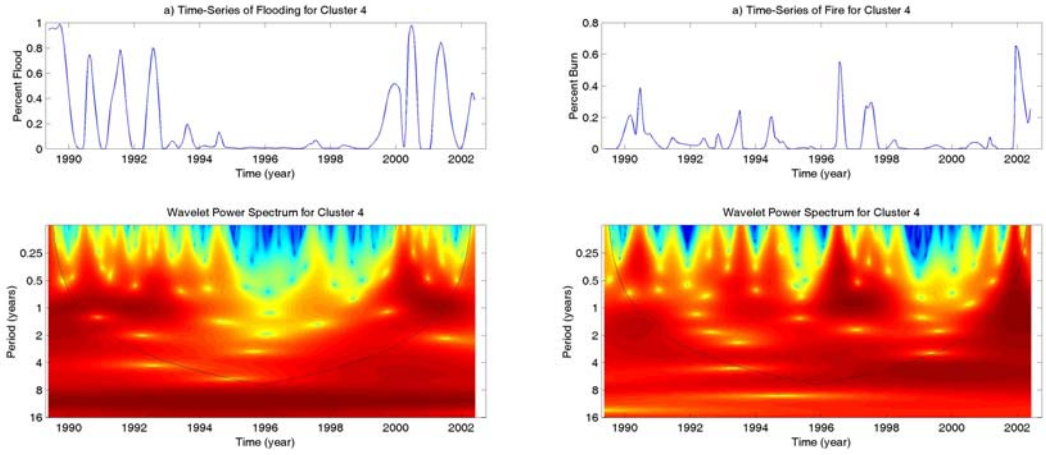

c) d)

Figure A.1-4 Wavelet power spectrum for EVI cluster 4 for a) Mean EVI trajectory b) Residual EVI trajectory c) Flooding trajectory, and d) Fire trajectory

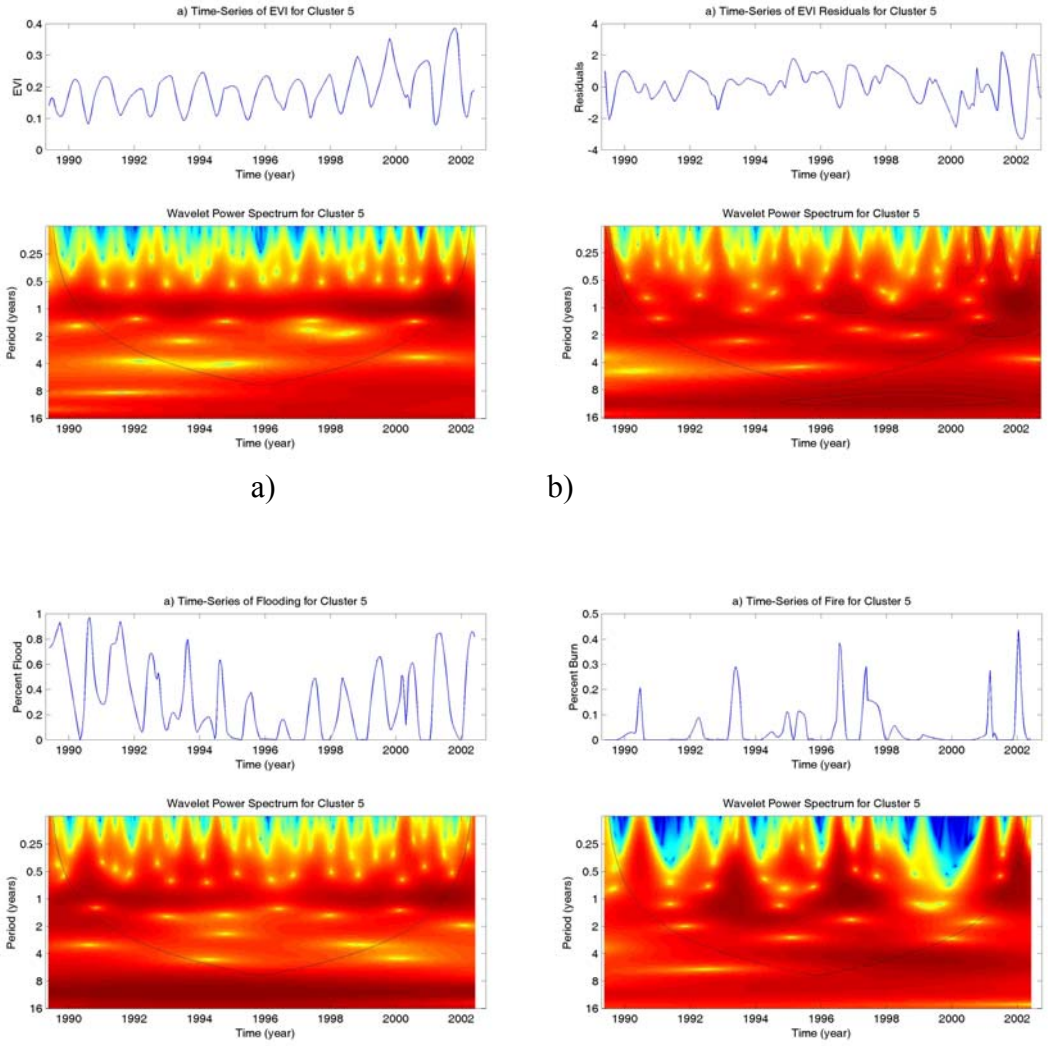

Figure A.1-5 Wavelet power spectrum for EVI cluster 5 for a) Mean EVI trajectory b) Residual EVI trajectory c) Flooding trajectory, and d) Fire trajectory

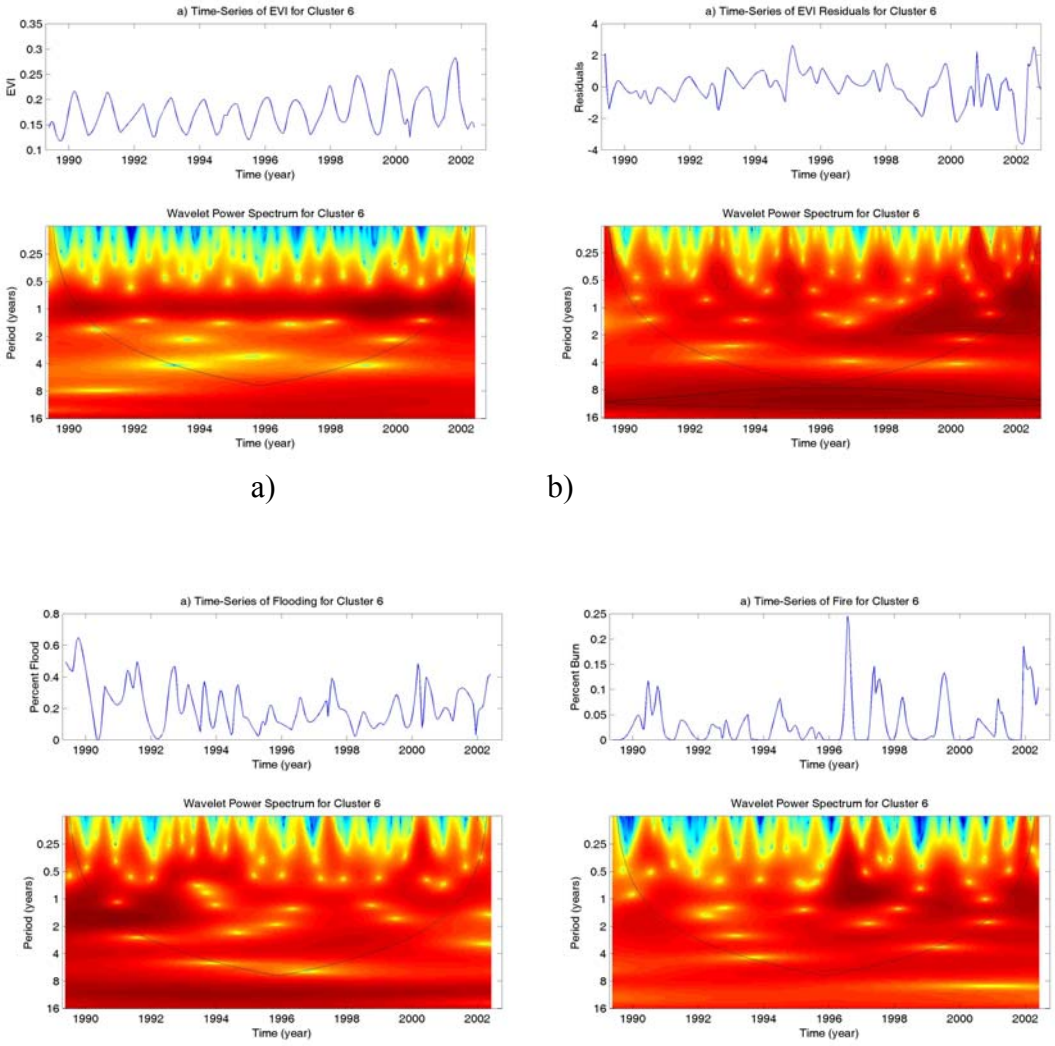

Figure A.1-6 Wavelet power spectrum for EVI cluster 6 for a) Mean EVI trajectory b) Residual EVI trajectory c) Flooding trajectory, and d) Fire trajectory

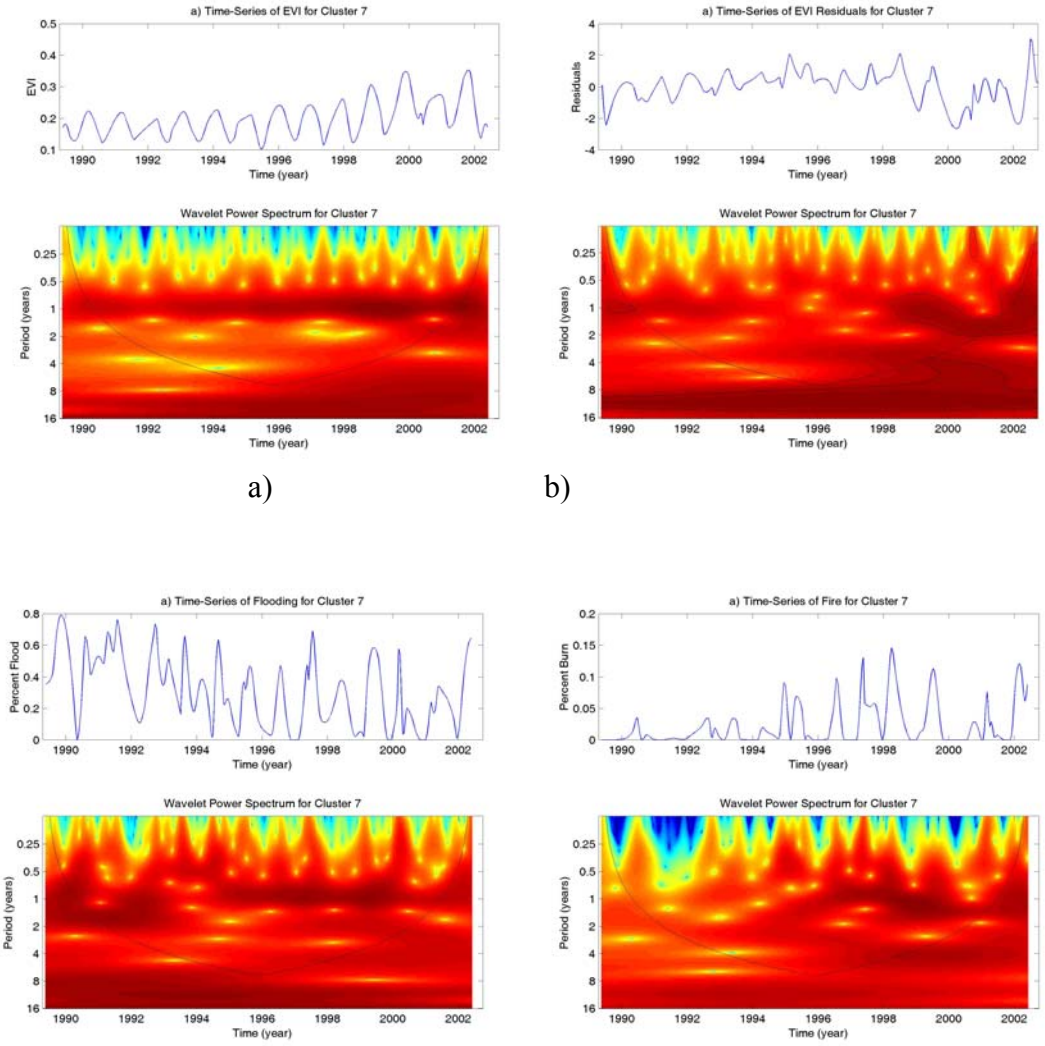

Figure A.1-7 Wavelet power spectrum for EVI cluster 7 for a) Mean EVI trajectory b) Residual EVI trajectory c) Flooding trajectory, and d) Fire trajectory

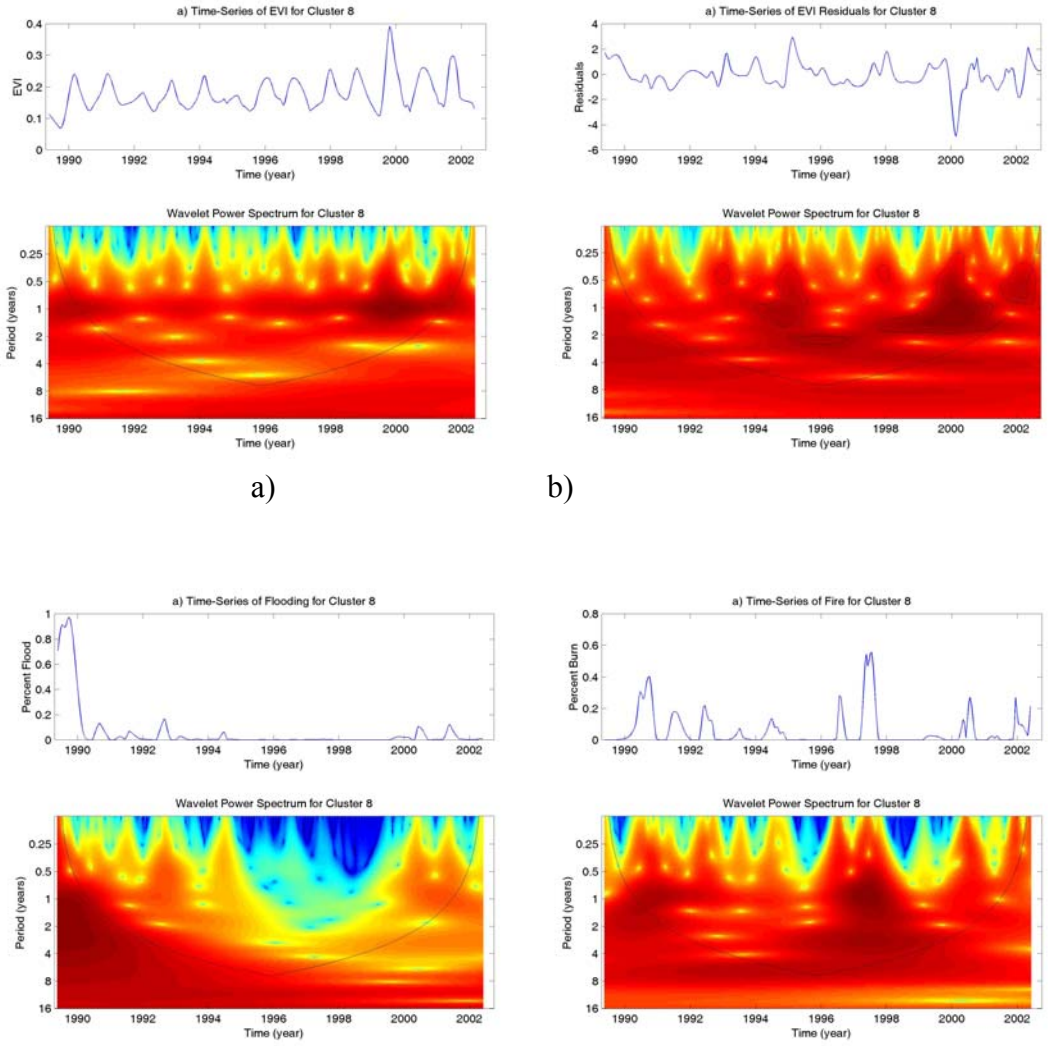

Figure A.1-8 Wavelet power spectrum for EVI cluster 8 for a) Mean EVI trajectory b) Residual EVI trajectory c) Flooding trajectory, and d) Fire trajectory

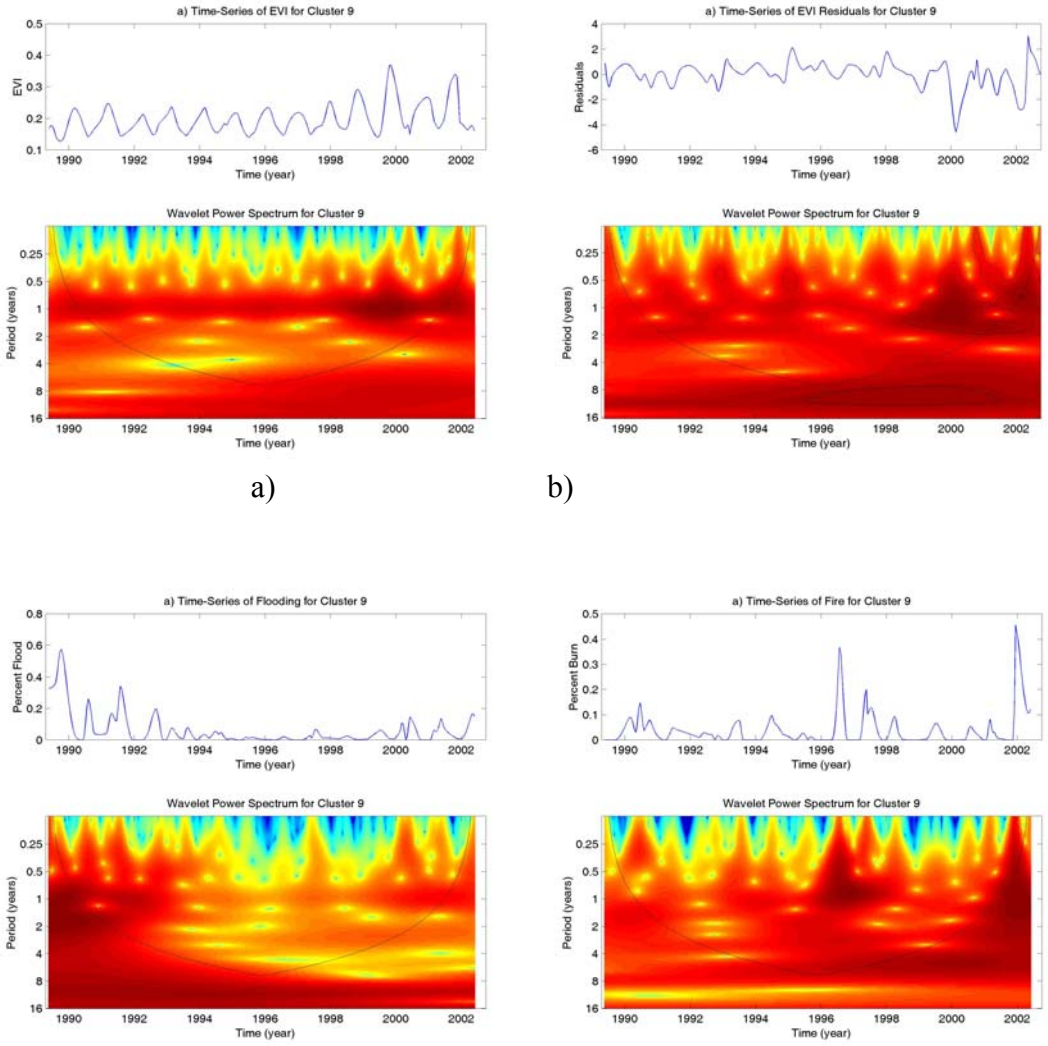

Figure A.1-9 Wavelet power spectrum for EVI cluster 9 for a) Mean EVI trajectory b) Residual EVI trajectory c) Flooding trajectory, and d) Fire trajectory

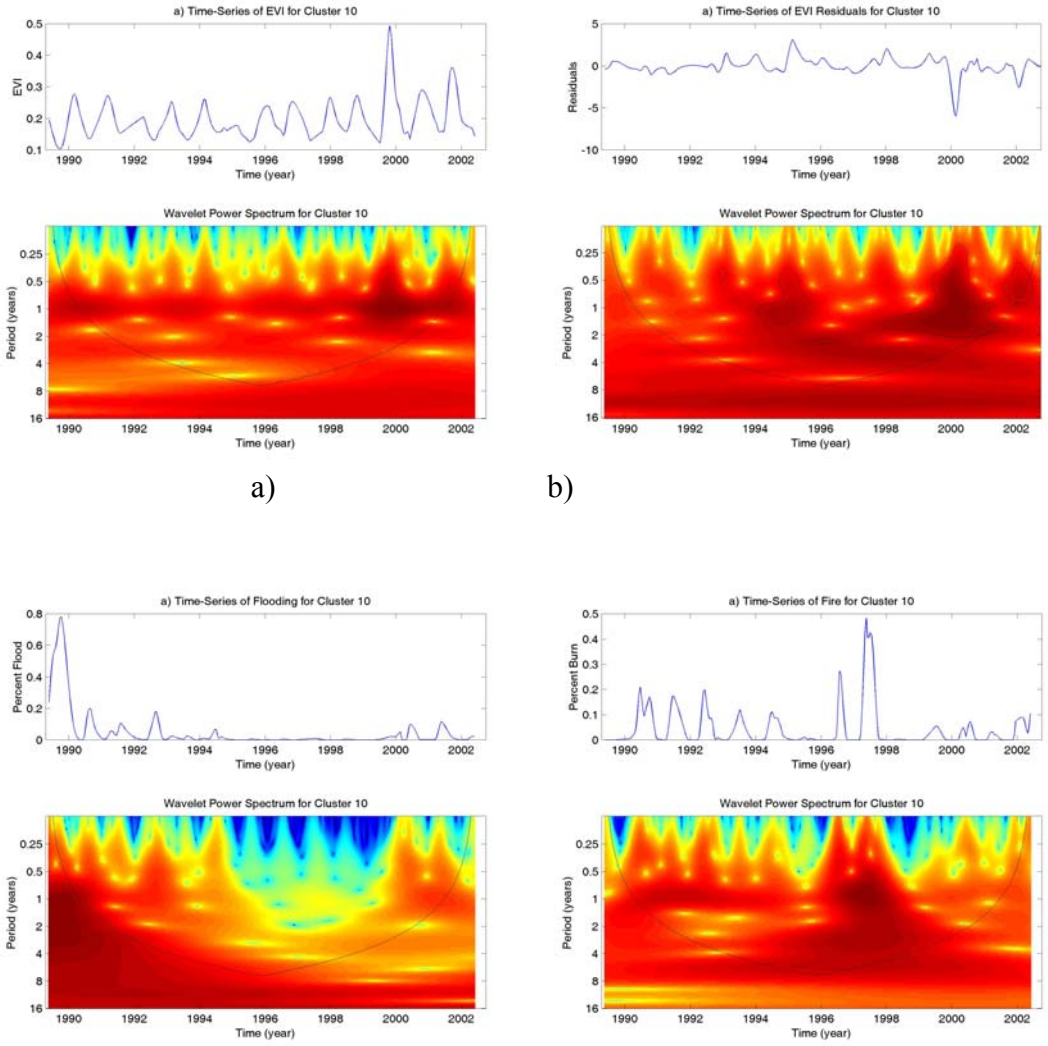

Figure A.1-10 Wavelet power spectrum for EVI cluster 10 for a) Mean EVI trajectory b) Residual EVI trajectory c) Flooding trajectory, and d) Fire trajectory

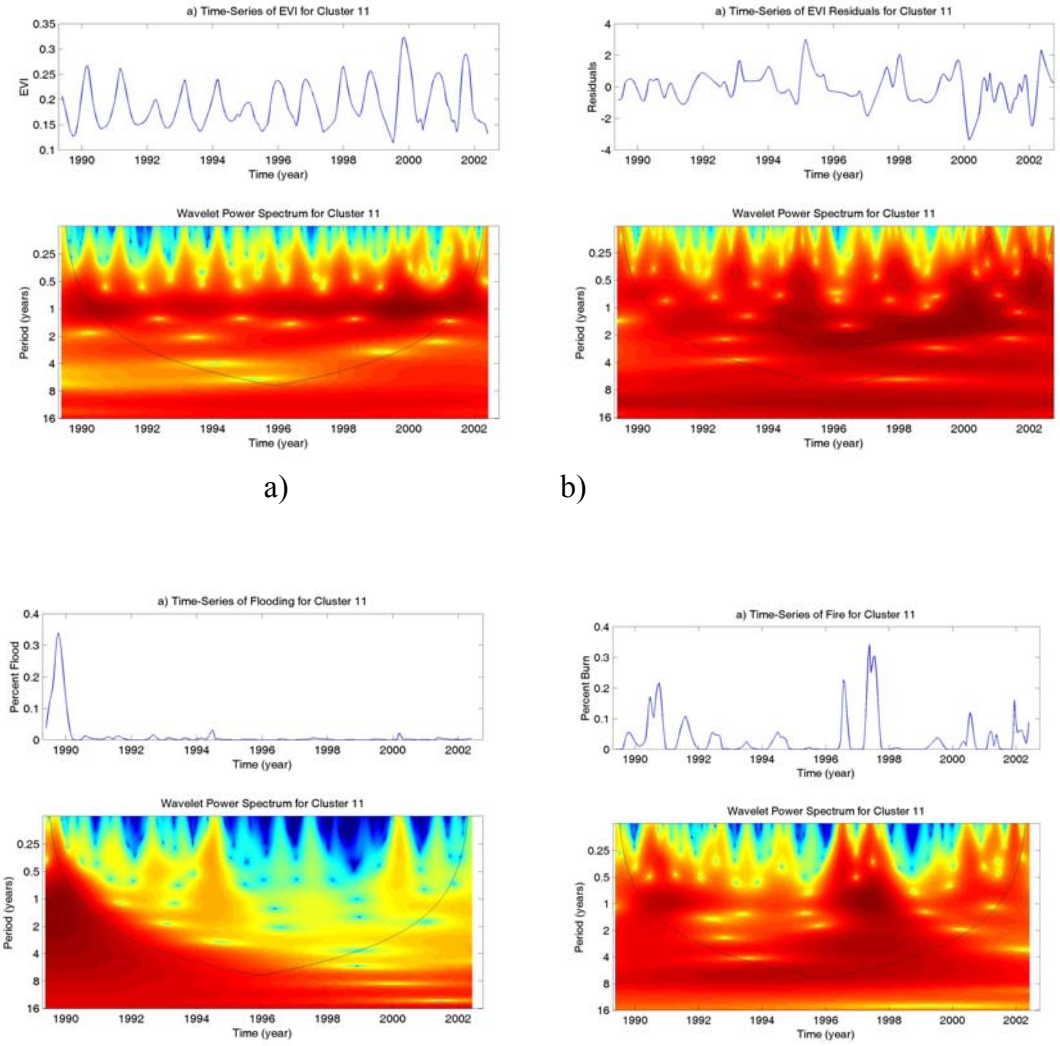

Figure A.1-11 Wavelet power spectrum for EVI cluster 11 for a) Mean EVI trajectory b) Residual EVI trajectory c) Flooding trajectory, and d) Fire trajectory

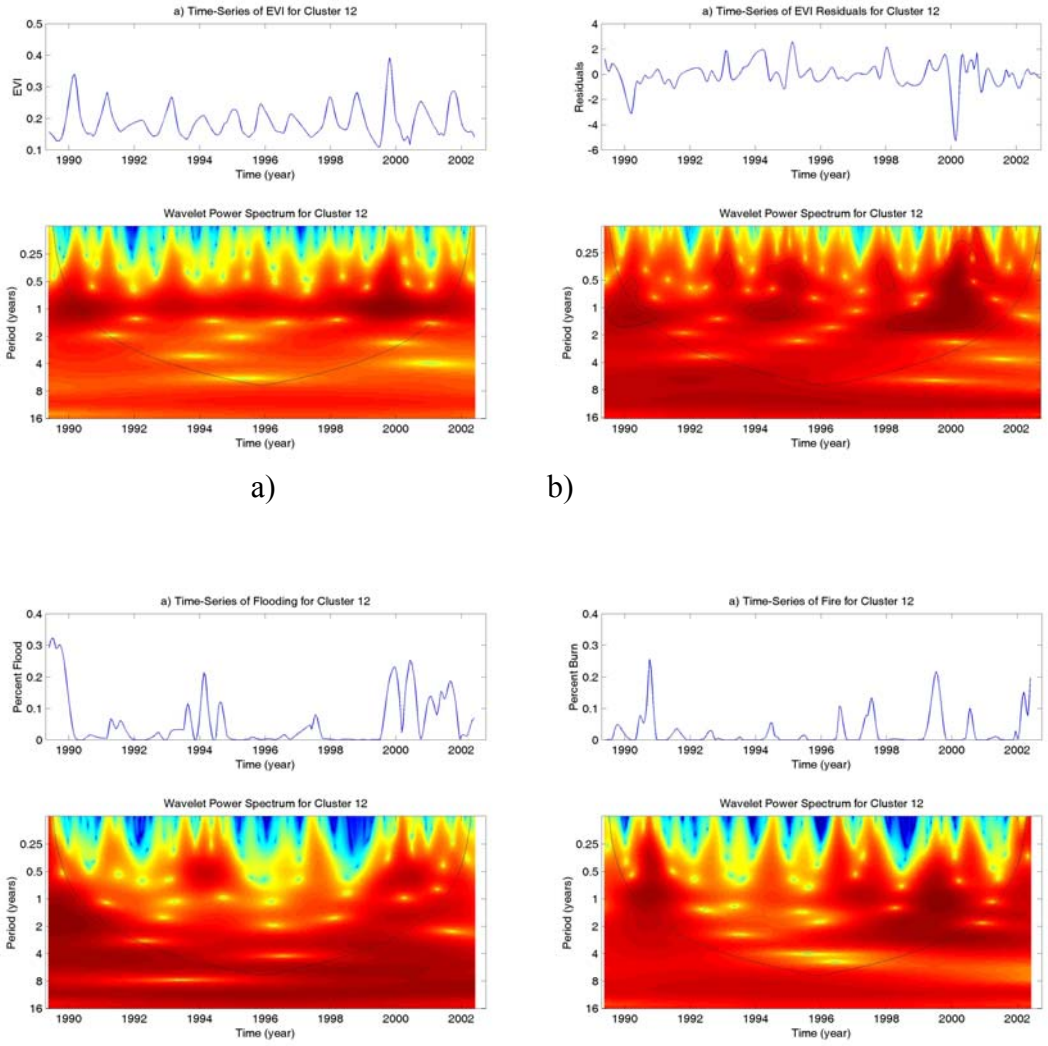

Figure A.1-12 Wavelet power spectrum for EVI cluster 12 for a) Mean EVI trajectory b) Residual EVI trajectory c) Flooding trajectory, and d) Fire trajectory

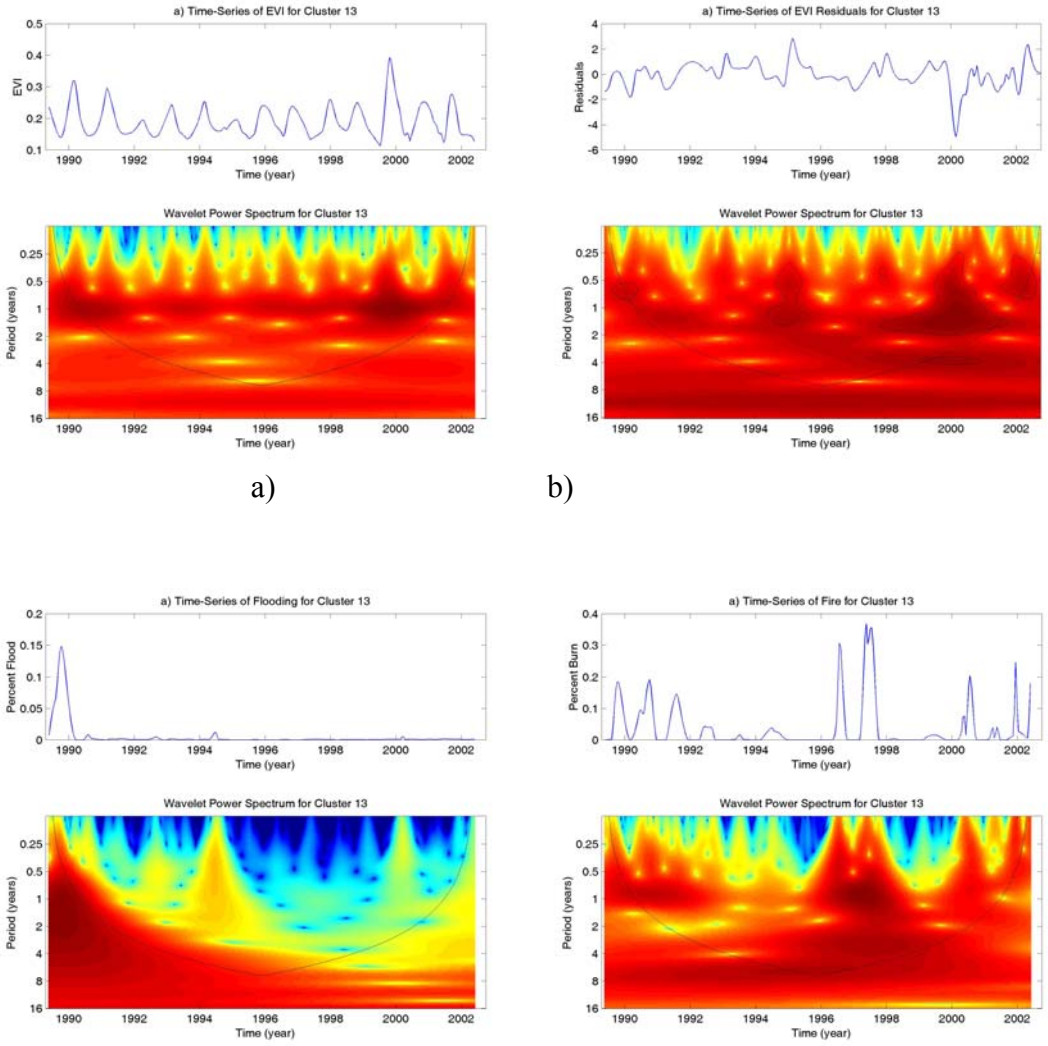

Figure A.1-13 Wavelet power spectrum for EVI cluster 13 for a) Mean EVI trajectory b) Residual EVI trajectory c) Flooding trajectory, and d) Fire trajectory

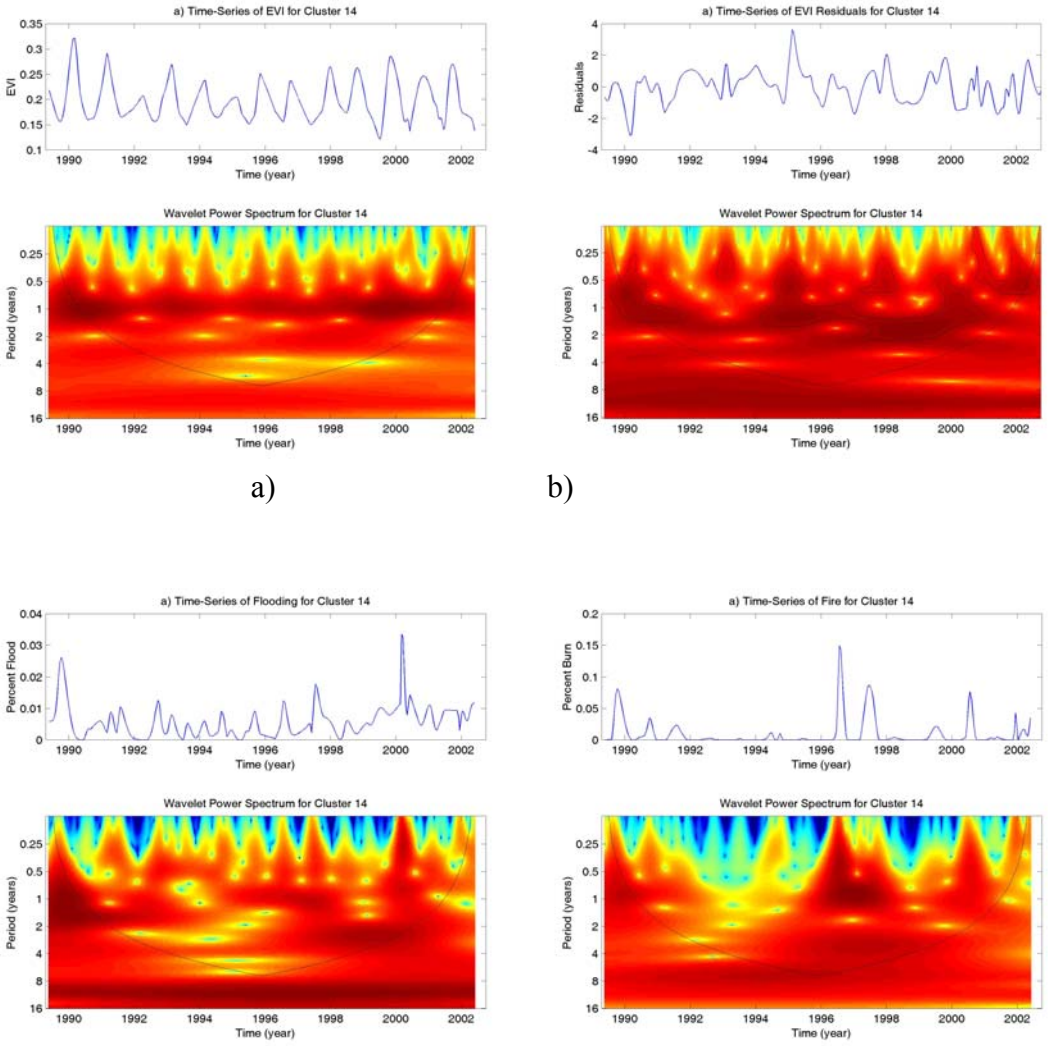

Figure A.1-14 Wavelet power spectrum for EVI cluster 14 for a) Mean EVI trajectory b) Residual EVI trajectory c) Flooding trajectory, and d) Fire trajectory

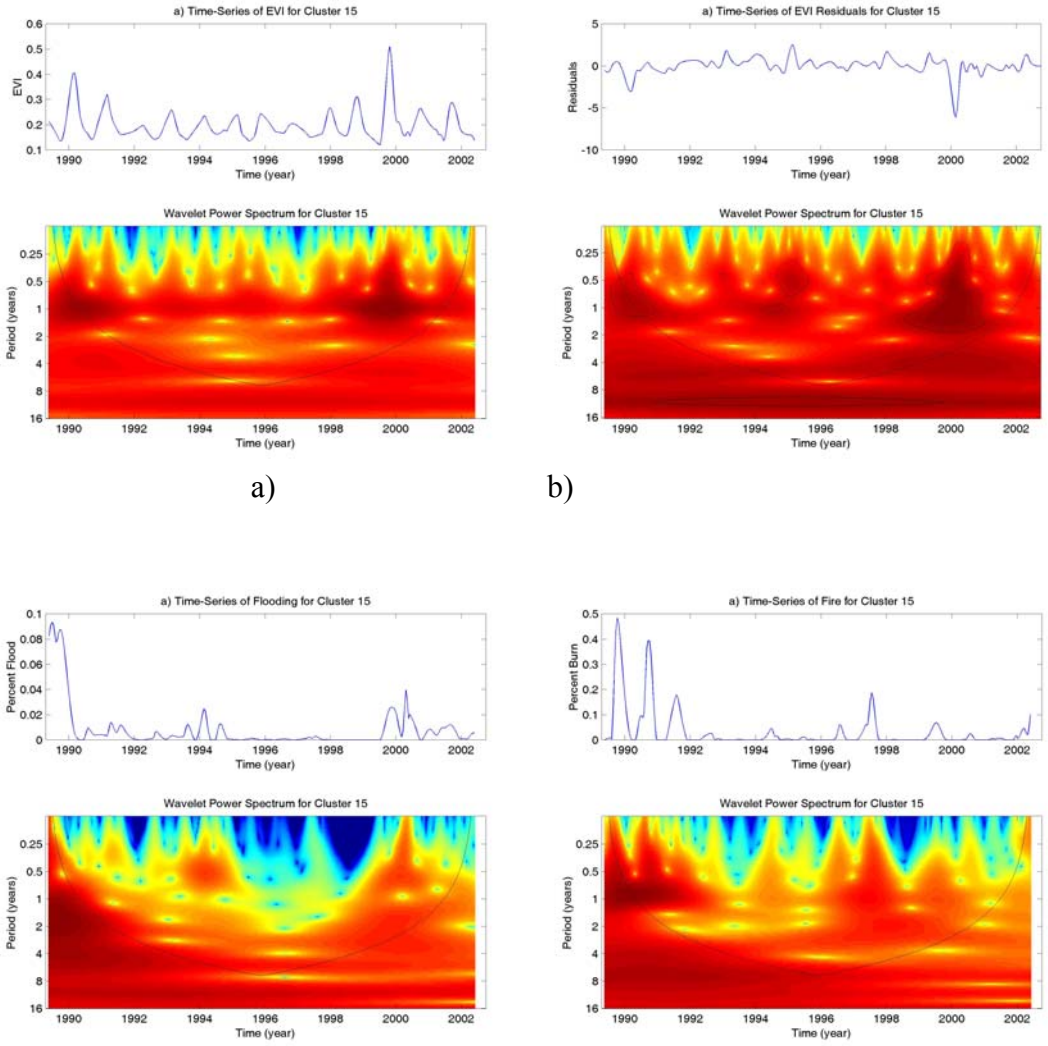

Figure A.1-15. Wavelet power spectrum for EVI cluster 15 for a) Mean EVI trajectory b) Residual EVI trajectory c) Flooding trajectory, and d) Fire trajectory

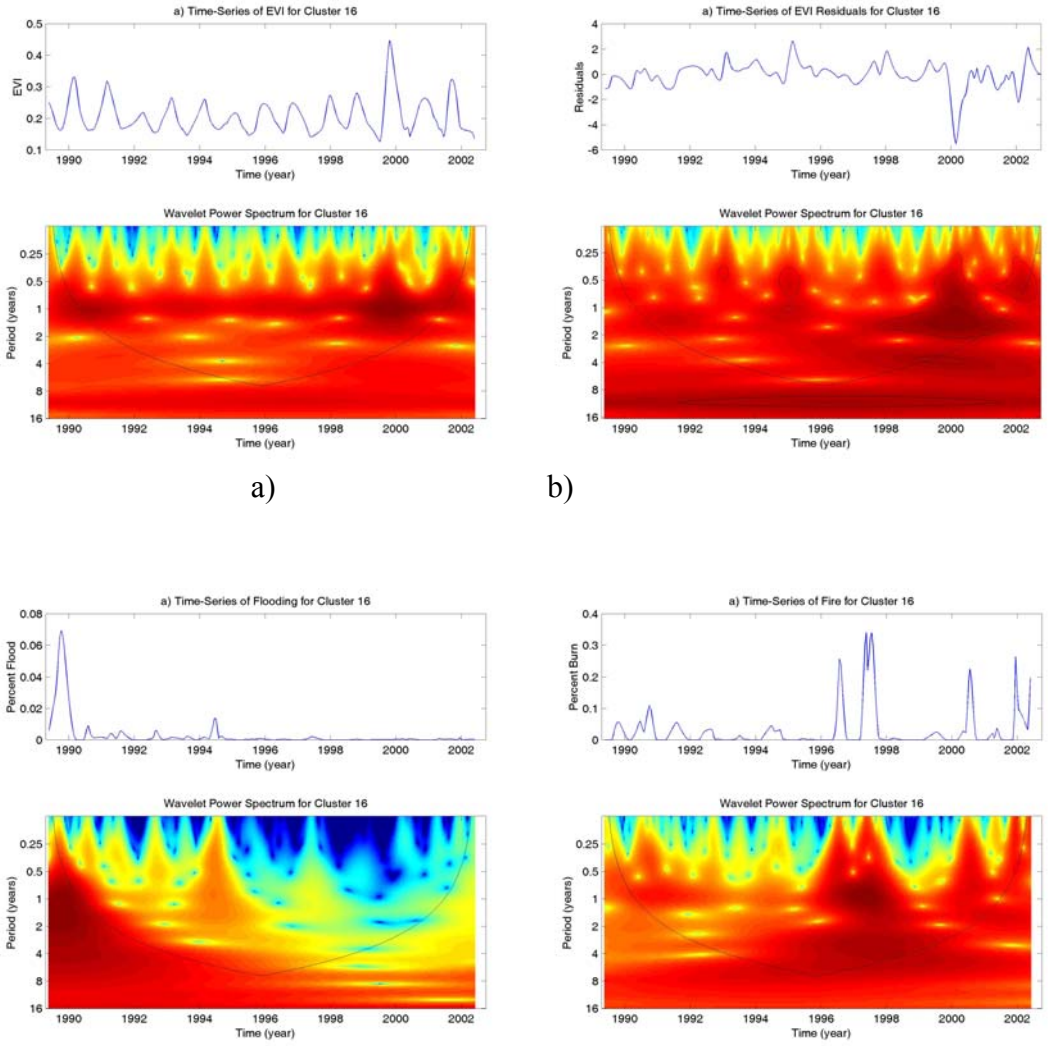

Figure A.1-16. Wavelet power spectrum for EVI cluster 16 for a) Mean EVI trajectory b) Residual EVI trajectory c) Flooding trajectory, and d) Fire trajectory

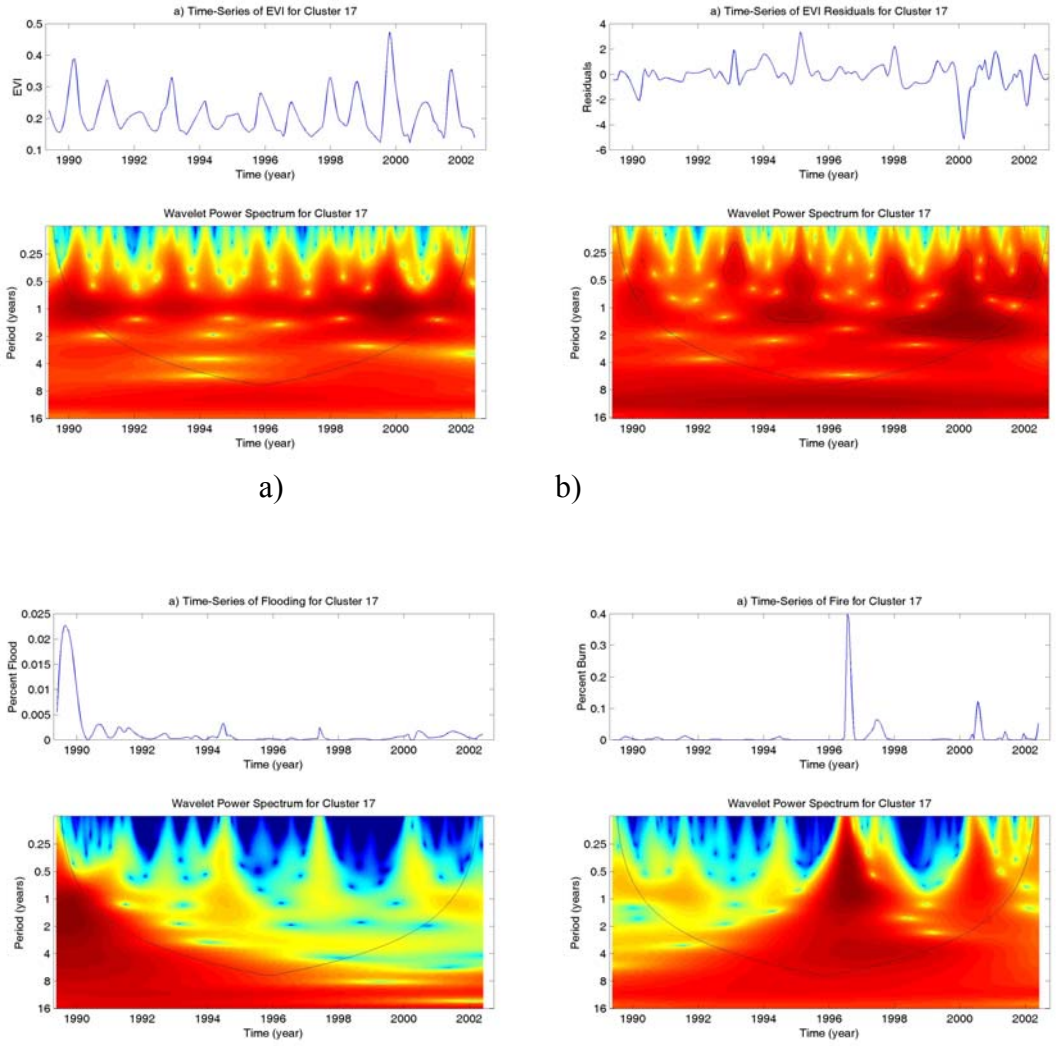

Figure A.1-17. Wavelet power spectrum for EVI cluster 17 for a) Mean EVI trajectory b) Residual EVI trajectory c) Flooding trajectory, and d) Fire trajectory

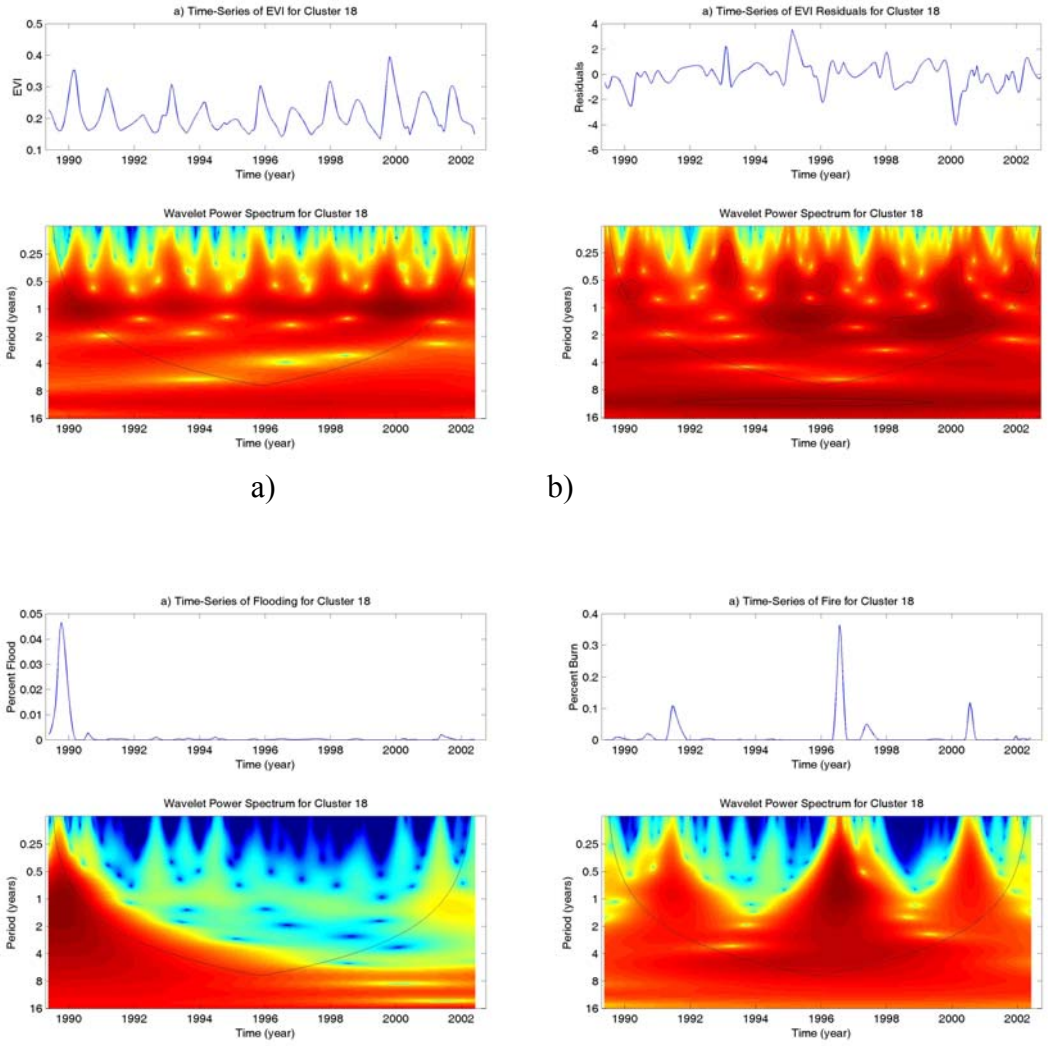

Figure A.1-18. Wavelet power spectrum for EVI cluster 18 for a) Mean EVI trajectory b) Residual EVI trajectory c) Flooding trajectory, and d) Fire trajectory

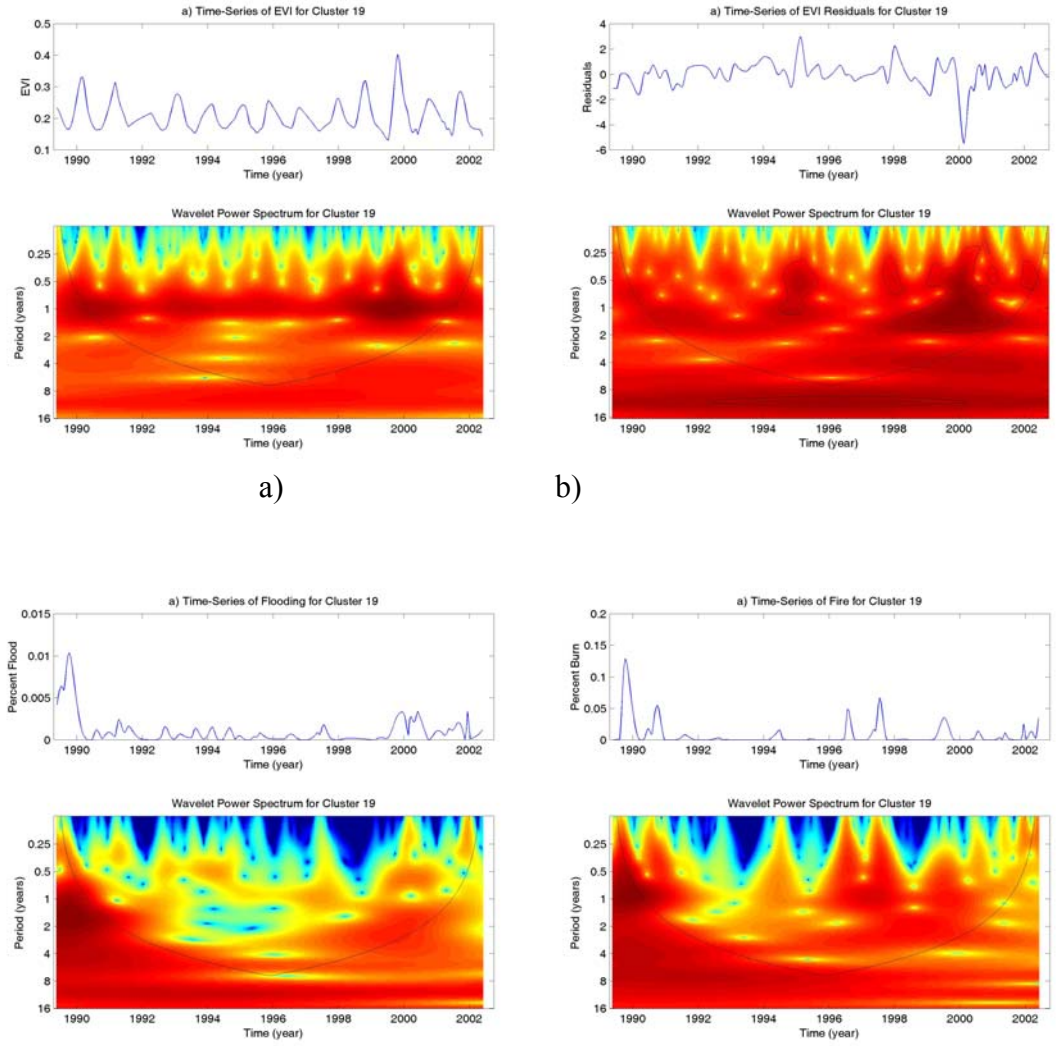

Figure A.1-19. Wavelet power spectrum for EVI cluster 19 for a) Mean EVI trajectory b) Residual EVI trajectory c) Flooding trajectory, and d) Fire trajectory

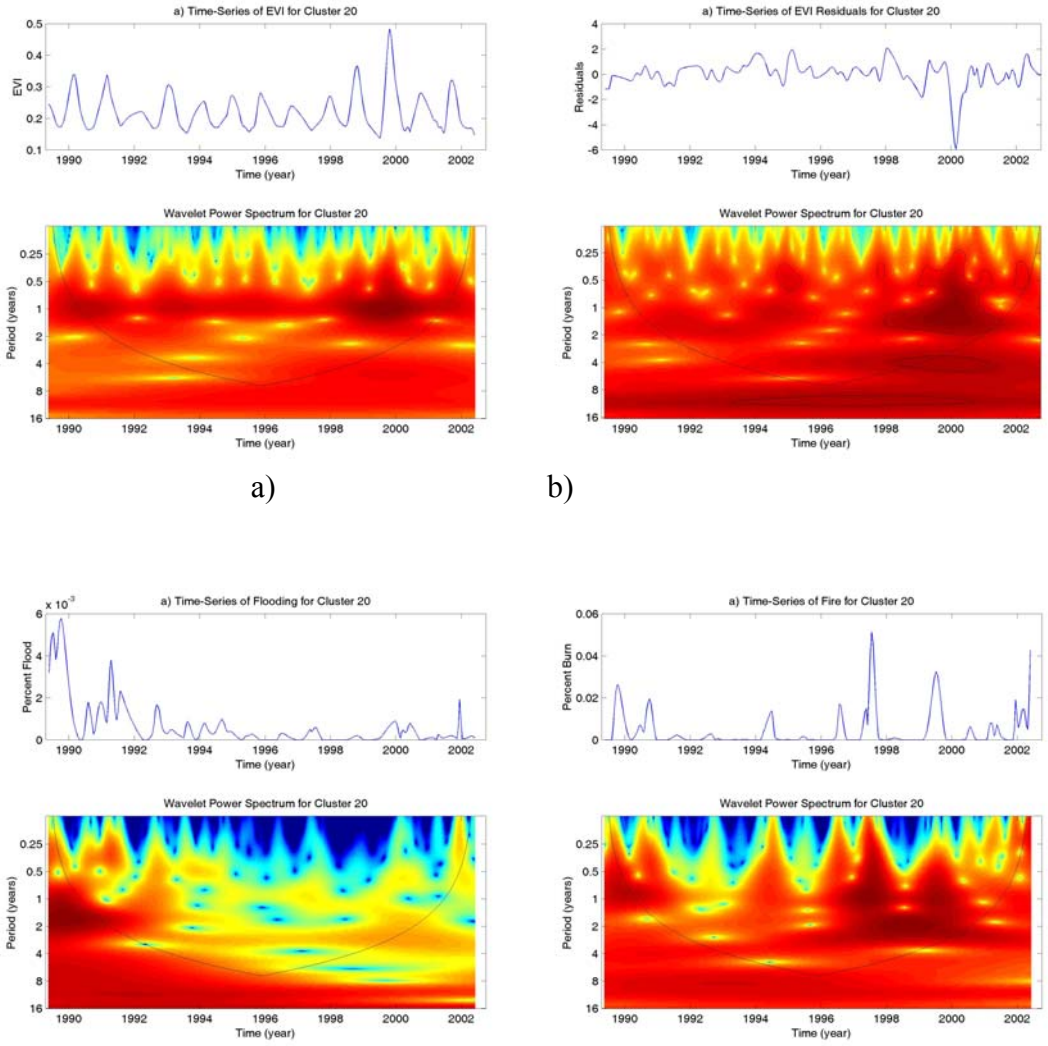

Figure A.1-20. Wavelet power spectrum for EVI cluster 20 for a) Mean EVI trajectory b) Residual EVI trajectory c) Flooding trajectory, and d) Fire trajectory

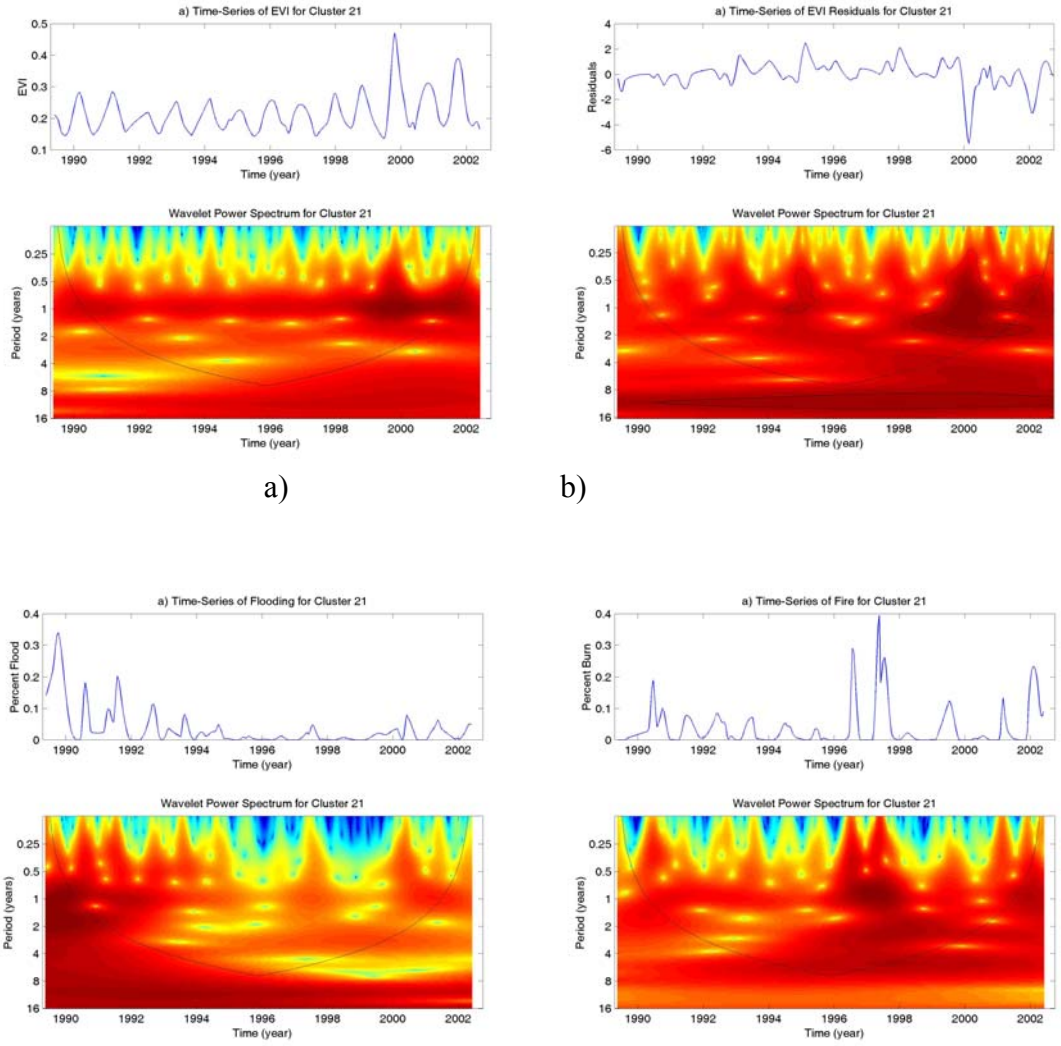

Figure A.1-21. Wavelet power spectrum for EVI cluster 21 for a) Mean EVI trajectory b) Residual EVI trajectory c) Flooding trajectory, and d) Fire trajectory

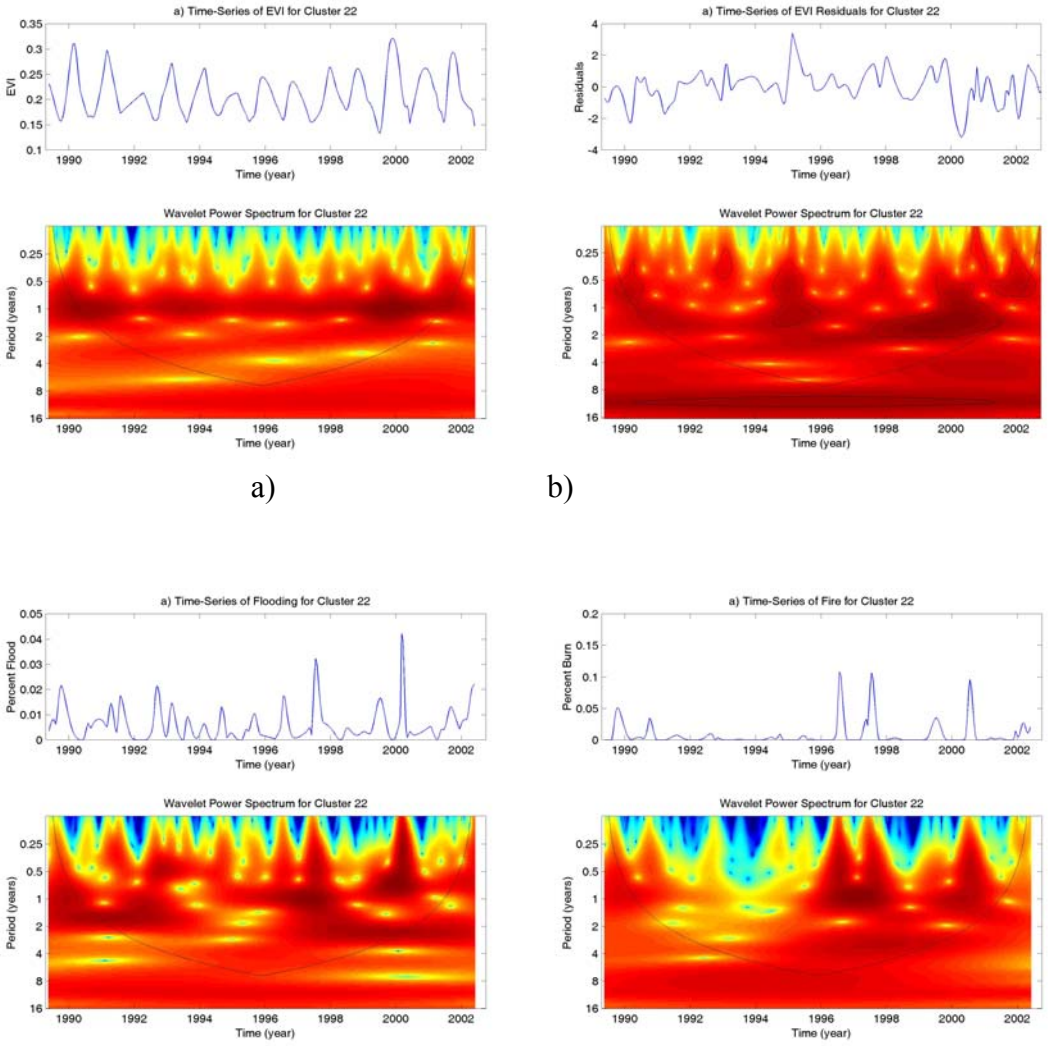

Figure A.1-22. Wavelet power spectrum for EVI cluster 22 for a) Mean EVI trajectory b) Residual EVI trajectory c) Flooding trajectory, and d) Fire trajectory

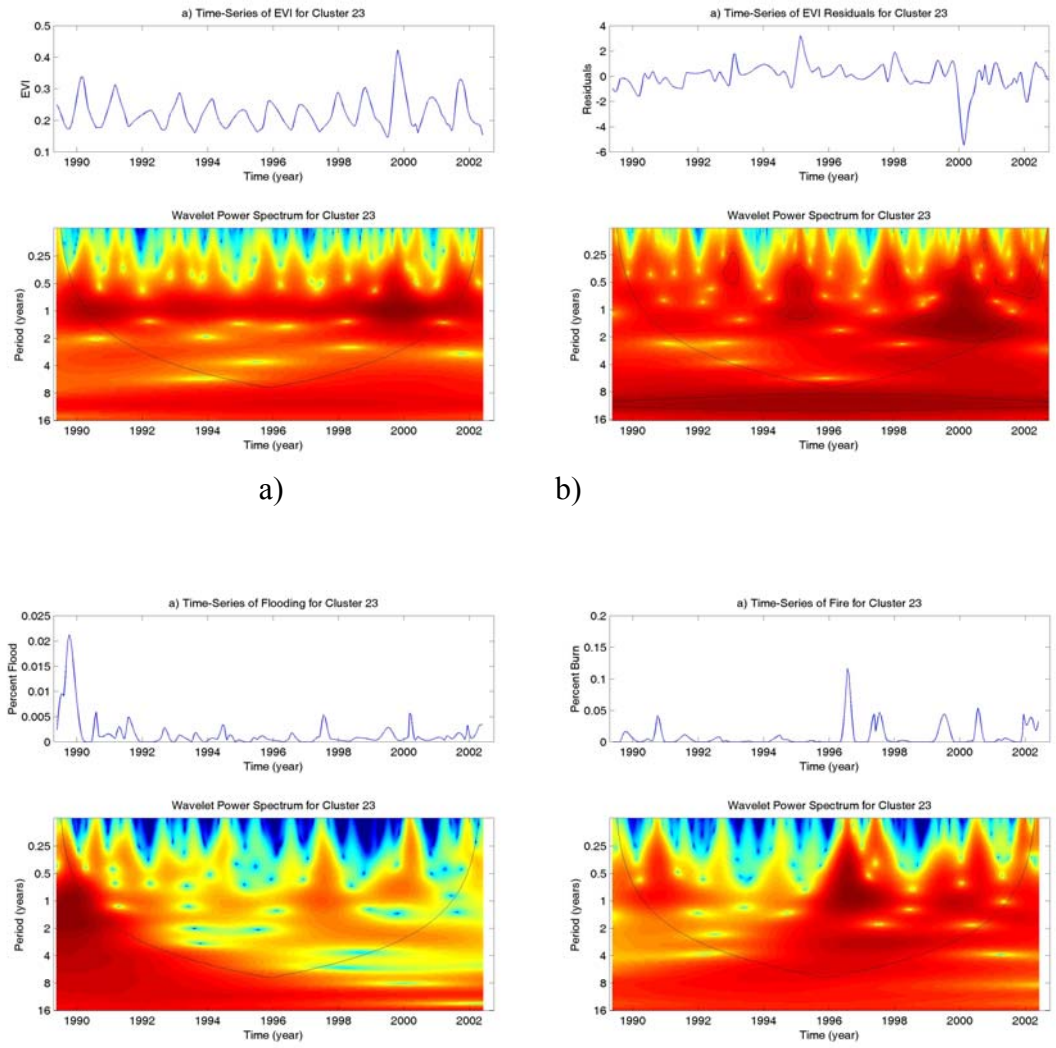

Figure A.1-23. Wavelet power spectrum for EVI cluster 23 for a) Mean EVI trajectory b) Residual EVI trajectory c) Flooding trajectory, and d) Fire trajectory

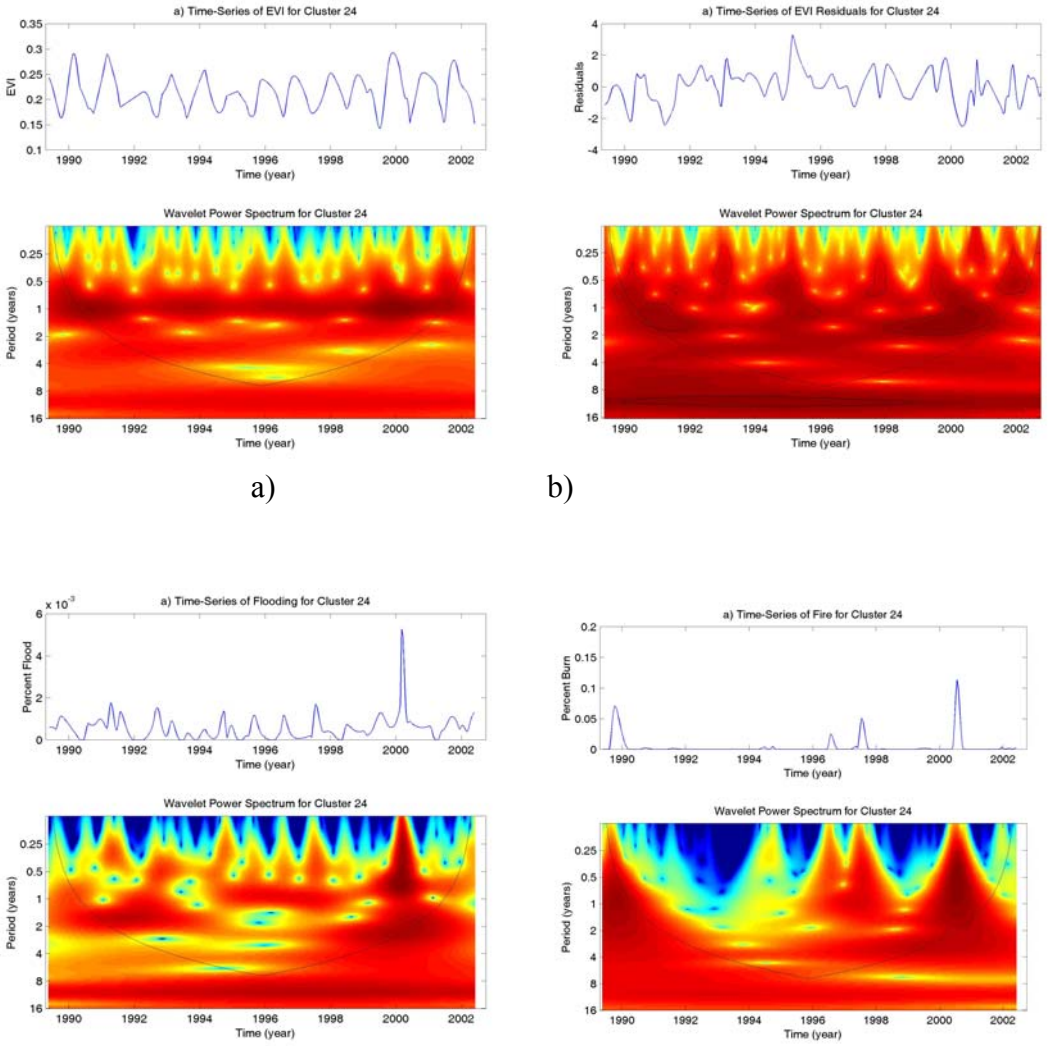

Figure A.1-24. Wavelet power spectrum for EVI cluster 24 for a) Mean EVI trajectory b) Residual EVI trajectory c) Flooding trajectory, and d) Fire trajectory

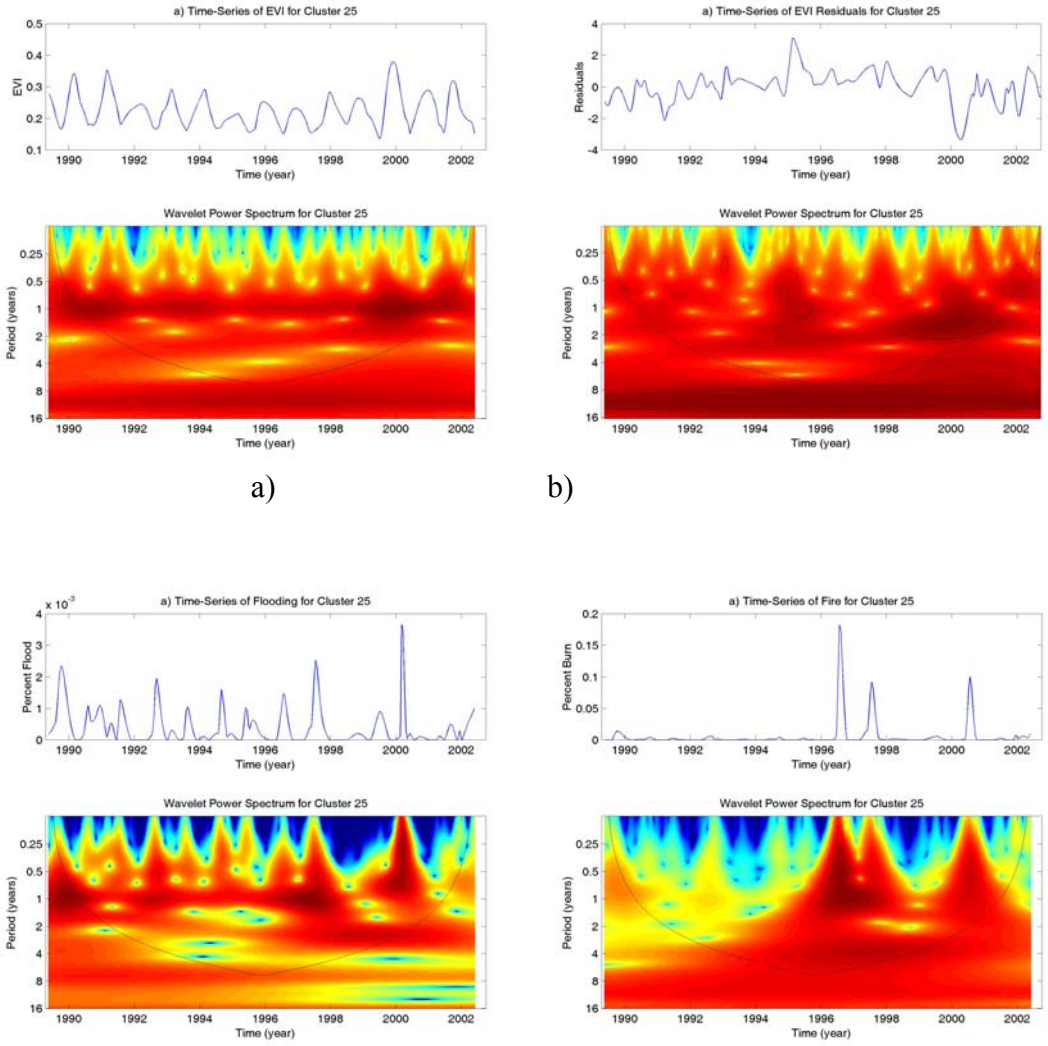

Figure A.1-25. Wavelet power spectrum for EVI cluster 25 for a) Mean EVI trajectory b) Residual EVI trajectory c) Flooding trajectory, and d) Fire trajectory

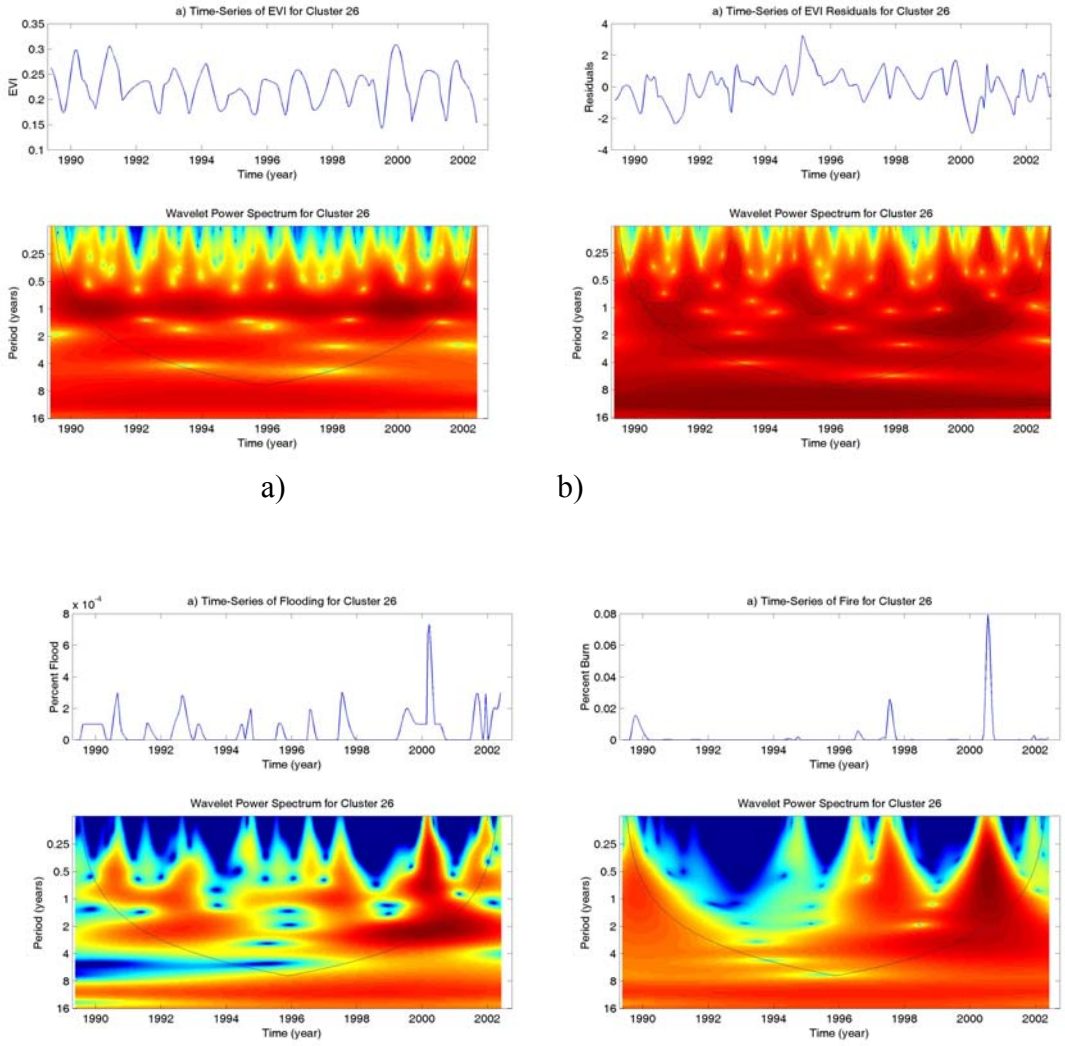

Figure A.1-26. Wavelet power spectrum for EVI cluster 26 for a) Mean EVI trajectory b) Residual EVI trajectory c) Flooding trajectory, and d) Fire trajectory

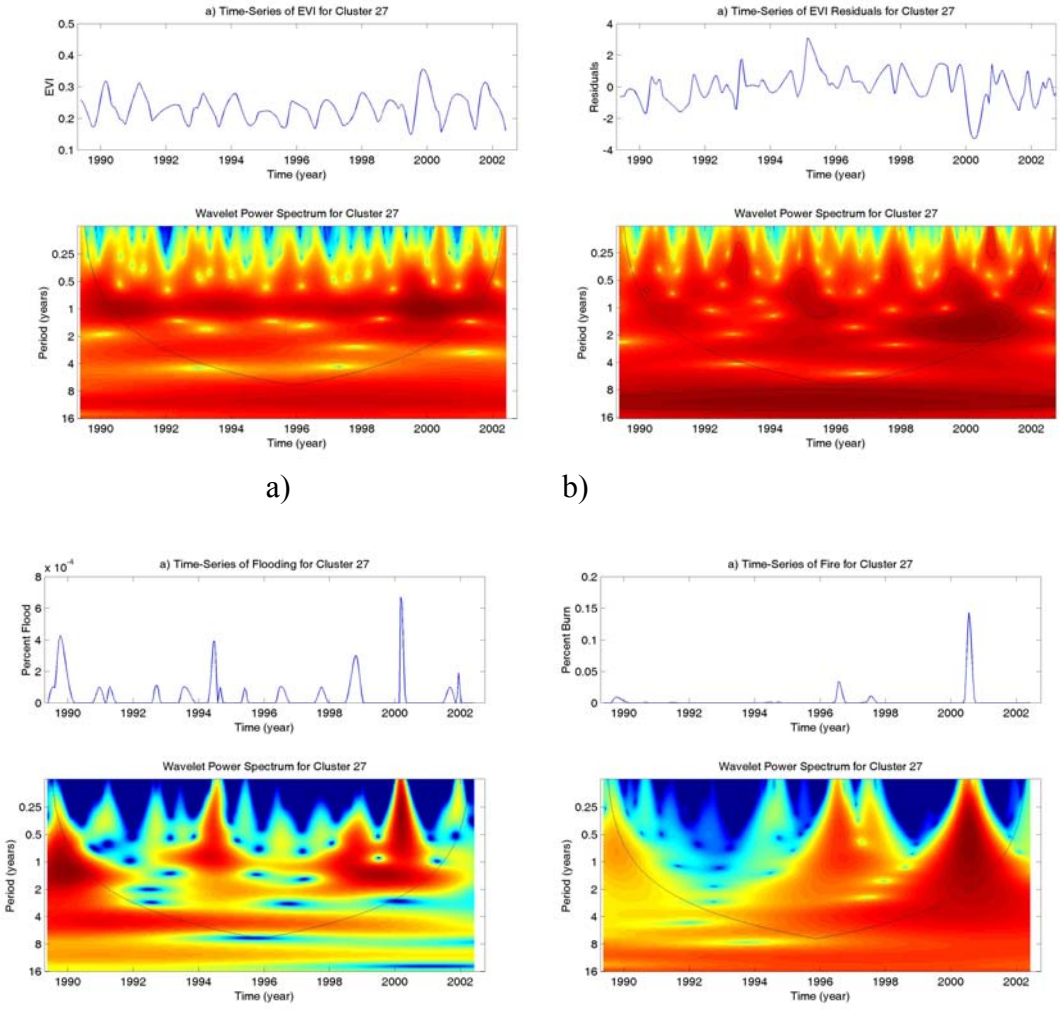

Figure A.1-27. Wavelet power spectrum for EVI cluster 27 for a) Mean EVI trajectory b) Residual EVI trajectory c) Flooding trajectory, and d) Fire trajectory

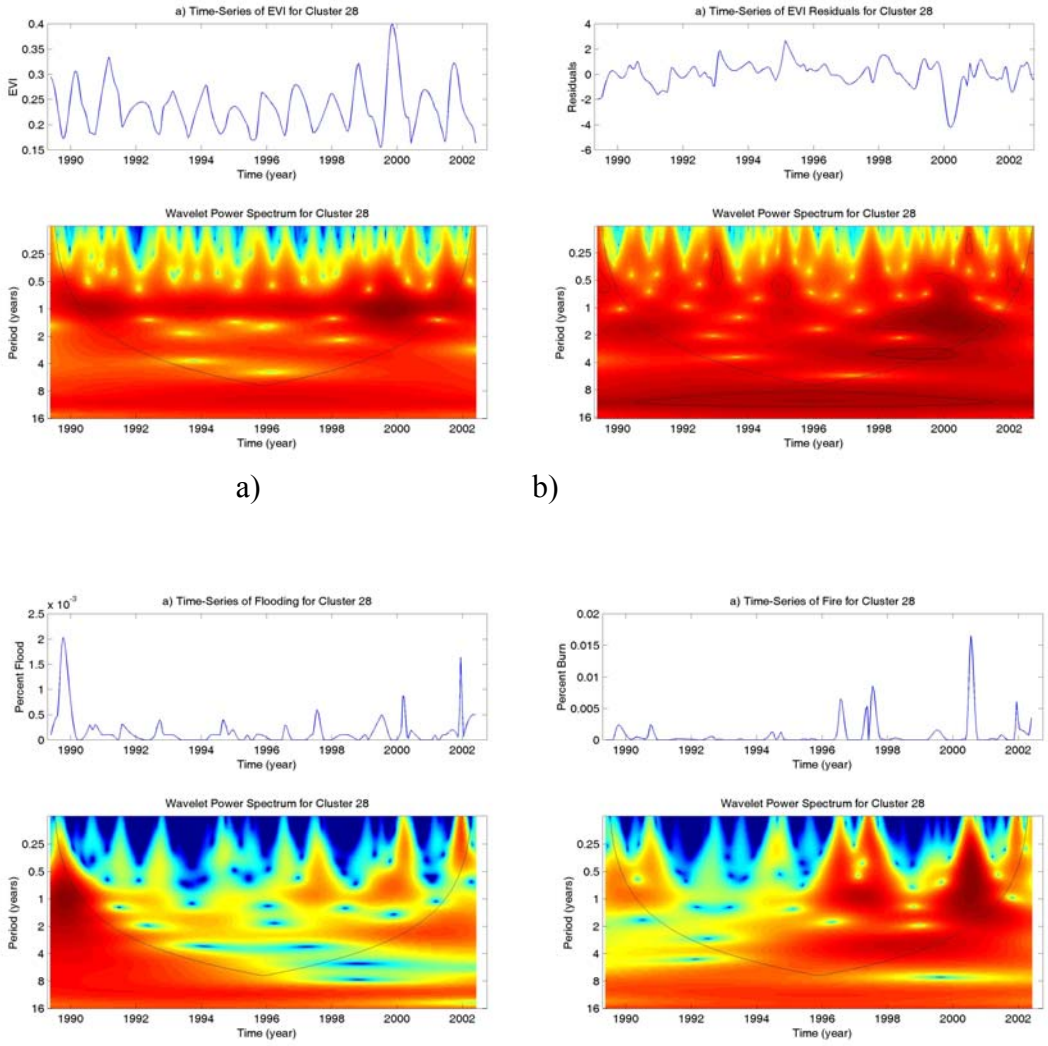

Figure A.1-28. Wavelet power spectrum for EVI cluster 28 for a) Mean EVI trajectory b) Residual EVI trajectory c) Flooding trajectory, and d) Fire trajectory

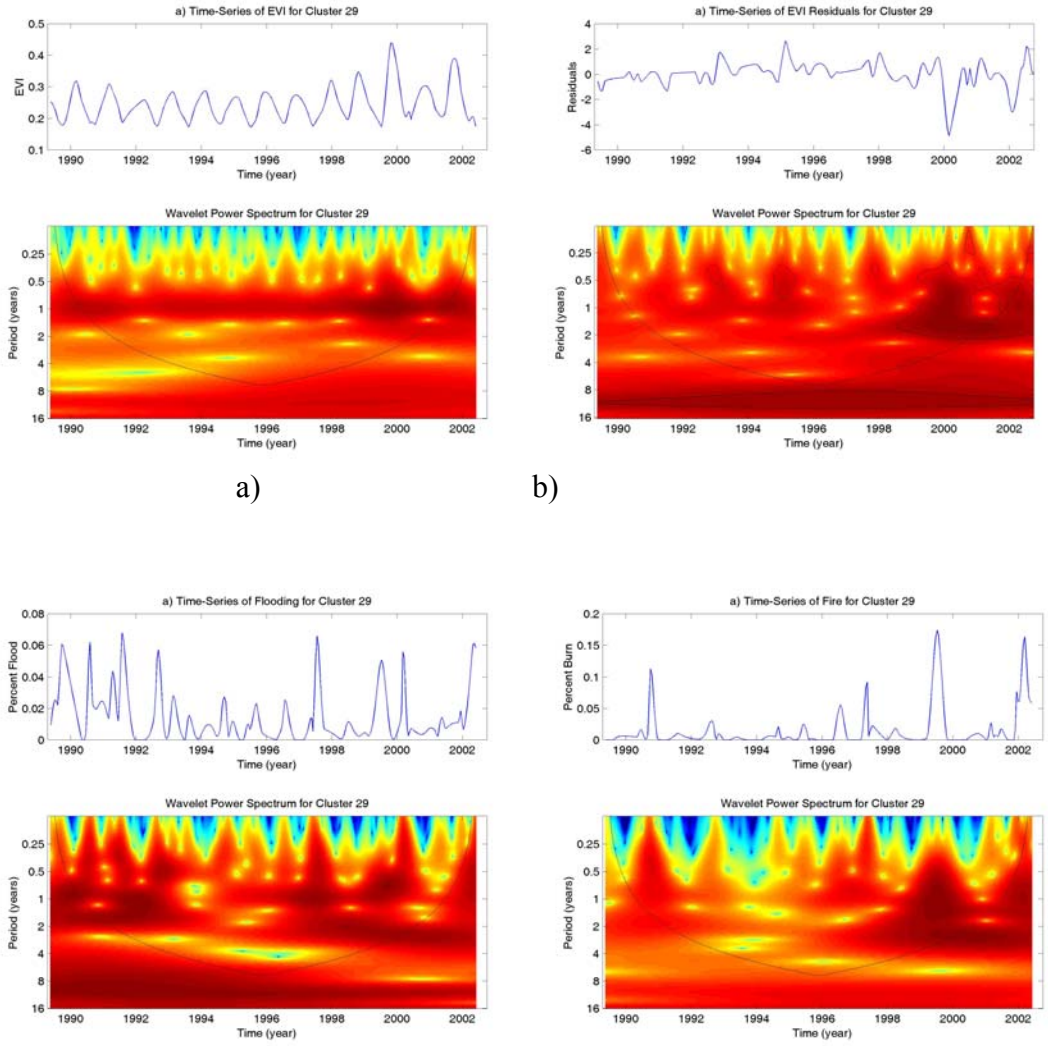

Figure A.1-29. Wavelet power spectrum for EVI cluster 29 for a) Mean EVI trajectory b) Residual EVI trajectory c) Flooding trajectory, and d) Fire trajectory

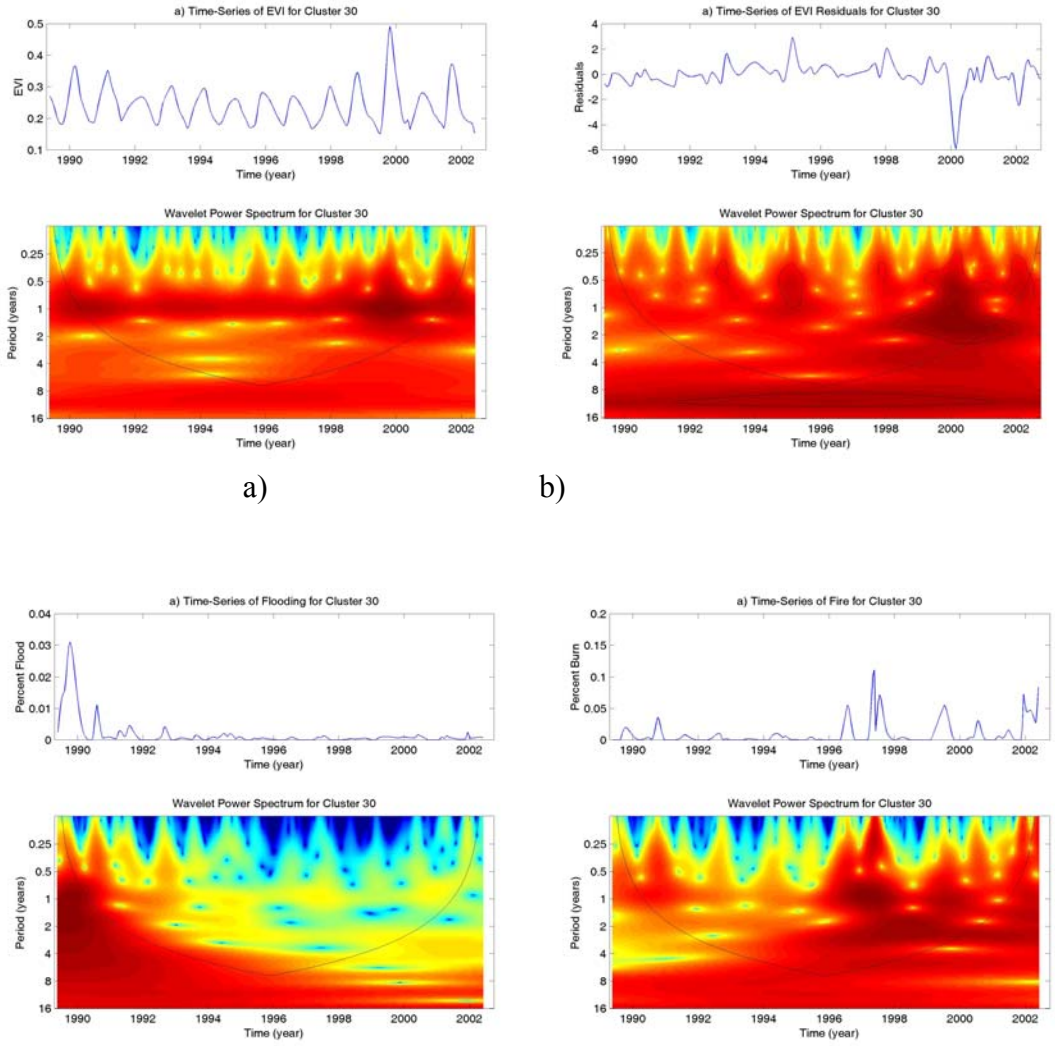

Figure A.1-30. Wavelet power spectrum for EVI cluster 30 for a) Mean EVI trajectory b) Residual EVI trajectory c) Flooding trajectory, and d) Fire trajectory

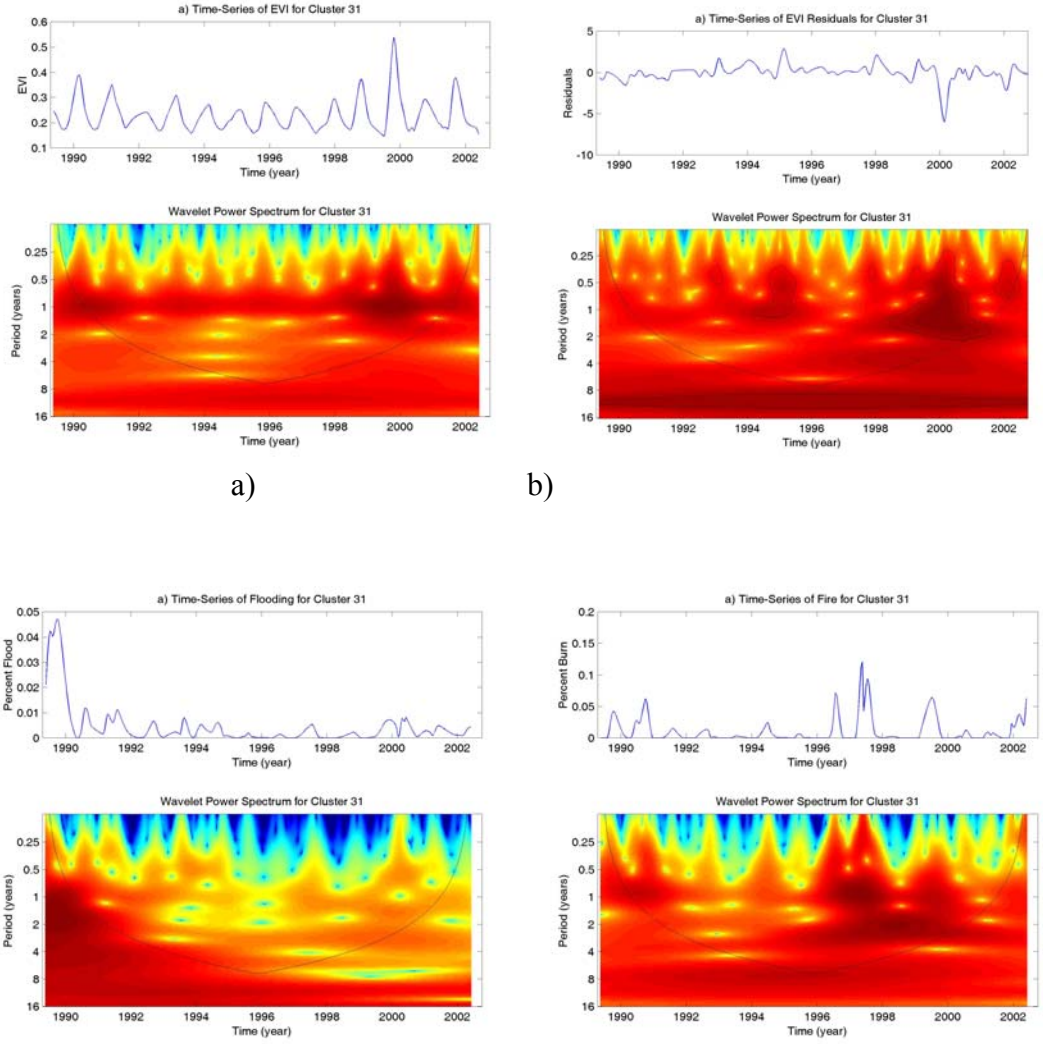

Figure A.1-31. Wavelet power spectrum for EVI cluster 31 for a) Mean EVI trajectory b) Residual EVI trajectory c) Flooding trajectory, and d) Fire trajectory

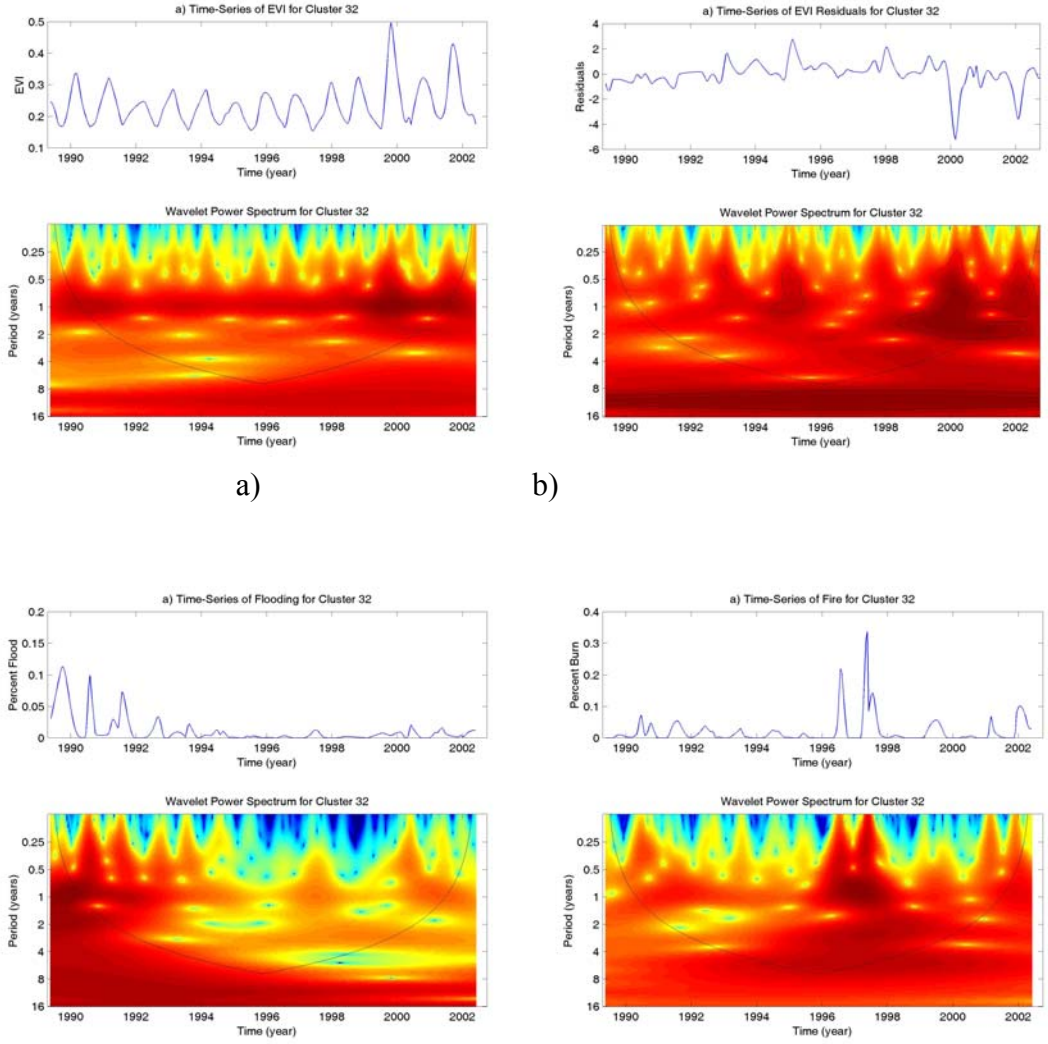

Figure A.1-32. Wavelet power spectrum for EVI cluster 32 for a) Mean EVI trajectory b) Residual EVI trajectory c) Flooding trajectory, and d) Fire trajectory

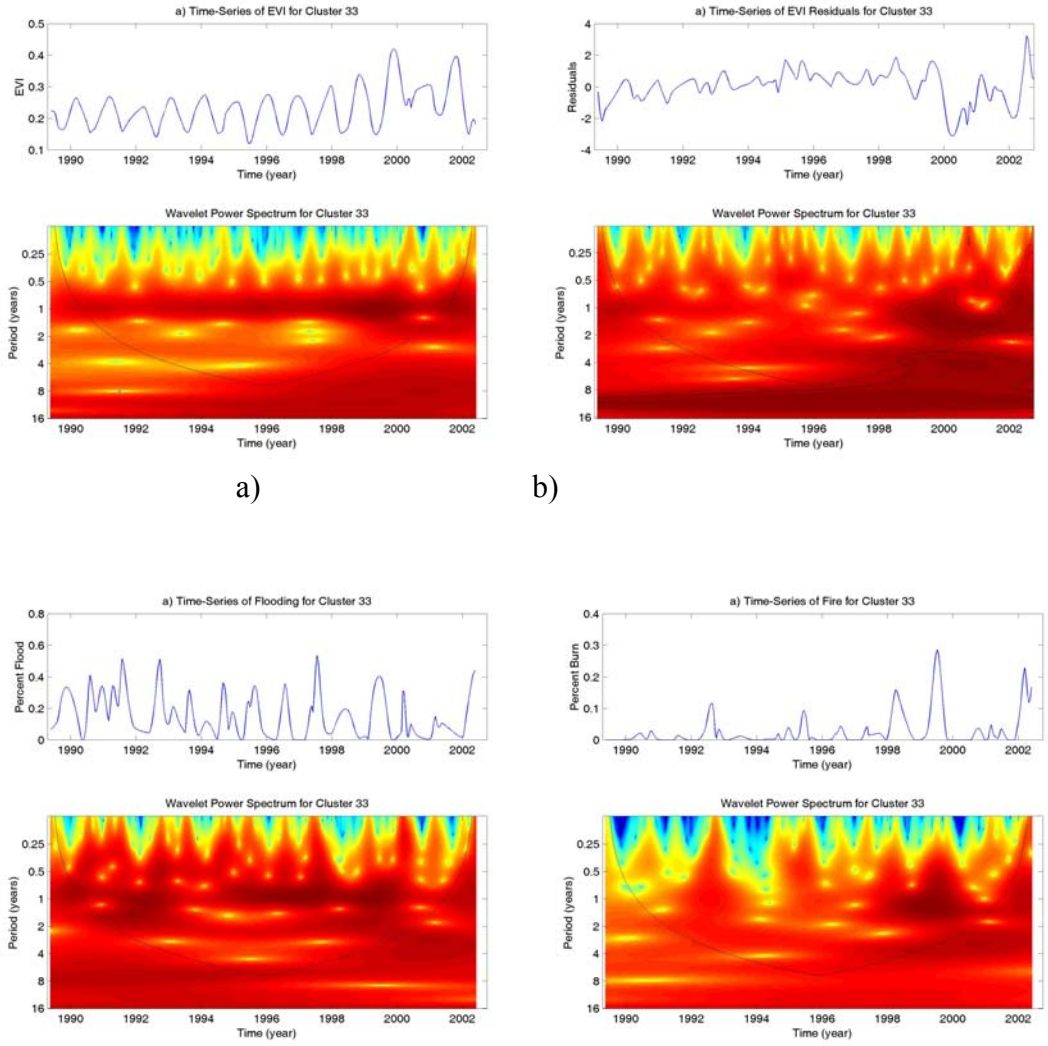

Figure A.1-33. Wavelet power spectrum for EVI cluster 33 for a) Mean EVI trajectory b) Residual EVI trajectory c) Flooding trajectory, and d) Fire trajectory

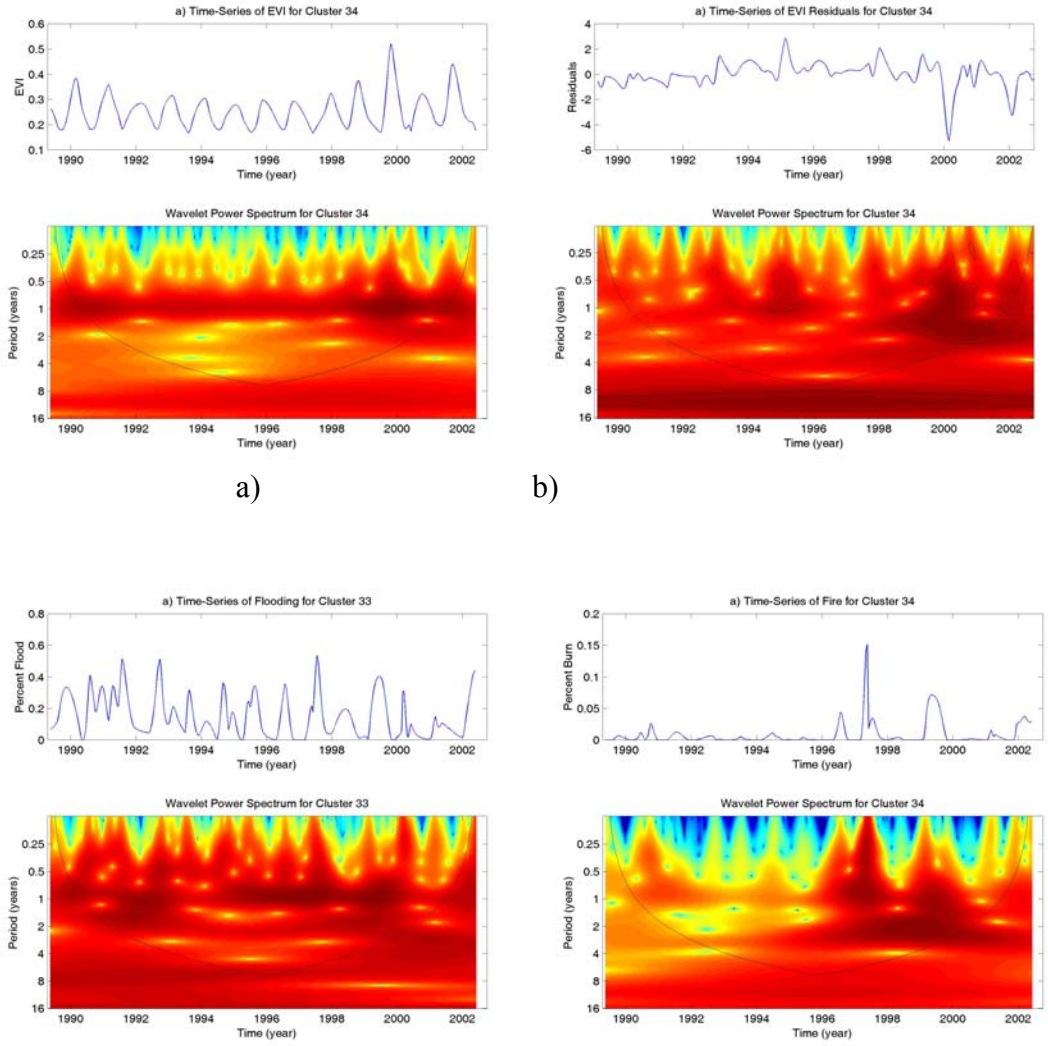

Figure A.1-34. Wavelet power spectrum for EVI cluster 34 for a) Mean EVI trajectory b) Residual EVI trajectory c) Flooding trajectory, and d) Fire trajectory

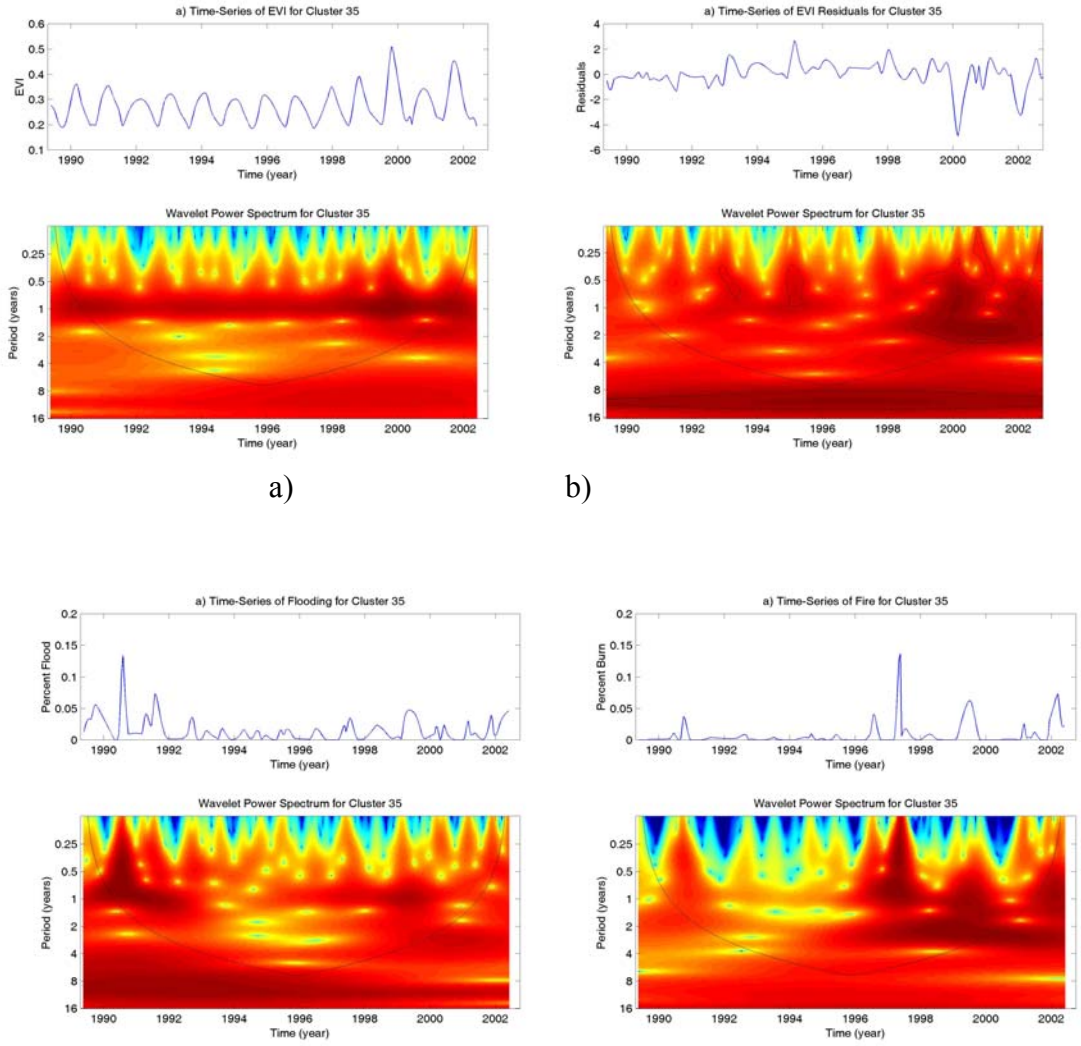

Figure A.1-35. Wavelet power spectrum for EVI cluster 35 for a) Mean EVI trajectory b) Residual EVI trajectory c) Flooding trajectory, and d) Fire trajectory

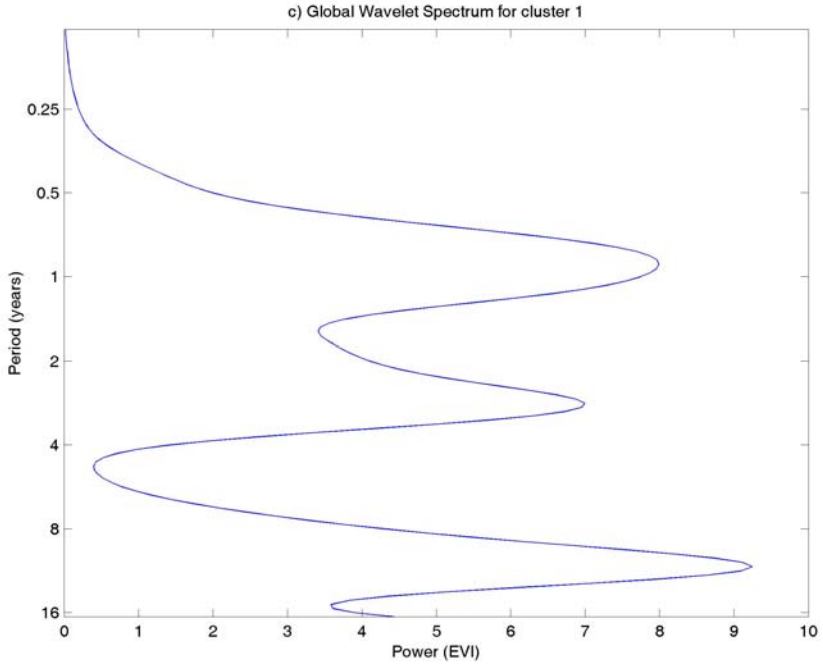

Figure A.1-36. Global Wavelet for Residuals of EVI Cluster 1

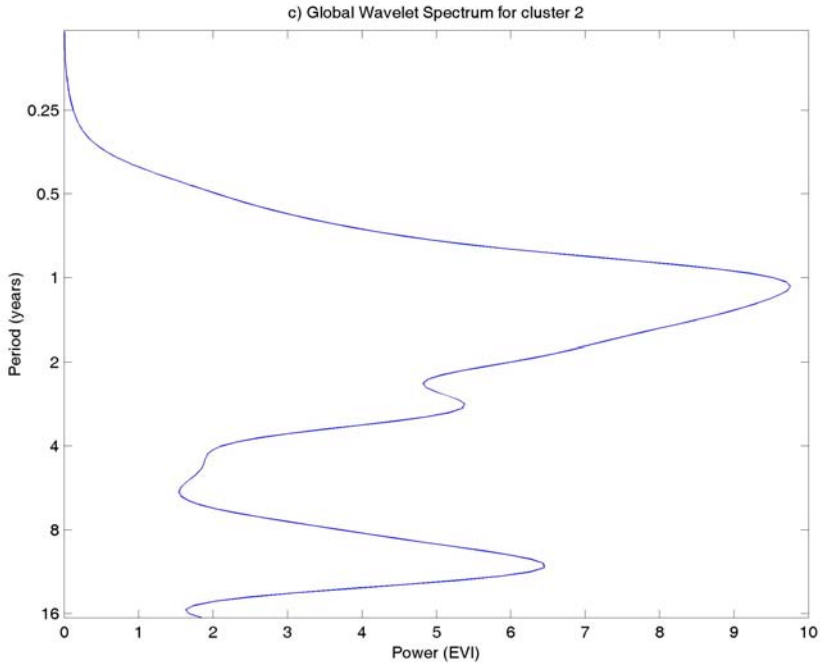

Figure A.1-37. Global Wavelet for Residuals of EVI Cluster 2

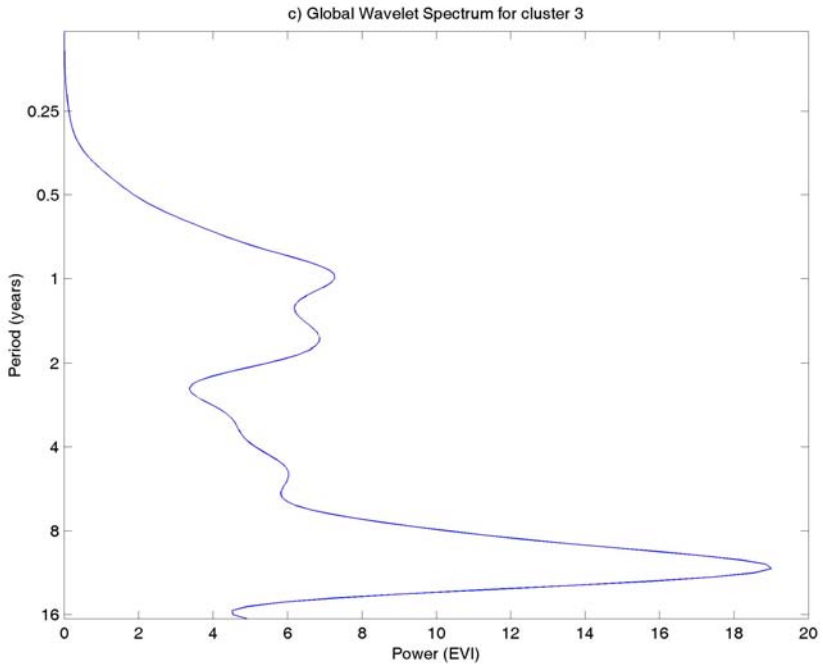

Figure A.1-38. Global Wavelet for Residuals of EVI Cluster 3

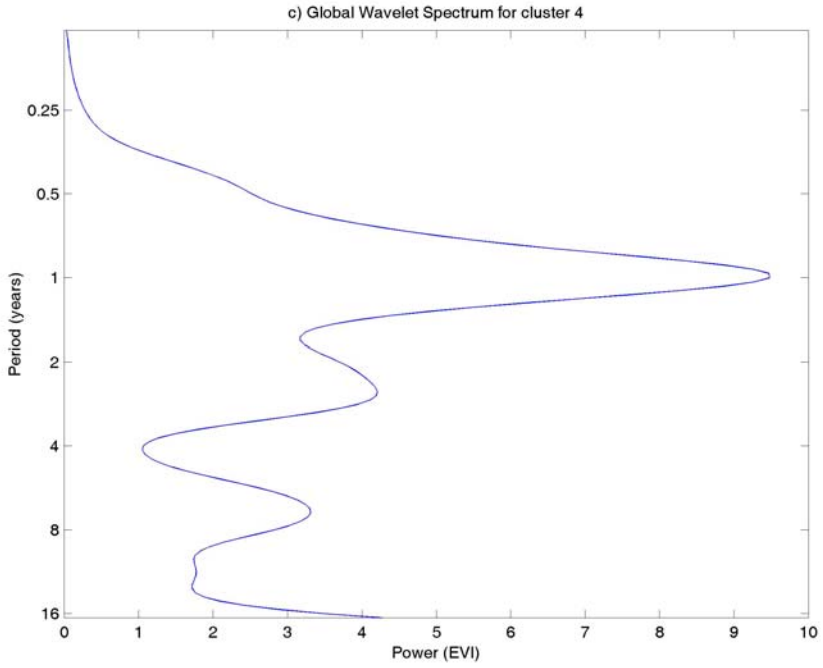

Figure A.1-39. Global Wavelet for Residuals of EVI Cluster 4

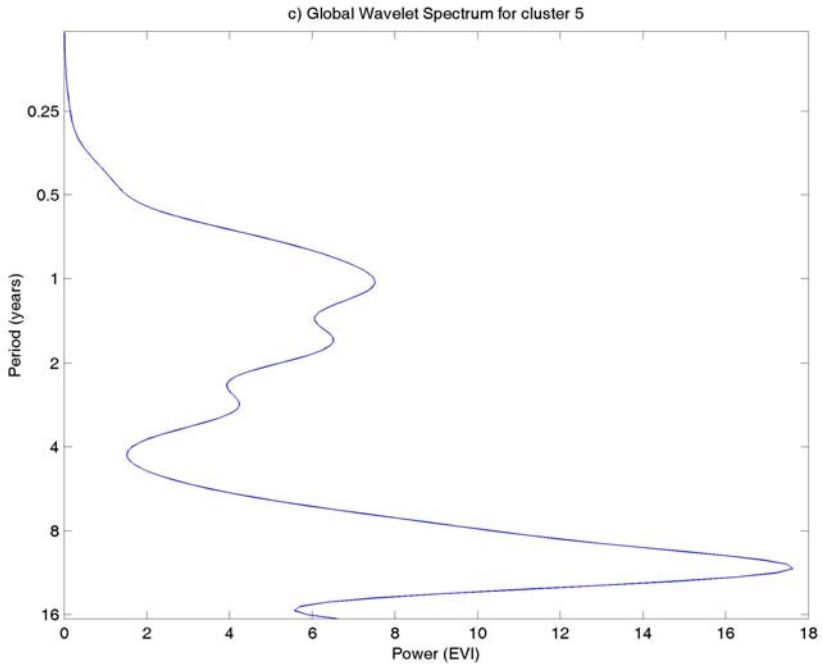

Figure A.1-40. Global Wavelet for Residuals of EVI Cluster 5

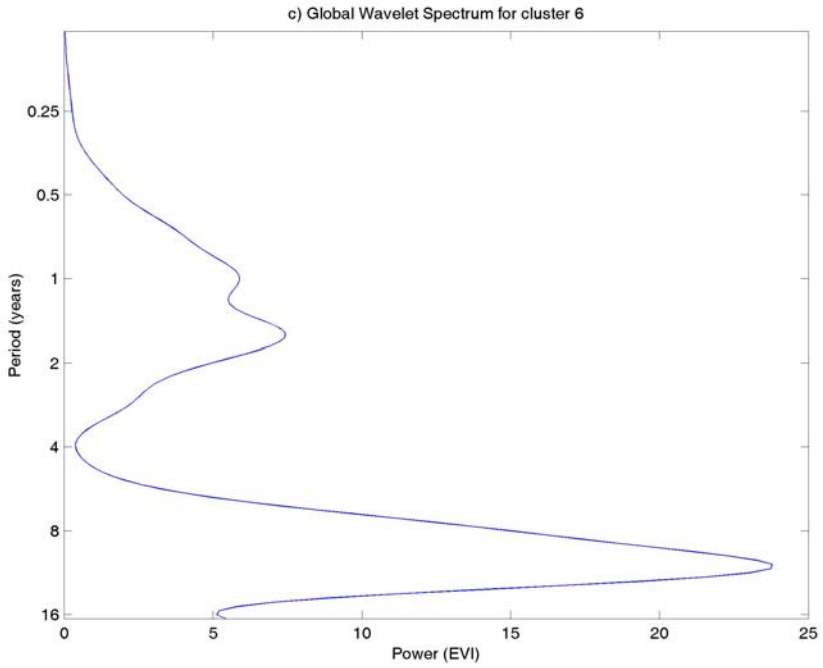

Figure A.1-41. Global Wavelet for Residuals of EVI Cluster 6

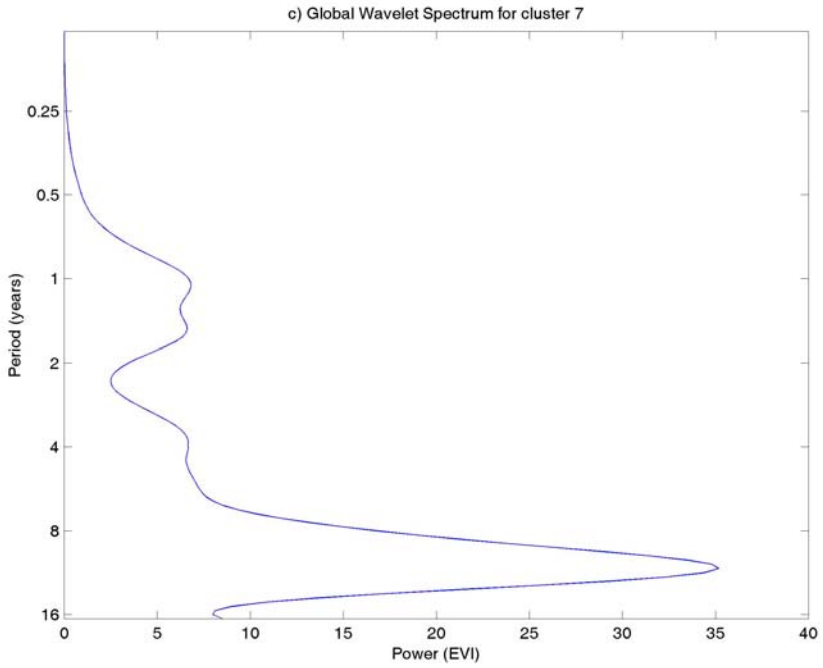

Figure A.1-42. Global Wavelet for Residuals of EVI Cluster 7

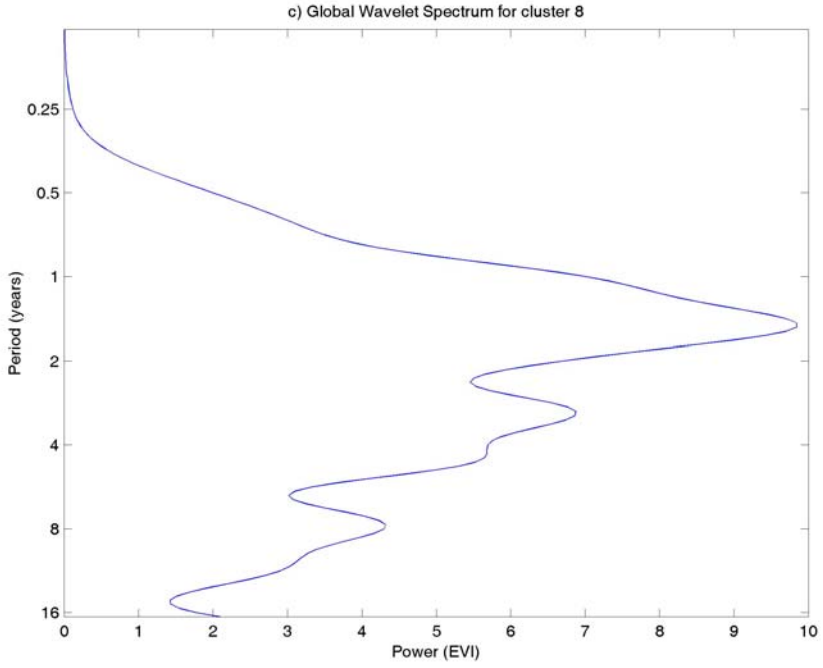

Figure A.1-43. Global Wavelet for Residuals of EVI Cluster 8

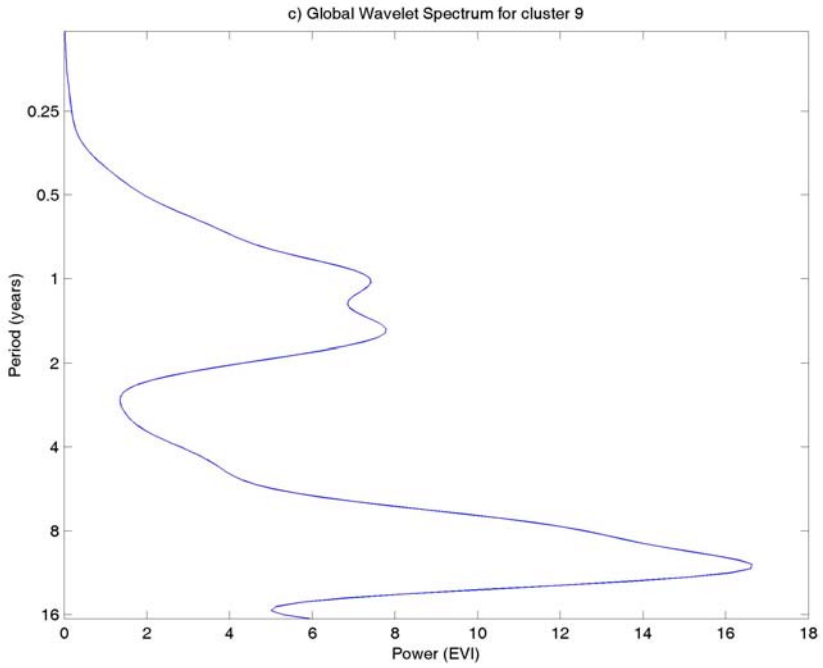

Figure A.1-44. Global Wavelet for Residuals of EVI Cluster 9

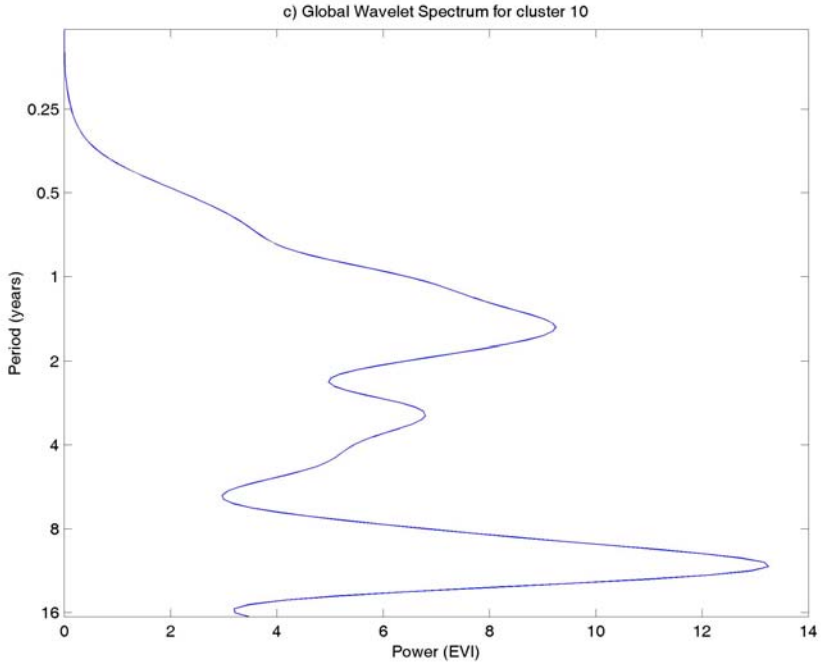

Figure A.1-45. Global Wavelet for Residuals of EVI Cluster 10

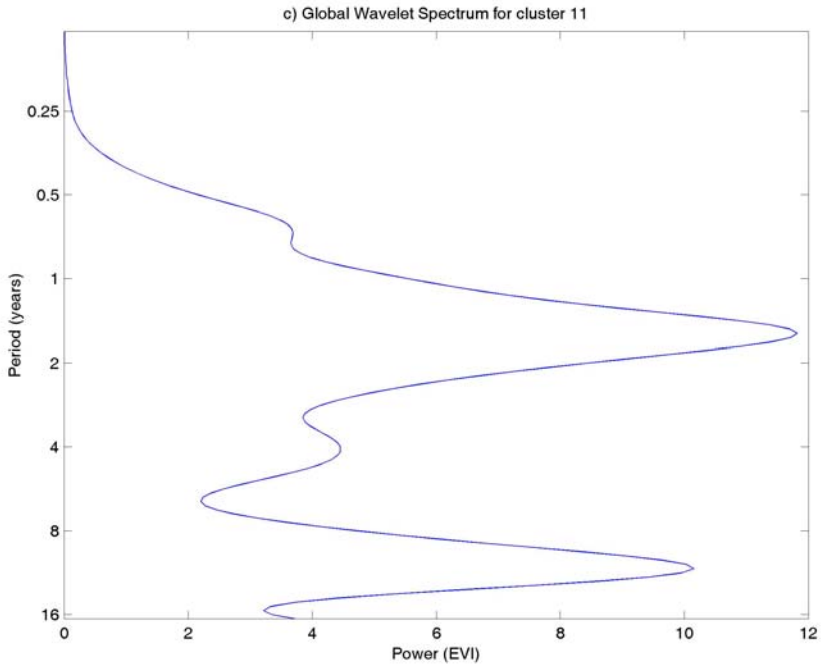

Figure A.1-46. Global Wavelet for Residuals of EVI Cluster 11

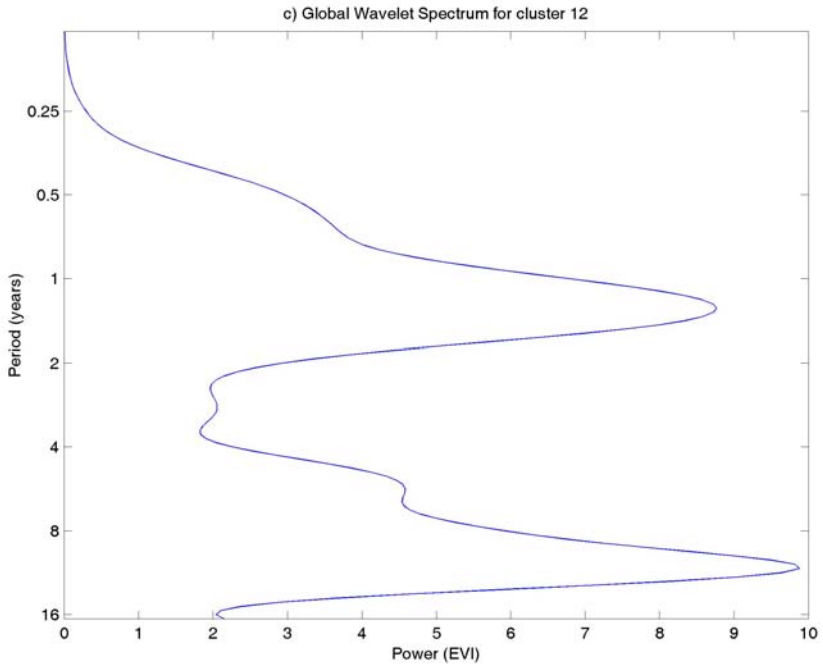

Figure A.1-47. Global Wavelet for Residuals of EVI Cluster 12

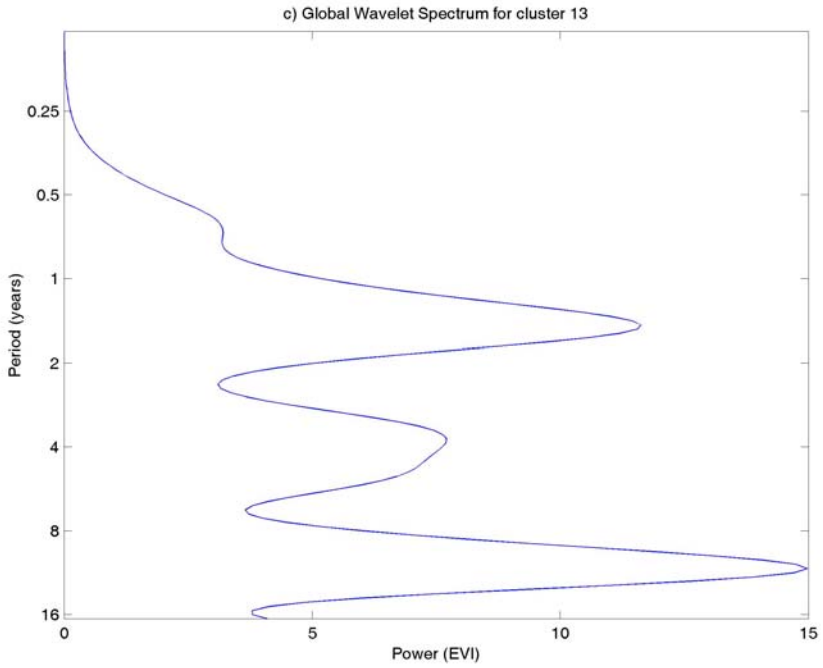

Figure A.1-48. Global Wavelet for Residuals of EVI Cluster 13

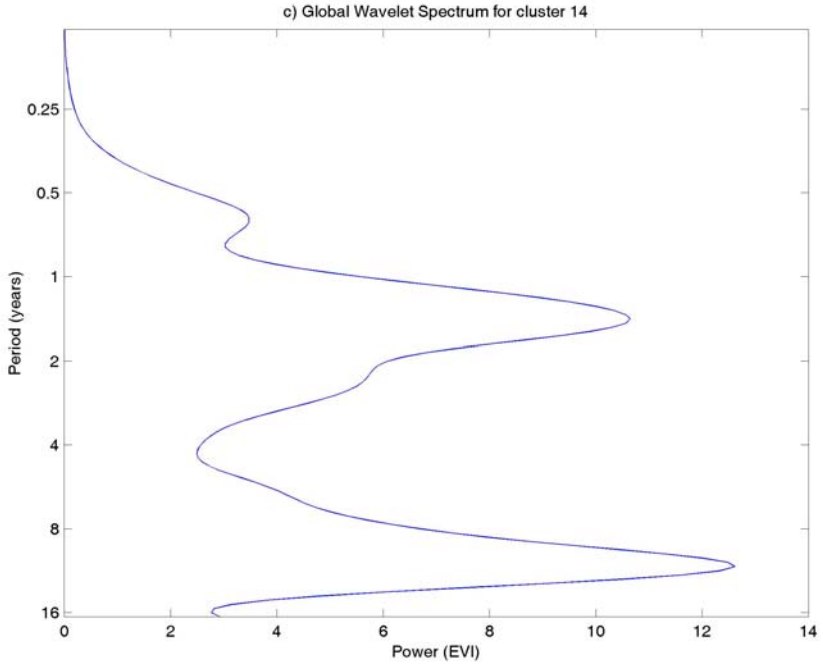

Figure A.1-49. Global Wavelet for Residuals of EVI Cluster 14

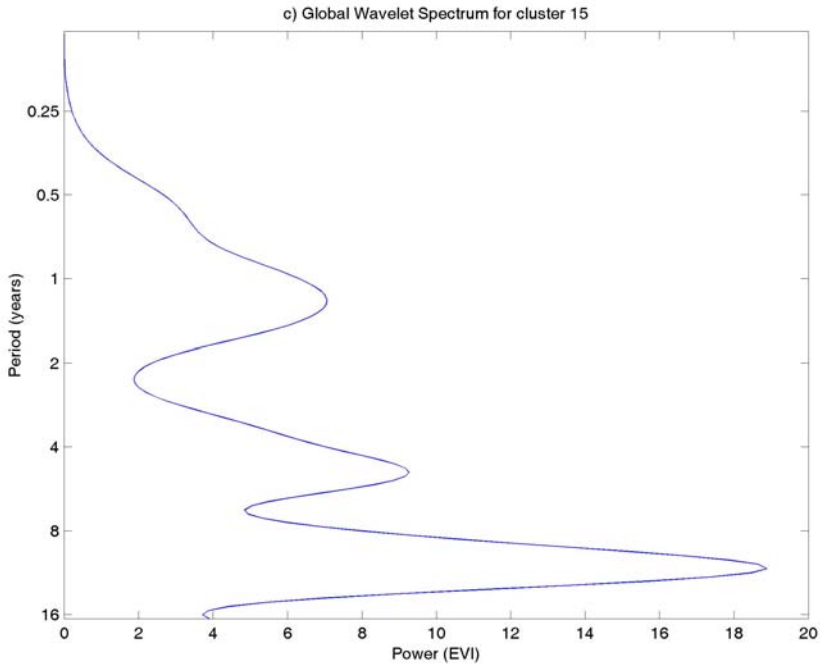

Figure A.1-50. Global Wavelet for Residuals of EVI Cluster 15

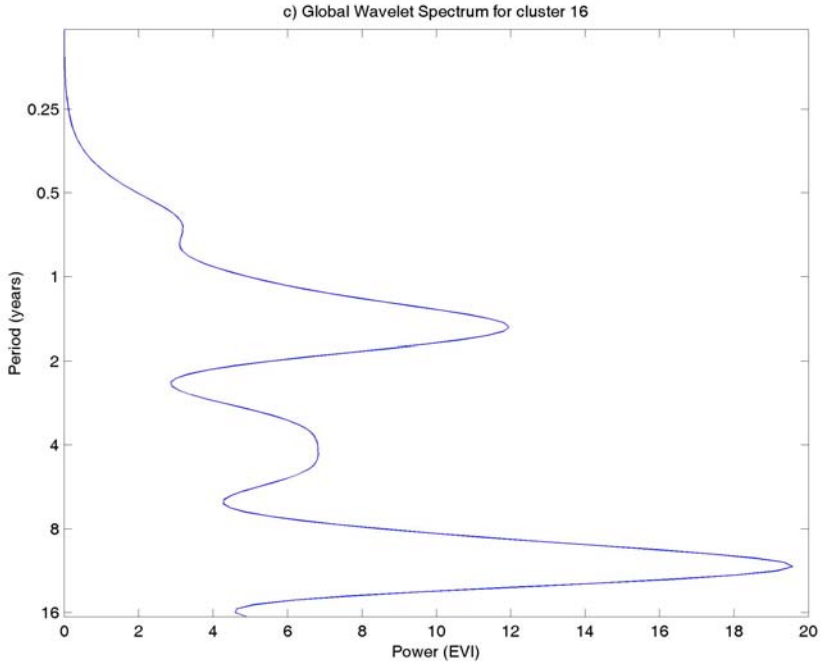

Figure A.1-51. Global Wavelet for Residuals of EVI Cluster 16

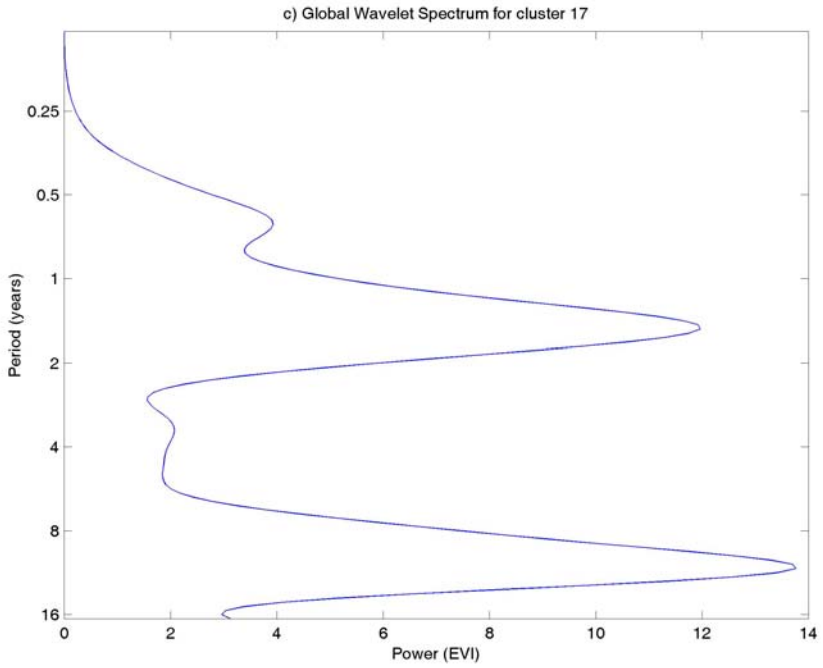

Figure A.1-52 Global Wavelet for Residuals of EVI Cluster 17

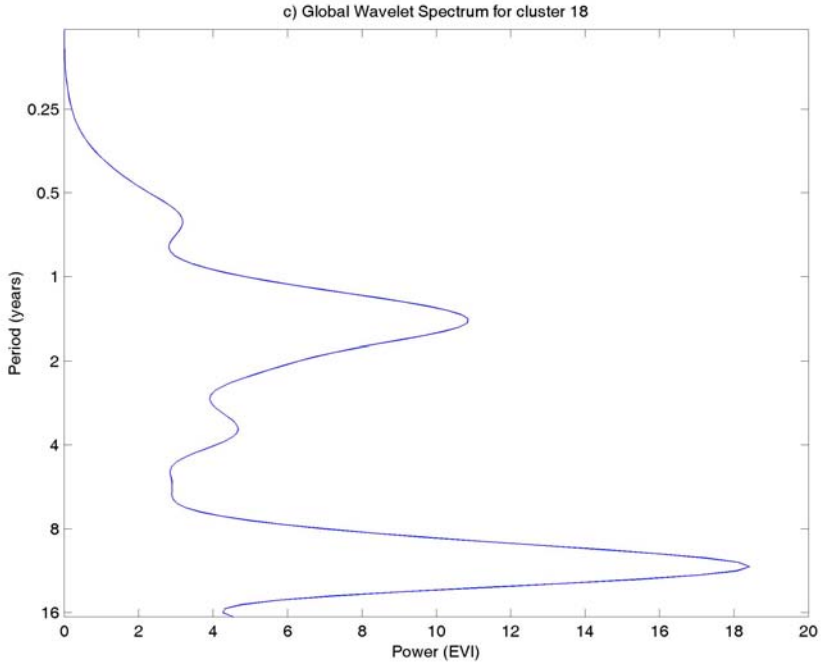

Figure A.1-53. Global Wavelet for Residuals of EVI Cluster 18

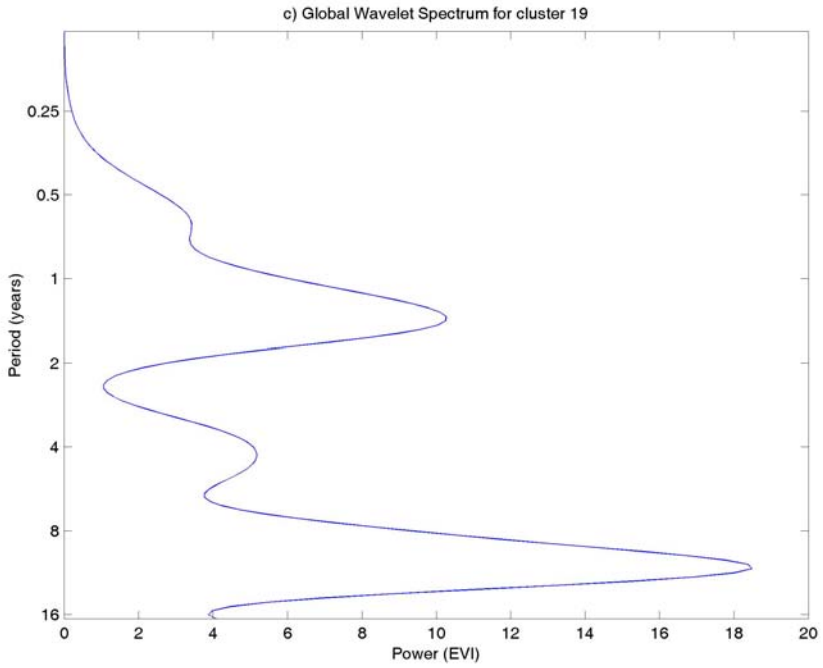

Figure A.1-54. Global Wavelet for Residuals of EVI Cluster 19

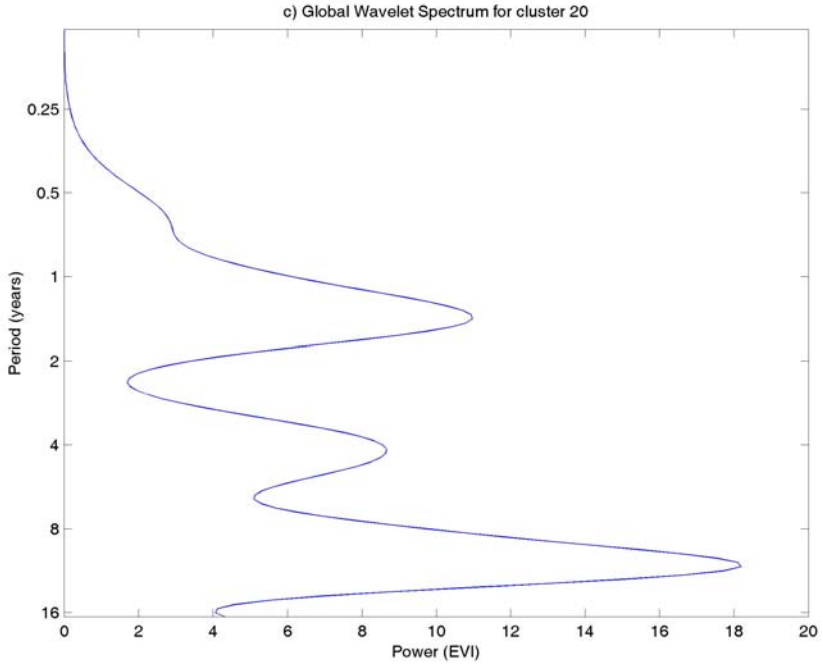

Figure A.1.55 Global Wavelet for Residuals of EVI Cluster 20

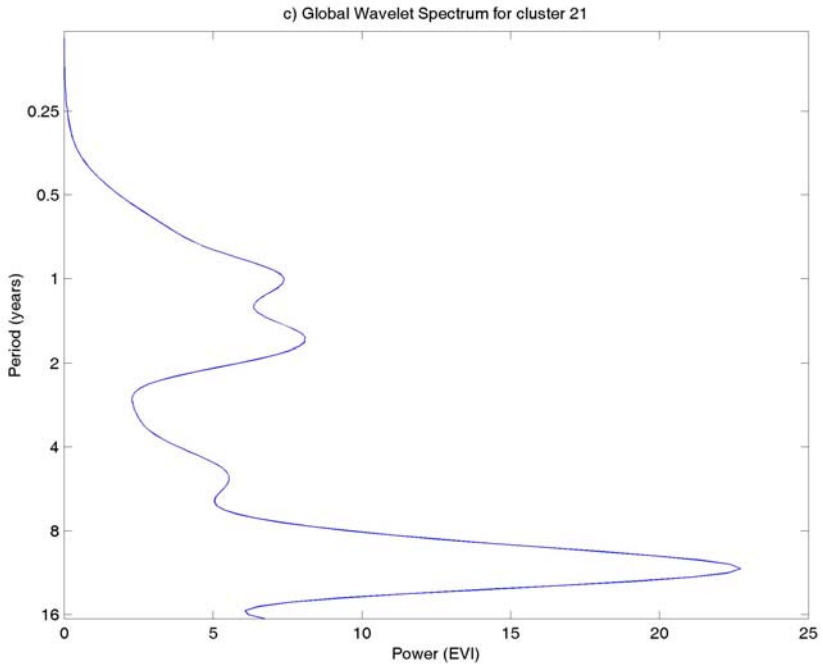

Figure A.1-56. Global Wavelet for Residuals of EVI Cluster 21

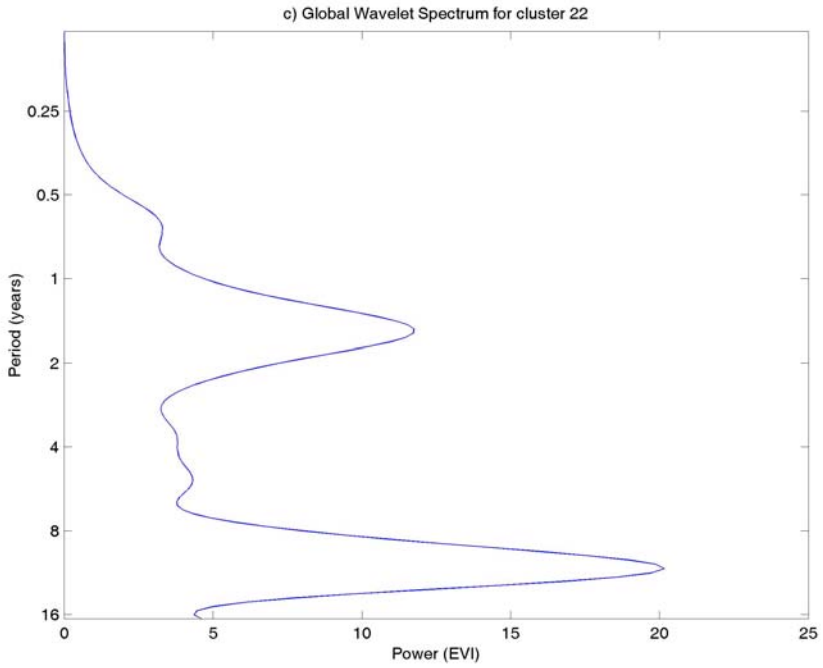

Figure A.1-57. Global Wavelet for Residuals of EVI Cluster 22

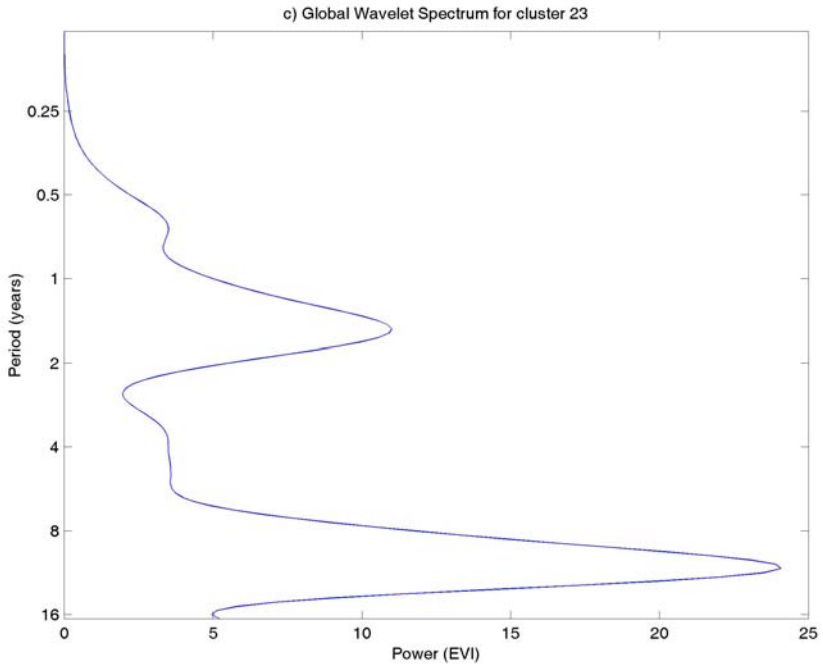

Figure A.1-58. Global Wavelet for Residuals of EVI Cluster 23

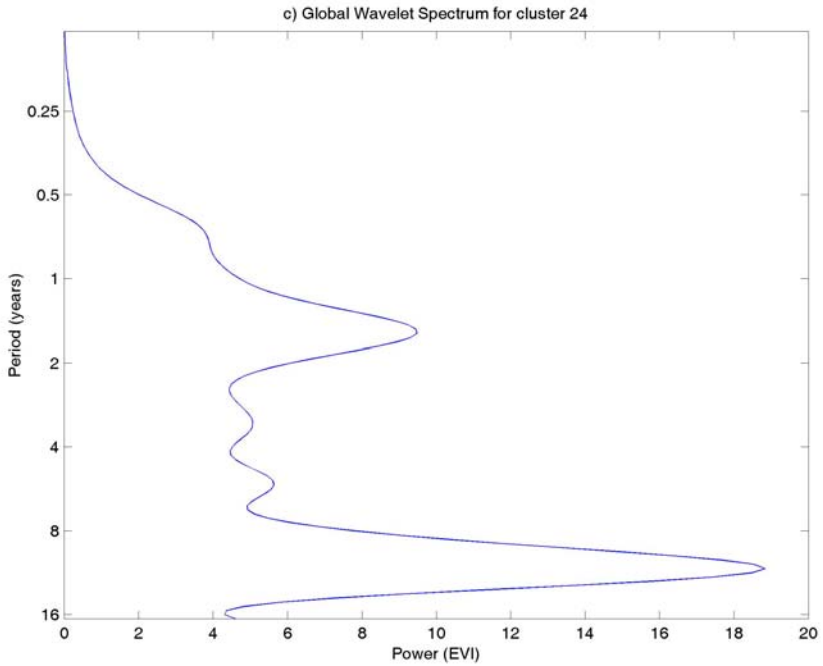

Figure A.1-59. Global Wavelet for Residuals of EVI Cluster 24

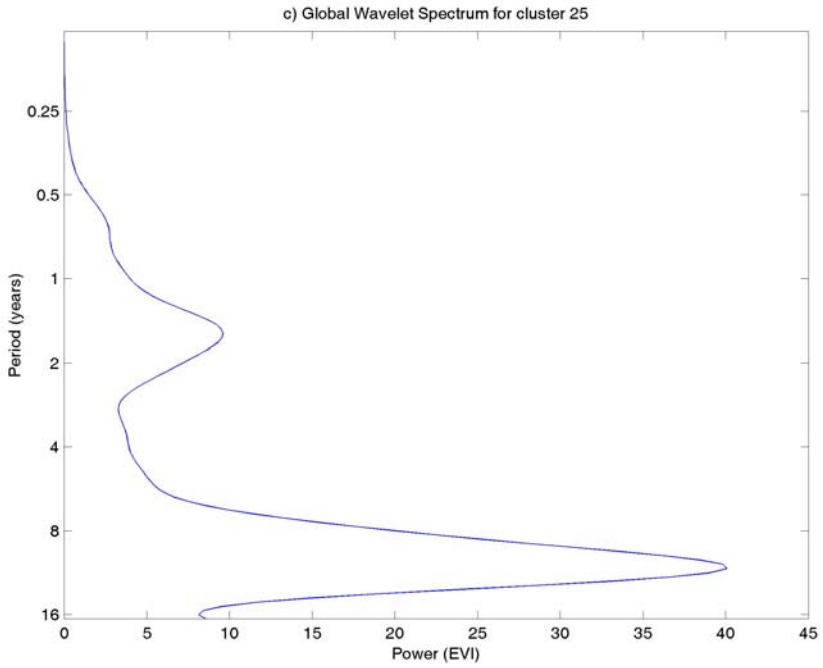

Figure A.1-60. Global Wavelet for Residuals of EVI Cluster 25

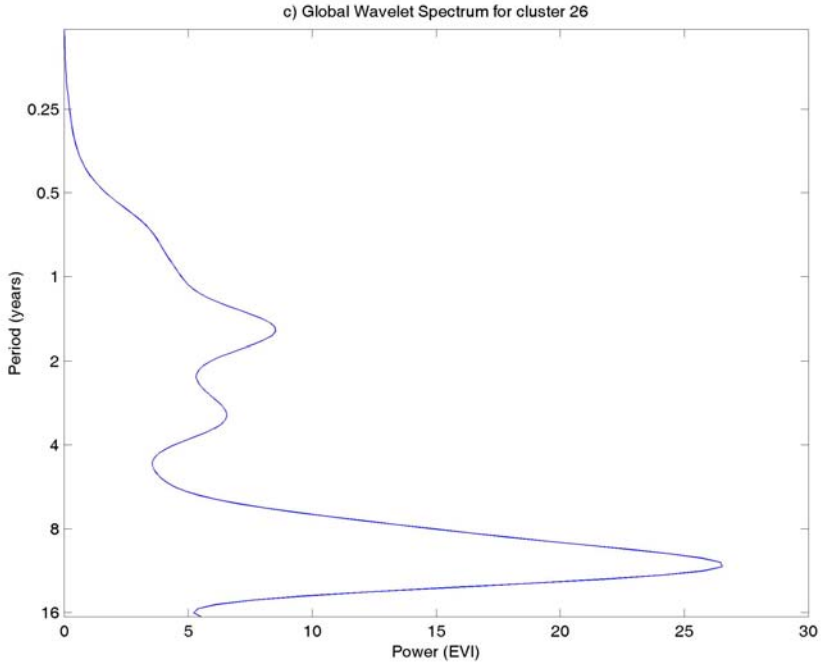

Figure A.1-61. Global Wavelet for Residuals of EVI Cluster 26

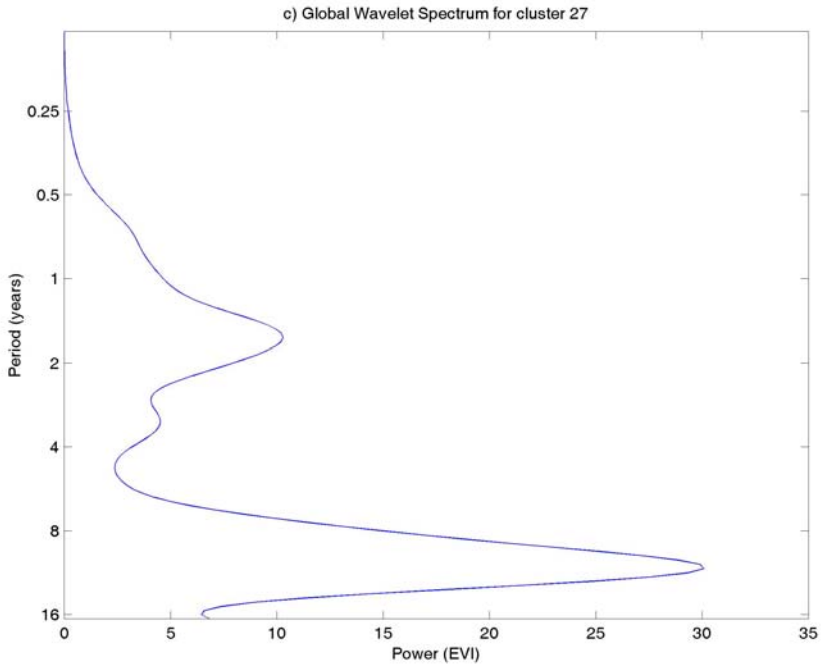

Figure A.1-62 Global Wavelet for Residuals of EVI Cluster 27

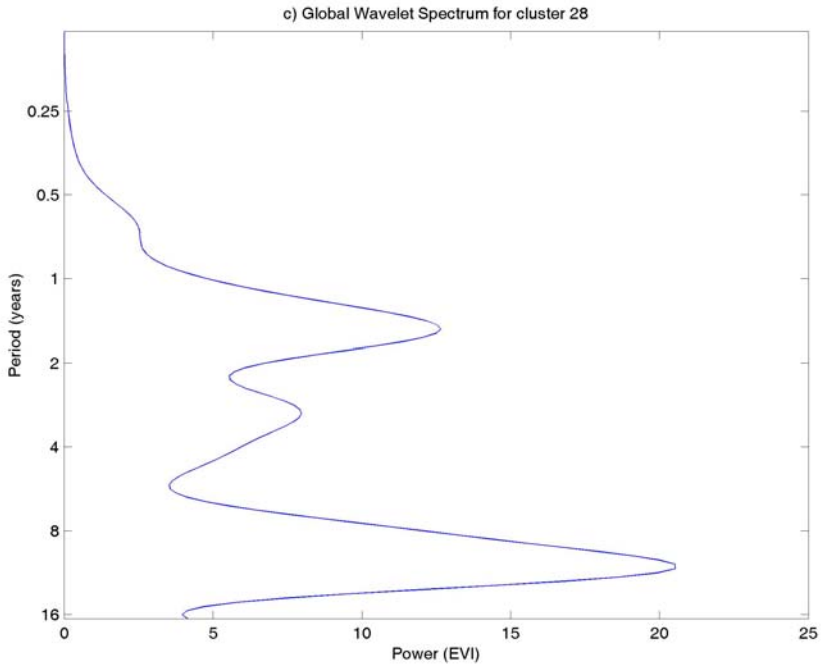

Figure A.1-63. Global Wavelet for Residuals of EVI Cluster 28

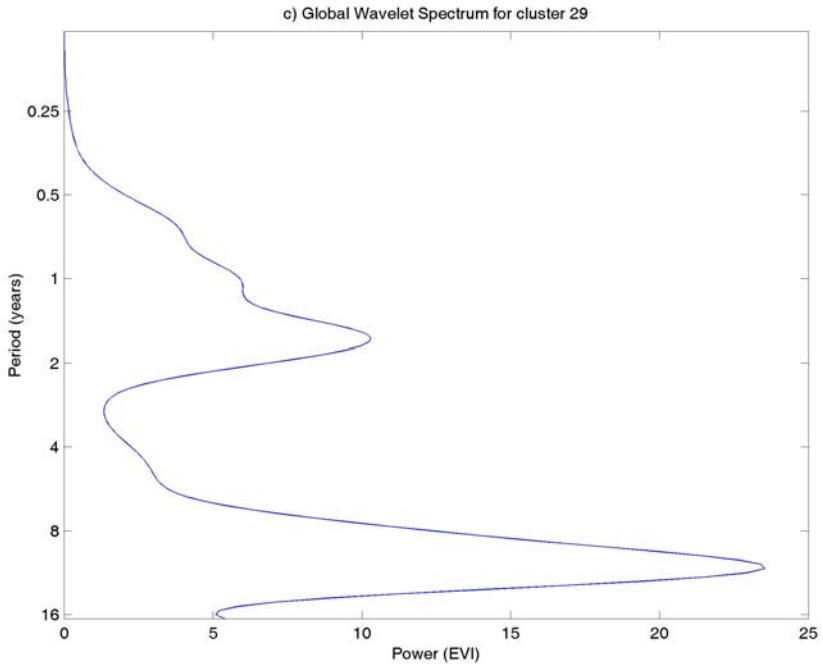

Figure A.1-64. Global Wavelet for Residuals of EVI Cluster 29

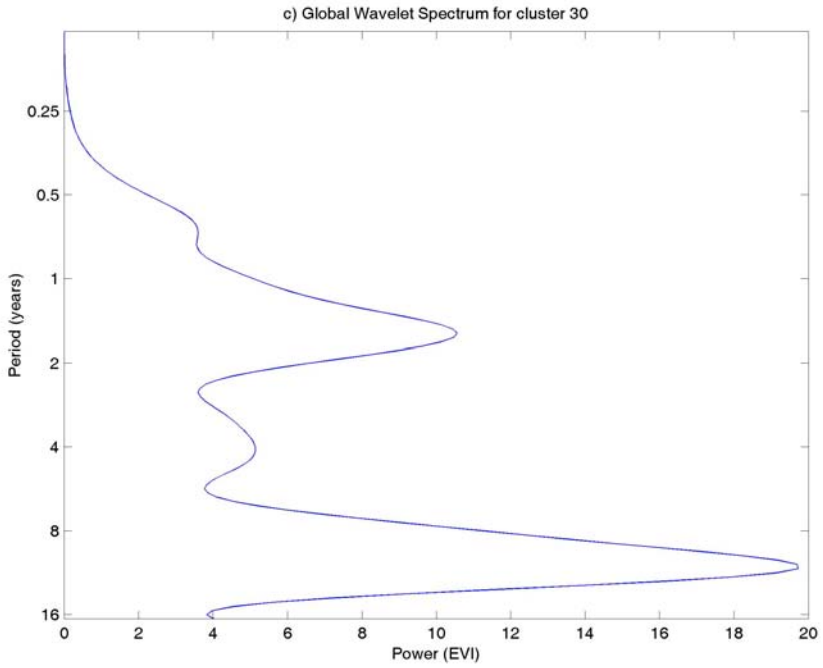

Figure A.1-65. Global Wavelet for Residuals of EVI Cluster 30

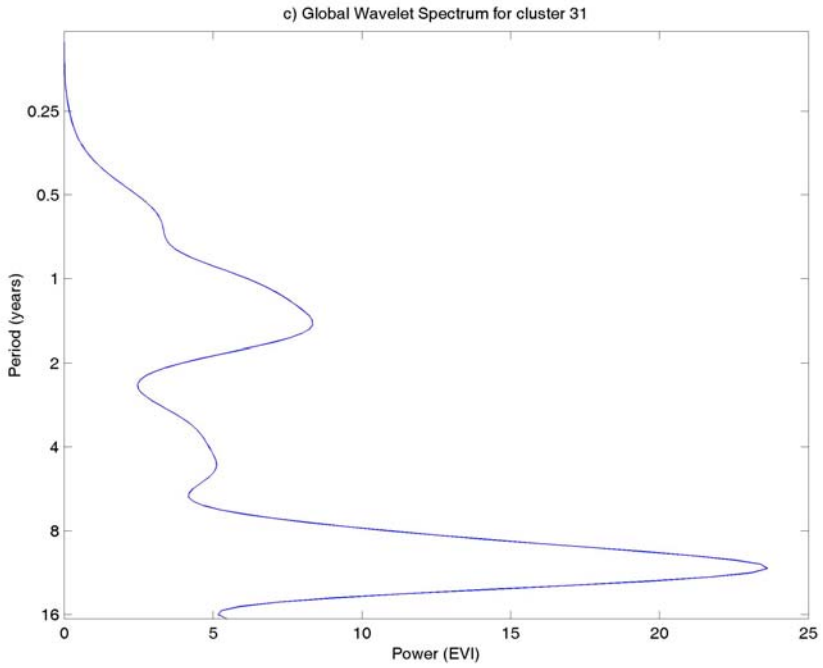

Figure A.1-66. Global Wavelet for Residuals of EVI Cluster 31

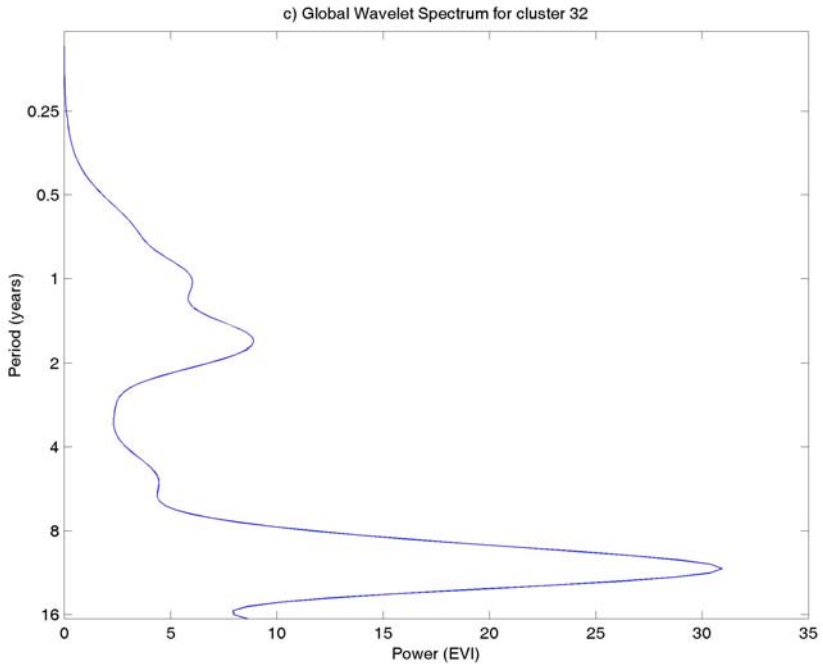

Figure A.1-67. Global Wavelet for Residuals of EVI Cluster 32

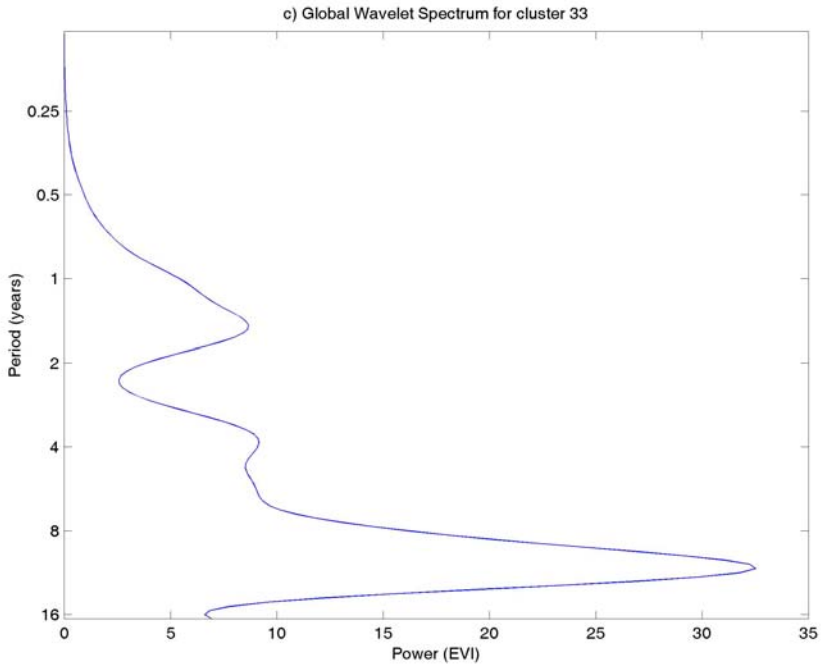

Figure A.1-68. Global Wavelet for Residuals of EVI Cluster 33

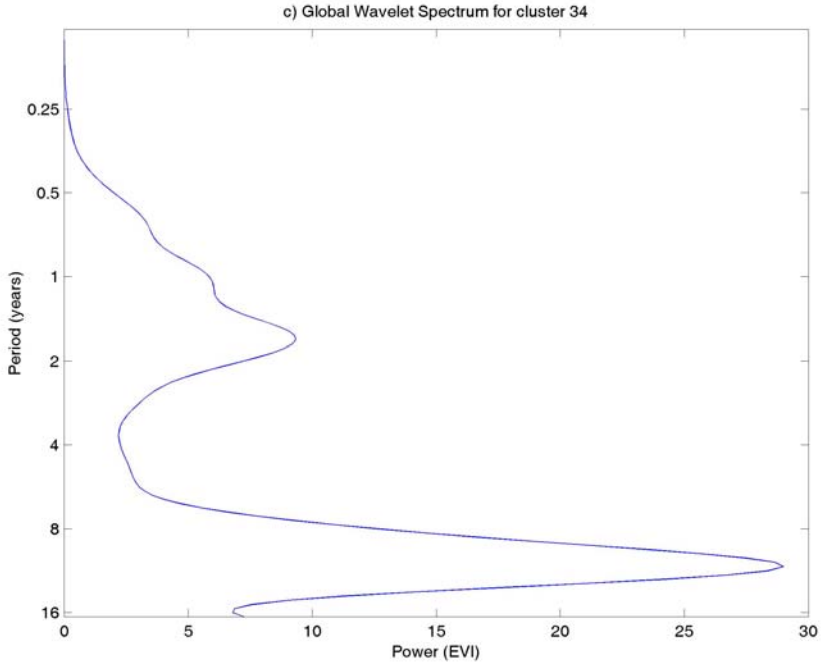

Figure A.1-69 Global Wavelet for Residuals of EVI Cluster 34

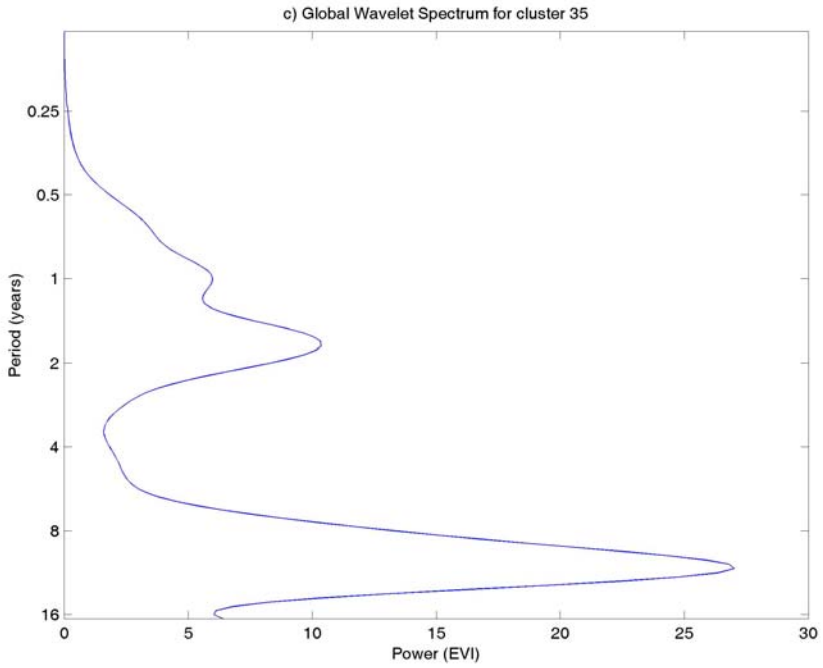

Figure A.1-70. Global Wavelet for Residuals of EVI Cluster 35

Appendix A.2. Wavelet Results for climate indices

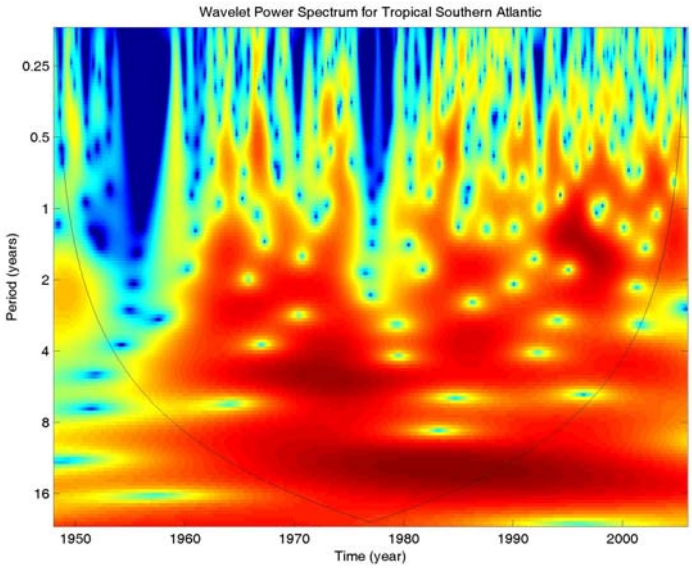

Figure A.2-1. Wavelet power spectrum for Tropical Southern Atlantic Index. Index is the anomaly of the average of the monthly SST from Eq-20S and 10E-30W

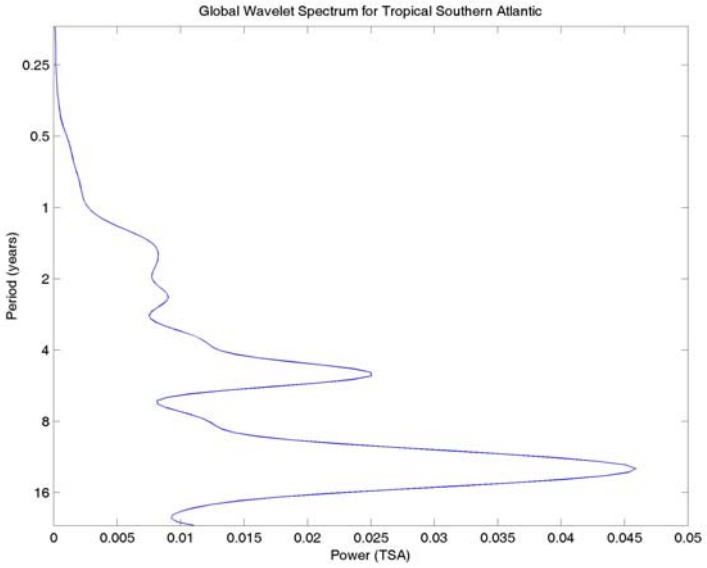

Figure A.2-2. Global Wavelet for Tropical Southern Atlantic Index

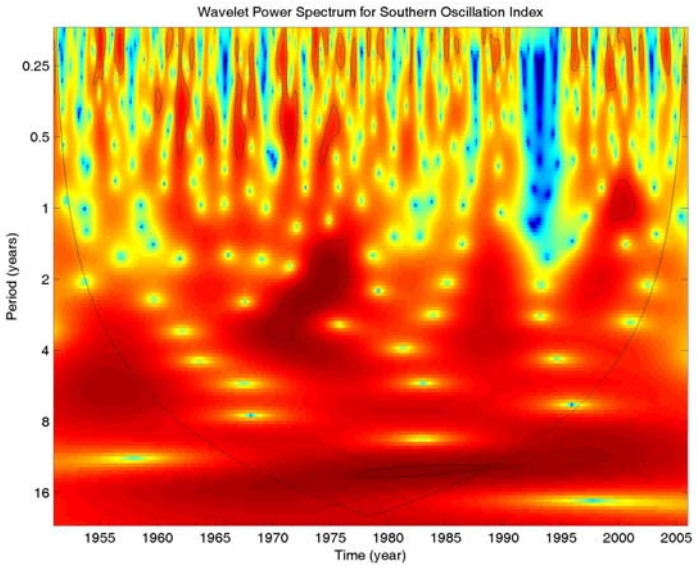

Figure A.2-3. Wavelet power spectrum for Southern Oscillation Index. Index is the Standardized Sea Level Pressure Difference from Tahiti to Darwin

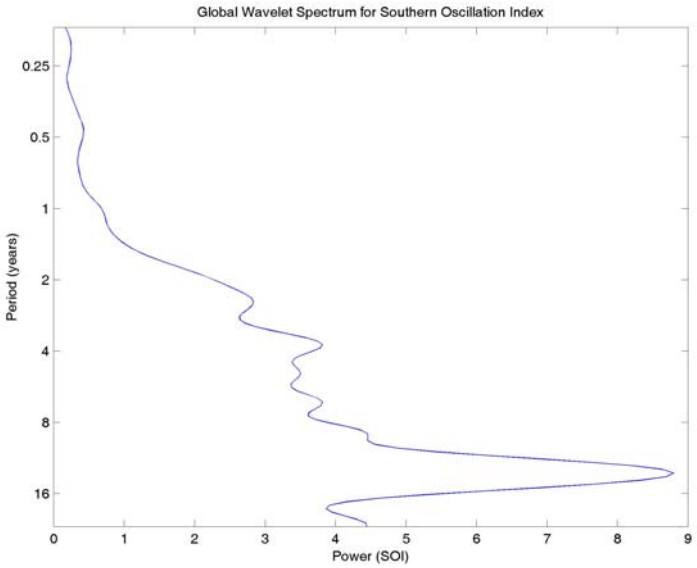

Figure A.2-4. Global Wavelet for Southern Oscillation Index

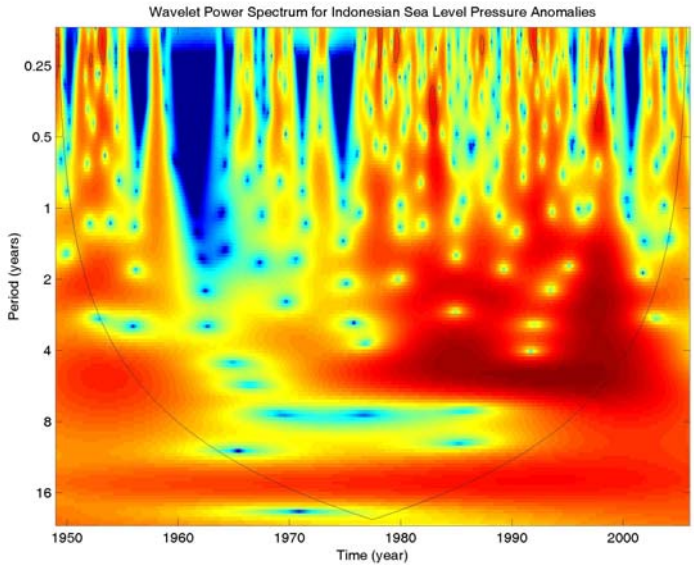

Figure A.2-5. Wavelet power spectrum for Indonesian Sea Level Pressure Index. Index is Equatorial SOI over Indonesia.

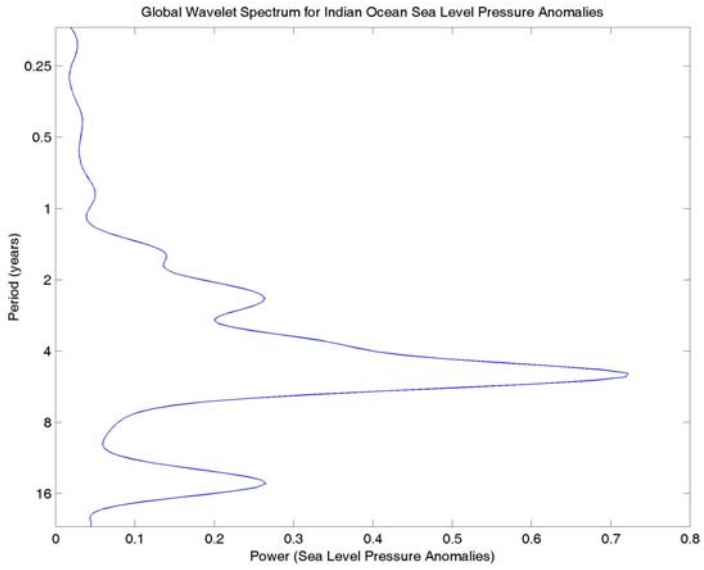

Figure A.2-6. Global Wavelet for Indonesian Sea Level Pressure Index

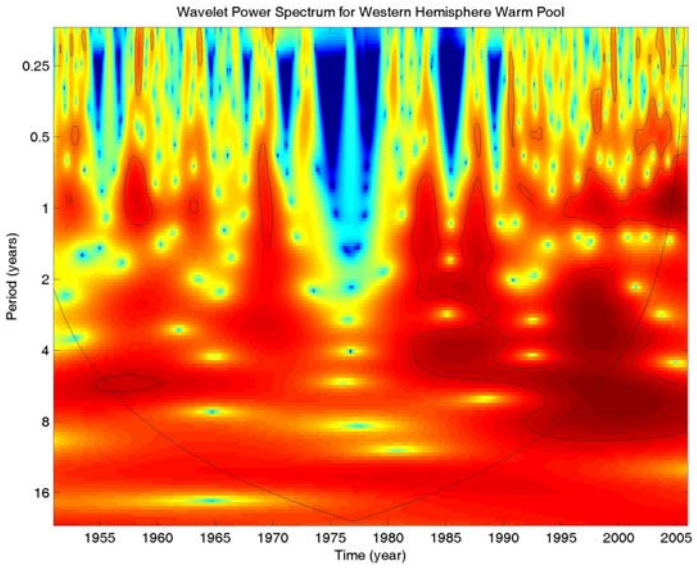

Figure A.2-7. Wavelet power spectrum for Western Hemisphere Warm Pool Index. Index is monthly anomaly of the ocean surface area warmer than 28.5°C in the Atlantic and eastern North Pacific.

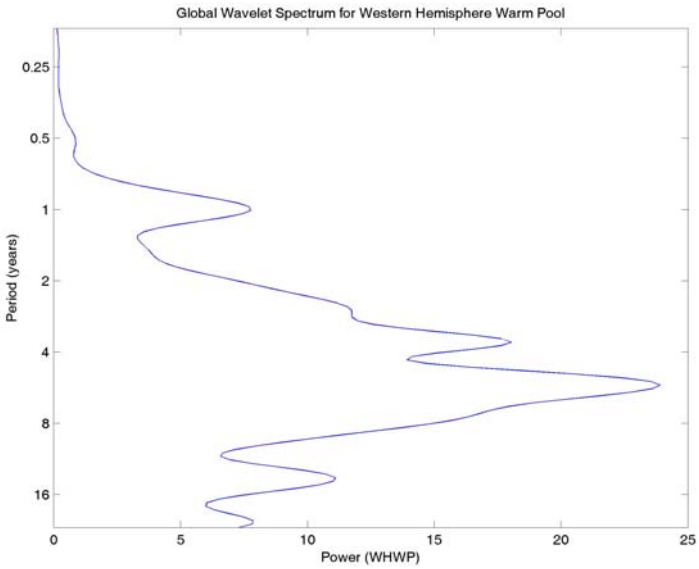

Figure A.2-8. Global Wavelet for Western Hemisphere Warm Pool Index

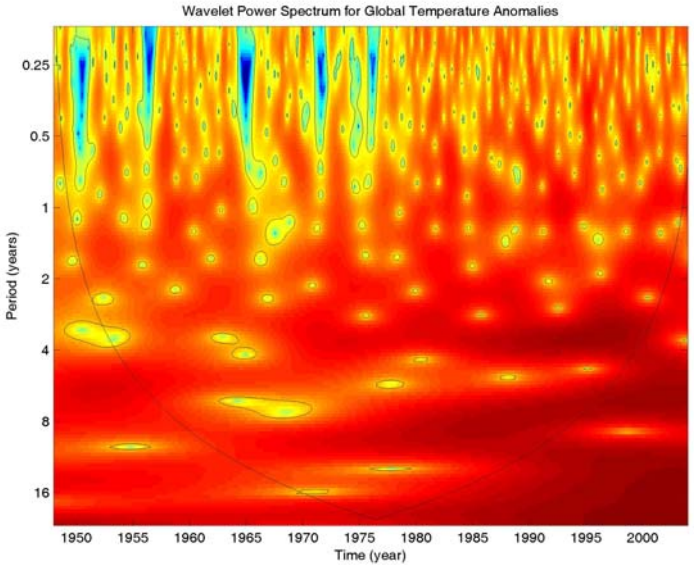

Figure A.2-9. Wavelet power spectrum for Global Temperature Anomalies Index

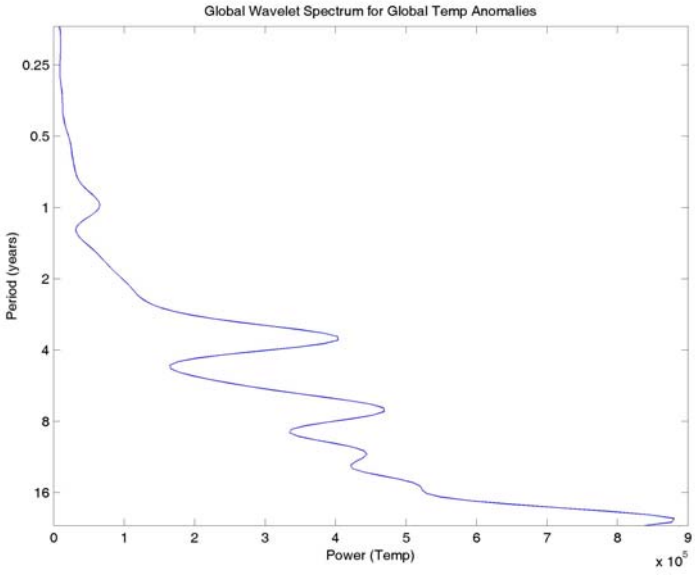

Figure A.2-10. Global Wavelet for Global Temperature Anomalies Index

Appendix A.3. Disturbance/ Management Clusters

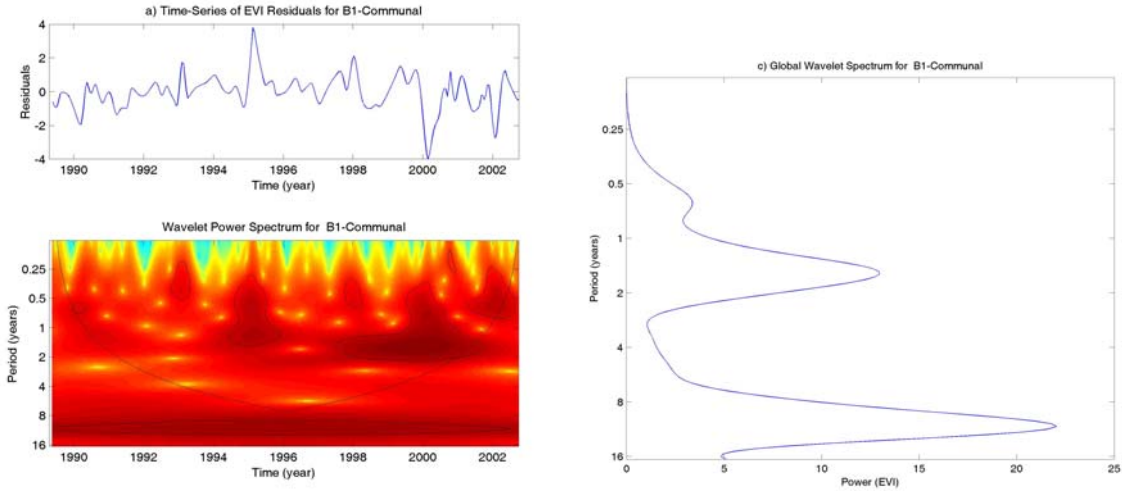

a) b)

Figure A.3-1. Burn 1-Communal a) Wavelet power spectrum b) Global Wavelet.

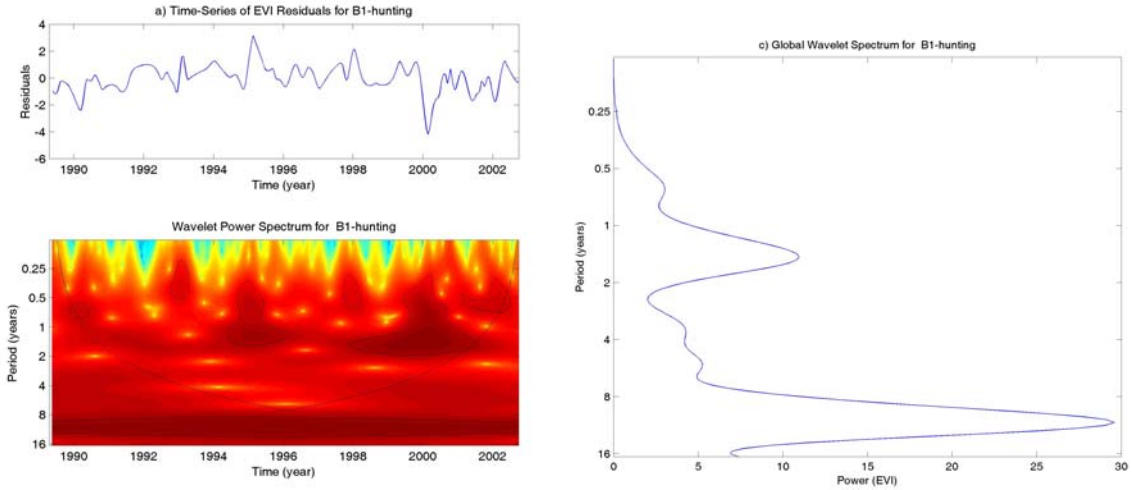

a) b)

Figure A.3-2. Burn 1-Hunting a) Wavelet power spectrum b) Global Wavelet.

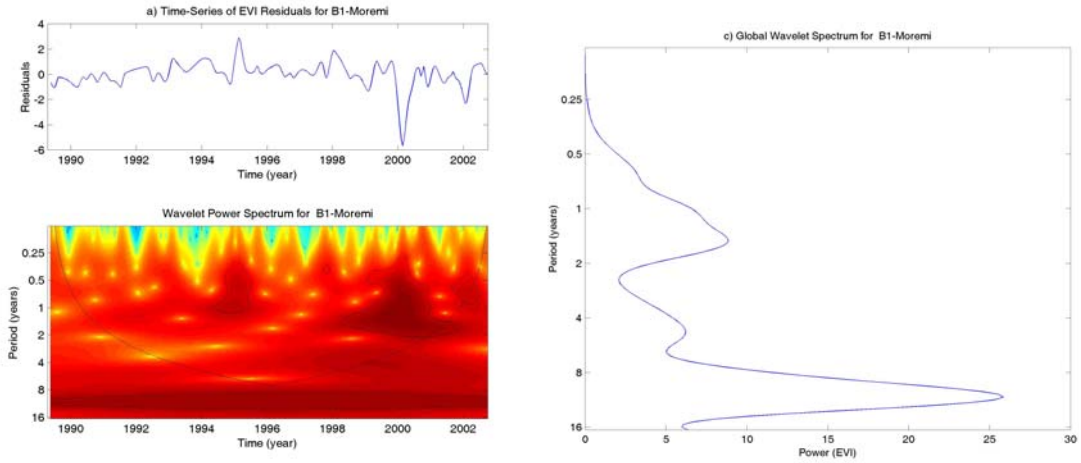

a) b)

Figure A.3-3. Burn 1-Moremi a) Wavelet power spectrum b) Global Wavelet.

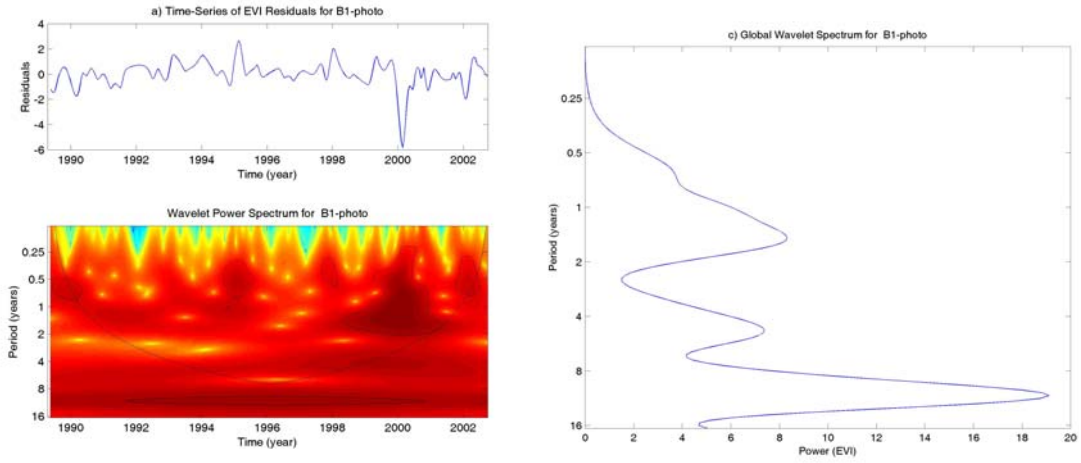

a) b)

Figure A.3-4. Burn 1-Photography a) Wavelet power spectrum b) Global Wavelet.

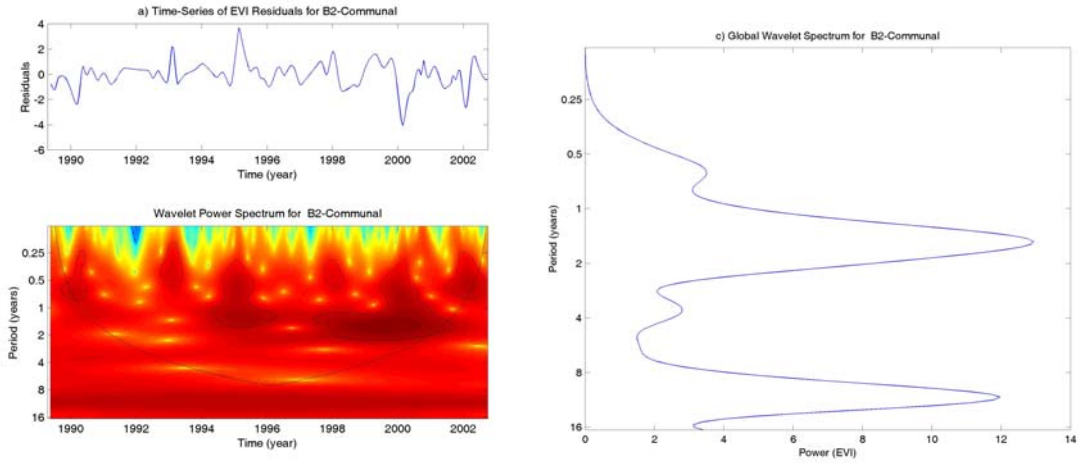

a) b)

Figure A.3-5. Burn 2-Communal a) Wavelet power spectrum b) Global Wavelet.

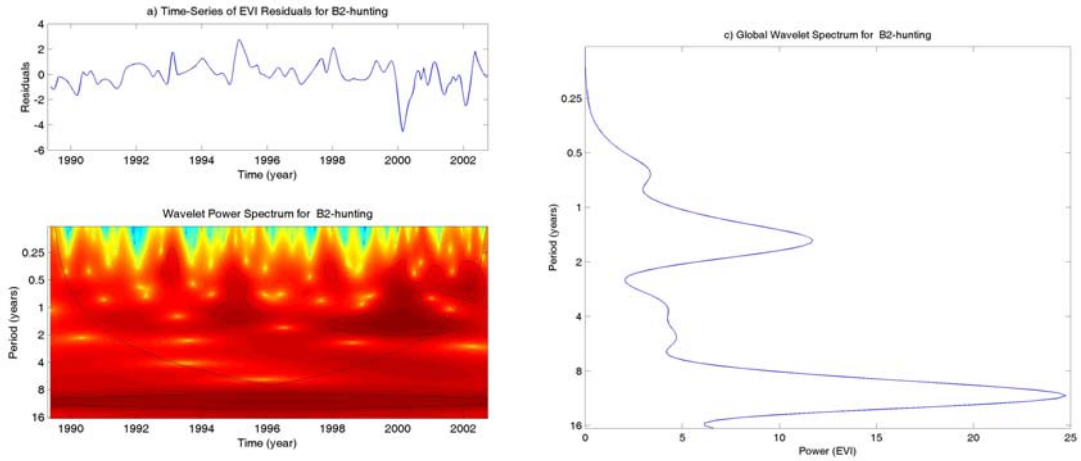

a) b)

Figure A.3-6. Burn 2-Hunting a) Wavelet power spectrum b) Global Wavelet.

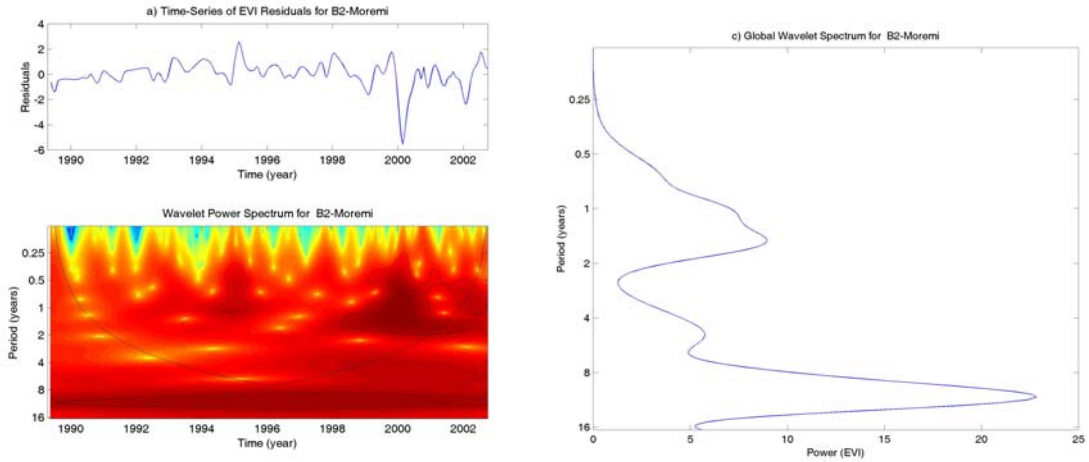

a) b)

Figure A.3-7. Burn 2-Moremi a) Wavelet power spectrum b) Global Wavelet.

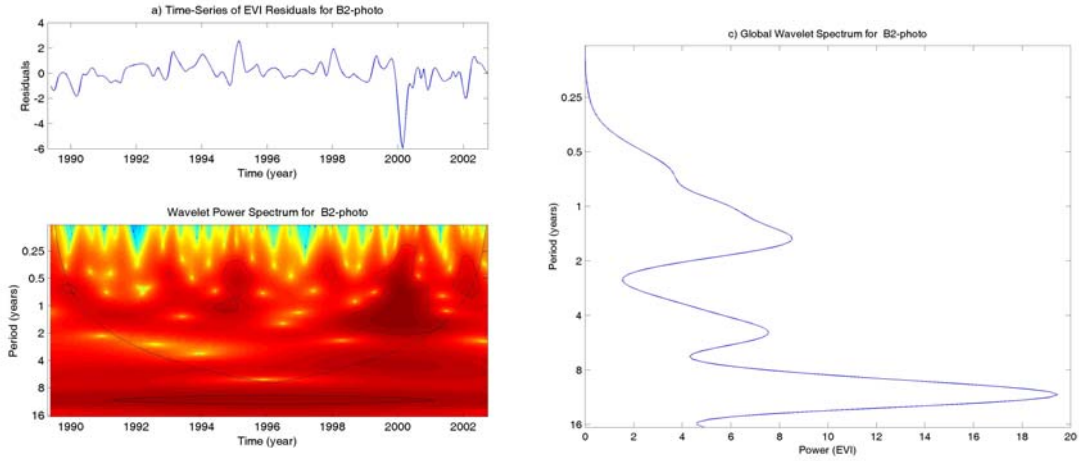

a) b)

Figure A.3-8. Burn 2-Photography a) Wavelet power spectrum b) Global Wavelet.

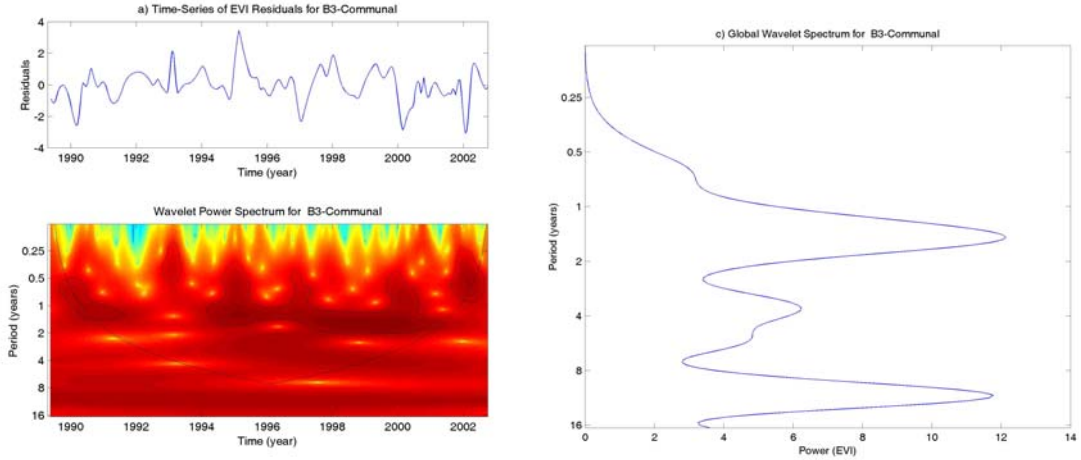

a) b)

Figure A.3-9. Burn 3-Communal a) Wavelet power spectrum b) Global Wavelet.

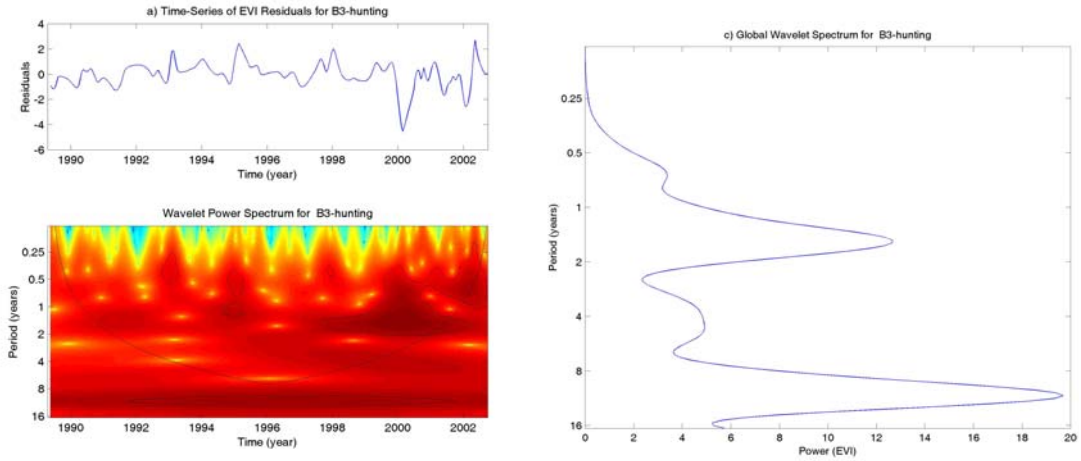

a) b)

Figure A.3-10. Burn 3-Hunting a) Wavelet power spectrum b) Global Wavelet.

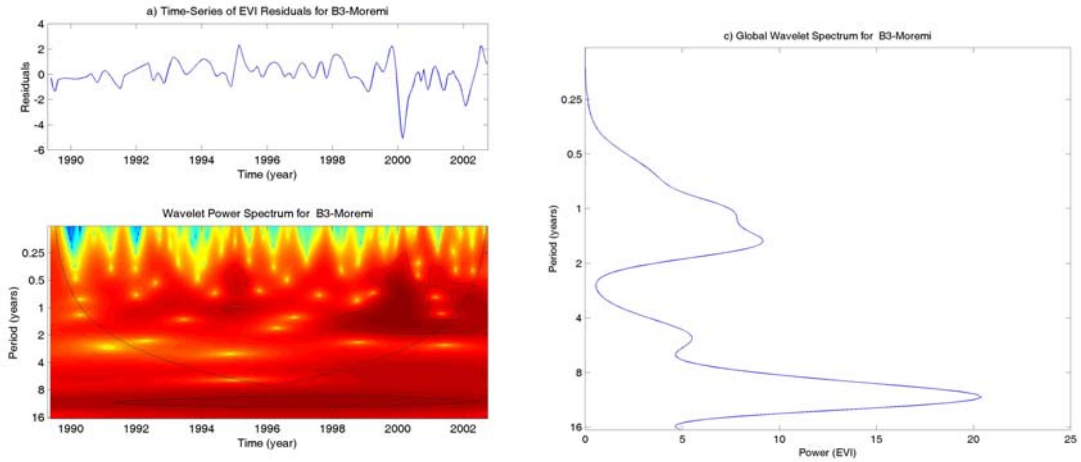

a) b)

Figure A.3-11. Burn 3-Moremi a) Wavelet power spectrum b) Global Wavelet.

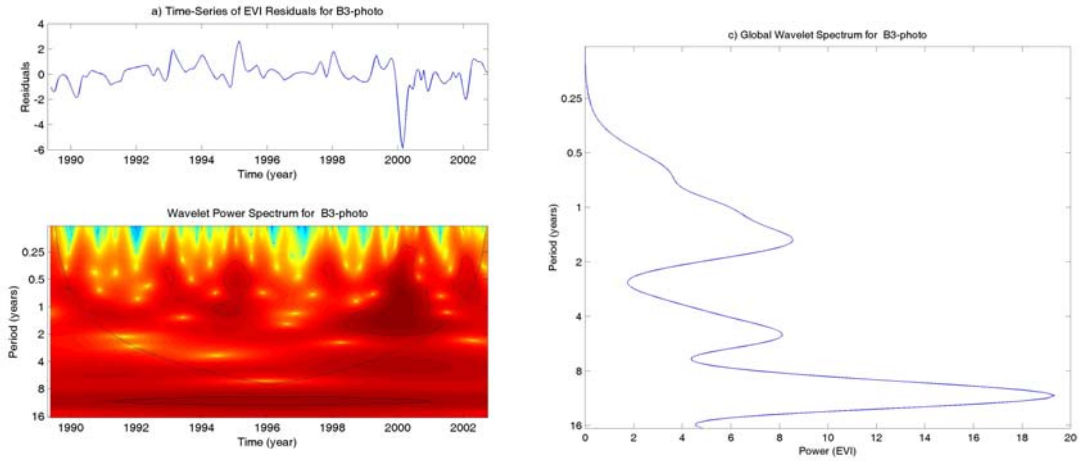

a) b)

Figure A.3-12. Burn 3-Photography a) Wavelet power spectrum b) Global Wavelet.

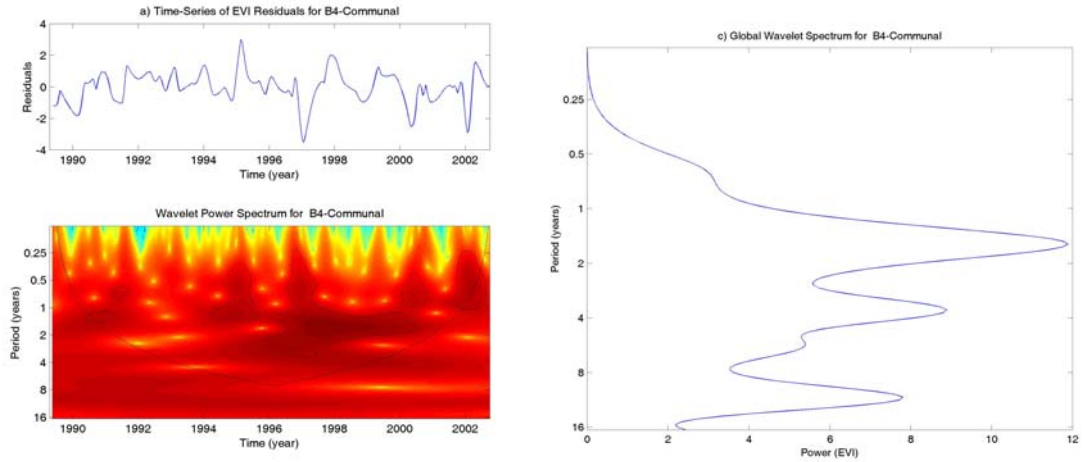

a) b)

Figure A.3-13. Burn 4-Communal a) Wavelet power spectrum b) Global Wavelet.

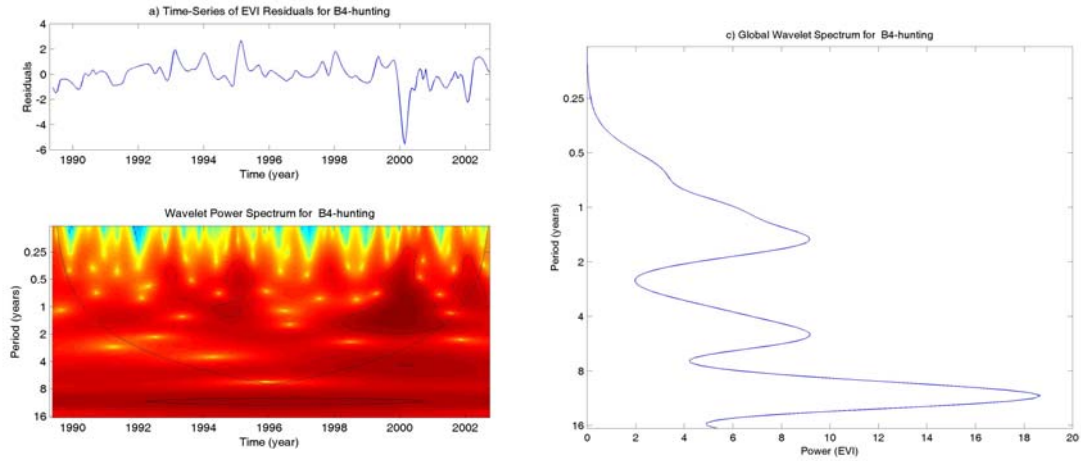

a) b)

Figure A.3-14. Burn 4-Hunting a) Wavelet power spectrum b) Global Wavelet.

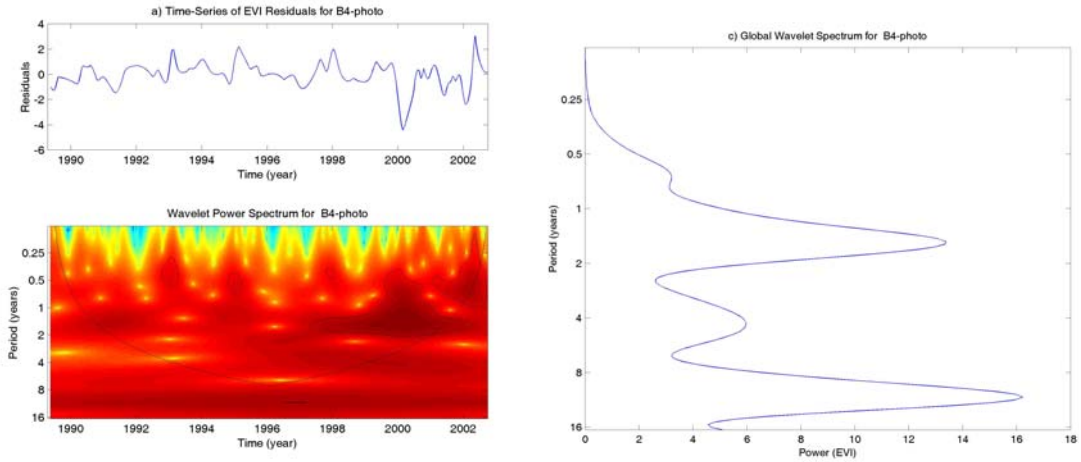

a) b)

Figure A.3-15. Burn 4-Photography a) Wavelet power spectrum b) Global Wavelet.

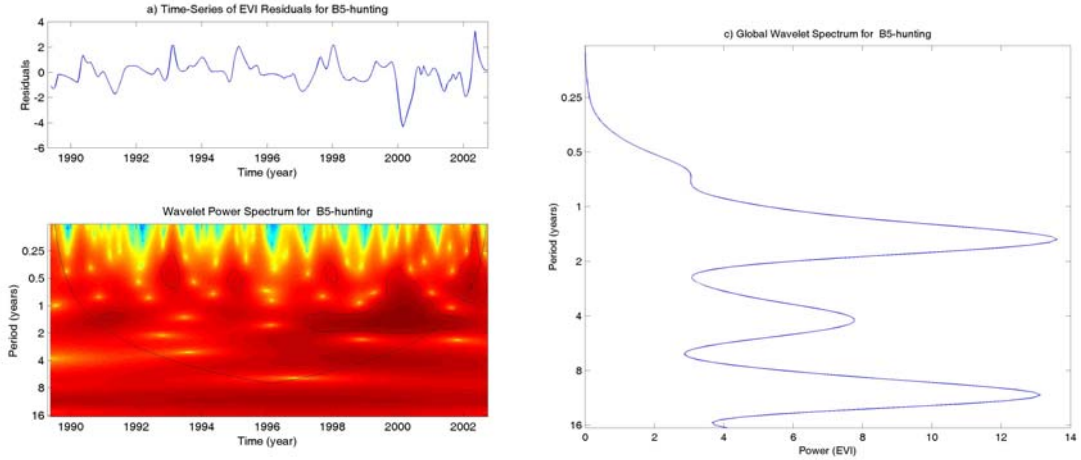

a) b)

Figure A.3-16. Burn 5-Hunting a) Wavelet power spectrum b) Global Wavelet.

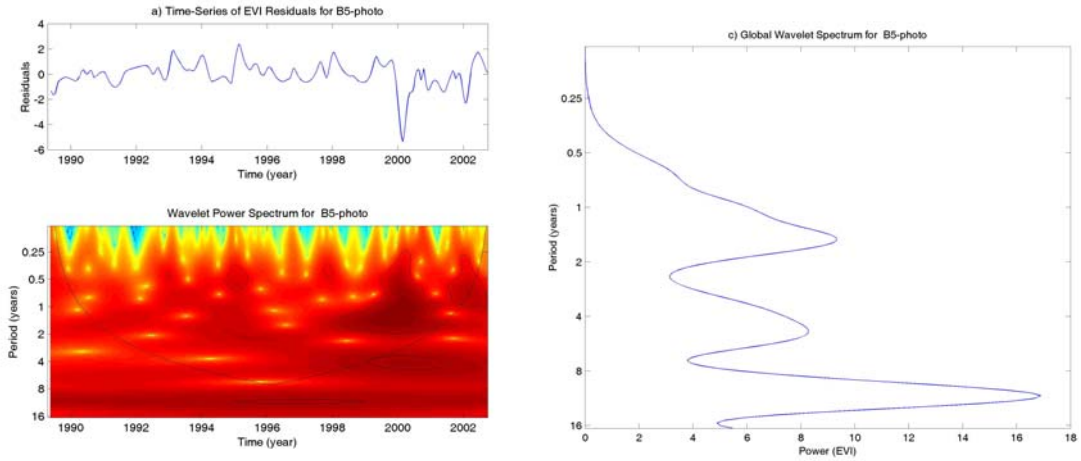

a) b)

Figure A.3-17. Burn 5-Photography a) Wavelet power spectrum b) Global Wavelet.

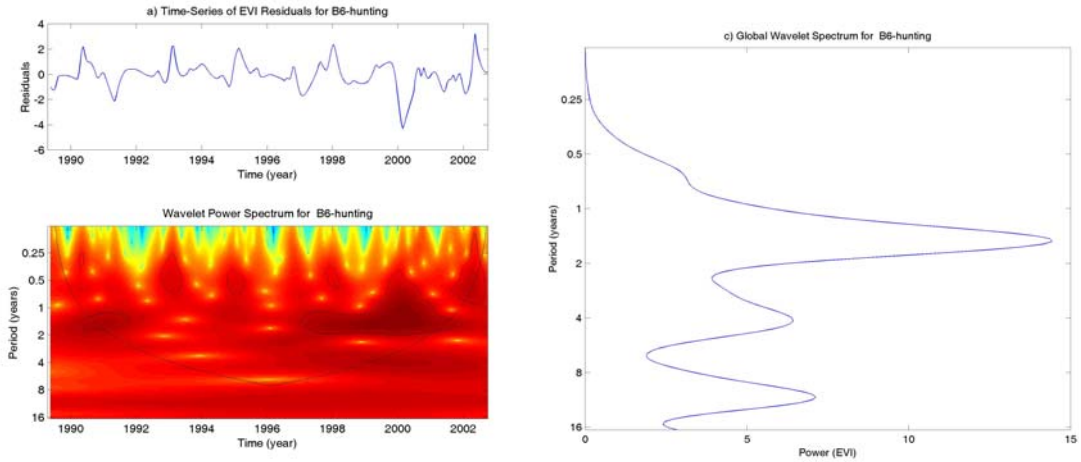

a) b)

Figure A.3-18. Burn 6-Hunting a) Wavelet power spectrum b) Global Wavelet.

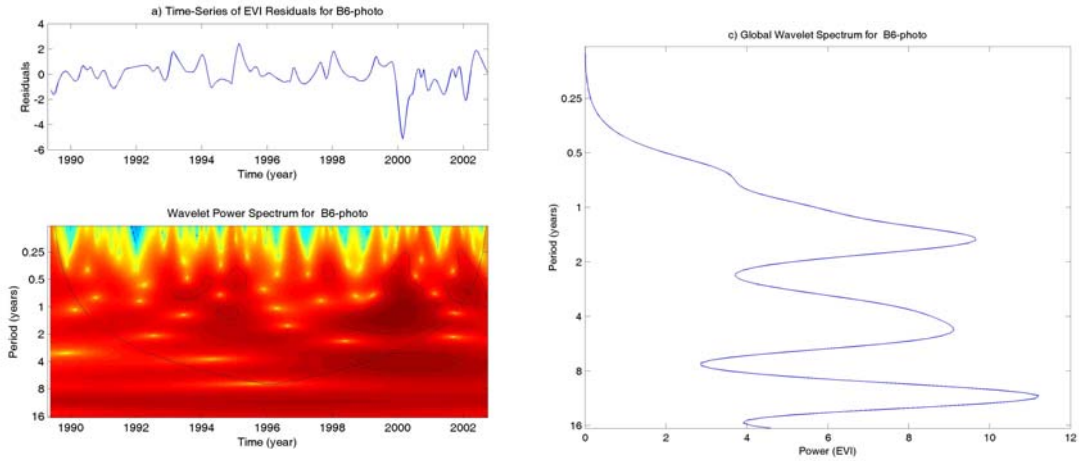

a) b)

Figure A.3-19. Burn 6-Photography a) Wavelet power spectrum b) Global Wavelet.

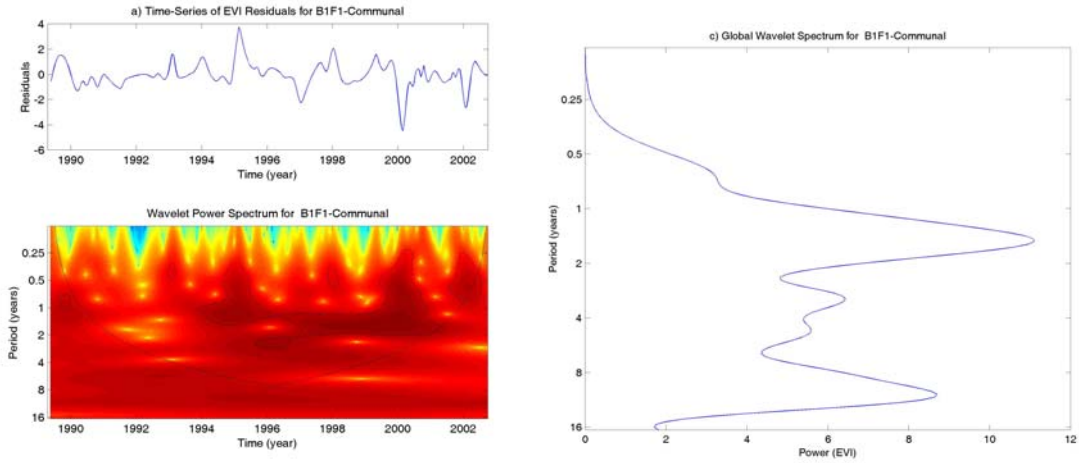

a) b)

Figure A.3-20. Burn 1 Flood 1-Communal a) Wavelet power spectrum b) Global Wavelet.

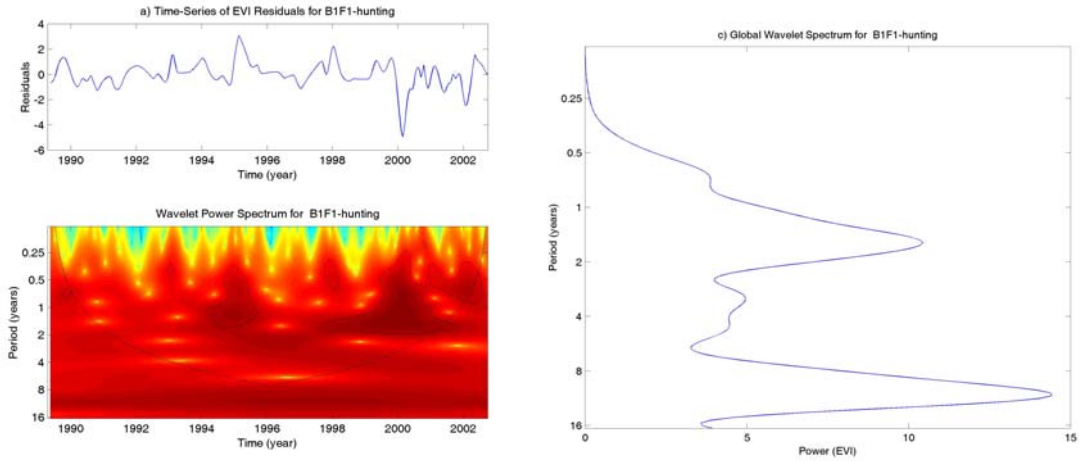

a) b)

Figure A.3-21. Burn 1 Flood 1-Hunting a) Wavelet power spectrum b) Global Wavelet.

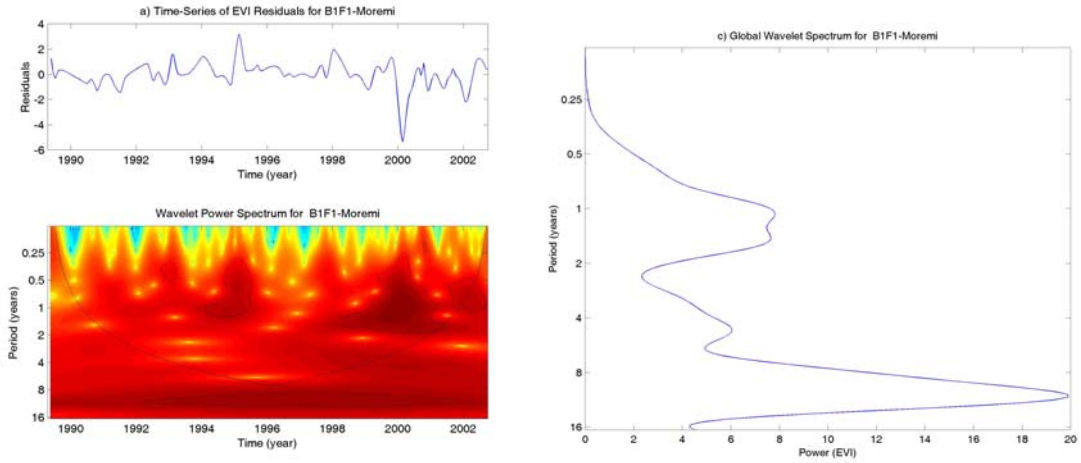

a) b)

Figure A.3-22. Burn 1 Flood 1-Moremi a) Wavelet power spectrum b) Global Wavelet.

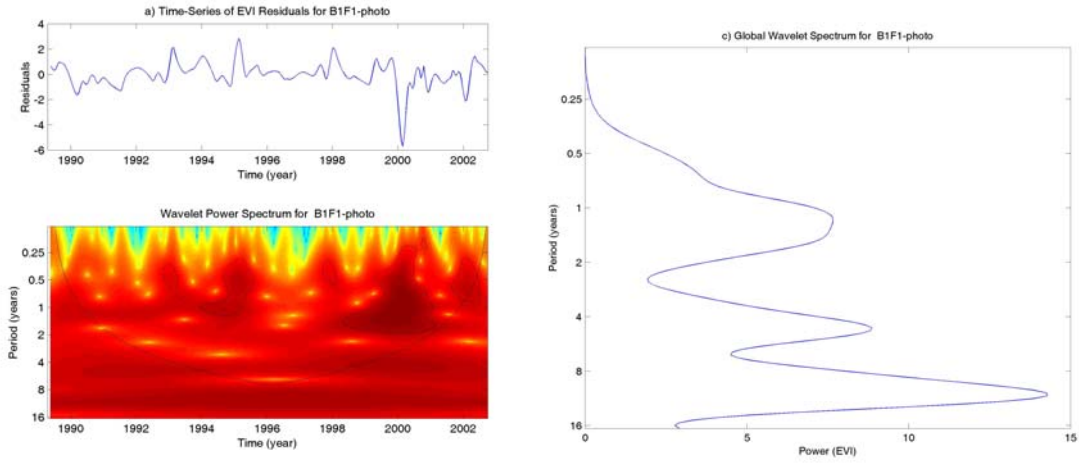

a) b)

Figure A.3-23. Burn 1 Flood 1-Photography a) Wavelet power spectrum b) Global Wavelet.

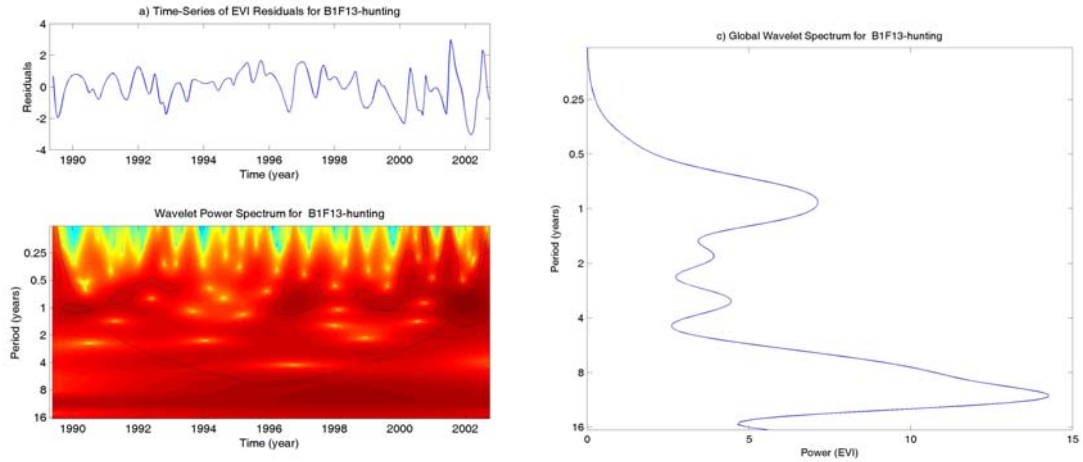

a) b)

Figure A.3-24. Burn 1 Flood 13-Hunting a) Wavelet power spectrum b) Global Wavelet.

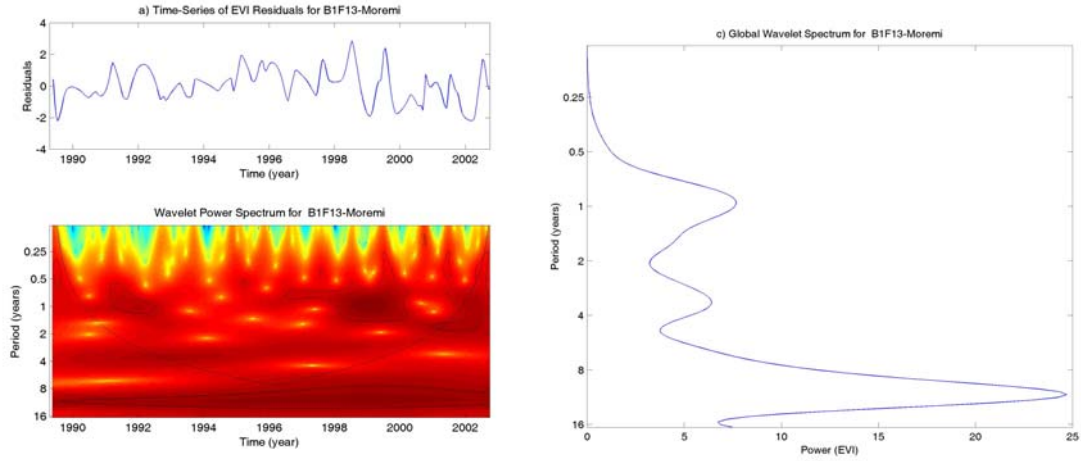

a) b)

Figure A.3-25. Burn 1 Flood 13-Moremi a) Wavelet power spectrum b) Global Wavelet.

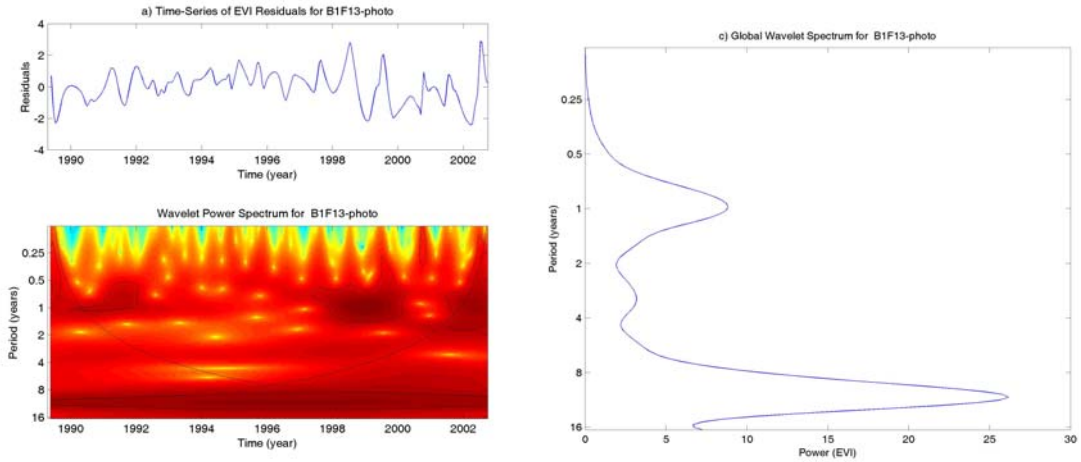

a) b)

Figure A.3-26. Burn 1 Flood 13-Photography a) Wavelet power spectrum b) Global Wavelet.

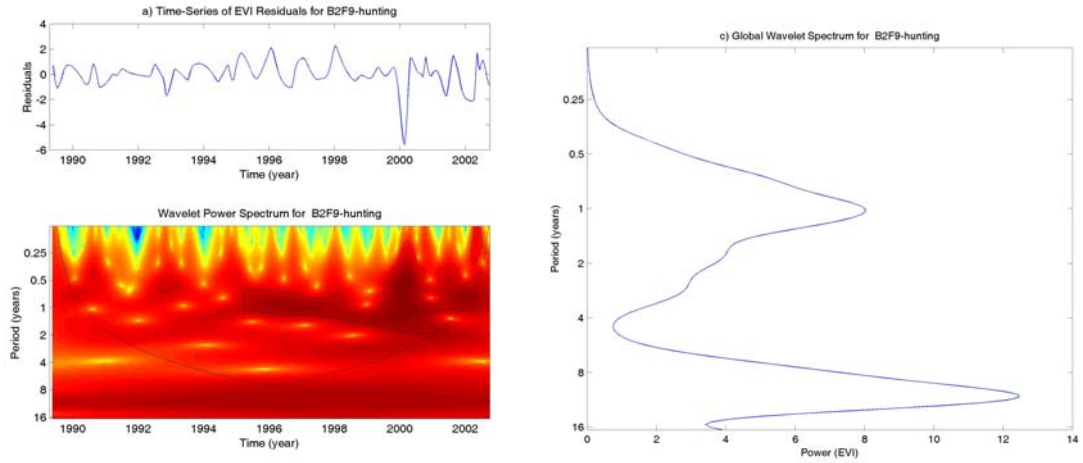

a) b)

Figure A.3-27. Burn 2 Flood 9-Hunting a) Wavelet power spectrum b) Global Wavelet.

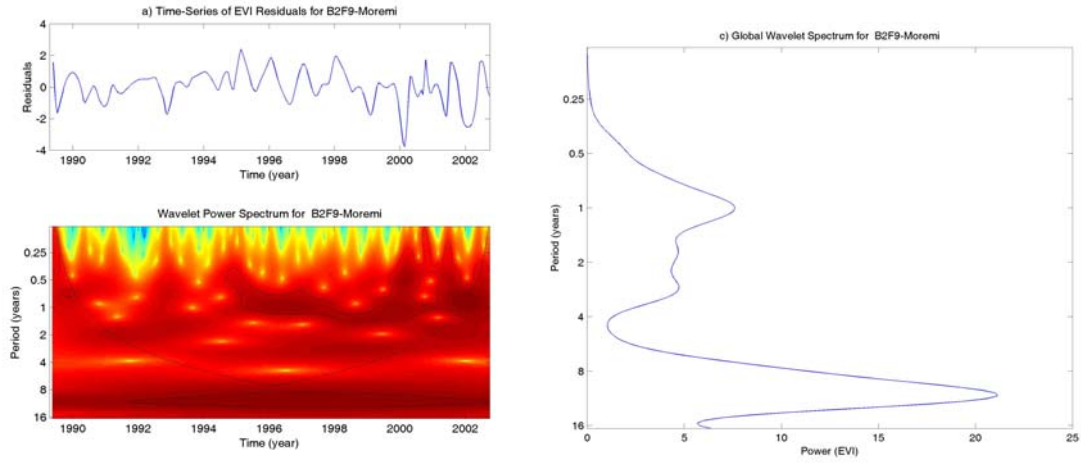

a) b)

Figure A.3-28. Burn 2 Flood 9 - Moremi a) Wavelet power spectrum b) Global Wavelet.

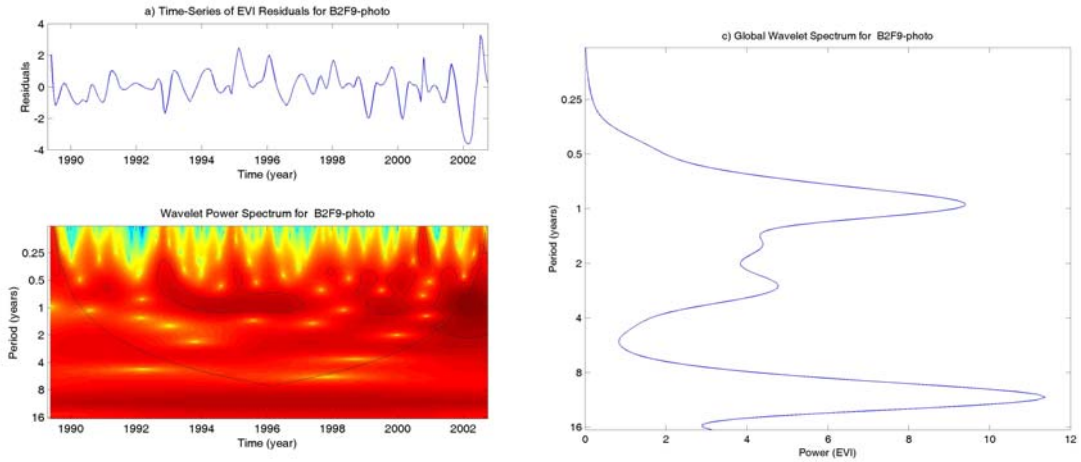

a) b)

Figure A.3-29. Burn 2 Flood 9-Photography a) Wavelet power spectrum b) Global Wavelet.

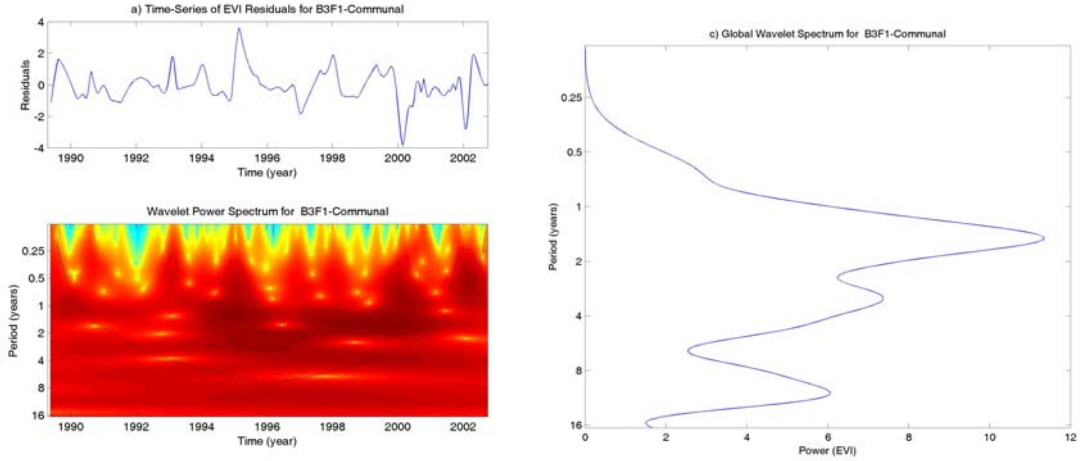

a) b)

Figure A.3-30. Burn 3 Flood 1 - Communal a) Wavelet power spectrum b) Global Wavelet.

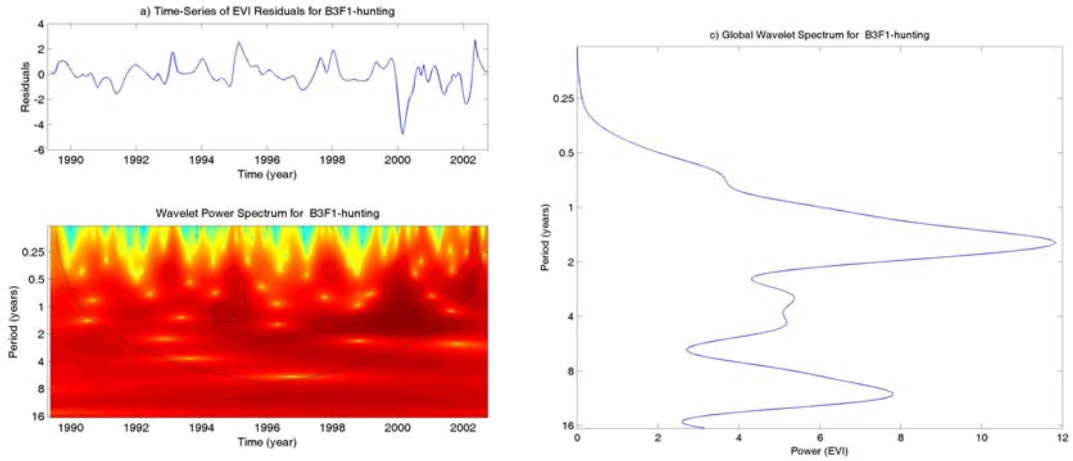

a) b)

Figure A.3-31. Burn 3 Flood 1 - Hunting a) Wavelet power spectrum b) Global Wavelet.

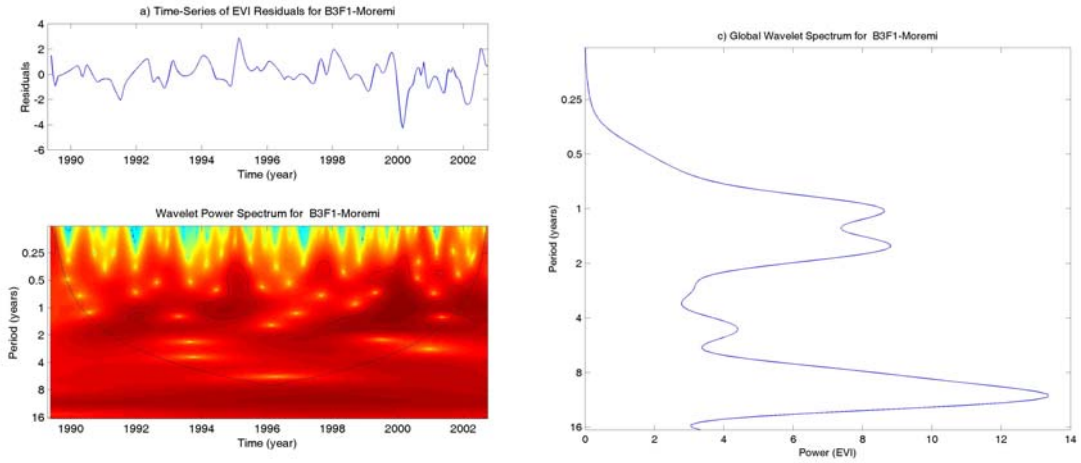

a) b)

Figure A.3-32. Burn 3 Flood 1 - Moremi a) Wavelet power spectrum b) Global Wavelet.

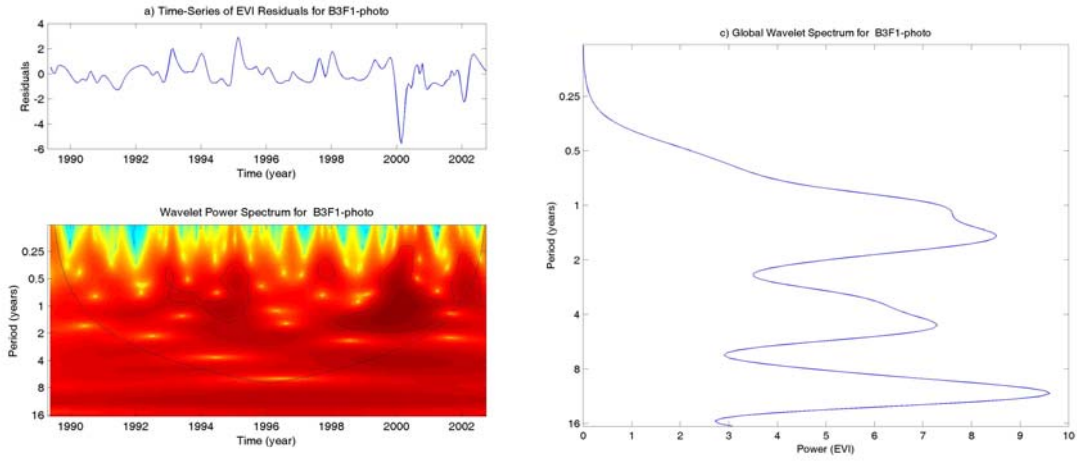

a) b)

Figure A.3-33. Burn 3 Flood 1 - Photography a) Wavelet power spectrum b) Global Wavelet.

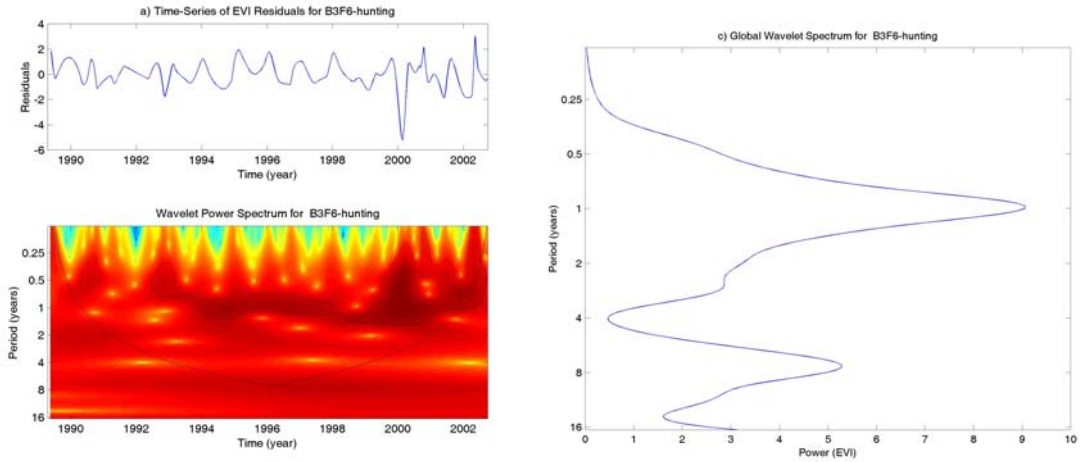

a) b)

Figure A.3-34. Burn 3 Flood 6 - Hunting a) Wavelet power spectrum b) Global Wavelet.

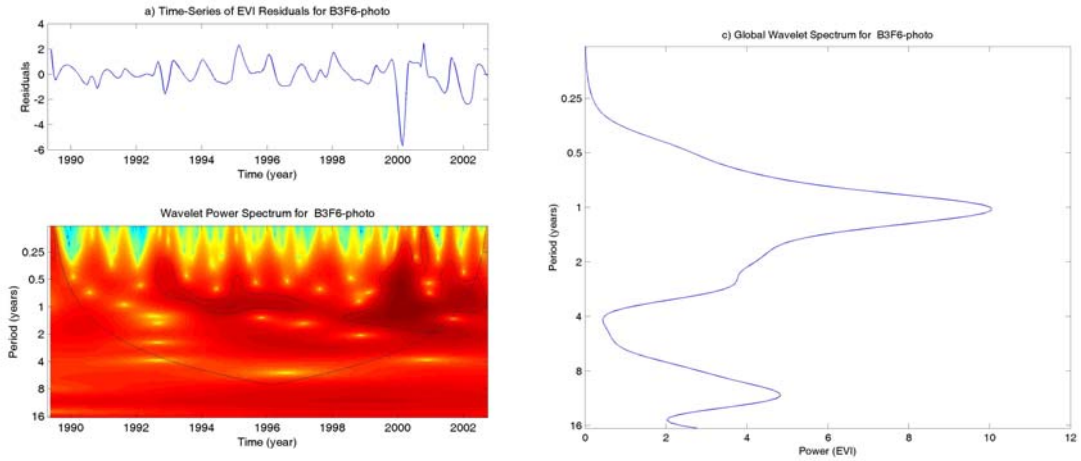

a) b)

Figure A.3-35. Burn 3 Flood 6 - Photography a) Wavelet power spectrum b) Global Wavelet.

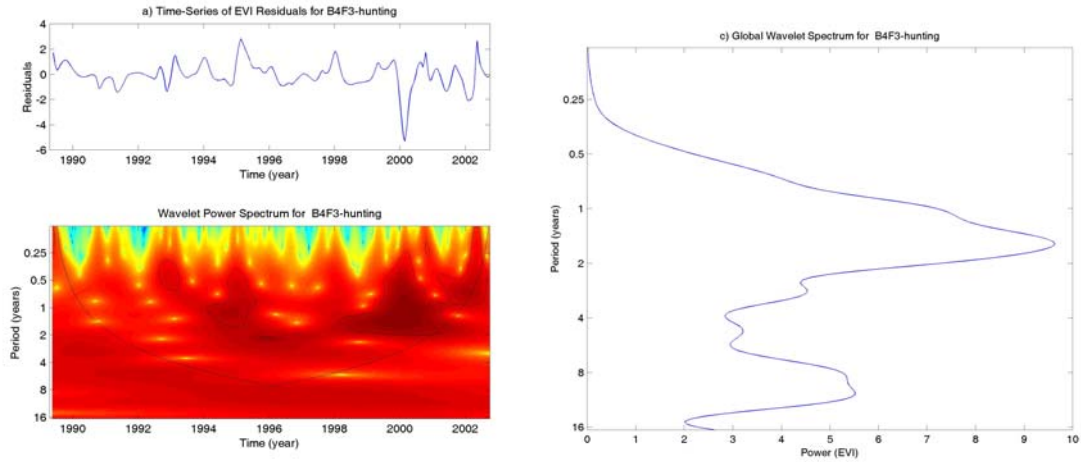

a) b)

Figure A.3-36. Burn 4 Flood 3 - Hunting a) Wavelet power spectrum b) Global Wavelet.

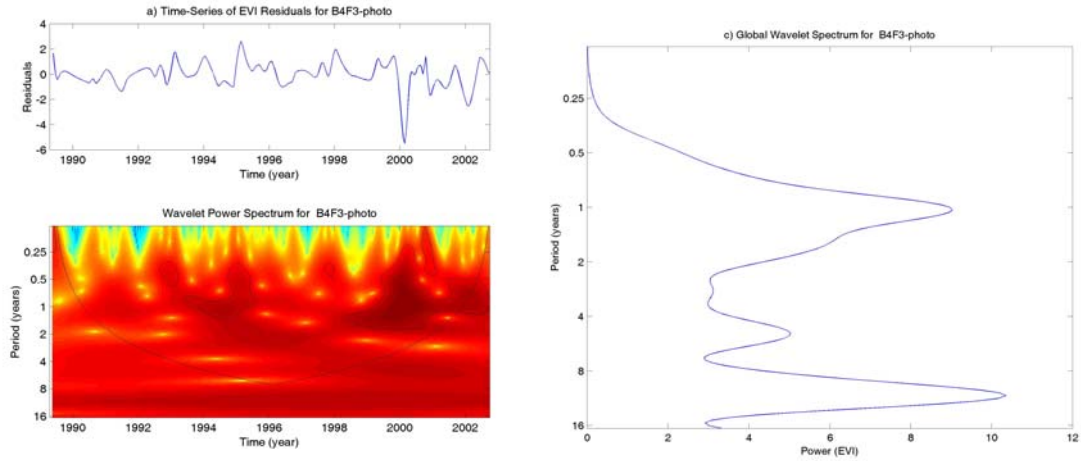

a) b)

Figure A.3-37. Burn 4 Flood 3 - Photography a) Wavelet power spectrum b) Global Wavelet.

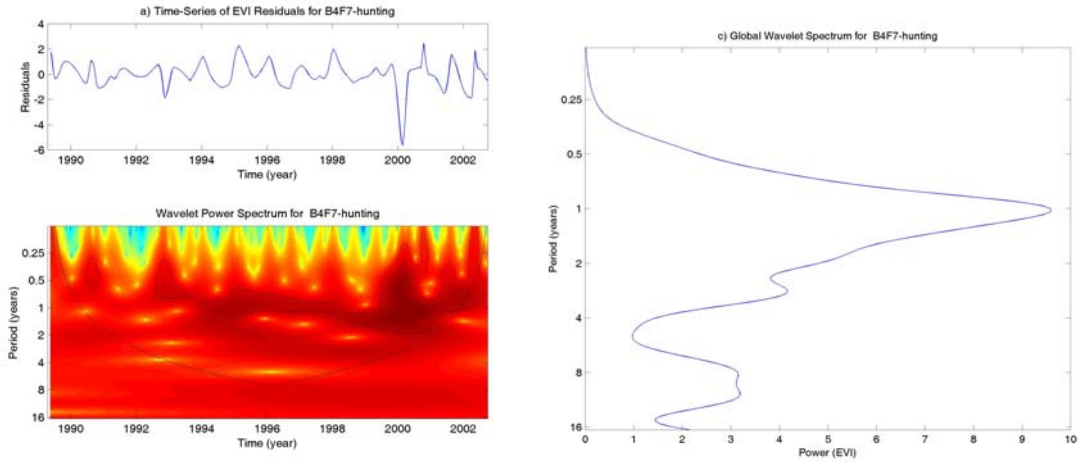

a) b)

Figure A.3-38. Burn 4 Flood 7 - Hunting a) Wavelet power spectrum b) Global Wavelet.

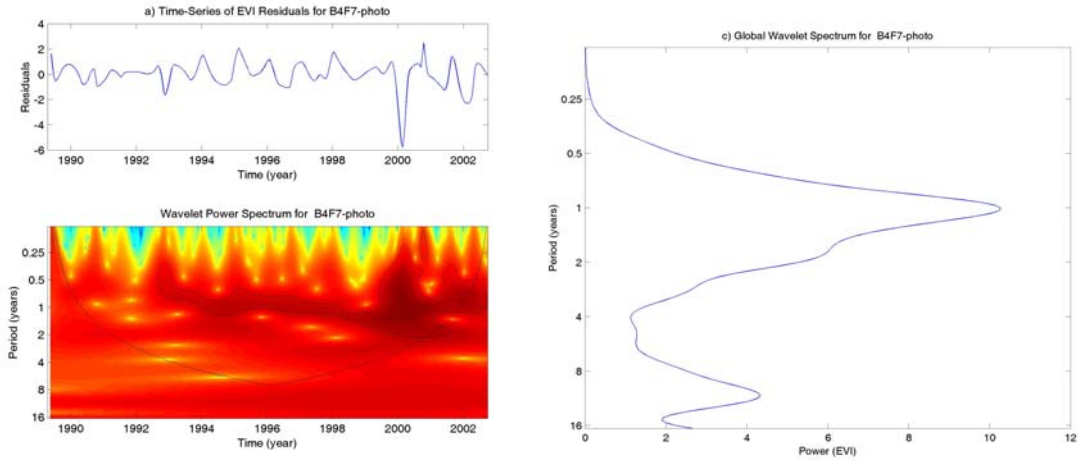

a) b)

Figure A.3-39. Burn 4 Flood 7 - Photography a) Wavelet power spectrum b) Global Wavelet.

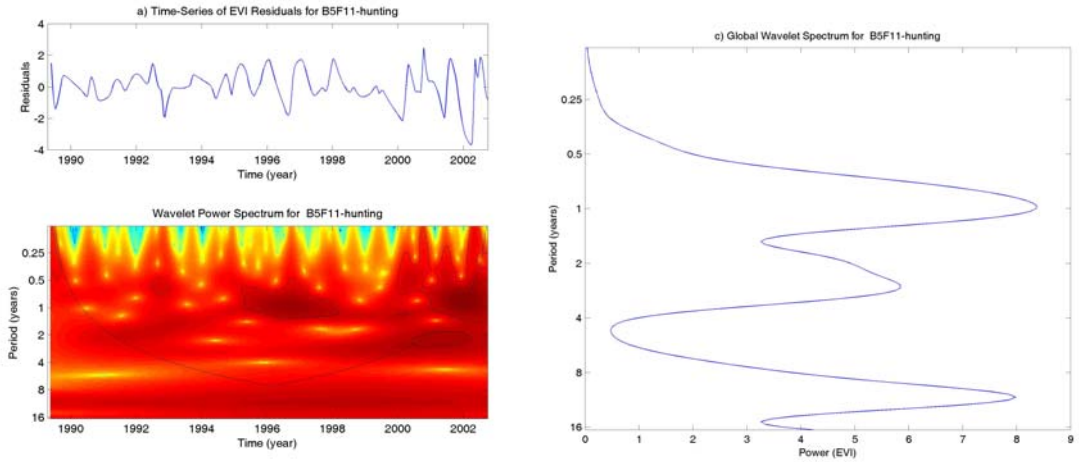

a) b)

Figure A.3-40. Burn 5 Flood 11 - Hunting a) Wavelet power spectrum b) Global Wavelet.

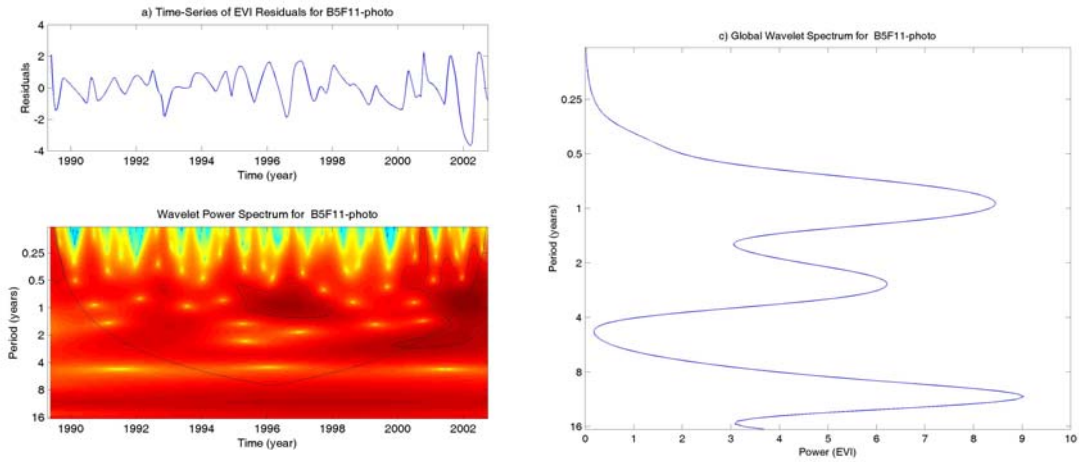

a) b)

Figure A.3-41. Burn 5 Flood 11 - Photography a) Wavelet power spectrum b) Global Wavelet.

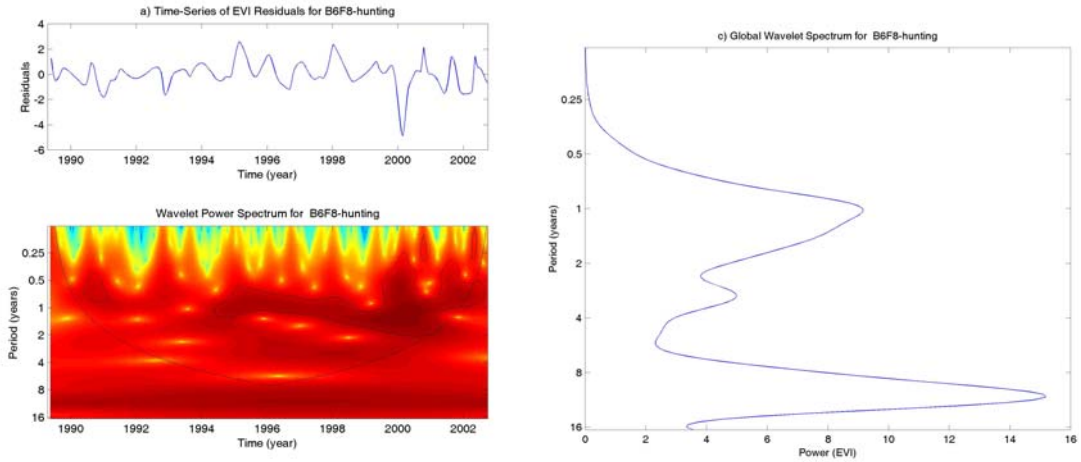

a) b)

Figure A.3-42. Burn 6 Flood 8 - Hunting a) Wavelet power spectrum b) Global Wavelet.

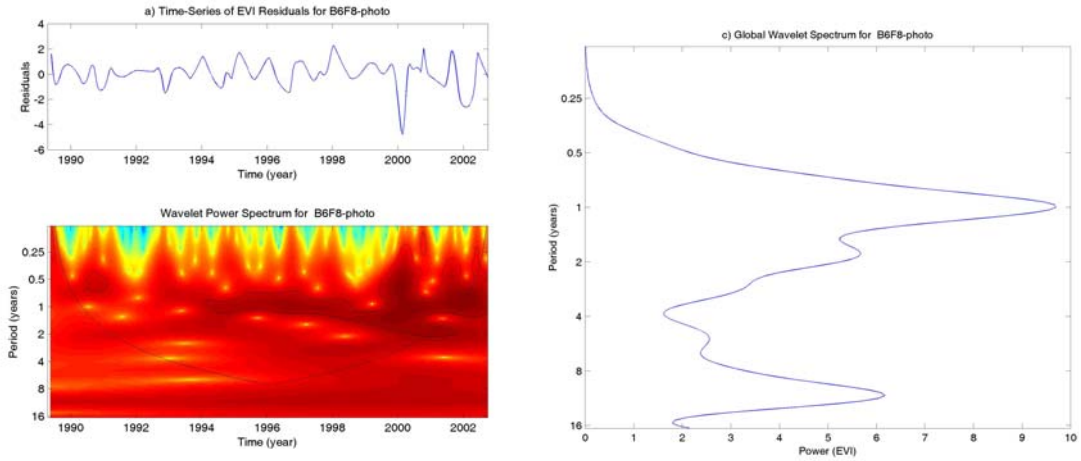

a) b)

Figure A.3-43. Burn 6 Flood 8 - Photography a) Wavelet power spectrum b) Global Wavelet.

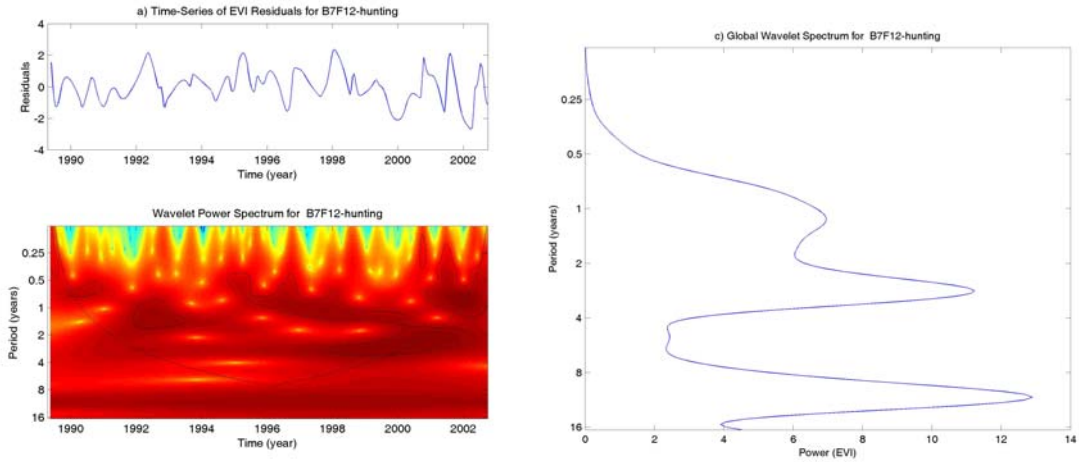

a) b)

Figure A.3-44. Burn 7 Flood 12 - Hunting a) Wavelet power spectrum b) Global Wavelet.

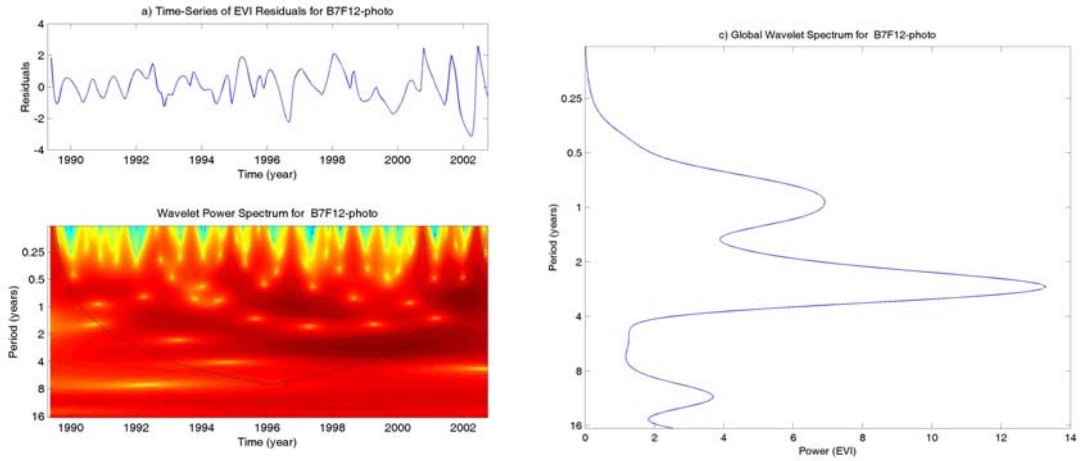

a) b)

Figure A.3-45. Burn 7 Flood 12 - Photography a) Wavelet power spectrum b) Global Wavelet.

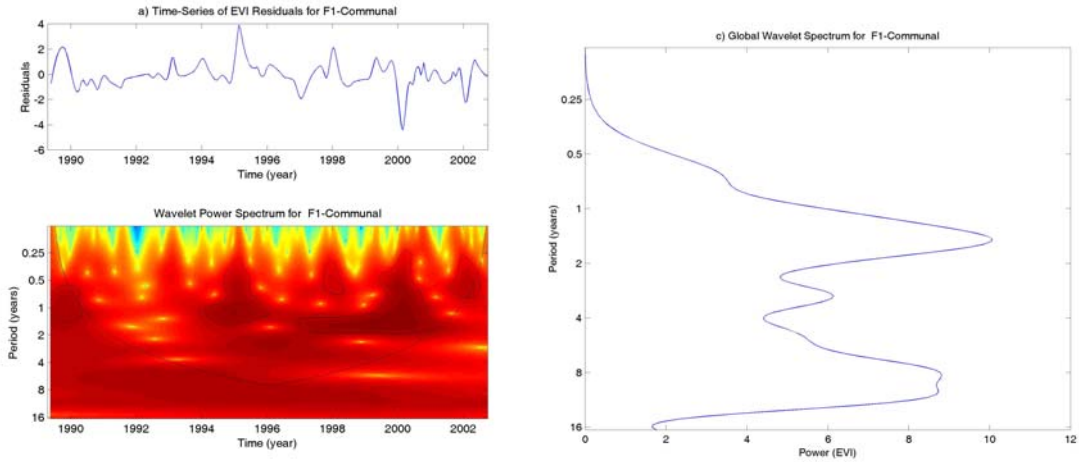

a) b)

Figure A.3-46. Flood1 - Communal a) Wavelet power spectrum b) Global Wavelet.

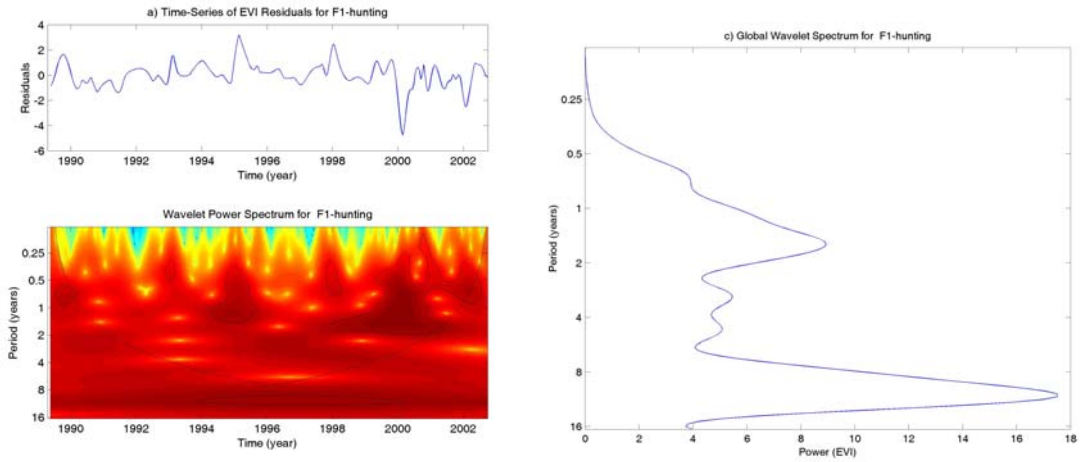

a) b)

Figure A.3-47. Flood1 – Hunting a) Wavelet power spectrum b) Global Wavelet.

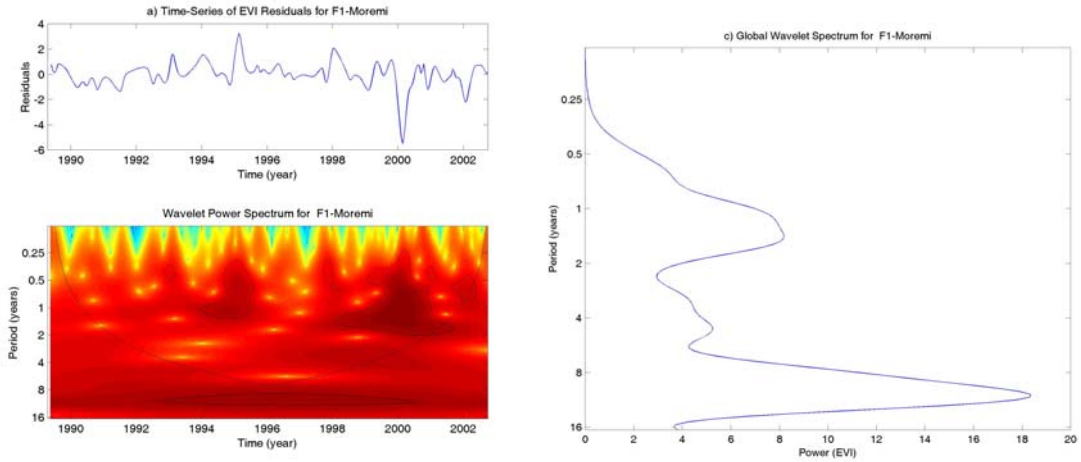

a) b)

Figure A.3-48. Flood1 - Moremi a) Wavelet power spectrum b) Global Wavelet.

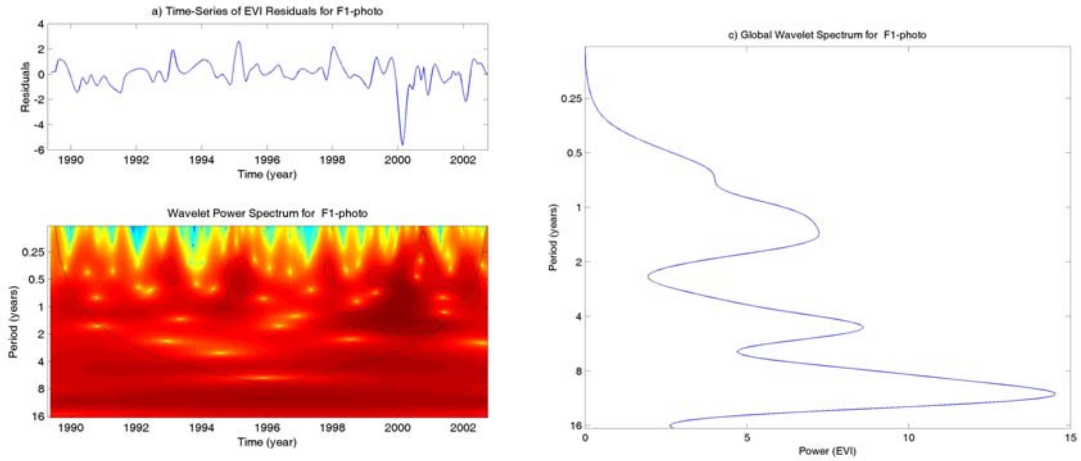

a) b)

Figure A.3-49. Flood1 - Photography a) Wavelet power spectrum b) Global Wavelet.

REFERENCES

Adger, W.N., 2000. Social and ecological resilience: are they related. *Progress in Human Geography*, 24(3): 347-364.

Adler, P.B., Raff, D.A. and Lauenroth, W.K., 2001. The effect of grazing on the spatial heterogeneity of vegetation. *Oecologia*, 128: 465-479.

Aguiar, M.R. and Sala, O.E., 1999. Patch structure, dynamics and implications for the functioning in arid ecosystems. *Trends in Ecology & Evolution*, 14(7): 273-277.

Albertson, A., 1998. Northern Botswana Veterinary Fences: critical ecological impacts. (http: //www.stud.ntnu.no/~skjetnep/owls/fences/index.html#buffalo)

Allan, J.D., 2004. Landscapes and riverscapes: the influence of land use on stream ecosystems. *Annual Review of Ecology, Evolution, and Systematics,* 35:257-284.

Allen, C.R., Gunderson, L., and Johnson, A.R., 2005. The use of discontinuities and functional groups to assess relative resilience in complex systems. *Ecosystems*, 8:958-966.

Alpin, P., 2006. On scales and dynamics in observing the environment. *International Journal of Remote Sensing*, 27(11): 2123-2140.

Andersson, J., 2006. Land cover change in the Okavango River Basin: Historical changes during the Angolan civil war, contributing causes and effects on water quality. Master's Thesis, Dept. of Water and Environmental Studies, Linkoping University.

Andersson, L., Wilk, J., Todd, M.C., Hughes, D.A., Earle, A., Kniveton, D., Layberry, R., and Savenije, H., 2006. Impact of climate change and development scenarios on flow patterns in the Okavango River. *Journal of Hydrology*; 331: 43-57.

Andersson, L., Gumbricht, T., Hughes, D., Kniveton, D., Ringrose, S., Savenije, H., Todd, M., Wilk, J., and P. Wolski, 2003. Water flow dynamics in the Okavango River Basin and Delta – a prerequisite for the ecosystems of the Delta. *Physics and Chemistry of the Earth*, 28:1165-1172.

Anderies, J.M., Ryan, P, and Walker, B.H., 2006. Loss of resilience, crisis, and institutional change: lessons from an intensive agricultural system in Southeastern Australia. *Ecosystems*, 9: 865-878.

Andres, L., Salas, W.A., and Skole, D.L., 1994. Fourier analysis of multi-temporal AVHRR data applied to a land cover classification. *International Journal of Remote Sensing*, 15: 1115-1121.

Arnell, N., Bates, B., Lang, H., Magnuson, JJ. And Mulholland, P., 1996. Hydrology and freshwater ecology. Cambridge University Press.

Ashton, P. and Neal, M., 2003. An Overview of key strategic issues in the Okavango Basin. In Turton, A., Ashton, P., and Cloete T.(eds). Transboundary rivers, sovereignty and development: Hydropolitical drivers in the Okavango River Basin. Pretoria and Geneva: AWIRU and Green Cross International.

Ashton, P., 2003, International Water in Southern Africa: water resources management and policy. M. Nakayama (editor), United Nations University Press, New York.

Asner, G.P., Elmore, A.J., Olander, L.P., Martin, R.E., and Harris, A.T., 2004. Grazing systems, ecosystem responses, and global change. *Annual Review of Environmental Resources*, 29:261-299.

Asrar, G., Myneni, R.B., and Choudhury, B.J., 1992. Spatial heterogeneity in vegetation canopies and remote sensing of absorbed photosynthetically active radiation. A modeling study. *Remote Sensing of Environment*, 41(2): 85-103.

Azzali, S. and Menenti, M., 2000. Mapping vegetation-soil-climate complexes in southern Africa using temporal Fourier analysis of NOAA-AVHRR NDVI data. *International Journal of Remote Sensing*, 21: 973-996.

Baidya Roy, S., 2006. Vegetation-Precipitation feedback in Rondonia. *EOS Transactions to American Geophysical Union*, 87.

Balling, R.C., 2005. Interactions of desertification and climate in Africa. In Low, P.S. (ed) Climate change and Africa. Cambridge University Press.

Barbier, E.B., 1994. Valuing environmental functions: tropical wetlands. *Land Economics*, 70(2): 155-173.

Barnes, M.E., 2001. Effects of large herbivores and fire on the regeneration of Acacia erioloba woodlands in Chobe National Park, Botswana. *African Journal of Ecology*, 39(4): 340-350.

Barnsley, M.J., Hobson, P.D., Hyman, A.H., Lucht, W., Muller, J-P, and Strahler, A.H., 1997. Characterizing the spatial variability of broadband albedo in a semidesert environment for MODIS validation. *Remote Sensing of Environment*, 74: 58-68.

Barnston, A.G. and Ropelewski, C.F., 1992. Prediction of ENSO episodes using canonical correlation analysis. *J. Climate*, 5(11): 1316-1345.

Bauer, P., Gumbricht, T. and Kinzelbach, W., 2006. A regional coupled surface water/groundwater model of the Okavango Delta, Botswana. Water Resources Research, 42, 15pg., doi:10.1029/2005WR004234.

Bauer P., Thabeng, G., Stauffer, F., and Kindzelbach, W., 2004. Estimation of the evapotranspiration rate from diurnal groundwater fluctuations in the Okavango Delta, Botswana. *Journal of Hydrology*, 288:344-355.

Bauer, P., Gumbricht, T. and Kinzelbach, W., 2002. Hydrological modelling and resource management in the Okavango Delta. Unpublished manuscript.

Baxter, P. and Getz, W., 2005. A model-framed evaluation of elephant effects on tree and fire dynamics in African savannas. *Ecological Applications*, 15(4): 1331-1341.

Bayley, P.B., 1995. Understanding large river floodplain ecosystems. Bioscience; 45(3):

Beckage, B. and Stout, I.J., 2000. Effects of repeated burning on species richness in a Florida pine savanna: a test of the intermediate disturbance hypothesis. *J. of Vegetation Science*, 11(1): 113-122.

Bengtsson, J., Angelstam, P., Elmqvist, T., Emanuelsson, U., Folke, C., Ihse, M., Moberg, F., and Nystrom, M., 2003. Reserves, resilience, and dynamic landscapes. *Ambio*, 32(6): 389-396.

Bennett, E.M., Cumming, G.S., and Peterson, G.D., 2005. A systems model approach to determining resilience surrogates for case studies. *Ecosystems*, 8:945 – 957.

Ben-Shahar, R., 1998. Changes in structure of savanna woodlands in northern Botswana following the impacts of elephants and fire. *Plant Ecology*, 136:189-194.

Ben-Shahar, R., 1996. Do elephants over-utilize mopane woodlands in northern Botswana. *Journal of Tropical Ecology*, 12: 505-515.

Bernard, T. and Moetapele, N., 2005. Desiccation of the Gomoti River: Biophysical process and indigeneous resource management in Northern Botswana. *Journal of Arid Environments*, 63:256-283.

Berryman, A. and Turchin, P., 2001. Identifying the density-dependent structure underlying ecological time series. *Oikos*, 92: 265-270.

Berryman, A., 1992. On choosing models for describing and analyzing ecological time-series. *Ecology*, 73(2): 694-698.

Bird, M.I. and J.A. Cali, 1998. A million-year record of fire in sub-Saharan Africa. *Nature*, 394:767-769.

Blackmore, A.C., Mentis, M.T., and Scholes, R.J., 1990. The origin and extent of nutrient-enriched patches within a nutrient-poor savanna in South Africa. *J. Biogeography*, 17: 463-470.

Bolaane, M., 2005. Chiefs, hunters and adventurers: the foundation of the Okavango/Moremi National Park, Botswana. Journal of Historical Geography, 31: 241-259.

Bolton, C., 1998. Healing knowledge and cultural practices in a modern Tswana village. Master's Thesis. Dept of Anthropology and Environmental Studies, Williams College, Williamstown Massachusetts.

Bonan, G.B., Levis, S., Sitch, S., Vertenstein, M., and Oleson, K., 2003, A dynamic global vegetation model for use with climate models: concepts and description of simulated vegetation dynamics. *Global Change Biology*, 9:1542-1566.

Bond, W.J. and Keeley, J.E., 2005. Fire as a global 'herbivore': the ecology and evolution of flammable ecosystems. *Trends in Ecology and Evolution*, 20(7): 387-394.

Bond, W.J., Woodward, F.I., and Midgley, G.F., 2005. The global distribution of ecosystems in a world without fire. *New Phytologist*, 165: 525-538.

Bond, W.J., Midgley, G.F., and Woodward, F.I., 2003a. The importance of low atmospheric CO2 and fire in promoting the spread of grasslands and savannas. *Global Change Biology*, 9: 973-982.

Bond, W.J., Midgley, G.F., and Woodward, F.I., 2003b. What controls South African vegetation – climate or fire? *South African Journal of Botany*, 69(1):79-91.

Bond, W.J. and van Wilgen, B.W., 1996. Fire and Plants. Chapman and Hall, New York.

Bonyongo, M.C. and Mubyana, T., 2004. Soil nutrient status in vegetation communities of the Okavango Delta floodplains. *South African Journal of Science*, 100: 337-340

Bonyongo, M.C., Bredenkamp, G.J., and Veenendaal, E., 2000. Floodplain vegetation in the Nxaraga lagoon area, Okavango Delta, Botswana. *South African Journal of Botany*, 66(1):15-21.
Boone, R.B. and Hobbs, N.T., 2004. Lines around fragments: effects of fencing on large herbivores. *African Journal of Range and Forage Science*, 21(3): 147-158.
Borak, J.S., Lambin, E.F., and Strahler, A.H., 2000. The use of temporal metrics for land cover change detection at coarse spatial scales. *International Journal of Remote Sensing*, 21: 1415-1432.
Bradley, B.A., Jacob, R.W., Hermance, J.F., and Mustard, J.F., 2007. A curve fitting procedure to derive interannual phenologies from time series of noisy satellite NDVI data. *Remote Sensing of Environment*; 106(2): 137-145.
Bradley, B.A. and Mustard, J.F., 2005. Identifying land cover variability distinct from land cover change: Cheatgrass in the great basin. *Remote Sensing of Environment*, 94: 204-213.
Brain, C.K. and A. Sillent, 1988. Evidence from the Swartkrans cave for the earliest use of fire. *Nature*, 336:464-466.
Braswell, B.H., Schimel, D.S., Linder, E., and Moore III, B., 1997. The response of global terrestrial ecosystems to interannual temperature variability. *Science*, 278: 870-873.
Briske, D.D., Fuhlendorf, S.D., and Smeins, F.E., 2003. Vegetation dynamics on rangelands: a critique of the current paradigms. *J. of Applied Ecology*; 40: 601-614.
Broge, N.H. and Mortensen, J.V. ,2000. Comparing prediction power and stability of broadband and hyperspectral vegetation indices for estimation of green leaf area index and canopy chlorophyll density. *Remote Sensing of Environment* 76: 156-172.
Brown, T.J., Hall, B.L., and Westerling, A.L., 2004. The impact of twenty-first century clmate change on wildland fire danger in the western US. *Climate Change*, 62(1-3): 365-388.
Bunn, S.E. and Arthington, A.H., 2002. Basic principles and ecological consequences of altered flow regimes for aquatic biodiversity. *Environmental Management*, 30(4): 492-507.
Butzer, K.W., 1984. Archeogeology and quaternary environment in the interior of southern Africa. In Klein, R.G. and Balkema, A.A. (eds) Southern African Prehistory and paleoenvironments.
Cairns, J., 2000. Setting ecological restoration goals for technical feasibility and scientific validity. *Ecological Engineerin*g, 15: 171-180.
Camill, P. and Clark, J.S., 2000. Long-term perspectives on lagged ecosystem responses to climate change: permafrost in Boreal peatlands and the grassland/woodland boundary. *Ecosystems,* 3: 534-544.
Campbell, B.M., Gordon, I.J., Luckert, M.K., Petheram, L., and Vetter, S., 2006. In search of optimal stocking regimes in semi-arid grazing lands: one size does not fit all. *Ecological Economics*, 60: 75-85.
Canty, M.J., Nielsen, A.A., and Schmidt, M., 2004. Automatic radiometric normalization of multi-temporal satellite imagery. *Remote Sensing of Environment*, 91(3/4): 441.
Capon, S.J., 2005. Flood variability and spatial variations in plant community composition and structure on a large arid floodplain. *Journal of Arid Environments*, 60:283-302.
Carpenter, S. and Brock, W.A., 2006. Rising variance: a leading indicator of ecological transition. *Ecology Letters*, 9:311-318.
Carpenter, S., Walker, B., Anderies, J.M. and Abel, N., 2001. From metaphor to measurement: Resilience of what to what? *Ecosystems*, 4: 765-781.
Casanova, M.T. and Brock, M.A., 2000, How do depth, duration and frequency of flooding influence the establishment of wetland plant communities? *Plant Ecology*, 147: 237-250.
Cassidy, L. 2000. CBNRM and Legal rights to resources in Botswana. IUCN, Occasional Paper No. 4., 34 pg.
Caylor, K.K., Dowty, P.R., Shugart, H.H., and Ringrose, S., 2004. Relationship between small-scale structural variability and simulated vegetation productivity across a regional moisture gradient in southern Africa. *Global Change Biology*, 10(3): 374-382.
Chaneton, E.J. and Facelli, J.M., 1991. Disturbance effects on plant community diversity: spatial scales and dominance hierarchies. *Plant Ecology*, 93(2): 143-155.
Chapin, F.S., Matson, P.A., and Mooney, H.A. 2002. Principles of Terrestrial Ecology. Springer.
Chapin, F.S., Walker, B.H., Hobbs, R.J., Hooper, D.U., Lawton, J.H., Sala, O.E., and Tilman, D., 1997. Biotic control over the functioning of ecosystems. *Science*, 277(5325): 500-504.

Chavez, P., and MacKinnon, D. J., 1994. Automatic detection of vegetation changes in the southwestern United States using remotely sensed images. *Photogrammetric Engineering and Remote Sensing,* 60(5), 567-585.

Chavez, P.S., 1988. An improved dark-object subtraction technique for atmospheric scattering of multispectral data. *Remote Sensing of Environment,* 24(3):459-479.

Chen, X., Vierling, L., and Deering, D., 2005. A simple and effective radiometric correction method to improve landscape change detection across sensors and across time. *Remote Sensing of Environment*, 98: 63-79.

Cheng, Y-B, Zarco-Tejada, P.J., Riano, D., Rueda, C.A, and Ustin, S., 2006. Estimating vegetation water content with hyperspectral data for different canopy scenarios between AVIRIS and MODIS indexes. *Remote Sensing of Environment*, 105(4): 354-366.

Chipps, S.R., Hubbard, D.E., Werlin, K.B., Haugerud, N.J., Powell, K.A.,Thompson, J., and Johnson, T., 2006. Association between wetland disturbance and biological attributes in floodplain wetlands. *Wetlands*, 26(2): 497-508.

Choudhury, B.J., 1987. Relationships between vegetation indices, radiation absorption, and net photosynthesis evaluated by a sensitivity analysis. *Remote Sensing of Environment*, 22: 209-233.

Clark, D.L., and Wilson, M.V., 2001. Fire, mowing, and hand-removal of woody species in restoring a native wetland prairie in the Willamette Valley of Oregon. *Wetlands*, 21(1): 135-144.

Clark, J.S., 1996. Testing disturbance theory with long-term data: alternative life-history solutions to the distribution of events. *The American Naturalist*, 148(6): 976-996.

Clifford, B., 1929. A journey by motor lorry from Mahalapye through the Kalahari desert. *Geographical Journal*, 73(4): 342-358.

Cohen, W.B. and Goward, S.N., 2004. Landsat's role in ecological applications of remote sensing. *Bioscience*, 54(6): 535-545.

Collins, S.L., Glenn, S.M., 1997. Effects of organismal and distance scaling on analysis of species distribution and abundance. *Ecological Applications*, 7(2): 543-551.

Collins, S.L., Glenn, S.M. and Gibson, D.J., 1995. Experimental analysis of intermediate disturbance and initial floristic composition: decoupling cause and effect. *Ecology*, 76(2): 486-492.

Collins, S.L., 1992. Fire frequency and community heterogeneity in tallgrass prairie vegetation. *Ecology*, 73: 2001-2006.

Collin, S.L., 1987. Interaction of disturbances in tallgrass prairie: A field experiment. *Ecology*, 68(5): 1243-1250.

Connell, J.H., 1978. Diversity in tropical forest and coral reefs. *Science*, 199: 1302-1310.

Coppin, P., Jonckheere, I., Nackaerts, K., Muys, B., and Lambin, E., 2004. Digital change detection methods in ecosystem monitoring: a review. *International Journal of Remote Sensing*, 25(9):1565-1596.

Coppin, P. and Bauer, M., 1996. Digital change detection in forest ecosystems with remote sensing imagery. Remote Sensing Reviews, 13(3/4):207-234.

Corbin, J.D. and D'Antonio, C.M., 2004. Competition between native perennial grasses: implications for an historical invasion. Ecology, 85(5): 1273-1283.

Costanza, R., 1999. Ecological sustainability, indicators, and climate change. International Proceedings on Climate Change.

Cowling, R.M., Richardson, D.M., and Pierce, S.M. (eds.). 1997. Vegetation of Southern Africa. Cambridge University Press, Cambridge, UK.

Cox, P.M., Betts, R.A., Jones, C.D., Spall, S.A., Totterdell, I.J., 2000. Acceleration of global warming due to carbon-cycle feedbacks in a coupled climate model. *Nature*, 408: 184-187.

Cramer, W., Bondeau, A., Woodward, F.I., Prentice, C., Betts, R.A., Brovkin, V., Cox, P.M., Fisher, V., Foley, J.A., Friend, A.D., Kucharik, C., Lomas, M.R., Ramankutty, N., Sitch, S., Smith, B., White, A., and Young-Molling, C., 2001. Global response of terrestrial ecosystem structure and function to CO2 and climate change: results from six dynamic global vegetation models. *Global Change Biology*, 7(4): 357-373.

Crawford, M.M., S. Kumar, M.R. Ricard, J.C. Gibeaut, and A.L. Neuenschwander, 1999. Fusion of airborne polarimetric and interferometric SAR data for classification of coastal environments. *IEEE Trans. Geosci. Rem. Sens*., 37:1306-1315.

Crews-Meyer, K.A., 2006. Temporal extensions of landscape ecology theory and practice: examples from the Peruvian Amazon. *Professional Geographer*, 58(4): 421-435.

Crews-Meyer, K.A., 2002. Characterizing landscape dynamism using paneled-pattern metrics. *Photogrammetric Eng. & Remote Sensing*, 68(10):1031-1040.

Cullinan, V.I., Simmons, M.A., and Thomas, J.M., 1997. A Bayesian test of hierarchy theory: scaling up variability in plant cover from field to remotely sensed data. *Landscape Ecology*, 12:273-285.

Cumming, G.S., Barnes, G., Perz, S., Schmink, M., Sieving, K.E., Southworth, J., Binford, M., Holt, R.D., Stickler, C., and Van Holt, T., 2005. An exploratory framework for the empirical measurement of resilience. *Ecosystems*, 8:975-987.

Cumming, D.H.M, Brock Fenton, M., Rautenbach, I.L., Taylor, R.D., Cumming, G.S., Cumming, M.S., Dunlop, J.M., Ford, A.G., Hovorka, M.D. Johnston, D.S., Kalcounis. M. Mahlangu, Z. and Protfors C.V.R., 1997. Elephants, woodlands and biodiversity in southern Africa. *South African Journal of Science*; 93: 231-236

Cummings, D.A.T., Irizarry, R.A., Huang, N.E., Endy, T.P., Nisalak, A., Ungchusak, K., and Burke, D.S., 2004. Travelling waves in the occurrence of denge haemorrhagic fever in Thailand. Nature, 427: 344-347.

Dale, V., 1997. The relationship between land-use change and climate change. *Ecological Applications*, 7(3): 753-769.

Daniels, L.D., and Veblen, T.T., 2003. Regional and local effects of disturbance and climate on altitudinal treelines in northern Patagonia. *Journal of Vegetation Science*, 14(5): 733-742.

DeAngelis, D.L. and Waterhouse, J.C., 1987. Equilibrium and nonequilibrium concepts in ecological models. *Ecological Monographs*, 57:1-21

DeBano, L.F., Neary, D.G., and Ffolliott, P.F., 1998. Fire's effects on ecosystems. Wiley & Sons, Inc. New York.

DeFries, R.S. and Townshend, J.G.R., 1994. NDVI derived land cover classifications at a global scale. *International Journal of Remote Sensing*, 5: 3567-3586.

Denny, P. 2001. Research, capacity-building and empowerment for sustainable management of African wetland ecosystems. *Hydrobiologia*, 458:21-31.

Dia, X. and Khorram, S., 1998. The effects of image misregistration on the accuracy of remotely sensed change detection. *IEEE Transactions on Geoscience and Remote Sensing*, 36(5): 1566-1577.

Diouf, A. and Lambin, E.F. 2001. Monitoring land-cover changes in semi-arid regions: remote sensing data and field observations in the Ferlo, Senegal. *Journal of Arid Environments*, 48:129-148.

Doraiswamy, P.C., Hatfield, J.L, Jackson, T.J., Akhmedov, B., Prueger, J., and Stern, A., 2004. Crop condition and yield simulations using Landsat and Modis. *Remote Sensing of Environment*, 92(4): 548-559.

Dougill, A. and Trodd, N., 1999. Monitoring and modelling open savannas using multisource information: analyses of Kalahari studies. *Global Ecology and Biogeography*, 8(3/4): 211-221.

Du, Y., Teillet, P.M., and Cihlar, J., 2002. Radiometric normalization of multi-temporal high-resolution satellite images with quality control for land cover change detection. *Remote Sensing of Environment*, 82: 123-134.

Dublin, H.T., Sinclair, A.R.E., and McGlade, J., 1990. Elephants and fire as causes of multiple stable states in the Serengeti-Mara woodlands. *Journal of Animal Ecology*, 59(3):1147-1164.

Dyer, T.G.J. and Tyson, P.D., 1977. Estimating above and below normal rainfall periods over south Africa, 1972-2000. *Journal of Applied Meteorology*, 16: 145-147.

Eastman, J.R. and Fulk, M., 1993. Long sequence time-series evaluation using standardized principal components. *Photogrammetric Engineering & Remote Sensing*, 59(8): 1307-1312.

Ellery, W.N., Dahlberg, A.C., Strydom, R., Neal, M.J., and Jackson, J., 2003a. Diversion of water flow from a floodplain wetland stream: an analysis of geomorphological setting and hydrological and ecological consequences. *Journal of Environmental Management*, 68: 51-71.

Ellery, W.N., McCarthy, T.S., and Smith, N.D. 2003b. Vegetation, hydrology, and sedimentation patterns on the major distributary systems of the Okavango Fan, Botswana. *Wetlands*, 23(2): 357-375.
Ellery, W.N., McCarthy, T.S., and Dangerfield, J.M., 1998. Biotic factors in mima mound development: evidence from the floodplains of the Okavango Delta, Botswana. *Int. Journal of Ecology and Environmental Sciences*, 24:293-313.
Ellery, W.N. and McCarthy, T.S., 1998. Environmental change over two decades since dredging and excavation of the lower Boro River, Okavango Delta, Botswana. *Journal of Biogeography*, 25:361-378.
Ellery, W.N. and McCarthy, T.S., 1994. Principles for the sustainable utilization of the Okavango Delta ecosystem, Botswana. *Biological Conservation*, 70:159-168.
Ellery, K., Ellery, W.N., Rogers, K.H., and Walker, B.H., 1991. Water depth and biotic insulation: major determinants of backswamp plant community composition. *Wetlands Ecology and Management*, 1(3): 149-162.
Ellison, A.M., 1996. An introduction to Bayesian inference for ecological research and environmental decision-making. *Ecological Applications*, 6(4): 1036-1046.
Eva, H. and Lambin, E.F., 2000. Fire and land-cover change in the tropics: a remote sensing analysis at the landscape scale. *Journal of Biogeography*, 27: 765-776.
Fang, H., Liang, S., McClaran, M.P., van Leeuwen W.J.D., Drake, S., Marsh, S.E., Thomson, A.M., Izaurralde, R.C., and Rosenberg, N.J., 2005. Biophysical characterization and management effects on semiarid rangeland observed from Landsat ETM+ data. *IEEE Transactions on Geoscience and Remote Sensing*, 42(1): 125-134.
Fensholt, R. and Sandholt, I., 2003. Derivation of a shortwave infrared water stress index from MODIS near- and shortwave infrared data in a semiarid environment. *Remote Sensing of Environment*, 87: 111-121.
Ferreira, L.G. and Huete, A.R., 2004. Assessing the seasonal dynamics of the Brazilian Cerrado vegetation through the use of spectral vegetation indices. *International Journal of Remote Sensing*, 25(10): 1837-1860.
Field, C.B., Randerson, J.T., and Malmstrom, C.M., 1995. Global net primary production: combining ecology and remote sensing. *Remote Sensing of Environment*, 51: 74-88.
Foley, J.A., Coe, M.T., Scheffer, M., and Wang, G., 2003. Regime shifts in the Sahara and Sahel: Interactions between ecological and climatic systems in Northern Africa. *Ecosystems*, 6:524-539.
Folke, C., Hahn, T., Olsson, P., and Norberg. 2005. Adaptive governance of social-ecological systems. Annual Review of Environment and Resources. 33pp (in press)
Folke, C., Carpenter, S., Walker, B., Scheffer, M., Elmqvist, T., Gunderson, L., and Holling, C.S., 2004. Regime shifts, resilience, and biodiversity in ecosystem management. *Annual Review of Ecology, Evolution, and Systematics*, 35:557-581.
Folke, C., Holling, C.S., and Perrings, C., 1996. Biological diversity, ecosystems and the human scale. *Ecological Applications*; 6(4): 1018-1024.
Forbes, B.C., Fresco, N., Shvidenko, A., Danell, J., and Chapin, F.S.III., 2004. Geographic variations in anthropogenic drivers that influence the vulnerability and resilience of social-ecological systems. *Ambio*, 35(6): 377-382.
Forman, R.T.T, 1995. Some general principles of landscape and regional ecology. *Landscape Ecology*, 10(3): 133-142.
Forman, R.T.T. 1995. Land mosaics: the ecology of landscapes and regions. Cambridge University Press, Cambridge, UK
Forman, R.T.T., and Godron, M. 1986. Landscape Ecology. Wiley and Sons Press.
Fortin, M-J.and Dale, M. 2005. Spatial Analysis: a guide for ecologists. Cambridge University Press.
Foster, D.R., Aber, J.D., Melillo, J.M., Bowden, R.D., and Bazzaz, F., 1997. Forest response to disturbance and anthropogenic stress. *BioScience*, 47(7): 437-445.
Friedl, M.A., McIver, D.K., Hodges, J.C.F., Zhang, X.Y., Muchoney, D., Strahler, A.H., Woodcock, C.E., Gopal, S., Schneider, A., Cooper, A., Baccini, A., Gao, F., and Schaaf, C., 2002. Global land cover mapping from MODIS: algorithms and early results. *Remote Sensing of Environment*, 83: 287-302.

Friis-Christensen, E. and Lassen, K., 1991. Length of the solar cycle: an indicator of solar activity closely associated with climate. Science, 254(5032): 698-700.
Fuhlendorf, S.D. and Engle, D.M., 2004. Application of the fire-grazing interaction to restore a shifting mosaic on tallgrass prairie. *Journal of Applied Ecology*, 41: 604-614.
Fuhlendorf, S. D. and F. E. Smeins, 1998. The influence of soil depth on plant species response to grazing within a semi-arid savanna. *Plant Ecology*, 138: 89-96.
Fuhlendorf, S. D. and F. E. Smeins, 1997. Long-term vegetation dynamics mediated by herbivores, weather, and fire in a Juniperus-Quercus savanna. *J. of Vegetation Science*, 8(6): 819-828.
Fuhlendorf, S. D., F. E. Smeins, and W. E. Grant. 1996. Simulation of a fire sensitive ecological threshold: a case study of Ashe juniper on the Edwards Plateau of Texas, USA. *Ecological Modelling* 90:245-255.
Fuhlendorf, S. D., and F. E. Smeins, 1996. Spatial scale influence on longterm temporal patterns of a semi-arid grassland. *Landscape Ecology*, 11(2): 107-113.
Fuller, D.O., 1999. Canopy phenology of some mopane and miombo woodlands in eastern Zambia. *Global Ecology and Biogeography*, 8: 199-209.
Fuller, D.O., Prince, S.D., and Astle, W.L., 1997. The influence of canopy strata on remotely sensed observations of savanna-woodlands. *International Journal of Remote Sensing*, 18(14): 2985-3009.
Furley, P.A. 2006. Tropical savannas. *Progress in Physical Geography*, 30(1): 105-121.
Gao, X., Heute, A., Ni, W., and Miura, T., 2000. Optical-biophysical relationships of vegetation spectra without background contamination. *Remote Sensing of Environment,* 74: 609-620.
Gao, B-C, 1996. NDWI-A normalized difference water index for remote sensing of vegetation liquid water from space. *Remote Sensing of Environment*; 58:257-266.
Garstang, M., Ellery, W.N., McCarthy, T.S., Scholes, M.C., Scholes, R.J., Swap, R.J., and Tyson, P.D., 1998. The contribution of aerosol- and water-borne nutrients to the functioning of the Okavango Delta ecosystem, Botswana. *South African Journal of Science*, 94(5):13pp
Gieske, A., 1997. Modelling outflow from the Jao/Boro river system in the Okavango Delta, Botswana. *Hydrology*, 193:214-239.
Gignoux, J., Clobert, J., and Menaut, J., 1997. Alternative fire resistance strategies in savanna trees. Oecologia, 110(4): 576-583.
Gillson, L. and Hoffman, M.T., 2007. Rangeland ecology in a changing world. *Science*, 315: 53-54.
Gillson, L. and Lindsay, K., 2003. Ivory and ecology-changing perspectives on elephant management in the international trade in ivory. *Environmental Science and Policy*, 6: 411-419.
Glenn, S.M., Collins, S.L, and Gibson, D.J., 1992. Disturbances in tallgrass prairie: local and regional effects on community heterogeneity. *Landscape Ecology*, 7(4): 243-251.
Gong, D-Y. and Shi, PJ., 2003. Northern hemispheric NDVI variations associated with large-scale climate indices in spring. *International Journal of Remote Sensing*, 24(12): 2559-2566.
Goward, S., Waring, R., Dye, D.G., and Yang, J., 1994. Ecological remote sensing at OTTER: Satellite macroscale observations. *Ecological Applications*, 4(2): 322-343.
Goward, S.N. and Huemmrich, K.F. 1992. Vegetation canopy PAR absorptance and the normalized difference vegetation index: as assessment using the SAIL model. *Remote Sensing of Environment*, 39: 119-140.
Grunblatt, J., Ottichilo, W.K. and Sinage, R.K., 1989. A hierarchical approach to vegetation classification in Kenya. *African Journal of Ecology*, 27: 45-51.
Gumbricht, T., McCarthy, T.S., and Bauer, P., 2005. The micro-topography of the wetlands of the Okavango Delta, Botswana*. Earth Surface Processes and Landforms*, 30: 27-39.
Gumbricht, T., Wolski, P., Frost, P.E, and McCarthy, T.S., 2004a. Forecasting the spatial extent of the annual flood in the Okavango delta, Botswana. *Journal of Hydrology*, 290:178-191.
Gumbricht, T., McCarthy, J., McCarthy, T.S., 2004b. Channels, wetlands and islands in the Okavango Delta, Botswana and their relation to hydrological and sedimentational processes. *Earth Surface Processes and Landforms*, 29:15-29.
Gumbricht, T., McCarthy, T.S., and Merry, C.L. 2001. The topography of the Okavango Delta, Botswana, and its tectonic and sedimentological implications. *South African Journal of Geology*, 104:243-264.

Gunderson, L.H., 2000. Ecological resilience in theory and application. *Annual Review of Ecological Systems*, 31:425-439.

Gupta, R.K., Prasad, T.S., Krishna Rao, P.V., and Bala Manikavelu, P.M., 2000. Problems in upscaling of high resolution remote sensing data to coarse spatial resolution over land surface. *Advances in Space Research*, 26(7): 1111-1121.

Hall, F.G., Strebel, D.E., Nickeson, J.E., and Goetz, S.J., 1991b. Radiometric rectification – toward a common radiometric response among multidate, multisensor images. *Remote Sensing of Environment*, 35: 11-27.

Harris, A.T., and Asner, G.P. 2003. Grazing gradient detection with airborne imaging spectroscopy on a semi-arid rangeland. *Journal of Arid Environments*, 55: 391-404.

Harris, J.A. and Hobbs, R.J., 2001. Clinical practice for ecosystem health: the role of ecological restoration. *Ecosystem Health*, 7(4): 195-202.

Hay, S.I., Snow, R.W., and Rogers, D.J., 1998. Predicting malaria seasons in Kenya using multi-temporal meteorological satellite sensor data. *Trans. To the Royal Soceity of Tropical Medicine and Hygiene*, 92: 12-20.

Hayes, D.J. and Sader, S.A., 2001. Comparison of change-detection techniques for monitoring tropical forest clearing regrowth in a time series. *Photogrammetric engineering and remote sensing*, 67(9): 1067-1075.

Heinl, M., Neuenschwander, A.L., and Silva, J., 2006. Interactions between fire and flooding in a southern African floodplain (Okavango Delta, Botswana). *Landscape Ecology*, 21(5): 699-709.

Heinl, M., Sliva, J., and Tacheba, B., 2004. Vegetation changes after single fire-events in the Okavango Delta wetland, Botswana. *South African Journal of Botany*, 70(5): 695:704.

Heinl, M., 2002. Fire and its effects on vegetation in the Okavango Delta, Botswana. Master's Thesis, Techniche Universitat Munchen.

Heyen, H., Fock, H. and Greve, W., 1998. Detecting relationships between interannual variability in ecological time series and climate using a multivariate statistical approach – a case study on Helgoland Roads zooplankton. *Climate Research*, 10: 179-191.

Hiernaux, P., Bielders, C.L., Valentin, C., Bationo, A., and Fernandez-Rivera, S., 1999. Effects of livestock grazing on physical and chemical properties of sandy soils in Sahelian rangelands. *Journal of Arid Environments*, 41:231-245.

Higgins, S.I., Bond, W.J., and Trollope, W.S., 2000. Fire, resprouting and variability: a recipe for grass-tree coexistence in savanna. *Journal of Ecology*; 88: 213-229.

Hirosawa, Y., Marsh, S.E., and Kliman, D.H., 1996. Application of standardized principal component analysis to land-cover characterization using multi-temporal AVHRR data. *Remote Sensing of Environment*, 58: 267-281.

Hoekman, D.H. and Quiriones, M.J., 2000. Land cover type and biomass classification using AirSAR data for evaluation and monitoring scenarios in the Colombian Amazon. *IEEE Transactions on Geoscience and Remote Sensing*, 38(2): 685-696.

Holechek, J.L., Gomez, H., Molinar, F., and Galt, D., 1999. Grazing studies: what we've learned. *Rangelands*, 21(2):12-16.

Holling, C.S., 2001. Understanding the complexity of Economic, Ecological, and Social Systems. *Ecosystems*, 4:390-405.

Holling, C.S. and Meffe, G.K., 1996. Command and control and the pathology of natural resource management. *Conservation Biology*, 10(2): 328-337.

Holling, C.S., 1992. Cross-scale morphology, geometry and dynamics of ecosystems. *Ecological Monographs*, 62: 447-502.

Holling, C.S., 1973. Resilience and stability of ecological systems. *Annual Review of Ecology and Systematics*. 4:1-23.

Hooper, D.U., Chapin, F.S., Ewel, J.J., Hector, A., Inchausti, P., Lavorel, S., Lawton, J.H., Lodge, D.M., Loreau, M., Naeem, S., Schmid, B, Setala, H., Symstad, A.J., Vandermeer, J., and Wardle, D.A., 2005. Effects of biodiversity on ecosystem functioning: a consensus of current knowledge. *Ecological Monographs*, 75(1): 3-35.

Howe, H. F. 1994. Response of Early- and Late-Flowering Plants to Fire Season in Experimental Prairies. *Ecological Applications,* 4:121-133.
Huang, Y., Street-Perrott, F.A., Metcalfe, S.E., Brenner, M., Moreland, M., and Freeman, K.H., 2001. Dominant control on glacial-interglacial variations in C3 and C4 plant abundance. *Science*, 293: 1647-1651.
Huete, A.R., Didan, K., Miura, T., Rodriguez, E.P., Gao, X. and Ferriera, L.G., 2002. Overview of the radiometric and biophysical performance of the MODIS vegetation indices. *Remote Sensing of Environment*, 83: 195-213.
Huete, A.R., Liu, H.Q., Batchily, K., van Leeuwen, W., 1997. A comparison of vegetation indices over a global set of TM images. *Remote Sensing of Environment*, 59:440-451.
Huete, A.R., Jackson, R.D., 1987. Suitability of spectral indices for evaluating vegetation characteristics on arid rangelands. *Remote Sensing of Environment*, 23:213-232.
Hulme, M., Doherty, R., Ngara, T., and New, M., 2005. Global warming and African climate change: a reassessment. In Low, P.S. (ed) Climate Change and Africa. Cambridge University Press.
Hulme, M., Doherty, R., Ngara, T., New, M. and Lister, D., 2001. African Climate Change: 1900-2100. *Climate Research*, 17:145-168
Hurrell, J.W. and Trenberth, K.W., 1996. Satellite versus surface estimates of air temperature since 1979. *J. Climate*, 9(9): 2222-2232.
Hurtt, G.C., Moorcroft, P.R., Pacala, S.W., and Levin, S.A., 1998. Terrestrial models and global change: challenges for the future. *Global Change Biology*, 4:581-590.
Illius, A.W. and O'Conner, T.G., 1999. On the relevance of nonequilibrium concepts to arid and semi-arid grazing systems. *Ecological Applications*, 9(3): 798-813.
Immerzeel, W.W., Quiroz, R.A., and DeJong, S.M., 2005. Understanding precipitation patterns and land use interaction in Tibet using harmonic analysis of SPOT VGT-S10 NDVI time series. *International Journal of Remote Sensing*, 26(11): 2281-2296.
Intergovernmental Panel on Climate Change (IPCC), 1996. Climate change, 1995: the science of climate change. Contribution of the working group I to the second assessment report of the IPCC. Cambridge University Press.
IUCN, 2000. The Ecosystem Approach. UNEP/CBD/COP/5/23. Adopted by the 5th Convention on Biological Diversity, Nairobi, Kenya.
Jakubauskas, M.E., Legates, D.R., and Kastens, J.H., 2001. Harmonic analysis of time-series AVHRR NDVI data. *Photogrammetric Engineering & Remote Sensing*, 67(4): 461-470.
Jansen, R. and Madzwamuse, M., 2003. The Okavango Delta Management Plan Project: the need for environmental parternerships. In Turton, A., Ashton, P., and Cloete T.(eds). Transboundary rivers, sovereignty and development: Hydropolitical drivers in the Okavango River Basin. Pretoria and Geneva: AWIRU and Green Cross International.
Jansen, R., 2002. The Okavango Delta Management Plan Project – application of an ecosystem based planning approach. *17th Global Diversity Forum*. Available online http://www.iucn.org/themes/cem/documents/ecosapproach/esa_gbf_ramsar_okavango_2002.pdf
Jassby, A.D. and Powell, T.M., 1990. Detecting changes in ecological time series. Ecology; 71(6): 2044-2052.
Jellema, A., Ringrose, S., and Matheson, W., 2001. Northern Botswana Vegetation Mapping Project. HOORC, University of Botswana (www.orc.ub.bw).
Jeltsch, F., Weber, G.E. and Grimm, V., 2000. Ecological buffering mechanisms in savannas: a unifying theory of long-term tree-grass coexistence. *Plant Ecology*, 161:161-171.
Junk, W.J., 2002. Long-term environmental trends and the future of tropical wetlands. *Environmental Conservation*, 29: 414-435.
Junk, W.J. and Furch, K., 1993. A general review of tropical South American floodplains. *Wetlands Ecology and Management*, 2(4): 231-238
Junk, W.J., Bayley, P.B. and Sparks, R.E., 1989. The floodpulse concept in river-floodplain ecosystems. In Key Environments: Amazonia (eds) Prance, G.T and Lovejoy, T.E. Pergamon Press.

Justice, C.O., L. Giglio, S. Korontzi, J. Owens, J. T. Morisette, D. Roy, J. Descloitres, S. Alleaume, F. Petitcolin and Y. Kaufman. 2002. The MODIS fire products. *Remote Sensing of Environment,* 83: 244-262.

Justice, C.O., Townshend, J.R.G., Holben, B.N., and Tucker, C.J., 1985. Analysis of the phenology of global vegetation using meteorological satellite data. *International Journal of Remote Sensing*, 6(8): 1271-1318.

Justice, C.O., Holben, B.N., and Gwynne, M.D., 1986. Monitoring east African vegetation using AVHRR data. *International Journal of Remote Sensing*, 7: 1453-1474.

Kaufman, Y.J., Tanre, D., Gordon, H.R., Nakajima, T., Lenoble, J., Frouin, R., Grassl, H., Herman, B.M., King, M.D., and Teillet, P.M., 1997. Passive remote sensing of tropospheric aerosol and atmospheric correction for the aerosol effect. Journal of Geophysical Research; 102(D14): 16815-16830.

Kaufman, Y., 1989. The atmospheric effects on remote sensing and its correction. In Theory and Applications of Optical Remote Sensing (ed. Asrar, G). Wiley Publishing, New York.

Kay, J.J., Regier, H.A., Boyle, M. and Francis, G., 1999. An ecosystem approach for sustainability: addressing the challenge of complexity. *Futures*, 31:721-742.

Kgathi, D.L., Kniveton, D., Ringrose, S., Turton, A.R., Vanderpost, C.H.M., Lundqvist, J., and Seely, M., 2006. The Okavango; a river supporting its people, environment and economic development. *Journal of Hydrology*, 331: 3-17.

Kgathi, D.L., Mmopelwa, G., and Mosepele, K., 2005. Natural resource assessment in the Okavango Delta, Botswana: case studies of some key resources. *Natural Resources Forum*, 29:70-81.

Keddy, P., 2000. Wetland Ecology: principles and conservation, Cambridge University Press, Cambridge, UK.

Kennedy, A.D. and Potgieter, A.L.F, 2003. Fire season affects size and architecture of Colophospermum mopane in southern Africa savannas. *Plant Ecology*, 167: 179-192

Kerr, J.T. and Ostrovsky, M., 2003. From space to species: ecological applications for remote sensing. *Trends in Ecology & Evolution*, 18(6): 299-305.

Keshava, N. and Mustard, J.F., 2002. Spectral unmixing. *IEEE Signal Processing*, 19: 44-57.

Kestin, T.S., Karoly, D.J., Yano, J., and Rayner, N.A., 1998. Time-frequency variability of ENSO and stochastic simulations. Journal of Climate, 11: 2258-2272.

Kingsford, R.T., 2000. Ecological impacts of dams, water diversions and river management on floodplain wetlands in Australia. *Austral Ecology*, 25: 109-127.

Kinzig, A.P., Ryan, P., Etienne, M., Allison, H., Elmqvist, T., and Walker, B.H., 2006. Resilience and regime shifts: assessing cascading effects. *Ecology and Society*, 11(1): 20.

Knoop, W.T. and Walker, B.H., 1985. Interactions of woody and herbaceous vegetation is a southern African savanna. *Journal of Ecology*, 73:235-253.

Korontzi, S., Justice, C.O., and Scholes, R.J., 2003. Influence of timing and spatial extent of savanna fires in southern Africa on atmospheric emissions. *Journal of Arid Environments*, 54:395-404.

Krah, M., McCarthy, T.S., Huntsman-Mapila, P., Wolski, P., Annegarn, H., and Sethebe, K. 2006. Nutrient budget in the seasonal wetland of the Okavango Delta, Botswana. *Wetlands Ecology and Management*, 14:253-267.

Krah, M., McCarthy, T.S., Annegarn, H., and Ramberg, L., 2004. Airborne dust deposition in the Okavango Delta, Botswana and its impact on landforms. *Earth Surface Processes and Landforms*, 29:565-577.

Labat, E., Ronchail, J., Callede, J., Guyot J.L., De Oliveira, E., and Guimaraes, W., 2004. Wavelet analysis of the Amazon hydrological regime variability. *Geophysical Research Letters*, 31, L02501, doi:10.1029/2003GL018741.

Lambin, E.F., Geist, H.J., and Lepers, E., 2003. Dynamics of land-use and land-cover change in tropical regions. *Annual Review of Environmental Resources*, 28:205-241.

Lambin, E.F., Turner, B.L., Geist, H.J., Agbola, S.B., Angelsen, A., Bruce, J.W., Coomes, O.T., Dirzo, R., Fischer, G., Folke, C., George, P.S., Homewood, K., Imbernon, J., Leemans, R., Li, X., Moran, E.F., Mortimore, M., Ramakrishnan, PS., Richards, J.F., Skanes, H., Steffen, W., Stone, G.D., Svedin, U., Veldkamp, T.A., Vogel, C., and Xu, J., 2001. The causes of land-luse and land-cover change: moving beyond the myths. *Global Environmental Change*, 11: 261-269.

Lambin, E.F., 1999. Monitoring forest degradation in tropical regions by remote sensing: some methodological issues. *Global Ecology and Biogeography*, 8:191-198.
Lambin, E.F. and Ehrlich, D., 1997. Land cover changes in sub-Saharan Africa (1982-1991): Application of a change index based upon remotely sensed surface temperature and vegetation indices at a continental scale. *Remote Sensing of Environment*, 61:181-200.
Lambin, E. F. 1996. Change detection at multiple temporal scales: seasonal and annual variations in landscape variables. *Photogrammetric Engineering & Remote Sensing*, 62: 931–938.
Landres, P.B., Morgan, P., and Swanson, F.J., 1999. Overview of the use of natural variability concepts in managing ecological systems. *Ecological Applications*, 9(4): 1179-1188.
Lankford, B. and Beale, T., 2007. Equilibrium and non-equilibrium theories of sustainable water resources in management: dynamic river basin and irrigation behavior in Tanzania. *Global Environmental Change*, 17: 168-180.
Lasaponara, R., On the use of principal components analysis (PCA) for evaluating interannual vegetation anomalies from SPOT/VEGETATION NDVI temporal series. *Ecological Modeling*, 194: 429-434.
Laurance, W.F. and Williamson, G.B., 2001. Positive feedbacks among forest fragmentation, drought, and climate change in the Amazon. *Conservation Biology*, 15(6): 1529-1535.
Lawrence, R.L. and Ripple, W.J., 1999. Calculating change curves for multi-temporal satellite imagery: Mt. St. Helens. *Remote Sensing of Environment*, 67: 309-319.
Lee, M.A., Snyder, K.L., Valentine-Darby, P., Miller, S.J., and Ponzio, K.J., 2005. Dormant season prescribed fire as a management tool for the control of Salix caroliniana Michx. in a floodplain marsh. *Wetlands Ecology and Management*, 13: 479-487.
Lefsky, M.A., Cohen, W.B., Parker, G.G., and Harding, D.J., 2002. Lidar remote sensing for ecosystem studies. BioScience, 52: 19-30.
Leprieur, C., Kerr, Y.H., Mastorchio, S., and Meunier, J.C., 2000. Monitoring vegetation cover across semi-arid regions : comparison of remote observations from various scales. *International Journal of Remote Sensing*, 21(2): 281-300.
Levin, S.A., 1998. Ecosystems and the biosphere as complex adaptive systems. *Ecosystems*, 1:431-436.
Levin, S.A. 1993. Concepts of scale at the local level, in Scaling Physiological Processes: Leaf to Globe, ed. Ehleringer, J.R. and Field, C.B., Academic Press.
Levin, S.A., 1992. The problem of pattern and scale in ecology. *Ecology*, 73(6): 1943-1967.
Li, Z., Zhu, Q., and Gold, C., 2005. Digital Terrain Modeling: principles and methodology. CRC Press.
Liang, S. (2004) Quantitative remote sensing of land surfaces. John Wiley Press, New Jersey.
Linn, F., Masie, M., and Rana, A., 2003. The impacts on groundwater development on shallow aquifers in the lower Okavango Delta, northwestern Botswana. *Environmental Geology*, 44:112-118.
Loreau, M., 1998. Biodiversity and ecosystem functioning: a mechanistic model. *PNAS*, 95: 5632-5636.
Loveland, T.R. and Belward, A.S., 1997. The IGBP-DIS global 1km land cover dataset, DISCover: preliminary results. *International Journal of Remote Sensing*, 18(15): 3289-3295.
Lundberg, P., Ranta, E., Ripa, J., and Kaitala, V., 2000. Population variability in space and time. *Trends in Ecology and Evolution*, 15(11): 460-464.
Ludwig, D., Walker, B., and Holling, C.S., 1997. Sustainability, stability, and resilience. Conservation Ecology 1(1), online at http://www.consecol.org/vol1/iss1/art7
Lunetta, R.S., Knight, J.F., Ediriwickrema, J., Lyon, J.G., and Worthy, L.D., 2006. Land-cover change detection using multi-temporal MODIS NDVI data. *Remote Sensing of Environment*, 105: 142-154.
Lunetta, R.S., Johnson, D.M, Lyon, J.G, and Crotwell, J., 2004. Impacts of image temporal frequency on land-cover change detection monitoring. *Remote Sensing of Environment*, 89: 444-454.
Lunetta, R.S., Ediriwickrema, J., Johnson, D.M., Lyon, J.G., and McKerrow, A., 2002. Impacts of vegetation dynamics on the identification of land-cover change in a biologically complex community in North Carolina, USA. *Remote Sensing of Environment*, 82: 258-270.
Lyon, J.G., Yuan, D., Lunetta, R.S., and Elvidge, C.D., 1998. A change detection experiment using vegetation indices. *Photogrammetric engineering and Remote Sensing*, 64(2):143-150.
Manolakis, D., Siracusa, C., and Shaw, G., 2001. Hyperspectral subpixel target detection using the linear mixing model. *IEEE Transactions on Geoscience and Remote Sensing*, 39(7): 1392-1409.
Mantua, N.J. and Hare, S.R., 2002. The Pacific decadal oscillation. *J. Oceanography*, 58: 35-44.

Markham, B.L., Storey, J.C., Williams, D.L and Irons, J.R., 2004. Landsat sensor performance: history and current status. *IEEE Transactions on Geoscience and Remote Sensing*, 42(12): 2691-2694.

Markon, C.J., Fleming, M.D., and Binnian, E.F., 1995. Characteristics of vegetation phenology over the Alaskan landscape using AVHRR time-series data. *Polar Record*, 31(177): 179-190.

Mas, J.F., 1999. Monitoring land-cover changes: a comparison of change detection techniques. *Int. Journal of Remote Sensing*, 20: 139-152.

Masek, J.G., Lindsay, F.E., Goward, S.N., 2000. Dynamics of urban growth in the Washington DC metropolitan area, 1973-1996, from Landsat observations. *International Journal of Remote Sensing*, 21: 3473-3486.

Masek, J.G., Honzak, M., Goward, S.N., Liu, P., and Pak, E., 2001. Landsat-7 ETM+ as an observatory for landcover. Initial radiometric and geometric comparisons with Landsat-5 Thematic Mapper. *Remote Sensing of Environment*, 78: 118-130.

Mayaux, P., Bartholome, E., Fritz, S., and Belward, A. 2004. A new land cover map of Africa for the year 2000. *Journal of Biogeography*, 31:861-877.

Mbaiwa, J.E. and Mbaiwa, O.I., 2006. The effects of veterinary fences on wildlife populations in Okavango Delta, Botswana. Int. Journal of Wildnerness, 12(3): 17-24.

Mbaiwa, J.E., 2005. Enclave tourism and its socio-economic impacts in the Okavango Delta, Botswana. *Tourism Management*, 26: 157-172.

Mbaiwa, J.E., 2004a. Causes and possible solutions to water resource conflicts in the Okavango River Basin: The case of Angola, Namibia, and Botswana. *Physics and Chemistry of the Earth*, 29: 1319-1326.

Mbaiwa, J.E., 2004b. Prospects of basket production in promoting sustainable rural livelihoods in the Okavango Delta, Botswana. *International Journal of Tourism Research*, 6(4): 221-235.

Mbaiwa, J.E., 2004c. The social-economic benefits and challenges of a community-based safari hunting tourism in the Okavango Delta, Botswana. *Journal of Tourism Studies*, 15: 37-50.

Mbaiwa, J.E., 2003. The socio-economic and environmental impacts of tourism development on the Okavango Delta, northwestern Botswana. *Journal of Arid Environments*, 54: 447-467.

Mbaiwa, J.E., Bernand, F.E. and Orford, C.E., 2002. Limits of acceptable change for tourism in the Okavango Delta. Presented at Environmental Monitoring of Tropical Wetlands conference. Available online http://www.ees.ufl.edu/homepp/brown/hoorc/docs/5%20Papers%20&%20Paper%20Abstracts/Mbaiwa,%20Bernard,%20Orford%205.4.doc

McCarthy, J.M., 2002, Remote sensing for detection of landscape form and function of the Okavango Delta, Ph.D. Dissertation, Kungl Tekniska, Hœgskolan, Stockholm, Sweden.

McCarthy, J.M., Gumbricht, T., McCarthy, T.S., Frost, P., Wessels, K., and Seidel, F., 2003, Flooding patterns of the Okavango Wetland in Botswana between 1972 and 2000. *Ambio*, 32(7): 453-457.

McCarthy, T.S., 2006. Groundwater in the wetlands of the Okavango Delta, Botswana and its contribution to the structure and function of the ecosystem. *Journal of Hydrology*; 320:264-282

McCarthy, T.S., G.R.J. Cooper, P.D. Tyson, and W.N. Ellery, 2000. Seasonal flooding in the Okavango Delta, Botswana – recent history and future prospects. *South African Journal of Scienc*e, 96: 25 – 33.

McCarthy, T.S., A. Bloem, and P.A. Larkin, 1998a. Observations on the hydrology and geohydrology of the Okavango Delta, Botswana. *J. Geology*, vol. 101(2), 101-117.

McCarthy, T. S., Ellery, W. N. and Bloem, A., 1998b. Some observations on the geomorphological impact of hippopotamus *(Hippopotamus amphibius* L.) in the Okavango Delta, Botswana. *African Journal of Ecology*, 36, 44-56.

McCarthy, T. S., Ellery, W. N., and Dangerfield, J. M., 1998c. The role of biota in the initiation and growth of islands on the floodplains of the Okavango alluvial fan, Botswana. *Earth Surface Processes and Landforms*, 23, 291-316.

McCarthy, T. S., Barry, M., Bloem, A., Ellery, W. N., Heister, H., Merry, C. L., Ruther, H. and Sternberg, H., 1997. The gradient of the Okavango Fan, Botswana, and its sedimentological and tectonic implications. *Journal of African Earth Sciences*, 24, 65-78.

McCarthy, T. S. and Ellery, W. N., 1997. The fluvial dynamics of the Maunachira channel system, northeastern Okavango swamps, Botswana. *South African Journal of Hydrology*, 23(2):115-125.

McCarthy, T. S. and Ellery, W. N., 1993, The Okavango Delta. *Geobulletin*, 36(2), 5-8.
McCarty, J.P., 2001. Ecological consequences of recent climate change. *Conservation Biology*, 15(2): 320-331.
McNaughton, S.J., Ruess, R.W. and Seagle, S.W., 1988. Large mammals and process dynamics in African ecosystems. BioScience, 38(11): 794-800.
McNaughton, S.J., 1985. Ecology of a grazing ecosystem: The Serengeti. *Ecological Monographs*, 55(3): 259-294.
Menenti, M., Azzali, S., Verhoef, W., and van Swol, R., 1993. Mapping agroecological zones and time lag in vegetation growth by means for Fourier analysis of time series of NDVI images. *Advanced Space Research*, 13(5): 233-237.
Mensing, S.A., Michaelsen, J., and Byrne, R., 1999. A 560-year record of Santa Ana fires reconstructed from charcoal deposited in the Santa Barbara basin. *Quaternary Research*, 51: 295-305.
Meyer, T. and Bendsen, H., 2003. The dynamics of the land use systems in Ngamiland: Changing livelihood options and strategies. In Environmental Monitoring of Tropical and Subtropical wetlands (eds Bernard, T., Mosepele, K., and Ramberg, L). Okavango Report Series No 1., Maun Botswana.
Mi, X., Ren, H., Ouyang, Z., Wei, W., and Ma, K. 2005. The use of the Mexican Hat and the Morlet wavelets for detection of ecological patterns. *Plant Ecology*; 179: 1-19.
Midgley, G.F., Hannah, L., Millar, D., Rutherford, M.C., and Lowrie, L.W., 2002. Assessing the vulnerability of species richness to anthropogenic climate change in a biodiversity hotspot. *Global Ecology and Biogeography*, 11: 445-451.
Mildrexler, D.J., Zhao, M., Heinsch, F.A., and Running, S.W., 2007. A new satellite-based methodology for continental-scale disturbance detection. Ecological Applications, 17(1): 235-250.
Ministry of Local Government, Lands, and Housing, (MLGLH), 1989, Ecological zoning of Okavango Delta, Maun, Internal Report, Gaborone, Botswana, 221pp. Nakayama, M. (Ed.), International Waters on Southern Africa, United Nations University Press, Tokyo, pp. 306, 2003.
Mitsch, W.J., Day, J.W., Gilliam, J.W., Groffman, P.M., Hey, D.L., Randall, G.W., and Wang, N., 2001. Reducing nitrogen loading to the Gulf of Mexico from the Mississippi River Basin: Strategies to counter a persistent ecological problem. *Bioscience*, 51(5): 373-388.
Mitsch, W.J. and Gosselink, J.G. 2000. Wetlands. Wiley and Sons, New York.
Miura, T., Huete, A.R., Yoshioka, H., and Holben, B.N., 2001. An error and sensitivity analysis of atmospheric resistant vegetation indices derived from dark target-based atmospheric correction. *Remote Sensing of Environment*, 78: 284-298.
Mlambo, D., 2007. Influence of soil fertility on the physiognomy of the African savanna tree Colophospermum mopane. *African Journal of Ecology*, 45(1): 109-111.
Mlambo, D., and Mapaure, I., 2006. Post-fire resprouting of Colophospermum mopane saplings in a southern African savanna. *Journal of Tropical Ecology*, 22:231-234.
Moleele, N.M., Reed, M.S., Motoma, L., and Seabe, O., 2005. Seed weight patterns of Acacia tortilis from seven seed provenances across Botswana. *African Journal of Ecology*, 43: 146-149.
Moody, A. and Johnson, D.M., 2001. Land-surface phenologies from AVHRR using the discrete fourier transform. *Remote Sensing of Environment*, 75:305-323.
Moon, T.K., 1996. The expectation-maximization algorithm. *IEEE Signal Processing*, 13: 47-60.
Mosugelo, D.K., Moe, S.R., Ringrose, S., and Nellemann, C., 2002. Vegetation changes during a 36-year period in northern Chobe National Park, Botswana. *African Journal of Ecology*, 40: 232-240.
Moss, R.H., Brenkert, A.L., and Malone, E.L., 2001. Vulnerability to climate change: a quantitative approach. Pacific Northwest National Laboratory. http://www.globalchange.umd.edu/data/publications/PNNL-13765.pdf
Moulin, S., Kergoat, L., Viovy, N., and Dedieu, G., 1997. Global scale assessment of vegetation phenology using NOAA/AVHRR satellite measurements. *Journal of Climate*, 10(6): 1154-1170.
Mubyana, T, Krah, M., Totolo, O., and Bonyongo, M., 2003. Influence of seasonal flooding on soil total nitrogen, organic phosphorus and microbial populations in the Okavango Delta, Botswana. *Journal of Arid Environments*, 54:359-369.

Muchoney, D. and Williamson, J., 2001. A Gaussian adaptive resonance theory neural network classification algorithm applied to supervised land cover mapping using multi-temporal vegetation index data. *IEEE Transactions on Geoscience and Remote Sensing*, 39(9): 1969-1977.

Murray-Hudson, M., Wolski, P., and Ringrose, S., 2006. Scenarios of the impact of local and upstream changes in climate and water use on hydro-ecology in the Okavango Delta, Botswana. Journal of Hydrology; (in press)

Murwira, A. and Skidmore, A.K., 2006. Monitoring change in the spatial heterogeneity of vegetation cover in an African savanna. *International Journal of Remote Sensing*, 27(11): 2255-2269.

Myneni, R., Hall, F.G., Sellers, P.J., and Marshak, A.L., 1995. Interpretation of spectral vegetation indices. *IEEE Transactions on Geoscience and Remote Sensing*, 33(2): 481-486.

Nash, D.J., Meadows, M.E. and Gulliver, V.L., 2006. Holocene environmental change in the Okavango panhandle, northwest Botswana. Quaternary Science Reviews, 25: 1302-1322.

National Research Council, 2007. Earth Science and applications from space: National Imperatives for the next decade and beyond. National Academies Press.

National Research Council, 2000. Ecological indicators for the Nation. National Academies Press.

Neme, L.A., 1997. The power of a few: bureaucratic decision-making in the Okavango Delta. *Journal of Modern African Studies*, 35:37-51.

Neuenschwander, A.L. and Crews-Meyer, K.A., 2006. Multi-temporal mapping of disturbances in the Okavango Delta, Botswana using Landsat TM and ETM+ data. *Proceedings to the IGARRS conference*, Denver, CO.

Neuenschwander, A.L., Crawford, M.M., Ringrose, S., 2005. Results of the EO-1 experiment: Use of Earth Observing-1 Advanced Land Imager (ALI) data to assess the vegetational response to flooding in the Okavango Delta, Botswana, *International Journal of Remote Sensing, Remote Sensing, NASA/Safari 2000 special issue,* 26(19): 4321-4337.

Neuenschwander, A.L., Crawford, M.M. and S. Ringrose, 2002. Monitoring of Seasonal Flooding in the Okavango Delta using EO-1 Data. in *Proc. 2002 Intl. Geosci. Rem. Sens. Symp.*, Toronto, Canada, June 24-28, pp 3124-3126.

Neuenschwander, A.L. 2003. Characterization of the vegetation of the Okavango Delta, Botswana using EO-1 Data. Master's Thesis, Department of Aerospace Engineering, University of Texas at Austin.

Nichol, A., 2003. The dynamics of river basin cooperation: The Nile and Okavango basins. In Turton, A., Ashton, P., and Cloete T.(eds). Transboundary rivers, sovereignty and development: Hydropolitical drivers in the Okavango River Basin. Pretoria and Geneva: AWIRU and Green Cross International.

Nicholson, S.E. and Farrar, T.J., 1994. The influence of soil type on the relationships between NDVI, rainfall, and soil moisture in semi-arid Botswana. 1. NDVI response to rainfall. *Remote Sensing of Environment*, 50: 107-120.

Niemi, G.J. and McDonald, M.E., 2004. Application of ecological indicators. *Annual Review of Ecological and Evolutionary Systems*, 35: 89-111.

Noy-Meir, I., 1975. Stability of grazing systems: an application of predator-prey graphs. *J. of Ecology*, 63(2): 459-481.

Nystrom, M. and Folke, C., 2001. Spatial resilience of coral reefs. *Ecosystems*, 4:406-417.

O'Conner, T.G., 2001. Effect of small catchment dams on downstream vegetation of a seasonal river in semi-arid African savanna. *Journal of Applied Ecology*, 38(6): 1314-1325.

Obasi, G.O.P., 2005. The impacts of ENSO in Africa. In Low, P.S. (ed) Climate Change and Africa. Cambridge University Press.

Ogden, J.C., 2005. Everglades ridge and slough conceptual ecological model. Wetlands, 25(4): 810-820.

Ogden, J.C., Davis, S.M., Barnes, T.K., Jacobs, K.J., and Gentile, J.H., 2005. Total system conceptual ecological model. *Wetlands*, 25(4): 955-979.

O'Neill, R.V., 1999. Recovery in complex ecosystems. *Journal of Aquatic Ecosystem Stress and Recovery*, 6: 181-187.

O'Neill, R.V., Johnson, A.R. and King, A.W., 1989. A hierarchical framework for the analysis of scale. *Landscape Ecology*, 3(3/4): 193-205.

Owen-Smith, N. and Danckwerts, D.E., 1997. Herbivory. In Vegetation of Southern Africa, eds (Cowling, R.M., Richardson, D.M., and Pierce, S.M), Cambridge University Press.

Perkins, J.S. 1996. Botswana: fencing out the equity issue. Cattleposts and cattle ranching in the Kalahari Desert. *Journal of Arid Environments*, 33:503-517.
Perry, G., 2002. Landscapes, space, and equilibrium: shifting viewpoints. *Progress in Physical Geography*, 26(3): 339-359.
Perry, C.A. and Hsu, K.J., 2000. Geophysical, archaeological, and historical evidence support a solar-output model for climate change. PNAS, 97: 12433-12438.
Peterson, D.L. and Parker, V.T. (eds), 1998. Ecological scale: Theory and applications. Columbia University Press.
Peterson, G.D., 2003. Uncertainty and the management of multistate ecosystems: and apparently rational route to collapse. *Ecology*, 84(6): 1403-1411.
Peterson, G.D., 2002a. Estimating resilience across landscapes. *Conservation Ecology*, 6(1): 17.
Peterson, G.D., 2002b. Contagious disturbance, ecological memory, and the emergence of landscape pattern. *Ecosystems*, 5:329-338.
Peterson, G.D., 2000a. Political ecology and ecological resilience: An integration of human and ecological dynamics. *Ecological Economics*, 35: 323-336.
Peterson, G.D., 2000b. Scaling ecological dynamics: self organization, hierarchical structure, and ecological resilience. *Climate Change*, 44:291-309.
Peterson, G.D, Allen, C.R., and Holling, C.S., 1998. Ecological resilience, biodiversity, and scale. *Ecosystems*, 1:6-18.
Petit, C.C and Lambin, E.F., 2001. Integration of multi-source remote sensing data for land cover change detection. *International Journal of Geographical Information Science*, 15(8): 785-803.
Petit, C.C., Scudder, T. and Lambin, E.F., 2001. Quantifying process of land cover change by remote sensing: resettlement and rapid land cover changes in southeastern Zambia. *International Journal of Remote Sensing*, 22(17):3435-3456.
Petit, J.R., Jouzel, J., Raynaud, D., Barkov, N.I., Barnola, J.M., Basile, I, Benders, M., Chappellaz, J., Davis, M., Delaygue, G., Delmotte, M., Kotlyakov, V.M., Legrand, M., Lipenkov, V.Y., Lorius, C., Pepin, L., Ritz, C., Saltzman, E., and Stievenard, M., 1999. Climate and atmospheric history of the past 420,000 years from the Vostok ice core, Antarctica. *Nature*, 399: 429-436.
Pettit, N.E. and Froend, R.H., 2001. Variability in flood disturbance and the impact on riparian tree recruitment in two contrasting river systems. *Wetlands Ecology and Management*, 9:13-25.
Pickett, S.T.A., Cadenasso, M.L., and Grove, J.M., 2005. Biocomplexity in coupled natural-human systems: a multidimensional framework. *Ecosystems*, 8:225-232.
Pickett, S.T.A. and Cadenasso, M.L., 2002. The ecosystem as a multidimensional concept: meaning, model, and metaphor. *Ecosystems*; 5:1-10.
Pickett, S.T.A., Kolasa, J, Armesto, J.J., and Collins, S.L., 1989. The ecological concept of disturbance and its expression at various hierarchical levels. *Oikos*, 54: 129-136.
Pickett, S.T.A. and White, P.S. (eds), 1985. The ecology of natural disturbance and patch dynamics. Academic Press, San Diego, CA.
Pielke Sr., R.A., Walko, R.L., Steyaert, L.T., Vidale, P.L., Liston, G.E., Lyons, W.A., and Chase, T.N., 1999. The influence of anthropogenic landscape changes on weather in South Florida. *Monthly Weather Review*, 127: 1663-1673.
Pielke Sr., R.A., Avissar, R., Raupach, M., Dolman, A.J., Zeng, X., and Denning, A.S., 1998. Interactions between the atmosphere and terrestrial ecosystems: influence on weather and climate. *Global Change Biology*, 4: 461-475.
Pietola, L., Horn, R., and Yli-Halla, M., 2005. Effects of trampling by cattle on hydraulic and mechanical properties of soil. *Soil and Tillage Research*, 82: 99-108.
Pimm, S.L., 1984. The complexity and stability of ecosystems. *Nature*, 307: 321-326.
Pinheiro, I., Gabaake, G. and Heyns, P., 2003. Cooperation in the Okavango River Basin: the OKACOM perspective. In Turton, A., Ashton, P., and Cloete T.(eds). Transboundary rivers, sovereignty and development: Hydropolitical drivers in the Okavango River Basin. Pretoria and Geneva: AWIRU and Green Cross International.
Ponzio, K.J., Miller, S.J., and Lee, M.A., 2004. Long-term effects of prescribed fire on *Cladium jamaicence* crantz and *Typha domingensis* pers. densities. *Wetlands Ecology and Management*, 12: 123-133.

Pons, X., Sole-Sugranes, L., 1994. A simple radiometric correction model to improve automatic mapping of vegetation from multispectral satellite data. *Remote Sensing of Environment*, 48: 191-205.
Pope, V.D., Gallani, M.L., Rowntree, P.R., 2000. The impact of new physical parametrizations in the Hadley centre climate model: HadAM3. *Climate Dynamics*, 16: 123-146.
Price, J.C., 1987. Calibration of satellite radiometers and comparison of vegetation indices. *Remote Sensing of Environment*, 18: 35-48.
Privette, J.L., Tian, Y., Roberts, G., Scholes, R.J., Wang, Y., Caylor, K.K., Frost, P., and Mukelabai, M., 2004. Vegetation structure characteristics and relationships of Kalahari woodlands and savannas. *Global Change Biology*, 10: 281-291.
Privette, J.L., Myneni, R.B., Knyazikhim, Y., Mukelabai, M., Roberts, G., Tian, Y., Wang, Y., and Leblanc, S.G., 2002. Early spatial and temporal validation of MODIS LAI product in the Southern Africa Kalahari. *Remote Sensing of Environment*, 83: 232-243.
Ramberg, L., Hancock, P., Lindholm, M., Meyer, T., Ringrose, S., Silva, J., van As, J., and Vanderpost, C., 2006a. Species diversity of the Okavango Delta, Botswana. *Aquatic Science*, 68: 310-337.
Ramberg, L., Wolski, P., and Krah, M., 2006b. Water balance and infiltration in a seasonal floodplain in the Okavango Delta, Botswana. *Wetlands*, 26(3): 677-690.
Rappaport, D.J., Costanza, R., and McMichael, A.J., 1998. Assessing ecosystem health. *Trends in Ecology and Evolution*, 13: 397-402.
Rey, C.F., 1932. Ngamiland and the Kalahari. *Geographical Journal*, 80(4): 281-307.
Richards, J.A. and Jia, X., 2006. Remote sensing digital image analysis: an introduction. 4th edition. Springer Press.
Ricotta, C. and Avena, G.C., 2000. The remote sensing approach in broad-scale phenological studies. *Applied Vegetation Science*, 3(1): 117-122.
Ridd, M.K., and Liu, J., 1998. A comparison of four algorithms for change detection in an urban environment – a remote sensing perspective. *Remote Sensing of Environment*, 63(2): 95-100.
Rietkerk, M., Boerlijst, M.C., van Langevelde, F., HilleRisLambers, R., van de Koppel, J., Kumar, L., Prins, H.H.T., and deRoos, A.M., 2002. Self-organization of vegetation in arid ecosystems. *American Naturalist*, 160: 524-530.
Ringrose, S., Vanderpost, C., Matheson, W., Wolski, P., Huntsman-Mapila, P, Murray-Hudson, M., and Jellema, A. 2006. Indicators of desiccation-driven change in the distal Okavango Delta, Botswana. Journal of Arid Environments; (in press)
Ringrose, S., Matheson, W., Wolski, P., and Huntsman-Mapila, P., 2003. Vegetation cover trends along the Botswana Kalahari transect. *Journal of Arid Environments*, 54: 297-317.
Ringrose, S., Matheson, W., and Vanderpost, C., 2003. Mapping ecological conditions in the Okavango Delta, Botswana, using fine and coarse resolution systems including simulated SPOT VEGETATION imagery. *International Journal of Remote Sensing*, 24(5): 1029-1052.
Ringrose, S., Jelema, Al, Huntsman-Mapila, P., Baker, L., and Brubaker, K., 2005. Use of remotely sensed data in the analysis of soil-vegetation changes along the drying gradient peripheral to the Okavango Delta, Botswana. *International Journal of Remote Sensing*, 26(19): 4293-4319.
Ringrose, S., Matheson, W., Jellema, A., and Ashworth, M., 2003. Characterization of riparian woodlands and their potential water loss in the distal Okavango Delta, Botswana. *Applied Geography*, 23(4): 281-302.
Ringrose, S., Chipanshi, A.C., Matheson, W., Chanda, R., Motoma, L., Magole, I., and Jellema, A., 2002a. Climate and human induced woody vegetation changes in Botswana and their implications for human adaptation. *Environmental Management*, 30(1):98-109.
Ringrose, S., Kampunzu, A. B., Vink, B., Matheson, W., and Downey, W.S., 2002b. Origin and paleo-environments of calcareous sediments in the Moshaweng dry valley, southeast Botswana. *Earth Surface Processes and Landforms*, 27(6): 591-611.
Ringrose, S., Downey, B., Genecke, D., Sefe, F., and Vink, B., 1999. Nature of sedimentary deposits in the western Makgadikgadi basin, Botswana. *Journal of Arid Environments*, 43:375-397.
Ringrose, S., Vanderpost, C., and Matheson, W., 1997. Use of image processing and GIS techniques to determine the extent and possible causes of land management/fenceline induced degradation problems in the Okavango area, northern Botswana. *International Journal of Remote Sensing*, 18(11), 2337-2364.

Ringrose, S., Matheson, W., and Boyle T., 1988. Differentiation of ecological zones in the Okavango Delta, Botswana, by classification and contextual analysis of Landsat MSS data. *Photogrammetric Engineering and Remote Sensing*, 54:325-332.

Robbins, L.H., Campbell, A.C., Murphy, M.L., Brook, G.A., Srivastava, P., and Badenhorst, S., 2005. The advent of herding in Southern Africa: early AMS dates on domestic livestock from the Kalahari desert. *Current Anthropology*, 46(4): 671-677.

Roberts, D.A., Keller, M., and Soares, J.V., 2003. Studies of land-cover, land-use, and biophysical properties of vegetation in the large scale biosphere atmosphere experiment in Amazonia. *Remote Sensing of Environment*, 87: 377-388.

Robertson, A.I., Bacon, P. and Heagney, G., 2001. The responses of floodplain primary production to flood frequency and timing. *Journal of Applied Ecology*. 38: 126-136.

Rodriguez-Arias, M.A. and Rodo, X., 2004. A primer on the study of transitory dynamics in ecological series using the scale-dependent correlation analysis. *Oecologica*, 138: 485-504.

Rodriguez-Trelles, F., Alvarez, G., and Zapata, C., 1996. Time-series analysis of seasonal changes in the O inversion polymorphism of Drosophila subobscura. *Genetics*, 142: 179-187.

Roerink, G.J. and Menenti, M., 2000. Reconstructing cloudfree NDVI composites using Fourier analysis of time series. *International Journal of Remote Sensing*, 21: 1911-1917.

Roerink, G.J., Menenti, M., Soepboer, W., and Su, Z., 2003. Assessment of climate impact on vegetation dynamics by using remote sensing. *Physics and Chemistry of the Earth*, 28: 103-109.

Rogan, J., Miller, J., Stow, D., Franklin, J., Levien, L. and Fischer, C., 2003. Landcover change monitoring with classification trees using Landsat TM and Ancillary data. *Photogrammetric Engineering & Remote Sensing*, 69(7): 793-804.

Rogan, J., Franklin, J., and Roberts, D.A., 2002. A comparison of methods for monitoring multi-temporal vegetation change using Thematic mapper. *Remote Sensing of Environment*, 80: 143-156.

Rogers, K.H., 1997. Freshwater wetlands. In Vegetation of Southern Africa, eds (Cowling, R.M., Richardson, D.M., and Pierce, S.M), Cambridge University Press.

Roodt, V. 1998. Trees and Shrubs of the Okavango Delta. Shell Field Guide, Part One. Shell Oil, Botswana.

Roques, K.G., O'Conner, T.G., and Watkinson, A.R., 2001. Dynamics of shrub encroachment in an African savanna: relative influences of fire, herbivory, rainfall, and density dependence. *Journal of Applied Ecology*, 38:268-280.

Ross, K., 1987. Okavango: Jewel of the Kalahari. Macmillan Publishing, New York.

Roy, D.P., Frost, P.G.H., Justice, C.O., Landmann, T. LeRoux, J.L., Gumbo, K., Makungwa, S., Dunham, K., Dutoit, R., Mhwandagara, K., Zacarias, A., Tacheba, B., Dube, O.P., Pereira, J.M., Mushove, P., Morisette, J.T., Vannan, S.K., Davies, D., 2005. The southern African Fire Network (SAFNET) regional burned (area product) validation protocol. *Int. J. of Remote Sensing*, 26(19): 4265-4292.

Roy, D.P. and Landmann, T., 2005. Characterizing the surface heterogeneity of fire effects using multi-temporal reflective wavelength data. *International Journal of Remote Sensing*, 26(19): 4197-4218.

Salomonson, V.V. and Appel, I., 2004. Estimating fractional snow cover from MODIS using the normalized difference snow index. Remote Sensing of Environment, 89: 351-360.

Sankaran, M., Ratnam, J., and Hanan, N.P., 2004. Tree-grass coexistence in savannas revisited – insights from an examination of assumptions and mechanisms invoked in existing models. *Ecology Letters*, 7:480-490.

Saunders, S.C., Chen, J., Drummer, T.D., Gustafson, E.J., and Brosofske, K.D., 2004. Identifying scales of pattern in ecological data: a comparison of lacunarity, spectral and wavelet analysis. *Ecological Complexity*; 2:87-105.

Sammy, J. and Opio, C. 2005. Problems and prospects for conservation and indigenous community development in rural Botswana. *Development Southern Africa*, 22(1): 67-85.

Scheffer, M. and Carpenter, S. 2003. Catastrophic regime shifts in ecosystems: linking theory to observation. *Trends in ecology & evolution*, 18(12): 648-656.

Scheffer, M., Carpenter, S., Foley, J.A., Folke, C., and Walker, B., 2001. Catastrophic shifts in ecosystems. *Nature*, 413:591-596.

Schiller, A., C. T. Hunsaker, M. A. Kane, A. K. Wolfe, V. H. Dale, G. W. Suter, C. S. Russell, G. Pion, M. H. Jensen, and V. C. Konar. 2001. Communicating ecological indicators to decision makers and the public. Conservation Ecology **5**(1): 19. [online] URL: http://www.consecol.org/vol5/iss1/art19/

Schneider, E.D. and Kay, J.J., 1994. Life as a manifestation of the second law of thermodynamics. *Mathematical and Computer Modeling*, 19(6/8):25-48.

Scholes, M. and Andreae, M.O., 2000. Biogenic and pyrogenic emissions from Africa and their impacts on the global atmosphere. *Ambio*, 29: 23-29.

Scholes, R.J., Dowty, P.R., Caylor, K., Parsons, D.A.B., Frost, PG.H., and Shugart, H.H., 2002. Trends in savanna structure and composition along an aridity gradient in the Kalahari. *Journal of Vegetation Science*, 13: 419-428.

Scholes, R.J., 2003. Convex relationships in ecosystems containing mixtures of trees and grass. *Environmental and Resource Economics*, 26:559-574.

Scholes, R.J. and Archer, S.R., 1997. Tree-grass interactions in savannas. *Annual Review of Ecological Systems*, 28:517-544.

Scholes, R.J., Pickett, G., Ellery, W.N. and A.C. Blackmore, 1997. Plant functional types in African savannas and grasslands in Plant Functional Types, *ed*. Smith, T.M., Shugart, H.H., and F.I. Woodward. IGBP book series, Cambridge Press.

Scholes, R.J. and Walker, B.H., 1993. An African Savanna: synthesis of the Nylsvley Study. Cambridge University Press.

Scholes, R.J., 1997. Savanna. In Vegetation of Southern Africa, eds (Cowling, R.M., Richardson, D.M., and Pierce, S.M), Cambridge University Press.

Schowengerdt, R.A., 1997. Remote Sensing: Models and Methods for Image Processing. Academic Press, 2nd Edition, San Diego.

Schroeder, T.A., Cohen, W.B., Song, C., Canty, M.J., and Yang, Z., 2006. Radiometric correction of multi-temporal Landsat data for characterization of early successional forest patterns in western Oregon. *Remote sensing of Environment*; 103: 16-26.

Schulze, R.E., 2006. River basin responses to global change and anthropogenic impacts. In Kabat, P., Claussen, M., Dirmeyer, P.A., Gash, J.H., DeGuenni, L., Meybeck, M., Pielke, R.A. Sr., Worosmarty, C.J., Hutjes, R., and Lutkemeier, S. (Eds) Vegetation, Water, Humans, and the Climate. Springer Press.

Scudder, T., Manley, R.E., Coley, R.W., Davis, R.K., Green, J., Howard, G.W., Lawry, S.W., Martz, D., Rogers, P.P., Taylor, A.R.D., Turner, S.D., White, G.F., and E.P. Wright, 1993. The IUCN Review of the Southern Kavango Integrated Water Development Project, Gland, Switzerland: IUCN – The World Conservation Union.

Shackleton, N.H., Hall, M.A., and Vincent, E., 2000. Phase relationships between millennial-scale events 64,000-24,000 years ago. *Paleoceanography*, 15(6): 565-569.

Shea, K., Roxburgh, S.H., Rauschert, E., 2004. Moving from pattern to process: coexistence mechanisms under intermediate disturbance regimes. *Ecology Letters*, 7(6): 491-508.

Sheuyange, A., Oba, G., and Weladji, R., 2005. Effects of anthropogenic fire history on savanna vegetation in northeastern Namibia. *Journal of Environmental Management*, (in press).

Singh, A., 1989. Digital change detection techniques using remotely sensed data. ***Int. Journal of Remote Sensing***, 10: 989-1003.

Skarpe, C., 1992. Dynamics of savanna ecosystems. ***J. of Vegetation Science***, 3(3): 239-300.

Shugart, H.H., 1993. Global Change in Vegetation Dynamics and Global Change, eds Solomon and Shugart, Chapman and Hall Press.

Shuman, C.S. and Ambrose, R.F., 2003. A comparison of remote sensing and ground-based methods for monitoring wetland restoration success. *Restoration Ecology*, 11(3): 325-333.

Slayback, D.A., Pinzon, J.E., Los, S.O., and Tucker, C.J., 2003. Northern hemisphere photosynthetic trends 1982 – 1999. *Global Change Biology*, 9(1): 1-15.

Smith, N.D., McCarthy, T.S., Ellery, W.N., Merry, C.L. and Ruther, H., 1997. Avulsion and anastomosis in the panhandle region of the Okavango Fan, Botswana. *Geomorphology*, 20:49-65.

Smith, T.M., Reynolds, R.W., Livezey, R.E., and Stokes, D., 1996. Reconstruction of historical sea surface temperatures using empirical orthogonal functions. *Journal of Climate*, 9: 1403-1420.

Song, C. and Woodcock, C.E., 2003. Monitoring forest succession with multi-temporal Landsat images: Factors of uncertainty. *IEEE Transactions on Geoscience and Remote Sensing*, 41(11): 2557-2567.
Song, C. and Woodcock, C.E., 2002. The spatial manifestation of forest succession in optical imagery: the potential of multi-resolution imagery. *Remote Sensing of Environment*, 82: 271-284.
Sparks, R.E., 1995. Need for ecosystem management of large rivers and their floodplains. Bioscience, 45(3): 18pgs.
Song, C., Woodcock, C.E., Seto, K.C., Pax-Lenney, M., and Macomber, S.A., 2001. Classification and change detection using Landsat TM data: when and how to correct atmospheric effects. *Remote Sensing of Environment*, 75: 230-244.
Sousa, W.P., 1984. The role of disturbance in natural communities. *Annual Review of Ecology & Systematics*, 15: 353-391.
Sporton, D., Thomas, D.S.G., and Morrison, J., 1999. Outcomes of social and environmental change in the Kalahari of Botswana: the role of migration. *Journal of Southern African Studies*, 25(3): 441-459.
Steneck, R.S., Graham, M.H., Bourque, B.J., Corbitt, D., Erlandson, J.M., Estes, J.A., and Tegner, M.J., 2002. Kelp forest ecosystems: biodiversity, stability, resilience, and future. *Environmental Conservation*, 29: 436-459.
Steven, M.D., Malthus, T.J., Baret, F., Xu, H., and Chopping, M.J., 2003. Intercalibration of vegetation indices from different sensor systems. *Remote Sensing of Environment*, 88:412-422.
Stockli, R. and Vidale, P.L., 2003. European plant phenology and climate as seen in a 20-year AVHRR land surface parameter dataset. *International Journal of Remote Sensing*, 25(17): 3303-3330.
Sullivan, S., 1996. Guest editorial: Towards a non-equilibrium ecology, perspectives from an arid land. *Journal of Biogeography*, 23(1): 1-5.
Swatuk, L.A., 2003. State interests and multilateral cooperation: thinking strategically about achieving wise use of the Okavango Delta system. *Physics and Chemistry of the Earth*, 28:897-905.
Tansley, A.G., 1935. The use and abuse of vegetational concepts and terms. *Ecology*, 16(3): 284-307.
Tiellet, P.M., Staenz, K., and Williams, D.J., 1997. Effects of spectral, spatial, and radiometric characteristics on remote sensing vegetation indices of forested regions. *Remote Sensing of Environment*, 61: 139-149.
Thai, B. and Healey, G., 2002. Invariant subpixel material detection in hyperspectral imagery. *IEEE Transactions on Geoscience and Remote Sensing*, 40(3): 599-608.
Thangarajan, M., Linn, F., Uhl, V., Bakaya, T.B., and Gabaake, G.G., 1999. Modelling an inland delta aquifer system to evolve pre-development management schemes: a case study in the Upper Thamalakane River valley, Botswana, southern Africa. *Environmental Geology*, 38(4): 285-295.
Theobald, D.M., Hobbs, N.T., Bearly, T., Zack, J.A., Shenk, T., and Riebsame, W.E., 2000. Incorporating biological information in local land-use decision making: designing a system for conservation planning. Landscape Ecology, 15(1): 35-45.
Thomas, A., 2003. NGOs' role in limiting national sovereignty over environmental resources of global significance: the 1990 campaign against the southern Okavango integrated water development project. *Journal of International Development*, 15: 215-229.
Thomas, D.S., Brook, G., Shaw, P., Bateman, M., Haberyan, K., Appleton, C., Nash, D., McLaren, S., and Davies, F., 2003. Late Pleistocene wetting and drying in the NW Kalahari: an integrated study from the Tsodilo Hills Botswana. *Quaternary International*, 104:53-67.
Tilman, D., Fargoine, J., Wolff, B., D'Antonio, C., Dobson, A., Howarth, R., Schindler, D., Schlesinger, W.H., Simberloff, D., and Swackhamer, D., 2001. Forecasting agriculturally driven global environmental change. *Science*, 292(5515): 281-284.
Tilman, D. and Lehman, C., 2001. Human-caused environmental change: Impacts on plant diversity and evolution. PNAS, 98(10): 5433-5440.
Tilman, D. 1999. The ecological consequences of changes in biodiversity: a search for general principles. *Ecology*, 80(5): 1455-1474.
Tilman, D. and Downing, J.A., 1994. Biodiversity and stability in grasslands. *Nature*, 367: 363-365
Tiner, R., 1991. A concept of hydrphyte for wetland identification. *Bioscience*, 41(4): 236-247.
Tooth, S. and McCarthy, T.S., 2002. Controls on the transition from meandering to straight channels in the wetlands of the Okavango Delta, Botswana. *Earth Surface Processes and Landforms*, 29:1627-1649.

Torrence, C and Compo, G.P, 1998. A practical guide to wavelet analysis. *Bulletin of the American Meteorological Society*, 79(1): 61-78.
Tottrup, C. and Rasmussen, M.S., 2004. Mapping long-term changes in savannah crop productivity in Senegal through trend analysis of time series of remote sensing data. *Agriculture, Ecosystems, and Environment*, 103: 545-560.
Toussaint, O. and Schneider, E.D., 1998. The thermodynamics and evolution of complexity in biological systems. *Comparative biochemistry and physiology, Part A*, 120(1): 3-9.
Townsend, C.R., Scarsbrook, M.R., and Doledec, S. 1997. The Intermediate disturbance hypothesis, refugia, and biodiversity in streams. *Limnology and Oceanography*, 42(5): 938-949.
Trigg, S.N., Curran, L.M., and McDonald, A.K., 2006. Utility of Landsat 7 satellite data for continued monitoring of forest cover change in protected areas in Southeast Asia. *Singaporae Journal of Tropical Geography*, 27(1): 49-66
Trodd, N.M. and Dougill, A.J. 1998. Monitoring vegetation dynamics in semi-arid African rangelands. *Applied Geography*, 18(4): 315-330.
Tso, B. and Mather, P.M. 2001. Classification Methods for Remotely Sensed Data. CRC Press
Turchin, P. and Taylor, A.D., 1992. Complex dynamics in ecological time series. *Ecology*, 73(1): 289-305.
Turner, M.D., 1999. Spatial and temporal scaling of grazing impact on the species composition and productivitiy of Sahelian annual grasslands. *Journal of Arid Environments*, 41:277-297.
Turner, M.G., Collins, S.L., Lugo, A.R., Magnuson, J.J., Rupp, T.S., and Swanson, F.J., 2003. Disturbance dynamics and ecological response: the contribution on long-term ecological research. *Bioscience*, 53(1):46-56.
Turner, M.G., Gardner, R.H., and R.V.O'Neill. 2001. Landscape ecology in theory and practice: pattern and process. Springer-Verlag, New York.
Turner, M.G., Romme, W.H., Gardner, R.H., O'Neill, R.V., and Kratz, T., 1993. A revised concept of landscape equilibrium: disturbance and stability on scales landscapes. *Landscape Ecology*, 8(3): 213-227.
Turner, M.G., O'Neill, R.V., Gardner, R.H., and Milne, B.T., 1989. Effects of changing spatial scale on the analysis of landscape pattern. *Landscape Ecology*, 3(3/4): 153-162.
Turner, M.G., 1988. Multiple disturbance in a Spartina alterniflora salt marsh: are the additive? *Bulletin of the Torrey Botanical Club*, 115(3): 196-202.
Turner, R.K, van de Bergh, J, Soderqvist, T., Barendregt, A., van der Straaten, J., Maltby, E., and Ierland, E.C., 2000. Ecological-economic analysis of wetlands: scientific integration for management and policy. *Ecological Economics*, 35: 7-23.
Turton, A., Ashton, P. and Cloete E., 2003. Introduction to the hydropolitical drivers in the Okavango River Basin. In Turton, A., Ashton, P., and Cloete T.(eds). Transboundary rivers, sovereignty and development: Hydropolitical drivers in the Okavango River Basin. Pretoria and Geneva: AWIRU and Green Cross International.
Turton, A. and Earle, A., 2003. Public participation in the development of a management plan for an international river basin: the Okavango case. International Symposium on Public participation and governance in water resources, Tokyo Japan. Available online at http://www.okavangochallenge.com/files/wp6/Public%20Participation%20in%20the%20Dev.pdf
Twyman, C., 2001. Natural resource use and livelihoods in Botswana's Wildlife Management Areas. *Applied Geography*, 21: 45-68.
Tyson, P.D., Cooper, G.R.J., and McCarthy, T.S., 2002. Millennial to multi-decadal variability in the climate of southern Africa. *International Journal of Climatology*, 22: 1105-1117.
Tyson, P.D. and Gatebe, C.K., 2001. The atmosphere, aerolos, trace gases and biogeochemical change in southern Africa: a regional integration. *South African Journal of Science;* 97: 106-118.
Tyson, P.D., Dyer, T.G.J., and Mametse, M.N., 1975. Secular changes in South African rainfall: 1880 to 1972. *Quarterly Journal of the Royal Meteorological Society*, 101:817-833.
Uhl, C. and Kauffman, J.B., 1990. Deforestation, fire susceptibility, and potential tree responses to fire in the eastern Amazon. *Ecology*, 71(2): 437-449.
Ungar, S.G. and Pearlman, J., 2002, Overview of the NASA EO-1 Mission, *Proceedings: International Geoscience and Remote Sensing Society Conference*, 24-28 June 2002, 568-571

US EPA, 2007. Report on the Environment. http://www.epa.gov/indicators/.
Uys, R.G., Bond, W.J., and Everson, T.M., 2004. The effect of different fire regimes on plant diversity in southern African grasslands. *Biological Conservation*, 118: 489-499.
van de Koppel and Rietkerk, M., 2004. Spatial interactions and resilience in arid ecosystems. *American Naturalist*, 163: 113-121.
van der Valk, A.G., 1994. Effects of prolonged flooding on the distribution and biomass of emergent species along a freshwater wetland coencline, *Vegetatio*, 110: 185-196.
van Langevelde, F., van De Vijver, C.A., Kumar, L., van de Koppel, J., de Ridder, N., van Andel, J., Skidmore, A.K., Hearne, J.W., Stroosnijder, L., Bond, W.J., Prins, H.H.T., and Rietkerk, M., 2003. Effects of fire and herbivory on the stability of savanna ecosystems. *Ecology*, 84(2):337-350.
van Wilgen, B.W., Govender, N., Biggs, H.C., Ntsala, D., and Funda, X.N., 2004. Response of savanna fire regimes to change fire-management policies in a large African national park. *Conservation Biology*, 18(6): 1533-1540.
Veenendaal, E.M., Kolle, O., and Lloyd, J., 2004. Seasonal variation in energy fluxes and carbon dioxide exchange for a broad-leaved semi-arid savanna (Mopane woodland) in Southern Africa. *Global Change Biology*, 10:318-328.
Verbyla, D.L. and Boles, S.H. 2000. Bias in land cover change estimates due to misregistration. *International Journal of Remote Sensing*, 21(18): 3553-3560.
Viedma, O., Melia, J., Segarra, D., and Garcia-Haro, J., 1997. Modeling rates of ecosystem recovery after fires by using Landsat TM data. *Remote Sensing of Environment*, 61:383-398.
Villa, F. and McLeod, H., 2002. Environmental vulnerability indicators for environmental planning and decision making: guidelines and applications. *Environmental Management*, 29(3): 335-348.
Vitousek, P.M., Mooney, H.A., Lubchenco, J., and Melillo, J.M., 1997. Human domination of Earth's ecosystems. *Science*, 277(5325): 494-499.
Vitousek, P.M., 1994. Beyond global warming: ecology and global change. *Ecology*, 75(7): 1861-1876.
Vogelmann, J.E., Helder, D., Morfitt, R., Choate, M.J., Merchant, J.W., and Bulley, H., 2001. Effects of Landsat 5 thematic mapper and Landsat 7 enhanced thematic mapper plus radiometric and geometric calibrations and corrections on landscape characterization. *Remote Sensing of Environment*, 78:55-70.
Walker, B., Gunderson, L., Kinzig, A., Folke, C., Carpenter, S. and Schultz, L., 2006. A handful of heuristics and some propositions for understanding resilience in social-ecological systems. Ecology and Society 11(1-13). Available online http://www.ecologyandsociety.org/vol11/iss1/art13
Walker, B.H., Ludwig, D., Holling, C.S., and Peterman, R.M., 1981. Stability of semi-arid savanna grazing systems. *Journal of Ecology*; 69: 473-498.
Wallace, J.M., Smith, C., and Bretherton, C.S., 1992. Singular value decomposition of wintertime sea surface temperature: 500-mb height anomalies. *Journal of Climate*, 5: 561-576.
Walter, H., 1971. Ecology of tropical and subtropical vegetation in: Burnett, J.H. (ed). Oliver and Boyd.
Walther, G-R., Post, E., Convey, P., Menzel, A., Parmesan, C., Beebee TJC., Fromentin, J-M., Hoegh-Guldberg, O., and Bairlein, F., 2002. Ecological responses to recent climate change. *Nature*, 416: 389-395.
Wang, Q., Adiku, S., Tenhunen, J., and Granier, A., 2005. On the relationship of NDVI with leaf area index in a deciduous forest site. *Remote Sensing of Environment*, 94: 244-255.
Wang, B. and Wang, Y., 1996. Temporal structure of the southern oscillation as revealed by waveform and wavelet analysis. *J. Climate*, 9(7): 1586-1598.
Waple, A.M., 1999. The sun-climate relationship in recent centuries: a review. *Progress in Physical Geography*, 23: 309-328.
Weber, G.E., Jeltsch, F., van Rooyen, N., and Milton, S.J., 1998. Simulated long-term vegetation response to grazing heterogeneity in semi-arid rangelands. *Journal of Applied Ecology*, 35:687-699.
Wellington, J.H., 1949. A new development scheme for the Okovango Delta, Northern Kalahari. *The Geographical Journal*, 113:62-69.
West, M., 1997. Time series decomposition. *Biometrika*, 84(2): 489-494.
Whelen, R.J., 1995. The ecology of fire. Cambridge Press.
White, P.S. and Jentsch, A., 2001. The search for generality in studies of disturbance and ecosystem dynamics. *Progress in Botany*, 62:399-449.

Wiegand, T. and Jeltsch, F., 2000. Long-term dynamics in arid and semi-arid ecosystems: synthesis of a workshop. *Plant Ecology*, 150(1/2): 3-6.
Wiens, J.A., 1989. Spatial scaling in Ecology. *Functional Ecology*, 3: 385-397.
Wiens, J.A., 1985. Vertebrate responses to environmental patchiness in arid and semi-arid ecosystems. In The Ecology of Natural Disturbance and Patch Dynamics, Pickett and White (eds), Academic Press.
Wigley, T.M.L. and Raper, S.C.B., 2001. Interpretation of high projections for global-mean warming. *Science*, 293(5529): 451-454.
Wilson, B.H., and Dincer, T., 1976. An introduction to the hydrology and hydrography of the Okavango Delta. *Symposium on the Okavango Delt*a, Botswana Society, Gaborone, pp 33-48.
Wolski, P. and Savenije, H.H.G., 2006. Dynamics of the floodplain-island groundwater flow in the Okavango Delta, Botswana. *Journal of Hydrology*, 320: 283-301.
Wolski, P. and Murray-Hudson, M. 2006. Flooding dynamics in a large low-gradiant alluvial fan, the Okavango Delta, Botswana, from analysis and interpretation of a 30 year hydrometric record. *Hydrology and Earth System Sciences*, 10: 127-137.
Wolski, P., Savenije, HHS, Murray-Hudson, M., Gumbricht, 2005. Modelling the hydrology of the Okavango Delta, Botswana using a hybrid reservoir-GIS model. *J. Hydrology*, 331: 58-72.
Woodward, F.I., 1987. Climate and Plant Distribution. Cambridge University Press.
Wu, J., and Loucks, O.L., 1995. From balance of nature to hierarchical patch dynamics: A paradigm shift in ecology. *Quarterly Review of Biology*, 70(4): 439-466.
Wyant, J.G., Meganck, R.A., and Ham, S.H., 1995. A planning and decision-making framework for ecological restoration. *Environmental Management*, 19(6): 789-796.
Xiao, J. and Moody, A. 2004. Trends in vegetation activity and their climatic correlates: China 1982 to 1998. International Journal of Remote Sensing, 25(24):5669-5689.
Xiao, X., Braswell, B., Zhang, Q., Boles, S., Frolking, S., and Moore III, B., 2003. Sensitivity of vegetation indices to atmospheric aerosols: continental-scale observations in northern Asia. *Remote Sensing of Environment*, 84: 385-392.
Yang, J. and Prince, S.D., 1997. A theoretical assessment of the relation between woody canopy cover and red reflectance. *Remote Sensing of Environment*, 59: 428-439.
Young, K.R. and Aspinall, R., 2006. Kaleidoscoping landscapes, shifting perspectives. *The Professional Geographer*, 58(4): 436-447.
Zhang, F., Wu, B., and Liu, C., 2003. Using time series of SPOT VGT NDVI for crop yield forecasting. Proceedings to 2003 IEEE Geoscience and Remote Sensing Symposium.

VITA

Amy Lynn Neuenschwander was born in Houston, Texas on November 29, 1968, the daughter of Linda Register Neuenschwander and Fredrick Richard Neuenschwander. After completing her work at Johnston High School, Austin, Texas, in 1987 she entered the University of Texas at Austin. She received the degree of Bachelor of Science in Aerospace Engineering from the University of Texas at Austin in December 1991. During the following years, she was employed as a research associate at the Center for Space Research at the University of Texas at Austin. In September 1997 she entered the Graduate School of the University of Texas at Austin and received a Master of Science in Aerospace Engineering in May 2003. In September 2003 she entered the PhD program in the department of Geography and the Environment. While enrolled in the PhD program, she has received several awards and fellowships including the NASA Earth Systems Science Fellowship # NNG04GR09H, National Science Foundation Doctoral Dissertation Research Improvement Grant # BCS—0503178, University of Texas Continuing fellowship (Miller Student Endowment), Department of Geography and Environment Outstanding Graduate Research Award, Department of Geography and Environment Veselka Award, Houston Advanced Research Center Summer Scholar, and the Prestigious Bruton Fellowship.

Permanent Address: 1717 Zydeco Drive, Round Rock, Texas 78664

This dissertation was typed by the author.